A Reproduced Copy

OF

Reproduced for NASA

by the

NASA Scientific and Technical Information Facility

(NASA-CR-124152) SINGLE-STAGE EARTH-ORBITAL REUSABLE VEHICLE SPACE SHUTTLE FEASIBILITY STUDY. VOLUME 4: VEHICLE DEFINITION, APPENDIXES (Chrysler Corp.) 454 p GP-0 CSCL 22B

G3/31 Unclas 05450

X73-10344

APPENDIX A
BASELINE TRAJECTORIES FOR VEHICLE DEFINITION

Appendix A

BASELINE TRAJECTORIES FOR VEHICLE DEFINITION

A.0 GENERAL

The baseline SERV selected for the vehicle definition task was of hybrid design because it was required to have the capability of delivering the MURP spacecraft plus 25,000 pounds of cargo to the reference space station mission and returning the Personnel Module (PM) plus 25,000 pounds of cargo. However, the baseline spacecraft was the PM, and the MURP was considered as an alternate spacecraft when large landing crossrange is required. Refer to section 1.4 of this volume for vehicle and mission details. Both ascent and reentry trajectory information are given in the following paragraphs.

A.1 ASCENT

A performance weight summary for the design reference trajectory (SERV-PM baseline vehicle) is given in table A-1, and the trajectory printout is reproduced as table A-2. In addition, performance weight summaries for other payloads of interest are included in tables A-3, A-4, and A-5.

A.2 REENTRY

Two reference reentry trajectories for SERV-PM plus 25,000 pounds of cargo were developed for vehicle definition analyses, one was the maximum loads trajectory, table A-6, and the other was the maximum total heating trajectory, table A-7. (Refer to section 1.4 of this volume for further details.)

Table A-1. Performance Weight Summary for SERV/PM*
Due East Launch

(Weight in Pounds)

Liftoff Weight		4,748,706
Ascent Propellants Consumed		-4,200,467
Weight Injected In 50 by 100 n mi Orbit		548,239
Auxiliary Propellants For Circularization		-3,443
Weight Injected Into 100 n mi Reference Orbit		544,796
SERV Weight In Parking Orbit		- 441,620
SERV Weight Empty	373,464	
Lift Engine Propellants	25,443	
RCS/ACS Propellants (1 Day Mission)	19,500	
Flight Propellant Reserve (1%)	11,934	
Residuals and Shutdown Propellants	11,279	
Payload Weight In Reference Orbit		103,176

- T/W at Liftoff = 1.1956
- q_{max} = 425 psf at 77 sec
- $a_{x_{max}}$ = 3.0 g at 139 sec

* PM in the retracted position.

Table A-2. SERV-PM Design Reference Trajectory - 50 by 100 n mi Injection Orbit - 28.5 Degree Inclination

PROJECT APOLLO STANDARD COORDINATE SYSTEM 1

FLIGHT TIME (SEC)	GEOCENTRIC RADIUS (FT)	INERTIAL VELOCITY (FT/S)	INERTIAL PATH ANGLE (DEG)	INERTIAL AZIMUTH (DEG)	GEOCENTRIC LATITUDE (DEG)	LONGITUDE (POS. EAST) (DEG)
.00	20909846.	1341.8	.00	90.00	28.36	-80.56
5.00	20909927.	1342.1	1.43	90.00	28.36	-80.56
10.00	20910134.	1343.5	3.01	89.99	28.36	-80.56
15.00	20910637.	1346.0	4.75	89.99	28.36	-80.56
20.00	20911304.	1350.2	6.65	89.98	28.36	-80.56
25.00	20912208.	1358.0	8.72	89.98	28.36	-80.56
30.00	20913370.	1371.3	10.92	89.97	28.36	-80.56
35.00	20914813.	1390.6	13.24	89.96	28.36	-80.56
40.00	20916560.	1416.6	15.63	89.96	28.36	-80.56
45.00	20918636.	1451.6	18.05	89.95	28.36	-80.56
50.00	20921064.	1497.3	20.41	89.95	28.36	-80.56
55.00	20923863.	1554.8	22.64	89.94	28.36	-80.56
60.00	20927052.	1624.7	24.64	89.94	28.36	-80.56
62.00	20928438.	1655.9	25.35	89.94	28.36	-80.56
64.00	20929887.	1688.7	25.99	89.94	28.36	-80.55
66.00	20931398.	1723.1	26.57	89.94	28.36	-80.55
68.00	20932969.	1758.9	27.07	89.94	28.36	-80.55
70.00	20934599.	1796.1	27.51	89.94	28.36	-80.55
72.00	20936287.	1834.7	27.88	89.95	28.36	-80.55
74.00	20938029.	1873.5	28.15	89.95	28.36	-80.55
76.00	20939821.	1912.5	28.33	89.95	28.36	-80.55
78.00	20941658.	1951.5	28.42	89.96	28.36	-80.54
80.00	20943535.	1990.9	28.44	89.96	28.36	-80.54
82.00	20945449.	2031.8	28.41	89.97	28.36	-80.54
84.00	20947401.	2074.5	28.35	89.97	28.36	-80.54
86.00	20949389.	2119.7	28.26	89.98	28.36	-80.53
88.00	20951415.	2167.8	28.14	89.98	28.36	-80.53
90.00	20953479.	2218.8	28.01	89.99	28.36	-80.52
92.00	20955582.	2272.9	27.85	90.00	28.36	-80.52
94.00	20957726.	2330.3	27.67	90.00	28.36	-80.52
96.00	20959911.	2391.2	27.48	90.01	28.36	-80.51
98.00	20962139.	2455.5	27.26	90.02	28.36	-80.51
100.00	20964410.	2523.4	27.02	90.03	28.36	-80.50
105.00	20970261.	2711.0	26.35	90.05	28.36	-80.49
110.00	20976457.	2932.3	25.63	90.08	28.36	-80.47

Table A-2. SERV-PM Design Reference Trajectory - 50 by 100 n mi Injection Orbit - 28.5 Degree Inclination (continued)

PROJECT APOLLO STANDARD COORDINATE SYSTEM 1

FLIGHT TIME (SEC)	GEOCENTRIC RADIUS (FT)	INERTIAL VELOCITY (FT/S)	INERTIAL PATH ANGLE (DEG)	INERTIAL AZIMUTH (DEG)	GEOCENTRIC LATITUDE (DEG)	LONGITUDE (POS. EAST) (DEG)
115.00	20982978.	3189.2	24.86	90.10	28.36	-80.45
120.00	20989870.	3478.9	24.02	90.14	28.36	-80.42
125.00	20997141.	3800.5	23.12	90.17	28.36	-80.39
130.00	21004794.	4153.9	22.19	90.20	28.36	-80.35
135.00	21012828.	4540.2	21.24	90.24	28.36	-80.31
138.00	21017828.	4786.8	20.66	90.27	28.36	-80.28
139.00	21019525.	4871.2	20.47	90.27	28.36	-80.27
140.00	21021235.	4955.8	20.28	90.28	28.36	-80.26
141.00	21022960.	5040.6	20.09	90.29	28.36	-80.25
142.00	21024698.	5125.5	19.89	90.30	28.36	-80.24
145.00	21029984.	5381.2	19.31	90.33	28.36	-80.21
150.00	21039006.	5810.0	18.34	90.37	28.36	-80.15
155.00	21048240.	6242.1	17.37	90.42	28.36	-80.08
160.00	21057626.	6677.1	16.43	90.47	28.36	-80.01
170.00	21076651.	7555.5	14.64	90.58	28.36	-79.84
180.00	21095576.	8443.9	12.61	90.79	28.35	-79.64
190.00	21113368.	9344.5	10.57	91.06	28.35	-79.41
200.00	21129838.	10256.1	8.66	91.33	28.34	-79.15
210.00	21144961.	11176.6	7.43	91.60	28.34	-78.87
220.00	21158726.	12104.5	6.21	91.87	28.33	-78.56
230.00	21171129.	13038.5	5.16	92.14	28.31	-78.21
240.00	21182177.	13977.9	4.26	92.42	28.30	-77.84
250.00	21191893.	14921.8	3.48	92.71	28.28	-77.44
260.00	21200311.	15869.5	2.81	93.01	28.26	-77.01
270.00	21207476.	16820.7	2.23	93.31	28.24	-76.55
280.00	21213447.	17774.8	1.74	93.63	28.21	-76.07
290.00	21218296.	18731.4	1.32	93.95	28.18	-75.55
300.00	21222107.	19693.1	.97	94.29	28.14	-75.00
310.00	21224977.	20050.6	.68	94.64	28.10	-74.43
320.00	21227017.	21612.6	.44	95.00	28.05	-73.83
330.00	21228350.	22575.7	.26	95.37	27.99	-73.20
340.00	21229113.	23539.7	.13	95.75	27.93	-72.54
350.00	21229456.	24504.3	.04	96.14	27.87	-71.85
360.00	21229543.	25469.2	.00	96.55	27.79	-71.13
364.42	21229544.	25895.7	.00	96.73	27.76	-70.81

Table A-2. SERV-PM Design Reference Trajectory - 50 by 100 n mi Injection Orbit - 28.5 Degree Inclination (continued)

PROJECT APOLLO STANDARD COORDINATE SYSTEM 1

FLIGHT TIME (SEC)	ALTITUDE (FT)	EARTH - FIXED VELOCITY (FT/S)	EARTH - FIXED PATH ANGLE (DEG)	EARTH - FIXED AZIMUTH (DEG)	RANGE (NMI)	GEODETIC LATITUDE (DEG)
.00	-0.	.0	.00	.00	.00	28.52
5.00	81.	33.4	89.82	336.19	.00	28.52
10.00	339.	70.5	89.79	319.50	.00	28.52
15.00	791.	111.4	89.74	308.93	.00	28.52
20.00	1459.	156.4	89.70	302.02	.00	28.52
25.00	2362.	205.8	89.81	33.00	.00	28.52
30.00	3524.	259.8	89.01	80.71	.00	28.52
35.00	4967.	318.6	87.91	85.67	.01	28.52
40.00	6715.	382.3	86.70	87.30	.02	28.52
45.00	8791.	451.3	85.19	88.19	.05	28.52
50.00	11218.	525.7	83.36	88.74	.08	28.52
55.00	14018.	605.5	81.23	89.09	.15	28.52
60.00	17207.	690.5	78.82	89.33	.24	28.52
62.00	18592.	725.4	77.78	89.41	.29	28.52
64.00	20041.	760.5	76.71	89.48	.34	28.52
66.00	21552.	795.7	75.59	89.54	.40	28.52
68.00	23123.	831.0	74.44	89.59	.47	28.52
70.00	24754.	866.5	73.25	89.64	.55	28.52
72.00	26441.	902.0	72.03	89.68	.64	28.52
74.00	28183.	936.2	70.77	89.72	.73	28.52
76.00	29975.	969.2	69.48	89.76	.84	28.52
78.00	31812.	1000.8	68.15	89.80	.96	28.52
80.00	33689.	1031.7	66.78	89.83	1.08	28.52
82.00	35604.	1063.5	65.38	89.86	1.22	28.52
84.00	37555.	1096.4	63.94	89.89	1.37	28.52
86.00	39544.	1131.5	62.48	89.92	1.54	28.52
88.00	41569.	1169.2	60.99	89.94	1.72	28.52
90.00	43633.	1209.6	59.47	89.96	1.91	28.52
92.00	45737.	1252.8	57.95	89.99	2.12	28.52
94.00	47880.	1299.3	56.41	90.01	2.35	28.52
96.00	50066.	1349.2	54.86	90.03	2.60	28.52
98.00	52294.	1402.4	53.32	90.05	2.86	28.52
100.00	54564.	1459.1	51.78	90.07	3.15	28.52
105.00	60435.	1619.3	48.00	90.11	3.96	28.52
110.00	66611.	1814.7	44.35	90.16	4.93	28.52

Table A-2. SERV-PM Design Reference Trajectory - 50 by 100 n mi Injection Orbit - 28.5 Degree Inclination (continued)

PROJECT APOLLO STANDARD COORDINATE SYSTEM 1

FLIGHT TIME (SEC)	ALTITUDE (FT)	* * * EARTH - FIXED * * * VELOCITY (FT/S)	PATH ANGLE (DEG)	AZIMUTH (DEG)	RANGE (NMI)	GEODETIC LATITUDE (DEG)
115.00	73132.	2047.4	40.91	90.20	6.10	28.52
120.00	80023.	2314.6	37.73	90.23	7.48	28.52
125.00	87295.	2615.5	34.80	90.27	9.11	28.52
130.00	94948.	2950.1	32.12	90.31	11.01	28.52
135.00	102931.	3319.6	29.70	90.36	13.21	28.52
138.00	107981.	3556.9	28.35	90.38	14.69	28.52
139.00	109678.	3636.3	27.92	90.39	15.21	28.52
140.00	111339.	3720.1	27.50	90.40	15.74	28.52
141.00	113113.	3802.0	27.09	90.41	16.29	28.52
142.00	114850.	3884.2	26.65	90.42	16.85	28.52
145.00	120137.	4131.8	25.51	90.44	18.62	28.52
150.00	129158.	4546.4	23.69	90.49	21.64	28.52
155.00	138391.	4969.4	22.03	90.54	25.43	28.52
160.00	147777.	5394.6	20.50	90.60	29.38	28.52
170.00	166800.	6256.3	17.78	90.72	38.37	28.52
180.00	185723.	7129.1	14.99	90.94	48.84	28.51
190.00	203510.	8016.7	12.34	91.25	60.84	28.51
200.00	219974.	8919.0	10.20	91.54	74.37	28.50
210.00	235091.	9833.0	8.45	91.82	89.43	28.50
220.00	248846.	10756.1	6.99	92.11	106.03	28.49
230.00	261236.	11686.6	5.76	92.39	124.16	28.47
240.00	272270.	12623.4	4.72	92.68	143.83	28.46
250.00	281968.	13565.3	3.83	92.98	165.04	28.44
260.00	290364.	14511.7	3.07	93.29	187.79	28.42
270.00	297504.	15461.9	2.43	93.60	212.08	28.40
280.00	303447.	16415.3	1.93	93.93	237.92	28.37
290.00	308232.	17371.4	1.42	94.26	265.31	28.34
300.00	312035.	18329.8	1.04	94.61	294.25	28.30
310.00	314861.	19290.2	.72	94.97	324.74	28.26
320.00	316853.	20252.1	.47	95.33	356.79	28.21
330.00	318131.	21215.3	.23	95.71	390.40	28.15
340.00	318832.	22179.3	.14	96.10	425.57	28.09
350.00	319107.	23144.1	.05	96.51	462.30	28.03
360.00	319118.	24109.2	.00	96.92	500.60	27.95
364.42	319084.	24535.7	.00	97.10	518.02	27.92

Table A-2. SERV-PM Design Reference Trajectory - 50 by 100 n mi Injection Orbit - 28.5 Degree Inclination (continued)

FLIGHT TIME (SEC)	THRUST (LB)	WEIGHT (LB)	LONGITUDINAL ACCELERATION (G'S)	INERTIAL ATTITUDE ANGLES PITCH (DEG)	YAW (DEG)	INCLINATION (DEG)
.00	5677510.	4748706.	1.1956	90.00	.00	28.36
5.00	5678592.	4663706.	1.2173	90.00	.00	28.36
10.00	5687318.	4578706.	1.2405	90.00	.00	28.36
15.00	5704537.	4493706.	1.2655	90.00	.00	28.36
20.00	5728923.	4408705.	1.2915	90.00	.00	28.36
25.00	5764687.	4323705.	1.3196	89.18	.00	28.36
30.00	5807172.	4238705.	1.3484	88.37	.00	28.36
35.00	5857126.	4153705.	1.3779	87.55	.00	28.36
40.00	5914962.	4068704.	1.4081	86.74	.00	28.36
45.00	5985108.	3983704.	1.4402	85.03	.00	28.36
50.00	6050813.	3898704.	1.4702	83.18	.00	28.36
55.00	6117504.	3813704.	1.4981	81.03	.00	28.36
60.00	6161095.	3728703.	1.5179	78.60	.00	28.36
62.00	6172694.	3694703.	1.5185	77.55	.00	28.36
64.00	6185406.	3660703.	1.5168	76.47	.00	28.36
66.00	6191032.	3626703.	1.5125	75.34	.00	28.36
68.00	6201589.	3592703.	1.5091	74.18	.00	28.36
70.00	6219557.	3558703.	1.5073	72.99	.00	28.36
72.00	6239161.	3524703.	1.4904	71.76	.00	28.36
74.00	6266943.	3490703.	1.4618	70.49	.00	28.36
76.00	6309780.	3456703.	1.4378	69.19	.00	28.36
78.00	6347500.	3422702.	1.4027	67.85	.00	28.36
80.00	6395127.	3388702.	1.4007	66.47	.00	28.36
82.00	6445792.	3354702.	1.4067	65.06	.00	28.36
84.00	6493555.	3320702.	1.4203	63.61	.00	28.36
86.00	6545306.	3286702.	1.4479	62.14	.00	28.36
88.00	6593595.	3252702.	1.4753	60.63	.00	28.36
90.00	6639349.	3218702.	1.5057	59.11	.00	28.36
92.00	6679369.	3184702.	1.5391	57.57	.00	28.36
94.00	6711048.	3150702.	1.5763	56.02	.00	28.36
96.00	6742459.	3116701.	1.6142	54.47	.00	28.36
98.00	6762531.	3082701.	1.6500	52.91	.00	28.36
100.00	6782978.	3048701.	1.6908	51.36	.00	28.36
105.00	6928970.	2963701.	1.8381	47.54	.00	28.36
110.00	7180549.	2878701.	2.0243	43.86	.00	28.36

Table A-2. SERV-PM Design Reference Trajectory - 50 by 100 n mi Injection Orbit - 28.5 Degree Inclination (continued)

FLIGHT TIME (SEC)	THRUST (LB)	WEIGHT (LB)	LONGITUDINAL ACCELERATION (G'S)	INERTIAL ATTITUDE ANGLES PITCH (DEG)	INERTIAL ATTITUDE ANGLES YAW (DEG)	INCLINATION (DEG)
115.00	7392970.	2793701.	2.2038	40.39	.00	28.36
120.00	7556354.	2708700.	2.3759	37.16	.00	28.36
125.00	7664275.	2623700.	2.5390	34.19	.00	28.36
130.00	7768599.	2533700.	2.7133	31.46	.00	28.36
135.00	7840542.	2453699.	2.8895	28.98	.00	28.36
138.00	7851286.	2402699.	2.9865	27.60	.00	28.36
139.00	7808318.	2385750.	3.0000	27.16	.00	28.36
140.00	7733463.	2368935.	3.0000	26.72	.00	28.36
141.00	7659341.	2352258.	3.0000	26.30	.00	28.36
142.00	7586037.	2335808.	3.0000	25.88	.00	28.36
145.00	7371729.	2287349.	3.0000	24.67	.00	28.36
150.00	7039315.	2209591.	3.0000	22.78	.00	28.36
155.00	6735000.	2135644.	3.0000	21.04	.00	28.36
160.00	6456956.	2064892.	3.0000	19.42	.00	28.36
170.00	5965910.	1931977.	3.0000	16.51	.00	28.36
180.00	5537563.	1808854.	3.0000	7.63	-1.36	28.36
190.00	5155302.	1694398.	3.0000	6.64	-1.44	28.37
200.00	4809525.	1587693.	3.0000	5.86	-1.51	28.37
210.00	4466294.	1488765.	3.0000	4.87	-1.58	28.38
220.00	4187790.	1395930.	3.0000	3.89	-1.66	28.38
230.00	3926468.	1308823.	3.0000	2.90	-1.73	28.39
240.00	3681290.	1227097.	3.0000	1.91	-1.80	28.40
250.00	3451278.	1150426.	3.0000	.92	-1.87	28.40
260.00	3235511.	1078504.	3.0000	-.07	-1.95	28.41
270.00	3033123.	1011041.	3.0000	-1.06	-2.02	28.42
280.00	2843299.	947766.	3.0000	-2.05	-2.09	28.42
290.00	2665271.	888424.	3.0000	-3.04	-2.16	28.43
300.00	2498315.	832772.	3.0000	-4.04	-2.23	28.44
310.00	2341744.	780581.	3.0000	-5.03	-2.30	28.45
320.00	2194853.	731618.	3.0000	-6.03	-2.37	28.46
330.00	2057031.	685677.	3.0000	-7.02	-2.44	28.47
340.00	1927735.	642579.	3.0000	-8.02	-2.50	28.48
350.00	1806455.	602152.	3.0000	-9.02	-2.57	28.49
360.00	1692706.	564235.	3.0000	-10.01	-2.64	28.50
364.42	1644716.	548239.	3.0000	-10.45	-2.67	28.50

Table A-2. SERV-PM Design Reference Trajectory - 50 by 100 n mi Injection Orbit - 28.5 Degree Inclination (continued)

FLIGHT TIME (SEC)	MACH NO.	DYNAMIC PRESSURE (LB/FT2)	NORMAL FORCE (LB)	AXIAL FORCE (LB)	ANGLE OF ATTACK (DEG)	AERO. HEATING INDICATOR (LB-FT/FT2)	AERO. LOAD INDICATOR (LB-DEG/FT2)
.00	.000	0.	.0	.0	.000	0.	0.
5.00	.029	1.	.0	1638.5	.053	33.	0.
10.00	.062	6.	.0	7254.5	.101	599.	1.
15.00	.098	14.	.0	17965.4	.145	3416.	2.
20.00	.136	27.	.0	34908.2	.185	12111.	5.
25.00	.182	46.	.0	59150.9	.619	33062.	28.
30.00	.231	70.	.0	91587.6	.543	76149.	38.
35.00	.285	101.	.0	133643.9	.231	155270.	23.
40.00	.344	138.	.0	185923.7	.184	288855.	25.
45.00	.406	181.	.0	247948.7	.001	500361.	0.
50.00	.479	227.	.0	318743.9	.002	817928.	0.
55.00	.557	276.	.0	404375.8	.003	1272101.	1.
60.00	.642	325.	.0	501297.8	.005	1893644.	1.
62.00	.678	343.	.0	562455.0	.005	2195084.	2.
64.00	.714	361.	.0	632860.4	.006	2528226.	2.
66.00	.752	376.	.0	705526.0	.007	2893390.	2.
68.00	.791	390.	.0	779344.1	.007	3290436.	3.
70.00	.830	403.	.0	855473.1	.008	3718968.	3.
72.00	.871	413.	.0	985862.6	.009	4178373.	4.
74.00	.912	420.	.0	1164306.7	.010	4666294.	4.
76.00	.952	424.	.0	1339682.7	.011	5178818.	5.
78.00	.992	425.	.0	1546393.7	.012	5711875.	5.
80.00	1.032	423.	.0	1648533.2	.013	6260759.	6.
82.00	1.074	420.	.0	1726826.8	.015	6823241.	6.
84.00	1.118	416.	.0	1777137.5	.016	7398268.	7.
86.00	1.164	411.	.0	1788315.8	.017	7984609.	7.
88.00	1.213	405.	.0	1794734.3	.019	8582345.	8.
90.00	1.265	398.	.0	1792537.3	.020	9190773.	8.
92.00	1.319	391.	.0	1778179.6	.022	9809235.	8.
94.00	1.376	382.	.0	1744048.2	.023	10430760.	9.
96.00	1.435	372.	.0	1711583.6	.024	11072192.	9.
98.00	1.496	361.	.0	1576113.9	.026	11713908.	9.
100.00	1.558	348.	.0	1629139.7	.027	12359806.	10.
105.00	1.714	313.	.0	1481274.0	.031	13977060.	10.
110.00	1.899	283.	.0	1353210.3	.034	15597014.	10.

Table A-2. SERV-PM Design Reference Trajectory - 50 by 100 n mi Injection Orbit - 28.5 Degree Inclination (continued)

FLIGHT TIME (SEC)	MACH NO.	DYNAMIC PRESSURE (LB/FT2)	NORMAL FORCE (LB)	AXIAL FORCE (LB)	ANGLE OF ATTACK (DEG)	AERO. HEATING INDICATOR (LB-FT/FT2)	AERO. LOAD INDICATOR (LB-DEG/FT2)
115.00	2.118	256.	.0	1236215.9	.037	17248327.	10.
120.00	2.369	232.	.0	1120736.7	.041	18937769.	9.
125.00	2.655	207.	.0	1002826.3	.044	20655743.	9.
130.00	2.968	183.	.0	880315.0	.047	22381026.	9.
135.00	3.300	158.	.0	750464.5	.050	24077490.	8.
138.00	3.510	144.	.0	675656.2	.052	25067634.	7.
139.00	3.581	139.	.0	651069.9	.052	25391501.	7.
140.00	3.651	134.	.0	625658.8	.053	25711741.	7.
141.00	3.722	130.	.0	602476.7	.054	26027868.	7.
142.00	3.792	125.	.0	578611.0	.054	26339466.	7.
145.00	4.000	111.	.0	509682.7	.056	27243571.	6.
150.00	4.342	91.	.0	410240.8	.060	28633506.	5.
155.00	4.679	73.	.0	328067.0	.064	29864902.	5.
160.00	5.021	58.	.0	262281.6	.068	30939284.	4.
170.00	5.796	38.	.0	169978.6	.076	32673474.	3.
180.00	6.766	25.	.0	111101.8	5.810	34024539.	143.
190.00	7.851	16.	.0	72107.7	3.942	35040290.	63.
200.00	9.026	10.	.0	46445.7	2.580	35761603.	27.
210.00	.000	0.	.0	.0	1.228	0.	0.
220.00	.000	0.	.0	.0	1.197	0.	0.
230.00	.000	0.	.0	.0	1.327	0.	0.
240.00	.000	0.	.0	.0	1.477	0.	0.
250.00	.000	0.	.0	.0	1.593	0.	0.
260.00	.000	0.	.0	.0	1.662	0.	0.
270.00	.000	0.	.0	.0	1.685	0.	0.
280.00	.000	0.	.0	.0	[illegible]	0.	0.
290.00	.000	0.	.0	.0	1.619	0.	0.
300.00	.000	0.	.0	.0	1.547	0.	0.
310.00	.000	0.	.0	.0	1.462	0.	0.
320.00	.000	0.	.0	.0	1.375	0.	0.
330.00	.000	0.	.0	.0	1.304	0.	0.
340.00	.000	0.	.0	.0	1.262	0.	0.
350.00	.000	0.	.0	.0	1.269	0.	0.
360.00	.000	0.	.0	.0	1.333	0.	0.
364.42	.000	0.	.0	.0	1.361	0.	0.

Table A-3. Performance Weight Summary for SERV/MURP Due East Launch

(Weight in Pounds)

Liftoff Weight		4,752,640
Ascent Propellant Consumed		-4,200,414
Weight Injected In 50 by 100 n mi Orbit		551,923
Auxiliary Propellants For Circularization		-3,466
Weight Injected into 100 n mi Reference Orbit		548,457
SERV Weight in Parking Orbit		-441,646
SERV Weight Empty	373,464	
Lift Engine Propellants	25,443	
RCS/ACS Propellants (1 Day Mission)	19,500	
Flight Propellant Reserve (1%)	11,960	
Residuals and Shutdown Propellants	11,279	
Payload Weight in Reference Orbit		106,811

- T/W at Liftoff = 1.1946
- q_{max} = 426 psf at 77 sec
- $a_{x_{max}}$ = 3.0 g at 138 sec

3

Table A-4. Performance Weight Summary for SERV/LPL (Reusable)*
Due East Launch

(Weight in Pounds)

Liftoff Weight		4,765,288
Ascent Propellants Consumed		-4,200,193
Weight Injected in 50 by 100 n mi Orbit		565,095
Auxiliary Propellants for Circularization		-3,549
Weight Injected into 100 n mi Reference Orbit		561,546
SERV Weight in Parking Orbit		-441,894
SERV Weight Empty	373,464	
Lift Engine Propellants	25,443	
RCS/ACS Propellants (1 Day Mission)	19,500	
Flight Propellant Reserve (1%)	12,208	
Residuals and Shutdown Propellants	11,279	
Payload Weight in Reference Orbit		119,652

- T/W at Liftoff = 1.1914
- q_{max} = 430 psf at 78 sec
- $a_{x_{max}}$ = 3.0 g at 135 sec

* Baseline SERV in the reusable configuration with a large payload (LPL).

Table A-5. Performance Weight Summary for SERV/LPL (Expendable)*
Due East Launch

(Weight in Pounds)

Liftoff Weight		4,771,576
Ascent Propellants Consumed		-4,200,112
Weight Injected in 50 by 100 n mi orbit		571,464
Auxiliary Propellants for Circularization		-3,589
Weight Injected into 100 n mi Reference Orbit		567,875
SERV Weight in Parking Orbit		-397,032
SERV Weight Empty	373,464	
Lift Engine Propellants	NA	
RCS/ACS Propellants (1 Day Mission)	NAA	
Flight Propellant Reserve (1%)	12,289	
Residuals and Shutdown Propellants	11,279	
Payload Weight in Reference Orbit		170,843

- T/W at Liftoff = 1.899
- q_{max} = 449 psf at 76 sec
- $a_{x_{max}}$ = 3.0 g at 134 sec

* Baseline SERV in the expendable configuration with a large payload (LPL). The 170,843-pound payload quoted here does not consider SERV subsystems that are removed when flying as an expendable vehicle. The purpose of this trajectory was to provide an input to subsystem analysis so that removable weights associated with reusable operation could be identified. When this total weight (102,700 lb) was converted to payload weight, the total payload capability was 273,500 pounds. (Refer to section 3.1 of this volume for expendable vehicle details.)

Table A-6. SERV-PM Maximum Loads Trajectory

W/CDA = 62. L/D = .255

TIME (SEC)	ALTITUDE (FT)	VELOCITY (FT/SEC)	GAMMA (DEG)	RANGE (N MI)	ACCEL (G)
0.	400000.	25928.	-1.99	.0	-.00
25.	377700.	25955.	-1.95	104.7	-.00
50.	355750.	25980.	-1.92	209.7	-.00
75.	334176.	26004.	-1.88	314.8	-.00
100.	313013.	26024.	-1.84	420.2	-.01
125.	292325.	26029.	-1.80	525.7	-.04
150.	272283.	25991.	-1.73	631.2	-.13
175.	253316.	25844.	-1.61	736.6	-.33
200.	236292.	25475.	-1.41	841.0	-.70
205.	233235.	25363.	-1.35	861.7	-.79
210.	230324.	25235.	-1.29	882.3	-.89
215.	227571.	25092.	-1.22	902.7	-.99
220.	224987.	24933.	-1.15	923.1	-1.09
225.	222595.	24759.	-1.07	943.3	-1.19
230.	220372.	24570.	-.99	963.4	-1.28
235.	218357.	24366.	-.90	983.3	-1.37
240.	216544.	24149.	-.81	1003.1	-1.45
245.	214936.	23920.	-.72	1022.7	-1.51
250.	213532.	23682.	-.63	1042.0	-1.57
255.	212328.	23435.	-.54	1061.2	-1.61
260.	211317.	23183.	-.45	1080.2	-1.64
265.	210490.	22927.	-.37	1099.0	-1.66
270.	209835.	22668.	-.29	1117.6	-1.66
275.	209336.	22410.	-.22	1135.9	-1.66
280.	208978.	22153.	-.15	1154.1	-1.64
285.	208742.	21899.	-.09	1172.0	-1.62
290.	208609.	21649.	-.05	1189.8	-1.59
295.	208559.	21403.	-.01	1207.3	-1.56
300.	208574.	21162.	.02	1224.7	-1.52
310.	208715.	20699.	.05	1258.8	-1.45
320.	208879.	20258.	.04	1292.1	-1.38
330.	208928.	19837.	-.01	1324.8	-1.32
340.	208738.	19433.	-.10	1356.8	-1.28
350.	208205.	19040.	-.22	1388.1	-1.25
360.	207246.	18653.	-.37	1418.8	-1.25
370.	205796.	18264.	-.54	1448.9	-1.26
380.	203816.	17868.	-.72	1478.4	-1.31
390.	201283.	17455.	-.92	1507.2	-1.37
400.	198199.	17018.	-1.13	1535.3	-1.47
410.	194589.	16549.	-1.34	1562.6	-1.59
420.	190499.	16038.	-1.54	1589.2	-1.74
430.	185998.	15478.	-1.73	1614.9	-1.91
440.	181172.	14862.	-1.91	1639.6	-2.10
445.	178668.	14531.	-1.99	1651.6	-2.20
450.	176120.	14186.	-2.07	1663.3	-2.30
455.	173543.	13825.	-2.15	1674.7	-2.40

Table A-6. SERV-PM Maximum Loads Trajectory (continued)

TIME (SEC)	ALTITUDE (FT)	VELOCITY (FT/SEC)	GAMMA (DEG)	RANGE (N MI)	ACCEL (G)
460.	170947.	13449.	-2.22	1685.9	-2.50
465.	168345.	13059.	-2.28	1696.7	-2.59
470.	165747.	12656.	-2.35	1707.2	-2.67
475.	163161.	12241.	-2.41	1717.3	-2.74
480.	160595.	11816.	-2.48	1727.1	-2.80
485.	158053.	11381.	-2.55	1736.6	-2.87
490.	155540.	10937.	-2.62	1745.7	-2.92
495.	153059.	10486.	-2.69	1754.4	-2.96
500.	150612.	10030.	-2.78	1762.8	-2.98
505.	148197.	9571.	-2.88	1770.8	-3.00
510.	145808.	9112.	-2.99	1778.4	-2.99
515.	143440.	8655.	-3.13	1785.7	-2.98
520.	141084.	8203.	-3.29	1792.6	-2.95
525.	138730.	7756.	-3.48	1799.1	-2.91
530.	136368.	7316.	-3.71	1805.2	-2.86
535.	133987.	6885.	-3.99	1811.0	-2.80
540.	131575.	6465.	-4.31	1816.5	-2.74
545.	129123.	6055.	-4.69	1821.6	-2.67
550.	126619.	5657.	-5.14	1826.3	-2.61
555.	124056.	5271.	-5.65	1830.8	-2.53
560.	121427.	4899.	-6.25	1834.9	-2.46
565.	118725.	4539.	-6.93	1838.8	-2.38
570.	115947.	4194.	-7.72	1842.3	-2.31
575.	113089.	3863.	-8.63	1845.6	-2.23
580.	110153.	3547.	-9.66	1848.6	-2.15
585.	107138.	3246.	-10.84	1851.3	-2.07
590.	104047.	2961.	-12.20	1853.8	-1.99
595.	100885.	2693.	-13.73	1856.0	-1.91
600.	97656.	2441.	-15.49	1858.1	-1.83
610.	91032.	1991.	-19.72	1861.5	-1.67
620.	84246.	1615.	-25.06	1864.2	-1.52
630.	77391.	1310.	-31.53	1866.3	-1.41
640.	70598.	1069.	-38.90	1867.9	-1.32
650.	64025.	881.	-46.64	1869.1	-1.27
660.	57831.	736.	-54.01	1870.0	-1.24
670.	52139.	624.	-60.38	1870.6	-1.20
680.	46962.	543.	-65.44	1871.0	-1.16
690.	42241.	484.	-69.09	1871.3	-1.12
700.	37904.	439.	-71.49	1871.6	-1.10
710.	33886.	405.	-72.97	1871.8	-1.08
720.	30135.	378.	-73.84	1872.0	-1.07
730.	26613.	355.	-74.35	1872.1	-1.06
740.	23238.	335.	-74.65	1872.3	-1.05
750.	20138.	318.	-74.83	1872.4	-1.05
760.	17143.	303.	-74.96	1872.6	-1.04
770.	14288.	289.	-75.05	1872.7	-1.04
780.	11559.	276.	-75.12	1872.8	-1.03
790.	8944.	265.	-75.17	1872.9	-1.03
800.	6433.	255.	-75.22	1873.0	-1.03
825.	550.	233.	-75.33	1873.3	-1.02

Table A-6. SERV-PM Maximum Loads Trajectory (continued)

W/CDA = 62. L/D = .255

TIME (SEC)	DYN PRES (PSF)	MACH	AHI	TAHT
0.	.01	19.735	1.1	0.
25.	.03	22.346	2.1	39.
50.	.09	24.844	4.3	116.
75.	.25	26.660	8.4	266.
100.	.77	28.200	16.7	566.
125.	2.58	29.445	33.3	1164.
150.	7.89	29.399	58.2	2270.
175.	19.85	28.015	83.3	4017.
200.	42.02	26.660	109.3	6419.
205.	47.61	26.377	113.7	6975.
210.	53.44	26.087	117.8	7552.
215.	59.41	25.793	121.2	8148.
220.	65.41	25.494	124.1	8760.
225.	71.29	25.192	126.4	9385.
230.	76.91	24.886	127.9	10021.
235.	82.13	24.578	128.8	10662.
240.	86.83	24.270	129.0	11307.
245.	90.89	23.962	128.5	11951.
250.	94.24	23.656	127.3	12592.
255.	96.82	23.353	125.6	13225.
260.	98.62	23.055	123.4	13849.
265.	99.66	22.763	120.8	14461.
270.	99.97	22.477	117.8	15059.
275.	99.64	22.199	114.6	15641.
280.	98.75	21.929	111.2	16208.
285.	97.39	21.667	107.6	16756.
290.	95.68	21.414	104.1	17287.
295.	93.70	21.168	100.5	17801.
300.	91.55	20.931	97.1	18296.
310.	87.10	20.478	90.4	19237.
320.	82.89	20.048	84.4	20113.
330.	79.33	19.634	79.0	20932.
340.	76.70	19.227	74.3	21700.
350.	75.19	18.818	70.3	22425.
360.	74.92	18.401	67.0	23113.
370.	75.99	17.967	64.2	23770.
380.	78.51	17.509	61.8	24401.
390.	82.57	17.022	59.7	25009.
400.	88.25	16.501	57.8	25597.
410.	95.59	15.941	56.0	26167.
420.	104.55	15.340	54.0	26719.
430.	114.97	14.695	51.8	27249.
440.	126.45	14.008	49.1	27755.
445.	132.41	13.648	47.5	27997.
450.	138.39	13.278	45.9	28232.
455.	144.28	12.899	44.1	28457.

Table A-6. SERV-PM Maximum Loads Trajectory (continued)

TIME (SEC)	DYN PRES (PSF)	MACH	AHI	TAHI
460.	149.96	12.512	42.2	28674.
465.	155.32	12.116	40.1	28881.
470.	160.22	11.714	37.9	29077.
475.	164.56	11.306	35.7	29262.
480.	168.35	10.896	33.4	29436.
485.	172.25	10.505	31.3	29599.
490.	175.43	10.109	29.1	29751.
495.	177.81	9.710	27.0	29893.
500.	179.33	9.308	24.8	30023.
505.	179.98	8.904	22.6	30143.
510.	179.78	8.499	20.5	30251.
515.	178.77	8.096	18.5	30350.
520.	177.04	7.696	16.5	30438.
525.	174.66	7.299	14.7	30517.
530.	171.75	6.909	13.0	30587.
535.	168.38	6.525	11.4	30648.
540.	164.67	6.148	9.9	30702.
545.	160.69	5.780	8.6	30749.
550.	156.51	5.421	7.4	30790.
555.	152.19	5.072	6.4	30825.
560.	147.75	4.733	5.4	30855.
565.	143.22	4.405	4.6	30880.
570.	138.62	4.088	3.9	30902.
575.	133.96	3.782	3.2	30920.
580.	129.23	3.488	2.7	30935.
585.	124.45	3.207	2.2	30947.
590.	119.62	2.939	1.8	30958.
595.	114.78	2.685	1.5	30966.
600.	109.96	2.446	1.2	30973.
610.	100.44	2.014	.7	30982.
620.	91.55	1.644	.5	30988.
630.	84.51	1.346	.3	30992.
640.	79.56	1.110	.2	30994.
650.	76.43	.927	.1	30996.
660.	74.79	.785	.1	30997.
670.	72.04	.666	.1	30998.
680.	69.45	.574	.0	30998.
690.	67.43	.503	.0	30999.
700.	65.97	.449	.0	30999.
710.	64.92	.406	.0	30999.
720.	64.19	.372	.0	31000.
730.	63.63	.343	.0	31000.
740.	63.20	.319	.0	31000.
750.	62.86	.299	.0	31000.
760.	62.58	.281	.0	31000.
770.	62.35	.266	.0	31000.
780.	62.15	.252	.0	31000.
790.	61.97	.240	.0	31000.
800.	61.80	.229	.0	31000.
825.	61.42	.205	.0	31000.

Table A-7. SERV-PM Maximum Total Heating Trajectory

W/CDA = 62. L/D = .300

TIME (SEC)	ALTITUDE (FT)	VELOCITY (FT/SEC)	GAMMA (DEG)	RANGE (N MI)	ACCEL (G)
0.	400000.	25969.	-1.64	.0	-.00
25.	381573.	25991.	-1.61	104.9	-.00
50.	363563.	26012.	-1.57	210.0	-.00
75.	345988.	26031.	-1.53	315.2	-.00
100.	328873.	26049.	-1.48	420.6	-.01
125.	312251.	26062.	-1.44	526.2	-.01
150.	296184.	26064.	-1.39	631.8	-.03
175.	280796.	26040.	-1.32	737.6	-.08
200.	266344.	25959.	-1.22	843.1	-.18
225.	253284.	25782.	-1.08	948.3	-.33
250.	242265.	25461.	-.88	1052.5	-.54
255.	240371.	25377.	-.83	1073.2	-.59
260.	238594.	25285.	-.78	1093.8	-.63
265.	236938.	25187.	-.73	1114.3	-.67
270.	235407.	25082.	-.67	1134.8	-.71
275.	234004.	24971.	-.61	1155.2	-.75
280.	232732.	24854.	-.56	1175.4	-.79
285.	231590.	24732.	-.50	1195.6	-.82
290.	230579.	24605.	-.44	1215.7	-.85
295.	229697.	24474.	-.38	1235.7	-.87
300.	228941.	24339.	-.33	1255.5	-.89
305.	228308.	24202.	-.27	1275.3	-.90
310.	227793.	24063.	-.22	1294.9	-.91
315.	227387.	23923.	-.17	1314.5	-.92
320.	227086.	23782.	-.12	1333.9	-.92
325.	226879.	23641.	-.08	1353.2	-.91
330.	226758.	23500.	-.04	1372.4	-.91
335.	226713.	23361.	-.00	1391.4	-.90
340.	226734.	23224.	.03	1410.4	-.89
345.	226811.	23088.	.05	1429.3	-.87
350.	226932.	22954.	.07	1448.0	-.86
360.	227265.	22693.	.09	1485.2	-.83
370.	227648.	22442.	.10	1521.9	-.80
380.	227997.	22200.	.08	1558.2	-.77
390.	228238.	21966.	.04	1594.2	-.75
400.	228300.	21740.	-.01	1629.8	-.73
410.	228124.	21517.	-.08	1665.0	-.72
420.	227657.	21297.	-.17	1699.8	-.72
430.	226857.	21075.	-.27	1734.3	-.73
440.	225694.	20850.	-.37	1768.4	-.75
450.	224145.	20617.	-.49	1802.2	-.78
460.	222199.	20373.	-.60	1835.6	-.83
470.	219857.	20113.	-.72	1868.5	-.89
480.	217134.	19833.	-.84	1901.1	-.96
490.	214054.	19527.	-.95	1933.1	-1.06
500.	210658.	19191.	-1.06	1964.7	-1.17

Table A-7. SERV-PM Maximum Total Heating Trajectory (continued)

TIME (SEC)	ALTITUDE (FT)	VELOCITY (FT/SEC)	GAMMA (DEG)	RANGE (N MI)	ACCEL (G)
510.	206998.	18817.	-1.15	1995.6	-1.30
520.	203138.	18403.	-1.23	2026.0	-1.44
530.	199151.	17943.	-1.29	2055.6	-1.59
540.	195113.	17434.	-1.33	2084.4	-1.75
550.	191099.	16878.	-1.35	2112.4	-1.91
560.	187175.	16275.	-1.36	2139.4	-2.05
565.	185261.	15958.	-1.36	2152.6	-2.11
570.	183386.	15631.	-1.36	2165.5	-2.17
575.	181552.	15296.	-1.36	2178.1	-2.22
580.	179759.	14954.	-1.36	2190.4	-2.27
585.	178005.	14605.	-1.36	2202.5	-2.31
590.	176288.	14251.	-1.37	2214.2	-2.34
595.	174604.	13892.	-1.38	2225.7	-2.36
600.	172947.	13531.	-1.39	2236.9	-2.38
605.	171309.	13167.	-1.42	2247.8	-2.39
610.	169683.	12803.	-1.45	2258.4	-2.40
615.	168060.	12438.	-1.50	2268.7	-2.40
620.	166431.	12073.	-1.55	2278.7	-2.40
625.	164786.	11708.	-1.62	2288.4	-2.39
630.	163116.	11345.	-1.70	2297.8	-2.38
635.	161412.	10983.	-1.80	2306.9	-2.38
640.	159665.	10622.	-1.91	2315.7	-2.37
645.	157870.	10262.	-2.03	2324.3	-2.37
650.	156021.	9902.	-2.17	2332.5	-2.38
655.	154113.	9542.	-2.33	2340.4	-2.38
660.	152145.	9182.	-2.50	2348.1	-2.38
665.	150113.	8822.	-2.68	2355.4	-2.38
670.	148017.	8462.	-2.88	2362.5	-2.39
675.	145855.	8102.	-3.10	2369.2	-2.39
680.	143630.	7743.	-3.34	2375.7	-2.39
685.	141340.	7384.	-3.60	2381.9	-2.39
690.	138939.	7026.	-3.89	2387.7	-2.39
695.	136578.	6670.	-4.20	2393.3	-2.38
700.	134109.	6316.	-4.54	2398.6	-2.37
705.	131584.	5964.	-4.91	2403.6	-2.36
710.	129006.	5616.	-5.32	2408.3	-2.34
715.	126376.	5273.	-5.78	2412.8	-2.31
720.	123695.	4935.	-6.29	2416.9	-2.28
725.	120966.	4605.	-6.87	2420.8	-2.24
730.	118138.	4282.	-7.52	2424.4	-2.20
740.	112486.	3667.	-9.10	2430.8	-2.09
750.	106539.	3098.	-11.16	2436.3	-1.96
760.	100497.	2585.	-13.85	2440.8	-1.81
770.	94216.	2134.	-17.36	2444.5	-1.67
780.	87774.	1749.	-21.86	2447.5	-1.52
790.	81215.	1431.	-27.44	2449.9	-1.40
800.	74622.	1175.	-34.00	2451.7	-1.32
825.	58830.	748.	-51.70	2454.6	-1.22
850.	45716.	520.	-64.54	2455.9	-1.14
875.	35079.	412.	-70.20	2456.6	-1.08

Table A-7. SERV-PM Maximum Total Heating Trajectory (continued)

TIME (SEC)	ALTITUDE (FT)	VELOCITY (FT/SEC)	GAMMA (DEG)	RANGE (N MI)	ACCEL (G)
900.	26125.	350.	-71.91	2457.1	-1.06
925.	18341.	307.	-72.43	2457.5	-1.04
950.	11433.	274.	-72.65	2457.9	-1.03
975.	5213.	248.	-72.80	2458.2	-1.03

Table A-7. SERV-PM Maximum Total Heating Trajectory (continued)

W/CDA = 62. L/D = .300

TIME (SEC)	DYN PRES (PSF)	MACH	AHI	TAHI
0.	.01	19.766	1.1	0.
25.	.03	21.965	1.9	37.
50.	.06	24.123	3.4	100.
75.	.14	25.659	5.8	212.
100.	.33	27.211	10.2	404.
125.	.81	28.292	17.2	735.
150.	2.07	29.417	29.8	1302.
175.	4.92	29.457	46.1	2233.
200.	10.62	28.950	65.3	3625.
225.	19.78	27.946	82.8	5468.
250.	32.15	26.975	98.0	7729.
255.	34.78	26.781	100.4	8224.
260.	37.38	26.587	102.5	8731.
265.	39.92	26.394	104.3	9247.
270.	42.35	26.202	105.8	9771.
275.	44.63	26.010	106.9	10303.
280.	46.73	25.821	107.8	10839.
285.	48.61	25.634	108.2	11379.
290.	50.25	25.449	108.4	11921.
295.	51.63	25.268	108.2	12463.
300.	52.74	25.090	107.8	13003.
305.	53.57	24.916	107.1	13541.
310.	54.13	24.746	106.1	14074.
315.	54.43	24.582	104.9	14602.
320.	54.48	24.422	103.5	15124.
325.	54.31	24.267	102.0	15638.
330.	53.94	24.117	100.3	16145.
335.	53.40	23.972	98.6	16643.
340.	52.73	23.831	96.7	17132.
345.	51.94	23.696	94.9	17612.
350.	51.08	23.564	93.0	18083.
360.	49.23	23.312	89.2	18996.
370.	47.37	23.072	85.7	19872.
380.	45.67	22.840	82.3	20713.
390.	44.26	22.611	79.4	21523.
400.	43.24	22.380	76.8	22305.
410.	42.68	22.143	74.6	23062.
420.	42.64	21.895	72.9	23800.
430.	43.20	21.632	71.4	24521.
440.	44.40	21.350	70.5	25231.
450.	46.33	21.045	69.8	25933.
460.	49.05	20.713	69.5	26629.
470.	52.64	20.351	69.4	27324.
480.	57.19	19.956	69.4	28017.
490.	62.75	19.527	69.5	28712.
500.	69.36	19.060	69.4	29406.

Table A-7. SERV-PM Maximum Total Heating Trajectory (continued)

TIME (SEC)	DYN PRES (PSF)	MACH	AHI	TAHI
510.	76.98	18.554	69.1	30099.
520.	85.48	18.010	68.4	30787.
530.	94.62	17.428	67.2	31466.
540.	104.03	16.810	65.3	32130.
550.	113.24	16.160	62.7	32772.
560.	121.73	15.482	59.4	33385.
565.	125.56	15.134	57.5	33678.
570.	129.03	14.781	55.5	33962.
575.	132.11	14.425	53.4	34235.
580.	134.77	14.066	51.1	34497.
585.	137.00	13.705	48.8	34748.
590.	138.81	13.342	46.4	34987.
595.	140.21	12.979	44.0	35215.
600.	141.22	12.616	41.6	35430.
605.	141.89	12.255	39.3	35633.
610.	142.24	11.895	36.9	35825.
615.	142.34	11.536	34.6	36005.
620.	142.23	11.181	32.4	36174.
625.	141.97	10.828	30.3	36331.
630.	141.59	10.478	28.2	36479.
635.	141.13	10.132	26.3	36616.
640.	140.99	9.798	24.5	36744.
645.	141.04	9.473	22.8	36862.
650.	141.11	9.150	21.2	36973.
655.	141.23	8.828	19.7	37076.
660.	141.37	8.509	18.2	37172.
665.	141.54	8.190	16.8	37260.
670.	141.71	7.873	15.5	37341.
675.	141.86	7.557	14.2	37416.
680.	141.95	7.241	13.0	37485.
685.	141.95	6.926	11.8	37547.
690.	141.81	6.611	10.7	37604.
695.	141.49	6.297	9.7	37656.
700.	140.94	5.984	8.7	37702.
705.	140.11	5.672	7.7	37744.
710.	138.95	5.362	6.8	37781.
715.	137.44	5.055	6.0	37813.
720.	135.55	4.752	5.2	37842.
725.	133.26	4.452	4.5	37867.
730.	130.57	4.159	3.9	37888.
740.	124.07	3.593	2.8	37922.
750.	116.31	3.063	1.9	37946.
760.	107.76	2.580	1.3	37962.
770.	99.06	2.149	.8	37973.
780.	90.54	1.774	.5	37980.
790.	83.41	1.463	.3	37984.
800.	78.25	1.212	.2	37987.
825.	72.48	.794	.1	37991.
850.	67.42	.548	.0	37992.
875.	64.11	.414	.0	37993.

Table A-7. SERV-PM Maximum Total Heating Trajectory (continued)

TIME (SEC)	DYN PRES (PSF)	MACH	AHI	TAHI
900.	62.66	.337	.0	37994.
925.	61.85	.286	.0	37994.
950.	61.34	.250	.0	37994.
975.	60.95	.222	.0	37994.

APPENDIX B

COMMON BULKHEAD HEAT TRANSFER

APPENDIX B

COMMON BULKHEAD HEAT TRANSFER

The heat transfer from the LO_2 to the LH_2 across the SERV common bulkhead influences the boiloff rate of the LH_2 on the launch pad. Also, the LO_2 temperature at the wall may decrease below the freezing temperature and result in local freezing. An analysis was conducted to compare SERV boiloff rate with the rates experienced with S-II and S-IVB and determine the minimum LO_2 temperature. The analysis was conducted for the steady state condition because this condition will result in the highest boiloff rates and lowest LO_2 temperature.

The steady state heat transfer across a honeycomb wall is calculated from the following equation:

$$q = \frac{K_e A}{\Delta X} \left(T_{w_{LO_2}} - T_{w_{LH_2}} \right)$$

where K_e (from reference B-1) represents the effective conductivity of the core:

$$K_e = K_c \left(\frac{A_w}{A_c} \right) + K_a + K_\lambda$$

The term $K_c \left(\frac{A_w}{A_c} \right)$ is the heat transfer through the metal core. K_a is the heat transfer through the gas inside of the honeycomb (if any is present). K_λ is the effect of radiation heat transfer and is represented by the following equation:

$$K_\lambda = 1.78 \psi L \left(\frac{T_m}{1000} \right) \left(\frac{\Delta T_F}{1000} \right)^2 + 7.12 \psi L \left(\frac{T_m}{1000} \right)^3$$

ψ is a parameter defined by equation 9 of reference B-1 and is a function of core height, cell size, and emissivity.

The SERV common bulkhead analyzed was a 4-inch thick Inconel 718 honeycomb, with a 0.002-inch-thick, 0.50-inch-square cell core. The core was welded to 0.050-inch-inch-thick face sheet. The temperature of the LH_2 and LO_2 sides of the bulkhead were -423°F and -297°F, respectively. Therefore, T_m = -360°F and ΔT_F = 126°F.

C

The thermal conductivity (K_c) of Inconel 718 at -360°F is 4.31 Btu/hr-ft-°R. The area ratio A_w/A_c = 0.00798. Therefore, the conduction through the metal core is:

$$K_c \left(\frac{A_w}{A_c} \right) = 0.0344 \text{ Btu/hr-ft-°R.}$$

K_a is zero for an evacuated honeycomb core because the honeycomb will be evacuated prior to filling the tanks as is done on the S-II and the S-IVB.

The analysis of the radiation contribution to the effective conductivity (K_λ) was based on an emissivity of 1.0. A lower emissivity would reduce the amount of boiloff. Using the above equation:

$$K_\lambda = 0.000494 \text{ Btu/hr-ft-°R.}$$

Comparing the radiation to conduction conductivity, the radiation is less 1.5 percent of the conduction. This is due to the very low temperatures, which reduces radiation.

The total effective conductivity (K_e) for SERV is:

$$K_e = 0.0349 \text{ Btu/hr-ft-°R.}$$

A comparison of the SERV LH_2/LO_2 common bulkhead heat transfer with that of the proven S-II and S-IVB bulkheads is depicted in figure B-1. The SERV effective thermoconductivity was determined analytically as described previously. The corresponding values for the S-II and S-IVB vehicles were obtained from McDonnell Douglas and MSFC, respectively.

In steady state;

$$Q = hA \left(T_{LO_2} - T_{W_{LO_2}} \right) = \frac{K_e A}{\Delta X} \left(T_{W_{LO_2}} - T_{W_{LH_2}} \right)$$

The lowest LO_2 wall temperature ($T_{W_{LO_2}}$) will occur when the LH_2 wall temperature ($T_{W_{LH_2}}$) is equal to -423°F. Rearranging the above equation and substituting in that $T_{W_{LH_2}}$ = -423°F and T_{LO_2} = -297°F gives:

$$T_{W_{LO_2}} = \frac{-297h - 423 \frac{K_e}{\Delta X}}{h + \frac{K_e}{\Delta X}}$$

Reference B-2 shows that the value for h in a LO_2 tank is equal to 72 Btu/hr-ft^2-°R. Using the above data for the honeycomb conductivity

$$\frac{K_e}{\Delta X} = \frac{0.0349}{4/12} = 0.1045 \text{ Btu/hr-ft}^2\text{-F}$$

LH_2/LOX COMMON BULKHEAD HEAT TRANSFER COMPARISON

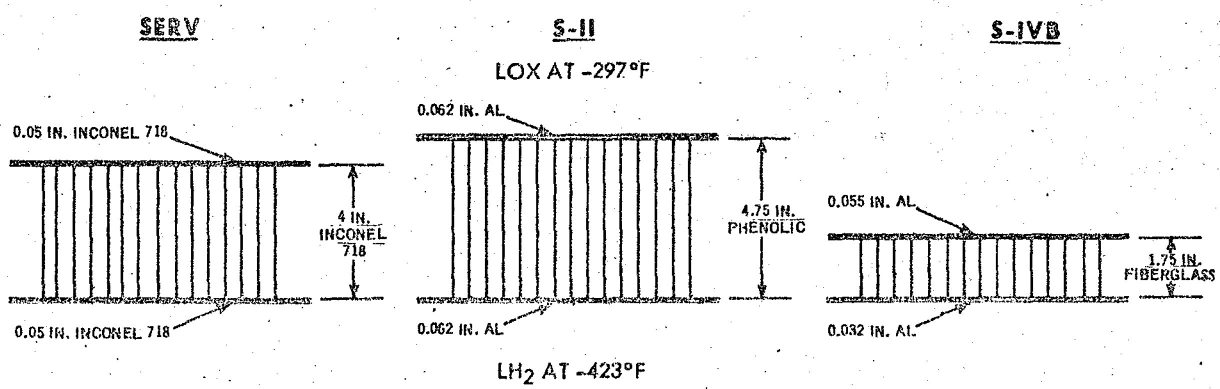

PARAMETER	SERV	S-II	S-IVB
EFFECTIVE K, BTU/HR-FT-°F	0.04	0.020	0.004
HEAT TRANSFER RATE, $BTU/HR\text{-}FT^2$	15.0	6.32	3.45
LH_2 BOIL-OFF RATE, $LBM/HR\text{-}FT^2$	0.078	0.033	0.018
% BOIL-OFF OF TOTAL VOLUME PER HR	0.069	-	0.020

Figure B-1. LH_2/LO_2 Common Bulkhead Heat Transfer Comparison

Substituting these values into the above equation gives a $T_{W_{LO_2}}$ equal to -297.2^oF. The freezing temperature for LO_2 is about -360^oF and, therefore, the LO_2 will not freeze.

REFERENCES:

B-1. Elam, B.F., Heat Transfer in Honeycomb-Core Sandwich Panels, ASME 65-HT-13, August 1965.

B-2. Piske, W. E., Internal Heat Transfer Coefficients of the SI/IB LOX Tanks, CCSD TB-AE-65-184, June 1965.

APPENDIX C

LOADS AND STRESS ANALYSIS

APPENDIX C

LOADS AND STRESS ANALYSIS

The primary objective of this task was to obtain preliminary size definition of the vehicle primary structure and a corresponding weight estimate. To accomplish these objectives, a math model was constructed that was used to determine the internal load distributions in the vehicle under static and dynamic conditions. Because the math model had to be based on a unique structure, it was constructed utilizing the structural sizes and geometry previously used in the work described in both paragraph 4.2.2 and appendix E of volume 3. It had been planned to base the math model on the vehicle configuration output described in volume 3, section 10; however, because these data were not available when the work described herein commenced, the decision was made to continue with the reference vehicle geometry. Because the reference vehicle was 90 feet in diameter, and the point design vehicle, when finally released, was 88 feet, the geometric changes were confined primarily to the lower frustum and the outer cylindrical bulkhead. With reference to the lower frustum, examination of the equation for the critical hoop buckling stress given in paragraph 9.3.2 of volume 3, appendix E, reveals that a decrease in the radius at the large end of the frustum will increase the buckling allowable. Similarly, examination of the equation for the critical meridional buckling stress shown in paragraph 9.3.1 of volume 3, appendix E, reveals that a decrease in radius at the small end of the frustum will increase the buckling allowable. On the other hand, the meridional loadings in the lower frustum will tend to increase directly with the reduction in radius. Because these two effects are somewhat self-compensating, it is believed that the continued use of the reference vehicle geometry will have minor impact on the final objectives of this Phase A study, namely; to establish the feasibility of the concept.

1.0 MATH MODEL CONSTRUCTION

Using the Chrysler-developed digital computer program described in reference 1, a math model was constructed in which the vehicle was idealized as a series of segments joined at circumferential node lines. The program calculates a stiffness matrix for each segment and then assembles them to produce a stiffness matrix for the total vehicle. It should be noted here that the toroidal propellant tank bulkheads were omitted from the math model primarily to provide as many nodes as possible, within the capacity of the program, and to describe the discontinuity effects expected at the points of common attachment between the cylinders and frustums comprising the vehicle primary structure. Because the toroidal bulkheads were designed as thin membranes which attach tangentially at the comparatively much stiffer supporting cylinders, it is believed that their omission from the model has negligible effect on the overall stiffness of the vehicle.

The assembled stiffness matrix is then converted to a flexibility matrix by the use of a factorized inverse table which mathematically provides the same result as the true inverse of the stiffness matrix. Multiplying the flexibility matrix by a load column corresponding to a single design condition, results in a compatible set of nodal deflections for this loading. Three degrees of freedom are provided at each node corresponding, in this instance, to translational loads acting parallel to the longitudinal axis of the vehicle; translational loads whose vectors are oriented radially in a plane normal to the longitudinal vehicle axis; and a moment whose vector is tangential to the nodal circle acting normal to the plane containing the translation vectors. The nodal deflections for each segment are then extracted, multiplied by the segmental stiffness matrix, and a set of compatible internal forces is obtained for each segment.

The input data required to obtain the vehicle stiffness matrix consist of the primary structural sizing of the reference vehicle configuration obtained from section 4.2.2 of volume 3 and appendix E to that volume. The node and segment idealization used to describe the vehicle primary structure configuration are illustrated in figures 1-1 through 1-6, inclusive. The meridional distance between nodes, "L_s", is purely arbitrary; the only requirement being that at the end regions of a given component, the node spacing be sufficiently small to define the discontinuity bending moment variation. Table 1-1 was set up to record the input data that were used to define the single curved segments.

The aft heat shield bulkhead is an assembly of I-beams and sandwich plates assumed to be fabricated from PH15-7 Mo stainless steel with the following physical characteristics.

$$E = 29.0 \times 10^6 \text{ lb/in.}^2$$

$$G = 11.0 \times 10^6 \text{ lb/in.}^2$$

In order to simulate the stiffness of a spherical cap reinforced by a spider beam network, it was believed that a reasonable approximation could be achieved by assuming a 12-in. I-beam with an area of 7.65 in.^{2} and a section modulus of 32.5 in.^{3} acting with a sandwich with $t = 2.50$, $t_f = 0.013$ in. and a width "W" in. The expressions for an effective thickness and effective modulus of elasticity of an equivalent plate were developed as follows:

The elastic properties of the beam section above are:

$$(EI)_{\text{Beam}} = (29.0 \times 10^6)\left(\frac{12}{2}\right)(32.5) = 5655.0 \times 10^6$$

$$(EA)_{\text{Beam}} = (29.0 \times 10^6)(7.625) = 221.85 \times 10^6$$

$$\text{Poisson's ratio} = \mu = \frac{E-2G}{2G} = \frac{29.0 - 22.0}{22.0} = 0.318 \qquad \mu^2 = (0.318)^2 = 0.101$$

The elastic properties of the sandwich plate above are:

$$(EI)_s = WD = W\left[\frac{E}{12(1-\mu^2)}\right](t^3 - tc^3)$$ (refer to paragraph 9.2.3, volume 3, appendix E.)

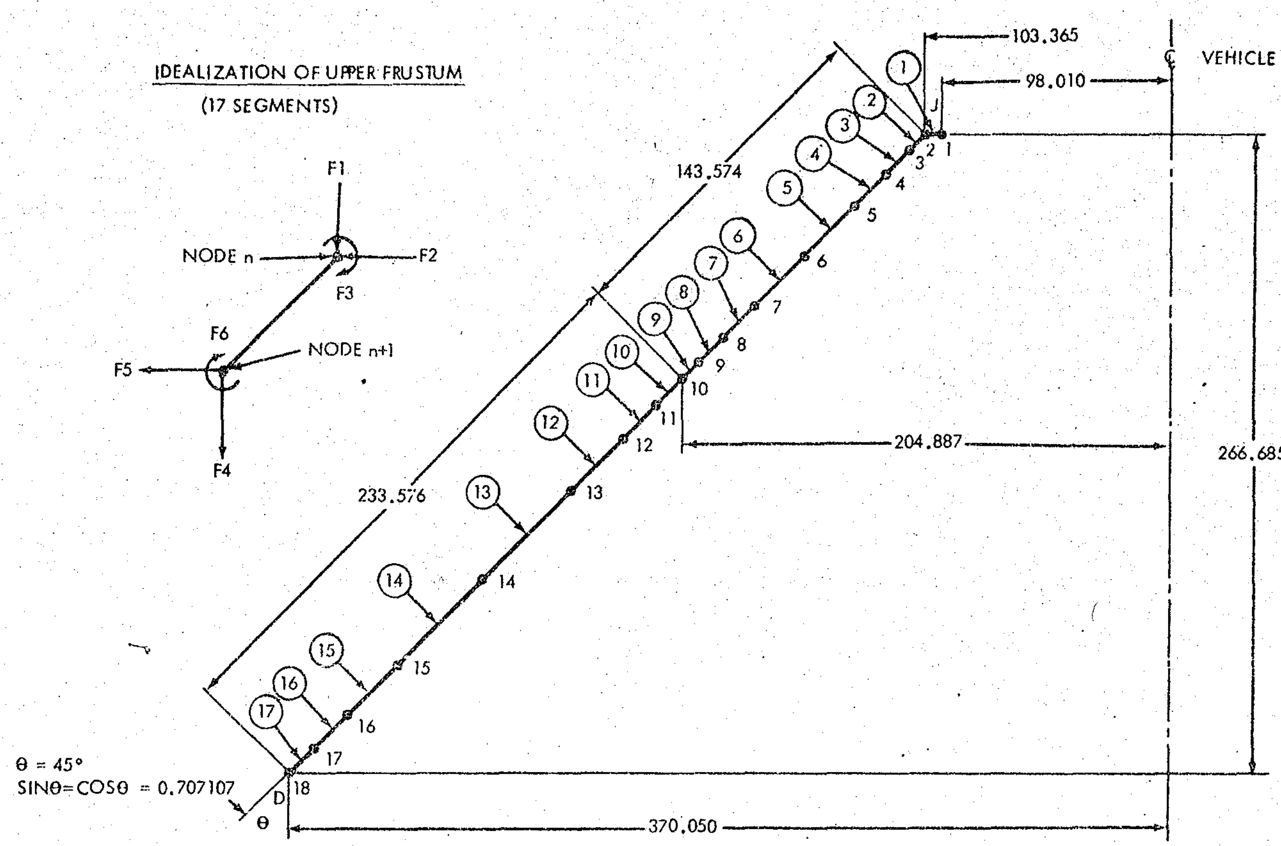

Figure 1-1. Idealization of Upper Frustum (17 Segments)

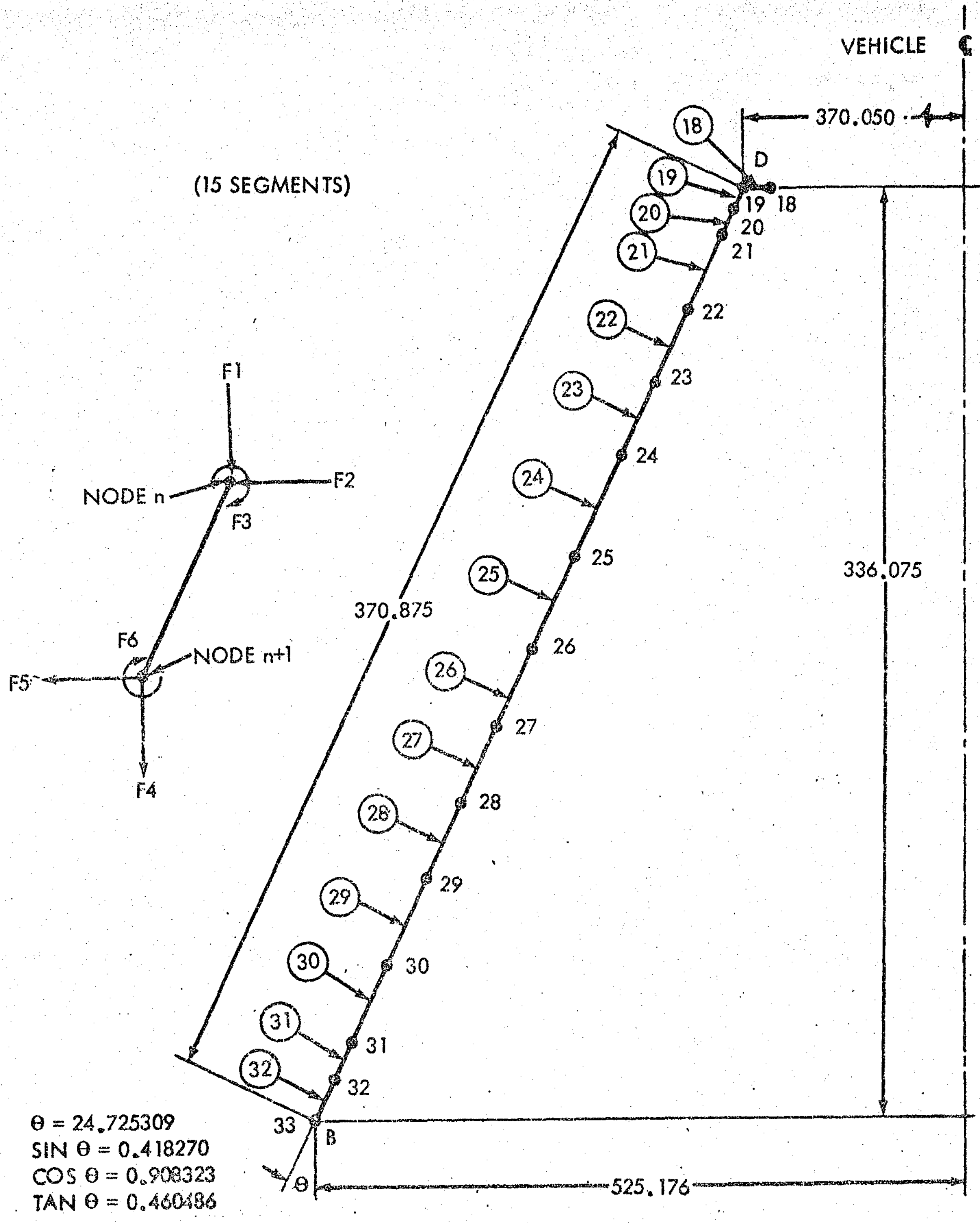

Figure 1-2. Idealization of Lower Frustum (15 Segments)

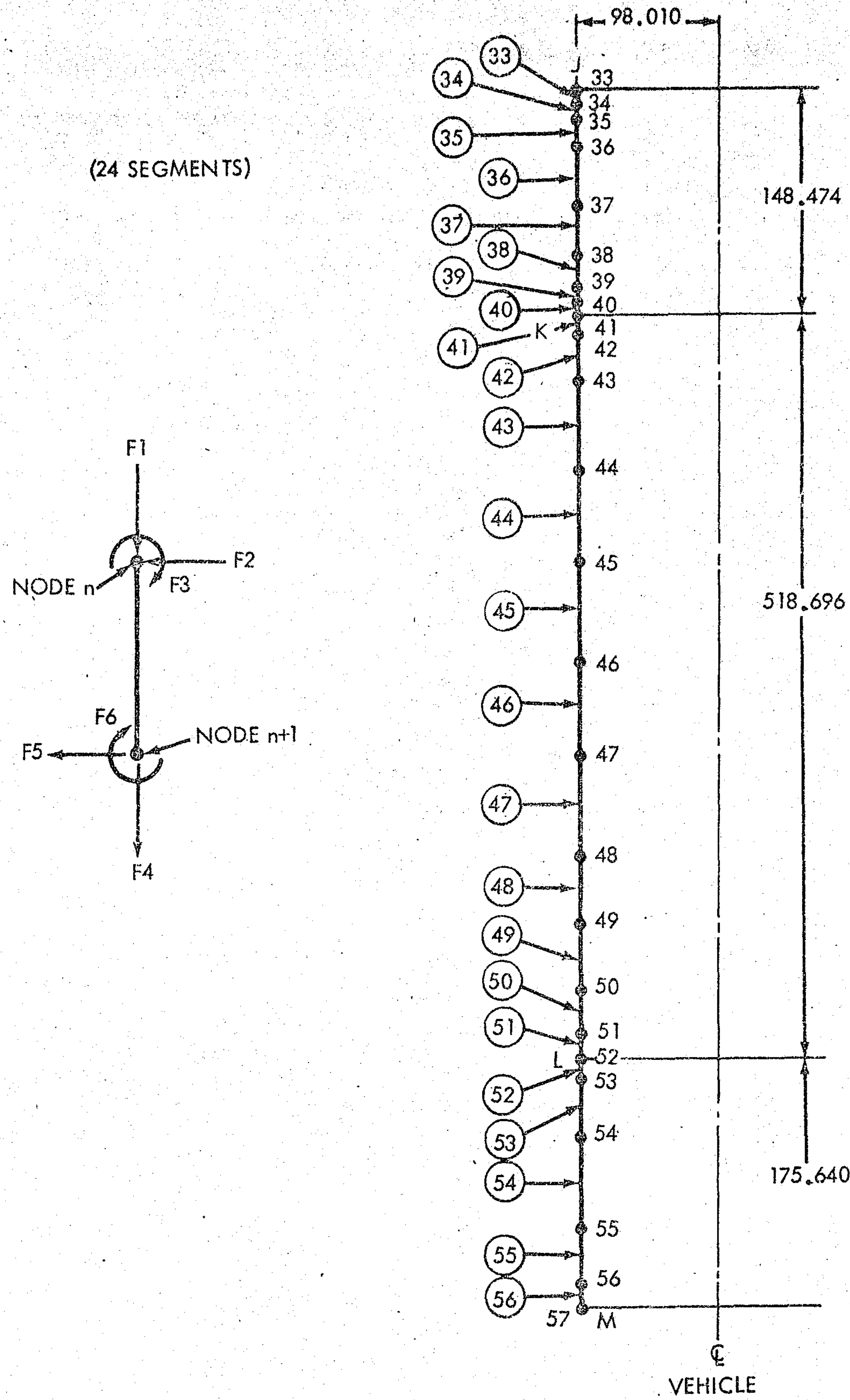

Figure 1-3. Idealization of Inner Cylindrical Bulkhead (24 Segments)

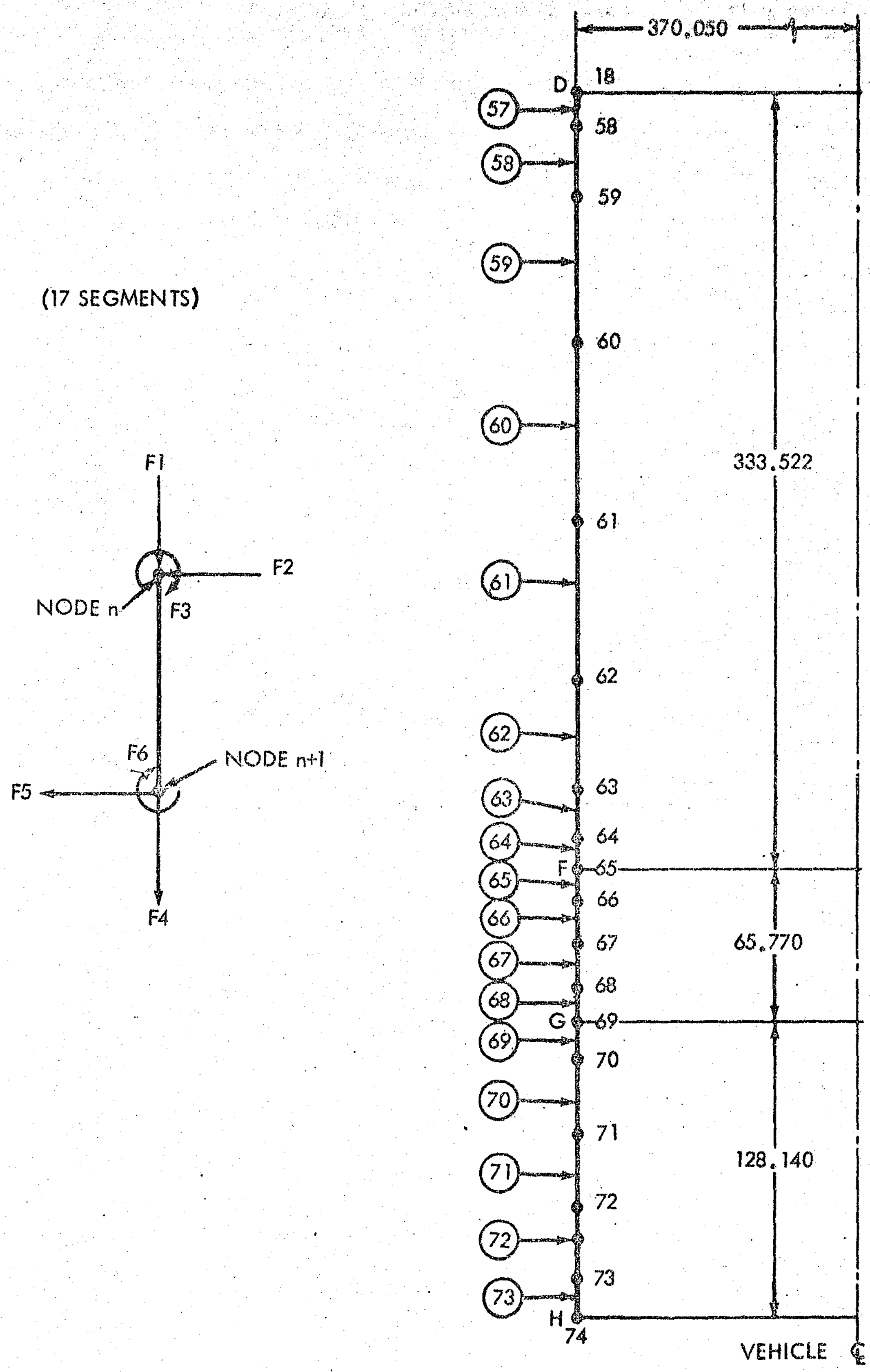

Figure 1-4. Idealization of Outer Cylindrical Bulkhead (17 Segments)

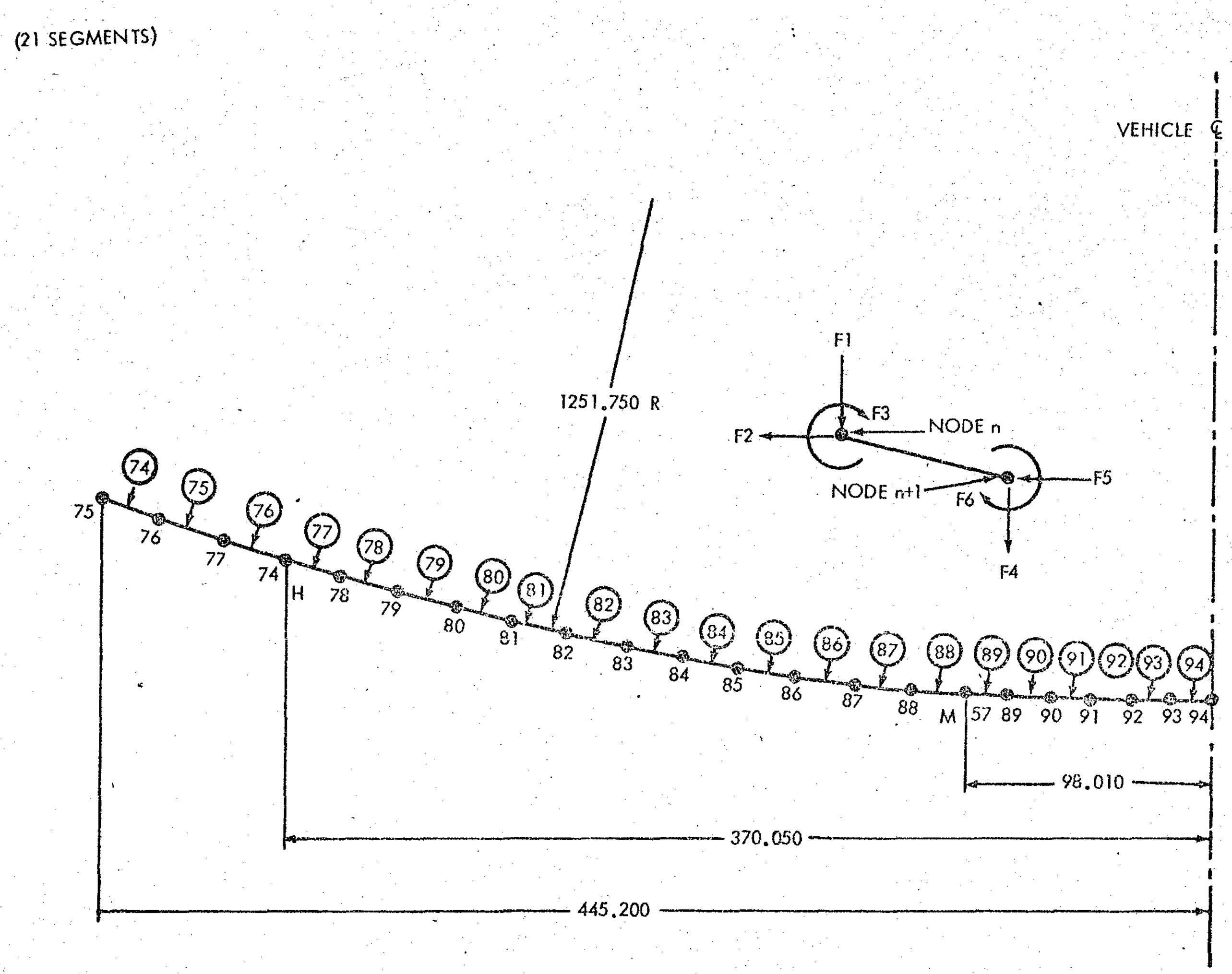

Figure 1-5. Idealization of Heat Shield Bulkhead (21 Segments)

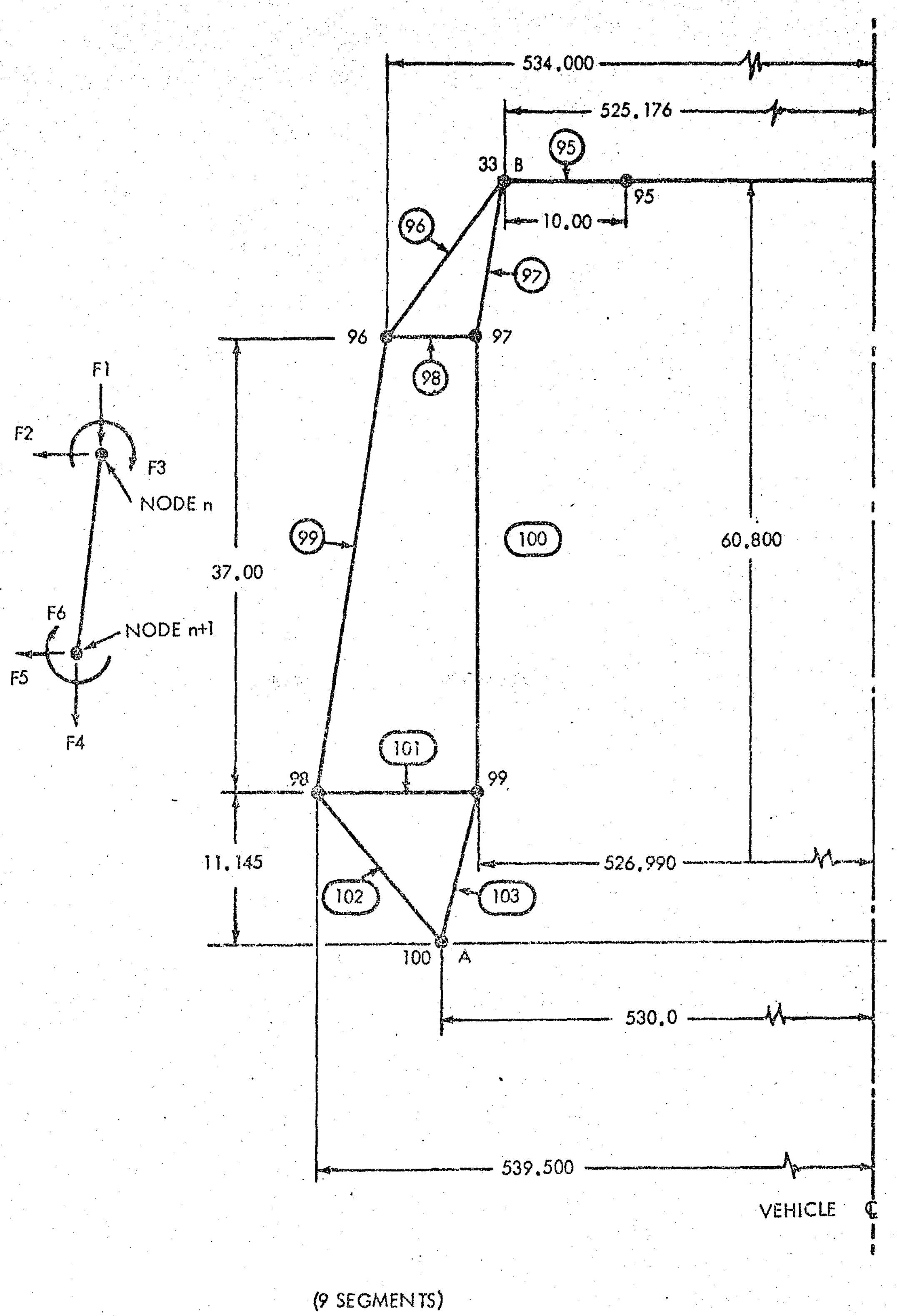

Figure 1-6. Idealization of Engine Thrust Ring (9 Segments)

Table 1-1. Input Data for Single Curved Segments

①	②	③	④	⑤	⑥	⑦	⑧	⑨	⑩
					Actual Sandwich		Equivalent Plate		
Comp.	Seg. No.	ϕ	R_F	L_s	t	t_F	t_e	E_e	Poisson's Ratio μ
Upper Frustum	1	90.0	98.010	5.355	N.A.	N.A.	.246000	29700000	.284
	2	45.0	103.365	9.493	1.600	.016	2.743618	346391	
	3		110.078	14.293					
	4		120.146	16.985					
	5		133.570	29.070					
	6		154.126	29.070					
	7		174.682	18.985					
	8		188.106	14.239					
	9		198.174	9.493	1.600	.016	2.743618	346391	
	10		204.887	15.000	4.000	.020	6.893591	172319	
	11		215.494	20.000					
	12		229.636	30.000					
	13		250.849	51.788					
	14		287.469	51.788					
	15		324.089	30.000					
	16		345.302	20.000					
	17	45.0	359.444	15.000	4.000	.020	6.893591	172319	
Lower Frustum	18	-90.0	370.050	10.000	N.A.	N.A.	.482000	29700000	
	19	24.725309	370.050	8.093	2.700	.016	4.648885	204425	
	20		373.435	10.000					
	21		377.610	29.494					
	22		389.954	32.906					
	23		403.718	32.907		.016	4.648885	204425	
	24		417.482	36.019		.018	4.645395	230175	
	25		432.548	38.690					
	26		448.731	38.691		.018	4.645395	230175	
	27		464.914	32.179		.020	4.641939	255925	
	28		478.374	32.179					
	29		491.834	30.352					
	30		504.529	18.690		.020	4.641939	255925	
	31		512.346	15.675		.027	4.629851	346391	
	32	24.725309	518.902	15.000	2.700	.027	4.629851	346391	
Inner Cylindrical Bulkhead	33	0	98.010	5.000	.375	.010	.632258	939500	
	34			10.000					
	35			20.000					
	36			39.237					
	37			39.237					
	38			20.000					
	39			10.000					
	40			5.000	.375		.632258	939500	
	41			15.000	3.400		5.871661	101158	
	42			30.000					
	43	0	98.010	60.000	3.400	.010	5.871661	101159	.284

Table 1-1. Input Data for Single Curved Segments (continued)

①	②	③	④	⑤	⑥	⑦	⑧	⑨	⑩
					ACTUAL SANDWICH		EQUIVALENT PLATE		POISSON'S RATIO
COMP.	SEG. No.	ϕ	R_F	L_s	t	t_F	t_e	E_e	μ
INNER CYLINDRICAL BULKHEAD	44	0	98.010	67.466	3.400	.010	5.071661	101158	.204
	45			67.467					
	46			68.375					
	47			68.375	3.400		5.071661	101158	
	48			48.507	3.800		6.564480	90496	
	49			48.506					
	50			30.000					
	51			15.000	3.800		6.564480	90496	
	52			14.413	.375		.632258	939500	
	53			40.000					
	54			66.814					
	55			40.000					
	56		98.010	14.413	.375	.010	.632258	939500	
OUTER CYLINDRICAL BULKHEAD	57		370.050	13.588	4.000	.036	6.865943	311464	
	58			27.176					
	59			54.352					
	60			71.645		.036	6.865943	311464	
	61			71.645		.070	6.807320	610810	
	62			54.352					
	63			27.176					
	64			13.588	4.000	.070	6.807320	610810	
	65			13.457	.680	.014	1.153628	720849	
	66			19.428					
	67			19.428					
	68			13.457					
	69			15.870					
	70			32.133					
	71			32.134					
	72			32.133					
	73	0	370.050	15.870	.680	.014	1.153628	720849	
ENGINE THRUST RING	95	-90.0	525.176	10.000	N.A.	N.A.	.478000	29700000	-
	96	34.006977	525.176	15.428	1.000	.020	1.697528	699841	
	97	8.137389	525.176	14.467					
	98	-90.0	534.000	7.010					
	99	8.548793	534.000	37.407					
	100	0	526.990	37.000					
	101	-90.0	539.500	12.510					
	102	-40.444333	539.500	14.644					
	103	15.113763	526.990	11.544	1.000	.020	1.697528	699841	.204

$$(EI)_s = \frac{(29.0 \times 10^6)(W)\ (2.50)^3 - (2.474)^3}{12\ (1 - 0.101)} = (1.296 \times 10^6)\ W$$

$(EA)_s = WH = W\ E\ (t - t_c)$ (refer to paragraph 9.2.3, volume 3, appendix E.)

$$(EA)_s = (29.0 \times 10^6)(0.026)(W) = (0.754 \times 10^6)W$$

The elastic properties of the combined beam and sandwich may then be found as follows:

Item	EA	$\bar{y}$	EAy	EAy^2	EI.
Beam	221.85×10^6	8.50	1885.725×10^6	16028.663×10^6	5655.0×10^6
Sandwich	$(0.754 \times 10^6)W$	1.250	$(0.942500 \times 10^6)W$	$(1.178125 \times 10^6)W$	$(1.296 \times 10^6)W$

$$(\bar{y})_{B\&S} = (1885.725 + 0.942500W)10^6/(221.85 + 0.754W)10^6$$

$$(EI)_{B\&S} = (16028.663 + 5655.0 + 1.178125W + 1.296W)10^6 - (221.85 + 0.754W)10^6 \times \left[\frac{1885.725 + 0.942500W}{(221.85 + 0.754W)}\right]^2$$

$$= \left[\frac{1254561.861 + 13343.775W + 0.977184W^2}{221.850 + 0.754W}\right] 10^6$$

$$(EA)_{B\&S} = (221.85 + 0.754W)10^6$$

Assuming an equivalent plate of width "W" and a thickness "te", we can write:

$$(EI)_e = E_e \frac{Wt_e^3}{12(1-\mu^2)} = \frac{E_e\ Wt_e^3}{10.788}$$

$$(EA)_e = E_e\ W\ t_e$$

Setting the elastic properties of the beam-sandwich combination equal to those of the equivalent plate, we can write:

$$(EI)_e = (EI)_{B\&S}$$

$$\frac{E_e\ Wt_e^3}{10.788} = \left[\frac{1254562 + 13343.775W + 0.977184\ W^2}{221.850 + 0.754W}\right] 10^6$$

and $(EA)_e = (EA)_{B\&S}$

$$E_e\ Wt_e = (221.85 + 0.754W)\ 10^6$$

Solving each of the previous expressions for "E_e" and setting the two expressions equal to each other, we get:

$$\frac{(10.788 \times 10^6)\ 1254562 + 13343.775W + 0.977184\ W^2}{W\ t_e^3\ (221.850 + 0.754W)} = \frac{(221.85 + 0.754W)\ 10^6}{Wt_e}$$

from which

$$t_e = \frac{10.788(1254562 + 13343.775W + 0.977184\ W^2)^{\frac{1}{2}}}{(221.85 + 0.754\ W)}$$

Because there are eight major radial beams in the aft heat shield bulkhead, the circumferential width "W" associated with each radial beam at a radius "R_s" from the centerline of the vehicle is:

$$W = \frac{2\pi \quad R_s}{8} = 0.785398\ R_s$$

If "R_s" is now defined as a point midway between two nodes on the idealized aft heat shield bulkhead (refer to figure 1-5), it can be evaluated from:

$$R_s = R_B \sin \quad \theta s$$

where

R_B = spherical radius of bulkhead = 1251.750 in.

θ_s = angle between line connecting origin of spherical radius to point midway between nodes and longitudinal centerline of the vehicle.

Table 1-2 was set up to summarize the results of a calculations made to evaluate "t_e" and "E_e" for the aft heat shield bulkhead. With these data available, it was then possible to complete table 1-3 which summarizes all of the input data required to define segments with double curvature.

The individual segmental stiffness matrices were then stacked to create the desired stiffness matrix for the vehicle assembly as illustrated in table 1-4. The singular 300 by 300 matrix thus assembled is then made nonsingular by elimination of those rows and columns which correspond to degrees of freedom at which the final deflections are zero. In this case, it was assumed that the attachment ring in the payload at the connection with SERV (point J on figure 3, volume 3, appendix E, would be quite stiff in the radial direction, so the corresponding deflection at node no. 1 (refer to figure 1-1) was arbitrarily set equal to zero. With reference to figure 1-5, the requirements of symmetry demand that the radial and rotational deflections at node no. 94 also be set equal to zero. Finally, in order to provide static equilibrium in the longitudinal direction, the corresponding deflection vector at node no. 100 was made equal to zero. With the construction of the nonsingular stiffness matrix for the complete vehicle, the math model is essentially complete. The final stiffness matrix was output on tape which was subsequently used as part of the input data to the computer program utilized to study the dynamic behavior of the vehicle structure.

2.0 DYNAMIC LOADS ANALYSIS

2.1 NORMAL MODES AND FREQUENCIES

A longitudinal dynamic model was constructed by adding two bulkhead models (LH_2 and LO_2) to the axisymmetric-shell model of the structures study (paragraph 1). The dynamic model had a total of 116 degrees of freedom. Four mass conditions were considered for the free-free case: Full (t = 0),

Table 1-2. Summary of t_e and E_e Calculations - Aft Heat Shield Bulkhead

①	②	③	④	⑤	⑥
SEGMENT No.	θ_n	R_s	W	t_e	E_e
74	20.834074	432.789	339.912	16.690	84282
75	19.621049	407.826	320.306	16.818	86016
76	18.408024	382.690	300.564	16.945	88056
77	17.195000	358.981	281.943	17.064	90299
78	16.136307	336.767	264.496	17.174	92743
79	15.077614	314.428	246.951	17.281	95617
80	14.018921	291.994	229.332	17.385	99013
81	12.960228	269.450	211.625	17.484	103084
82	11.901535	246.824	193.855	17.575	108018
83	10.842842	224.107	176.013	17.658	114080
84	9.784149	201.311	158.109	17.728	121749
85	8.725456	178.452	140.156	17.781	131426
86	7.666763	155.531	122.154	17.813	144285
87	6.608070	132.552	104.106	17.816	161933
88	5.549377	109.176	85.747	17.782	187901
89	4.490690	89.859	70.575	17.716	219997
90	3.742242	73.545	57.762	17.626	260681
91	2.993794	57.206	44.929	17.498	325282
92	2.245346	40.867	32.097	17.322	442551
93	1.496898	24.528	19.264	17.086	718149
94	.748450	8.176	6.421	16.774	2104720

Table 1-3. Input Data for Double Curved Segments

① Segment No.	② R_M	③ R_c	④ θ_1	⑤ θ_2	⑥ t_e	⑦ E_e	⑧ Poisson's Ratio μ
74	1251.750	0	159.165926	160.378951	16.690	84282	.318
75	↑	↑	160.378951	161.591976	16.818	86016	↑
76			161.591976	162.805000	16.945	88056	
77			162.805000	163.863693	17.064	90299	
78			163.863693	164.922386	17.174	92743	
79			164.922386	165.981079	17.281	95617	
80			165.981079	167.039772	17.385	99015	
81			167.039772	168.098465	17.484	103084	
82			168.098465	169.157158	17.575	108018	
83			169.157158	170.215851	17.658	114080	
84			170.215851	171.274544	17.728	121749	
85			171.274544	172.333237	17.781	131426	
86			172.333237	173.391930	17.813	144285	
87			173.391930	174.450623	17.816	161933	
88			174.450623	175.509310	17.782	187901	
89			175.509310	176.257758	17.716	219997	
90			176.257758	177.006206	17.626	260681	
91			177.006206	177.754654	17.498	325282	
92			177.754654	178.503102	17.322	442551	
93	↓	↓	178.503102	179.251550	17.086	718149	↓
94	1251.750	0	179.251550	180.0	16.774	2164720	.318

Table 1-4. Construction of Vehicle Stiffness Matrix

Sing. Matrix Row No.	Node No.	Vector	Vector	Vector	Vector	Non-Singular Matrix Row No.
1		F1, 1		F1, 33		1
2	1	F2, 1		F2, 33		Eliminated
3		F3, 1		F3, 33		2
4		F4, 1	F1, 2			3
5	2	F5, 1	F2, 2			4
6		F6, 1	F3, 2			5
7		F1, 3	F4, 2			6
8	3	F2, 3	F5, 2			7
9		F3, 3	F6, 2			8
10		F4, 3	F1, 4			9
11	4	F5, 3	F2, 4			10
12		F6, 3	F3, 4			11
13		F1, 5	F4, 4			12
14	5	F2, 5	F5, 4			13
15		F3, 5	F6, 4			14
16		F4, 5	F1, 6			15
17	6	F5, 5	F2, 6			16
18		F6, 5	F3, 6			17
19		F1, 7	F4, 6			18
20	7	F2, 7	F5, 6			19
21		F3, 7	F6, 6			20
22		F4, 7	F1, 8			21
23	8	F5, 7	F2, 8			22
24		F6, 7	F3, 8			23
25		F1, 9	F4, 8			24
26	9	F2, 9	F5, 8			25
27		F3, 9	F6, 8			26
28		F4, 9	F1, 10			27
29	10	F5, 9	F2, 10			28
30		F6, 9	F3, 10			29
31		F1, 11	F4, 10			30
32	11	F2, 11	F5, 10			31
33		F3, 11	F6, 10			32
34		F4, 11	F1, 12			33
35	12	F5, 11	F2, 12			34
36		F6, 11	F3, 12			35
37		F1, 13	F4, 12			36
38	13	F2, 13	F5, 12			37
39		F3, 13	F6, 12			38
40		F4, 13	F1, 14			39
41	14	F5, 13	F2, 14			40
42		F6, 13	F3, 14			41
43		F1, 15	F4, 14			42
44	15	F2, 15	F5, 14			43
45		F3, 15	F6, 14			44
46		F4, 15	F1, 16			45
47	16	F5, 15	F2, 16			46
48		F6, 15	F3, 16			47

Table 1-4. Construction of Vehicle Stiffness Matrix (continued)

Sing. Matrix Row No.	Node No.	Vector	Vector	Vector	Vector	Non-Singular Matrix Row No.
49		F1,17	F4,16			48
50	17	F2,17	F5,16			49
51		F3,17	F6,16			50
52		F4,17	F1,18	F1,19	F1,57	51
53	18	F5,17	F2,18	F2,19	F2,57	52
54		F6,17	F3,18	F3,19	F3,57	53
55			F4,18			54
56	19		F5,18			55
57			F6,18			56
58		F1,20		F4,19		57
59	20	F2,20		F5,19		58
60		F3,20		F6,19		59
61		F4,20	F1,21			60
62	21	F5,20	F2,21			61
63		F6,20	F3,21			62
64		F1,22	F4,21			63
65	22	F2,22	F5,21			64
66		F3,22	F6,21			65
67		F4,22	F1,23			66
68	23	F5,22	F2,23			67
69		F6,22	F3,23			68
70		F1,24	F4,23			69
71	24	F2,24	F5,23			70
72		F3,24	F6,23			71
73		F4,24	F1,25			72
74	25	F5,24	F2,25			73
75		F6,24	F3,25			74
76		F1,26	F4,25			75
77	26	F2,26	F5,25			76
78		F3,26	F6,25			77
79		F4,26	F1,27			78
80	27	F5,26	F2,27			79
81		F6,26	F3,27			80
82		F1,28	F4,27			81
83	28	F2,28	F5,27			82
84		F3,28	F6,27			83
85		F4,28	F1,29			84
86	29	F5,28	F2,29			85
87		F6,28	F3,29			86
88		F1,30	F4,29			87
89	30	F2,30	F5,29			88
90		F3,30	F6,29			89
91		F4,30	F1,31			90
92	31	F5,30	F2,31			91
93		F6,30	F3,31			92
94		F1,32	F4,31			93
95	32	F2,32	F5,31			94
96		F3,32	F6,31			95

Table 1-4. Construction of Vehicle Stiffness Matrix (continued)

SING. MATRIX Row No.	NODE No	VECTOR	VECTOR	VECTOR	VECTOR	NON-SINGULAR MATRIX Row No.
97		F4, 32	F1, 97	F1, 95	F1, 96	96
98	33	F5, 32	F2, 97	F2, 95	F2, 96	97
99		F6, 32	F3, 97	F3, 95	F3, 96	98
100		F4, 33	F1, 34			99
101	34	F5, 33	F2, 34			100
102		F6, 33	F3, 34			101
103		F1, 35	F4, 34			102
104	35	F2, 35	F5, 34			103
105		F3, 35	F6, 34			104
106		F4, 35	F1, 36			105
107	36	F5, 35	F2, 36			106
108		F6, 35	F3, 36			107
109		F1, 37	F4, 36			108
110	37	F2, 37	F5, 36			109
111		F3, 37	F6, 36			110
112		F4, 37	F1, 38			111
113	38	F5, 37	F2, 38			112
114		F6, 37	F3, 38			113
115		F1, 39	F4, 38			114
116	39	F2, 39	F5, 38			115
117		F3, 39	F6, 38			116
118		F4, 39	F1, 40			117
119	40	F5, 39	F2, 40			118
120		F6, 39	F3, 40			119
121		F1, 41	F4, 40			120
122	41	F2, 41	F5, 40			121
123		F3, 41	F6, 40			122
124		F4, 41	F1, 42			123
125	42	F5, 41	F2, 42			124
126		F6, 41	F3, 42			125
127		F1, 43	F4, 42			126
128	43	F2, 43	F5, 42			127
129		F3, 43	F6, 42			128
130		F4, 43	F1, 44			129
131	44	F5, 43	F2, 44			130
132		F6, 43	F3, 44			131
133		F1, 45	F4, 44			132
134	45	F2, 45	F5, 44			133
135		F3, 45	F6, 44			134
136		F4, 45	F1, 46			135
137	46	F5, 45	F2, 46			136
138		F6, 45	F3, 46			137
139		F1, 47	F4, 46			138
140	47	F2, 47	F5, 46			139
141		F3, 47	F6, 46			140
142		F4, 47	F1, 48			141
143	48	F5, 47	F2, 48			142
144		F6, 47	F3, 48			143

Table 1-4. Construction of Vehicle Stiffness Matrix (continued)

SING. MATRIX ROW NO.	NODE NO.	VECTOR	VECTOR	VECTOR	VECTOR	NON-SINGULAR MATRIX ROW NO.
145		F1, 49	F4, 48			144
146	49	F2, 49	F5, 48			145
147		F3, 49	F6, 48			146
148		F4, 49	F1, 50			147
149	50	F5, 49	F2, 50			148
150		F6, 49	F3, 50			149
151		F1, 51	F4, 50			150
152	51	F2, 51	F5, 50			151
153		F3, 51	F6, 50			152
154		F4, 51	F1, 52			153
155	52	F5, 51	F2, 52			154
156		F6, 51	F3, 52			155
157		F1, 53	F4, 52			156
158	53	F2, 53	F5, 52			157
159		F3, 53	F6, 52			158
160		F4, 53	F1, 54			159
161	54	F5, 53	F2, 54			160
162		F6, 53	F3, 54			161
163		F1, 55	F4, 54			162
164	55	F2, 55	F5, 54			163
165		F3, 55	F6, 54			164
166		F4, 55	F1, 56			165
167	56	F5, 55	F2, 56			166
168		F6, 55	F3, 56			167
169			F4, 56	F4, 88	F1, 89	168
170	57		F5, 56	F5, 88	F2, 89	169
171			F6, 56	F6, 88	F3, 89	170
172		F4, 57	F1, 58			171
173	58	F5, 57	F2, 58			172
174		F6, 57	F3, 58			173
175		F1, 59	F4, 58			174
176	59	F2, 59	F5, 58			175
177		F3, 59	F6, 58			176
178		F4, 59	F1, 60			177
179	60	F5, 59	F2, 60			178
180		F6, 59	F3, 60			179
181		F1, 61	F4, 60			180
182	61	F2, 61	F5, 60			181
183		F3, 61	F6, 60			182
184		F4, 61	F1, 62			183
185	62	F5, 61	F2, 62			184
186		F6, 61	F3, 62			185
187		F1, 63	F4, 62			186
188	63	F2, 63	F5, 62			187
189		F3, 63	F6, 62			188
190		F4, 63	F1, 64			189
191	64	F5, 63	F2, 64			190
192		F6, 63	F3, 64			191

Table 1-4. Construction of Vehicle Stiffness Matrix (continued)

SING. MATRIX ROW No.	NODE No.	VECTOR	VECTOR	VECTOR	VECTOR	NON-SINGULAR MATRIX ROW No.
193		F1, 65	F4, 64			192
194	65	F2, 65	F5, 64			193
195		F3, 65	F6, 64			194
196		F4, 65	F1, 66			195
197	66	F5, 65	F2, 66			196
198		F6, 65	F3, 66			197
199		F1, 67	F4, 66			198
200	67	F2, 67	F5, 66			199
201		F3, 67	F6, 66			200
202		F4, 67	F1, 68			201
203	68	F5, 67	F2, 68			202
204		F6, 67	F3, 68			203
205		F1, 69	F4, 68			204
206	69	F2, 69	F5, 68			205
207		F3, 69	F6, 68			206
208		F4, 69	F1, 70			207
209	70	F5, 69	F2, 70			208
210		F6, 69	F3, 70			209
211		F1, 71	F4, 70			210
212	71	F2, 71	F5, 70			211
213		F3, 71	F6, 70			212
214		F4, 71	F1, 72			213
215	72	F5, 71	F2, 72			214
216		F6, 71	F3, 72			215
217		F1, 73	F4, 72			216
218	73	F2, 73	F5, 72			217
219		F3, 73	F6, 72			218
220		F4, 73		F4, 76	F1, 77	219
221	74	F5, 73		F5, 76	F2, 77	220
222		F6, 73		F6, 76	F3, 77	221
223		F1, 74				222
224	75	F2, 74				223
225		F3, 74				224
226		F4, 74	F1, 75			225
227	76	F5, 74	F2, 75			226
228		F6, 74	F3, 75			227
229		F1, 76	F4, 75			228
230	77	F2, 76	F5, 75			229
231		F3, 76	F6, 75			230
232		F4, 77	F1, 78			231
233	78	F5, 77	F2, 78			232
234		F6, 77	F3, 78			233
235		F1, 79	F4, 78			234
236	79	F2, 79	F5, 78			235
237		F3, 79	F6, 78			236
238		F4, 79	F1, 80			237
239	80	F5, 79	F2, 80			238
240		F6, 79	F3, 80			239

Table 1-4. Construction of Vehicle Stiffness Matrix (continued)

SING. MATRIX Row No.	NODE No.	VECTOR	VECTOR	VECTOR	VECTOR	NON-SINGULAR MATRIX Row No.
241		F1, 81	F4, 80			240
242	81	F2, 81	F5, 80			241
243		F3, 81	F6, 80			242
244		F4, 81	F1, 82			243
245	82	F5, 81	F2, 82			244
246		F6, 81	F3, 82			245
247		F1, 83	F4, 82			246
248	83	F2, 83	F5, 82			247
249		F3, 83	F6, 82			248
250		F4, 83	F1, 84			249
251	84	F5, 83	F2, 84			250
252		F6, 83	F3, 84			251
253		F1, 85	F4, 84			252
254	85	F2, 85	F5, 84			253
255		F3, 85	F6, 84			254
256		F4, 85	F1, 86			255
257	86	F5, 85	F2, 86			256
258		F6, 85	F3, 86			257
259		F1, 87	F4, 86			258
260	87	F2, 87	F5, 86			259
261		F3, 87	F6, 86			260
262		F4, 87	F1, 88			261
263	88	F5, 87	F2, 88			262
264		F6, 87	F3, 88			263
265		F4, 89	F1, 90			264
266	89	F5, 89	F2, 90			265
267		F6, 89	F3, 90			266
268		F1, 91	F4, 90			267
269	90	F2, 91	F5, 90			268
270		F3, 91	F6, 90			269
271		F4, 91	F1, 92			270
272	91	F5, 91	F2, 92			271
273		F6, 91	F3, 92			272
274		F1, 93	F4, 92			273
275	92	F2, 93	F5, 92			274
276		F3, 93	F6, 92			275
277		F4, 93	F2, 94			276
278	93	F5, 93	F3, 94			277
279		F6, 93	F4, 94			278
280			F1, 94			279
281	94		F5, 94			Eliminated
282			F6, 94			Eliminated
283		F4, 95				280
284	95	F5, 95				281
285		F6, 95				282
286		F4, 96	F1, 98	F1, 99		283
287	96	F5, 96	F2, 98	F2, 99		284
288		F6, 96	F3, 98	F3, 99		285

Table 1-4. Construction of Vehicle Stiffness Matrix (continued)

SING. MATRIX Row No	Node No	VECTOR	VECTOR	VECTOR	VECTOR	NON-SINGULAR MATRIX Row No.
289		F4, 97	F4, 98	F1, 100		286
290	97	F5, 97	F5, 98	F2, 100		287
291		F6, 97	F6, 98	F3, 100		288
292		F4, 99	F1, 101	F1, 102		289
293	98	F5, 99	F2, 101	F2, 102		290
294		F6, 99	F3, 101	F3, 102		291
295		F4, 100	F4, 101	F1, 103		292
296	99	F5, 100	F5, 101	F2, 103		293
297		F6, 100	F6, 101	F3, 103		294
298		F4, 103		F4, 102		Eliminated
299	100	F5, 103		F5, 102		295
300		F6, 103		F6, 102		296

NOTE: 1) In the above table $F_{n,m}$ corresponds to the force or deflection component "n" contributed by segment "m". Refer to segment sketches on figures 1-1 through 1-6 inclusive

Q (t = 77 sec), Accel (t - 138), empty. The "Full" configuration was also investigated in the supported-on-pad mode. The normal frequencies are summarized in table 2-1. A representative sample of the modes is given in figure 2-1 thru 2-7. The bulkheads are quite flexible compared to the primary structure and the bulkhead modes predominate at the lower frequencies.

2.2 POGO

POGO instability exists in a launch vehicle if disturbances in the propulsion system occur at a natural frequency of the structure/fuel dynamic system. Conventional high length-to-diameter ratio vehicles with long liquid pipe lines are possibly vulnerable to the POGO phenomenon for some flight configuration. Probability is increased if the number of engines and transfer pumps is small, because a pulse resonance is more likely. Considering the above, the SERV configuration has certain inherent longitudinal-stability advantages over the conventional vehicle: liquid lines are short, the aerospike engine, a "large-order" combustion-chamber/liquid-pump propulsion system. A detailed POGO analysis for SERV is deferred for future study; however, a preliminary appraisal of the structural/liquid dynamic model showed neither a significant payload displacement relative to the tank bulkheads (figures 2-3 and 2-4), nor a payload structural gain factor for a sinusoidal forcing function at the thrust vector (figure 2-8).

3.0 RIGID BODY ANALYSIS

For this analysis the vehicle was assumed to be a rigid body with the external aerodynamic and thrust loads balanced by vehicle inertia, all of which are time dependent. Critical time points were selected in the same manner as discussed previously in paragraph 1.0, volume 3, appendix E.

3.1 TRAJECTORY DATA AT SELECTED CRITICAL TIME POINTS

References 2 and 3 were used as the sources of trajectory data in the same manner as discussed in paragraph 2.0, volume 3, appendix E. The trajectory data thus abstracted and used in this portion of the analysis are summarized in table 3.1.

It should be noted at this point that a limit value of acceleration of 3g was used in the landing condition throughout the major part of the work that follows. However, reference 7 indicated that a decision had been made to revise the design criteria to specify a limit landing acceleration of 2g maximum. Because the major portion of this analysis had been completed when this change was made, no attempt was made towards its incorporation and the now conservative data were retained. Only when use of the conservative data would result in a negative margin of safety (refer to paragraph 3.8.4.5) was recourse made to the reduced load factor.

3.2 CALCULATION OF WEIGHT DISTRIBUTION TO NODES - FIXED WEIGHT ITEMS

The vehicle weight distribution used in this analysis is summarized in table 3-2. Reference 4 was used to provide a more detailed weight breakdown of the vehicle primary structure than was available from the sizing program printout, reference 2. Updating adjustments were made to the weights of the outer cylindrical bulkhead and the upper frustum which had been increased in

Table 2-1. SERV Longitudinal Normal Frequencies (Radians per Second)

MODE	FREE - FREE				SUPPORTED
	FULL t = 0	MAX Q t = 77	MAX. ACCEL t = 138	EMPTY	FULL t = 0
1	4.904	5.916	7.405	82.155	4.893
2	8.252	9.955	12.462	123.507	8.196
3	10.276	12.215	15.053	132.122	10.269
4	13.154	15.748	19.471	139.423	11.281
5	16.209	19.345	23.812	218.161	15.889
6	19.721	23.555	29.030	219.653	17.890
7	22.711	27.347	34.124	231.731	20.976
8	29.399	35.282	43.583	271.782	28.542

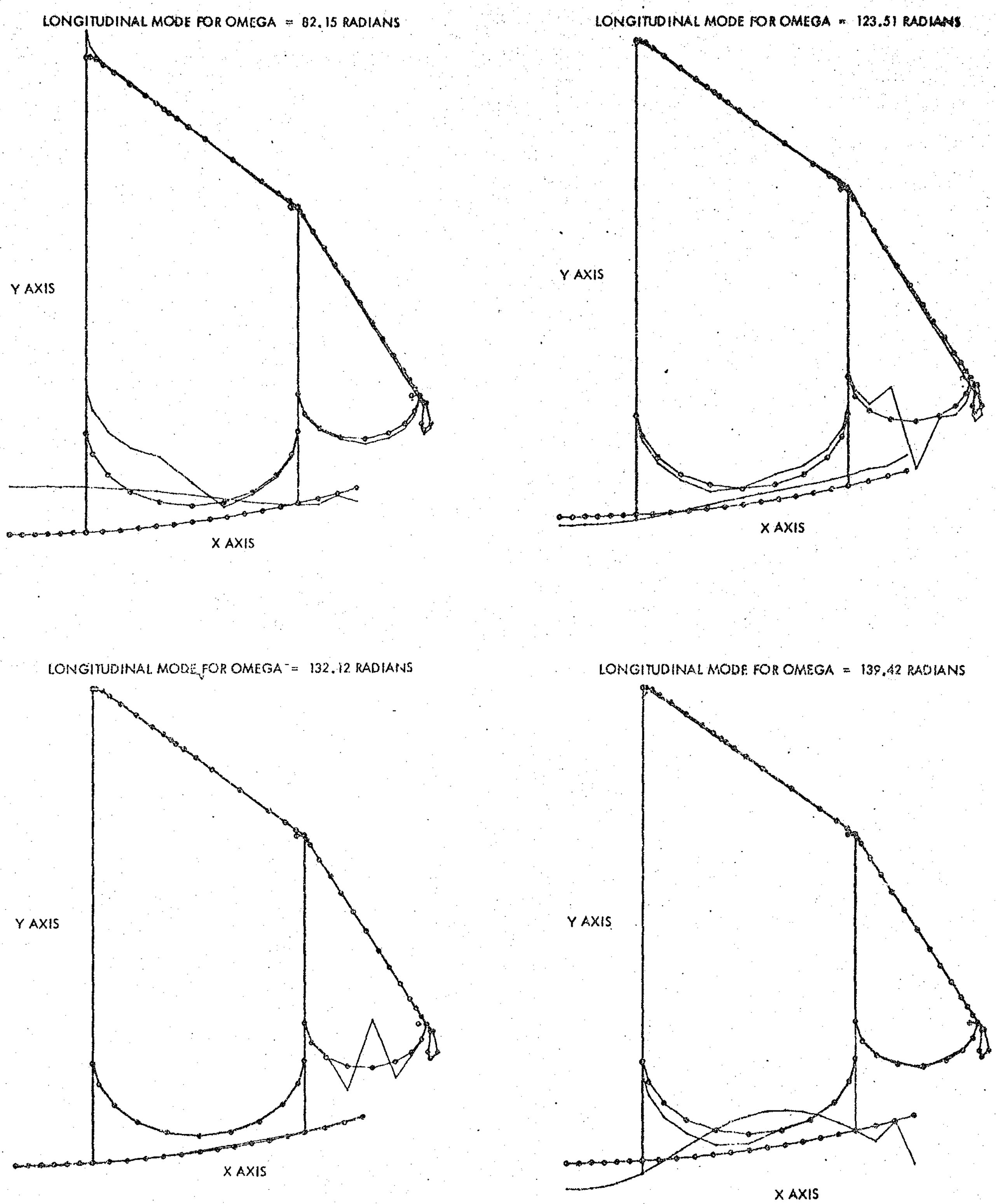

Figure 2-1. SERV Normal Modes - Empty/Free-Free

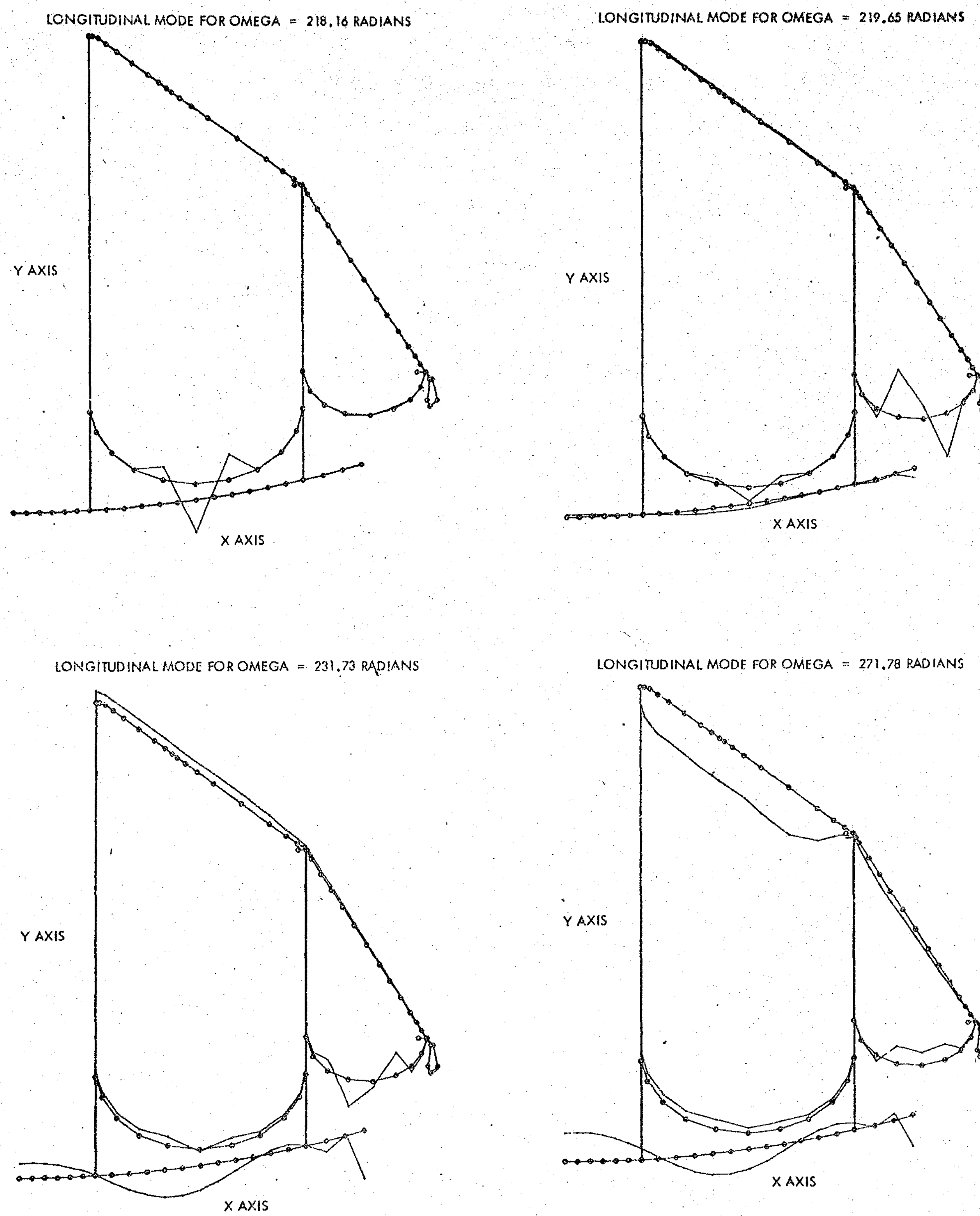

Figure 2-2. SERV Normal Modes - Empty/Free-Free

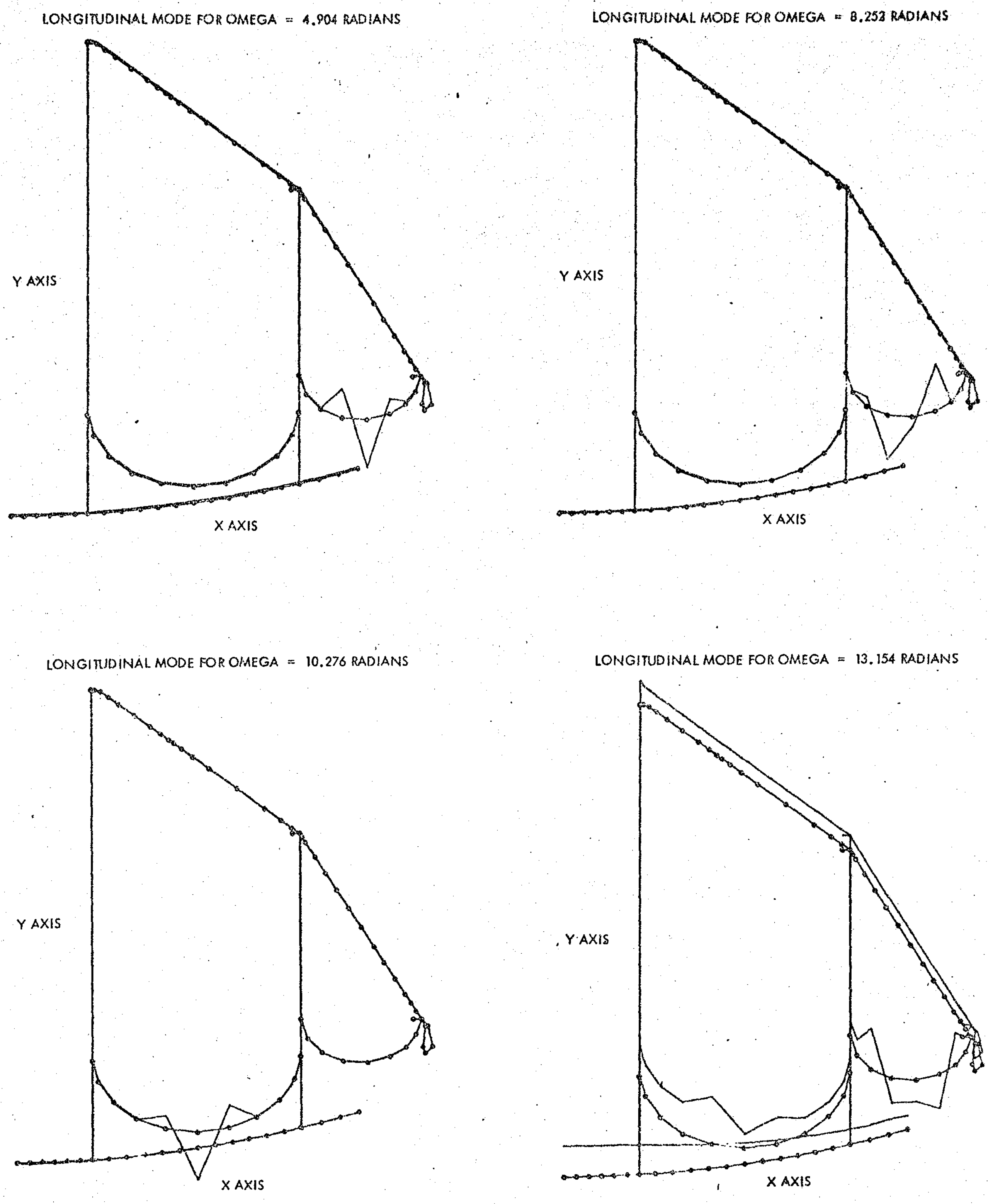

Figure 2-3. SERV Normal Modes - Full/Free-Free

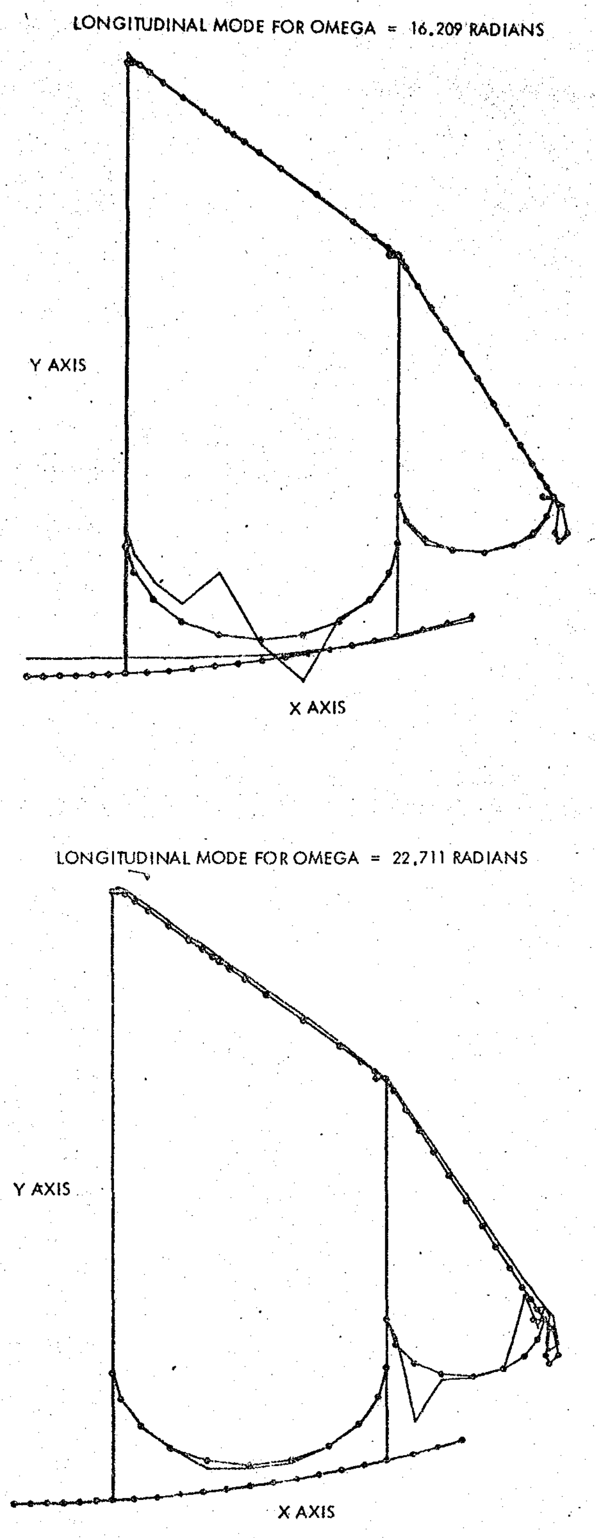

Figure 2-4. SERV Normal Modes - Full/Free-Free

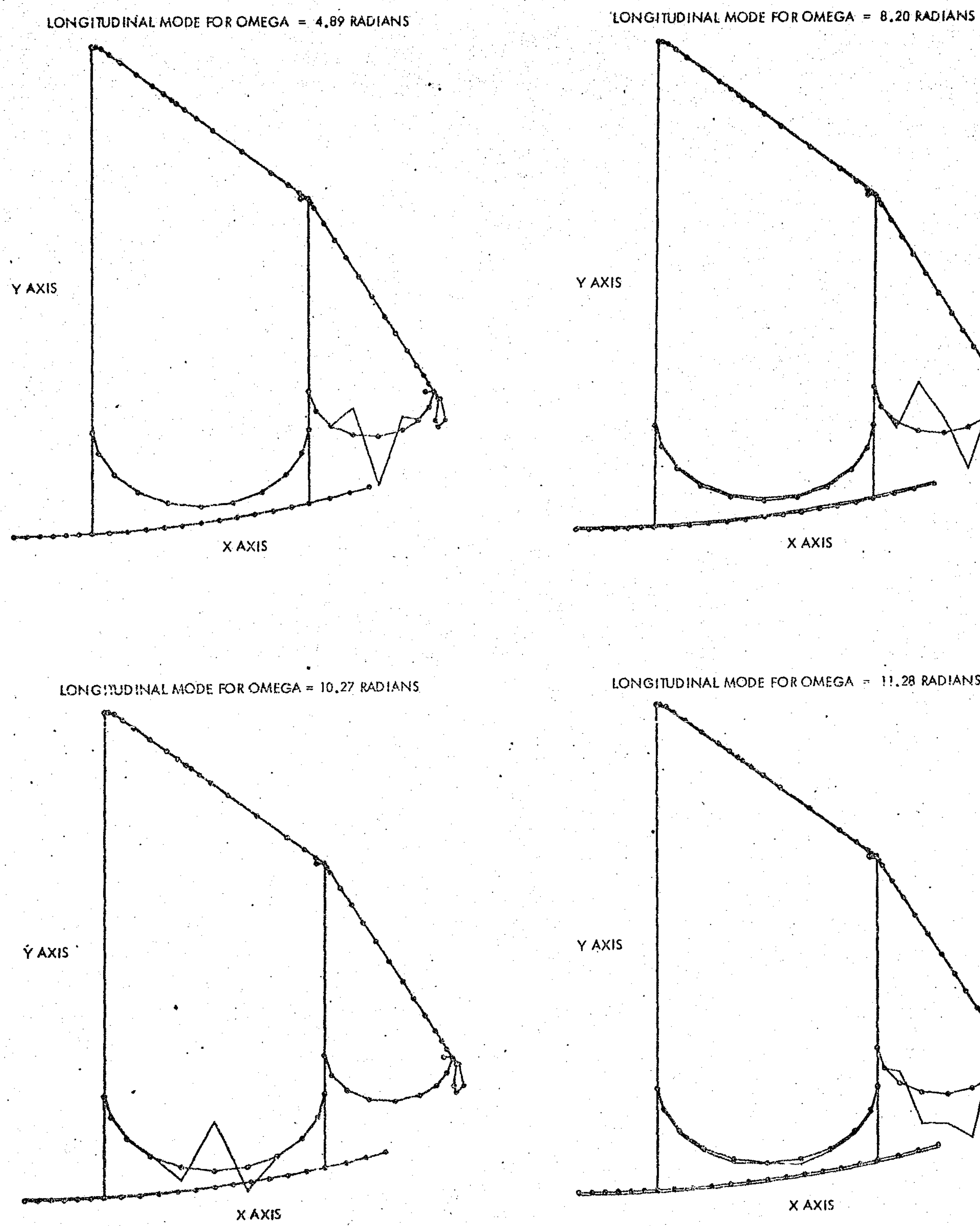

Figure 2-5. SERV Normal Modes - Full/Supported

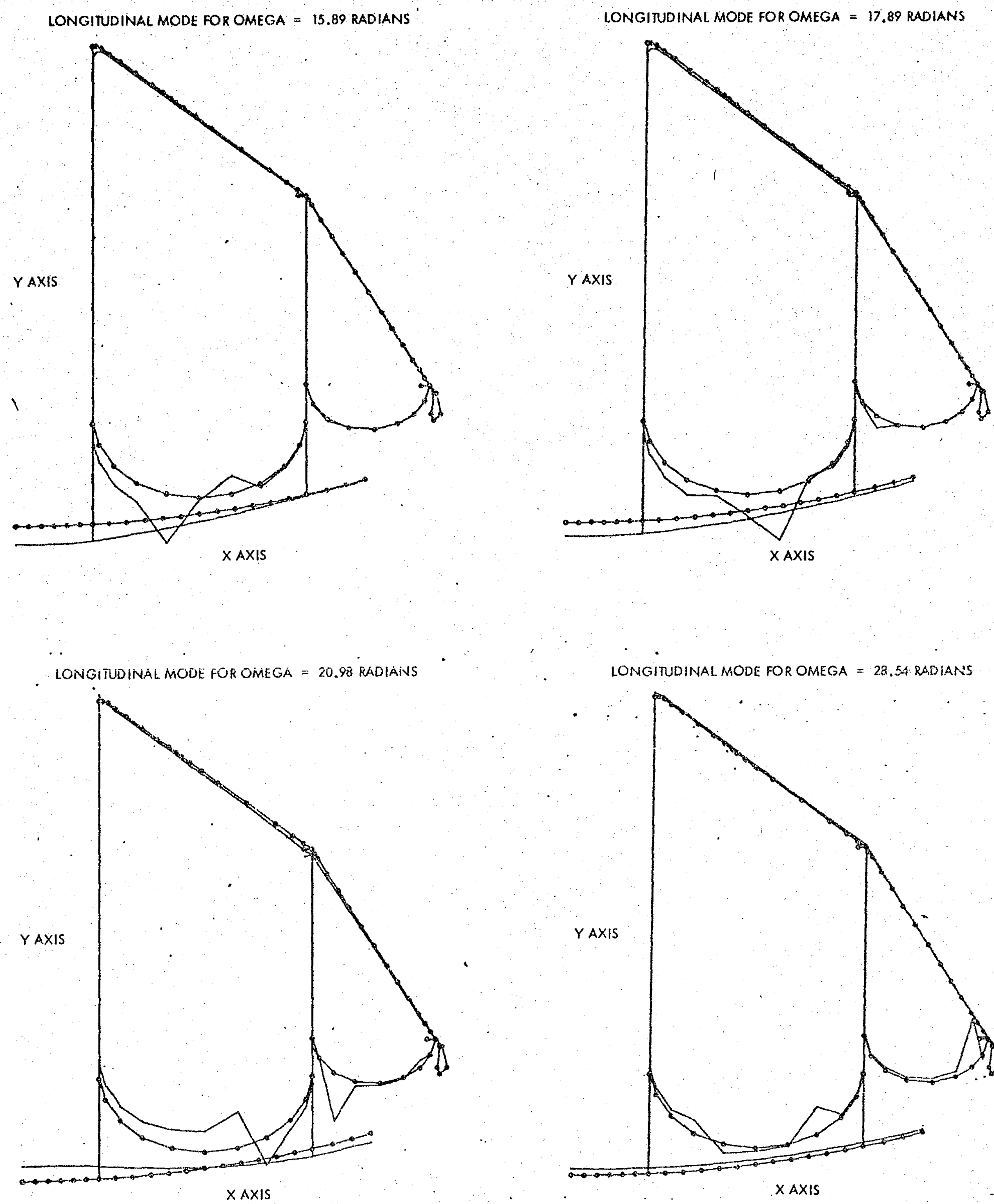

Figure 2-6. SERV Normal Modes - Full/Supported

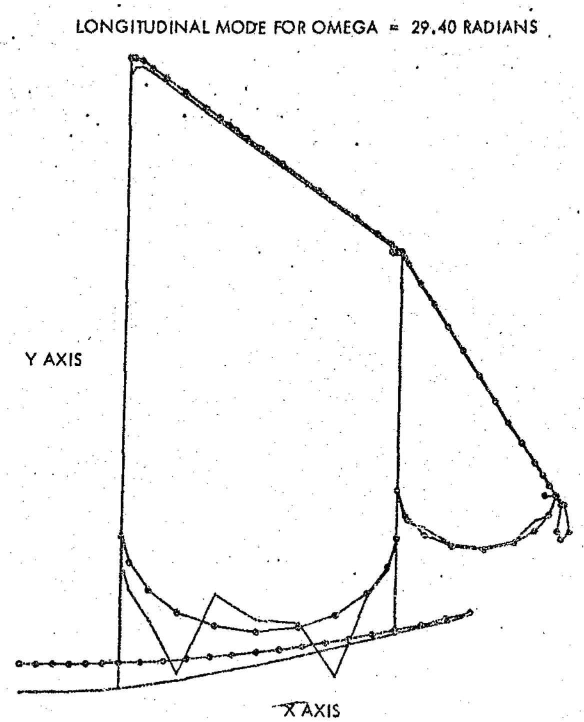

Figure 2-7. SERV Normal Modes - Full/Supported

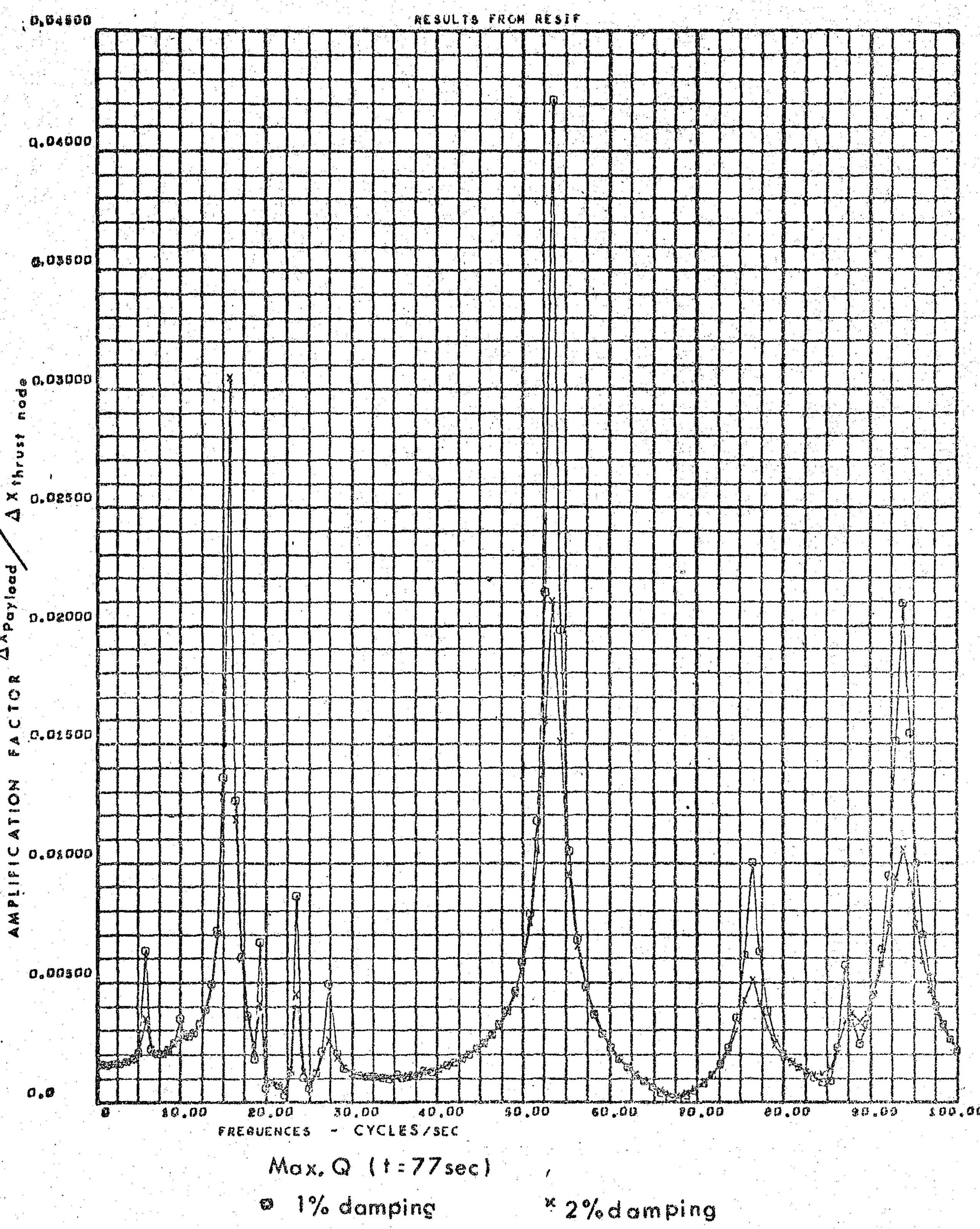

Figure 2-8. Payload Frequency Response

Table 3-1. Trajectory Data at Selected Critical Time Points

No.	ITEM	DESIGN COND. / UNITS	LIFT-OFF (T=0)	MAX. DYNAMIC PRESSURE (T=77)	MAX. LONG. ACCELERATION (T=138)
①	Long. Acceleration	g	1.200	1.430	3.000 (1)
②	Vehicle Weight	lb	4732740	3428748	2402699
③	Thrust	lb	5679290	6421706	7051206
④	Ambient Pressure	psi	14.75	3.95	.12
⑤	Weight of LO_2	lb	3618610	2500286	1593219
⑥	Weight of LH_2	lb	603100	416696	265535
⑦	LO_2 Ullage Pressure	psia	14.75	10.0	10.0
⑧	LH_2 Ullage Pressure	psia	14.75	5.0	5.0
⑨	Mach Number	—	0	.990	3.510
⑩	Dynamic Pressure	lb / sq.ft	0	425	144
⑪	Drag	lb	0	1443039	675656

NOTE 1) This limit longitudinal acceleration was also assumed to apply to the Reentry and Landing Conditions.

Table 3-2. SERV Weight Breakdown - Ascent Phase

ITEM	WEIGHT
Inner Cylindrical Bulkhead	6177.0 (1)
Outer Cylindrical Bulkhead	36145.0 (2)
Upper Frustum (Point D to I)	7995.0 (2)
Upper Frustum (Point I to J)	2290.0 (1)
Lower Frustum	18437.0 (1)
Lower LH_2 Bulkhead	2165.0 (1)
Lower LO_2 Bulkhead	8150.0 (1)
Upper LH_2 Bulkhead	300.0 (1)
Heat Shield Structure	18040.0 (1)
Engine Thrust Ring	8883.0 (1)
Upper Kick Ring	225.0 (1)
Center Kick Ring	2986.0 (1)
Lower Kick Ring	4215.0 (1)
Aerospike Doors	11725.0 (1)
Joints, Baffles & Brackets	13292.0 (1)
Landing Gear & Supports	11910.45 (3)
Misc.	9196.706 (6)
Contingency (10%)	16221.216
Sub-Total (Structures)	178433.372
Thermal Protection System	31218.154 (5)
RCS/Retro	4962.69 (3)
Pressurization System	387.36 (3)
GN&C, Power & Communications	5000.00 (3)
Propulsion Feed System	1257.13 (3)
Hydraulics & Pneumatic Systems	2977.61 (3)
Main Engines	84346.0 (4)
Lift Engines & Supports	47226.70 (4)
Contingency (10%)	17737.564
Sub-Total (Equipment)	195113.208
Sub-Total (SERV DRY WEIGHT)	373546.580 (4)
LH_2 (Main Engine)	603100.0 (4)
LO_2 (Main Engine)	3618610.0 (4)
Lift Engine Fuel	25443.4 (4)
Aux. Propellant	23548.0 (4)
FPR Propellant	3367.02 (6)
Sub-Total (Propellants)	4274068.42
Payload	85125.0 (4)
Gross Lift-off Weight	4732740.0 (4)

NOTES:
1.) These data were taken from reference 4
2.) These data represent an update of reference 4 due to structural changes.
3.) These data taken from table 6, Volume 3, appendix E
4.) These data were taken from reference 2
5.) Calculated value based upon TPS weighing 2 lb/ft^2
6.) These were arbitrary values required to balance the sub-group in which they appear

weight due to structural changes that had been made after the release of reference 4. The weight estimate used for the thermal protection system was based on a system weighing 2.0 lb/sq.ft. applied to the outside surface of the vehicle (the aerospike doors were not included in this area determination). The weights for the main and lift engines and their supporting equipment were taken from reference 2. Because it was known that the structural weight that had been used exceded that shown by reference 2, the remaining items of fixed equipment were assumed to weigh the same as the corresponding items in the original reference vehicle. The total dry weight was then made to equal that shown in reference 2 by the inclusion of a miscellaneous item in the structures group. In the same manner the weight shown for FPR propellants was used to adjust the total weight of propellants so that the reference 2 values of GLOW, payload and SERV dry weight were compatible.

The reentry and landing weight breakdown that was used is summarized in table 3-3. In arriving at the weight of lift engine fuel, it was assumed that the fuel consumed was the difference between the reentry and landing total weights. The value of SERV dry weight is from table 3-2. The total reentry and landing weights and the lift engine fuel onboard at start of reentry were obtained from reference 2; the weight of unused propellants is that required for compatibility of the data.

The distribution of the total weight of a component to the individual nodes lying within the component is illustrated in detail for the upper frustum between points J and I (refer to figure 3, volume 3, appendix E) as follows:

The surface area of a frustum is given by:

$$S_{J-I} = L_s \ (R_u + R_L)/144$$

where

L_s = meridional length of surface = 143.574 in.

R_U = radius at small end = 103.365 in.

R_L = radius at large end = 204.887 in.

(refer to figure 1-1)

$$S_{J-I} = (3.141593)(143.574)(103.365 + 204.887)/144 = 965.537 \text{ sq. ft.}$$

Estimated weight of structure = 2290 lb (refer to table 3-2). Including the 10 percent contingency factor, this weight becomes 1.10(2290) = 2519.0 lb. Unit weight of structure = 2519.0/965.537 = 2.609 lb/ft^2.

The weight of the thermal protection system was assumed to be 2.0 lb ft^2 including the 10 percent contingency, this weight becomes 2.20 lb/ft.^{2}

The total unit weight of the frustum is then

$$W_{J-I} = 2.609 + 2.20 = 4.809 \text{ lb/ft}^2$$

The 1g weight of the frustum is then W_{J-I} = 4.809(965.537) = 4643.267 lb. The weight of each segment of the frustum (refer to figure 1-1) was then

Table 3-3. SERV Weight Breakdown - Reentry and Landing

ITEM	REENTRY WEIGHT	LANDING WEIGHT
SERV Dry Weight	373546.58	373546.58
Lift Engine Fuel	25443.4	16854.7
Unused Propellants	4286.12	4286.12
Payload	46758.0	46758.0
TOTAL	450034.1	441445.4

determined from

$$W_{SEG} = \pi L_S (R_n + R_{n+1}) W_{J-I}/144$$

where

W_{SEG} = total weight of segment

L_S = meridional length of segment

R_N = radius to node "n"

R_{N+1} = radius to node "n + 1"

$$W_{SEG} = (3.141593)(4.809)L_S(R_n + R_{n+1})/144 = 0.104916\ L_S(R_n + R_{n+1})$$

Table 3-4 was set up to show the evaluation of W_{SEG}. The weight of each of the remaining segments into which the primary structure of the vehicle had been subdivided was calculated in a similar manner; the results are shown in column ⑩ of table 3-5. This table was established to distribute the weight of an individual segment to its boundary nodes as follows:

$$W_n = W_{SEG}\ (R_n)/(R_n + R_{n+1})$$

$$W_{n+1} = W_{SEG}\ (R_{n+1})/(R_n + R_{n+1})$$

This distribution is made so that the running load acting on each nodal circle due to the weight of the segment is equalized. The remaining items which make up the SERV dry weight (refer to table 3-2) were distributed to nodes corresponding to panel points as illustrated in figure 3, volume 3, appendix E, due consideration being given to their actual installation in the vehicle. The total nodal load was then converted to a running load on the nodal circle in table 3-6. Note that the summation of column ⑥ agrees with the SERV dry weight shown in table 3-2.

3.3 CALCULATION OF WEIGHT DISTRIBUTION TO NODES - VARIABLE WEIGHT ITEMS

The variable load items include the inertia loadings due to payload, main engine propellant supply, thrust load, drag load and the auxiliary propellants. The methods used in distributing these inertia items to the appropriate nodes and the evaluation of the average local pressures acting on the individual segments were the same as previously described in paragraph 5.0, volume 3, appendix E. In determining nodal loads and segmental pressures representing the effects of the main engine propellant supply, the following basic assumption should be noted. Because the weights of propellants at the critical time points for the new trajectories differ from those investigated in volume 3, appendix E, and because of the geometric differencies between the reference vehicle being investigated and that output from the sizing program (refer to the opening paragraph of this appendix), it was assumed that the liquid levels in the main tanks remained the same as previously calculated. The proper weight of contained propellant was then obtained by adjustment of the propellant densities. This procedure produces peak pressure intensities reasonably close to those which should actually exist, but slight deviations result in pressure distributions.

Table 3-4. Calculation of W_{SEG} - Upper Frustum - Point J to I

(1)	(2)	(3)	(4)	(5)	(6)	(7)
SEGMENT No.	L_s	R_n	R_{n+1}	$R_n + R_{n+1}$	$L_s(R_n + R_{n+1})$	W_{SEG}
REF.	TABLE 1-1	TABLE 1-1	TABLE 1-1	(3) + (4)	(2) × (5)	.104916 (6)
2	9.493	103.365	110.078	213.443	2026.214	212.583
3	14.239	110.078	120.146	230.224	3278.160	343.932
4	18.985	120.146	133.570	253.716	4816.798	505.360
5	29.070	133.570	154.126	287.696	8363.323	877.447
6	29.070	154.126	174.682	328.808	9558.449	1002.838
7	18.985	174.682	188.106	362.788	6887.530	722.613
8	14.239	188.106	198.174	386.280	5500.241	577.064
9	9.493	198.174	204.887	403.061	3826.258	401.436

$\Sigma = 4643.270$ ✓

Table 3-5. Distribution of Segment Weight to Boundary Nodes

①		②	③	④	⑤	⑥	⑦	⑧	⑨	⑩	⑪	⑫
COMP		SEGMENT No.	NODE No. n	NODE No. n+1	R_n	R_{n+1}	$R_n + R_{n+1}$	$\frac{R_n}{(R_n+R_{n+1})}$	$\frac{R_{n+1}}{(R_n+R_{n+1})}$	W_{SEG}	W_n	W_{n+1}
REFERENCE			FIGS. 1 TO 6		TABLE 1-1	⑤ n+1	⑤ + ⑥	⑤ / ⑦	⑥ / ⑦		⑧ × ⑩	⑨ × ⑩
UPPER LOCK RING		1	1	2	98.010	103.365	201.375	.486704	.513296	247.500	120.459	127.041
UPPER FRUSTUM	POINT J TO F	2	2	3	103.365	110.078	213.443	.484274	.515726	212.583	102.948	109.635
		3	3	4	110.078	120.146	230.224	.478134	.521866	343.932	164.446	179.486
		4	4	5	120.146	133.570	253.716	.473545	.526455	505.360	239.311	266.049
		5	5	6	133.570	154.126	287.696	.464275	.535725	877.447	407.377	470.070
		6	6	7	154.126	174.682	328.808	.468742	.531258	1002.838	470.072	532.766
		7	7	8	174.682	188.106	362.788	.481499	.518501	722.613	347.937	374.676
		8	8	9	188.106	198.174	386.280	.486968	.513032	577.064	281.012	296.052
		9	9	10	198.174	204.887	403.061	.491672	.508328	401.436	197.375	204.061
	POINT F TO D	10	10	11	204.887	215.494	420.381	.487384	.512616	715.773	348.856	366.917
		11	11	12	215.494	229.636	445.130	.484115	.515885	1010.551	489.223	521.328
		12	12	13	229.636	250.849	480.485	.477925	.522075	1636.222	781.991	854.231
		13	13	14	250.849	287.469	538.318	.465987	.534013	3164.531	1474.630	1689.901
		14	14	15	287.469	324.089	611.558	.470060	.529940	3595.056	1689.892	1905.164
		15	15	16	324.089	345.302	669.391	.484155	.515845	2279.515	1103.639	1175.876
		16	16	17	345.302	359.444	704.746	.489967	.510033	1599.941	783.918	816.023
		17	17	18	359.444	370.050	729.494	.492731	.507269	1242.093	612.018	630.075 ✓
[illegible]		18	18	19	370.050	360.050	730.100	.506848	.493152	3284.600	1664.793 ✓	1619.807
LOWER FRUSTUM	POINT D TO NODE 24	19	18	20	370.050	373.435	743.485	.497724	.502276	620.783	308.979 ✓	311.804
		20	20	21	373.435	377.618	751.053	.497215	.502785	774.869	385.216	389.593
		21	21	22	377.618	389.954	767.572	.491964	.508036	2335.662	1149.062	1186.600
		22	22	23	389.954	403.718	793.672	.491329	.508671	2694.469	1323.871	1370.598
		23	23	24	403.718	417.482	821.200	.491620	.508380	2788.011	1370.642	1417.369
	NODE 24 TO 27	24	24	25	417.482	432.548	850.030	.491138	.508862	3283.715	1612.757	1670.958
		25	25	26	432.548	448.731	881.279	.490818	.509182	3656.888	1794.866	1862.022
		26	26	27	448.731	464.914	913.645	.491144	.508856	3791.290	1862.069	1929.221
	NODE 27 TO 31	27	27	28	464.914	478.374	943.288	.492863	.507135	3380.649	1666.204	1714.445
		28	28	29	478.374	491.834	970.208	.493063	.506937	3477.127	1714.443	1762.684
		29	29	30	491.834	504.529	996.363	.493629	.506371	3368.124	1662.604	1705.520
		30	30	31	504.529	512.346	1016.875	.496156	.503844	2116.704	1050.215	1066.579
	[illegible]	31	31	32	512.346	518.902	1031.248	.496821	.503179	1995.358	991.336	1004.022
		32	32	33	518.902	525.176	1044.078	.496995	.503005	1953.189	960.785	972.404

E

Table 3-5. Distribution of Segment Weight to Boundary Nodes (continued)

①	②	③	④	⑤	⑥	⑦	⑧	⑨	⑩	⑪	⑫
COMP.	SEGMENT NO.	NODE NO. n	NODE NO. n+1	R_n	R_{n+1}	$R_n + R_{n+1}$	$\frac{R_n}{(R_n+R_{n+1})}$	$\frac{R_{n+1}}{(R_n+R_{n+1})}$	W_{SEG}	W_n	W_{n+1}
REFERENCE		FIGS. 1-6		TABLE 1-1	③ n+1	⑤ + ⑥	⑤/⑦	⑥/⑦		⑧ × ⑩	⑨ × ⑩
INNER CYLINDRICAL BULKHEAD	33	1	34	98.010	98.010	196.020	.500	.500	22.078	11.039	11.039
	34	34	35						44.156	22.078	22.078
	35	35	36						88.312	44.156	44.156
	36	36	37						173.254	86.627	86.627
	37	37	38						173.254	86.627	86.627
	38	38	39						88.312	44.156	44.156
	39	39	40						44.156	22.078	22.078
	40	40	41						22.078	11.039	11.039
	41	41	42						149.592	74.796	74.796
	42	42	43						299.177	149.588	149.589
	43	43	44						595.355	299.177	299.178
	44	44	45						672.810	336.405	336.405
	45	45	46						672.820	336.410	336.410
	46	46	47						681.875	340.937	340.938
	47	47	48						681.875	340.937	340.938
	48	48	49						516.996	258.498	258.498
	49	49	50						516.986	258.498	258.498
	50	50	51						319.745	159.872	159.873
	51	51	52						159.873	79.936	79.937
	52	52	53						71.310	35.655	35.655
	53	53	54						197.905	98.952	98.953
	54	54	55						330.570	165.285	165.285
	55	55	56						197.905	98.952	98.953
	56	56	57	98.010	98.010	196.020			71.310	35.655	35.655
OUTER CYLIN. BULK	57	18	58	370.050	370.050	740.100			1069.287	534.643 ✓	534.644
	58	58	59						2138.573	1069.286	1069.287
	59	59	60						4277.147	2138.573	2138.574
	60	60	61						5637.993	2818.996	2818.997
	61	61	62						9317.102	4658.551	4658.551
	62	62	63						7068.227	3534.113	3534.114
	63	63	64						3534.113	1767.056	1767.057
	64	64	65						1767.058	883.529	883.529
	65	65	66	370.050	370.050	740.100	.500	.500	343.521	171.760	171.761

Table 3-5. Distribution of Segment Weight to Boundary Nodes (continued)

①	②	③	④	⑤	⑥	⑦	⑧	⑨	⑩	⑪	⑫
COMP.	SEGMENT NO	NODE NO n	n+1	R_n	R_{n+1}	$R_n + R_{n+1}$	$\frac{R_n}{R_n+R_{n+1}}$	$\frac{R_{n+1}}{R_n+R_{n+1}}$	W_{SEG}	W_n	W_{n+1}
REFERENCE		FIGS. 1-6		TABLE 1-1	⑤ n+1	⑤ + ⑥	⑤/⑦	⑥/⑦		⑧ × ⑩	⑨ × ⑩
OUTER CYLIN. BULK.	66	66	67	370.050	370.050	740.100	.500	.500	495.945	247.972	247.973
	67	67	68	↕	↕	↕	↕	↕	495.945	247.972	247.973
	68	68	69	↕	↕	↕	↕	↕	343.521	171.760	171.761
	69	69	70	↕	↕	↕	↕	↕	405.118	202.559	202.559
	70	70	71	↕	↕	↕	↕	↕	820.269	410.134	410.135
	71	71	72	↕	↕	↕	↕	↕	820.294	410.147	410.147
	72	72	73	↕	↕	↕	↕	↕	820.269	410.134	410.135
	73	73	74	370.050	370.050	740.100	.500	.500	405.118	202.559	202.559
AFT HEAT SHIELD BULKHEAD.	74	75	76	445.200	420.339	865.539	.514362	.485638	3322.588	1709.013	1613.575
	75	76	77	420.339	395.284	815.623	.515359	.484641	3130.975	1613.576	1517.399
	76	77	74	395.284	370.050	765.334	.516486	.483514	2937.948	1517.409	1420.539
	77	74	78	370.050	347.886	717.936	.515436	.484564	2405.437	1239.849	1165.588
	78	78	79	347.886	325.610	673.496	.516538	.483462	2256.623	1165.632	1090.991
	79	79	80	325.610	302.871	628.481	.518090	.481910	2105.817	1091.003	1014.814
	80	80	81	302.871	280.732	583.603	.518968	.481032	1955.310	1014.743	940.567
	81	81	82	280.732	258.145	538.877	.520957	.479043	1805.573	940.626	864.947
	82	82	83	258.145	235.473	493.618	.522965	.477035	1653.844	864.903	788.941
	83	83	84	235.473	212.715	448.188	.525389	.474611	1501.651	788.951	712.700
	84	84	85	212.715	189.814	402.529	.528446	.471554	1348.694	712.712	635.982
	85	85	86	189.814	166.998	356.812	.531972	.468028	1195.577	636.013	559.564
	86	86	87	166.998	144.051	311.049	.536886	.463114	1042.156	559.519	482.637
	87	87	88	144.051	121.043	265.094	.543396	.456604	888.276	482.686	405.590
	88	88	57	121.043	98.010	219.053	.552574	.447426	733.931	405.551	328.380
	89	57	89	98.010	81.695	179.705	.545394	.454606	425.706	232.177	193.529
	90	89	90	81.695	65.381	147.076	.555461	.444539	348.408	193.527	154.881
	91	90	91	65.381	49.042	114.423	.571397	.428603	270.996	154.846	116.150
	92	91	92	49.042	32.703	81.745	.599939	.400061	193.585	116.139	77.446
	93	92	93	32.703	16.352	49.055	.666660	.333340	116.174	77.449	38.725
	94	93	94	16.352	0	16.352	1.000	0	38.762	38.762	0

Table 3-5. Distribution of Segment Weight to Boundary Nodes (continued)

①	②	③	④	⑤	⑥	⑦	⑧	⑨	⑩	⑪	⑫
COMP.	SEGMENT No	NODE No. n	NODE No. n+1	R_n	R_{n+1}	$R_n + R_{n+1}$	$\frac{R_n}{R_n + R_{n+1}}$	$\frac{R_{n+1}}{(R_n + R_{n+1})}$	W_{SEG}	W_n	W_{n+1}
REFERENCE		FIGS. 1-6		TABLE 1-1	⑤$_{n+1}$	⑤ + ⑥	⑤/⑦	⑥/⑦		⑧ × ⑩	⑨ × ⑩
ENGINE THRUST RING	95	33	95	525.176	515.176	1040.352	.504806	.495194	4636.500	2340.533	2295.967
	96	33	96	525.176	534.000	1059.176	.495834	.504166	1025.521	508.488	517.033
	97	33	97	525.176	526.990	1052.166	.499138	.500862	961.642	479.992	481.650
	98	96	97	534.000	526.990	1060.990	.503304	.496696	465.965	234.522	231.443
	99	96	98	534.000	539.500	1073.500	.497438	.502562	2486.497	1236.878	1249.619
	100	97	99	526.990	526.990	1053.980	.500	.500	2459.443	1229.721	1229.722
	101	98	99	539.500	526.990	1066.490	.505865	.494135	631.479	319.443	312.036
	102	98	100	539.500	530.000	1069.500	.504441	.495559	973.408	491.027	482.381
	103	99	100	526.990	530.000	1056.990	.498576	.501424	767.346	382.580	384.766

Table 3-6. Calculation of Running Load at Nodes

①	②	③	④	⑤	⑥	⑦	⑧	⑨
Node No.	Load Contributions				Total Load	R_n	C_n	P_n
REF					②+③+④+⑤	Table 3-5	6.283185 ⑦	⑥/⑧
1	120.459	11.039			131.498	98.010	615.815	.213538
2	127.041	102.948			229.989	103.365	649.461	.354123
3	109.635	164.446			274.081	110.078	691.640	.396277
4	179.486	239.311			418.797	120.146	754.900	.554771
5	266.049	407.377			673.426	133.570	839.245	.802419
6	470.070	470.072			940.142	154.126	968.402	.970818
7	532.766	347.937			880.703	174.602	1097.559	.802420
8	374.676	281.012			655.688	188.106	1181.905	.554772
9	296.052	197.375			493.427	198.174	1245.164	.396275
10	204.061	348.856	280.529		833.446	204.887	1287.343	.647416
11	366.917	489.223			856.140	215.494	1353.989	.632309
12	521.328	781.991			1303.319	229.636	1442.845	.903298
13	854.231	1474.630			2328.861	250.849	1576.131	1.477581
14	1689.901	1689.892			3379.793	287.469	1806.221	1.871196
15	1905.164	1103.639			3008.803	324.089	2036.311	1.477575
16	1175.876	783.918			1959.794	345.302	2169.596	.903299
17	816.023	612.018			1428.041	359.444	2258.453	.632309
18	630.075	1664.793	308.979	534.643	3138.490	370.050	2325.093	1.349834
19	1619.807				1619.807	360.050	2262.261	.716012
20	311.804	385.276			697.080	373.435	2346.361	.297090
21	389.593	1149.062			1538.655	377.618	2372.644	.648498
22	1186.600	1323.871			2510.471	389.954	2450.153	1.024618
23	1370.598	1370.642			2741.240	403.718	2536.635	1.080660
24	1417.369	1612.757			3030.126	417.482	2623.117	1.155162
25	1670.958	1794.866			3465.824	432.548	2717.779	1.275241
26	1862.022	1862.069			3724.091	448.731	2819.460	1.320853
27	1929.221	1666.204			3595.425	464.919	2921.172	1.230816
28	1714.445	1714.443			3428.888	478.374	3005.712	1.140791
29	1762.684	1662.604			3425.288	491.834	3090.284	1.108406
30	1705.520	1050.215			2755.735	504.529	3170.049	.869304
31	1066.579	991.336			2057.915	512.346	3219.165	.639270
32	1004.022	960.785	{5458.959	{5241.344	1914.807	518.902	3260.357	.602636
33	972.404	2340.533	508.488}	479.992	18001.720	525.176	3299.778	4.546282

Table 3-6. Calculation of Running Load at Nodes (continued)

①	②	③	④	⑤	⑥	⑦	⑧	⑨
NODE No	LOAD CONTRIBUTIONS				TOTAL LOAD	R_n	C_n	P_n
REF					②+③+④+⑤	TABLE 3-5	6.283185 ⑦	⑥/⑧
34	11.039	22.078			33.117	98.010	615.815	.053778
35	22.078	44.156			66.234			.107555
36	44.156	86.627			130.783			.212374
37	86.627	86.627			173.254			.281341
38	86.627	44.156			130.783			.212374
39	44.156	22.078			66.234			.107555
40	22.078	11.039	137.471		170.588			.277012
41	11.039	74.796			85.835			.139384
42	74.796	149.588			224.384			.364369
43	149.589	299.177			448.766			.728735
44	299.178	336.405			635.583			1.032100
45	336.405	336.410			672.815			1.092560
46	336.410	340.937			677.347			1.099919
47	340.938	340.937			681.875			1.107272
48	340.938	258.498			599.436			0.973403
49	258.498	258.498			516.996			.839531
50	258.498	159.872			418.370			.679376
51	159.873	79.936			239.809			.389417
52	79.937	35.655	2750.000	506.656	3372.248			5.476013
53	35.655	98.952			134.607			.218583
54	98.953	165.285			264.238			.429087
55	165.285	98.952			264.237			.429085
56	98.953	35.655			134.608			.218585
57	35.655	328.380	232.177	{2750.000 / 3061.684}	6407.896	98.010	615.815	10.405456
58	534.644	1069.286			1603.930	370.050	2325.093	.689834
59	1069.287	2138.573			3207.860			1.379669
60	2138.574	2818.996			4957.570			2.132201
61	2818.997	4658.551			7477.548			3.216019
62	4658.551	3534.113			8192.664			3.523583
63	3534.114	1767.056			5301.170			2.279980
64	1767.057	883.529			2650.586			1.139991
65	883.529	171.760	3723.656		4778.945			2.055377
66	171.761	247.972			419.733	370.050	2325.093	.180523

Table 3-6. Calculation of Running Load at Nodes (continued)

①	②	③	④	⑤	⑥	⑦	⑧	⑨
Node No.	Load Contributions				Total Load	R_n	C_n	P_n
Ref.					②+③+④+⑤	Table 3-5	6.283185⑦	⑥/⑧
67	247.973	247.972			495.945	370.050	2325.093	.213301
68	247.973	171.760			419.733	↑	↑	.180523
69	171.761	202.559	32523.482	1876.849	34774.596	│	│	14.955357
70	202.559	410.134			612.693	│	│	.263513
71	410.135	410.147			820.282	│	│	.352795
72	410.147	410.134			820.281	│	│	.352795
73	410.135	202.559			612.694	↓	↓	.263514
74	202.559	1420.539	1239.040	{32523.433 4658.840 11559.876 10440.681}	62044.883	370.050	2325.093	26.684903
75	1709.013				1709.013	445.200	2797.274	.610957
76	1613.575	1613.576			3227.151	420.339	2641.068	1.221911
77	1517.399	1517.409			3034.808	395.284	2483.642	1.221918
78	1165.588	1165.632			2331.220	347.886	2185.832	1.066514
79	1090.991	1091.003			2181.994	325.610	2045.868	1.066537
80	1014.814	1014.743			2029.557	302.871	1902.995	1.066507
81	940.567	940.626			1881.193	280.732	1763.891	1.066502
82	864.947	864.903			1729.850	258.145	1621.973	1.066510
83	788.941	788.951			1577.892	235.473	1479.520	1.066489
84	712.700	712.712			1425.412	212.715	1336.528	1.066504
85	635.982	636.013			1271.995	189.814	1192.636	1.066541
86	559.564	559.519			1119.083	166.998	1049.279	1.066526
87	482.637	482.686			965.323	144.051	905.099	1.066539
88	405.590	405.551			811.141	121.043	760.536	1.066539
89	193.529	193.527			387.056	81.695	513.308	.754047
90	154.881	154.846			309.727	65.301	410.301	.753959
91	116.150	116.139			232.289	49.042	308.140	.753842
92	77.446	77.449			154.895	32.703	205.479	.753824
93	38.762	0			38.762	16.352	102.743	.377271
94	0				0	0	0	0
95	2295.967				2295.967	515.176	3236.946	.709300
96	517.033	234.522	1236.878		1988.433	534.000	3355.221	.592638
97	481.650	231.443	1229.721		1942.814	526.990	3311.176	.586744
98	1249.619	319.443	491.027	12897.500	14957.589	539.500	3389.778	4.412557
99	1229.722	312.036	382.580		1924.338	526.990	3311.176	.581165
100	482.381	384.766	92780.600		93647.747	530.000	3330.088	28.121703

Σ = [illegible]

Because the calculations involved in determining these nodal loadings and pressure variations were quite voluminous, only the results are summarized herein. They can be seen in the segmental pressures shown in column ⑥ of tables 3-7 through 3-11, inclusive, and the ultimate nodal loadings shown in column ⑤ of tables 3-12 through 3-16, inclusive.

3.4 CONSTRUCTION OF LOAD COLUMNS

The reference 1 computer program requires that the pressure acting on a segment be input on the first of two cards which are used to specify the geometry and physical (elastic) properties of the segment. Tables 3-7 through 3-11 were set up to show how these data actually were entered on the data cards Columns ② to ⑥ are input on the first card while the remainder of the data is placed on the second card.

The final data required consist of the load column corresponding to the running loads on the nodes. Tables 3-12 through 3-16, inclusive, show the calculations resulting in the ultimate nodal loadings for each design condition. For a given design condition, these tables show the 1g nodal loading corresponding to the SERV dry weight, the product of these values times the ultimate load factor, the ultimate nodal loadings due to the variable weight items, and the algebraic sum of the two ultimate increments.

3.5 ULTIMATE INTERNAL FORCE AND DELECTION DISTRIBUTIONS

Tables 3-17 through 3-21 summarize the internal forces and deflections calculated at each boundary node defining an individual segment for each design condition investigated. Figure 3-1 is provided to show the positive sense of these data with respect to the vehicle. It should be noted that all radial deflections are with respect to the longitudinal centerline of the vehicle and longitudinal deflections are with respect to a horizontal plane passing through node 100 (point A). Translational deflections are in inches, rotational deflections are in radians, forces are in pounds, and moments are in inch-pounds.

3.6 CALCULATION OF STRESSES

3.6.1 MERIDIONAL STRESS DISTRIBUTION

The meridional stress in the inner and outer faces of the sandwich structure is the algebraic sum of the stress component due to the meridional loading and that due to the discontinuity bending moment. Because the internal forces output by the reference 1 computer program are referred to the longitudinal centerline of the vehicle, the forces acting at each end of the segment in the upper and lower frustums must now be converted into components parallel and perpendicular to the meridian. The component parallel to the meridian (P) corresponds to the axial load on the segment while the component perpendicular to the meridian (S) corresponds to the transverse shear loading acting on the segment. If "θ" is equal to 1/2 the cone angle of the frustum, these components are evaluated as follows:

$$P_n = (F1)\cos\theta + (F2)\sin\theta$$

$$S_n = (F1)\sin\theta - (F2)\cos\theta$$

Table 3-7. Summary of CR0033 Input Data - Liftoff Condition (T = 0 Seconds)

①	②	③	④	⑤	⑥	⑦	⑧	⑨	⑩	⑪
SEG No.	CURVE OPTION	No. OF SEGMENTS	R_m OR ϕ	R_c OR R_F	PRESSURE	∠ To n=1 OR L To n=1	∠ To n=2 OR L_{SEG}	t_e	E_e	μ
REF	NOTE (1)	NOTE (2)	NOTE (3)	NOTE (3)	NOTE (4)	NOTE (5)	NOTE (3)	NOTE (3)	NOTE (3)	NOTE (3)
1	1	1	90.0°	98.010	0	0	5.355	.246	29700000	.284
2			45.0°	103.365			9.493	2.743616	346391	
3				110.078			14.239			
4				120.146			18.985			
5				133.570			29.070			
6				154.126			29.070			
7				174.682			18.985			
8				188.106			14.239			
9				198.174	0		9.493	2.743618	346391	
10				204.887	0.700		15.000	6.893591	172319	
11				215.494	0.700		20.000			
12				229.636	0.700		30.000			
13				250.849	0.780		51.788			
14				287.469	0.941		51.788			
15				324.089	1.065		30.000			
16				345.302	1.146		20.000			
17			45.0°	359.444	1.200		15.000	6.893591	172319	
18			-90.0°	370.050	0		10.000	.482	29700000	
19			24.725309°	370.050	1.400		8.093	4.648085	204425	
20				373.435			10.000			
21				377.618			29.494			
22				389.954			32.906			
23				403.718	1.400		32.907	4.648085	204425	
24				417.482	2.357		36.019	4.645395	230175	
25				432.548	4.341		38.690			
26				448.731	6.397		38.691	4.645395	230175	
27				464.914	8.280		32.179	4.641939	255925	
28				478.394	9.989		32.179			
29				491.834	11.651		30.352			
30				504.529	12.953		18.690	4.641939	255925	
31				512.346	13.866		15.675	4.629851	346391	
32	1	1	24.725309°	518.902	14.681	0	15.000	4.629851	346391	.284

Table 3-7. Summary of CR0033 Input Data - Liftoff Condition (T = 0 Seconds) (continued)

①	②	③	④	⑤	⑥	⑦	⑧	⑨	⑩	⑪
SEG No.	CURV. OPTION	No. of SEGMENTS	R_m or ϕ	R_c or R_F	PRESSURE	∡ To n=1 or L To n=1	∡ To n+2 $L_{SEG.}$	t_e	E_e	μ
REF.	NOTE (1)	NOTE (2)	NOTE (3)	NOTE (3)	NOTE (4)	NOTE (5)	NOTE (3)	NOTE (3)	NOTE (3)	NOTE (3)
33	1	1	0°	98.010	0	0	5.000	.632258	939500	.284
34	↑	↑	↑	↑	↑	↑	10.000	↑	↑	↑
35							20.000			
36							37.237			
37							37.237			
38							20.000			
39					↓		10.000	↓	↓	
40					0		5.000	.632256	939500	
41					-0.733		15.000	5.871661	101159	
42					-0.832		30.000	↑	↑	
43					-1.029		60.000			
44					-1.309		67.466			
45					-1.606		67.467			
46					-1.904		68.315	↓	↓	
47					-2.205		68.315	5.871661	101158	
48					-2.461		48.507	6.564460	80436	
49					-2.674		48.506	↑	↑	
50					-2.847		30.000	↓	↓	
51					-2.946		15.000	6.564450	70496	
52					0		14.413	.632255	939500	
53					↑		40.000	↑	↑	
54							66.514			
55				↓	↓		40.000	↓	↓	
56				98.010	0		14.413	.632258	939500	
57				370.050	-0.133		13.588	6.865943	311464	
58				↑	-0.044		27.176	↑	↑	
59					0.135		54.352	↓	↓	
60					-2.219		71.645	6.865943	311164	
61					-6.933		71.645	6.807320	610810	
62					-11.079		54.352	↑	↑	
63					-13.762		27.176	↓	↓	
64					-15.101		13.558	6.807320	610810	
65	↓	↓	↓	↓	2.731	↓	13.457	1.153629	720849	↓
66	1	1	0°	370.050	2.804	0	19.428	1.153629	720849	.284

Table 3-7. Summary of CR0033 Input Data - Liftoff Condition (T = 0 Seconds) (continued)

①	②	③	④	⑤	⑥	⑦	⑧	⑨	⑩	⑪
SEG. No.	CURV. OPTION	No. OF SEGMENTS	R_m OR ϕ	R_c OR R_p	PRESSURE	ϕ To n=1 OR L To n=1	ϕ To n=2 OR LONG.	t_e	E_e	μ
REF.	NOTE (1)	NOTE (2)	NOTE (3)	NOTE (3)	NOTE (4)	NOTE (5)	NOTE (3)	NOTE (3)	NOTE (3)	NOTE (3)
67	1	1	0°	370.050	2.899	0	19.428	1.153628	720849	.284
68					2.961		13.457			
69					0		15.810			
70							32.133			
71							32.134			
72							32.135			
73	1		0°	370.050	0	0	15.810	1.153628	720849	.284
74	2		1251.750 in.	0	0.392	159.165926	160.378951	16.690	84282	.318
75						160.378951	161.591976	16.818	86016	
76						161.591976	162.805000	16.945	88056	
77						162.805000	163.863693	17.064	90299	
78						163.863693	164.922386	17.174	92743	
79						164.922386	165.981079	17.281	95617	
80						165.981079	167.039772	17.385	99015	
81						167.039772	168.098465	17.484	103084	
82						168.098465	169.157158	17.575	108015	
83						169.157158	170.215851	17.658	114080	
84						170.215851	171.274544	17.728	121743	
85						171.274544	172.333237	17.781	131426	
86						172.333237	173.391930	17.813	144285	
87						173.391930	174.450623	17.816	161933	
88						174.450623	175.509310	17.782	187901	
89						175.509310	176.257958	17.716	219997	
90						176.257958	177.006206	17.626	260681	
91						177.006206	177.754654	17.498	325282	
92						177.754654	178.503102	17.322	442551	
93	2		1251.750	0	0.392	178.503102	179.251550	17.086	718149	
94	1		-90.0	32.703	0	0	32.703	16.774	2104720	.318
95			-90.0	525.176			10.000	.418	29700000	.289
96			34.886977°	525.176			15.428	1.697528	699841	
97			8.157389°	525.176			14.467			
98			-90.0°	534.000			7.010			
99	1	1	8.548793°	534.000	0	0	37.407	1.697528	699841	.289

Table 3-7. Summary of CR0033 Input Data - Liftoff Condition (T = 0 Seconds) (continued)

①	②	③	④	⑤	⑥	⑦	⑧	⑨	⑩	⑪
SEG. No.	CURVE OPTION	No. OF SEGMENTS	R_m OR ϕ	R_c OR R_ϕ	PRESSURE	∡ To n=1 OR L To n=1	∡ To n=2 OR $L_{SEG.}$	t_e	E_e	μ
REF	NOTE (1)	NOTE (2)	NOTE (3)	NOTE (3)	NOTE (4)	NOTE (5)	NOTE (3)	NOTE (3)	NOTE (3)	NOTE (3)
100	1	1	0°	526.990	0	0	37.000	1.697528	697841	.284
101	↕	↕	-90°	539.500	↕	↕	9.500	↕	↕	↕
102	↕	↕	-40.444333	539.500	↕	↕	14.644	↕	↕	↕
103	1	1	15.113963	526.990	0	0	11.544	1.697528	697841	.284

NOTES:

1) Under curve option "1" corresponds to a segment with single curvature and "2" corresponds to a segment with double curvature (refer to figures 1-1 through 1-6 inclusive)

2) The program option was selected to define each segment individually therefore a "1" is required

3) These data are from table 1-1 for single curved segments and from table 1-3 for segments with double curvature.

4) Ultimate average pressure (lb/in²) acting on segment

5.) These data correspond to angle defining Node 1 for a double curved segment, otherwise "0".

Table 3-8. Summary of CR0033 Input Data - Maximum Dynamic Pressure Condition (T = 77 Seconds)

①	②	③	④	⑤	⑥	⑦	⑧	⑨	⑩	⑪
SEG No.	CURVE OPTION	No. OF SEGMENTS	R_m OR ϕ	R_c OR R_F	PRESSURE	∠ To n=1 OR ∠ To n≠1	∠ To n=2 OR L_{SEG}	t_e	E_e	μ
REF	NOTE (1)	NOTE (2)	NOTE (3)	NOTE (3)	NOTE (4)	NOTE (5)	NOTE (3)	NOTE (3)	NOTE (3)	NOTE (3)
1	1	1	90.0°	98.010	0	0	5.355	.246	29700000	.284
2			45.0°	103.363	-1.148		9.493	2.743618	346391	
3				110.078			14.239			
4				120.146			18.985			
5				133.570			29.070			
6				154.126			29.070			
7				174.682			18.985			
8				188.106			14.239			
9				198.174	-1.148		9.493	2.743618	346391	
10				204.887	1.021		15.000	6.893591	172319	
11				215.494	0.985		20.000			
12				229.636	0.880		30.000			
13				250.849	0.378		51.788			
14				287.469	-0.733		51.788			
15				324.089	-1.880		30.000			
16				345.302	-2.651		20.000			
17			45.0°	359.444	-3.225		15.000	6.893591	172319	
18			-90.0°	370.050	0		10.000	.482	29700000	
19			24.725309°	370.050	8.257		8.093	4.640085	204425	
20				373.435	8.248		10.000			
21				377.618	8.221		29.494			
22				389.954	8.177		32.906			
23				403.718	8.132		32.907	4.640085	204425	
24				417.482	8.096		36.019	4.645395	230175	
25				432.548	8.060		38.690			
26				448.731	8.033		38.691	4.645395	230175	
27				464.914	8.015		32.179	4.641939	255925	
28				478.374	9.277		32.179			
29				491.834	11.754		30.352			
30				504.529	13.700		18.690	4.641939	255925	
31				512.346	15.068		15.675	4.629851	346391	
32	1	1	24.725309°	518.902	16.296	0	15.000	4.629851	346391	.284

Table 3-8. Summary of CR0033 Input Data - Maximum Dynamic Pressure Condition (T = 77 Seconds) (continued)

(1)	(2)	(3)	(4)	(5)	(6)	(7)	(8)	(9)	(10)	(11)
SEG NO.	CURV. OPTION	NO. OF SEGMENTS	R_m OR ϕ	R_c OR R_F	PRESSURE	℄ TO n=1 OR L TO n=1	℄ TO n=2 $L_{SEG.}$	t_e	E_e	μ
REF.	NOTE (1)	NOTE (2)	NOTE (3)	NOTE (3)	NOTE (4)	NOTE (4)	NOTE (3)	NOTE (3)	NOTE (3)	NOTE (3)
33	1	1	0°	98.010	0	0	5.000	.632258	939500	.284
34	↑	↑	↑	↑	↑	↑	10.000	↑	↑	↑
35							20.000			
36							37.237			
37							37.237			
38							20.000			
39					↓		10.000	↓	↓	
40					0		5.000	.632258	939500	
41					-2.170		15.000	5.871661	101155	
42					↑		30.000	↑	↑	
43							60.000			
44					↓		67.466			
45					-2.170		67.467			
46					-2.359		68.315	↓	↓	
47					-2.736		68.315	5.871661	101158	
48					-3.059		48.507	6.564460	[illegible]	
49					-3.326		48.506	↑	↑	
50					-3.543		30.000	↓	↓	
51					-3.667		15.000	6.564460	[illegible]	
52					0		14.413	.632258	939500	
53					↑		40.000	↑	↑	
54							66.5[illegible]			
55				↓	↓		40.000	↓	↓	
56				98.010	0		14.413	.632258	939500	
57				370.050	-7.700		13.588	6.865943	311464	
58				↑	-7.700		27.176	↑	↑	
59					-7.700		54.352	↓	↓	
60					-7.643		71.645	6.865943	311464	
61					-7.247		71.645	6.807320	[illegible]	
62					-8.546		54.352	↑	↑	
63					-11.915		27.176	↓	↓	
64					-13.600		13.5[illegible]	6.807320	[illegible]	
65	↓	↓	↓	↓	3.383	↓	13.457	1.153625	720[illegible]	↓
66	1	1	0°	370.050	3.474	0	19.428	1.153628	720849	.284

Table 3-8. Summary of CR0033 Input Data - Maximum Dynamic Pressure Condition (T = 77 Seconds) (continued)

①	②	③	④	⑤	⑥	⑦	⑧	⑨	⑩	⑪
SEG. No.	CURV. OPTION	No. OF SEGMENTS	R_m OR ϕ	R_c OR R_F	PRESSURE	ℓ To n=1 OR L To n=1	ℓ To n=2 OR LSEG.	t_e	E_e	μ
REF.	NOTE (1)	NOTE (2)	NOTE (3)	NOTE (3)	NOTE (4)	NOTE (5)	NOTE (3)	NOTE (3)	NOTE (3)	NOTE (3)
67	1	1	0°	370.050	3.581	0	13.428	1.153628	720849	.284
68	↕	↕	↕	↕	3.672	↕	13.457	↕	↕	↕
69	↕	↕	↕	↕	0	↕	15.810	↕	↕	↕
70	↕	↕	↕	↕	↕	↕	32.133	↕	↕	↕
71	↕	↕	↕	↕	↕	↕	32.134	↕	↕	↕
72	↕	↕	↕	↕	↕	↕	32.133	↕	↕	↕
73	1	↕	0°	370.050	0	0	15.810	1.153628	720849	.284
74	2	↕	1251.750 in.	0	1.441	159.165926	160.378951	16.690	84282	.318
75	↕	↕	↕	↕	↕	160.378951	161.591976	16.818	86016	↕
76	↕	↕	↕	↕	↕	161.591976	162.805000	16.945	88056	↕
77	↕	↕	↕	↕	↕	162.805000	163.863693	17.064	90279	↕
78	↕	↕	↕	↕	↕	163.863693	164.922386	17.174	92743	↕
79	↕	↕	↕	↕	↕	164.922386	165.981079	17.281	95617	↕
80	↕	↕	↕	↕	↕	165.981079	167.039772	17.385	99015	↕
81	↕	↕	↕	↕	↕	167.039772	168.098465	17.484	103084	↕
82	↕	↕	↕	↕	↕	168.098465	169.157158	17.575	108018	↕
83	↕	↕	↕	↕	↕	169.157158	170.215851	17.658	114080	↕
84	↕	↕	↕	↕	↕	170.215851	171.274544	17.728	121749	↕
85	↕	↕	↕	↕	↕	171.274544	172.333237	17.781	131426	↕
86	↕	↕	↕	↕	↕	172.333237	173.391930	17.813	144285	↕
87	↕	↕	↕	↕	↕	173.391930	174.450623	17.816	161933	↕
88	↕	↕	↕	↕	↕	174.450623	175.509310	17.782	187901	↕
89	↕	↕	↕	↕	↕	175.509310	176.257758	17.716	219997	↕
90	↕	↕	↕	↕	↕	176.257758	177.006206	17.626	260681	↕
91	↕	↕	↕	↕	↕	177.006206	177.754654	17.498	325282	↕
92	↕	↕	↕	↕	↕	177.754654	178.503102	17.322	442551	↕
93	2	↕	1251.750	0	1.441	178.503102	179.251550	17.086	718149	↕
94	1	↕	-90.0	32.703	0	0	32.703	16.774	2104720	.318
95	↕	↕	-90.0°	525.176	0	↕	10.800	.478	29700000	.284
96	↕	↕	34.806977°	525.176	-1.935	↕	15.428	1.697528	699841	↕
97	↕	↕	8.157389°	525.176	0	↕	14.467	↕	↕	↕
98	↕	↕	-90.0°	534.000	0	↕	7.010	↕	↕	↕
99	1	1	8.548993°	534.000	-1.944	0	37.407	1.697528	699841	.284

Table 3-8. Summary of CR0033 Input Data - Maximum Dynamic Pressure Condition (T = 77 Seconds) (continued)

①	②	③	④	⑤	⑥	⑦	⑧	⑨	⑩	⑪
SEG. No.	CURVE OPTION	No. OF SEGMENTS	R_m OR ϕ	R_c OR R_ϕ	PRESSURE	∡ TO n=1 OR L TO n=1	∡ TO n=2 OR L SEG.	t_e	E_e	μ
REF	NOTE (1)	NOTE (2)	NOTE (3)	NOTE (3)	NOTE (4)	NOTE (5)	NOTE (3)	NOTE (3)	NOTE (3)	NOTE (3)
100	1	1	0°	526.990	0	0	37.000	1.697528	699841	.284
101	↕	↕	-90°	539.500	↕	↕	9.500	↕	↕	↕
102	↕	↕	-40.444333	539.500	↕	↕	14.644	↕	↕	↕
103	1	1	15.113763	526.990	0	0	11.544	1.697528	699841	.284

NOTES:

1) Under curve option "1" corresponds to a segment with single curvature and "2" corresponds to a segment with double curvature (refer to figures 1-1 through 1-6 inclusive)

2) The program option was selected to define each segment individually therefore a "1" is required

3) These data are from table 1-1 for single curved segments and from table 1-3 for segments with double curvature.

4) Ultimate average pressure (lb/in²) acting on segment

5.) These data correspond to angle defining Node 1 for a double curved segment, otherwise "0".

Table 3-9. Summary of CR0033 Input Data - Maximum Longitudinal Acceleration Condition (T = 138 Seconds)

①	②	③	④	⑤	⑥	⑦	⑧	⑨	⑩	⑪
SEG No.	CURVE OPTION	No. OF SEGMENTS	R_m OR ϕ	R_c OR R_F	PRESSURE	∠ To n=1 OR L To n=1	∠ To n=2 OR L_{SEG}	t_e	E_e	μ
REF	NOTE (1)	NOTE (2)	NOTE (3)	NOTE (3)	NOTE (4)	NOTE (5)	NOTE (3)	NOTE (3)	NOTE (3)	NOTE (3)
1	1	1	90.0°	98.010	0	0	5.355	.246	29700000	.284
2			45.0°	103.365	-0.543		9.493	2.743618	346391	
3				110.078			14.239			
4				120.146			18.985			
5				133.570			29.070			
6				154.126			29.070			
7				174.682			18.985			
8				188.106			14.239			
9				198.174	-0.543		9.493	2.743618	346391	
10				204.887	6.988		15.000	6.893591	172319	
11				215.494	6.971		20.000			
12				229.636	6.922		30.000			
13				250.849	6.684		51.788			
14				287.469	6.158		51.788			
15				324.089	5.616		30.000			
16				345.302	5.251		20.000			
17			45.0°	359.444	4.979		15.000	6.893591	172319	
18			-90.0°	370.050	0		10.000	.482	29700000	
19			24.725309°	370.050	14.469		8.073	4.648885	204425	
20				373.435	14.464		10.000			
21				377.618	14.452		29.494			
22				389.954	14.431		32.906			
23				403.718	14.410		32.907	4.648085	204425	
24				419.482	14.393		36.019	4.645395	230175	
25				432.548	14.376		38.690			
26				448.731	14.363		38.691	4.645395	230175	
27				464.914	14.354		32.179	4.641939	255925	
28				478.374	14.341		32.179			
29				491.834	14.329		30.352			
30				504.527	14.320		18.690	4.641939	255925	
31				512.346	15.619		15.675	4.629851	346391	
32	1	1	24.725309°	518.902	18.169	0	15.000	4.629851	346391	.284

Table 3-9. Summary of CR0033 Input Data - Maximum Longitudinal Acceleration Condition (T = 138 Seconds) (continued)

①	②	③	④	⑤	⑥	⑦	⑧	⑨	⑩	⑪
SEG No.	CURV. OPTION	No. of SEGMENTS	R_m or ϕ	R_c or R_F	PRESSURE	X To n=1 or L To n=1	X To n=2 Lseg.	t_e	E_e	μ
REF.	NOTE (1)	NOTE (2)	NOTE (3)	NOTE (3)	NOTE (4)	NOTE (5)	NOTE (3)	NOTE (3)	NOTE (3)	NOTE (3)
33	|	|	0°	98.010	0	0	5.000	.632258	939500	.284
34	↑	↑	↑	↑	↑	↑	10.000	↑	↑	↑
35							20.000			
36							37.237			
37							37.237			
38							20.000			
39					↓		10.000	↓	↓	
40					0		5.000	.632258	939500	
41					-7.532		15.000	5.871661	101155	
42					↑		30.000	↑	↑	
43							60.000			
44							67.466			
45							67.467			
46					↓		68.375	↓	↓	
47					-7.532		68.375	5.871661	101155	
48					-7.810		48.507	6.564480	90436	
49					-8.366		48.506	↑	↑	
50					-8.816		30.000	↓	↓	
51					-9.074		15.000	6.564480	90436	
52					0		14.413	.632258	939500	
53					↑		40.000	↑	↑	
54							66.514			
55				↓	↓		40.000	↓	↓	
56				98.010	0		14.413	.632258	939500	
57				370.050	-7.700		13.588	6.565943	311464	
58				↑	↑		27.176	↑	↑	
59							54.352	↓	↓	
60					↓		71.645	6.865943	311464	
61					-7.700		71.645	6.807320	610810	
62					-7.605		54.352	↑	↑	
63					-7.209		27.176	↓	↓	
64					-10.706		13.555	6.807320	610810	
65	↓	↓	↓	↓	8.483	↓	13.457	1.153628	720849	↓
66	|	|	0°	370.050	8.671	0	19.428	1.153628	720849	.284

Table 3-9. Summary of CR0033 Input Data - Maximum Longitudinal Acceleration Condition (T = 138 Seconds) (continued)

①	②	③	④	⑤	⑥	⑦	⑧	⑨	⑩	⑪
SEG. No.	CURV. OPTION	No. OF SEGMENTS	R_m OR ϕ	R_c OR R_F	PRESSURE	4 To n=1 OR L To n=1	4 To n=2 OR LSEG.	t_e	E_e	μ
REF.	NOTE(1)	NOTE (2)	NOTE (3)	NOTE (3)	NOTE (4)	NOTE (5)	NOTE (3)	NOTE (3)	NOTE (3)	NOTE (3)
67	1	1	0°	370.050	8.894	0	19.428	1.153628	720847	.284
68	↕	↕	↕	↕	9.083	↕	13.457	↕	↕	↕
69	↕	↕	↕	↕	0	↕	15.810	↕	↕	↕
70	↕	↕	↕	↕	↕	↕	32.133	↕	↕	↕
71	↕	↕	↕	↕	↕	↕	32.134	↕	↕	↕
72	↕	↕	↕	↕	↕	↕	32.133	↕	↕	↕
73	1	↕	0°	370.050	0	0	15.810	1.153628	720849	.284
74	2	↕	1251.750 in.	0	-1.540	159.165926	160.378951	16.690	84282	.318
75	↕	↕	↕	↕	↕	160.378951	161.591976	16.818	86016	↕
76	↕	↕	↕	↕	↕	161.591976	162.805000	16.945	88056	↕
77	↕	↕	↕	↕	↕	162.805000	163.863693	17.064	90299	↕
78	↕	↕	↕	↕	↕	163.863693	164.922386	17.174	92743	↕
79	↕	↕	↕	↕	↕	164.922386	165.981079	17.281	95617	↕
80	↕	↕	↕	↕	↕	165.981079	167.039772	17.383	99015	↕
81	↕	↕	↕	↕	↕	167.039772	168.098465	17.484	103084	↕
82	↕	↕	↕	↕	↕	168.098465	169.157158	17.575	108016	↕
83	↕	↕	↕	↕	↕	169.157158	170.215851	17.658	114080	↕
84	↕	↕	↕	↕	↕	170.215851	171.274544	17.728	121749	↕
85	↕	↕	↕	↕	↕	171.274544	172.333237	17.781	131426	↕
86	↕	↕	↕	↕	↕	172.333237	173.391930	17.813	144285	↕
87	↕	↕	↕	↕	↕	173.391930	174.450623	17.816	161933	↕
88	↕	↕	↕	↕	↕	174.450623	175.509310	17.782	187901	↕
89	↕	↕	↕	↕	↕	175.509310	176.257758	17.716	219997	↕
90	↕	↕	↕	↕	↕	176.257758	177.006206	17.626	260681	↕
91	↕	↕	↕	↕	↕	177.006206	177.754654	17.498	325282	↕
92	↕	↕	↕	↕	↕	177.754654	178.503102	17.322	442551	↕
93	2	↕	1251.750	0	-1.540	178.503102	179.251550	17.006	718149	↕
94	1	↕	-90.0	32.703	0	0	32.703	16.774	2104120	.318
95	↕	↕	-90.0°	525.176	0	↕	10.000	.478	29700000	.284
96	↕	↕	34.886977°	525.176	-.916	↕	15.428	1.697528	699841	↕
97	↕	↕	8.157389°	525.176	0	↕	14.467	↕	↕	↕
98	↕	↕	-90.0°	534.000	0	↕	7.010	↕	↕	↕
99	1	1	8.548793°	534.000	-.920	0	37.407	1.697528	699841	.284

Table 3-9. Summary of CR0033 Input Data - Maximum Longitudinal Acceleration Condition (T = 138 Seconds) (continued)

①	②	③	④	⑤	⑥	⑦	⑧	⑨	⑩	⑪
SEG. No.	CURVE OPTION	No. OF SEGMENTS	R_m OR ϕ	R_c OR R_F	PRESSURE	ϕ TO n=1 OR L TO n=1	ϕ TO n=2 OR L SEG.	t_e	E_e	μ
REF	NOTE (1)	NOTE (2)	NOTE (3)	NOTE (3)	NOTE (4)	NOTE (5)	NOTE (3)	NOTE (3)	NOTE (3)	NOTE (3)
100	1	1	0°	526.990	0	0	37.000	1.697528	699841	.284
101	↑	↑	-90°	539.500	↑	↑	9.500	↑	↑	↑
102	↓	↓	-40.444333	539.500	↓	↓	14.644	↓	↓	↓
103	1	1	15.113763	526.990	0	0	11.544	1.697525	699841	.284

NOTES: 1) Under curve option "1" corresponds to a segment with single curvature and "2" corresponds to a segment with double curvature (refer to figures 1-1 through 1-6 inclusive.

2) The program option was selected to define each segment individually therefore a "1" is required

3) These data are from table 1-1 for single curved segments and from table 1-3 for segments with double curvature.

4). Ultimate average pressure (lb/in²) acting on segment

5.) These data correspond to angle defining Node 1 for a double curved segment, otherwise "0".

Table 3-10. Summary of CR0033 Input Data - Reentry Condition (T_R = 505 Seconds)

①	②	③	④	⑤	⑥	⑦	⑧	⑨	⑩	⑪
SEG No.	CURVE OPTION	No. OF SEGMENTS	R_m OR ϕ	R_c OR R_F	PRESSURE	∠ To n=1 - OR L To n=1	∠ To n=2 OR L_{SEG}	t_e	E_e	μ
REF	NOTE (1)	NOTE (2)	NOTE (3)	NOTE (3)	NOTE (4)	NOTE (5)	NOTE (3)	NOTE (3)	NOTE (3)	NOTE (3)
1	1	1	90.0°	98.030	0	0	5.355	.246	29700000	.284
2			45.0°	103.365			9.493	2.743618	346391	
3				110.078			14.239			
4				120.146			18.985			
5				133.570			29.070			
6				154.126			29.070			
7				174.692			18.985			
8				188.106			14.239			
9				198.174	0		9.493	2.743618	346391	
10				204.887	7.700		15.000	6.893591	172319	
11				215.494			20.000			
12				229.636			30.000			
13				250.849			51.788			
14				287.469			51.788			
15				324.089			30.000			
16				345.302			20.000			
17			45.0°	359.444	7.700		15.000	6.893591	172319	
18			-90.0°	370.050	0		10.000	.482	29700000	
19			24.725309°	370.050	7.000		8.093	4.648885	204425	
20				373.435			10.000			
21				377.615			29.494			
22				389.954			32.906			
23				403.718			32.907	4.648885	204425	
24				417.482			36.019	4.645395	230175	
25				432.548			38.690			
26				448.731			38.691	4.645395	230175	
27				464.914			32.179	4.641939	255925	
28				478.374			32.179			
29				491.834			30.352			
30				504.527			18.690	4.641939	255925	
31				512.346			15.675	4.629851	346391	
32	1	1	24.725309°	518.902	7.000	0	15.000	4.629851	346391	.284

Table 3-10. Summary of CR0033 Input Data - Reentry Condition (T_R = .505 Seconds) (continued)

① SEG No.	② CURV. OPTION	③ No. of SEGMENTS	④ R_m or ϕ	⑤ R_c or R_F	⑥ PRESSURE	⑦ $\measuredangle$ To n=1 or L To n=1	⑧ $\measuredangle$ To n=2 Degs.	⑨ t_e	⑩ E_e	⑪ μ
REF.	NOTE (1)	NOTE (2)	NOTE (3)	NOTE (3)	NOTE (4)	NOTE (5)	NOTE (3)	NOTE (3)	NOTE (3)	NOTE (3)
33	1	1	0°	98.010	0	0	5.000	.632258	939500	.284
34	↑	↑	↑	↑	↑	↑	10.000	↑	↑	↑
35							20.000			
36							37.237			
37							37.237			
38							20.000			
39					↓		10.000	↓	↓	
40					0		5.000	.632258	939500	
41					-7.700		15.000	5.871661	101158	
42					↑		30.000	↑	↑	
43							60.000			
44							67.466			
45							67.467			
46							68.315	↓	↓	
47							68.315	5.871661	101158	
48							48.507	6.564480	90436	
49							48.506	↑	↑	
50					↓		30.000	↓	↓	
51					-7.700		15.000	6.564480	90476	
52					0		14.413	.632258	939500	
53					↑		40.000	↑	↑	
54							66.514			
55				↓	↓		40.000	↓	↓	
56				98.010	0		14.413	.632258	939500	
57				370.050	0.700		13.588	6.865943	311464	
58				↑	↑		27.176	↑	↑	
59							54.352	↓	↓	
60							71.645	6.865943	311464	
61							71.645	6.807320	610810	
62							54.352	↑	↑	
63					↓		27.176	↓	↓	
64					0.700		13.555	6.807320	610810	
65	↓	↓	↓	↓	7.700	↓	12.457	1.153628	720849	↓
66	1	1	0°	370.050	7.700	0	17.428	1.153628	720849	.284

Table 3-10. Summary of CR0033 Input Data - Reentry Condition (T_R = 505 Seconds) (continued)

①	②	③	④	⑤	⑥	⑦	⑧	⑨	⑩	⑪
SEG. No.	CURV. OPTION	No. OF SEGMENTS	R_m OR ϕ	R_c OR R_F	PRESSURE	∡ To n=1 OR L To n=1	∡ To n=2 OR LSEG.	t_e	E_e	μ
REF.	NOTE(1)	NOTE(2)	NOTE(3)	NOTE(3)	NOTE(4)	NOTE(5)	NOTE(3)	NOTE(3)	NOTE(3)	NOTE(3)
67	1	1	0°	370.050	7.700	0	19.428	1.153628	720849	.284
68					7.700		13.457			
69					0		16.810			
70							32.133			
71							32.134			
72							32.133			
73	1		0°	370.050	0	0	15.810	1.153628	720849	.284
74	2		1251.750 in.	0	-2.075	159.165926	160.378951	16.690	84282	.318
75						160.378951	161.591976	16.818	86016	
76						161.591976	162.808000	16.945	88056	
77						162.808000	162.863693	17.064	90299	
78						163.863693	164.922386	17.174	92743	
79						164.922386	165.981079	17.281	95617	
80						165.981079	167.039772	17.385	99015	
81						167.039772	168.098465	17.484	103084	
82						168.098465	169.157158	17.575	108018	
83						169.157158	170.215851	17.658	114080	
84						170.215851	171.274544	17.728	121749	
85						171.274544	172.333237	17.781	131426	
86						172.333237	173.391930	17.813	144285	
87						173.391930	174.450623	17.816	161933	
88						174.450623	175.509310	17.782	187901	
89						175.509310	176.257158	17.716	219997	
90						176.257158	177.006206	17.626	260681	
91						177.006206	177.754654	17.498	325282	
92						177.754654	178.503102	17.322	442551	
93	2		1251.750	0	-2.075	178.503102	179.251550	17.086	718149	
94	1		-90.0	32.703	0	0	32.703	16.774	2104720	.318
95			-90.0°	525.176			10.000	.478	29700000	.289
96			34.696977°	525.176			15.428	1.697528	698841	
97			8.157309°	525.176			14.467			
98			-90.0°	534.000			7.010			
99	1	1	8.548953°	534.000	0	0	37.407	1.697528	699841	.284

Table 3-10. Summary of CR0033 Input Data - Reentry Condition (T_R = 505 Seconds) (continued)

①	②	③	④	⑤	⑥	⑦	⑧	⑨	⑩	⑪
SEG. No.	CURVE OPTION	No. OF SEGMENTS	R_m OR ϕ	R_c OR R_P	PRESSURE	∢ To n=1 OR L To n=1	∢ To n=2 OR $L_{SEG.}$	t_e	E_e	μ
REF	NOTE (1)	NOTE (2)	NOTE (3)	NOTE (3)	NOTE (4)	NOTE (5)	NOTE (3)	NOTE (3)	NOTE (3)	NOTE (3)
100	1	1	0°	526.990	0	0	37.000	1.697528	697841	.284
101	↕	↕	-90°	539.500	↕	↕	9.500	↕	↕	↕
102	↕	↕	-40.444333	539.500	↕	↕	14.644	↕	↕	↕
103	1	1	15.113963	526.990	0	0	11.544	1.697528	697841	.284

NOTES: 1) Under curve option "1" corresponds to a segment with single curvature and "2" corresponds to a segment with double curvature (refer to figures 1-1 through 1-6 inclusive.

2) The program option was selected to define each segment individually therefore a "1" is required

3) These data are from table 1-1 for single curved segments and from Table 1-3 for segments with double curvature.

4). Ultimate average pressure (lb/in²) acting on segment

5.) These data correspond to angle defining Node 1 for a double curved segment, otherwise "0".

Table 3-11. Summary of CR0033 Input Data - Landing Condition

①	②	③	④	⑤	⑥	⑦	⑧	⑨	⑩	⑪
SEG No.	CURVE OPTION	No. OF SEGMENTS	R_m OR ϕ	R_c OR R_F	PRESSURE	∠ To n=1 OR L To n=1	∠ To n=2 OR L_{SEG}	t_e	E_e	μ
REF	NOTE (1)	NOTE (2)	NOTE (3)	NOTE (3)	NOTE (4)	NOTE (5)	NOTE (3)	NOTE (3)	NOTE (3)	NOTE (3)
1	1	1	90.0°	98.010	0	0	5.355	.246	29700000	.284
2			45.0°	103.365			9.493	2.743618	346391	
3				110.078			14.239			
4				120.146			18.985			
5				133.570			29.070			
6				154.126			29.070			
7				174.682			18.985			
8				188.106			14.239			
9				198.174	0		9.493	2.743618	346391	
10				204.887	0.700		15.000	6.893591	172319	
11				215.494			20.000			
12				229.636			30.000			
13				250.849			51.788			
14				287.469			51.788			
15				324.089			30.000			
16				345.302			20.000			
17			45.0°	359.444	0.700		15.000	6.893591	172319	
18			-90.0°	370.050	0		10.000	.482	29700000	
19			24.725309°	370.050	1.400		8.093	4.648085	204425	
20				373.435			10.000			
21				377.618			29.494			
22				389.954			32.906			
23				403.718			32.907	4.648085	204425	
24				417.482			36.019	4.645395	230175	
25				432.548			38.690			
26				446.731			38.691	4.645395	230175	
27				464.914			32.179	4.641939	255925	
28				478.374			32.179			
29				491.834			30.352			
30				504.527			18.690	4.641939	255925	
31				512.346			15.675	4.629851	346391	
32	1	1	24.725309°	518.902	1.400	0	15.000	4.629851	346391	.284

Table 3-11. Summary of CR0033 Input Data - Landing Condition (continued)

①	②	③	④	⑤	⑥	⑦	⑧	⑨	⑩	⑪
SEG No.	CURV. OPTION	No. of SEGMENTS	R_m or ϕ	R_c or R_F	PRESSURE	∡ To n=1 or L To n=1	∡ To n=2 Lseg.	t_e	E_e	μ
REF.	NOTE (1)	NOTE (2)	NOTE (3)	NOTE (3)	NOTE (4)	NOTE (5)	NOTE (3)	NOTE (3)	NOTE (3)	NOTE (3)
33	1	1	0°	98.010	0	0	5.000	.632258	939500	.264
34							10.000			
35							20.000			
36							37.237			
37							37.237			
38							20.000			
39							10.000			
40					0		5.000	.632258	939500	
41					-0.700		15.000	5.871661	101158	
42							30.000			
43							60.000			
44							67.466			
45							67.467			
46							68.375			
47							68.375	5.871661	101158	
48							48.507	6.564460	90496	
49							48.506			
50							30.000			
51					-0.700		15.000	6.564480	90496	
52					0		14.413	.632258	939500	
53							40.000			
54							66.914			
55							40.000			
56				98.010	0		14.413	.632258	939500	
57				370.050	-0.700		13.588	6.865943	311464	
58							27.176			
59							54.352			
60							71.645	6.865943	311464	
61							71.645	6.807320	610810	
62							54.352			
63							27.176			
64					-0.700		13.565	6.807320	610810	
65					0.700		13.457	1.153628	720849	
66	1	1	0°	370.050	0.700	0	19.428	1.153628	720849	.284

Table 3-11. Summary of CR0033 Input Data - Landing Condition (continued)

①	②	③	④	⑤	⑥	⑦	⑧	⑨	⑩	⑪
SEG. No.	CURV. OPTION	No. OF SEGMENTS	R_m OR ϕ	R_c OR R_f	PRESSURE	ϕ To n=1 OR L To n=1	ϕ To n=2 OR LONG.	t_e	E_e	μ
REF.	NOTE (1)	NOTE (2)	NOTE (3)	NOTE (3)	NOTE (4)	NOTE (5)	NOTE (3)	NOTE (3)	NOTE (3)	NOTE (3)
67	1	1	0°	370.050	0.700	0	19.428	1.153628	720849	.284
68					0.700		13.457			
69					0		15.870			
70							32.133			
71							32.134			
72							32.133			
73	1		0°	370.050		0	15.870	1.153628	720849	.284
74	2		1251.750 in.	0		159.165926	160.378951	16.690	84282	.318
75						160.378951	161.591976	16.818	86016	
76						161.591976	162.805000	16.945	88056	
77						162.805000	163.863693	17.064	90299	
78						163.863693	164.922386	17.174	92743	
79						164.922386	165.981079	17.281	95617	
80						165.981079	167.039772	17.385	99015	
81						167.039772	168.098465	17.484	103054	
82						168.098465	169.157158	17.575	108016	
83						169.157158	170.215851	17.658	114080	
84						170.215851	171.274544	17.728	121749	
85						171.274544	172.333237	17.781	131426	
86						172.333237	173.391930	17.813	144285	
87						173.391930	174.450623	17.816	161933	
88						174.450623	175.509310	17.782	187901	
89						175.509310	176.257758	17.716	219997	
90						176.257758	177.006206	17.626	260681	
91						177.006206	177.754654	17.498	325202	
92						177.754654	178.503102	17.322	442551	
93	2		1251.750	0		178.503102	179.251550	17.086	718149	
94	1		-90.0	32.703		0	32.703	16.774	2104720	.318
95			-90.0°	525.176			10.000	.478	29700000	.289
96			34.886777°	525.176			15.428	1.697528	693841	
97			8.157389°	525.176			14.467			
98			-90.0°	534.000			7.010			
99	1	1	8.548793°	534.000	0	0	37.407	1.697528	699841	.289

Table 3-11. Summary of CR0033 Input Data - Landing Condition (continued)

①	②	③	④	⑤	⑥	⑦	⑧	⑨	⑩	⑪
SEG. No.	CURVE OPTION	No. OF SEGMENTS	R_m OR ϕ	R_c OR R_ϕ	PRESSURE	∡ To n=1 OR L To n=1	∡ To n=2 OR L SEG.	t_e	E_e	μ
REF	NOTE (1)	NOTE (2)	NOTE (3)	NOTE (3)	NOTE (4)	NOTE (5)	NOTE (3)	NOTE (3)	NOTE (3)	NOTE (3)
100	1	1	0°	526.990	0	0	37.000	1.697528	699841	.284
101	↑	↑	-90° l	539.500	↑	↑	9.500	↑	↑	↑
102	↓	↓	-40.444353	539.500	↓	↓	14.644	↓	↓	↓
103	1	1	15.113963	526.990	0	0	11.544	1.697528	699841	.284

NOTES:

1) Under curve option "1" corresponds to a segment with single curvature and "2" corresponds to a segment with double curvature (refer to figures 1-1 through 1-6 inclusive.

2) The program option was selected to define each segment individually therefore a "1" is required

3) These data are from table 1-1 for single curved segments and from table 1-3 for segments with double curvature.

4). Ultimate average pressure (lb/in²) acting on segment

5.) These data correspond to angle defining Node 1 for a double curved segment, otherwise "0".

Table 3-12. Load Column - Liftoff Condition (T = 0 Seconds) (continued)

①	②	③	④	⑤	⑥
Node No.	Matrix Element No.	Fixed Weight Items P (n=1.0)	Fixed Weight Items P (n=1.680)	Ultimate Variable Weight	Ultimate Nodal Loading
Ref.	Note (1)	Table 3-6	1.680 x ③		④ + ⑤
37	108	.281341	.473		.473
38	111	.212374	.357		.357
39	114	.107555	.181		.181
40	117	.277012	.465		.465
41	120	.139384	.234	-57.387	-57.153
	121	0	0	0	0
	122	-.372000	-.625	108.461	107.836
42	123	.364369	.612		.612
43	126	.728735	1.224		1.224
44	129	1.032100	1.734		1.734
45	132	1.092560	1.836		1.836
46	135	1.099919	1.848		1.848
47	138	1.107272	1.860		1.860
48	141	.973403	1.635		1.635
49	144	.839531	1.410		1.410
50	147	.679376	1.141		1.141
51	150	.389417	.654		.654
52	153	5.476073	9.200	829.814	839.014
	154	0	0	0	0
	155	-1.533000	-2.575	-1568.348	-1570.923
53	156	.218583	.367		.367
54	159	.429037	.721		.721
55	162	.429085	.721		.721
56	165	.218585	.367		.367
57	168	10.405456	17.481		17.481
58	171	.689834	1.159		1.159
59	174	1.379669	2.318		2.318
60	177	2.132201	3.582		3.582
61	180	3.216019	5.403		5.403
62	183	3.523583	5.920		5.920
63	186	2.279980	3.830		3.830
64	189	1.139991	1.915		1.915
65	192	2.055377	3.453	1915.347	1918.800
	193	0	0	0	0
	194	-3.186000	-5.352	-4309.531	-4314.883
66	195	.180523	.303		.303
67	198	.213301	.358		.358
68	201	.180523	.303		.303
69	204	14.955357	25.125	364.796	389.921
	205	0	0	0	0
	206	.274000	.460	820.791	821.251
70	207	.263313	.443		.443

PRECEDING PAGE BLANK NOT FILMED

C2

Table 3-12. Load Column - Liftoff Condition (T = 0 Seconds) (continued)

①	②	③	④	⑤	⑥
NODE NO.	MATRIX ELEMENT NO.	FIXED WEIGHT ITEMS P (n = 1.00)	P (n = 1.680)	ULTIMATE VARIABLE WEIGHT	ULTIMATE NODAL LOADING
REF.	NOTE (1)	TABLE 3-6	1.680 x ③		④ + ⑤
71	210	.352795	.593		.593
72	213	.352795	.593		.593
73	216	.263514	.443		.443
74	219	26.604903	44.081	18.384	63.215
75	222	.610957	1.026		1.026
76	225	1.221911	2.053		2.053
77	228	1.221910	2.053		2.053
78	231	1.066514	1.792		1.792
79	234	1.066537	↑		↑
80	237	1.066507			
81	240	1.066502			
82	243	1.066510			
83	246	1.066409			
84	249	1.066504			
85	252	1.066541			
86	255	1.066526			
87	258	1.066539	↓		↓
88	261	1.066539	1.792		1.792
89	264	.754047	1.267		1.267
90	267	.753969	1.267		1.267
91	270	.753842	1.266		1.266
92	273	.753824	1.266		1.266
93	276	.377271	.633	2.556	3.189
94	279	0	0	131.324	1.278 (2)
95	280	.709300	1.192		1.192
96	283	.592688	.996		.996
97	286	.586744	.986		.986
98	289	4.412557	7.413		7.413
99	292	.581165	.976		.976

NOTES: 1) The matrix element number corresponds to the non-singular matrix row number shown in table 1-4

2.) An error in the program requires that this entry be 131.324/102.743 = 1.278 where 102.743 ins. is the circumference at Node 93.

Table 3-13. Load Column - Maximum Pressure Condition (T = 77 Seconds)

Ultimate load factor = (1.400) (1.430) = 2.002 (refer to table 3-1)

①	②	③	④	⑤	⑥
Node No.	Matrix Element No.	Fixed Weight Items: P (n = 1.0)	Fixed Weight Items: P (n = 2.002)	Ultimate Variable Weight	Ultimate Nodal Loading
Ref.	Note (1)	Table 3-6	2.002 × ③		④ + ⑤
1	1	.213535	.427		.427
2	3	.354123	.709	321.709	322.418
3	6	.396277	.793		.793
4	9	.554771	1.111		1.111
5	12	.802419	1.606		1.606
6	15	.970818	1.944		1.944
7	18	.802420	1.606		1.606
8	21	.554772	1.111		1.111
9	24	.396275	.793		.793
10	27	.647416	1.296	-84.352	-83.056
10	28	0	0	-84.352	-84.352
10	29	.310000	.621	-238.582	-237.961
11	30	.632309	1.266		1.266
12	33	.903298	1.808		1.808
13	36	1.477581	2.958		2.958
14	39	1.871196	3.746		3.746
15	42	1.477575	2.958		2.958
16	45	.903299	1.808		1.808
17	48	.632309	1.266		1.266
18	51	1.349834	2.702	4.055	6.757
19	54	.716012	1.433		1.433
20	57	.297090	.595		.595
21	60	.648498	1.298		1.298
22	63	1.024618	2.051		2.051
23	66	1.080660	2.163		2.163
24	69	1.155162	2.313		2.313
25	72	1.275241	2.553		2.553
26	75	1.320853	2.644		2.644
27	78	1.230816	2.464		2.464
28	81	1.140791	2.284		2.284
29	84	1.108406	2.219		2.219
30	87	.869304	1.740		1.740
31	90	.639270	1.280		1.280
32	93	.602636	1.206		1.206
33	96	4.546282	9.102	1566.072 -33.822	1541.352
33	97	0	0	0	0
33	98	2.367000	4.739	2154.915	2159.654
34	99	.053778	.108		.108
35	102	.107893	.215		.215
36	105	.212374	.425		.425

Table 3-13. Load Column - Maximum Pressure Condition (T = 77 Seconds) (continued)

①	②	③	④	⑤	⑥
NODE NO.	MATRIX ELEMENT NO.	FIXED WEIGHT ITEMS P (n = 1.0)	FIXED WEIGHT ITEMS P (n = 2.002)	ULTIMATE VARIABLE WEIGHT	ULTIMATE NODAL LOADING
REF.	NOTE (1)	TABLE 3-6	2.002 × ③		④ + ⑤
37	108	.281341	.563		.563
38	111	.212374	.425		.425
39	114	.107555	.215		.215
40	117	.277012	.555		.555
	120	.139384	.279	-177.899	-177.620
41	121	0	0	0	0
	122	-.372000	-.745	336.229	335.484
42	123	.364369	.729		.729
43	126	.728735	1.459		1.459
44	129	1.032100	2.066		2.066
45	132	1.092560	2.187		2.187
46	135	1.099919	2.202		2.202
47	138	1.107272	2.217		2.217
48	141	.973403	1.949		1.949
49	144	.839531	1.681		1.681
50	147	.679376	1.360		1.360
51	150	.389417	.780		.780
	153	5.476073	10.963	1031.453	1042.416
52	154	0	0	0	0
	155	-1.533000	-3.069	-1949.446	-1952.515
53	156	.218583	.438		.438
54	159	.429087	.859		.859
55	162	.429085	.859		.859
56	165	.218585	.438		.438
57	168	10.403456	20.832		20.832
58	171	.689834	1.381		1.381
59	174	1.379669	2.762		2.762
60	177	2.132201	4.269		4.269
61	180	3.216019	6.438		6.438
62	183	3.523583	7.054		7.054
63	186	2.279980	4.565		4.565
64	189	1.139991	2.282		2.282
	192	2.055377	4.115	1951.090	1955.205
65	193	0	0	0	0
	194	-3.186000	-6.378	-4389.953	-4396.331
66	195	.180523	.361		.361
67	198	.213301	.427		.427
68	201	.180525	.361		.361
	204	14.955337	29.941	453.013	482.954
69	205	0	0	0	0
	206	.274000	.549	1019.279	1019.828
70	207	.263813	.528		.528

Table 3-13. Load Column - Maximum Pressure Condition (T = 77 Seconds) (continued)

①	②	③	④	⑤	⑥
NODE NO.	MATRIX ELEMENT NO.	FIXED WEIGHT ITEMS P (n = 1.00)	P (n = 2.002)	ULTIMATE VARIABLE WEIGHT	ULTIMATE NODAL LOADING
REF.	NOTE (1)	TABLE 3-6	2.002 x ③		④ + ⑤
71	210	.352795	.706		.706
72	213	.352795	.706		.706
73	216	.263514	.528		.528
74	219	26.684903	53.423	21.908	75.331
75	222	.610957	1.223		1.223
76	225	1.221911	2.446		2.446
77	228	1.221918	2.446		2.446
78	231	1.066514	2.135		2.135
79	234	1.066537	↑		↑
80	237	1.066507			
81	240	1.066502			
82	243	1.066510			
83	246	1.066489			
84	249	1.066504			
85	252	1.066541			
86	255	1.066526			
87	258	1.066539	↓		↓
88	261	1.066539	2.135		2.135
89	264	.754047	1.510		1.510
90	267	.753959	1.509		1.509
91	270	.753842	1.509		1.509
92	273	.753824	1.509		1.509
93	276	.377271	.755	8.356	9.111
94	279	0	0	429.252	4.178 (2)
95	280	.709300	1.420		1.420
96	283	.592638	1.186		1.186
97	286	.586744	1.175		1.175
98	289	4.412557	8.834	69.399	78.233
99	292	.581165	1.163		1.163

NOTES: 1) The matrix element number corresponds to the non-singular matrix row number shown in Table 1-4.

2). An error in the program requires that this entry be 429.252/102.743 = 4.178 where 102.743 ins. is the circumference at Node 93

Table 3-14. Load Column - Maximum Longitudinal Acceleration Condition (T = 138 Seconds)

Ultimate load factor = (1.400)(3.000) = 4.200 (refer to Table 3-1.)

①	②	③	④	⑤	⑥
Node No.	Matrix Element No.	Fixed Weight Items P (n = 1.0)	Fixed Weight Items P (n = 4.200)	Ultimate Variable Weight	Ultimate Nodal Loading
Ref.	Note (1)	Table 3-6	4.200 × ③		④ + ⑤
1	1	.213535	.897		.897
2	3	.354123	1.487	578.558	580.045
3	6	.396277	1.664		1.664
4	9	.554771	2.330		2.330
5	12	.802419	3.370		3.370
6	15	.970818	4.077		4.077
7	18	.802420	3.370		3.370
8	21	.554772	2.330		2.330
9	24	.396278	1.664		1.664
10	27	.647416	2.719	-292.783	-290.064
10	28	0	0	-292.783	-292.783
10	29	.310000	1.302	-828.114	-826.812
11	30	.632309	2.656		2.656
12	33	.903298	3.794		3.794
13	36	1.477581	6.206		6.206
14	39	1.871196	7.859		7.859
15	42	1.477578	6.206		6.206
16	45	.903299	3.794		3.794
17	48	.632309	2.656		2.656
18	51	1.349834	5.669	14.943	20.612
19	54	.716012	3.007		3.007
20	57	.297090	1.248		1.248
21	60	.648498	2.724		2.724
22	63	1.024618	4.303		4.303
23	66	1.080660	4.539		4.539
24	69	1.155162	4.852		4.852
25	72	1.275241	5.356		5.356
26	75	1.320853	5.548		5.548
27	78	1.230816	5.169		5.169
28	81	1.140791	4.791		4.791
29	84	1.108406	4.655		4.655
30	87	.869304	3.651		3.651
31	90	.639270	2.685		2.685
32	93	.602636	2.531		2.531
33	96	4.546282	19.094	2125.049 37.225	2181.368
33	97	0	0	0	0
33	98	2.367000	9.941	2924.067	2934.008
34	99	.053778	.226		.226
35	102	.107555	.452		.452
36	105	.212374	.892		.892

Table 3-14. Load Column - Maximum Longitudinal Acceleration Condition (T = 138 Seconds) (continued)

①	②	③	④	⑤	⑥
NODE NO.	MATRIX ELEMENT NO.	FIXED WEIGHT ITEMS P (n = 1.0)	FIXED WEIGHT ITEMS P (n = 4.200)	ULTIMATE VARIABLE WEIGHT	ULTIMATE NODAL LOADING
REF.	NOTE (1)	TABLE 3-6	4.200 × ③		④ + ⑤
37	108	.281341	1.182		1.182
38	111	.212374	.892		.892
39	114	.107555	.452		.452
40	117	.277012	1.163		1.163
	120	.139384	.585	-617.481	-616.896
41	121	0	0	0	0
	122	-.372000	-1.562	1167.039	1165.477
42	123	.364369	1.530		1.530
43	126	.728735	3.061		3.061
44	129	1.032100	4.335		4.335
45	132	1.092560	4.589		4.589
46	135	1.099919	4.620		4.620
47	138	1.107272	4.651		4.651
48	141	.973403	4.088		4.088
49	144	.839531	3.526		3.526
50	147	.679376	2.853		2.853
51	150	.389417	1.636		1.636
	153	5.476073	23.000	2474.438	2497.438
52	154	0	0	0	0
	155	-1.533000	-6.439	-4676.688	-4683.127
53	156	.218583	.918		.918
54	159	.429087	1.802		1.802
55	162	.429085	1.802		1.802
56	165	.218585	.918		.918
57	168	10.405456	43.703		43.703
58	171	.689834	2.897		2.897
59	174	1.379669	5.795		5.795
60	177	2.132201	8.955		8.955
61	180	3.216019	13.507		13.507
62	183	3.523583	14.799		14.799
63	186	2.279980	9.576		9.576
64	189	1.139991	4.788		4.788
	192	2.055377	8.633	2708.684	2717.317
65	193	0	0	0	0
	194	-3.186000	-13.381	-6094.539	-6107.920
66	195	.180523	.758		.758
67	198	.213301	.896		.896
68	201	.180523	.758		.758
	204	14.955337	62.812	1099.496	1162.308
69	205	0	0	0	0
	206	.274000	1.151	2473.866	2475.017
70	207	.263313	1.107		1.107

Table 3-14. Load Column - Maximum Longitudinal Acceleration Condition (T = 138 Seconds) (continued)

①	②	③	④	⑤	⑥
NODE NO.	MATRIX ELEMENT NO.	FIXED WEIGHT ITEMS P (n = 1.00)	P (n = 4.200)	ULTIMATE VARIABLE WEIGHT	ULTIMATE NODAL LOADING
REF.	NOTE (1)	TABLE 3-6	4.200 x ③		④ + ⑤
71	210	.352795	1.482		1.482
72	213	.352795	1.482		1.482
73	216	.263514	1.107		1.107
74	219	26.684903	112.077	45.960	158.037
75	222	.610957	2.566		2.566
76	225	1.221911	5.132		5.132
77	228	1.221918	5.132		5.132
78	231	1.066514	4.479		4.479
79	234	1.066537	↑		↑
80	237	1.066507			
81	240	1.066502			
82	243	1.066510			
83	246	1.066409			
84	249	1.066504			
85	252	1.066541			
86	255	1.066526			
87	258	1.066559	↓		↓
88	261	1.066539	4.479		4.479
89	264	.754047	3.167		3.167
90	267	.753959	3.167		3.167
91	270	.753842	3.166		3.166
92	273	.753884	3.166		3.166
93	276	.377271	1.583	-7.337	-5.754
94	279	0	0	-376.891	-3.668 (2)
95	280	.709300	2.979		2.979
96	283	.592638	2.489		2.489
97	286	.586744	2.464		2.464
98	289	4.412557	18.533	1.703	20.236
99	292	.581165	2.441		2.441

NOTES: 1) The matrix element number corresponds to the non-singular matrix row number shown in table 1-4

2) An error in the program requires that this entry be -376.891/102.743 = -3.668 where 102.743 ins. is the circumference at Node 93.

Table 3-15. Load Column - Reentry Condition (T_R = 505 Seconds)

Ultimate load factor = (1.400) (3.000) = 4.200 (refer to table 3-1)

①	②	③	④	⑤	⑥
NODE No.	MATRIX ELEMENT No.	FIXED WEIGHT ITEMS P, (n=1.0)	P (n=4.200)	ULTIMATE VARIABLE WEIGHT	ULTIMATE NODAL LOADING
REF.	NOTE (1)	TABLE 3-6	4.200 × ③		④ + ⑤
1	1	.213535	.897		.897
2	3	.354123	1.487	372.379	373.866
3	6	.396277	1.664		1.664
4	9	.554771	2.330		2.330
5	12	.802419	3.370		3.370
6	15	.970818	4.077		4.077
7	18	.802420	3.370		3.370
8	21	.554772	2.330		2.330
9	24	.396278	1.664		1.664
10	27	.647416	2.719	-299.313	-296.594
	28	0	0	-299.313	-299.313
	29	.310000	1.302	-846.584	-845.282
11	30	.632309	2.656		2.656
12	33	.903298	3.794		3.794
13	36	1.477581	6.206		6.206
14	39	1.871196	7.859		7.859
15	42	1.477575	6.206		6.206
16	45	.903299	3.794		3.794
17	48	.632309	2.656		2.656
18	51	1.349834	5.669	15.829	21.498
19	54	.716012	3.007		3.007
20	57	.297090	1.248		1.248
21	60	.648498	2.724		2.724
22	63	1.024618	4.303		4.303
23	66	1.080660	4.539		4.539
24	69	1.155162	4.852		4.852
25	72	1.275241	5.356		5.356
26	75	1.320853	5.548		5.548
27	78	1.230816	5.169		5.169
28	81	1.140791	4.791		4.791
29	84	1.108406	4.655		4.655
30	87	.869304	3.651		3.651
31	90	.639270	2.685		2.685
32	93	.602636	2.531		2.531
33	96	4.546282	19.094	494.947 19.223	533.264
	97	0	0	0	0
	98	2.367000	9.941	681.542	691.483
34	99	.053778	.226		.226
35	102	.107855	.452		.452
36	105	.212374	.892		.892

Table 3-15. Load Column - Reentry Condition (T_R = 505 Seconds) (continued)

(1)	(2)	(3)	(4)	(5)	(6)
NODE NO.	MATRIX ELEMENT NO.	FIXED WEIGHT ITEMS P (n = 1.0)	FIXED WEIGHT ITEMS P (n = 4.200)	ULTIMATE VARIABLE WEIGHT	ULTIMATE NODAL LOADING
REF.	NOTE (1)	TABLE 3-6	4.200 × (3)		(4) + (5)
37	108	.281341	1.182		1.182
38	111	.212374	.892		.892
39	114	.107555	.452		.452
40	117	.277012	1.163		1.163
41	120	.139384	.585	-631.254	-630.669
	121	0	0	0	0
	122	-.372000	-1.562	1193.070	1191.508
42	123	.364369	1.530		1.530
43	126	.728735	3.061		3.061
44	129	1.032100	4.335		4.335
45	132	1.092360	4.589		4.589
46	135	1.099919	4.620		4.620
47	138	1.107272	4.651		4.651
48	141	.973403	4.088		4.088
49	144	.839531	3.526		3.526
50	147	.679376	2.853		2.853
51	150	.389417	1.636		1.636
52	153	5.476073	23.000	1757.528	1780.528
	154	0	0	0	0
	155	-1.533000	-6.439	-3321.690	-3328.129
53	156	.218503	.918		.918
54	159	.429087	1.802		1.802
55	162	.429005	1.802		1.802
56	165	.218505	.918		.918
57	168	10.405456	43.703		43.703
58	171	.689034	2.897		2.897
59	174	1.379669	5.795		5.795
60	177	2.132201	8.955		8.955
61	180	3.216019	13.507		13.507
62	183	3.523503	14.799		14.799
63	186	2.279980	9.576		9.576
64	189	1.139991	4.788		4.788
65	192	2.055377	8.633	592.107	600.740
	193	0	0	0	0
	194	-3.186000	-13.381	-1331.101	-1344.482
66	195	.180523	.758		.758
67	198	.213301	.896		.896
68	201	.180523	.758		.758
69	204	14.955357	62.812	839.845	902.657
	205	0	0	0	0
	206	.274000	1.151	1887.021	1888.172
70	207	.263313	1.107		1.107

Table 3-15. Load Column - Reentry Condition (T_R = 505 Seconds) (continued)

①	②	③	④	⑤	⑥
NODE NO.	MATRIX ELEMENT NO.	FIXED WEIGHT ITEMS P (n = 1.00)	FIXED WEIGHT ITEMS P (n = 4.200)	ULTIMATE VARIABLE WEIGHT	ULTIMATE NODAL LOADING
REF.	NOTE (1)	TABLE 3-6	4.200 x ③		④ + ⑤
71	210	.352795	1.482		1.482
72	213	.352795	1.482		1.482
73	216	.263514	1.107		1.107
74	219	26.684903	112.077	45.960	158.037
75	222	.610957	2.566		2.566
76	225	1.221911	5.132		5.132
77	228	1.221918	5.132		5.132
78	231	1.066514	4.479		4.479
79	234	1.066537	↑		↑
80	237	1.066507			
81	240	1.066502			
82	243	1.066510			
83	246	1.066489			
84	249	1.066504			
85	252	1.066541			
86	255	1.066526			
87	258	1.066539	↓		↓
88	261	1.066539	4.479		4.479
89	264	.754047	3.167		3.167
90	267	.753959	3.167		3.167
91	270	.753842	3.166		3.166
92	273	.753824	3.166		3.166
93	276	.377271	1.583	-10.253	-8.670
94	279	0	0	-526.695	-5.126 (2)
95	280	.709300	2.979		2.979
96	283	.592638	2.489		2.489
97	286	.586744	2.464		2.464
98	289	4.412557	18.533	-179.609	-161.076
99	292	.581165	2.441		2.441

NOTES: 1) The matrix element number corresponds to the non-singular matrix row number shown in table 1-4.

2.) An error in the program requires that this entry be -526.695/102.743 = -5.126 where 102.743 ins. is the circumference at Node 93.

Table 3-16. Load Column - Landing Condition

Ultimate load factor = (1.400) (3.000) = 4.200 (refer to table 3-1)

①	②	③	④	⑤	⑥
Node No.	Matrix Element No.	Fixed Weight Items P (n=1.0)	Fixed Weight Items P (n=4.200)	Ultimate Variable Weight	Ultimate Nodal Loading
Ref.	Note (1)	Table 3-6	4.200 × ③		④ + ⑤
1	1	.213535	.897		.897
2	3	.354123	1.487	302.379	303.866
3	6	.396277	1.664		1.664
4	9	.554771	2.330		2.330
5	12	.802419	3.370		3.370
6	15	.970818	4.077		4.077
7	18	.802420	3.370		3.370
8	21	.554772	2.330		2.330
9	24	.396275	1.664		1.664
10	27	.647416	2.719	-27.210	-24.491
	28	0	0	-27.210	-27.210
	29	.310000	1.302	-76.962	-75.660
11	30	.632309	2.656		2.656
12	33	.903298	3.794		3.794
13	36	1.477581	6.206		6.206
14	39	1.871196	7.859		7.859
15	42	1.477575	6.206		6.206
16	45	.903299	3.794		3.794
17	48	.632309	2.656		2.656
18	51	1.349834	7.108		7.108
19	54	.716012	3.007		3.007
20	57	.297090	1.248		1.248
21	60	.648498	2.724		2.724
22	63	1.024618	4.303		4.303
23	66	1.080660	4.539		4.539
24	69	1.155162	4.852		4.852
25	72	1.275241	5.356		5.356
26	75	1.320853	5.548		5.548
27	78	1.230816	5.169		5.169
28	81	1.140791	4.791		4.791
29	84	1.108406	4.655		4.655
30	87	.869304	3.651		3.651
31	90	.639270	2.685		2.685
32	93	.602636	2.531		2.531
33	96	4.546282	19.094	102.449 3.845	125.388
	97	0	0	0	0
	98	2.367000	9.941	141.465	151.406
34	99	.053778	.226		.226
35	102	.107638	.452		.452
36	105	.212374	.892		.892

Table 3-16. Load Column - Landing Condition (continued)

①	②	③	④	⑤	⑥
NODE NO.	MATRIX ELEMENT NO.	FIXED WEIGHT ITEMS P (n = 1.0)	P (n = 4.200)	ULTIMATE VARIABLE WEIGHT	ULTIMATE NODAL LOADING
REF.	NOTE (1)	TABLE 3-6	4.200 x ③		④ + ⑤
37	108	.281341	1.182		1.182
38	111	.212374	.892		.892
39	114	.107555	.452		.452
40	117	.277012	1.163		1.163
41	120	.139384	.585	-57.387	-56.802
	121	0	0	0	0
	122	-.372000	-1.562	108.461	106.899
42	123	.364369	1.530		1.530
43	126	.728735	3.061		3.061
44	129	1.032100	4.335		4.335
45	132	1.092560	4.589		4.589
46	135	1.099919	4.620		4.620
47	138	1.107272	4.651		4.651
48	141	.973403	4.088		4.088
49	144	.839531	3.526		3.526
50	147	.679376	2.853		2.853
51	150	.389417	1.636		1.636
52	153	5.476073	23.000	161.053	184.053
	154	0	0	0	0
	155	-1.533000	-6.439	-304.352	-310.791
53	156	.218583	.918		.918
54	159	.429087	1.802		1.802
55	162	.429085	1.802		1.802
56	165	.218585	.918		.918
57	168	10.405456	43.703		43.703
58	171	.689834	2.897		2.897
59	174	1.379669	5.795		5.795
60	177	2.132201	8.955		8.955
61	180	3.216019	13.507		13.507
62	183	3.523583	14.799		14.799
63	186	2.279980	9.576		9.576
64	189	1.139991	4.788		4.788
65	192	2.055377	8.633	121.911	130.544
	193[4]	0	0	0	0
	194	-3.186000	-13.381	-273.160	-286.541
66	195	.180523	.758		.758
67	198	.213301	.896		.896
68	201	.180523	.758		.758
69	204	14.955337	62.812	77.602	140.414
	205	0	0	0	0
	206	.274000	1.151	171.974	173.125
70	207	.263513	1.107		1.107

Table 3-16. Load Column - Landing Condition (continued)

①	②	③	④	⑤	⑥
NODE NO.	MATRIX ELEMENT NO.	FIXED WEIGHT ITEMS P (n = 1.00)	FIXED WEIGHT ITEMS P (n = 4.200)	ULTIMATE VARIABLE WEIGHT	ULTIMATE NODAL LOADING
REF.	NOTE (1)	TABLE 3-6	4.200 × ③		④ + ⑤
71	210	.352795	1.482		1.482
72	213	.352795	1.482		1.482
73	216	.263514	1.107		1.107
74	219	26.604903	112.077	30.446 / -797.418	-654.095
75	222	.610957	2.566		2.566
76	225	1.221911	5.132		5.132
77	228	1.221918	5.132		5.132
78	231	1.066514	4.479		4.479
79	234	1.066537			
80	237	1.066507			
81	240	1.066502			
82	243	1.066510			
83	246	1.066409			
84	249	1.066504			
85	252	1.066541			
86	255	1.066526			
87	258	1.066539			
88	261	1.066539	4.479		4.479
89	264	.754047	3.167		3.167
90	267	.753959	3.167		3.167
91	270	.753042	3.166		3.166
92	273	.753024	3.166		3.166
93	276	.377271	1.583	0.587	2.170
94	279	0	0	54.322	0.529 (2)
95	280	.709300	2.979		2.979
96	283	.592638	2.489		2.489
97	286	.586744	2.464		2.464
98	289	4.412557	18.533		18.533
99	292	.581165	2.441		2.441

NOTES: 1) The matrix element number corresponds to the non-singular matrix row number shown in table 1-4.

2) An error in the program requires that this entry be 54.322/102.743 = 0.529 where 102.743 ins. is the circumference at Node 93.

B

Table 3-17. Summary of Deflections and Forces on Segments Liftoff Condition (T = 0 Seconds)

PAGE

Segment	DEFLECTION COLUMN		NODAL FORCES	
SEGMENT 1	D(1) =	2.2603657+00	F(1) =	7.6242397+02
	D(2) =	0.0000000	F(2) =	1.1748336+03
	D(3) =	1.4510829-01	F(3) =	-1.1752071+03
	D(4) =	1.6986222+00	F(4) =	-7.1344337+02
	D(5) =	-7.7043735-04	F(5) =	-1.1323296+03
	D(6) =	3.6808101-02	F(6) =	-2.7161808+03
SEGMENT 2	D(1) =	1.6986222+00	F(1) =	9.3423543+02
	D(2) =	-7.7043735-04	F(2) =	1.1323282+03
	D(3) =	3.6808101-02	F(3) =	2.7161869+03
	D(4) =	1.5430576+00	F(4) =	-8.7726547+02
	D(5) =	1.3384611-01	F(5) =	-1.0489176+03
	D(6) =	7.9701679-03	F(6) =	-1.1948014+03
SEGMENT 3	D(1) =	1.5430576+00	F(1) =	8.7792879+02
	D(2) =	1.3384611-01	F(2) =	1.0489131+03
	D(3) =	7.9701679-03	F(3) =	1.1948008+03
	D(4) =	1.5206847+00	F(4) =	-8.0435677+02
	D(5) =	1.2509100-01	F(5) =	-8.7653662+02
	D(6) =	-4.9771107-03	F(6) =	-1.0322378+01
SEGMENT 4	D(1) =	1.5206847+00	F(1) =	8.0529190+02
	D(2) =	1.2509100-01	F(2) =	8.7654041+02
	D(3) =	-4.9771107-03	F(3) =	1.0324180+01
	D(4) =	1.5545992+00	F(4) =	-7.2435649+02
	D(5) =	5.7410274-02	F(5) =	-7.3285823+02
	D(6) =	-2.3325722-03	F(6) =	1.7753651+02
SEGMENT 5	D(1) =	1.5545992+00	F(1) =	7.2570791+02
	D(2) =	5.7410274-02	F(2) =	7.3286135+02
	D(3) =	-2.3325722-03	F(3) =	-1.7753598+02
	D(4) =	1.5380376+00	F(4) =	-6.2892091+02
	D(5) =	3.2654835-02	F(5) =	-6.2821407+02
	D(6) =	1.3880815-03	F(6) =	-5.0668204+00
SEGMENT 6	D(1) =	1.5380376+00	F(1) =	6.3189821+02
	D(2) =	3.2654835-02	F(2) =	6.2821146+02
	D(3) =	1.3880815-03	F(3) =	5.0677569+00
	D(4) =	1.4949031+00	F(4) =	-5.5753983+02
	D(5) =	3.9899951-02	F(5) =	-5.5906682+02
	D(6) =	1.0632874-03	F(6) =	-7.3445125+00
SEGMENT 7	D(1) =	1.4949031+00	F(1) =	5.5753905+02
	D(2) =	3.9899951-02	F(2) =	5.5906579+02
	D(3) =	1.0632874-03	F(3) =	7.3454064+00
	D(4) =	1.4697606+00	F(4) =	-5.1774967+02
	D(5) =	4.3541635-02	F(5) =	-5.1890490+02
	D(6) =	1.1110642-03	F(6) =	1.1794358+01

Table 3-17. Summary of Deflections and Forces on Segments (continued) Liftoff Condition (T = 0 Seconds)

	DEFLECTION COLUMN		NODAL FORCES	
SEGMENT 8	D(1) =	1.4697606+00	F(1) =	5.1868279+02
	D(2) =	4.3541635-02	F(2) =	5.1890602+02
	D(3) =	1.1110642-03	F(3) =	-1.1793502+01
	D(4) =	1.4499274+00	F(4) =	-4.9233049+02
	D(5) =	4.8106959-02	F(5) =	-4.9092426+02
	D(6) =	1.3051410-03	F(6) =	7.5986919+00
SEGMENT 9	D(1) =	1.4499274+00	F(1) =	4.9299594+02
	D(2) =	4.8106959-02	F(2) =	4.9092430+02
	D(3) =	1.3051410-03	F(3) =	-7.5944254+00
	D(4) =	1.4363483+00	F(4) =	-4.7684425+02
	D(5) =	5.1863245-02	F(5) =	-4.7291727+02
	D(6) =	1.2619354-03	F(6) =	-1.1638143+01
SEGMENT 10	D(1) =	1.4363483+00	F(1) =	4.4694499+02
	D(2) =	5.1863245-02	F(2) =	4.4948410+02
	D(3) =	1.2619354-03	F(3) =	-6.4787708+01
	D(4) =	1.4163542+00	F(4) =	-4.2494634+02
	D(5) =	6.0159626-02	F(5) =	-4.1750813+02
	D(6) =	1.4004125-03	F(6) =	4.3201788+01
SEGMENT 11	D(1) =	1.4163542+00	F(1) =	4.1729997+02
	D(2) =	6.0159626-02	F(2) =	4.2621687+02
	D(3) =	1.4004125-03	F(3) =	-4.3184029+01
	D(4) =	1.3878683+00	F(4) =	-3.9160057+02
	D(5) =	7.3704269-02	F(5) =	-3.8308290+02
	D(6) =	1.5727384-03	F(6) =	5.8668668+01
SEGMENT 12	D(1) =	1.3878683+00	F(1) =	3.8061910+02
	D(2) =	7.3704269-02	F(2) =	3.9558559+02
	D(3) =	1.5727384-03	F(3) =	-5.8641988+01
	D(4) =	1.3407510+00	F(4) =	-3.4843184+02
	D(5) =	9.9584852-02	F(5) =	-3.2862799+02
	D(6) =	1.8621253-03	F(6) =	5.5121931+01
SEGMENT 13	D(1) =	1.3407510+00	F(1) =	3.2872198+02
	D(2) =	9.9584852-02	F(2) =	3.5082040+02
	D(3) =	1.8621253-03	F(3) =	-5.5120241+01
	D(4) =	1.2871430+00	F(4) =	-2.8684722+02
	D(5) =	1.2064913-01	F(5) =	-2.4045318+02
	D(6) =	-3.6743737-05	F(6) =	-4.0502684+02
SEGMENT 14	D(1) =	1.2871430+00	F(1) =	2.5835452+02
	D(2) =	1.2064913-01	F(2) =	2.7208934+02
	D(3) =	-3.6743737-05	F(3) =	4.0502859+02
	D(4) =	1.4232440+00	F(4) =	-2.2916236+02
	D(5) =	-3.6813161-02	F(5) =	-2.2684678+02
	D(6) =	-8.2620753-03	F(6) =	-1.2201184+03

Table 3-17. Summary of Deflections and Forces on Segments (continued)
Liftoff Condition (T = 0 Seconds)

	DEFLECTION COLUMN		NODAL FORCES	
SEGMENT 15	D(1) =	1.4232440+00	F(1) =	2.0352170+02
	D(2) =	-3.6813161-02	F(2) =	2.5497027+02
	D(3) =	-8.2620753-03	F(3) =	1.2201219+03
	D(4) =	1.6347193+00	F(4) =	-1.9101860+02
	D(5) =	-2.5356964-01	F(5) =	-2.9086916+02
	D(6) =	-1.1477540-02	F(6) =	3.8895460+01
SEGMENT 16	D(1) =	1.6347193+00	F(1) =	1.7325606+02
	D(2) =	-2.5356964-01	F(2) =	3.1014785+02
	D(3) =	-1.1477540-02	F(3) =	-3.8877853+01
	D(4) =	1.7668485+00	F(4) =	-1.6643939+02
	D(5) =	-3.8615894-01	F(5) =	-3.6329393+02
	D(6) =	-6.7860322-03	F(6) =	2.2819317+03
SEGMENT 17	D(1) =	1.7668485+00	F(1) =	1.5307866+02
	D(2) =	-3.8615894-01	F(2) =	3.7771903+02
	D(3) =	-6.7860322-03	F(3) =	-2.2818953+03
	D(4) =	1.7850962+00	F(4) =	-1.4869104+02
	D(5) =	-4.0428195-01	F(5) =	-4.2354942+02
	D(6) =	3.7231946-03	F(6) =	4.8577711+03
SEGMENT 18	D(1) =	1.7850962+00	F(1) =	-1.1705212+00
	D(2) =	-4.0428195-01	F(2) =	-4.3181757+02
	D(3) =	3.7231946-03	F(3) =	-1.1760660+01
	D(4) =	1.8235706+00	F(4) =	1.2030312+00
	D(5) =	-4.0729568-01	F(5) =	-3.5417818-02
	D(6) =	3.9511599-03	F(6) =	4.2822206-04
SEGMENT 19	D(1) =	1.7850962+00	F(1) =	2.6851405+03
	D(2) =	-4.0428195-01	F(2) =	1.0144617+03
	D(3) =	3.7231946-03	F(3) =	-3.1861104+03
	D(4) =	1.7357296+00	F(4) =	-2.6608008+03
	D(5) =	-3.4504586-01	F(5) =	-1.0436275+03
	D(6) =	1.4299380-02	F(6) =	1.6946318+03
SEGMENT 20	D(1) =	1.7357296+00	F(1) =	2.6559970+03
	D(2) =	-3.4504586-01	F(2) =	1.0551389+03
	D(3) =	1.4299380-02	F(3) =	-1.6946167+03
	D(4) =	1.6404290+00	F(4) =	-2.6265778+03
	D(5) =	-1.9902526-01	F(5) =	-1.0831281+03
	D(6) =	1.9795462-02	F(6) =	3.7642175+02
SEGMENT 21	D(1) =	1.6404290+00	F(1) =	2.6160203+03
	D(2) =	-1.9902526-01	F(2) =	1.1084176+03
	D(3) =	1.9795462-02	F(3) =	-3.7640995+02
	D(4) =	1.3369164+00	F(4) =	-2.5332612+03
	D(5) =	2.6625377-01	F(5) =	-1.1283026+03
	D(6) =	1.6486692-02	F(6) =	-7.6201167+02

Table 3-17. Summary of Deflections and Forces on Segments (continued)
Liftoff Condition (T = 0 Seconds)

	DEFLECTION COLUMN		NODAL FORCES	
SEGMENT 22	D(1) =	1.3369164+00	F(1) =	2.5166918+03
	D(2) =	2.6625377-01	F(2) =	1.1680280+03
	D(3) =	1.6486692-02	F(3) =	7.6201329+02
	D(4) =	1.0899432+00	F(4) =	-2.4308928+03
	D(5) =	5.7130806-01	F(5) =	-1.1101726+03
	D(6) =	7.1570159-03	F(6) =	-2.8482812+02
SEGMENT 23	D(1) =	1.0899432+00	F(1) =	2.4134355+03
	D(2) =	5.7130806-01	F(2) =	1.1520168+03
	D(3) =	7.1570159-03	F(3) =	2.8482798+02
	D(4) =	9.1044320-01	F(4) =	-2.3338670+03
	D(5) =	7.2645105-01	F(5) =	-1.0545140+03
	D(6) =	6.4589013-03	F(6) =	2.0871314+02
SEGMENT 24	D(1) =	9.1044320-01	F(1) =	2.3083118+03
	D(2) =	7.2645105-01	F(2) =	1.1142280+03
	D(3) =	6.4589013-03	F(3) =	-2.0871407+02
	D(4) =	6.9317491-01	F(4) =	-2.2279135+03
	D(5) =	9.6471460-01	F(5) =	-9.5776433+02
	D(6) =	1.0653204-02	F(6) =	2.8805241+02
SEGMENT 25	D(1) =	6.9317491-01	F(1) =	2.1769424+03
	D(2) =	9.6471460-01	F(2) =	1.0730921+03
	D(3) =	1.0653204-02	F(3) =	-2.8805421+02
	D(4) =	3.9171105-01	F(4) =	-2.0984343+03
	D(5) =	1.3630283+00	F(5) =	-8.4919071+02
	D(6) =	1.4381088-02	F(6) =	1.3140005+02
SEGMENT 26	D(1) =	3.9171105-01	F(1) =	2.0135661+03
	D(2) =	1.3630283+00	F(2) =	1.0383112+03
	D(3) =	1.4381088-02	F(3) =	-1.3140335+02
	D(4) =	4.0243720-02	F(4) =	-1.9434758+03
	D(5) =	1.8604203+00	F(5) =	-7.4050788+02
	D(6) =	1.6545507-02	F(6) =	1.2024877+02
SEGMENT 27	D(1) =	4.0243720-02	F(1) =	1.8381239+03
	D(2) =	1.8604203+00	F(2) =	9.7378729+02
	D(3) =	1.6545507-02	F(3) =	-1.2025422+02
	D(4) =	-2.5482541-01	F(4) =	-1.7864067+03
	D(5) =	2.2867760+00	F(5) =	-6.3351201+02
	D(6) =	1.4845749-02	F(6) =	-3.4266632+02
SEGMENT 28	D(1) =	-2.5482541-01	F(1) =	1.6652691+03
	D(2) =	2.2867760+00	F(2) =	9.0073743+02
	D(3) =	1.4845749-02	F(3) =	3.4265937+02
	D(4) =	-4.5659333-01	F(4) =	-1.6196976+03
	D(5) =	2.5102425+00	F(5) =	-5.2526611+02
	D(6) =	2.2150211-03	F(6) =	-1.4601218+03

Table 3-17. Summary of Deflections and Forces on Segments (continued)
Liftoff Condition (T = 0 Seconds)

	DEFLECTION COLUMN	NODAL FORCES
SEGMENT 29	D(1) = -4.5659333-01	F(1) = 1.4803572+03
	D(2) = 2.5102425+00	F(2) = 8.3190629+02
	D(3) = 2.2150211-03	F(3) = 1.4601055+03
	D(4) = -4.1146915-01	F(4) = -1.4431076+03
	D(5) = 2.2245167+00	F(5) = -4.9832979+02
	D(6) = -2.0908386-02	F(6) = -2.0816725+03
SEGMENT 30	D(1) = -4.1146915-01	F(1) = 1.3203414+03
	D(2) = 2.2245167+00	F(2) = 7.6810493+02
	D(3) = -2.0908386-02	F(3) = 2.0816507+03
	D(4) = -2.3774132-01	F(4) = -1.3001955+03
	D(5) = 1.7468021+00	F(5) = -6.0219742+02
	D(6) = -3.2735199-02	F(6) = -8.8981347+02
SEGMENT 31	D(1) = -2.3774132-01	F(1) = 1.2052482+03
	D(2) = 1.7468021+00	F(2) = 8.1072038+02
	D(3) = -3.2735199-02	F(3) = 8.8979974+02
	D(4) = -5.0468016-02	F(4) = -1.1900199+03
	D(5) = 1.2789801+00	F(5) = -6.7011704+02
	D(6) = -3.0782240-02	F(6) = 1.6109009+03
SEGMENT 32	D(1) = -5.0468016-02	F(1) = 1.0995282+03
	D(2) = 1.2789801+00	F(2) = 8.6883126+02
	D(3) = -3.0782240-02	F(3) = -1.6109326+03
	D(4) = 7.1172229-02	F(4) = -1.0863927+03
	D(5) = 9.6554021-01	F(5) = -7.7069253+02
	D(6) = -1.2884679-02	F(6) = 5.7794489+03
SEGMENT 33	D(1) = 2.2603557+00	F(1) = -7.5207146+02
	D(2) = 0.0000000	F(2) = 1.9665212+02
	D(3) = 1.4510829-01	F(3) = 1.1752080+02
	D(4) = 2.2640577+00	F(4) = 7.5207146+02
	D(5) = 2.9235711-01	F(5) = -1.4055946+02
	D(6) = -1.5699537-02	F(6) = -2.0927509+02
SEGMENT 34	D(1) = 2.2640577+00	F(1) = -7.5198455+02
	D(2) = 2.9235711-01	F(2) = 1.4055852+02
	D(3) = -1.5699537-02	F(3) = 2.0927778+02
	D(4) = 2.2712293+00	F(4) = 7.5198455+02
	D(5) = 1.5952707-02	F(5) = -2.3443279+01
	D(6) = -3.0412755-02	F(6) = 1.4594069+02
SEGMENT 35	D(1) = 2.2712293+00	F(1) = -7.5179885+02
	D(2) = 1.5952707-02	F(2) = 2.3443699+01
	D(3) = -3.0412755-02	F(3) = -1.4594077+02
	D(4) = 2.2952130+00	F(4) = 7.5179885+02
	D(5) = -4.0542022-02	F(5) = 4.9201334+00
	D(6) = 1.4709253-02	F(6) = -4.8820724+01

Table 3-17. Summary of Deflections and Forces on Segments (continued) Liftoff Condition (T = 0 Seconds)

	DEFLECTION COLUMN	NODAL FORCES
SEGMENT 36	D(1) = 2.2952130+00	F(1) = -7.5143834+02
	D(2) = -4.0542022-02	F(2) = -4.9197403+00
	D(3) = 1.4709253-02	F(3) = 4.8820761+01
	D(4) = 2.3450941+00	F(4) = 7.5143834+02
	D(5) = -3.4190950-02	F(5) = -3.0761530-01
	D(6) = -6.8976312-03	F(6) = 2.5115388+01
SEGMENT 37	D(1) = 2.3450941+00	F(1) = -7.5096521+02
	D(2) = -3.4190950-02	F(2) = 3.0807166-01
	D(3) = -6.8976312-03	F(3) = -2.5115401+01
	D(4) = 2.3946983+00	F(4) = 7.5096521+02
	D(5) = -3.6176477-02	F(5) = -2.9318344-01
	D(6) = 2.7851585-03	F(6) = -1.4492206+01
SEGMENT 38	D(1) = 2.3946983+00	F(1) = -7.5061181+02
	D(2) = -3.6176477-02	F(2) = 2.9351091-01
	D(3) = 2.7851586-03	F(3) = 1.4492217+01
	D(4) = 2.4199480+00	F(4) = 7.5061181+02
	D(5) = -3.3374337-02	F(5) = 1.9852060-01
	D(6) = -1.4829353-03	F(6) = 5.3056251+00
SEGMENT 39	D(1) = 2.4199480+00	F(1) = -7.5043871+02
	D(2) = -3.3374337-02	F(2) = -1.9811720-01
	D(3) = -1.4829353-03	F(3) = -5.3056095+00
	D(4) = 2.4327026+00	F(4) = 7.5043871+02
	D(5) = -4.5312560-02	F(5) = -2.3856793+00
	D(6) = -1.1405545-03	F(6) = -3.8317375+00
SEGMENT 40	D(1) = 2.4327026+00	F(1) = -7.4998235+02
	D(2) = -4.5312560-02	F(2) = 2.3860528+00
	D(3) = -1.1405545-03	F(3) = 3.8318154+00
	D(4) = 2.4391834+00	F(4) = 7.4998235+02
	D(5) = -4.8157484-02	F(5) = -5.9698802+00
	D(6) = 2.5674355-04	F(6) = 1.5861922+01
SEGMENT 41	D(1) = 2.4391834+00	F(1) = -8.0711930+02
	D(2) = -4.8157484-02	F(2) = 4.7274335-01
	D(3) = 2.5674355-04	F(3) = 9.1974497+01
	D(4) = 2.4600067+00	F(4) = 8.0711930+02
	D(5) = -4.7750026-02	F(5) = -9.8682705+00
	D(6) = -1.6690445-04	F(6) = -1.2875373+01
SEGMENT 42	D(1) = 2.4600067+00	F(1) = -8.0650163+02
	D(2) = -4.7750026-02	F(2) = -8.1088374+00
	D(3) = -1.6690445-04	F(3) = 1.2875854+01
	D(4) = 2.5018318+00	F(4) = 8.0650163+02
	D(5) = -5.2924258-02	F(5) = -1.5156982+01
	D(6) = -1.5342426-04	F(6) = 1.4543983+01

Table 3-17. Summary of Deflections and Forces on Segments (continued)
Liftoff Condition (T = 0 Seconds)

	DEFLECTION COLUMN	NODAL FORCES
SEGMENT 43	D(1) = 2.5018318+00	F(1) = -8.0527535+02
	D(2) = -5.2924258-02	F(2) = -2.8192620+01
	D(3) = -1.5342426-04	F(3) = -1.4543766+01
	D(4) = 2.5861604+00	F(4) = 8.0527535+02
	D(5) = -5.6865570-02	F(5) = -3.5461522+01
	D(6) = -1.4783308-05	F(6) = -5.9656057+00
SEGMENT 44	D(1) = 2.5861604+00	F(1) = -8.0354086+02
	D(2) = -5.6865570-02	F(2) = -3.9564537+01
	D(3) = -1.4783308-05	F(3) = 5.9657137+00
	D(4) = 2.6816072+00	F(4) = 8.0354086+02
	D(5) = -6.1168953-02	F(5) = -4.9546196+01
	D(6) = -9.7935237-05	F(6) = 1.3901849+00
SEGMENT 45	D(1) = 2.6816072+00	F(1) = -8.0170500+02
	D(2) = -6.1168953-02	F(2) = -4.8785850+01
	D(3) = -9.7935237-05	F(3) = -1.3901106+00
	D(4) = 2.7777469+00	F(4) = 8.0170500+02
	D(5) = -6.5902205-02	F(5) = -5.9534101+01
	D(6) = -4.1748967-05	F(6) = 1.7015542+00
SEGMENT 46	D(1) = 2.7777469+00	F(1) = -7.9985571+02
	D(2) = -6.5902205-02	F(2) = -5.9734532+01
	D(3) = -4.1748967-05	F(3) = -1.7014955+00
	D(4) = 2.8759324+00	F(4) = 7.9985571+02
	D(5) = -7.0733956-02	F(5) = -7.0629260+01
	D(6) = -1.1464565-04	F(6) = -5.6593893+00
SEGMENT 47	D(1) = 2.8759324+00	F(1) = -7.9799799+02
	D(2) = -7.0733956-02	F(2) = -6.9846775+01
	D(3) = -1.1464565-04	F(3) = 5.6594728+00
	D(4) = 2.9747496+00	F(4) = 7.9799799+02
	D(5) = -7.4263864-02	F(5) = -7.8561067+01
	D(6) = 5.3208313-05	F(6) = 1.4773036+01
SEGMENT 48	D(1) = 2.9747496+00	F(1) = -7.9636350+02
	D(2) = -7.4263864-02	F(2) = -5.6509735+01
	D(3) = 5.3208313-05	F(3) = -1.4772932+01
	D(4) = 3.0454255+00	F(4) = 7.9636350+02
	D(5) = -8.0760142-02	F(5) = -6.4076919+01
	D(6) = -4.0644259-04	F(6) = -5.8749849+01
SEGMENT 49	D(1) = 3.0454265+00	F(1) = -7.9495180+02
	D(2) = -8.0760142-02	F(2) = -6.0462961+01
	D(3) = -4.0644259-04	F(3) = 5.8750010+01
	D(4) = 3.1157094+00	F(4) = 7.9495180+02
	D(5) = -7.0212687-02	F(5) = -5.4243362+01
	D(6) = 1.1508196-03	F(6) = 2.0774349+02

Table 3-17. Summary of Deflections and Forces on Segments (continued)
Liftoff Condition (T = 0 Seconds)

	DEFLECTION COLUMN	NODAL FORCES
SEGMENT 50	D(1) = 3.1157094+00	F(1) = -7.9381165+02
	D(2) = -7.0212687-02	F(2) = -5.3313860+01
	D(3) = 1.1508196-03	F(3) = -2.0774321+02
	D(4) = 3.1578824+00	F(4) = 7.9381165+02
	D(5) = -5.2156932-02	F(5) = 8.8046720+00
	D(6) = -4.2007050-04	F(6) = -4.5075402+02
SEGMENT 51	D(1) = 3.1578824+00	F(1) = -7.9316491+02
	D(2) = -5.2156932-02	F(2) = -7.3604201+01
	D(3) = -4.2007050-04	F(3) = 4.5075511+02
	D(4) = 3.1796486+00	F(4) = 7.9316491+02
	D(5) = -1.0218279-01	F(5) = 3.6493065+01
	D(6) = -6.6145651-03	F(6) = -1.4657752+03
SEGMENT 52	D(1) = 3.1796486+00	F(1) = 4.5851820+01
	D(2) = -1.0218279-01	F(2) = -5.8587768+01
	D(3) = -6.6145651-03	F(3) = -1.0514715+02
	D(4) = 3.1808774+00	F(4) = -4.5851820+01
	D(5) = -5.6485228-03	F(5) = 8.6198617+00
	D(6) = 1.4536890-02	F(6) = -4.1973465+01
SEGMENT 53	D(1) = 3.1808774+00	F(1) = 4.6225673+01
	D(2) = -5.6485228-03	F(2) = -8.6195886+00
	D(3) = 1.4536890-02	F(3) = 4.1973467+01
	D(4) = 3.1781915+00	F(4) = -4.6225673+01
	D(5) = 2.6155259-03	F(5) = -4.8940526-01
	D(6) = -7.9558162-03	F(6) = 1.7766958+01
SEGMENT 54	D(1) = 3.1781915+00	F(1) = 4.6946910+01
	D(2) = 2.6155259-03	F(2) = 4.8978103-01
	D(3) = -7.9558162-03	F(3) = -1.7766956+01
	D(4) = 3.1728914+00	F(4) = -4.6946910+01
	D(5) = 1.9851466-03	F(5) = -7.4920662-02
	D(6) = 3.0295617-03	F(6) = -1.0689161+01
SEGMENT 55	D(1) = 3.1728914+00	F(1) = 4.7666444+01
	D(2) = 1.9851466-03	F(2) = 7.5339803-02
	D(3) = 3.0295617-03	F(3) = 1.0689161+01
	D(4) = 3.1696717+00	F(4) = -4.7666444+01
	D(5) = 2.6523902-03	F(5) = 1.3523973-01
	D(6) = -1.2663256-03	F(6) = 6.0659542+00
SEGMENT 56	D(1) = 3.1696717+00	F(1) = 4.8030566+01
	D(2) = 2.6523902-03	F(2) = -1.3481989-01
	D(3) = -1.2663256-03	F(3) = -6.0659540+00
	D(4) = 3.1684199+00	F(4) = -4.8030566+01
	D(5) = 5.9847384-03	F(5) = 1.9778837+00
	D(6) = 1.5953748-03	F(6) = 2.4811745+00

Table 3-17. Summary of Deflections and Forces on Segments (continued)
Liftoff Condition (T = 0 Seconds)

	DEFLECTION COLUMN		NODAL FORCES
SEGMENT 57	D(1) =	1.7850962+00	F(1) =	-2.5406122+03
	D(2) =	-4.0428195-01	F(2) =	-1.4851064+02
	D(3) =	3.7231946-03	F(3) =	-1.6598906+03
	D(4) =	1.8038397+00	F(4) =	2.5406122+03
	D(5) =	-3.4415692-01	F(5) =	9.5596619+01
	D(6) =	4.9934195-03	F(6) =	4.8567096+01
SEGMENT 58	D(1) =	1.8038397+00	F(1) =	-2.5394484+03
	D(2) =	-3.4415692-01	F(2) =	-9.7094946+01
	D(3) =	4.9934195-03	F(3) =	-4.8587848+01
	D(4) =	1.8395024+00	F(4) =	2.5394484+03
	D(5) =	-2.3064810-01	F(5) =	2.8086515+01
	D(6) =	3.1379720-03	F(6) =	-1.2963792+03
SEGMENT 59	D(1) =	1.8395024+00	F(1) =	-2.5371201+03
	D(2) =	-2.3064810-01	F(2) =	-2.5015858+01
	D(3) =	3.1379720-03	F(3) =	1.2963875+03
	D(4) =	1.9075305+00	F(4) =	2.5371201+03
	D(5) =	-1.8867397-01	F(5) =	-4.7111993+01
	D(6) =	-1.2210155-03	F(6) =	-1.6932637+02
SEGMENT 60	D(1) =	1.9075305+00	F(1) =	-2.5335376+03
	D(2) =	-1.8867397-01	F(2) =	-2.8709177+01
	D(3) =	-1.2210155-03	F(3) =	1.6932801+02
	D(4) =	1.9984311+00	F(4) =	2.5335376+03
	D(5) =	-2.7933460-01	F(5) =	-9.3800829+01
	D(6) =	-1.1549644-03	F(6) =	1.8617696+02
SEGMENT 61	D(1) =	1.9984311+00	F(1) =	-2.5281393+03
	D(2) =	-2.7933460-01	F(2) =	-2.3404626+02
	D(3) =	-1.1549644-03	F(3) =	-1.8617480+02
	D(4) =	2.0557514+00	F(4) =	2.5281393+03
	D(5) =	-3.4891599-01	F(5) =	-3.1030536+02
	D(6) =	-8.3695169-04	F(6) =	-3.1127469+01
SEGMENT 62	D(1) =	2.0557514+00	F(1) =	-2.5222317+03
	D(2) =	-3.4891599-01	F(2) =	-2.3913414+02
	D(3) =	-8.3695169-04	F(3) =	3.1133490+01
	D(4) =	2.1018762+00	F(4) =	2.5222317+03
	D(5) =	-4.0931340-01	F(5) =	-2.8132883+02
	D(6) =	-1.4419600-03	F(6) =	-3.5768859+02
SEGMENT 63	D(1) =	2.1018762+00	F(1) =	-2.5184225+03
	D(2) =	-4.0931340-01	F(2) =	-2.0675028+02
	D(3) =	-1.4419600-03	F(3) =	3.5771112+02
	D(4) =	2.1262069+00	F(4) =	2.5184225+03
	D(5) =	-4.7273442-01	F(5) =	-1.0464655+02
	D(6) =	-3.3788328-03	F(6) =	-2.1318376+03

Table 3-17. Summary of Deflections and Forces on Segments (continued)
Liftoff Condition (T = 0 Seconds)

	DEFLECTION COLUMN	NODAL FORCES
SEGMENT 64	D(1) = 2.1262069+00	F(1) = -2.5165682+03
	D(2) = -4.7273442-01	F(2) = -1.8494026+02
	D(3) = -3.3788328-03	F(3) = 2.1319124+03
	D(4) = 2.1390124+00	F(4) = 2.5165682+03
	D(5) = -5.3314160-01	F(5) = 3.6795307+00
	D(6) = -5.5717903-03	F(6) = -3.5055015+03
SEGMENT 65	D(1) = 2.1390124+00	F(1) = -5.9767287+02
	D(2) = -5.3314160-01	F(2) = -8.7910232+01
	D(3) = -5.5717903-03	F(3) = -8.0933104+02
	D(4) = 2.1519403+00	F(4) = 5.9767287+02
	D(5) = -2.4850417-01	F(5) = 6.2144102+01
	D(6) = 4.0985200-02	F(6) = -1.1518796+02
SEGMENT 66	D(1) = 2.1519403+00	F(1) = -5.9736287+02
	D(2) = -2.4850417-01	F(2) = -1.6530421+01
	D(3) = 4.0985200-02	F(3) = 1.1518847+02
	D(4) = 2.1647649+00	F(4) = 5.9736287+02
	D(5) = 2.4925116-01	F(5) = 2.6481348+01
	D(6) = 9.2031189-03	F(6) = -2.1303268+02
SEGMENT 67	D(1) = 2.1647649+00	F(1) = -5.9700963+02
	D(2) = 2.4925116-01	F(2) = 2.9820623+01
	D(3) = 9.2031189-03	F(3) = 2.1303261+02
	D(4) = 2.1742502+00	F(4) = 5.9700963+02
	D(5) = 1.9840755-01	F(5) = 5.4888899+00
	D(6) = -1.2235155-02	F(6) = -8.3655738+00
SEGMENT 68	D(1) = 2.1742502+00	F(1) = -5.9670705+02
	D(2) = 1.9840755-01	F(2) = 4.2498136+01
	D(3) = -1.2235155-02	F(3) = 8.3654057+00
	D(4) = 2.1810949+00	F(4) = 5.9670705+02
	D(5) = 1.9519398-01	F(5) = -2.0252571+01
	D(6) = 1.4896906-02	F(6) = 4.1289178+02
SEGMENT 69	D(1) = 2.1810949+00	F(1) = -2.0678527+02
	D(2) = 1.9519398-01	F(2) = 4.0175856+01
	D(3) = 1.4896906-02	F(3) = 4.0835907+02
	D(4) = 2.1824380+00	F(4) = 2.0678527+02
	D(5) = 1.8000246-01	F(5) = -1.9577437+01
	D(6) = -1.2699859-02	F(6) = 5.9465002+01
SEGMENT 70	D(1) = 2.1824380+00	F(1) = -2.0633173+02
	D(2) = 1.8000246-01	F(2) = 1.9577643+01
	D(3) = -1.2699859-02	F(3) = -5.9465046+01
	D(4) = 2.1878643+00	F(4) = 2.0633173+02
	D(5) = -2.5633619-02	F(5) = 5.7226842-01
	D(6) = -9.0501496-04	F(6) = 1.4181649+01

Table 3-17. Summary of Deflections and Forces on Segments (continued)
Liftoff Condition (T = 0 Seconds)

	DEFLECTION COLUMN		NODAL FORCES
SEGMENT 71	D(1) =	2.1878643+00	F(1) =	-2.0574166+02
	D(2) =	-2.5633619-02	F(2) =	-5.7206903-01
	D(3) =	-9.0501496-04	F(3) =	-1.4181631+01
	D(4) =	2.1958193+00	F(4) =	2.0574166+02
	D(5) =	-2.6768580-02	F(5) =	5.3299974-01
	D(6) =	4.8396919-04	F(6) =	-5.5091201+00
SEGMENT 72	D(1) =	2.1958193+00	F(1) =	-2.0514628+02
	D(2) =	-2.6768580-02	F(2) =	-5.3282139-01
	D(3) =	4.8396919-04	F(3) =	5.5091553+00
	D(4) =	2.2045930+00	F(4) =	2.0514628+02
	D(5) =	-9.3756170-02	F(5) =	-6.1675339+00
	D(6) =	-5.0749523-03	F(6) =	-2.9200603+01
SEGMENT 73	D(1) =	2.2045930+00	F(1) =	-2.0471155+02
	D(2) =	-9.3756170-02	F(2) =	6.1677185+00
	D(3) =	-5.0749523-03	F(3) =	2.9200692+01
	D(4) =	2.2095352+00	F(4) =	2.0471155+02
	D(5) =	-1.2802023-01	F(5) =	-1.4361313+01
	D(6) =	2.0632645-03	F(6) =	1.1944611+02
SEGMENT 74	D(1) =	2.1588687+00	F(1) =	5.8065993+00
	D(2) =	-1.3380563-01	F(2) =	1.7625171+00
	D(3) =	7.1085929-05	F(3) =	-1.6511556-02
	D(4) =	2.1627676+00	F(4) =	-6.1501065+00
	D(5) =	-1.3537188-01	F(5) =	-2.9244497+01
	D(6) =	1.7692545-04	F(6) =	2.8763876+02
SEGMENT 75	D(1) =	2.1627676+00	F(1) =	1.7985275+01
	D(2) =	-1.3537188-01	F(2) =	3.2734463+01
	D(3) =	1.7692545-04	F(3) =	-2.8768877+02
	D(4) =	2.1743734+00	F(4) =	-1.9125263+01
	D(5) =	-1.3501949-01	F(5) =	-6.6146528+01
	D(6) =	7.0115496-04	F(6) =	1.1996036+03
SEGMENT 76	D(1) =	2.1743734+00	F(1) =	3.1059262+01
	D(2) =	-1.3501949-01	F(2) =	6.9431540+01
	D(3) =	7.0115496-04	F(3) =	-1.1994215+03
	D(4) =	2.2095352+00	F(4) =	-3.3177042+01
	D(5) =	-1.2802023-01	F(5) =	-1.0920360+02
	D(6) =	2.0632645-03	F(6) =	2.8105529+03
SEGMENT 77	D(1) =	2.2095352+00	F(1) =	-9.9038320+01
	D(2) =	-1.2802023-01	F(2) =	1.2646178+02
	D(3) =	2.0632645-03	F(3) =	-2.9300539+03
	D(4) =	2.2719373+00	F(4) =	1.0534616+02
	D(5) =	-1.1431123-01	F(5) =	-1.6549048+02
	D(6) =	3.4244873-03	F(6) =	1.7250863+03

Table 3-17. Summary of Deflections and Forces on Segments (continued)
Liftoff Condition (T = 0 Seconds)

	DEFLECTION COLUMN		NODAL FORCES	
SEGMENT 78	D(1) =	2.2719373+00	F(1) =	-9.4850947+01
	D(2) =	-1.1431123-01	F(2) =	1.6800782+02
	D(3) =	3.4244873-03	F(3) =	-1.7258348+03
	D(4) =	2.3582103+00	F(4) =	1.0133999+02
	D(5) =	-9.5419096-02	F(5) =	-2.0994376+02
	D(6) =	4.1814516-03	F(6) =	7.6903510+02
SEGMENT 79	D(1) =	2.3582103+00	F(1) =	-9.0782532+01
	D(2) =	-9.5419096-02	F(2) =	2.1230499+02
	D(3) =	4.1814516-03	F(3) =	-7.6974969+02
	D(4) =	2.4568604+00	F(4) =	9.7486072+01
	D(5) =	-7.5141065-02	F(5) =	-2.5596379+02
	D(6) =	4.5000767-03	F(6) =	4.0262771+01
SEGMENT 80	D(1) =	2.4568604+00	F(1) =	-8.6900808+01
	D(2) =	-7.5141065-02	F(2) =	2.5816256+02
	D(3) =	4.5000767-03	F(3) =	-4.0925157+01
	D(4) =	2.5596490+00	F(4) =	9.3862813+01
	D(5) =	-5.5840898-02	F(5) =	-3.0278399+02
	D(6) =	4.5189761-03	F(6) =	-4.9160428+02
SEGMENT 81	D(1) =	2.5596490+00	F(1) =	-8.3236686+01
	D(2) =	-5.5840898-02	F(2) =	3.0481926+02
	D(3) =	4.5189761-03	F(3) =	4.9084007+02
	D(4) =	2.6610372+00	F(4) =	9.0519519+01
	D(5) =	-3.8825448-02	F(5) =	-3.5000092+02
	D(6) =	4.3480747-03	F(6) =	-8.6305249+02
SEGMENT 82	D(1) =	2.6610372+00	F(1) =	-7.9850521+01
	D(2) =	-3.8825448-02	F(2) =	3.5187473+02
	D(3) =	4.3480747-03	F(3) =	8.6227567+02
	D(4) =	2.7575953+00	F(4) =	8.7539726+01
	D(5) =	-2.4670229-02	F(5) =	-3.9750197+02
	D(6) =	4.0689703-03	F(6) =	-1.1153320+03
SEGMENT 83	D(1) =	2.7575953+00	F(1) =	-7.6841394+01
	D(2) =	-2.4670229-02	F(2) =	3.9921041+02
	D(3) =	4.0689703-03	F(3) =	1.1145744+03
	D(4) =	2.8474199+00	F(4) =	8.5061423+01
	D(5) =	-1.3483534-02	F(5) =	-4.4539776+02
	D(6) =	3.7366984-03	F(6) =	-1.2951470+03
SEGMENT 84	D(1) =	2.8474199+00	F(1) =	-7.4336449+01
	D(2) =	-1.3483534-02	F(2) =	4.4694258+02
	D(3) =	3.7366984-03	F(3) =	1.2942626+03
	D(4) =	2.9295769+00	F(4) =	8.3272913+01
	D(5) =	-5.1068051-03	F(5) =	-4.9398892+02
	D(6) =	3.3818957-03	F(6) =	-1.4558680+03

Table 3-17. Summary of Deflections and Forces on Segments (continued)
Liftoff Condition (T = 0 Seconds)

	DEFLECTION COLUMN		NODAL FORCES	
SEGMENT 85	D(1) =	2.9295769+00	F(1) =	-7.2507760+01
	D(2) =	-5.1068051-03	F(2) =	4.9536898+02
	D(3) =	3.3818957-03	F(3) =	1.4549200+03
	D(4) =	3.0035735+00	F(4) =	8.2447451+01
	D(5) =	7.2942128-04	F(5) =	-5.4370457+02
	D(6) =	3.0118976-03	F(6) =	-1.6619732+03
SEGMENT 86	D(1) =	3.0035735+00	F(1) =	-7.1695618+01
	D(2) =	7.2942128-04	F(2) =	5.4491759+02
	D(3) =	3.0118976-03	F(3) =	1.6607576+03
	D(4) =	3.0688730+00	F(4) =	8.3118193+01
	D(5) =	4.3306020-03	F(5) =	-5.9517278+02
	D(6) =	2.6145500-03	F(6) =	-1.9972701+03
SEGMENT 87	D(1) =	3.0688730+00	F(1) =	-7.2313720+01
	D(2) =	4.3306020-03	F(2) =	5.9622185+02
	D(3) =	2.6145500-03	F(3) =	1.9957581+03
	D(4) =	3.1244577+00	F(4) =	8.6053144+01
	D(5) =	5.9865711-03	F(5) =	-6.4937433+02
	D(6) =	2.1584222-03	F(6) =	-2.5797625+03
SEGMENT 88	D(1) =	3.1244577+00	F(1) =	-7.5115121+01
	D(2) =	5.9865711-03	F(2) =	6.5026356+02
	D(3) =	2.1584222-03	F(3) =	2.5794252+03
	D(4) =	3.1684199+00	F(4) =	9.2773424+01
	D(5) =	5.9847384-03	F(5) =	-7.0823757+02
	D(6) =	1.5953740-03	F(6) =	-3.5935060+03
SEGMENT 89	D(1) =	3.1684199+00	F(1) =	-1.9603691+01
	D(2) =	5.9847384-03	F(2) =	7.0689352+02
	D(3) =	1.5953748-03	F(3) =	3.5901405+03
	D(4) =	3.1913195+00	F(4) =	2.3517032+01
	D(5) =	5.2048328-03	F(5) =	-7.5299687+02
	D(6) =	1.1789485-03	F(6) =	-3.5463393+03
SEGMENT 90	D(1) =	3.1913195+00	F(1) =	-1.5811239+01
	D(2) =	5.2048328-03	F(2) =	7.5342120+02
	D(3) =	1.1789485-03	F(3) =	3.5425683+03
	D(4) =	3.2079108+00	F(4) =	1.9758942+01
	D(5) =	4.0192010-03	F(5) =	-8.0784636+02
	D(6) =	8.2423991-04	F(6) =	-3.6521221+03
SEGMENT 91	D(1) =	3.2079108+00	F(1) =	-1.2114064+01
	D(2) =	4.0192010-03	F(2) =	8.0818613+02
	D(3) =	8.2423991-04	F(3) =	3.6476135+03
	D(4) =	3.2190900+00	F(4) =	1.6148855+01
	D(5) =	2.6765718-03	F(5) =	-8.7880971+02
	D(6) =	5.1718027-04	F(6) =	-4.0210402+03

Table 3-17. Summary of Deflections and Forces on Segments (continued)
Liftoff Condition (T = 0 Seconds)

	DEFLECTION COLUMN	NODAL FORCES
SEGMENT 92	D(1) = 3.2190900+00	F(1) = -8.3908900+00
	D(2) = 2.6765718-03	F(2) = 8.7907015+02
	D(3) = 5.1718027-04	F(3) = 4.0152748+03
	D(4) = 3.2255309+00	F(4) = 1.2584454+01
	D(5) = 1.3964531-03	F(5) = -9.8742453+02
	D(6) = 2.4234711-04	F(6) = -4.8821686+03
SEGMENT 93	D(1) = 3.2255309+00	F(1) = -4.7216181+00
	D(2) = 1.3964531-03	F(2) = 9.8760783+02
	D(3) = 2.4234711-04	F(3) = 4.8749831+03
	D(4) = 3.2275898+00	F(4) = 9.4422251+00
	D(5) = 3.9251202-04	F(5) = -1.2425207+03
	D(6) = -3.2614367-06	F(6) = -6.0756476+03
SEGMENT 94	D(1) = 3.2269208+00	F(1) = 1.3764054+00
	D(2) = 3.2275898+00	F(2) = -1.3764054+00
	D(3) = 3.9251202-04	F(3) = 1.2425923+03
	D(4) = -3.2614367-05	F(4) = 6.2324434+05
	D(5) = 0.0000000	F(5) = 0.0000000
	D(6) = 0.0000000	F(6) = 0.0000000
SEGMENT 95	D(1) = 7.1172229-02	F(1) = -1.1691695+00
	D(2) = 9.6554021-01	F(2) = 5.0450891+02
	D(3) = -1.2884679-02	F(3) = -1.1711166+01
	D(4) = -5.6926170-02	F(4) = 1.1918641+00
	D(5) = 9.7065859-01	F(5) = 3.9716111-02
	D(6) = -1.2756777-02	F(6) = 3.8616644-04
SEGMENT 96	D(1) = 7.1172229-02	F(1) = 8.1905882+02
	D(2) = 9.6554021-01	F(2) = 3.5258329+02
	D(3) = -1.2884679-02	F(3) = -1.7264269+03
	D(4) = 9.5481314-02	F(4) = -8.0552413+02
	D(5) = 8.9944560-01	F(5) = -2.9327197+02
	D(6) = -4.5440812-03	F(6) = -1.3777969+03
SEGMENT 97	D(1) = 7.1172229-02	F(1) = 1.6056827+03
	D(2) = 9.6554021-01	F(2) = 1.3191974+01
	D(3) = -1.2884679-02	F(3) = -1.9059158+03
	D(4) = 5.4966953-02	F(4) = -1.5994310+03
	D(5) = 9.0216231-01	F(5) = 3.2365953+01
	D(6) = -4.3973122-03	F(6) = -1.5383926+03
SEGMENT 98	D(1) = 9.5481314-02	F(1) = 2.9553302+02
	D(2) = 8.9944560-01	F(2) = 1.3491558+02
	D(3) = -4.5440812-03	F(3) = 1.0315513+03
	D(4) = 5.4966953-02	F(4) = -2.9946419+02
	D(5) = 9.0216231-01	F(5) = -1.0941116+02
	D(6) = -4.3973122-03	F(6) = 1.0539460+03

Table 3-17. Summary of Deflections and Forces on Segments (continued)
Liftoff Condition (T = 0 Seconds)

	DEFLECTION COLUMN	NODAL FORCES
SEGMENT 99	D(1) = 9.5481314-02	F(1) = 5.1095982+02
	D(2) = 8.9944560-01	F(2) = 1.5835167+02
	D(3) = -4.5440812-03	F(3) = 3.4624659+02
	D(4) = 1.2421835-01	F(4) = -5.0569396+02
	D(5) = 5.1366729-01	F(5) = -5.8302566+01
	D(6) = -1.2305734-02	F(6) = 2.1536925+02
SEGMENT 100	D(1) = 5.4966953-02	F(1) = 1.9006065+03
	D(2) = 9.0216231-01	F(2) = 7.7040346+01
	D(3) = -4.3973122-03	F(3) = 4.8514410+02
	D(4) = -1.3555022-02	F(4) = -1.9006065+03
	D(5) = 5.1233892-01	F(5) = -2.9974489+00
	D(6) = -1.0977949-02	F(6) = 3.7476495+03
SEGMENT 101	D(1) = 1.2421835-01	F(1) = -4.4597605+01
	D(2) = 5.1366729-01	F(2) = 4.9930392+02
	D(3) = -1.2305734-02	F(3) = -3.1499592+02
	D(4) = -1.3555022-02	F(4) = 4.5656289+01
	D(5) = 5.1233892-01	F(5) = -4.8071675+02
	D(6) = -1.0977949-02	F(6) = -2.4891433+02
SEGMENT 102	D(1) = 1.2421835-01	F(1) = 5.5776099+02
	D(2) = 5.1366729-01	F(2) = -4.4099326+02
	D(3) = -1.2305734-02	F(3) = 9.9601716+01
	D(4) = 0.0000000	F(4) = -5.6776826+02
	D(5) = 3.8600113-01	F(5) = 4.7078364+02
	D(6) = -1.1324785-02	F(6) = 1.4503898+02
SEGMENT 103	D(1) = -1.3555022-02	F(1) = 1.8559266+03
	D(2) = 5.1233892-01	F(2) = 4.8371463+02
	D(3) = -1.0977949-02	F(3) = -1.2585133+02
	D(4) = 0.0000000	F(4) = -1.8453866+03
	D(5) = 3.8600113-01	F(5) = -4.7078449+02
	D(6) = -1.1324785-02	F(6) = -1.4504006+02

Table 3-18. Summary of Forces and Deflections on Segments
Maximum Dynamic Pressure Condition (T = 77 Seconds)

	DEFLECTION COLUMN	NODAL FORCES
SEGMENT 1	D(1) = 2.7554455+00	F(1) = 1.0072844+03
	D(2) = 0.0000000	F(2) = 1.6156868+03
	D(3) = 1.9340579-01	F(3) = -1.5665668+03
	D(4) = 2.0103455+00	F(4) = -9.5510033+02
	D(5) = -1.0595488-03	F(5) = -1.5572332+03
	D(6) = 4.7560685-02	F(6) = -3.6426850+03
SEGMENT 2	D(1) = 2.0103455+00	F(1) = 1.2814493+03
	D(2) = -1.0595488-03	F(2) = 1.5532927+03
	D(3) = 4.7560685-02	F(3) = 3.6426921+03
	D(4) = 1.8126072+00	F(4) = -1.2033061+03
	D(5) = 1.6822119-01	F(5) = -1.4445778+03
	D(6) = 9.2228845-03	F(6) = -1.5611310+03
SEGMENT 3	D(1) = 1.8126072+00	F(1) = 1.2138307+03
	D(2) = 1.6822119-01	F(2) = 1.4348452+03
	D(3) = 9.2228845-03	F(3) = 1.5611342+03
	D(4) = 1.7933296+00	F(4) = -1.1121095+03
	D(5) = 1.4564019-01	F(5) = -1.2190625+03
	D(6) = -7.3807505-03	F(6) = 1.2016947+01
SEGMENT 4	D(1) = 1.7933296+00	F(1) = 1.1268344+03
	D(2) = 1.4564019-01	F(2) = 1.2054568+03
	D(3) = -7.3807505-03	F(3) = -1.2015733+01
	D(4) = 1.8452306+00	F(4) = -1.0135825+03
	D(5) = 4.8381693-02	F(5) = -1.0391326+03
	D(6) = -3.4309201-03	F(6) = 2.3995092+02
SEGMENT 5	D(1) = 1.8452306+00	F(1) = 1.0350445+03
	D(2) = 4.8381693-02	F(2) = 1.0192844+03
	D(3) = -3.4309201-03	F(3) = -2.3994955+02
	D(4) = 1.8316800+00	F(4) = -8.9700156+02
	D(5) = 6.0116550-03	F(5) = -9.1954903+02
	D(6) = 1.2649124-03	F(6) = -2.1433324+01
SEGMENT 6	D(1) = 1.8316800+00	F(1) = 9.2254140+02
	D(2) = 6.0116550-03	F(2) = 8.9594833+02
	D(3) = 1.2649124-03	F(3) = 2.1434369+01
	D(4) = 1.7800463+00	F(4) = -8.1398169+02
	D(5) = 8.4181117-03	F(5) = -8.4152027+02
	D(6) = 1.4903719-03	F(6) = 3.1813712+01
SEGMENT 7	D(1) = 1.7800463+00	F(1) = 8.3482475+02
	D(2) = 8.4181117-03	F(2) = 8.2227864+02
	D(3) = 1.4903719-03	F(3) = -3.1812744+01
	D(4) = 1.7359208+00	F(4) = -7.7524657+02
	D(5) = 2.2320695-02	F(5) = -7.8024614+02
	D(6) = 2.8672945-03	F(6) = 6.4721040+01

Table 3-18. Summary of Forces and Deflections on Segments (continued)
Maximum Dynamic Pressure Condition (T = 77 Seconds)

	DEFLECTION COLUMN		NODAL FORCES	
SEGMENT 8	D(1) =	1.7359208+00	F(1) =	7.8976402+02
	D(2) =	2.2320695-02	F(2) =	7.7484197+02
	D(3) =	2.8872945-03	F(3) =	-8.4719940+01
	D(4) =	1.6927254+00	F(4) =	-7.4963911+02
	D(5) =	4.3451848-02	F(5) =	-7.4603867+02
	D(6) =	3.4269827-03	F(6) =	-8.3498838+00
SEGMENT 9	D(1) =	1.6927254+00	F(1) =	7.6001173+02
	D(2) =	4.3451848-02	F(2) =	7.3646191+02
	D(3) =	3.4269827-03	F(3) =	8.3554509+00
	D(4) =	1.6660821+00	F(4) =	-7.3511197+02
	D(5) =	5.5625072-02	F(5) =	-7.1524232+02
	D(6) =	2.2492105-03	F(6) =	-1.4750949+02
SEGMENT 10	D(1) =	1.6660821+00	F(1) =	6.5035532+02
	D(2) =	5.5625072-02	F(2) =	6.3258799+02
	D(3) =	2.2492105-03	F(3) =	-9.0439866+01
	D(4) =	1.6342939+00	F(4) =	-6.1834481+02
	D(5) =	7.1107735-02	F(5) =	-5.9403703+02
	D(6) =	2.1741852-03	F(6) =	-1.1669155+02
SEGMENT 11	D(1) =	1.6342939+00	F(1) =	6.0716955+02
	D(2) =	7.1107735-02	F(2) =	6.0647982+02
	D(3) =	2.1741852-03	F(3) =	1.1669743+02
	D(4) =	1.5978289+00	F(4) =	-5.6977703+02
	D(5) =	8.6644944-02	F(5) =	-5.5297971+02
	D(6) =	1.4888268-03	F(6) =	-2.1495086+02
SEGMENT 12	D(1) =	1.5978289+00	F(1) =	5.5514423+02
	D(2) =	3.6644944-02	F(2) =	5.6942413+02
	D(3) =	1.4888268-03	F(3) =	2.1495594+02
	D(4) =	1.5657804+00	F(4) =	-5.0819816+02
	D(5) =	8.9657771-02	F(5) =	-4.9453646+02
	D(6) =	1.8102431-04	F(6) =	-2.2353451+02
SEGMENT 13	D(1) =	1.5657804+00	F(1) =	4.9482781+02
	D(2) =	8.9657771-02	F(2) =	5.1086603+02
	D(3) =	1.8102431-04	F(3) =	2.2353694+02
	D(4) =	1.6098269+00	F(4) =	-4.3179340+02
	D(5) =	5.3763972-03	F(5) =	-4.3832994+02
	D(6) =	-3.7778146-03	F(6) =	-5.5920941+02
SEGMENT 14	D(1) =	1.6098269+00	F(1) =	4.4290236+02
	D(2) =	5.3763972-03	F(2) =	4.3096598+02
	D(3) =	-3.7778146-03	F(3) =	5.5921030+02
	D(4) =	1.8426046+00	F(4) =	-3.9285764+02
	D(5) =	-2.5227250-01	F(5) =	-4.8061229+02
	D(6) =	-9.5233051-03	F(6) =	-6.1925880+02

Table 3-18. Summary of Forces and Deflections on Segments (continued)
Maximum Dynamic Pressure Condition (T = 77 Seconds)

	DEFLECTION COLUMN	NODAL FORCES
SEGMENT 15	D(1) = 1.8426046+00	F(1) = 4.2910656+02
	D(2) = -2.5227250-01	F(2) = 4.4732084+02
	D(3) = -9.5233051-03	F(3) = 6.1928428+02
	D(4) = 2.0381427+00	F(4) = -4.0274495+02
	D(5) = -4.5588673-01	F(5) = -5.4370642+02
	D(6) = -8.8471351-03	F(6) = 7.6736071+02
SEGMENT 16	D(1) = 2.0381427+00	F(1) = 4.4308380+02
	D(2) = -4.5588673-01	F(2) = 5.0517264+02
	D(3) = -8.8471351-03	F(3) = -7.6733251+02
	D(4) = 2.1204942+00	F(4) = -4.2565091+02
	D(5) = -5.4201809-01	F(5) = -5.8969154+02
	D(6) = -2.7787448-03	F(6) = 2.2858911+03
SEGMENT 17	D(1) = 2.1204942+00	F(1) = 4.6268476+02
	D(2) = -5.4201809-01	F(2) = 5.5392176+02
	D(3) = -2.7787448-03	F(3) = -2.2858320+03
	D(4) = 2.1033521+00	F(4) = -4.4942303+02
	D(5) = -5.2814671-01	F(5) = -6.1720381+02
	D(6) = 5.8753895-03	F(6) = 3.6160963+03
SEGMENT 18	D(1) = 2.1033521+00	F(1) = -1.3943799+00
	D(2) = -5.2814671-01	F(2) = -5.6410646+02
	D(3) = 5.8753895-03	F(3) = -1.4014455+01
	D(4) = 2.1636450+00	F(4) = 1.4331073+00
	D(5) = -5.3208379-01	F(5) = -5.6666241-02
	D(6) = 6.1587934-03	F(6) = -8.2881689-05
SEGMENT 19	D(1) = 2.1033521+00	F(1) = 3.3807667+03
	D(2) = -5.2814671-01	F(2) = 1.0396136+03
	D(3) = 5.8753895-03	F(3) = -8.0456483+03
	D(4) = 2.0139325+00	F(4) = -3.3580489+03
	D(5) = -3.9280974-01	F(5) = -1.0773097+03
	D(6) = 3.2819595-02	F(6) = 4.3839655+03
SEGMENT 20	D(1) = 2.0139325+00	F(1) = 3.3273910+03
	D(2) = -3.9280974-01	F(2) = 1.1451638+03
	D(3) = 3.2819595-02	F(3) = -4.3839404+03
	D(4) = 1.8147926+00	F(4) = -3.2905351+03
	D(5) = -3.7253783-02	F(5) = -1.1732342+03
	D(6) = 4.7426415-02	F(6) = 1.1132730+03
SEGMENT 21	D(1) = 1.8147926+00	F(1) = 3.2233925+03
	D(2) = -3.7253783-02	F(2) = 1.3218741+03
	D(3) = 4.7426415-02	F(3) = -1.1132585+03
	D(4) = 1.1568024+00	F(4) = -3.1214188+03
	D(5) = 1.1282562+00	F(5) = -1.2537489+03
	D(6) = 4.0389989-02	F(6) = -1.9212667+03

Table 3-18. Summary of Forces and Deflections on Segments (continued)
Maximum Dynamic Pressure Condition (T = 77 Seconds)

	DEFLECTION COLUMN	NODAL FORCES
SEGMENT 22	D(1) = 1.1568024+00	F(1) = 3.0163637+03
	D(2) = 1.1282562+00	F(2) = 1.4863498+03
	D(3) = 4.0389989-02	F(3) = 1.9212663+03
	D(4) = 6.7097155-01	F(4) = -2.9135299+03
	D(5) = 1.8503625+00	F(5) = -1.2219673+03
	D(6) = 1.2712068-02	F(6) = -1.1874628+03
SEGMENT 23	D(1) = 6.7097155-01	F(1) = 2.8034575+03
	D(2) = 1.8503625+00	F(2) = 1.4856946+03
	D(3) = 1.2712068-02	F(3) = 1.1874583+03
	D(4) = 4.6018407-01	F(4) = -2.7110303+03
	D(5) = 1.9721235+00	F(5) = -1.1370199+03
	D(6) = 4.0183671-04	F(6) = -2.0766179+02
SEGMENT 24	D(1) = 4.6018407-01	F(1) = 2.5962749+03
	D(2) = 1.9721235+00	F(2) = 1.3912493+03
	D(3) = 4.0183671-04	F(3) = 2.0765679+02
	D(4) = 3.3754857-01	F(4) = -2.5058469+03
	D(5) = 1.9182727+00	F(5) = -1.0015463+03
	D(6) = 9.1702263-05	F(6) = 1.6812478+02
SEGMENT 25	D(1) = 3.3754857-01	F(1) = 2.3820903+03
	D(2) = 1.9182727+00	F(2) = 1.2758387+03
	D(3) = 9.1702263-05	F(3) = -1.6812837+02
	D(4) = 1.9182651-01	F(4) = -2.2961838+03
	D(5) = 1.9157222+00	F(5) = -8.9162359+02
	D(6) = 2.8885349-03	F(6) = 1.3637886+02
SEGMENT 26	D(1) = 1.9182651-01	F(1) = 2.1686127+03
	D(2) = 1.9157222+00	F(2) = 1.1743994+03
	D(3) = 2.8885349-03	F(3) = -1.3638223+02
	D(4) = -7.6175377-03	F(4) = -2.0931254+03
	D(5) = 2.0480810+00	F(5) = -8.0308561+02
	D(6) = 7.8850688-03	F(6) = 4.0723074+02
SEGMENT 27	D(1) = -7.6175377-03	F(1) = 1.9768870+03
	D(2) = 2.0480810+00	F(2) = 1.0608694+03
	D(3) = 7.8850688-03	F(3) = -4.0723534+02
	D(4) = -2.2720503-01	F(4) = -1.9212656+03
	D(5) = 2.2967927+00	F(5) = -7.0409492+02
	D(6) = 1.1646046-02	F(6) = 1.4909011+02
SEGMENT 28	D(1) = -2.2720503-01	F(1) = 1.8070973+03
	D(2) = 2.2967927+00	F(2) = 9.5698059+02
	D(3) = 1.1646046-02	F(3) = -1.4909926+02
	D(4) = -4.2482719-01	F(4) = -1.7576445+03
	D(5) = 2.5022528+00	F(5) = -5.8250154+02
	D(6) = 4.0709123-03	F(6) = -1.2215199+03

Table 3-18. Summary of Forces and Deflections on Segments (continued) Maximum Dynamic Pressure Condition (T = 77 Seconds)

	DEFLECTION COLUMN		NODAL FORCES	
SEGMENT 29	D(1) =	-4.2482719-01	F(1) =	1.6227480+03
	D(2) =	2.5022528+00	F(2) =	8.8034199+02
	D(3) =	4.0709123-03	F(3) =	1.2215027+03
	D(4) =	-4.1124887-01	F(4) =	-1.5819154+03
	D(5) =	2.2757953+00	F(5) =	-5.4503884+02
	D(6) =	-1.8647234-02	F(6) =	-2.2529753+03
SEGMENT 30	D(1) =	-4.1124887-01	F(1) =	1.4558468+03
	D(2) =	2.2757953+00	F(2) =	8.2259509+02
	D(3) =	-1.8647234-02	F(3) =	2.2529619+03
	D(4) =	-2.5006434-01	F(4) =	-1.4336333+03
	D(5) =	1.8187968+00	F(5) =	-6.5210426+02
	D(6) =	-3.2485193-02	F(6) =	-1.2158327+03
SEGMENT 31	D(1) =	-2.5006434-01	F(1) =	1.3320311+03
	D(2) =	1.8187968+00	F(2) =	8.7552834+02
	D(3) =	-3.2485193-02	F(3) =	1.2158110+03
	D(4) =	-6.1117932-02	F(4) =	-1.3152009+03
	D(5) =	1.3429270+00	F(5) =	-7.2891961+02
	D(6) =	-3.2036019-02	F(6) =	1.3380898+03
SEGMENT 32	D(1) =	-6.1117932-02	F(1) =	1.2158939+03
	D(2) =	1.3429270+00	F(2) =	9.4720238+02
	D(3) =	-3.2036019-02	F(3) =	-1.3381138+03
	D(4) =	6.8981634-02	F(4) =	-1.2013682+03
	D(5) =	1.0072760+00	F(5) =	-8.4459200+02
	D(6) =	-1.4709890-02	F(6) =	5.8115834+03
SEGMENT 33	D(1) =	2.7554455+00	F(1) =	-1.0068592+03
	D(2) =	0.0000000	F(2) =	2.6219405+02
	D(3) =	1.9340579-01	F(3) =	1.5665675+03
	D(4) =	2.7604146+00	F(4) =	1.0068592+03
	D(5) =	3.8961715-01	F(5) =	-1.8737422+02
	D(6) =	-2.0940283-02	F(6) =	-2.7885575+02
SEGMENT 34	D(1) =	2.7604146+00	F(1) =	-1.0067571+03
	D(2) =	3.8961715-01	F(2) =	1.8737275+02
	D(3) =	-2.0940283-02	F(3) =	2.7885945+02
	D(4) =	2.7700489+00	F(4) =	1.0067571+03
	D(5) =	2.1005387-02	F(5) =	-3.1241398+01
	D(6) =	-4.0567519-02	F(6) =	1.9436862+02
SEGMENT 35	D(1) =	2.7700469+00	F(1) =	-1.0065368+03
	D(2) =	2.1005387-02	F(2) =	3.1241757+01
	D(3) =	-4.0567519-02	F(3) =	-1.9436868+02
	D(4) =	2.8021659+00	F(4) =	1.0065368+03
	D(5) =	-5.4224436-02	F(5) =	6.5486390+00
	D(6) =	1.9670105-02	F(6) =	-6.4713966+01

Table 3-18. Summary of Forces and Deflections on Segments (continued)
Maximum Dynamic Pressure Condition (T = 77 Seconds)

	DEFLECTION COLUMN		NODAL FORCES	
SEGMENT 36	D(1) =	2.8021659+00	F(1) =	-1.0061104+03
	D(2) =	-5.4224436-02	F(2) =	-6.5482539+00
	D(3) =	1.9670105-02	F(3) =	6.4714025+01
	D(4) =	2.8689509+00	F(4) =	1.0061104+03
	D(5) =	-4.5810927-02	F(5) =	-4.1976172-01
	D(6) =	-9.3588448-03	F(6) =	3.2865746+01
SEGMENT 37	D(1) =	2.8689509+00	F(1) =	-1.0055508+03
	D(2) =	-4.5810927-02	F(2) =	4.2024507-01
	D(3) =	-9.3588448-03	F(3) =	-3.2865756+01
	D(4) =	2.9353651+00	F(4) =	1.0055508+03
	D(5) =	-4.8299467-02	F(5) =	-2.6397311-01
	D(6) =	4.0667653-03	F(6) =	-1.8136232+01
SEGMENT 38	D(1) =	2.9353651+00	F(1) =	-1.0051273+03
	D(2) =	-4.8299467-02	F(2) =	2.6433009-01
	D(3) =	4.0667653-03	F(3) =	1.8136241+01
	D(4) =	2.9691816+00	F(4) =	1.0051273+03
	D(5) =	-4.5012351-02	F(5) =	2.8454692-01
	D(6) =	-2.6071301-03	F(6) =	3.7714317+00
SEGMENT 39	D(1) =	2.9691816+00	F(1) =	-1.0049215+03
	D(2) =	-4.5012351-02	F(2) =	-2.8417468-01
	D(3) =	-2.6071301-03	F(3) =	-3.7714171+00
	D(4) =	2.9864919+00	F(4) =	1.0049215+03
	D(5) =	-7.6265583-02	F(5) =	-8.0940900+00
	D(6) =	-3.9920898-03	F(6) =	-9.7333550+00
SEGMENT 40	D(1) =	2.9864919+00	F(1) =	-1.0043803+03
	D(2) =	-7.6265583-02	F(2) =	8.0945408+00
	D(3) =	-3.9920898-03	F(3) =	9.7334826+00
	D(4) =	2.9954375+00	F(4) =	1.0043803+03
	D(5) =	-8.5688891-02	F(5) =	-1.8579820+01
	D(6) =	1.0322594-03	F(6) =	5.2990876+01
SEGMENT 41	D(1) =	2.9954375+00	F(1) =	-1.1819786+03
	D(2) =	-8.5688891-02	F(2) =	2.3052880+00
	D(3) =	1.0322594-03	F(3) =	2.8249414+02
	D(4) =	3.0264952+00	F(4) =	1.1819786+03
	D(5) =	-8.0676477-02	F(5) =	-2.8082181+01
	D(6) =	-2.5310631-04	F(6) =	-3.5624657+01
SEGMENT 42	D(1) =	3.0264952+00	F(1) =	-1.1812443+03
	D(2) =	-8.0676477-02	F(2) =	-2.0742425+01
	D(3) =	-2.5310631-04	F(3) =	3.5625865+01
	D(4) =	3.0887272+00	F(4) =	1.1812443+03
	D(5) =	-8.9159071-02	F(5) =	-3.4093853+01
	D(6) =	-2.4783960-04	F(6) =	3.6277597+01

Table 3-18. Summary of Forces and Deflections on Segments (continued)
Maximum Dynamic Pressure Condition (T = 77 Seconds)

Segment	Deflection Column		Nodal Forces	
SEGMENT 43	D(1) =	3.0887272+00	F(1) =	-1.1797816+03
	D(2) =	-8.9159091-02	F(2) =	-6.3555746+01
	D(3) =	-2.4783960-04	F(3) =	-3.6277230+01
	D(4) =	3.2139161+00	F(4) =	1.1797816+03
	D(5) =	-9.0576882-02	F(5) =	-6.4736177+01
	D(6) =	1.1005339-04	F(6) =	-1.4133241+01
SEGMENT 44	D(1) =	3.2139161+00	F(1) =	-1.1777151+03
	D(2) =	-9.0576882-02	F(2) =	-7.3564111+01
	D(3) =	1.1005339-04	F(3) =	1.4133343+01
	D(4) =	3.3545674+00	F(4) =	1.1777151+03
	D(5) =	-9.0187978-02	F(5) =	-7.3241703+01
	D(6) =	-6.0384726-05	F(6) =	4.7547967+00
SEGMENT 45	D(1) =	3.3545674+00	F(1) =	-1.1755288+03
	D(2) =	-9.0187978-02	F(2) =	-7.3160206+01
	D(3) =	-6.0384726-05	F(3) =	-4.7547117+00
	D(4) =	3.4951059+00	F(4) =	1.1755288+03
	D(5) =	-9.1737774-02	F(5) =	-7.6496660+01
	D(6) =	2.1933755-06	F(6) =	-1.3113277+00
SEGMENT 46	D(1) =	3.4951059+00	F(1) =	-1.1733261+03
	D(2) =	-9.1737774-02	F(2) =	-7.7353016+01
	D(3) =	2.1933755-06	F(3) =	1.3114326+00
	D(4) =	3.6379019+00	F(4) =	1.1733261+03
	D(5) =	-9.6235609-02	F(5) =	-8.7538580+01
	D(6) =	-1.4471239-04	F(6) =	-6.6647536+00
SEGMENT 47	D(1) =	3.6379019+00	F(1) =	-1.1711098+03
	D(2) =	-9.6235609-02	F(2) =	-8.6646301+01
	D(3) =	-1.4471239-04	F(3) =	6.6648472+00
	D(4) =	3.7813480+00	F(4) =	1.1711098+03
	D(5) =	-1.0066821-01	F(5) =	-9.7562662+01
	D(6) =	6.5716216-05	F(6) =	1.8089981+01
SEGMENT 48	D(1) =	3.7813480+00	F(1) =	-1.1691611+03
	D(2) =	-1.0066821-01	F(2) =	-7.0165426+01
	D(3) =	6.5716216-05	F(3) =	-1.8089819+01
	D(4) =	3.8838352+00	F(4) =	1.1691611+03
	D(5) =	-1.0879894-01	F(5) =	-7.9681448+01
	D(6) =	-5.0655860-04	F(6) =	-7.2841982+01
SEGMENT 49	D(1) =	3.8838352+00	F(1) =	-1.1674797+03
	D(2) =	-1.0879894-01	F(2) =	-7.5175017+01
	D(3) =	-5.0655860-04	F(3) =	7.2842248+01
	D(4) =	3.9858482+00	F(4) =	1.1674797+03
	D(5) =	-9.5746613-02	F(5) =	-6.7523241+01
	D(6) =	1.4289782-03	F(6) =	2.5802774+02

Table 3-18. Summary of Forces and Deflections on Segments (continued)
Maximum Dynamic Pressure Condition (T = 77 Seconds)

	DEFLECTION COLUMN		NODAL FORCES	
SEGMENT 50	D(1) =	3.9858482+00	F(1) =	-1.1661202+03
	D(2) =	-9.5746613-02	F(2) =	-6.6286905+01
	D(3) =	1.4289782-03	F(3) =	-2.5802738+02
	D(4) =	4.0473338+00	F(4) =	1.1661202+03
	D(5) =	-7.3270991-02	F(5) =	1.0869807+01
	D(6) =	-5.1754136-04	F(6) =	-5.5914668+02
SEGMENT 51	D(1) =	4.0473338+00	F(1) =	-1.1653557+03
	D(2) =	-7.3270991-02	F(2) =	-9.1516605+01
	D(3) =	-5.1754136-04	F(3) =	5.5914846+02
	D(4) =	4.0789192+00	F(4) =	1.1653557+03
	D(5) =	-1.3533182-01	F(5) =	4.5414462+01
	D(6) =	-8.2103859-03	F(6) =	-1.8209601+03
SEGMENT 52	D(1) =	4.0789192+00	F(1) =	-1.2293833+02
	D(2) =	-1.3533182-01	F(2) =	-7.2916332+01
	D(3) =	-8.2103859-03	F(3) =	-1.3155363+02
	D(4) =	4.0848128+00	F(4) =	1.2293833+02
	D(5) =	-1.5578676-02	F(5) =	1.0800303+01
	D(6) =	1.7946026-02	F(6) =	-5.3431478+01
SEGMENT 53	D(1) =	4.0848128+00	F(1) =	-1.2248783+02
	D(2) =	-1.5578676-02	F(2) =	-1.0799571+01
	D(3) =	1.7946026-02	F(3) =	5.3431489+01
	D(4) =	4.0935966+00	F(4) =	1.2248783+02
	D(5) =	-5.1418612-03	F(5) =	-6.2941348-01
	D(6) =	-9.4333179-03	F(6) =	2.3966009+01
SEGMENT 54	D(1) =	4.0935966+00	F(1) =	-1.2162349+02
	D(2) =	-5.1418612-03	F(2) =	6.2995420-01
	D(3) =	-9.4333179-03	F(3) =	-2.3966009+01
	D(4) =	4.1072557+00	F(4) =	1.2162349+02
	D(5) =	-6.0387319-03	F(5) =	-1.8001714-01
	D(6) =	2.4620919-03	F(6) =	-1.6301887+01
SEGMENT 55	D(1) =	4.1072557+00	F(1) =	-1.2077037+02
	D(2) =	-6.0387319-03	F(2) =	1.8061068-01
	D(3) =	2.4620919-03	F(3) =	1.6301888+01
	D(4) =	4.1153026+00	F(4) =	1.2077037+02
	D(5) =	-3.8011915-03	F(5) =	1.6479666+00
	D(6) =	8.3517825-04	F(6) =	1.4551014+01
SEGMENT 56	D(1) =	4.1153026+00	F(1) =	-1.2034206+02
	D(2) =	-3.8011915-03	F(2) =	-1.6471756+00
	D(3) =	8.3517825-04	F(3) =	-1.4551012+01
	D(4) =	4.1178282+00	F(4) =	1.2034206+02
	D(5) =	1.1408013-02	F(5) =	1.0063004+01
	D(6) =	1.1235039-04	F(6) =	-1.6709904+01

Table 3-18. Summary of Forces and Deflections on Segments (continued)
Maximum Dynamic Pressure Condition (T = 77 Seconds)

	DEFLECTION COLUMN	NODAL FORCES
SEGMENT 57	D(1) = 2.1033521+00	F(1) = -2.9282765+03
	D(2) = -5.2814671-01	F(2) = 1.0293094+02
	D(3) = 5.8753895-03	F(3) = 4.4436151+03
	D(4) = 2.1257374+00	F(4) = 2.9282765+03
	D(5) = -4.8442433-01	F(5) = -1.7982680+02
	D(6) = 7.2158212-04	F(6) = -2.4882729+03
SEGMENT 58	D(1) = 2.1257374+00	F(1) = -2.9268893+03
	D(2) = -4.8442433-01	F(2) = 2.2886527+01
	D(3) = 7.2158212-04	F(3) = 2.4882781+03
	D(4) = 2.1703972+00	F(4) = 2.9268893+03
	D(5) = -5.1907884-01	F(5) = -1.7478348+02
	D(6) = -2.8461433-03	F(6) = 8.8975270+01
SEGMENT 59	D(1) = 2.1703972+00	F(1) = -2.9241163+03
	D(2) = -5.1907884-01	F(2) = -1.3909979+02
	D(3) = -2.8461433-03	F(3) = -8.8959303+01
	D(4) = 2.2617558+00	F(4) = 2.9241163+03
	D(5) = -5.8529761-01	F(5) = -2.0762051+02
	D(6) = 7.5029166-04	F(6) = 1.1203456+03
SEGMENT 60	D(1) = 2.2617558+00	F(1) = -2.9198468+03
	D(2) = -5.8529761-01	F(2) = -2.7542562+02
	D(3) = 7.5029166-04	F(3) = -1.1203415+03
	D(4) = 2.3797988+00	F(4) = 2.9198468+03
	D(5) = -4.3718851-01	F(5) = -1.3603272+02
	D(6) = 2.6154919-03	F(6) = -6.4454769+02
SEGMENT 61	D(1) = 2.3797988+00	F(1) = -2.9134180+03
	D(2) = -4.3718851-01	F(2) = -3.9736346+02
	D(3) = 2.6154919-03	F(3) = 6.4455132+02
	D(4) = 2.4470271+00	F(4) = 2.9134180+03
	D(5) = -3.2945642-01	F(5) = -2.7633788+02
	D(6) = 4.4444968-04	F(6) = -4.1394113+02
SEGMENT 62	D(1) = 2.4470271+00	F(1) = -2.9063694+03
	D(2) = -3.2945642-01	F(2) = -2.1551277+02
	D(3) = 4.4444968-04	F(3) = 4.1394597+02
	D(4) = 2.4961377+00	F(4) = 2.9063694+03
	D(5) = -3.5059417-01	F(5) = -2.2441534+02
	D(6) = -1.2695724-03	F(6) = -6.8760893+02
SEGMENT 63	D(1) = 2.4961377+00	F(1) = -2.9018253+03
	D(2) = -3.5059417-01	F(2) = -1.6972994+02
	D(3) = -1.2695724-03	F(3) = 6.8762828+02
	D(4) = 2.5215479+00	F(4) = 2.9018253+03
	D(5) = -4.1405999-01	F(5) = -8.5235271+01
	D(6) = -3.5338574-03	F(6) = -2.2227598+03

Table 3-18. Summary of Forces and Deflections on Segments (continued)
Maximum Dynamic Pressure Condition (T = 77 Seconds)

	DEFLECTION COLUMN	NODAL FORCES
SEGMENT 64	D(1) = 2.5215479+00	F(1) = -2.8995734+03
	D(2) = -4.1405999-01	F(2) = -1.6905724+02
	D(3) = -3.5338574-03	F(3) = 2.2228292+03
	D(4) = 2.5349054+00	F(4) = 2.8995734+03
	D(5) = -4.7699803-01	F(5) = 1.5477125+01
	D(6) = -5.7882468-03	F(6) = -3.5725096+03
SEGMENT 65	D(1) = 2.5349054+00	F(1) = -9.4429928+02
	D(2) = -4.7699803-01	F(2) = -8.5121916+01
	D(3) = -5.7882468-03	F(3) = -8.2377175+02
	D(4) = 2.5523939+00	F(4) = 9.4429928+02
	D(5) = -1.8920357-01	F(5) = 6.7652827+01
	D(6) = 4.1541487-02	F(6) = -1.1810742+02
SEGMENT 66	D(1) = 2.5523939+00	F(1) = -9.4393510+02
	D(2) = -1.8920357-01	F(2) = -1.1143726+01
	D(3) = 4.1541487-02	F(3) = 1.1810767+02
	D(4) = 2.5718246+00	F(4) = 9.4393510+02
	D(5) = 3.0231177-01	F(5) = 3.1890437+01
	D(6) = 7.8557594-03	F(6) = -2.2977289+02
SEGMENT 67	D(1) = 2.5718246+00	F(1) = -9.4350285+02
	D(2) = 3.0231177-01	F(2) = 3.6641997+01
	D(3) = 7.8557594-03	F(3) = 2.2977274+02
	D(4) = 2.5882695+00	F(4) = 9.4350285+02
	D(5) = 2.1005846-01	F(5) = 7.6512609+00
	D(6) = -1.4941462-02	F(6) = -5.6576063+00
SEGMENT 68	D(1) = 2.5882695+00	F(1) = -9.4314588+02
	D(2) = 2.1005846-01	F(2) = 5.1841755+01
	D(3) = -1.4941462-02	F(3) = 5.6593980+00
	D(4) = 2.6001258+00	F(4) = 9.4314588+02
	D(5) = 2.1112162-01	F(5) = -2.4891405+01
	D(6) = 1.8949483-02	F(6) = 5.1095761+02
SEGMENT 69	D(1) = 2.6001258+00	F(1) = -4.6018879+02
	D(2) = 2.1112162-01	F(2) = -4.9598618+01
	D(3) = 1.8949483-02	F(3) = 5.0887021+02
	D(4) = 2.6057138+00	F(4) = 4.6018879+02
	D(5) = 1.9706543-01	F(5) = -2.4324057+01
	D(6) = -1.5617065-02	F(6) = 7.1860146+01
SEGMENT 70	D(1) = 2.6057138+00	F(1) = -4.5965454+02
	D(2) = 1.9706543-01	F(2) = 2.4324270+01
	D(3) = -1.5617065-02	F(3) = -7.1860194+01
	D(4) = 2.6203123+00	F(4) = 4.5965454+02
	D(5) = -5.6743231-02	F(5) = 7.0229060-01
	D(6) = -1.1279079-03	F(6) = 1.8609719+01

Table 3-18. Summary of Forces and Deflections on Segments (continued) ~~PAGE 11~~
Maximum Dynamic Pressure Condition (T = 77 Seconds)

	DEFLECTION COLUMN		NODAL FORCES	
SEGMENT 71	D(1) =	2.6203123+00	F(1) =	-4.5894772+02
	D(2) =	-5.6743231-02	F(2) =	-7.0209634-01
	D(3) =	-1.1279079-03	F(3) =	-1.8609679+01
	D(4) =	2.6380354+00	F(4) =	4.5894772+02
	D(5) =	-5.8335948-02	F(5) =	7.9203216-01
	D(6) =	5.5323511-04	F(6) =	-8.1129929+00
SEGMENT 72	D(1) =	2.6380354+00	F(1) =	-4.5824080+02
	D(2) =	-5.8335948-02	F(2) =	-7.9189467-01
	D(3) =	5.5323511-04	F(3) =	8.1130451+00
	D(4) =	2.6571759+00	F(4) =	4.5824080+02
	D(5) =	-1.7377825-01	F(5) =	-1.0554539+01
	D(6) =	-8.4501489-03	F(6) =	-4.8103845+01
SEGMENT 73	D(1) =	2.6571759+00	F(1) =	-4.5772595+02
	D(2) =	-1.7377825-01	F(2) =	1.0554744+01
	D(3) =	-8.4501489-03	F(3) =	4.8103983+01
	D(4) =	2.6676432+00	F(4) =	4.5772595+02
	D(5) =	-2.2633645-01	F(5) =	-2.4260423+01
	D(6) =	4.0623750-03	F(6) =	2.0629446+02
SEGMENT 74	D(1) =	2.6345340+00	F(1) =	1.8804026+01
	D(2) =	-2.1706510-01	F(2) =	6.4785291+00
	D(3) =	-1.0514406-03	F(3) =	-1.6623271-02
	D(4) =	2.6127013+00	F(4) =	-1.9916436+01
	D(5) =	-2.3009201-01	F(5) =	-5.2383365+01
	D(6) =	-8.0177866-04	F(6) =	7.4637922+02
SEGMENT 75	D(1) =	2.6127013+00	F(1) =	5.8325694+01
	D(2) =	-2.3009201-01	F(2) =	6.5212559+01
	D(3) =	-8.0177866-04	F(3) =	-7.4642238+02
	D(4) =	2.6099568+00	F(4) =	-6.2022639+01
	D(5) =	-2.3732161-01	F(5) =	-1.2357451+02
	D(6) =	5.3556202-04	F(6) =	3.1258926+03
SEGMENT 76	D(1) =	2.6099568+00	F(1) =	1.0071987+02
	D(2) =	-2.3732161-01	F(2) =	1.3564314+02
	D(3) =	5.3556202-04	F(3) =	-3.1255988+03
	D(4) =	2.6676432+00	F(4) =	-1.0758747+02
	D(5) =	-2.2633645-01	F(5) =	-2.0669532+02
	D(6) =	4.0623750-03	F(6) =	7.3471589+03
SEGMENT 77	D(1) =	2.6676432+00	F(1) =	-2.4061154+02
	D(2) =	-2.2633645-01	F(2) =	2.4160744+02
	D(3) =	4.0623750-03	F(3) =	-7.5535195+03
	D(4) =	2.7984982+00	F(4) =	2.5593631+02
	D(5) =	-1.7641161-01	F(5) =	-3.1013754+02
	D(6) =	7.4523978-03	F(6) =	4.1156428+03

Table 3-18. Summary of Forces and Deflections on Segments (continued)
Maximum Dynamic Pressure Condition (T = 77 Seconds)

	DEFLECTION COLUMN		NODAL FORCES	
SEGMENT 78	D(1) =	2.7984982+00	F(1) =	-2.2178187+02
	D(2) =	-1.9641161-01	F(2) =	3.1940252+02
	D(3) =	7.4523978-03	F(3) =	-4.1185248+03
	D(4) =	2.9860979+00	F(4) =	2.3695465+02
	D(5) =	-1.5346670-01	F(5) =	-3.9068052+02
	D(6) =	9.1094985-03	F(6) =	1.3363124+03
SEGMENT 79	D(1) =	2.9860979+00	F(1) =	-2.0263539+02
	D(2) =	-1.5346670-01	F(2) =	3.9935824+02
	D(3) =	9.1094985-03	F(3) =	-1.3369654+03
	D(4) =	3.1971211+00	F(4) =	2.1759611+02
	D(5) =	-1.0804664-01	F(5) =	-4.6943003+02
	D(6) =	9.4846508-03	F(6) =	-8.2731255+02
SEGMENT 80	D(1) =	3.1971211+00	F(1) =	-1.8313026+02
	D(2) =	-1.0804664-01	F(2) =	4.7751037+02
	D(3) =	9.4846508-03	F(3) =	8.2652525+02
	D(4) =	3.4071821+00	F(4) =	1.9780163+02
	D(5) =	-6.6675162-02	F(5) =	-5.4358520+02
	D(6) =	8.9640368-03	F(6) =	-2.4337538+03
SEGMENT 81	D(1) =	3.4071821+00	F(1) =	-1.6318425+02
	D(2) =	-6.6675162-02	F(2) =	5.5106943+02
	D(3) =	8.9640368-03	F(3) =	2.4330883+03
	D(4) =	3.5995636+00	F(4) =	1.7746213+02
	D(5) =	-3.2836383-02	F(5) =	-6.1137805+02
	D(6) =	7.8677031-03	F(6) =	-3.5488116+03
SEGMENT 82	D(1) =	3.5995636+00	F(1) =	-1.4273542+02
	D(2) =	-3.2836383-02	F(2) =	6.1825869+02
	D(3) =	7.8677031-03	F(3) =	3.5459041+03
	D(4) =	3.7639230+00	F(4) =	1.5648013+02
	D(5) =	-7.8275843-03	F(5) =	-6.7192954+02
	D(6) =	6.4533742-03	F(6) =	-4.2271649+03
SEGMENT 83	D(1) =	3.7639230+00	F(1) =	-1.2159751+02
	D(2) =	-7.8275843-03	F(2) =	6.7821026+02
	D(3) =	6.4533742-03	F(3) =	4.2263403+03
	D(4) =	3.8950880+00	F(4) =	1.3460528+02
	D(5) =	8.5394959-03	F(5) =	-7.2519508+02
	D(6) =	4.9248864-03	F(6) =	-4.5241623+03
SEGMENT 84	D(1) =	3.8950880+00	F(1) =	-9.9639499+01
	D(2) =	8.5394959-03	F(2) =	7.3086946+02
	D(3) =	4.9248864-03	F(3) =	4.5230707+03
	D(4) =	3.9920157+00	F(4) =	1.1161781+02
	D(5) =	1.7387601-02	F(5) =	-7.7190388+02
	D(6) =	3.4417455-03	F(6) =	-4.4705164+03

Table 3-18. Summary of Forces and Deflections on Segments (continued)
Maximum Dynamic Pressure Condition (T = 77 Seconds)

	DEFLECTION COLUMN		NODAL FORCES	
SEGMENT 85	D(1) =	3.9920157+00	F(1) =	-7.6537529+01
	D(2) =	1.7387601-02	F(2) =	7.7697324+02
	D(3) =	3.4417455-03	F(3) =	4.4692487+03
	D(4) =	4.0569087+00	F(4) =	8.7029638+01
	D(5) =	2.0327434-02	F(5) =	-8.1369158+02
	D(6) =	2.1257659-03	F(6) =	-4.0730197+03
SEGMENT 86	D(1) =	4.0569087+00	F(1) =	-5.1917631+01
	D(2) =	2.0327434-02	F(2) =	8.1815016+02
	D(3) =	2.1257659-03	F(3) =	4.0710478+03
	D(4) =	4.0945557+00	F(4) =	6.0189168+01
	D(5) =	1.9167112-02	F(5) =	-8.5321965+02
	D(6) =	1.0770022-03	F(6) =	-3.3038235+03
SEGMENT 87	D(1) =	4.0945557+00	F(1) =	-2.4713555+01
	D(2) =	1.9167112-02	F(2) =	8.5707428+02
	D(3) =	1.0770022-03	F(3) =	3.3011474+03
	D(4) =	4.1119075+00	F(4) =	2.9647068+01
	D(5) =	1.5669993-02	F(5) =	-8.9460951+02
	D(6) =	3.7934308-04	F(6) =	-2.0777953+03
SEGMENT 88	D(1) =	4.1119075+00	F(1) =	5.8481680+00
	D(2) =	1.5669993-02	F(2) =	8.9786422+02
	D(3) =	3.7934308-04	F(3) =	2.0773409+03
	D(4) =	4.1178282+00	F(4) =	-7.2229740+00
	D(5) =	1.1408013-02	F(5) =	-9.4365369+02
	D(6) =	1.1235039-04	F(6) =	-2.2072975+02
SEGMENT 89	D(1) =	4.1178282+00	F(1) =	-6.3691895+01
	D(2) =	1.1408013-02	F(2) =	9.3594177+02
	D(3) =	1.1235039-04	F(3) =	2.3593029+02
	D(4) =	4.1196393+00	F(4) =	7.6406239+01
	D(5) =	8.5080129-03	F(5) =	-9.7607846+02
	D(6) =	8.1797520-05	F(6) =	-2.8502922+02
SEGMENT 90	D(1) =	4.1196393+00	F(1) =	-5.1409857+01
	D(2) =	8.5080129-03	F(2) =	9.7762259+02
	D(3) =	8.1797520-05	F(3) =	2.7767101+02
	D(4) =	4.1209012+00	F(4) =	6.4245716+01
	D(5) =	5.8914447-03	F(5) =	-1.0307465+03
	D(6) =	5.2215421-05	F(6) =	-2.9687827+02
SEGMENT 91	D(1) =	4.1209012+00	F(1) =	-3.9205086+01
	D(2) =	5.8914447-03	F(2) =	1.0319987+03
	D(3) =	5.2215421-05	F(3) =	2.8699477+02
	D(4) =	4.1216704+00	F(4) =	5.2262910+01
	D(5) =	3.6239650-03	F(5) =	-1.1081470+03
	D(6) =	2.7910464-05	F(6) =	-2.8285549+02

Table 3-18. Summary of Forces and Deflections on Segments (continued)
Maximum Dynamic Pressure Condition (T = 77 Seconds)

	DEFLECTION COLUMN		NODAL FORCES	
SEGMENT 92	D(1) =	4.1216704+00	F(1) =	-2.6996675+01
	D(2) =	3.6239650-03	F(2) =	1.1091003+03
	D(3) =	2.7910464-05	F(3) =	2.7108657+02
	D(4) =	4.1220544+00	F(4) =	4.0488960+01
	D(5) =	1.7865135-03	F(5) =	-1.2359979+03
	D(6) =	1.0511986-05	F(6) =	-2.5635051+02
SEGMENT 93	D(1) =	4.1220544+00	F(1) =	-1.5498500+01
	D(2) =	1.7865135-03	F(2) =	1.2386513+03
	D(3) =	1.0511986-05	F(3) =	2.4196845+02
	D(4) =	4.1221656+00	F(4) =	3.0893691+01
	D(5) =	4.9000501-04	F(5) =	-1.5509284+03
	D(6) =	-1.5865674-06	F(6) =	-2.2315334+02
SEGMENT 94	D(1) =	4.1221402+00	F(1) =	4.3476046+00
	D(2) =	4.1221656+00	F(2) =	-4.3476048+00
	D(3) =	4.9000501-04	F(3) =	1.5512301+03
	D(4) =	-1.5865674-06	F(4) =	2.1262793+04
	D(5) =	0.0000000	F(5) =	0.0000000
	D(6) =	0.0000000	F(6) =	0.0000000
SEGMENT 95	D(1) =	6.8981634-02	F(1) =	-1.3927831+00
	D(2) =	1.0072760+00	F(2) =	5.2628975+02
	D(3) =	-1.4709890-02	F(3) =	-1.3951885+01
	D(4) =	-7.7207637-02	F(4) =	1.4198181+00
	D(5) =	1.0126157+00	F(5) =	5.9512157-02
	D(6) =	-1.4553891-02	F(6) =	6.5648295-04
SEGMENT 96	D(1) =	6.8981634-02	F(1) =	8.4515584+02
	D(2) =	1.0072760+00	F(2) =	3.7401630+02
	D(3) =	-1.4709890-02	F(3) =	-1.6958195+03
	D(4) =	1.1316318-01	F(4) =	-8.3118990+02
	D(5) =	9.1160971-01	F(5) =	-3.1286328+02
	D(6) =	-7.2663696-03	F(6) =	-1.3838302+03
SEGMENT 97	D(1) =	6.8981634-02	F(1) =	1.8566276+03
	D(2) =	1.0072760+00	F(2) =	4.2495316+01
	D(3) =	-1.4709890-02	F(3) =	-1.9421695+03
	D(4) =	5.3920733-02	F(4) =	-1.8493989+03
	D(5) =	9.1454116-01	F(5) =	2.8907568+00
	D(6) =	-6.8713896-03	F(6) =	-1.6024748+03
SEGMENT 98	D(1) =	1.1316318-01	F(1) =	3.1203973+02
	D(2) =	9.1160971-01	F(2) =	1.0414317+02
	D(3) =	-7.2663696-03	F(3) =	1.0781967+03
	D(4) =	5.3920733-02	F(4) =	-3.1619047+02
	D(5) =	9.1454116-01	F(5) =	-7.7980558+01
	D(6) =	-6.8713896-03	F(6) =	1.1238889+03

Table 3-18. Summary of Forces and Deflections on Segments (continued)
Maximum Dynamic Pressure Condition (T = 77 Seconds)

	DEFLECTION COLUMN	NODAL FORCES
SEGMENT 99	D(1) = 1.1316318-01	F(1) = 5.3425366+02
	D(2) = 9.1160971-01	F(2) = 1.6046193+02
	D(3) = -7.2663696-03	F(3) = 3.0563425+02
	D(4) = 1.5694326-01	F(4) = -5.2874774+02
	D(5) = 4.2627418-01	F(5) = -6.6573962+01
	D(6) = -1.5569064-02	F(6) = 1.6589326+02
SEGMENT 100	D(1) = 5.3920733-02	F(1) = 2.1676018+03
	D(2) = 9.1454116-01	F(2) = 7.5095988+01
	D(3) = -6.8713896-03	F(3) = 4.7931178+02
	D(4) = -2.1487061-02	F(4) = -2.1676018+03
	D(5) = 4.2383055-01	F(5) = -1.2401594+01
	D(6) = -1.4107315-02	F(6) = 3.5794128+02
SEGMENT 101	D(1) = 1.5694326-01	F(1) = -4.0839160+01
	D(2) = 4.2627418-01	F(2) = 5.5129431+02
	D(3) = -1.5569064-02	F(3) = -2.9520716+02
	D(4) = -2.1487061-02	F(4) = 4.1808623+01
	D(5) = 4.2383055-01	F(5) = -5.3822559+02
	D(6) = -1.4107315-02	F(6) = -2.2106116+02
SEGMENT 102	D(1) = 1.5694326-01	F(1) = 6.5326545+02
	D(2) = 4.2627418-01	F(2) = -5.2054353+02
	D(3) = -1.5569064-02	F(3) = 1.2929466+02
	D(4) = 0.0000000	F(4) = -6.6497453+02
	D(5) = 2.6109979-01	F(5) = 5.4426417+02
	D(6) = -1.4715561-02	F(6) = 1.7035065+02
SEGMENT 103	D(1) = -2.1487061-02	F(1) = 2.1269566+03
	D(2) = 4.2383055-01	F(2) = 5.5062718+02
	D(3) = -1.4107315-02	F(3) = -1.3688065+02
	D(4) = 0.0000000	F(4) = -2.1148774+03
	D(5) = 2.6109979-01	F(5) = -5.4426512+02
	D(6) = -1.4715561-02	F(6) = -1.7035129+02

Table 3-19. Summary of Forces and Deflections on Segments
Maximum Longitudinal Acceleration Condition (T = 138 Seconds)

	DEFLECTION COLUMN	NODAL FORCES
SEGMENT 1	D(1) = 3.0515481+00	F(1) = 1.2443928+03
	D(2) = 0.0000000	F(2) = 2.1656173+03
	D(3) = 2.4007708-01	F(3) = -1.9440095+03
	D(4) = 2.1219066+00	F(4) = -1.1799249+03
	D(5) = -1.4202044-03	F(5) = -2.0872679+03
	D(6) = 6.1015990-02	F(6) = -4.4917583+03
SEGMENT 2	D(1) = 2.1219066+00	F(1) = 1.7618285+03
	D(2) = -1.4202044-03	F(2) = 2.0854038+03
	D(3) = 6.1015990-02	F(3) = 4.4917676+03
	D(4) = 1.8617706+00	F(4) = -1.6543917+03
	D(5) = 2.2023899-01	F(5) = -1.9422270+03
	D(6) = 1.3319841-02	F(6) = -1.9764043+03
SEGMENT 3	D(1) = 1.8617706+00	F(1) = 1.6606559+03
	D(2) = 2.2023899-01	F(2) = 1.9376180+03
	D(3) = 1.3319841-02	F(3) = 1.9764064+03
	D(4) = 1.8207468+00	F(4) = -1.5214899+03
	D(5) = 2.0437473-01	F(5) = -1.6467785+03
	D(6) = -8.1079541-03	F(6) = -1.7739414+01
SEGMENT 4	D(1) = 1.8207468+00	F(1) = 1.5302626+03
	D(2) = 2.0437473-01	F(2) = 1.6403478+03
	D(3) = -8.1079541-03	F(3) = 1.7740657+01
	D(4) = 1.8722882+00	F(4) = -1.3764644+03
	D(5) = 9.0305769-02	F(5) = -1.3980282+03
	D(6) = -3.8054289-03	F(6) = 2.8970975+02
SEGMENT 5	D(1) = 1.8722882+00	F(1) = 1.3892299+03
	D(2) = 9.0305769-02	F(2) = 1.3886430+03
	D(3) = -3.8054289-03	F(3) = -2.8970929+02
	D(4) = 1.8470339+00	F(4) = -1.2039495+03
	D(5) = 3.8224943-02	F(5) = -1.2175154+03
	D(6) = 1.5501099-03	F(6) = -3.9564846+01
SEGMENT 6	D(1) = 1.8470339+00	F(1) = 1.2191864+03
	D(2) = 3.8224943-02	F(2) = 1.2063504+03
	D(3) = 1.5501099-03	F(3) = 3.9565027+01
	D(4) = 1.7652801+00	F(4) = -1.0757191+03
	D(5) = 5.2256246-02	F(5) = -1.0978114+03
	D(6) = 3.4708213-03	F(6) = 1.2343768+02
SEGMENT 7	D(1) = 1.7652801+00	F(1) = 1.0881851+03
	D(2) = 5.2256246-02	F(2) = 1.0887081+03
	D(3) = 3.4708213-03	F(3) = -1.2343709+02
	D(4) = 1.6644272+00	F(4) = -1.0105256+03
	D(5) = 1.1103224-01	F(5) = -1.0110495+03
	D(6) = 8.5234547-03	F(6) = 2.2820877+02

Table 3-19. Summary of Forces and Deflections on Segments (continued)
Maximum Longitudinal Acceleration Condition (T = 138 Seconds)

		DEFLECTION COLUMN		NODAL FORCES
SEGMENT 8	D(1) =	1.6644272+00	F(1) =	1.0191995+03
	D(2) =	1.1103224-01	F(2) =	1.0047118+03
	D(3) =	8.5234547-03	F(3) =	-2.2820889+02
	D(4) =	1.5482239+00	F(4) =	-9.6741784+02
	D(5) =	1.9562008-01	F(5) =	-9.2820366+02
	D(6) =	1.1148894-02	F(6) =	2.7356571+01
SEGMENT 9	D(1) =	1.5482239+00	F(1) =	9.7361193+02
	D(2) =	1.9562008-01	F(2) =	9.2367478+02
	D(3) =	1.1148894-02	F(3) =	-2.7352924+01
	D(4) =	1.4708893+00	F(4) =	-9.4171413+02
	D(5) =	2.5171059-01	F(5) =	-8.6187805+02
	D(6) =	8.4080215-03	F(6) =	-3.8508929+02
SEGMENT 10	D(1) =	1.4708893+00	F(1) =	6.1575372+02
	D(2) =	2.5171059-01	F(2) =	6.0499052+02
	D(3) =	8.4080215-03	F(3) =	-4.4171155+02
	D(4) =	1.3686259+00	F(4) =	-5.8544630+02
	D(5) =	3.3229279-01	F(5) =	-4.7672719+02
	D(6) =	8.7344525-03	F(6) =	-1.2578415+02
SEGMENT 11	D(1) =	1.3686259+00	F(1) =	5.0127827+02
	D(2) =	3.3229279-01	F(2) =	5.6354807+02
	D(3) =	8.7344525-03	F(3) =	1.2579684+02
	D(4) =	1.2373605+00	F(4) =	-4.7040707+02
	D(5) =	4.3488251-01	F(5) =	-3.6791961+02
	D(6) =	7.7761967-03	F(6) =	-2.8402383+02
SEGMENT 12	D(1) =	1.2373605+00	F(1) =	3.5024418+02
	D(2) =	4.3488251-01	F(2) =	4.9188126+02
	D(3) =	7.7761967-03	F(3) =	2.8403474+02
	D(4) =	1.0684021+00	F(4) =	-3.2062559+02
	D(5) =	5.6316128-01	F(5) =	-1.7258227+02
	D(6) =	6.2952655-03	F(6) =	-1.6261217+02
SEGMENT 13	D(1) =	1.0684021+00	F(1) =	1.2714501+02
	D(2) =	5.6316128-01	F(2) =	3.7227034+02
	D(3) =	6.2952655-03	F(3) =	1.6261393+02
	D(4) =	9.1451065-01	F(4) =	-1.1094844+02
	D(5) =	6.6119605-01	F(5) =	1.5372814+02
	D(6) =	2.7177864-04	F(6) =	-9.6974505+02
SEGMENT 14	D(1) =	9.1451065-01	F(1) =	-1.1591793+02
	D(2) =	6.6119605-01	F(2) =	8.0998308+01
	D(3) =	2.7177864-04	F(3) =	9.6974348+02
	D(4) =	1.2414296+00	F(4) =	1.0282005+02
	D(5) =	3.1219776-01	F(5) =	2.4737739+02
	D(6) =	-1.9402609-02	F(6) =	-2.9151591+03

Table 3-19. Summary of Forces and Deflections on Segments (continued)
Maximum Longitudinal Acceleration Condition (T = 138 Seconds)

	DEFLECTION COLUMN		NODAL FORCES	
SEGMENT 15	D(1) =	1.2414296+00	F(1) =	-2.6573049+02
	D(2) =	3.1219776-01	F(2) =	-7.7399979+01
	D(3) =	-1.9402609-02	F(3) =	2.9079783+03
	D(4) =	1.7580725+00	F(4) =	2.4944341+02
	D(5) =	-1.9743936-01	F(5) =	9.9774250+01
	D(6) =	-2.8002494-02	F(6) =	-2.2160564+02
SEGMENT 16	D(1) =	1.7580725+00	F(1) =	-3.4221500+02
	D(2) =	-1.9743936-01	F(2) =	-4.0192095+00
	D(3) =	-2.8002494-02	F(3) =	2.2213532+02
	D(4) =	2.1042923+00	F(4) =	3.2875074+02
	D(5) =	-5.3036081-01	F(5) =	-6.0133584+01
	D(6) =	-1.9030036-02	F(6) =	4.6186018+03
SEGMENT 17	D(1) =	2.1042923+00	F(1) =	-3.8940539+02
	D(2) =	-5.3036081-01	F(2) =	1.2344204+02
	D(3) =	-1.9030036-02	F(3) =	-4.6185455+03
	D(4) =	2.2005549+00	F(4) =	3.7824403+02
	D(5) =	-6.1453082-01	F(5) =	-1.9355458+02
	D(6) =	2.8160235-03	F(6) =	1.0193200+04
SEGMENT 18	D(1) =	2.2005549+00	F(1) =	-2.9261065+00
	D(2) =	-6.1453082-01	F(2) =	-6.5636605+02
	D(3) =	2.8160235-03	F(3) =	-2.9386093+01
	D(4) =	2.2315553+00	F(4) =	3.0073759+00
	D(5) =	-6.1911187-01	F(5) =	-5.6626923-02
	D(6) =	3.3324134-03	F(6) =	-1.1327164-03
SEGMENT 19	D(1) =	2.2005549+00	F(1) =	3.5279703+03
	D(2) =	-6.1453082-01	F(2) =	8.3886269+02
	D(3) =	2.8160235-03	F(3) =	-1.2631193+04
	D(4) =	2.0941756+00	F(4) =	-3.4959906+03
	D(5) =	-4.4217212-01	F(5) =	-8.8241281+02
	D(6) =	4.5448322-02	F(6) =	7.0272120+03
SEGMENT 20	D(1) =	2.0941756+00	F(1) =	3.4424522+03
	D(2) =	-4.4217212-01	F(2) =	1.0013650+03
	D(3) =	4.5448322-02	F(3) =	-7.0271762+03
	D(4) =	1.8208736+00	F(4) =	-3.4043219+03
	D(5) =	7.2846822-02	F(5) =	-1.0293638+03
	D(6) =	6.9423317-02	F(6) =	1.9846266+03
SEGMENT 21	D(1) =	1.8208736+00	F(1) =	3.2868009+03
	D(2) =	7.2846822-02	F(2) =	1.2905038+03
	D(3) =	6.9423317-02	F(3) =	-1.9846080+03
	D(4) =	8.7754079-01	F(4) =	-3.1828213+03
	D(5) =	1.8339660+00	F(5) =	-1.1487993+03
	D(6) =	6.1590026-02	F(6) =	-2.8508474+03

Table 3-19. Summary of Forces and Deflections on Segments (continued)
Maximum Longitudinal Acceleration Condition (T = 138 Seconds) PAGE 4

	DEFLECTION COLUMN	NODAL FORCES
SEGMENT 22	D(1) = 8.7754079-01	F(1) = 2.9984467+03
	D(2) = 1.8339660+00	F(2) = 1.5585482+03
	D(3) = 6.1590026-02	F(3) = 2.8508443+03
	D(4) = 1.7927445-01	F(4) = -2.8962238+03
	D(5) = 2.9672751+00	F(5) = -1.1141608+03
	D(6) = 1.9988650-02	F(6) = -1.8200030+03
SEGMENT 23	D(1) = 1.7927445-01	F(1) = 2.7022811+03
	D(2) = 2.9672751+00	F(2) = 1.5451815+03
	D(3) = 1.9988650-02	F(3) = 1.8199926+03
	D(4) = -1.0482476-01	F(4) = -2.6131896+03
	D(5) = 3.1924218+00	F(5) = -9.9850962+02
	D(6) = 1.2622265-03	F(6) = -3.0181023+02
SEGMENT 24	D(1) = -1.0482476-01	F(1) = 2.4102400+03
	D(2) = 3.1924218+00	F(2) = 1.4497820+03
	D(3) = 1.2622265-03	F(3) = 3.0180083+02
	D(4) = -2.6223028-01	F(4) = -2.3262915+03
	D(5) = 3.1579885+00	F(5) = -7.9561929+02
	D(6) = 1.2259636-03	F(6) = 2.9307174+02
SEGMENT 25	D(1) = -2.6223028-01	F(1) = 2.1067115+03
	D(2) = 3.1579885+00	F(2) = 1.2840904+03
	D(3) = 1.2259636-03	F(3) = -2.9308185+02
	D(4) = -4.5083229-01	F(4) = -2.0307362+03
	D(5) = 3.1972606+00	F(5) = -6.2846960+02
	D(6) = 4.4351867-03	F(6) = 5.9711528+01
SEGMENT 26	D(1) = -4.5083229-01	F(1) = 1.8037436+03
	D(2) = 3.1972606+00	F(2) = 1.1334614+03
	D(3) = 4.4351867-03	F(3) = -5.9721863+01
	D(4) = -6.5703064-01	F(4) = -1.7409570+03
	D(5) = 3.3030547+00	F(5) = -5.0697178+02
	D(6) = 4.9245691-03	F(6) = -8.9423499-01
SEGMENT 27	D(1) = -6.5703064-01	F(1) = 1.5337255+03
	D(2) = 3.3030547+00	F(2) = 9.6822976+02
	D(3) = 4.9245691-03	F(3) = 8.7852023-01
	D(4) = -8.0250724-01	F(4) = -1.4905728+03
	D(5) = 3.3657552+00	F(5) = -4.0766701+02
	D(6) = 2.1046695-03	F(6) = -3.9833037+02
SEGMENT 28	D(1) = -8.0250724-01	F(1) = 1.3022551+03
	D(2) = 3.3657552+00	F(2) = 8.2702824+02
	D(3) = 2.1046695-03	F(3) = 3.9831530+02
	D(4) = -8.3212581-01	F(4) = -1.2666178+03
	D(5) = 3.1990778+00	F(5) = -3.0410961+02
	D(6) = -1.1581793-02	F(6) = -1.5718472+03

Table 3-19. Summary of Forces and Deflections on Segments (continued)
Maximum Longitudinal Acceleration Condition (T = 138 Seconds)

	DEFLECTION COLUMN	NODAL FORCES
SEGMENT 29	D(1) = -8.3212581-01	F(1) = 1.0839030+03
	D(2) = 3.1990778+00	F(2) = 7.1100505+02
	D(3) = -1.1581793-02	F(3) = 1.5718354+03
	D(4) = -6.0716435-01	F(4) = -1.0566291+03
	D(5) = 2.5263964+00	F(5) = -3.0168589+02
	D(6) = -3.5122151-02	F(6) = -2.0506964+03
SEGMENT 30	D(1) = -6.0716435-01	F(1) = 9.1382661+02
	D(2) = 2.5263964+00	F(2) = 6.1972840+02
	D(3) = -3.5122151-02	F(3) = 2.0506742+03
	D(4) = -3.2502037-01	F(4) = -8.9988335+02
	D(5) = 1.8235449+00	F(5) = -4.3536644+02
	D(6) = -4.5090304-02	F(6) = -4.7565465+02
SEGMENT 31	D(1) = -3.2502037-01	F(1) = 7.9546088+02
	D(2) = 1.8235449+00	F(2) = 6.6796588+02
	D(3) = -4.5090304-02	F(3) = 4.7561654+02
	D(4) = -6.4337926-02	F(4) = -7.8541019+02
	D(5) = 1.2055438+00	F(5) = -5.2525993+02
	D(6) = -3.9600881-02	F(6) = 2.5853130+03
SEGMENT 32	D(1) = -6.4337926-02	F(1) = 6.7972846+02
	D(2) = 1.2055438+00	F(2) = 7.6025788+02
	D(3) = -3.9600881-02	F(3) = -2.5853439+03
	D(4) = 9.4152137-02	F(4) = -6.7160809+02
	D(5) = 8.2289556-01	F(5) = -6.6944087+02
	D(6) = -1.4210201-02	F(6) = 7.9070367+03
SEGMENT 33	D(1) = 3.0515481+00	F(1) = -1.2434990+03
	D(2) = 0.0000000	F(2) = 3.2529803+02
	D(3) = 2.4007708-01	F(3) = 1.9440107+03
	D(4) = 3.0576660+00	F(4) = 1.2434990+03
	D(5) = 4.8382466-01	F(5) = -2.3248581+02
	D(6) = -2.5925999-02	F(6) = -3.4615617+02
SEGMENT 34	D(1) = 3.0576660+00	F(1) = -1.2432779+03
	D(2) = 4.8382466-01	F(2) = 2.3248454+02
	D(3) = -2.5925999-02	F(3) = 3.4615946+02
	D(4) = 3.0695189+00	F(4) = 1.2432779+03
	D(5) = 2.6200860-02	F(5) = -3.8765546+01
	D(6) = -5.0454633-02	F(6) = 2.4056921+02
SEGMENT 35	D(1) = 3.0695189+00	F(1) = -1.2428223+03
	D(2) = 2.6200860-02	F(2) = 3.8765943+01
	D(3) = -5.0454633-02	F(3) = -2.4056935+02
	D(4) = 3.1091681+00	F(4) = 1.2428223+03
	D(5) = -6.6887318-02	F(5) = 8.1002457+00
	D(6) = 2.4653721-02	F(6) = -7.8907055+01

Table 3-19. Summary of Forces and Deflections on Segments (continued)
Maximum Longitudinal Acceleration Condition (T = 138 Seconds) PAGE 6

	DEFLECTION COLUMN	NODAL FORCES
SEGMENT 36	D(1) = 3.1091681+00	F(1) = -1.2419261+03
	D(2) = -6.6887318-02	F(2) = -8.0999006+00
	D(3) = 2.4653721-02	F(3) = 7.8907094+01
	D(4) = 3.1916080+00	F(4) = 1.2419261+03
	D(5) = -5.6622559-02	F(5) = -5.3513788-01
	D(6) = -1.2248046-02	F(6) = 3.8421379+01
SEGMENT 37	D(1) = 3.1916080+00	F(1) = -1.2407439+03
	D(2) = -5.6622559-02	F(2) = 5.3548211-01
	D(3) = -1.2248046-02	F(3) = -3.8421390+01
	D(4) = 3.2735319+00	F(4) = 1.2407439+03
	D(5) = -5.9073225-02	F(5) = 1.7477519-01
	D(6) = 6.4144807-03	F(6) = -1.7946334+01
SEGMENT 38	D(1) = 3.2735319+00	F(1) = -1.2398554+03
	D(2) = -5.9073225-02	F(2) = -1.7443984-01
	D(3) = 6.4144807-03	F(3) = 1.7946343+01
	D(4) = 3.3152610+00	F(4) = 1.2398554+03
	D(5) = -5.6559946-02	F(5) = 5.2371657-01
	D(6) = -5.6508877-03	F(6) = -8.0230055+00
SEGMENT 39	D(1) = 3.3152610+00	F(1) = -1.2394114+03
	D(2) = -5.6559946-02	F(2) = -5.2330535-01
	D(3) = -5.6508877-03	F(3) = 8.0230285+00
	D(4) = 3.3375210+00	F(4) = 1.2394114+03
	D(5) = -1.5586056-01	F(5) = -2.9240286+01
	D(6) = -1.4813090-02	F(6) = -3.1418195+01
SEGMENT 40	D(1) = 3.3375210+00	F(1) = -1.2382600+03
	D(2) = -1.5586056-01	F(2) = 2.9240779+01
	D(3) = -1.4813090-02	F(3) = 3.1418418+01
	D(4) = 3.3496176+00	F(4) = 1.2382600+03
	D(5) = -1.9122553-01	F(5) = -6.4957574+01
	D(6) = 3.5144401-03	F(6) = 1.8921021+02
SEGMENT 41	D(1) = 3.3496176+00	F(1) = -1.8551360+03
	D(2) = -1.9122553-01	F(2) = 8.4680721+00
	D(3) = 3.5144401-03	F(3) = 9.7626857+02
	D(4) = 3.4006383+00	F(4) = 1.8551360+03
	D(5) = -1.7457861-01	F(5) = -9.7475579+01
	D(6) = -9.0985441-04	F(6) = -1.1871246+02
SEGMENT 42	D(1) = 3.4006383+00	F(1) = -1.8536002+03
	D(2) = -1.7457861-01	F(2) = -7.1994263+01
	D(3) = -9.0985441-04	F(3) = 1.1871476+02
	D(4) = 3.5031771+00	F(4) = 1.8536002+03
	D(5) = -2.0430914-01	F(5) = -1.1828910+02
	D(6) = -8.5263637-04	F(6) = 1.2579521+02

Table 3-19. Summary of Forces and Deflections on Segments (continued)
Maximum Longitudinal Acceleration Condition (T = 138 Seconds)

	DEFLECTION COLUMN		NODAL FORCES	
SEGMENT 43	D(1) =	3.5031771+00	F(1) =	-1.8505364+03
	D(2) =	-2.0430914-01	F(2) =	-2.2065059+02
	D(3) =	-8.5263637-04	F(3) =	-1.2579447+02
	D(4) =	3.7109881+00	F(4) =	1.8505364+03
	D(5) =	-2.0929586-01	F(5) =	-2.2484885+02
	D(6) =	3.7051792-04	F(6) =	-5.0113996+01
SEGMENT 44	D(1) =	3.7109881+00	F(1) =	-1.8462012+03
	D(2) =	-2.0929586-01	F(2) =	-2.5518776+02
	D(3) =	3.7051792-04	F(3) =	5.0114237+01
	D(4) =	3.9445596+00	F(4) =	1.8462012+03
	D(5) =	-2.0793651-01	F(5) =	-2.5416036+02
	D(6) =	-1.9012907-04	F(6) =	1.9264010+01
SEGMENT 45	D(1) =	3.9445596+00	F(1) =	-1.8416124+03
	D(2) =	-2.0793651-01	F(2) =	-2.5399687+02
	D(3) =	-1.9012907-04	F(3) =	-1.9263806+01
	D(4) =	4.1775304+00	F(4) =	1.8416124+03
	D(5) =	-2.0801781-01	F(5) =	-2.5358994+02
	D(6) =	1.4742777-04	F(6) =	-6.8963727-01
SEGMENT 46	D(1) =	4.1775304+00	F(1) =	-1.8369946+03
	D(2) =	-2.0801781-01	F(2) =	-2.5799044+02
	D(3) =	1.4742777-04	F(3) =	6.8991241-01
	D(4) =	4.4131601+00	F(4) =	1.8369946+03
	D(5) =	-2.0805850-01	F(5) =	-2.5760045+02
	D(6) =	-1.8244695-04	F(6) =	-1.7220490+01
SEGMENT 47	D(1) =	4.4131601+00	F(1) =	-1.8323432+03
	D(2) =	-2.0805850-01	F(2) =	-2.5739915+02
	D(3) =	-1.8244695-04	F(3) =	1.7220736+01
	D(4) =	4.6483125+00	F(4) =	1.8323432+03
	D(5) =	-2.0816976-01	F(5) =	-2.5943455+02
	D(6) =	3.0369022-04	F(6) =	4.3615346+01
SEGMENT 48	D(1) =	4.6483125+00	F(1) =	-1.8282578+03
	D(2) =	-2.0816976-01	F(2) =	-1.8748470+02
	D(3) =	3.0369022-04	F(3) =	-4.3614986+01
	D(4) =	4.8158175+00	F(4) =	1.8282578+03
	D(5) =	-2.2243174-01	F(5) =	-2.0140174+02
	D(6) =	-1.1551222-03	F(6) =	-1.8318624+02
SEGMENT 49	D(1) =	4.8158175+00	F(1) =	-1.8247303+03
	D(2) =	-2.2243174-01	F(2) =	-1.9091778+02
	D(3) =	-1.1551222-03	F(3) =	1.8318697+02
	D(4) =	4.9817568+00	F(4) =	1.8247303+03
	D(5) =	-1.8970869-01	F(5) =	-1.7076717+02
	D(6) =	3.4404563-03	F(6) =	6.2287608+02

Table 3-19. Summary of Forces and Deflections on Segments (continued)
Maximum Longitudinal Acceleration Condition (T = 138 Seconds)

	DEFLECTION COLUMN		NODAL FORCES	
SEGMENT 50	D(1) =	4.9817568+00	F(1) =	-1.8218811+03
	D(2) =	-1.8970869-01	F(2) =	-1.6437267+02
	D(3) =	3.4404563-03	F(3) =	-6.2287548+02
	D(4) =	5.0804392+00	F(4) =	1.8218811+03
	D(5) =	-1.3464818-01	F(5) =	2.1861690+01
	D(6) =	-1.1776421-03	F(6) =	-1.3372780+03
SEGMENT 51	D(1) =	5.0804392+00	F(1) =	-1.8202536+03
	D(2) =	-1.3464818-01	F(2) =	-2.2215571+02
	D(3) =	-1.1776421-03	F(3) =	1.3372809+03
	D(4) =	5.1317597+00	F(4) =	1.8202536+03
	D(5) =	-2.8252360-01	F(5) =	1.0777994+02
	D(6) =	-1.9628691-02	F(6) =	-4.3713356+03
SEGMENT 52	D(1) =	5.1317597+00	F(1) =	6.7718981+02
	D(2) =	-2.8252360-01	F(2) =	-1.7583454+02
	D(3) =	-1.9628691-02	F(3) =	-3.1178941+02
	D(4) =	5.1223705+00	F(4) =	-6.7718981+02
	D(5) =	8.7503518-03	F(5) =	2.5550653+01
	D(6) =	4.3908484-02	F(6) =	-1.2202098+02
SEGMENT 53	D(1) =	5.1223705+00	F(1) =	6.7811695+02
	D(2) =	8.7503518-03	F(2) =	-2.5550041+01
	D(3) =	4.3908484-02	F(3) =	1.2202101+02
	D(4) =	5.0779705+00	F(4) =	-6.7811695+02
	D(5) =	3.2993432-02	F(5) =	-1.4216695+00
	D(6) =	-2.5176431-02	F(6) =	4.7672252+01
SEGMENT 54	D(1) =	5.0779705+00	F(1) =	6.7992194+02
	D(2) =	3.2993432-02	F(2) =	1.4224669+00
	D(3) =	-2.5176431-02	F(3) =	-4.7672253+01
	D(4) =	5.0014254+00	F(4) =	-6.7992194+02
	D(5) =	3.1423048-02	F(5) =	1.2986046-02
	D(6) =	1.2919744-02	F(6) =	-2.3127178+01
SEGMENT 55	D(1) =	5.0014254+00	F(1) =	6.8171904+02
	D(2) =	3.1423048-02	F(2) =	-1.2308077-02
	D(3) =	1.2919744-02	F(3) =	2.3127174+01
	D(4) =	4.9557052+00	F(4) =	-6.8171904+02
	D(5) =	2.9252221-02	F(5) =	-3.9635982+00
	D(6) =	-1.0899342-02	F(6) =	-2.5067780+00
SEGMENT 56	D(1) =	4.9557052+00	F(1) =	6.8263217+02
	D(2) =	2.9252221-02	F(2) =	3.9643528+00
	D(3) =	-1.0899342-02	F(3) =	2.5067772+00
	D(4) =	4.9397289+00	F(4) =	-6.8263217+02
	D(5) =	6.6106570-03	F(5) =	-1.6492143+01
	D(6) =	1.0299451-02	F(6) =	6.5821862+01

Table 3-19. Summary of Forces and Deflections on Segments (continued)
Maximum Longitudinal Acceleration Condition (T = 138 Seconds)

	DEFLECTION COLUMN		NODAL FORCES	
SEGMENT 57	D(1) =	2.2005549+00	F(1) =	-3.9334017+03
	D(2) =	-6.1453082-01	F(2) =	3.8298290+01
	D(3) =	2.8160235-03	F(3) =	2.4674097+03
	D(4) =	2.2298445+00	F(4) =	3.9334017+03
	D(5) =	-5.9612544-01	F(5) =	-1.2572792+02
	D(6) =	-1.3705602-05	F(6) =	-1.3385861+03
SEGMENT 58	D(1) =	2.2298445+00	F(1) =	-3.9305039+03
	D(2) =	-5.9612544-01	F(2) =	-3.1211982+01
	D(3) =	-1.3705602-05	F(3) =	1.3385977+03
	D(4) =	2.2884907+00	F(4) =	3.9305039+03
	D(5) =	-6.2421750-01	F(5) =	-1.4576602+02
	D(6) =	-1.8110928-03	F(6) =	1.2985187+02
SEGMENT 59	D(1) =	2.2884907+00	F(1) =	-3.9246922+03
	D(2) =	-6.2421750-01	F(2) =	-1.6811773+02
	D(3) =	-1.8110928-03	F(3) =	-1.2983028+02
	D(4) =	2.4066631+00	F(4) =	3.9246922+03
	D(5) =	-6.4481841-01	F(5) =	-2.0674645+02
	D(6) =	1.3145254-03	F(6) =	9.2116196+02
SEGMENT 60	D(1) =	2.4066631+00	F(1) =	-3.9157361+03
	D(2) =	-6.4481841-01	F(2) =	-2.7834167+02
	D(3) =	1.3145254-03	F(3) =	-9.2115634+02
	D(4) =	2.5582536+00	F(4) =	3.9157361+03
	D(5) =	-4.8219483-01	F(5) =	-1.3683300+02
	D(6) =	2.5612350-03	F(6) =	-6.0313337+02
SEGMENT 61	D(1) =	2.5582536+00	F(1) =	-3.9022337+03
	D(2) =	-4.8219483-01	F(2) =	-4.1483285+02
	D(3) =	2.5612350-03	F(3) =	6.0313660+02
	D(4) =	2.6428304+00	F(4) =	3.9022337+03
	D(5) =	-3.4572892-01	F(5) =	-2.7115279+02
	D(6) =	1.3934160-03	F(6) =	3.3766073+01
SEGMENT 62	D(1) =	2.6428304+00	F(1) =	-3.8874441+03
	D(2) =	-3.4572892-01	F(2) =	-2.1135295+02
	D(3) =	1.3934160-03	F(3) =	-3.3760966+01
	D(4) =	2.7025276+00	F(4) =	3.8874441+03
	D(5) =	-2.7662402-01	F(5) =	-1.4004059+02
	D(6) =	1.1058201-03	F(6) =	-2.1859123+02
SEGMENT 63	D(1) =	2.7025276+00	F(1) =	-3.8778856+03
	D(2) =	-2.7662402-01	F(2) =	-1.6458729+02
	D(3) =	1.1058201-03	F(3) =	2.1860698+02
	D(4) =	2.7315749+00	F(4) =	3.8778856+03
	D(5) =	-2.7439578-01	F(5) =	1.8122483+01
	D(6) =	-1.1552721-03	F(6) =	-2.6876774+03

Table 3-19. Summary of Forces and Deflections on Segments (continued)
Maximum Longitudinal Acceleration Condition (T = 138 Seconds)

	DEFLECTION COLUMN	NODAL FORCES
SEGMENT 64	D(1) = 2.7315749+00	F(1) = -3.8731512+03
	D(2) = -2.7439578-01	F(2) = -1.8880747+02
	D(3) = -1.1552721-03	F(3) = 2.6877475+03
	D(4) = 2.7462541+00	F(4) = 3.8731512+03
	D(5) = -3.0917507-01	F(5) = 1.0881152+02
	D(6) = -4.0535347-03	F(6) = -4.7627891+03
SEGMENT 65	D(1) = 2.7462541+00	F(1) = -1.1557504+03
	D(2) = -3.0917507-01	F(2) = -1.2447900+02
	D(3) = -4.0535347-03	F(3) = -1.3450751+03
	D(4) = 2.7639115+00	F(4) = 1.1557504+03
	D(5) = 2.1943991-01	F(5) = 1.3274865+02
	D(6) = 7.0896993-02	F(6) = -2.2759770+02
SEGMENT 66	D(1) = 2.7639115+00	F(1) = -1.1549800+03
	D(2) = 2.1943991-01	F(2) = 8.5594391+00
	D(3) = 7.0896993-02	F(3) = 2.2759759+02
	D(4) = 2.7797022+00	F(4) = 1.1549800+03
	D(5) = 9.8994122-01	F(5) = 8.0004544+01
	D(6) = 6.1218769-03	F(6) = -4.4135049+02
SEGMENT 67	D(1) = 2.7797022+00	F(1) = -1.1540821+03
	D(2) = 9.8994122-01	F(2) = 9.0622019+01
	D(3) = 6.1218769-03	F(3) = 4.4134980+02
	D(4) = 2.7922794+00	F(4) = 1.1540821+03
	D(5) = 6.4790060-01	F(5) = 2.3203989+01
	D(6) = -3.6580714-02	F(6) = 3.4998605-01
SEGMENT 68	D(1) = 2.7922794+00	F(1) = -1.1533310+03
	D(2) = 6.4790060-01	F(2) = 1.2430742+02
	D(3) = -3.6580714-02	F(3) = -3.5089999-01
	D(4) = 2.8027252+00	F(4) = 1.1533310+03
	D(5) = 6.5196673-01	F(5) = -5.9282374+01
	D(6) = 4.6399862-02	F(6) = 1.2368508+03
SEGMENT 69	D(1) = 2.8027252+00	F(1) = 8.9839513+00
	D(2) = 6.5196673-01	F(2) = 1.2039754+02
	D(3) = 4.6399862-02	F(3) = 1.2381653+03
	D(4) = 2.7948104+00	F(4) = -8.9839513+00
	D(5) = 6.2183473-01	F(5) = -5.9125401+01
	D(6) = -3.7787801-02	F(6) = 1.7381675+02
SEGMENT 70	D(1) = 2.7948104+00	F(1) = 1.0098500+01
	D(2) = 6.2183473-01	F(2) = 5.9125607+01
	D(3) = -3.7787801-02	F(3) = -1.7381709+02
	D(4) = 2.7867477+00	F(4) = -1.0098500+01
	D(5) = 2.9589906-03	F(5) = 1.5857107+00
	D(6) = -3.0592348-03	F(6) = 4.3027149+01

Table 3-19. Summary of Forces and Deflections on Segments (continued)
Maximum Longitudinal Acceleration Condition (T = 138 Seconds)

	DEFLECTION COLUMN		NODAL FORCES	
SEGMENT 71	D(1) =	2.7867477+00	F(1) =	1.1579252+01
	D(2) =	2.9589906-03	F(2) =	-1.5855716+00
	D(3) =	-3.0592348-03	F(3) =	-4.3027156+01
	D(4) =	2.7863377+00	F(4) =	-1.1579252+01
	D(5) =	-3.0689994-03	F(5) =	1.2892468+00
	D(6) =	1.6791669-03	F(6) =	-1.3441622+01
SEGMENT 72	D(1) =	2.7863377+00	F(1) =	1.3059114+01
	D(2) =	-3.0689994-03	F(2) =	-1.2890735+00
	D(3) =	1.6791669-03	F(3) =	1.3441668+01
	D(4) =	2.7873187+00	F(4) =	-1.3059114+01
	D(5) =	-1.1411647-01	F(5) =	-1.0466600+01
	D(6) =	-9.3364804-03	F(6) =	-5.5339743+01
SEGMENT 73	D(1) =	2.7873187+00	F(1) =	1.4159919+01
	D(2) =	-1.1411647-01	F(2) =	1.0466818+01
	D(3) =	-9.3364804-03	F(3) =	5.5339861+01
	D(4) =	2.7889288+00	F(4) =	-1.4159919+01
	D(5) =	-1.9107019-01	F(5) =	-2.5345510+01
	D(6) =	1.8546532-03	F(6) =	1.9682457+02
SEGMENT 74	D(1) =	2.5504329+00	F(1) =	-1.6230078+01
	D(2) =	-2.5593551-01	F(2) =	-6.9239836+00
	D(3) =	3.5122246-03	F(3) =	-5.8985802-02
	D(4) =	2.6393596+00	F(4) =	1.7190218+01
	D(5) =	-2.2859631-01	F(5) =	-4.1823857+01
	D(6) =	3.4879062-03	F(6) =	-2.6269420+02
SEGMENT 75	D(1) =	2.6393596+00	F(1) =	-5.0486234+01
	D(2) =	-2.2859631-01	F(2) =	2.8113572+01
	D(3) =	3.4879062-03	F(3) =	2.6261242+02
	D(4) =	2.7238887+00	F(4) =	5.3686279+01
	D(5) =	-2.0539228-01	F(5) =	-8.0012683+01
	D(6) =	3.0758695-03	F(6) =	-1.1321993+03
SEGMENT 76	D(1) =	2.7238887+00	F(1) =	-8.7244663+01
	D(2) =	-2.0539228-01	F(2) =	6.7121519+01
	D(3) =	3.0758695-03	F(3) =	1.1324970+03
	D(4) =	2.7889288+00	F(4) =	9.3193453+01
	D(5) =	-1.9107019-01	F(5) =	-1.2436091+02
	D(6) =	1.8546532-03	F(6) =	-2.7232249+03
SEGMENT 77	D(1) =	2.7889288+00	F(1) =	4.2370173+01
	D(2) =	-1.9107019-01	F(2) =	1.3831853+02
	D(3) =	1.8546532-03	F(3) =	2.5262722+03
	D(4) =	2.8219741+00	F(4) =	-4.5068769+01
	D(5) =	-1.8729603-01	F(5) =	-1.9804462+02
	D(6) =	1.0292317-03	F(6) =	-5.1547943+02

Table 3-19. Summary of Forces and Deflections on Segments (continued)
Maximum Longitudinal Acceleration Condition (T = 138 Seconds)

	DEFLECTION COLUMN	NODAL FORCES
SEGMENT 78	D(1) = 2.8219741+00	F(1) = 1.5342538+01
	D(2) = -1.8729603-01	F(2) = 1.8813636+02
	D(3) = 1.0292317-03	F(3) = 5.1457979+02
	D(4) = 2.8484512+00	F(4) = -1.6392169+01
	D(5) = -1.8697609-01	F(5) = -2.5923311+02
	D(6) = 1.2373900-03	F(6) = 1.2302930+03
SEGMENT 79	D(1) = 2.8484512+00	F(1) = -1.3504547+01
	D(2) = -1.8697609-01	F(2) = 2.4996261+02
	D(3) = 1.2373900-03	F(3) = -1.2309587+03
	D(4) = 2.8890674+00	F(4) = 1.4501598+01
	D(5) = -1.8462423-01	F(5) = -3.3608062+02
	D(6) = 2.2679206-03	F(6) = 2.6919843+03
SEGMENT 80	D(1) = 2.8890674+00	F(1) = -4.4584418+01
	D(2) = -1.8462423-01	F(2) = 3.2744474+02
	D(3) = 2.2679206-03	F(3) = -2.6927007+03
	D(4) = 2.9601325+00	F(4) = 4.8156271+01
	D(5) = -1.7694409-01	F(5) = -4.3167088+02
	D(6) = 3.9168540-03	F(6) = 3.8388968+03
SEGMENT 81	D(1) = 2.9601325+00	F(1) = -7.8376343+01
	D(2) = -1.7694409-01	F(2) = 4.2367573+02
	D(3) = 3.9168540-03	F(3) = -3.8397789+03
	D(4) = 3.0735504+00	F(4) = 8.5233918+01
	D(5) = -1.6247224-01	F(5) = -5.4849662+02
	D(6) = 5.9821532-03	F(6) = 4.6149133+03
SEGMENT 82	D(1) = 3.0735504+00	F(1) = -1.1560813+02
	D(2) = -1.6247224-01	F(2) = 5.4114432+02
	D(3) = 5.9821532-03	F(3) = -4.6157937+03
	D(4) = 3.2366708+00	F(4) = 1.2674061+02
	D(5) = -1.4125750-01	F(5) = -6.8833807+02
	D(6) = 8.2549655-03	F(6) = 4.9199715+03
SEGMENT 83	D(1) = 3.2366708+00	F(1) = -1.5722935+02
	D(2) = -1.4125750-01	F(2) = 6.8162843+02
	D(3) = 8.2549655-03	F(3) = -4.9211746+03
	D(4) = 3.4519110+00	F(4) = 1.7404880+02
	D(5) = -1.1457326-01	F(5) = -8.5210613+02
	D(6) = 1.0506760-02	F(6) = 4.5895963+03
SEGMENT 84	D(1) = 3.4519110+00	F(1) = -2.0466262+02
	D(2) = -1.1457326-01	F(2) = 8.4604272+02
	D(3) = 1.0506760-02	F(3) = -4.5908054+03
	D(4) = 3.7160898+00	F(4) = 2.2926644+02
	D(5) = -8.4643628-02	F(5) = -1.0396379+03
	D(6) = 1.2475842-02	F(6) = 3.3614776+03

E

Table 3-19. Summary of Forces and Deflections on Segments (continued)
Maximum Longitudinal Acceleration Condition (T = 138 Seconds)

	DEFLECTION COLUMN		NODAL FORCES	
SEGMENT 85	D(1) =	3.7160898+00	F(1) =	-2.5998127+02
	D(2) =	-8.4643628-02	F(2) =	1.0342239+03
	D(3) =	1.2475842-02	F(3) =	-3.3626945+03
	D(4) =	4.0194876+00	F(4) =	2.9562067+02
	D(5) =	-5.4378720-02	F(5) =	-1.2490450+03
	D(6) =	1.3855316-02	F(6) =	8.2753086+02
SEGMENT 86	D(1) =	4.0194876+00	F(1) =	-3.2650660+02
	D(2) =	-5.4378720-02	F(2) =	1.2442757+03
	D(3) =	1.3855316-02	F(3) =	-8.2935690+02
	D(4) =	4.3445395+00	F(4) =	3.7852576+02
	D(5) =	-2.7025178-02	F(5) =	-1.4767169+03
	D(6) =	1.4271915-02	F(6) =	-3.6553224+03
SEGMENT 87	D(1) =	4.3445395+00	F(1) =	-4.0939228+02
	D(2) =	-2.7025178-02	F(2) =	1.4726040+03
	D(3) =	1.4271915-02	F(3) =	3.6525779+03
	D(4) =	4.6641561+00	F(4) =	4.8717578+02
	D(5) =	-5.8030471-03	F(5) =	-1.7171772+03
	D(6) =	1.3271067-02	F(6) =	-1.1117283+04
SEGMENT 88	D(1) =	4.6641561+00	F(1) =	-5.1788741+02
	D(2) =	-5.8030471-03	F(2) =	1.7137267+03
	D(3) =	1.3271067-02	F(3) =	1.1117217+04
	D(4) =	4.9397289+00	F(4) =	6.3963404+02
	D(5) =	6.6106570-03	F(5) =	-1.9663523+03
	D(6) =	1.0299451-02	F(6) =	-2.3297051+04
SEGMENT 89	D(1) =	4.9397289+00	F(1) =	5.5200172+01
	D(2) =	6.6106570-03	F(2) =	1.9802865+03
	D(3) =	1.0299451-02	F(3) =	2.3229578+04
	D(4) =	5.0869817+00	F(4) =	-6.6219376+01
	D(5) =	9.8694130-03	F(5) =	-2.1703698+03
	D(6) =	7.6141505-03	F(6) =	-2.2790760+04
SEGMENT 90	D(1) =	5.0869817+00	F(1) =	4.4424658+01
	D(2) =	9.8694130-03	F(2) =	2.1687283+03
	D(3) =	7.6141505-03	F(3) =	2.2783957+04
	D(4) =	5.1938107+00	F(4) =	-5.5516474+01
	D(5) =	9.5989442-03	F(5) =	-2.3763693+03
	D(6) =	5.3375384-03	F(6) =	-2.3463951+04
SEGMENT 91	D(1) =	5.1938107+00	F(1) =	3.3513219+01
	D(2) =	9.5989442-03	F(2) =	2.3750437+03
	D(3) =	5.3375384-03	F(3) =	2.3456387+04
	D(4) =	5.2660254+00	F(4) =	-4.4675285+01
	D(5) =	7.2650811-03	F(5) =	-2.6234778+03
	D(6) =	3.3631615-03	F(6) =	-2.5959752+04

Table 3-19. Summary of Forces and Deflections on Segments (continued)
Maximum Longitudinal Acceleration Condition (T = 138 Seconds)

	DEFLECTION COLUMN		NODAL FORCES	
SEGMENT 92	D(1) =	5.2660254+00	F(1) =	2.2622413+01
	D(2) =	7.2650811-03	F(2) =	2.6224815+03
	D(3) =	3.3631615-03	F(3) =	2.5948608+04
	D(4) =	5.3078043+00	F(4) =	-3.3928548+01
	D(5) =	4.0941848-03	F(5) =	-2.9743188+03
	D(6) =	1.5834142-03	F(6) =	-3.1770229+04
SEGMENT 93	D(1) =	5.3078043+00	F(1) =	1.2188618+01
	D(2) =	4.0941848-03	F(2) =	2.9736502+03
	D(3) =	1.5834142-03	F(3) =	3.1753313+04
	D(4) =	5.3211929+00	F(4) =	-2.4374627+01
	D(5) =	1.1861782-03	F(5) =	-3.7555112+03
	D(6) =	-2.1258929-04	F(6) =	-3.9812261+04
SEGMENT 94	D(1) =	5.3168115+00	F(1) =	-3.4441334+00
	D(2) =	5.3211929+00	F(2) =	3.4441334+00
	D(3) =	1.1861782-03	F(3) =	3.7551357+03
	D(4) =	-2.1258929-04	F(4) =	4.0887753+06
	D(5) =	0.0000000	F(5) =	0.0000000
	D(6) =	0.0000000	F(6) =	0.0000000
SEGMENT 95	D(1) =	9.4152137-02	F(1) =	-2.9222041+00
	D(2) =	8.2289556-01	F(2) =	4.2996328+02
	D(3) =	-1.4210201-02	F(3) =	-2.9289546+01
	D(4) =	-4.5570564-02	F(4) =	2.9789265+00
	D(5) =	8.2725778-01	F(5) =	4.9615934+02
	D(6) =	-1.3788348-02	F(6) =	1.5446658+04
SEGMENT 96	D(1) =	9.4152137-02	F(1) =	1.0261031+03
	D(2) =	8.2289556-01	F(2) =	3.9925926+02
	D(3) =	-1.4210201-02	F(3) =	-2.4051164+03
	D(4) =	9.3530599-02	F(4) =	-1.0091470+03
	D(5) =	7.9024226-01	F(5) =	-3.4897390+02
	D(6) =	-1.0229429-03	F(6) =	-1.8557987+03
SEGMENT 97	D(1) =	9.4152137-02	F(1) =	1.7770927+03
	D(2) =	8.2289556-01	F(2) =	-4.2359593+01
	D(3) =	-1.4210201-02	F(3) =	-2.5386370+03
	D(4) =	7.2398211-02	F(4) =	-1.7701736+03
	D(5) =	7.9237404-01	F(5) =	7.8615788+01
	D(6) =	-1.2467483-03	F(6) =	-1.9778542+03
SEGMENT 98	D(1) =	9.3530599-02	F(1) =	4.2459315+02
	D(2) =	7.9024226-01	F(2) =	1.6525048+02
	D(3) =	-1.0229429-03	F(3) =	1.5020758+03
	D(4) =	7.2398211-02	F(4) =	-4.3024107+02
	D(5) =	7.9237404-01	F(5) =	-1.4329166+02
	D(6) =	-1.2467483-03	F(6) =	1.4939717+03

Table 3-19. Summary of Forces and Deflections on Segments (continued)
Maximum Longitudinal Acceleration Condition (T = 138 Seconds)

	DEFLECTION COLUMN		NODAL FORCES	
SEGMENT 99	D(1) =	9.3530599-02	F(1) =	5.9363182+02
	D(2) =	7.9024226-01	F(2) =	1.6088167+02
	D(3) =	-1.0229429-03	F(3) =	3.5372383+02
	D(4) =	1.0501185-01	F(4) =	-5.8751397+02
	D(5) =	5.1054376-01	F(5) =	-7.1107130+01
	D(6) =	-1.0126554-02	F(6) =	2.0074833+02
SEGMENT 100	D(1) =	7.2398211-02	F(1) =	2.2036814+03
	D(2) =	7.9237404-01	F(2) =	6.4646398+01
	D(3) =	-1.2467483-03	F(3) =	4.8477853+02
	D(4) =	-3.6683306-03	F(4) =	-2.2036814+03
	D(5) =	5.0845348-01	F(5) =	-5.6425765+00
	D(6) =	-8.4815659-03	F(6) =	3.6342657+02
SEGMENT 101	D(1) =	1.0501185-01	F(1) =	-4.3793967+01
	D(2) =	5.1054376-01	F(2) =	5.7488234+02
	D(3) =	-1.0126554-02	F(3) =	-3.1734843+02
	D(4) =	-3.6683306-03	F(4) =	4.4833573+01
	D(5) =	5.0845348-01	F(5) =	-5.5776131+02
	D(6) =	-8.4815659-03	F(6) =	-2.3626920+02
SEGMENT 102	D(1) =	1.0501185-01	F(1) =	6.5415918+02
	D(2) =	5.1054376-01	F(2) =	-5.2072486+02
	D(3) =	-1.0126554-02	F(3) =	1.1657666+02
	D(4) =	0.0000000	F(4) =	-6.6588428+02
	D(5) =	4.0771883-01	F(5) =	5.5153549+02
	D(6) =	-9.1304224-03	F(6) =	1.6234546+02
SEGMENT 103	D(1) =	-3.6683306-03	F(1) =	2.1612892+03
	D(2) =	5.0845348-01	F(2) =	5.6340490+02
	D(3) =	-8.4815659-03	F(3) =	-1.2715795+02
	D(4) =	0.0000000	F(4) =	-2.1490149+03
	D(5) =	4.0771883-01	F(5) =	-5.5153581+02
	D(6) =	-9.1304224-03	F(6) =	-1.6234644+02

Table 3-20. Summary of Forces and Deflections on Segments Maximum Reentry Dynamic Pressure Condition (T_R = 505 Seconds)

	DEFLECTION COLUMN	NODAL FORCES
SEGMENT 1	D(1) = 8.3869358-01	F(1) = 5.2226545+02
	D(2) = 0.0000000	F(2) = 1.0364437+03
	D(3) = 1.0124139-01	F(3) = -8.1941134+02
	D(4) = 4.4472193-01	F(4) = -4.9520860+02
	D(5) = -6.7970905-04	F(5) = -9.9894647+02
	D(6) = 2.6542098-02	F(6) = -1.8817669+03
SEGMENT 2	D(1) = 4.4472193-01	F(1) = 8.6907462+02
	D(2) = -6.7970905-04	F(2) = 9.9894630+02
	D(3) = 2.6542098-02	F(3) = 1.8817679+03
	D(4) = 3.2848427-01	F(4) = -8.1607819+02
	D(5) = 9.7053590-02	F(5) = -9.3391982+02
	D(6) = 6.3919369-03	F(6) = -8.4841039+02
SEGMENT 3	D(1) = 3.2848427-01	F(1) = 8.1773924+02
	D(2) = 9.7053590-02	F(2) = 9.3391613+02
	D(3) = 6.3919369-03	F(3) = 8.4840804+02
	D(4) = 3.0334577-01	F(4) = -7.4921123+02
	D(5) = 9.4790188-02	F(5) = -8.0066154+02
	D(6) = -2.9691014-03	F(6) = -2.0737825+01
SEGMENT 4	D(1) = 3.0334577-01	F(1) = 7.5154405+02
	D(2) = 9.4790188-02	F(2) = 8.0066523+02
	D(3) = -2.9691014-03	F(3) = 2.0738215+01
	D(4) = 3.1890096-01	F(4) = -6.7601054+02
	D(5) = 4.8587758-02	F(5) = -6.8314172+02
	D(6) = -1.4352290-03	F(6) = 1.1668842+02
SEGMENT 5	D(1) = 3.1890096-01	F(1) = 6.7938276+02
	D(2) = 4.8587758-02	F(2) = 6.8314362+02
	D(3) = -1.4352290-03	F(3) = -1.1668850+02
	D(4) = 3.0648614-01	F(4) = -5.8877409+02
	D(5) = 2.2820181-02	F(5) = -5.9356500+02
	D(6) = 3.7436260-04	F(6) = -3.0953613+01
SEGMENT 6	D(1) = 3.0648614-01	F(1) = 5.9284972+02
	D(2) = 2.2820181-02	F(2) = 5.9356341+02
	D(3) = 3.7436260-04	F(3) = 3.0953714+01
	D(4) = 2.6070222-01	F(4) = -5.2308635+02
	D(5) = 3.5056331-02	F(5) = -5.3358670+02
	D(6) = 2.8089215-03	F(6) = 1.3610223+02
SEGMENT 7	D(1) = 2.6070222-01	F(1) = 5.2645523+02
	D(2) = 3.5056331-02	F(2) = 5.3358535+02
	D(3) = 2.8089215-03	F(3) = -1.3610175+02
	D(4) = 1.7652488-01	F(4) = -4.8888418+02
	D(5) = 9.7669222-02	F(5) = -4.8174914+02
	D(6) = 8.2222292-03	F(6) = 2.3950201+02

Table 3-20. Summary of Forces and Deflections on Segments (continued)
Maximum Reentry Dynamic Pressure Condition (T_R = 505 Seconds)

	DEFLECTION COLUMN		NODAL FORCES	
SEGMENT 8	D(1) =	1.7652488-01	F(1) =	4.9121550+02
	D(2) =	9.7669222-02	F(2) =	4.8175043+02
	D(3) =	8.2222292-03	F(3) =	-2.3950273+02
	D(4) =	6.9437709-02	F(4) =	-4.6625871+02
	D(5) =	1.8762580-01	F(5) =	-4.2077591+02
	D(6) =	1.1073134-02	F(6) =	3.6372580+01
SEGMENT 9	D(1) =	6.9437709-02	F(1) =	4.6792376+02
	D(2) =	1.8762580-01	F(2) =	4.2077668+02
	D(3) =	1.1073134-02	F(3) =	-3.6373172+01
	D(4) =	-3.0513988-03	F(4) =	-4.5259349+02
	D(5) =	2.4812279-01	F(5) =	-3.6746673+02
	D(6) =	8.4121219-03	F(6) =	-3.8317736+02
SEGMENT 10	D(1) =	-3.0513988-03	F(1) =	1.1445869+02
	D(2) =	2.4812279-01	F(2) =	1.0969243+02
	D(3) =	8.4121219-03	F(3) =	-4.6341089+02
	D(4) =	-9.9981057-02	F(4) =	-1.0882503+02
	D(5) =	3.3473717-01	F(5) =	7.6008668+00
	D(6) =	8.7949681-03	F(6) =	-1.0860746+02
SEGMENT 11	D(1) =	-9.9981057-02	F(1) =	1.5677383+01
	D(2) =	3.3473717-01	F(2) =	8.8203629+01
	D(3) =	8.7949681-03	F(3) =	1.0859932+02
	D(4) =	-2.2557743-01	F(4) =	-1.4711892+01
	D(5) =	4.4595464-01	F(5) =	9.7656816+01
	D(6) =	7.9265574-03	F(6) =	-2.5448898+02
SEGMENT 12	D(1) =	-2.2557743-01	F(1) =	-1.1900926+02
	D(2) =	4.4595464-01	F(2) =	3.9858850+01
	D(3) =	7.9265574-03	F(3) =	2.5448367+02
	D(4) =	-3.9067310-01	F(4) =	1.0894518+02
	D(5) =	5.9019949-01	F(5) =	2.7377948+02
	D(6) =	6.7231458-03	F(6) =	-9.5933273+01
SEGMENT 13	D(1) =	-3.9067310-01	F(1) =	-3.2995399+02
	D(2) =	5.9019949-01	F(2) =	-4.6564964+01
	D(3) =	6.7231458-03	F(3) =	9.5929186+01
	D(4) =	-5.8233442-01	F(4) =	2.8792229+02
	D(5) =	7.5514857-01	F(5) =	5.9610014+02
	D(6) =	2.8102604-03	F(6) =	-6.1911366+02
SEGMENT 14	D(1) =	-5.8233442-01	F(1) =	-5.6203413+02
	D(2) =	7.5514857-01	F(2) =	-3.1412785+02
	D(3) =	2.8102604-03	F(3) =	6.1910960+02
	D(4) =	-4.0927444-01	F(4) =	4.9852840+02
	D(5) =	5.8115716-01	F(5) =	7.3420547+02
	D(6) =	-1.2993760-02	F(6) =	-2.4737057+03

Table 3-20. Summary of Forces and Deflections on Segments (continued)
Maximum Reentry Dynamic Pressure Condition (T_R = 505 Seconds)

	DEFLECTION COLUMN	NODAL FORCES
SEGMENT 15	D(1) = -4.0927444-01	F(1) = -7.1144992+02
	D(2) = 5.8115716-01	F(2) = -5.1507675+02
	D(3) = -1.2993760-02	F(3) = 2.4736975+03
	D(4) = -2.3785413-02	F(4) = 6.6774290+02
	D(5) = 2.1152812-01	F(5) = 6.3038787+02
	D(6) = -2.1927804-02	F(6) = -7.1452188+02
SEGMENT 16	D(1) = -2.3785413-02	F(1) = -7.9913852+02
	D(2) = 2.1152812-01	F(2) = -4.9519965+02
	D(3) = -2.1927804-02	F(3) = 7.1451722+02
	D(4) = 2.6668469-01	F(4) = 7.6769685+02
	D(5) = -6.0577835-02	F(5) = 5.0493586+02
	D(6) = -1.7069176-02	F(6) = 3.0422483+03
SEGMENT 17	D(1) = 2.6668469-01	F(1) = -8.6001230+02
	D(2) = -6.0577835-02	F(2) = -4.0996580+02
	D(3) = -1.7069176-02	F(3) = -3.0422485+03
	D(4) = 3.7584167-01	F(4) = 8.3536214+02
	D(5) = -1.5342346-01	F(5) = 3.9438163+02
	D(6) = -1.3100755-03	F(6) = 7.6188858+03
SEGMENT 18	D(1) = 3.7584167-01	F(1) = -2.9257108+00
	D(2) = -1.5342346-01	F(2) = -1.6386789+02
	D(3) = -1.3100755-03	F(3) = -2.9373953+01
	D(4) = 3.6541213-01	F(4) = 3.0069693+00
	D(5) = -1.5456716-01	F(5) = -1.4133628-02
	D(6) = -8.2765993-04	F(6) = 2.2447124-04
SEGMENT 19	D(1) = 3.7584167-01	F(1) = 5.5829344+02
	D(2) = -1.5342346-01	F(2) = -5.9152696+01
	D(3) = -1.3100755-03	F(3) = -5.3045876+03
	D(4) = 3.4603807-01	F(4) = -5.5323273+02
	D(5) = -9.5891941-02	F(5) = 4.8731407+01
	D(6) = 1.6721317-02	F(6) = 3.0067659+03
SEGMENT 20	D(1) = 3.4603807-01	F(1) = 5.2797523+02
	D(2) = -9.5891941-02	F(2) = 8.8287768+00
	D(3) = 1.6721317-02	F(3) = -3.0067595+03
	D(4) = 2.4858817-01	F(4) = -5.2212711+02
	D(5) = 1.0448864-01	F(5) = -1.2114660+01
	D(6) = 2.7190893-02	F(6) = 9.2446781+02
SEGMENT 21	D(1) = 2.4858817-01	F(1) = 4.6661798+02
	D(2) = 1.0448864-01	F(2) = 1.3857483+02
	D(3) = 2.7190893-02	F(3) = -9.2446514+02
	D(4) = -1.0668233-01	F(4) = -4.5185629+02
	D(5) = 8.1961311-01	F(5) = -5.8965525+01
	D(6) = 2.5130570-02	F(6) = -1.1343916+03

Table 3-20. Summary of Forces and Deflections on Segments (continued)
Maximum Reentry Dynamic Pressure Condition (T_R = 505 Seconds)

	DEFLECTION COLUMN	NODAL FORCES
SEGMENT 22	D(1) = -1.0668233-01	F(1) = 3.6469963+02
	D(2) = 8.1961311-01	F(2) = 2.5758599+02
	D(3) = 2.5130570-02	F(3) = 1.1343907+03
	D(4) = -3.6777361-01	F(4) = -3.5226630+02
	D(5) = 1.2966248+00	F(5) = -5.2323766+01
	D(6) = 8.3163950-03	F(6) = -7.5281864+02
SEGMENT 23	D(1) = -3.6777361-01	F(1) = 2.6045909+02
	D(2) = 1.2966248+00	F(2) = 2.6155222+02
	D(3) = 8.3163950-03	F(3) = 7.5281365+02
	D(4) = -4.6042047-01	F(4) = -2.5187202+02
	D(5) = 1.4022766+00	F(5) = -1.3342145+01
	D(6) = 5.2858715-04	F(6) = -1.2950531+02
SEGMENT 24	D(1) = -4.6042047-01	F(1) = 1.5571592+02
	D(2) = 1.4022766+00	F(2) = 2.3269505+02
	D(3) = 5.2858715-04	F(3) = 1.2949932+02
	D(4) = -5.0181136-01	F(4) = -1.5029235+02
	D(5) = 1.3988611+00	F(5) = 6.4870382+01
	D(6) = 5.0366479-04	F(6) = 1.2465558+02
SEGMENT 25	D(1) = -5.0181136-01	F(1) = 4.6184260+01
	D(2) = 1.3988611+00	F(2) = 1.7284386+02
	D(3) = 5.0366479-04	F(3) = -1.2466141+02
	D(4) = -5.5600174-01	F(4) = -4.4518695+01
	D(5) = 1.4283791+00	F(5) = 1.2800242+02
	D(6) = 1.9517394-03	F(6) = 3.4311085+01
SEGMENT 26	D(1) = -5.5600174-01	F(1) = -6.3213233+01
	D(2) = 1.4283791+00	F(2) = 1.1800257+02
	D(3) = 1.9517394-03	F(3) = -3.4317487+01
	D(4) = -6.2141532-01	F(4) = 6.1012841+01
	D(5) = 1.4919138+00	F(5) = 1.7212675+02
	D(6) = 2.4275755-03	F(6) = 1.9759994+01
SEGMENT 27	D(1) = -6.2141532-01	F(1) = -1.5939037+02
	D(2) = 1.4919138+00	F(2) = 5.2737887+01
	D(3) = 2.4275755-03	F(3) = -1.9766486+01
	D(4) = -6.6946729-01	F(4) = 1.5490578+02
	D(5) = 1.5365988+00	F(5) = 2.0867596+02
	D(6) = 1.1848538-03	F(6) = -1.9506227+02
SEGMENT 28	D(1) = -6.6946729-01	F(1) = -2.4432966+02
	D(2) = 1.5365988+00	F(2) = -4.0725656+00
	D(3) = 1.1848538-03	F(3) = 1.9505513+02
	D(4) = -6.5929197-01	F(4) = 2.3764336+02
	D(5) = 1.4632999+00	F(5) = 2.4953493+02
	D(6) = -6.0541729-03	F(6) = -8.4667180+02

Table 3-20. Summary of Forces and Deflections on Segments (continued)
Maximum Reentry Dynamic Pressure Condition (T_R = 505 Seconds)

	DEFLECTION COLUMN	NODAL FORCES
SEGMENT 29	D(1) = -6.5929197-01	F(1) = -3.2448265+02
	D(2) = 1.4632999+00	F(2) = -5.0843808+01
	D(3) = -6.0541729-03	F(3) = 8.4666244+02
	D(4) = -5.1046982-01	F(4) = 3.1631782+02
	D(5) = 1.1070982+00	F(5) = 2.4045412+02
	D(6) = -1.9588076-02	F(6) = -1.2345073+03
SEGMENT 30	D(1) = -5.1046982-01	F(1) = -3.8422858+02
	D(2) = 1.1070982+00	F(2) = -8.5046631+01
	D(3) = -1.9588076-02	F(3) = 1.2344916+03
	D(4) = -3.3188824-01	F(4) = 3.7836599+02
	D(5) = 7.1053272-01	F(5) = 1.6553239+02
	D(6) = -2.6620767-02	F(6) = -5.4030770+02
SEGMENT 31	D(1) = -3.3188824-01	F(1) = -4.2594934+02
	D(2) = 7.1053272-01	F(2) = -5.6371842+01
	D(3) = -2.6620767-02	F(3) = 5.4028548+02
	D(4) = -1.6012570-01	F(4) = 4.2056746+02
	D(5) = 3.3581880-01	F(5) = 1.0856816+02
	D(6) = -2.5568282-02	F(6) = 9.1541438+02
SEGMENT 32	D(1) = -1.6012570-01	F(1) = -4.6293520+02
	D(2) = 3.3581880-01	F(2) = -1.1065467+01
	D(3) = -2.5568282-02	F(3) = -9.1543217+02
	D(4) = -2.8645033-02	F(4) = 4.5740475+02
	D(5) = 5.5311344-02	F(5) = 3.1660272+01
	D(6) = -1.5094150-02	F(6) = 3.3986012+03
SEGMENT 33	D(1) = 8.3869358-01	F(1) = -5.2137012+02
	D(2) = 0.0000000	F(2) = 1.3708534+02
	D(3) = 1.0124139-01	F(3) = 8.1941177+02
	D(4) = 8.4124922-01	F(4) = 5.2137012+02
	D(5) = 2.0416205-01	F(5) = -9.7969503+01
	D(6) = -1.0885126-02	F(6) = -1.4594706+02
SEGMENT 34	D(1) = 8.4124922-01	F(1) = -5.2114516+02
	D(2) = 2.0416205-01	F(2) = 9.7969518+01
	D(3) = -1.0885126-02	F(3) = 1.4594717+02
	D(4) = 8.4619712-01	F(4) = 5.2114516+02
	D(5) = 1.1036879-02	F(5) = -1.6331903+01
	D(6) = -2.1370868-02	F(6) = 1.0080841+02
SEGMENT 35	D(1) = 8.4619712-01	F(1) = -5.2069153+02
	D(2) = 1.1036879-02	F(2) = 1.6332001+01
	D(3) = -2.1370868-02	F(3) = -1.0080843+02
	D(4) = 8.6280433-01	F(4) = 5.2069153+02
	D(5) = -2.7936732-02	F(5) = 3.3933918+00
	D(6) = 1.0620147-02	F(6) = -3.1951361+01

Table 3-20. Summary of Forces and Deflections on Segments (continued)
Maximum Reentry Dynamic Pressure Condition (T_R = 505 Seconds)

	DEFLECTION COLUMN	NODAL FORCES
SEGMENT 36	D(1) = 8.6280433-01	F(1) = -5.1979964+02
	D(2) = -2.7936732-02	F(2) = -3.3932869+00
	D(3) = 1.0620147-02	F(3) = 3.1951380+01
	D(4) = 8.9730947-01	F(4) = 5.1979964+02
	D(5) = -2.3766551-02	F(5) = -2.3187703-01
	D(6) = -5.7553191-03	F(6) = 1.3985506+01
SEGMENT 37	D(1) = 8.9730947-01	F(1) = -5.1861713+02
	D(2) = -2.3766551-02	F(2) = 2.3199830-01
	D(3) = -5.7553191-03	F(3) = -1.3985505+01
	D(4) = 9.3153013-01	F(4) = 5.1861713+02
	D(5) = -2.4195591-02	F(5) = 5.4698049-01
	D(6) = 3.9826822-03	F(6) = -3.3017369+00
SEGMENT 38	D(1) = 9.3153013-01	F(1) = -5.1772626+02
	D(2) = -2.4195591-02	F(2) = -5.4691115-01
	D(3) = 3.9826822-03	F(3) = 3.3017392+00
	D(4) = 9.4896955-01	F(4) = 5.1772626+02
	D(5) = -2.4592807-02	F(5) = 3.8140460-01
	D(6) = -4.6395422-03	F(6) = -1.5256629+01
SEGMENT 39	D(1) = 9.4896955-01	F(1) = -5.1727596+02
	D(2) = -2.4592807-02	F(2) = -3.8128700-01
	D(3) = -4.6395422-03	F(3) = 1.5256650+01
	D(4) = 9.5911410-01	F(4) = 5.1727596+02
	D(5) = -1.2302023-01	F(5) = -3.0269751+01
	D(6) = -1.5460713-02	F(6) = -3.1326056+01
SEGMENT 40	D(1) = 9.5911410-01	F(1) = -5.1611774+02
	D(2) = -1.2302023-01	F(2) = 3.0269872+01
	D(3) = -1.5460713-02	F(3) = 3.1326200+01
	D(4) = 9.6515872-01	F(4) = 5.1611774+02
	D(5) = -1.6005690-01	F(5) = -6.6553991+01
	D(6) = 3.5690267-03	F(6) = 1.9516370+02
SEGMENT 41	D(1) = 9.6515872-01	F(1) = -1.1467789+03
	D(2) = -1.6005690-01	F(2) = 8.8042802+00
	D(3) = 3.5690267-03	F(3) = 9.9634608+02
	D(4) = 9.9837612-01	F(4) = 1.1467789+03
	D(5) = -1.4329143-01	F(5) = -9.9636606+01
	D(6) = -9.4002343-04	F(6) = -1.1961151+02
SEGMENT 42	D(1) = 9.9837612-01	F(1) = -1.1452493+03
	D(2) = -1.4329143-01	F(2) = -7.3613423+01
	D(3) = -9.4002343-04	F(3) = 1.1961349+02
	D(4) = 1.0653353+00	F(4) = 1.1452493+03
	D(5) = -1.7375460-01	F(5) = -1.2088886+02
	D(6) = -8.6805846-04	F(6) = 1.2851894+02

Table 3-20. Summary of Forces and Deflections on Segments (continued)
Maximum Reentry Dynamic Pressure Condition (T_R = 505 Seconds) PAGE 7

	DEFLECTION COLUMN	NODAL FORCES
SEGMENT 43	D(1) = 1.0653353+00	F(1) = -1.1421874+03
	D(2) = -1.7375460-01	F(2) = -2.2561092+02
	D(3) = -8.6805846-04	F(3) = -1.2851840+02
	D(4) = 1.2020597+00	F(4) = 1.1421874+03
	D(5) = -1.7884329-01	F(5) = -2.2987433+02
	D(6) = 3.7496614-04	F(6) = -5.1608479+01
SEGMENT 44	D(1) = 1.2020597+00	F(1) = -1.1378517+03
	D(2) = -1.7884329-01	F(2) = -2.6086956+02
	D(3) = 3.7496614-04	F(3) = 5.1608673+01
	D(4) = 1.3557045+00	F(4) = 1.1378517+03
	D(5) = -1.7743750-01	F(5) = -2.5982265+02
	D(6) = -1.8735074-04	F(6) = 2.0666554+01
SEGMENT 45	D(1) = 1.3557045+00	F(1) = -1.1332629+03
	D(2) = -1.7743750-01	F(2) = -2.5966920+02
	D(3) = -1.8735074-04	F(3) = -2.0666376+01
	D(4) = 1.5087480+00	F(4) = 1.1332629+03
	D(5) = -1.7757141-01	F(5) = -2.5927493+02
	D(6) = 1.3582763-04	F(6) = -2.8833928+00
SEGMENT 46	D(1) = 1.5087480+00	F(1) = -1.1286428+03
	D(2) = -1.7757141-01	F(2) = -2.6371662+02
	D(3) = 1.3582763-04	F(3) = 2.8835641+00
	D(4) = 1.6633675+00	F(4) = 1.1286428+03
	D(5) = -1.7748988-01	F(5) = -2.6323780+02
	D(6) = -1.5382424-04	F(6) = -1.2842963+01
SEGMENT 47	D(1) = 1.6633675+00	F(1) = -1.1239921+03
	D(2) = -1.7748988-01	F(2) = -2.6324943+02
	D(3) = -1.5382424-04	F(3) = 1.2843139+01
	D(4) = 1.8173451+00	F(4) = 1.1239921+03
	D(5) = -1.7606033-01	F(5) = -2.6143203+02
	D(6) = 2.9845847-04	F(6) = 3.7399630+01
SEGMENT 48	D(1) = 1.8173451+00	F(1) = -1.1199039+03
	D(2) = -1.7606033-01	F(2) = -1.8856348+02
	D(3) = 2.9845847-04	F(3) = -3.7399455+01
	D(4) = 1.9265315+00	F(4) = 1.1199039+03
	D(5) = -1.8134470-01	F(5) = -1.9009936+02
	D(6) = -7.1591449-04	F(6) = -1.3444917+02
SEGMENT 49	D(1) = 1.9265315+00	F(1) = -1.1163778+03
	D(2) = -1.8134470-01	F(2) = -1.8340047+02
	D(3) = -7.1591449-04	F(3) = 1.3444949+02
	D(4) = 2.0338430+00	F(4) = 1.1163778+03
	D(5) = -1.5317959-01	F(5) = -1.6143189+02
	D(6) = 2.5526726-03	F(6) = 4.4717670+02

Table 3-20. Summary of Forces and Deflections on Segments (continued)
Maximum Reentry Dynamic Pressure Condition (T_R = 505 Seconds)

	DEFLECTION COLUMN		NODAL FORCES	
SEGMENT 50	D(1) =	2.0338430+00	F(1) =	-1.1135278+03
	D(2) =	-1.5317959-01	F(2) =	-1.4081591+02
	D(3) =	2.5526726-03	F(3) =	-4.4717603+02
	D(4) =	2.0968423+00	F(4) =	1.1135278+03
	D(5) =	-1.0684130-01	F(5) =	-3.5914349+00
	D(6) =	-4.3813650-04	F(6) =	-9.0984300+02
SEGMENT 51	D(1) =	2.0968423+00	F(1) =	-1.1118964+03
	D(2) =	-1.0684130-01	F(2) =	-1.6965808+02
	D(3) =	-4.3813650-04	F(3) =	9.0984511+02
	D(4) =	2.1294260+00	F(4) =	1.1118964+03
	D(5) =	-2.0479788-01	F(5) =	7.3441878+01
	D(6) =	-1.3410630-02	F(6) =	-3.1037473+03
SEGMENT 52	D(1) =	2.1294260+00	F(1) =	6.6863607+02
	D(2) =	-2.0479788-01	F(2) =	-1.3119173+02
	D(3) =	-1.3410630-02	F(3) =	-2.2430057+02
	D(4) =	2.1184804+00	F(4) =	-6.6863607+02
	D(5) =	1.4697737-02	F(5) =	1.8552412+01
	D(6) =	3.2247091-02	F(6) =	-8.8013245+01
SEGMENT 53	D(1) =	2.1184804+00	F(1) =	6.6955610+02
	D(2) =	1.4697737-02	F(2) =	-1.8552144+01
	D(3) =	3.2247091-02	F(3) =	8.8013273+01
	D(4) =	2.0743093+00	F(4) =	-6.6955610+02
	D(5) =	3.2240405-02	F(5) =	-1.0032211+00
	D(6) =	-1.8876590-02	F(6) =	3.2994285+01
SEGMENT 54	D(1) =	2.0743093+00	F(1) =	6.7136068+02
	D(2) =	3.2240405-02	F(2) =	1.0035722+00
	D(3) =	-1.8876590-02	F(3) =	-3.2994287+01
	D(4) =	1.9987421+00	F(4) =	-6.7136068+02
	D(5) =	3.1219491-02	F(5) =	1.1329640-01
	D(6) =	1.0758829-02	F(6) =	-1.3900412+01
SEGMENT 55	D(1) =	1.9987421+00	F(1) =	6.7316153+02
	D(2) =	3.1219491-02	F(2) =	-1.1310811-01
	D(3) =	1.0758829-02	F(3) =	1.3900409+01
	D(4) =	1.9536228+00	F(4) =	-6.7316153+02
	D(5) =	2.8229788-02	F(5) =	-4.3870896+00
	D(6) =	-1.0387640-02	F(6) =	-8.8572897+00
SEGMENT 56	D(1) =	1.9536228+00	F(1) =	6.7407789+02
	D(2) =	2.8229788-02	F(2) =	4.3873342+00
	D(3) =	-1.0387640-02	F(3) =	8.8572936+00
	D(4) =	1.9379660+00	F(4) =	-6.7407789+02
	D(5) =	1.4653442-03	F(5) =	-1.9306458+01
	D(6) =	9.5477647-03	F(6) =	6.8398979+01

Table 3-20. Summary of Forces and Deflections on Segments (continued)
Maximum Reentry Dynamic Pressure Condition (T_R = 505 Seconds)

	DEFLECTION COLUMN	NODAL FORCES
SEGMENT 57	D(1) = 3.7584167-01	F(1) = -1.4215640+03
	D(2) = -1.5342346-01	F(2) = -1.0033775+02
	D(3) = -1.3100755-03	F(3) = -2.2849261+03
	D(4) = 3.8574725-01	F(4) = 1.4215640+03
	D(5) = -1.5372198-01	F(5) = 8.2574800+01
	D(6) = 1.1634568-03	F(6) = 1.0419841+03
SEGMENT 58	D(1) = 3.8574725-01	F(1) = -1.4186675+03
	D(2) = -1.5372198-01	F(2) = -6.8308104+01
	D(3) = 1.1634568-03	F(3) = -1.0419737+03
	D(4) = 4.0501350-01	F(4) = 1.4186675+03
	D(5) = -1.0441330-01	F(5) = 4.3120801+01
	D(6) = 2.2407745-03	F(6) = -3.1747530+02
SEGMENT 59	D(1) = 4.0501350-01	F(1) = -1.4128702+03
	D(2) = -1.0441330-01	F(2) = -1.4586154+01
	D(3) = 2.2407745-03	F(3) = 3.1747881+02
	D(4) = 4.4077434-01	F(4) = 1.4128702+03
	D(5) = -2.7325730-02	F(5) = 1.7611777+01
	D(6) = 6.2625524-04	F(6) = -2.2540490+02
SEGMENT 60	D(1) = 4.4077434-01	F(1) = -1.4039147+03
	D(2) = -2.7325730-02	F(2) = 2.6487221+01
	D(3) = 6.2625524-04	F(3) = 2.2540532+02
	D(4) = 4.8516669-01	F(4) = 1.4039147+03
	D(5) = -1.4549922-02	F(5) = 2.7280596+01
	D(6) = -1.6068906-04	F(6) = 2.4663798+01
SEGMENT 61	D(1) = 4.8516669-01	F(1) = -1.3904091+03
	D(2) = -1.4549922-02	F(2) = 2.2870986+01
	D(3) = -1.6068906-04	F(3) = -2.4663602+01
	D(4) = 5.0819325-01	F(4) = 1.3904091+03
	D(5) = -2.1865421-02	F(5) = 1.3970833+01
	D(6) = -4.1527482-05	F(6) = 3.3433662+01
SEGMENT 62	D(1) = 5.0819325-01	F(1) = -1.3756134+03
	D(2) = -2.1865421-02	F(2) = 3.0128281+01
	D(3) = -4.1527482-05	F(3) = -3.3433398+01
	D(4) = 5.2472748-01	F(4) = 1.3756134+03
	D(5) = 2.1726377-02	F(5) = 2.7138201+01
	D(6) = 1.8434656-03	F(6) = 1.1780000+03
SEGMENT 63	D(1) = 5.2472748-01	F(1) = -1.3660402+03
	D(2) = 2.1726377-02	F(2) = 1.3967185+00
	D(3) = 1.8434656-03	F(3) = -1.1780010+03
	D(4) = 5.3175505-01	F(4) = 1.3660402+03
	D(5) = 9.1482908-02	F(5) = 7.3803052+01
	D(6) = 3.2419437-03	F(6) = 6.1952605+02

Table 3-20. Summary of Forces and Deflections on Segments (continued)
Maximum Reentry Dynamic Pressure Condition (T_R = 505 Seconds)

	DEFLECTION COLUMN		NODAL FORCES	
SEGMENT 64	D(1) =	5.3175505-01	F(1) =	-1.3612627+03
	D(2) =	9.1482908-02	F(2) =	-5.9537250+01
	D(3) =	3.2419437-03	F(3) =	-6.1954132+02
	D(4) =	5.3465815-01	F(4) =	1.3612627+03
	D(5) =	1.3609257-01	F(5) =	1.2067976+02
	D(6) =	3.2741122-03	F(6) =	-5.3684570+02
SEGMENT 65	D(1) =	5.3465815-01	F(1) =	-7.6050529+02
	D(2) =	1.3609257-01	F(2) =	-6.4111994+01
	D(3) =	3.2741122-03	F(3) =	-8.0764955+02
	D(4) =	5.4260757-01	F(4) =	7.6050529+02
	D(5) =	5.1548044-01	F(5) =	9.8590149+01
	D(6) =	4.5798220-02	F(6) =	-1.7363488+02
SEGMENT 66	D(1) =	5.4260757-01	F(1) =	-7.5974695+02
	D(2) =	5.1548044-01	F(2) =	2.8017137+01
	D(3) =	4.5798220-02	F(3) =	1.7363440+02
	D(4) =	5.4787554-01	F(4) =	7.5974695+02
	D(5) =	9.6671206-01	F(5) =	7.0747246+01
	D(6) =	-7.8632398-04	F(6) =	-3.0745531+02
SEGMENT 67	D(1) =	5.4787554-01	F(1) =	-7.4884972+02
	D(2) =	9.6671206-01	F(2) =	7.8848402+01
	D(3) =	-7.8632398-04	F(3) =	3.0745465+02
	D(4) =	5.5211286-01	F(4) =	7.4884972+02
	D(5) =	6.2233353-01	F(5) =	2.6056891+01
	D(6) =	-3.1457533-02	F(6) =	-9.2942666+00
SEGMENT 68	D(1) =	5.5211286-01	F(1) =	-7.4809457+02
	D(2) =	6.2233353-01	F(2) =	1.0055037+02
	D(3) =	-3.1457533-02	F(3) =	9.2935004+00
	D(4) =	5.5706028-01	F(4) =	7.4809457+02
	D(5) =	5.7482861-01	F(5) =	-4.3907120+01
	D(6) =	3.1534961-02	F(6) =	9.4848224+02
SEGMENT 69	D(1) =	5.5706028-01	F(1) =	1.5456529+02
	D(2) =	5.7482861-01	F(2) =	9.5716644+01
	D(3) =	3.1534961-02	F(3) =	9.3968891+02
	D(4) =	5.4777278-01	F(4) =	-1.5456529+02
	D(5) =	5.0495704-01	F(5) =	-4.5566836+01
	D(6) =	-3.0743040-02	F(6) =	1.5233484+02
SEGMENT 70	D(1) =	5.4777278-01	F(1) =	1.5567353+02
	D(2) =	5.0495704-01	F(2) =	4.5566910+01
	D(3) =	-3.0743040-02	F(3) =	-1.5233512+02
	D(4) =	5.3581358-01	F(4) =	-1.5567353+02
	D(5) =	1.6442119-02	F(5) =	1.4662811+00
	D(6) =	-1.8770194-03	F(6) =	2.7903557+01

Table 3-20. Summary of Forces and Deflections on Segments (continued)
Maximum Reentry Dynamic Pressure Condition (T_R = 505 Seconds)

	DEFLECTION COLUMN	NODAL FORCES
SEGMENT 71	D(1) = 5.3581358-01	F(1) = 1.5715618+02
	D(2) = 1.6442119-02	F(2) = -1.4662420+00
	D(3) = -1.8770194-03	F(3) = -2.7903574+01
	D(4) = 5.2982444-01	F(4) = -1.5715618+02
	D(5) = 1.6498132-02	F(5) = 8.0454604-01
	D(6) = 1.2329413-03	F(6) = -8.4856664+00
SEGMENT 72	D(1) = 5.2982444-01	F(1) = 1.5863800+02
	D(2) = 1.6498132-02	F(2) = -8.0451450-01
	D(3) = 1.2329413-03	F(3) = 8.4856664+00
	D(4) = 5.2446075-01	F(4) = -1.5863800+02
	D(5) = -3.8534865-02	F(5) = -5.2577384+00
	D(6) = -5.0549138-03	F(6) = -3.0775536+01
SEGMENT 73	D(1) = 5.2446075-01	F(1) = 1.5974238+02
	D(2) = -3.8534865-02	F(2) = 5.2577800+00
	D(3) = -5.0549138-03	F(3) = 3.0775559+01
	D(4) = 5.2242067-01	F(4) = -1.5974238+02
	D(5) = -8.6683443-02	F(5) = -1.3237373+01
	D(6) = 1.0085432-04	F(6) = 9.5957726+01
SEGMENT 74	D(1) = 3.1151705-01	F(1) = -2.2752924+01
	D(2) = -1.5158486-01	F(2) = -9.3291073+00
	D(3) = 3.7292721-03	F(3) = -4.6473662-03
	D(4) = 4.0399052-01	F(4) = 2.4098943+01
	D(5) = -1.2056650-01	F(5) = -1.7670508+01
	D(6) = 3.6053968-03	F(6) = -5.4900179+02
SEGMENT 75	D(1) = 4.0399052-01	F(1) = -7.0751253+01
	D(2) = -1.2056650-01	F(2) = -8.0298495-01
	D(3) = 3.6053968-03	F(3) = 5.4899157+02
	D(4) = 4.8460002-01	F(4) = 7.5235786+01
	D(5) = -9.5769795-02	F(5) = -2.4040012+01
	D(6) = 2.6766727-03	F(6) = -2.3299371+03
SEGMENT 76	D(1) = 4.8460002-01	F(1) = -1.2226244+02
	D(2) = -9.5769795-02	F(2) = 6.6663158+00
	D(3) = 2.6766727-03	F(3) = 2.3300021+03
	D(4) = 5.2242067-01	F(4) = 1.3059892+02
	D(5) = -8.6683443-02	F(5) = -3.1292128+01
	D(6) = 1.0085432-04	F(6) = -5.5345217+03
SEGMENT 77	D(1) = 5.2242067-01	F(1) = 1.3786814+02
	D(2) = -8.6683443-02	F(2) = 2.9188430+01
	D(3) = 1.0085432-04	F(3) = 5.4385399+03
	D(4) = 5.0047790-01	F(4) = -1.4664909+02
	D(5) = -9.5184640-02	F(5) = -5.7085787+01
	D(6) = -2.0527843-03	F(6) = -2.1640915+03

F

Table 3-20. Summary of Forces and Deflections on Segments (continued)
Maximum Reentry Dynamic Pressure Condition (T_R = 505 Seconds)

	DEFLECTION COLUMN	NODAL FORCES
SEGMENT 78	D(1) = 5.0047790-01	F(1) = 1.0503876+02
	D(2) = -9.5184640-02	F(2) = 4.3739790+01
	D(3) = -2.0527843-03	F(3) = 2.1639428+03
	D(4) = 4.4922369-01	F(4) = -1.1222479+02
	D(5) = -1.1223639-01	F(5) = -8.1085403+01
	D(6) = -2.5372822-03	F(6) = 5.9472589+02
SEGMENT 79	D(1) = 4.4922369-01	F(1) = 7.0371148+01
	D(2) = -1.1223639-01	F(2) = 6.8592590+01
	D(3) = -2.5372822-03	F(3) = -5.9480874+02
	D(4) = 4.0152803-01	F(4) = -7.5566702+01
	D(5) = -1.2842818-01	F(5) = -1.2039860+02
	D(6) = -1.7332430-03	F(6) = 2.8377102+03
SEGMENT 80	D(1) = 4.0152803-01	F(1) = 3.3489060+01
	D(2) = -1.2842818-01	F(2) = 1.0876339+02
	D(3) = -1.7332430-03	F(3) = -2.8377918+03
	D(4) = 3.8252153-01	F(4) = -3.6172015+01
	D(5) = -1.3802853-01	F(5) = -1.7904124+02
	D(6) = 1.1905701-05	F(6) = 4.5605648+03
SEGMENT 81	D(1) = 3.8252153-01	F(1) = -6.1131288+00
	D(2) = -1.3802853-01	F(2) = 1.6826784+02
	D(3) = 1.1905701-05	F(3) = -4.5606528+03
	D(4) = 4.1010521-01	F(4) = 6.6479999+00
	D(5) = -1.3825227-01	F(5) = -2.6005350+02
	D(6) = 2.3795263-03	F(6) = 5.7366758+03
SEGMENT 82	D(1) = 4.1010521-01	F(1) = -4.9121502+01
	D(2) = -1.3825227-01	F(2) = 2.5014373+02
	D(3) = 2.3795263-03	F(3) = -5.7367794+03
	D(4) = 4.9534012-01	F(4) = 5.3851656+01
	D(5) = -1.2861405-01	F(5) = -3.6544763+02
	D(6) = 5.0700664-03	F(6) = 6.2979351+03
SEGMENT 83	D(1) = 4.9534012-01	F(1) = -9.6501442+01
	D(2) = -1.2861405-01	F(2) = 3.5640667+02
	D(3) = 5.0700664-03	F(3) = -6.2980635+03
	D(4) = 6.4258675-01	F(4) = 1.0682458+02
	D(5) = -1.1037457-01	F(5) = -4.9609563+02
	D(6) = 7.7876355-03	F(6) = 6.1110515+03
SEGMENT 84	D(1) = 6.4258675-01	F(1) = -1.4963881+02
	D(2) = -1.1037457-01	F(2) = 4.8792401+02
	D(3) = 7.7876355-03	F(3) = -6.1112745+03
	D(4) = 8.4930934-01	F(4) = 1.6762786+02
	D(5) = -8.6060681-02	F(5) = -6.5154160+02
	D(6) = 1.0223560-02	F(6) = 4.9453912+03

Table 3-20. Summary of Forces and Deflections on Segments (continued)
Maximum Reentry Dynamic Pressure Condition (T_R = 505 Seconds)

	DEFLECTION COLUMN	NODAL FORCES
SEGMENT 85	D(1) = 8.4930934-01	F(1) = -2.1057553+02
	D(2) = -8.6060681-02	F(2) = 6.4424472+02
	D(3) = 1.0223560-02	F(3) = -4.9456661+03
	D(4) = 1.1055621+00	F(4) = 2.3944217+02
	D(5) = -5.9036930-02	F(5) = -8.2936190+02
	D(6) = 1.2042465-02	F(6) = 2.4236342+03
SEGMENT 86	D(1) = 1.1055621+00	F(1) = -2.8253361+02
	D(2) = -5.9036930-02	F(2) = 8.2293896+02
	D(3) = 1.2042465-02	F(3) = -2.4240916+03
	D(4) = 1.3930407+00	F(4) = 3.2754697+02
	D(5) = -3.3061680-02	F(5) = -1.0251103+03
	D(6) = 1.2856078-02	F(6) = -2.0635690+03
SEGMENT 87	D(1) = 1.3930407+00	F(1) = -3.7073227+02
	D(2) = -3.3061680-02	F(2) = 1.0195650+03
	D(3) = 1.2856078-02	F(3) = 2.0628089+03
	D(4) = 1.6836938+00	F(4) = 4.4117046+02
	D(5) = -1.1850304-02	F(5) = -1.2320001+03
	D(6) = 1.2207022-02	F(6) = -9.5109246+03
SEGMENT 88	D(1) = 1.6836938+00	F(1) = -4.8439828+02
	D(2) = -1.1850304-02	F(2) = 1.2273349+03
	D(3) = 1.2207022-02	F(3) = 9.5108588+03
	D(4) = 1.9379660+00	F(4) = 5.9827218+02
	D(5) = 1.4653442-03	F(5) = -1.4438706+03
	D(6) = 9.5477647-03	F(6) = -2.1608845+04
SEGMENT 89	D(1) = 1.9379660+00	F(1) = 7.7688079+01
	D(2) = 1.4653442-03	F(2) = 1.4597581+03
	D(3) = 9.5477647-03	F(3) = 2.1539892+04
	D(4) = 2.0743896+00	F(4) = -9.3196377+01
	D(5) = 5.6935098-03	F(5) = -1.6203314+03
	D(6) = 7.0592218-03	F(6) = -2.1110323+04
SEGMENT 90	D(1) = 2.0743896+00	F(1) = 6.2429943+01
	D(2) = 5.6935098-03	F(2) = 1.6180988+03
	D(3) = 7.0592218-03	F(3) = 2.1107864+04
	D(4) = 2.1733869+00	F(4) = -7.8017263+01
	D(5) = 6.5179004-03	F(5) = -1.7896767+03
	D(6) = 4.9507623-03	F(6) = -2.1736185+04
SEGMENT 91	D(1) = 2.1733869+00	F(1) = 4.7239121+01
	D(2) = 6.5179004-03	F(2) = 1.7878878+03
	D(3) = 4.9507623-03	F(3) = 2.1732159+04
	D(4) = 2.2403432+00	F(4) = -6.2972798+01
	D(5) = 5.2766926-03	F(5) = -1.9879931+03
	D(6) = 3.1215414-03	F(6) = -2.4067734+04

Table 3-20. Summary of Forces and Deflections on Segments (continued)
Maximum Reentry Dynamic Pressure Condition (T_R = 505 Seconds)

	DEFLECTION COLUMN		NODAL FORCES	
SEGMENT 92	D(1) =	2.2403432+00	F(1) =	3.2416771+01
	D(2) =	5.2766926-03	F(2) =	1.9866477+03
	D(3) =	3.1215414-03	F(3) =	2.4063218+04
	D(4) =	2.2791051+00	F(4) =	-4.8617890+01
	D(5) =	3.0788632-03	F(5) =	-2.2621954+03
	D(6) =	1.4707298-03	F(6) =	-2.9487991+04
SEGMENT 93	D(1) =	2.2791051+00	F(1) =	1.7755375+01
	D(2) =	3.0788632-03	F(2) =	2.2612773+03
	D(3) =	1.4707298-03	F(3) =	2.9481825+04
	D(4) =	2.2915317+00	F(4) =	-3.5506948+01
	D(5) =	9.0336709-04	F(5) =	-2.8603156+03
	D(6) =	-1.9738570-04	F(6) =	-3.6996925+04
SEGMENT 94	D(1) =	2.2874606+00	F(1) =	-5.0430351+00
	D(2) =	2.2915317+00	F(2) =	5.0430351+00
	D(3) =	9.0336709-04	F(3) =	2.8598283+03
	D(4) =	-1.9738570-04	F(4) =	3.8003120+06
	D(5) =	0.0000000	F(5) =	0.0000000
	D(6) =	0.0000000	F(6) =	0.0000000
SEGMENT 95	D(1) =	-2.8645033-02	F(1) =	-2.9222799+00
	D(2) =	5.5311344-02	F(2) =	2.8901143+01
	D(3) =	-1.5094150-02	F(3) =	-2.9289659+01
	D(4) =	-1.7723214-01	F(4) =	2.9790038+00
	D(5) =	5.5604517-02	F(5) =	2.6701277-03
	D(6) =	-1.4677303-02	F(6) =	-1.5446658-04
SEGMENT 96	D(1) =	-2.8645033-02	F(1) =	5.4091431+02
	D(2) =	5.5311344-02	F(2) =	2.1188494+02
	D(3) =	-1.5094150-02	F(3) =	-1.2755720+03
	D(4) =	2.1950312-02	F(4) =	-5.3197588+02
	D(5) =	-2.9137630-02	F(5) =	-2.1210873+02
	D(6) =	-3.3953007-03	F(6) =	-7.9687035+02
SEGMENT 97	D(1) =	-2.8645033-02	F(1) =	-4.8400535+02
	D(2) =	5.5311344-02	F(2) =	-2.2495009+02
	D(3) =	-1.5094150-02	F(3) =	-1.4022616+03
	D(4) =	-1.0685861-02	F(4) =	4.8212088+02
	D(5) =	-3.0378134-02	F(5) =	2.2883103+02
	D(6) =	-2.8958804-03	F(6) =	-8.7686201+02
SEGMENT 98	D(1) =	2.1950312-02	F(1) =	3.4087177+02
	D(2) =	-2.9137630-02	F(2) =	2.0668482+02
	D(3) =	-3.3953007-03	F(3) =	1.1756001+03
	D(4) =	-1.0685861-02	F(4) =	-3.4540603+02
	D(5) =	-3.0378134-02	F(5) =	-2.0953462+02
	D(6) =	-2.8958804-03	F(6) =	1.2299733+03

Table 3-20. Summary of Forces and Deflections on Segments (continued)
Maximum Reentry Dynamic Pressure Condition (T_R = 505 Seconds) PAGE 15

	DEFLECTION COLUMN		NODAL FORCES	
SEGMENT 99	D(1) =	2.1950312-02	F(1) =	1.9359369+02
	D(2) =	-2.9137630-02	F(2) =	5.4244653+00
	D(3) =	-3.3953007-03	F(3) =	-3.7872929+02
	D(4) =	1.6042758-02	F(4) =	-1.9159855+02
	D(5) =	-2.3686483-02	F(5) =	-1.3201521+01
	D(6) =	-1.0751598-03	F(6) =	-3.3822424+02
SEGMENT 100	D(1) =	-1.0685861-02	F(1) =	-1.3446867+02
	D(2) =	-3.0378134-02	F(2) =	-1.9400306+01
	D(3) =	-2.8958804-03	F(3) =	-3.5271383+02
	D(4) =	-6.2953501-03	F(4) =	1.3446867+02
	D(5) =	-2.3815368-02	F(5) =	1.7792818+01
	D(6) =	-1.2381272-03	F(6) =	-3.2490780+02
SEGMENT 101	D(1) =	1.6042758-02	F(1) =	4.4404914+01
	D(2) =	-2.3686483-02	F(2) =	-3.6120465+00
	D(3) =	-1.0751598-03	F(3) =	2.8295898+02
	D(4) =	-6.2953501-03	F(4) =	-4.5459023+01
	D(5) =	-2.3815368-02	F(5) =	2.4210168+00
	D(6) =	-1.2381272-03	F(6) =	2.7904495+02
SEGMENT 102	D(1) =	1.6042758-02	F(1) =	-1.3860758+01
	D(2) =	-2.3686483-02	F(2) =	1.6815081+01
	D(3) =	-1.0751598-03	F(3) =	5.5303288+01
	D(4) =	0.0000000	F(4) =	1.4109197+01
	D(5) =	-4.3293626-02	F(5) =	-1.9005236+01
	D(6) =	-2.2235050-03	F(6) =	7.3275935+00
SEGMENT 103	D(1) =	-6.2953501-03	F(1) =	-8.6568661+01
	D(2) =	-2.3815368-02	F(2) =	-2.0213905+01
	D(3) =	-1.2381272-03	F(3) =	4.5862891+01
	D(4) =	0.0000000	F(4) =	8.6077026+01
	D(5) =	-4.3293626-02	F(5) =	1.9005232+01
	D(6) =	-2.2235050-03	F(6) =	-7.3275378+00

Table 3-21. Summary of Forces and Deflections on Segments Landing Condition

	DEFLECTION COLUMN		NODAL FORCES	
SEGMENT 1	D(1) =	2.3529732-01	F(1) =	1.3214127+02
	D(2) =	0.0000000	F(2) =	4.7177703+02
	D(3) =	2.6070551-02	F(3) =	-2.1087843+02
	D(4) =	1.3194370-01	F(4) =	-1.2529547+02
	D(5) =	-3.0941476-04	F(5) =	-4.5470877+02
	D(6) =	7.6271419-03	F(6) =	-4.7268109+02
SEGMENT 2	D(1) =	1.3194370-01	F(1) =	4.2916135+02
	D(2) =	-3.0941476-04	F(2) =	4.5470865+02
	D(3) =	7.6271419-03	F(3) =	4.7268134+02
	D(4) =	9.4914523-02	F(4) =	-4.0299097+02
	D(5) =	2.8282024-02	F(5) =	-4.3157401+02
	D(6) =	2.3996496-03	F(6) =	-2.3324388+02
SEGMENT 3	D(1) =	9.4914523-02	F(1) =	4.0465351+02
	D(2) =	2.8282024-02	F(2) =	4.3157238+02
	D(3) =	2.3996496-03	F(3) =	2.3324326+02
	D(4) =	7.9823627-02	F(4) =	-3.7074282+02
	D(5) =	3.0958796-02	F(5) =	-3.8533287+02
	D(6) =	-3.3193593-04	F(6) =	-1.8472243+01
SEGMENT 4	D(1) =	7.9823627-02	F(1) =	3.7307431+02
	D(2) =	3.0958796-02	F(2) =	3.8533450+02
	D(3) =	-3.3193593-04	F(3) =	1.8472460+01
	D(4) =	7.6221888-02	F(4) =	-3.3557869+02
	D(5) =	1.9985075-02	F(5) =	-3.3933746+02
	D(6) =	-1.4276889-04	F(6) =	2.9439339+01
SEGMENT 5	D(1) =	7.6221888-02	F(1) =	3.3894979+02
	D(2) =	1.9985075-02	F(2) =	3.3933864+02
	D(3) =	-1.4276889-04	F(3) =	-2.9439326+01
	D(4) =	6.2972008-02	F(4) =	-2.9374437+02
	D(5) =	1.4189674-02	F(5) =	-2.9617190+02
	D(6) =	4.1043135-04	F(6) =	-3.1933394+00
SEGMENT 6	D(1) =	6.2972008-02	F(1) =	2.9782064+02
	D(2) =	1.4189674-02	F(2) =	2.9617113+02
	D(3) =	4.1043135-04	F(3) =	3.1933420+00
	D(4) =	4.5037408-02	F(4) =	-2.6277470+02
	D(5) =	1.5354593-02	F(5) =	-2.6576868+02
	D(6) =	5.4718016-04	F(6) =	9.6085985+00
SEGMENT 7	D(1) =	4.5037408-02	F(1) =	2.6614410+02
	D(2) =	1.5354593-02	F(2) =	2.6576806+02
	D(3) =	5.4718016-04	F(3) =	-9.6085670+00
	D(4) =	2.9992634-02	F(4) =	-2.4715043+02
	D(5) =	2.0224711-02	F(5) =	-2.4783579+02
	D(6) =	9.4538920-04	F(6) =	1.8492617+01

Table 3-21. Summary of Forces and Deflections on Segments (continued)
Landing Condition

	DEFLECTION COLUMN		NODAL FORCES	
SEGMENT 8	D(1) =	2.9992634-02	F(1) =	2.4948100+02
	D(2) =	2.0224711-02	F(2) =	2.4783636+02
	D(3) =	9.4538920-04	F(3) =	-1.8492698+01
	D(4) =	1.5697981-02	F(4) =	-2.3680682+02
	D(5) =	2.7148264-02	F(5) =	-2.3388674+02
	D(6) =	1.1385035-03	F(6) =	7.8513663-01
SEGMENT 9	D(1) =	1.5697981-02	F(1) =	2.3847043+02
	D(2) =	2.7148264-02	F(2) =	2.3388633+02
	D(3) =	1.1385035-03	F(3) =	-7.8519404-01
	D(4) =	6.4316807-03	F(4) =	-2.3065768+02
	D(5) =	3.1601212-02	F(5) =	-2.2412625+02
	D(6) =	8.7788668-04	F(6) =	-3.4733407+01
SEGMENT 10	D(1) =	6.4316807-03	F(1) =	2.0238970+02
	D(2) =	3.1601212-02	F(2) =	2.0069207+02
	D(3) =	8.7788668-04	F(3) =	-4.0926836+01
	D(4) =	-5.8130134-03	F(4) =	-1.9242807+02
	D(5) =	3.8325503-02	F(5) =	-1.8252713+02
	D(6) =	9.0102063-04	F(6) =	-1.5504589+01
SEGMENT 11	D(1) =	-5.8130134-03	F(1) =	1.8637435+02
	D(2) =	3.8325503-02	F(2) =	1.9123629+02
	D(3) =	9.0102063-04	F(3) =	1.5503983+01
	D(4) =	-2.1322614-02	F(4) =	-1.7489649+02
	D(5) =	4.6736703-02	F(5) =	-1.6602079+02
	D(6) =	7.8743576-04	F(6) =	-3.4333957+01
SEGMENT 12	D(1) =	-2.1322614-02	F(1) =	1.6618919+02
	D(2) =	4.6736703-02	F(2) =	1.7852231+02
	D(3) =	7.8743576-04	F(3) =	3.4333078+01
	D(4) =	-4.1202714-02	F(4) =	-1.5213531+02
	D(5) =	5.6630596-02	F(5) =	-1.4058721+02
	D(6) =	6.2446878-04	F(6) =	-1.5551045+01
SEGMENT 13	D(1) =	-4.1202714-02	F(1) =	1.3768565+02
	D(2) =	5.6630596-02	F(2) =	1.6124321+02
	D(3) =	6.2446878-04	F(3) =	1.5550656+01
	D(4) =	-7.2507565-02	F(4) =	-1.2014626+02
	D(5) =	7.2604473-02	F(5) =	-9.8870389+01
	D(6) =	6.9106962-04	F(6) =	3.1990805+01
SEGMENT 14	D(1) =	-7.2507565-02	F(1) =	1.0237139+02
	D(2) =	7.2604473-02	F(2) =	1.2450405+02
	D(3) =	6.9106962-04	F(3) =	-3.1991024+01
	D(4) =	-1.0627936-01	F(4) =	-9.0804172+01
	D(5) =	9.3074035-02	F(5) =	-6.5363979+01
	D(6) =	7.6389741-04	F(6) =	-1.1123105+01

Table 3-21. Summary of Forces and Deflections on Segments (continued)
Landing Condition

	DEFLECTION COLUMN	NODAL FORCES
SEGMENT 15	D(1) = -1.0647936-01	F(1) = 7.7089471+01
	D(2) = 9.3074035-02	F(2) = 8.5284676+01
	D(3) = 7.6389741-04	F(3) = 1.1122137+01
	D(4) = -1.2153545-01	F(4) = -7.2353577+01
	D(5) = 1.0150192-01	F(5) = -5.2557390+01
	D(6) = 3.1685023-04	F(6) = -1.3572120+02
SEGMENT 16	D(1) = -1.2153545-01	F(1) = 6.3857629+01
	D(2) = 1.0150192-01	F(2) = 6.4847224+01
	D(3) = 3.1685023-04	F(3) = 1.3571931+02
	D(4) = -1.2288509-01	F(4) = -6.1345186+01
	D(5) = 9.8760292-02	F(5) = -4.4805617+01
	D(6) = -4.3432400-04	F(6) = -2.4769100+02
SEGMENT 17	D(1) = -1.2288509-01	F(1) = 5.5367634+01
	D(2) = 9.8760292-02	F(2) = 5.3439306+01
	D(3) = -4.3432400-04	F(3) = 2.4768910+02
	D(4) = -1.1523171-01	F(4) = -5.3780656+01
	D(5) = 8.8390096-02	F(5) = -4.0362110+01
	D(6) = -1.2739522-03	F(6) = -3.2931726+02
SEGMENT 18	D(1) = -1.1523171-01	F(1) = -2.9257537+00
	D(2) = 8.8390096-02	F(2) = 9.4409989+01
	D(3) = -1.2739522-03	F(3) = -2.9374138+01
	D(4) = -1.2529858-01	F(4) = 3.0070133+00
	D(5) = 8.9049002-02	F(5) = 8.8517205-03
	D(6) = -7.9124687-04	F(6) = -1.1050892-04
SEGMENT 19	D(1) = -1.1523171-01	F(1) = -1.8790191+02
	D(2) = 8.8390096-02	F(2) = -1.1255342+02
	D(3) = -1.2739522-03	F(3) = -5.6667074+02
	D(4) = -1.1332659-01	F(4) = 1.8619866+02
	D(5) = 8.7038193-02	F(5) = 1.1773543+02
	D(6) = 7.1809848-04	F(6) = 3.5008604+02
SEGMENT 20	D(1) = -1.1332659-01	F(1) = -1.9025147+02
	D(2) = 8.7038193-02	F(2) = -1.0622304+02
	D(3) = 7.1809848-04	F(3) = -3.5009017+02
	D(4) = -1.1796796-01	F(4) = 1.8814415+02
	D(5) = 1.0045516-01	F(5) = 1.1296316+02
	D(6) = 2.0440488-03	F(6) = 1.4593190+02
SEGMENT 21	D(1) = -1.1796796-01	F(1) = -1.9706673+02
	D(2) = 1.0045516-01	F(2) = -8.7670576+01
	D(3) = 2.0440488-03	F(3) = -1.4593320+02
	D(4) = -1.4396313-01	F(4) = 1.9083242+02
	D(5) = 1.6479928-01	F(5) = 1.1430283+02
	D(6) = 2.4461162-03	F(6) = -9.0313431+01

Table 3-21. Summary of Forces and Deflections on Segments (continued)
Landing Condition

		DEFLECTION COLUMN		NODAL FORCES
SEGMENT 22	D(1) =	-1.4396313-01	F(1) =	-2.0482183+02
	D(2) =	1.6479928-01	F(2) =	-7.4578967+01
	D(3) =	2.4461162-03	F(3) =	9.0312636+01
	D(4) =	-1.6480730-01	F(4) =	1.9783905+02
	D(5) =	2.1619275-01	F(5) =	1.1426388+02
	D(6) =	9.4207286-04	F(6) =	-7.8053108+01
SEGMENT 23	D(1) =	-1.6480730-01	F(1) =	-2.1256886+02
	D(2) =	2.1619275-01	F(2) =	-7.2418041+01
	D(3) =	9.4207286-04	F(3) =	7.8052181+01
	D(4) =	-1.6966325-01	F(4) =	2.0556070+02
	D(5) =	2.3199023-01	F(5) =	1.1603100+02
	D(6) =	1.2018918-04	F(6) =	-1.4965273+01
SEGMENT 24	D(1) =	-1.6966325-01	F(1) =	-2.2091018+02
	D(2) =	2.3199023-01	F(2) =	-7.2160408+01
	D(3) =	1.2018918-04	F(3) =	1.4964411+01
	D(4) =	-1.6979619-01	F(4) =	2.1321590+02
	D(5) =	2.3645893-01	F(5) =	1.2436381+02
	D(6) =	1.3867758-04	F(6) =	1.6945690+01
SEGMENT 25	D(1) =	-1.6979619-01	F(1) =	-2.2975259+02
	D(2) =	2.3645893-01	F(2) =	-7.6820873+01
	D(3) =	1.3867758-04	F(3) =	-1.6946373+01
	D(4) =	-1.7177139-01	F(4) =	2.2146691+02
	D(5) =	2.4612091-01	F(5) =	1.3061549+02
	D(6) =	3.4484154-04	F(6) =	5.7479922+00
SEGMENT 26	D(1) =	-1.7177139-01	F(1) =	-2.3857489+02
	D(2) =	2.4612091-01	F(2) =	-8.1414454+01
	D(3) =	3.4484154-04	F(3) =	-5.7486103+00
	D(4) =	-1.7599506-01	F(4) =	2.3027033+02
	D(5) =	2.6122393-01	F(5) =	1.3407983+02
	D(6) =	4.8585577-04	F(6) =	6.6986588+00
SEGMENT 27	D(1) =	-1.7599506-01	F(1) =	-2.4581056+02
	D(2) =	2.6122393-01	F(2) =	-8.9106894+01
	D(3) =	4.5585577-04	F(3) =	-6.6995913+00
	D(4) =	-1.7942278-01	F(4) =	2.3889446+02
	D(5) =	2.7223320-01	F(5) =	1.3689749+02
	D(6) =	2.2001026-04	F(6) =	-3.9925548+01
SEGMENT 28	D(1) =	-1.7942278-01	F(1) =	-2.5294638+02
	D(2) =	2.7223320-01	F(2) =	-9.5976812+01
	D(3) =	2.2001026-04	F(3) =	3.9924332+01
	D(4) =	-1.7102991-01	F(4) =	2.4602428+02
	D(5) =	2.5852549-01	F(5) =	1.4103701+02
	D(6) =	-1.3130415-03	F(6) =	-1.8070249+02

Table 3-21. Summary of Forces and Deflections on Segments (continued)
Landing Condition

	DEFLECTION COLUMN	NODAL FORCES
SEGMENT 29	D(1) = -1.7102991-01	F(1) = -2.5966776+02
	D(2) = 2.5852549-01	F(2) = -1.0129856+02
	D(3) = -1.3130415-03	F(3) = 1.8070110+02
	D(4) = -1.3317361-01	F(4) = 2.5313384+02
	D(5) = 1.8311720-01	F(5) = 1.3535725+02
	D(6) = -4.3014873-03	F(6) = -2.7872829+02
SEGMENT 30	D(1) = -1.3317381-01	F(1) = -2.6379514+02
	D(2) = 1.8311720-01	F(2) = -1.0427663+02
	D(3) = -4.3014873-03	F(3) = 2.7872628+02
	D(4) = -9.0238946-02	F(4) = 2.5977012+02
	D(5) = 9.6249351-02	F(5) = 1.1757554+02
	D(6) = -6.0012255-03	F(6) = -1.4957912+02
SEGMENT 31	D(1) = -9.0238946-02	F(1) = -2.6713924+02
	D(2) = 9.6249351-02	F(2) = -9.5743478+01
	D(3) = -6.0012255-03	F(3) = 1.4957614+02
	D(4) = -4.8816716-02	F(4) = 2.6376392+02
	D(5) = 1.1274233-02	F(5) = 1.0204405+02
	D(6) = -5.9735900-03	F(6) = 1.5074411+02
SEGMENT 32	D(1) = -4.8816716-02	F(1) = -2.7021280+02
	D(2) = 1.1274233-02	F(2) = -8.2543694+01
	D(3) = -5.9735900-03	F(3) = -1.5074605+02
	D(4) = -1.4969864-02	F(4) = 2.6698470+02
	D(5) = -5.6055569-02	F(5) = 8.1875523+01
	D(6) = -3.9283273-03	F(6) = 6.9004829+02
SEGMENT 33	D(1) = 2.3529732-01	F(1) = -1.3124442+02
	D(2) = 0.0000000	F(2) = 3.5242413+01
	D(3) = 2.6070551-02	F(3) = 2.1087842+02
	D(4) = 2.3593190-01	F(4) = 1.3124442+02
	D(5) = 5.2600684-02	F(5) = -2.5209192+01
	D(6) = -2.7944949-03	F(6) = -3.7636643+01
SEGMENT 34	D(1) = 2.3593190-01	F(1) = -1.3101903+02
	D(2) = 5.2600684-02	F(2) = 2.5209199+01
	D(3) = -2.7944949-03	F(3) = 3.7636652+01
	D(4) = 2.3715341-01	F(4) = 1.3101903+02
	D(5) = 3.0491038-03	F(5) = -4.2065670+00
	D(6) = -5.4702369-03	F(6) = 2.6118184+01
SEGMENT 35	D(1) = 2.3715341-01	F(1) = -1.3056651+02
	D(2) = 3.0491038-03	F(2) = 4.2065836+00
	D(3) = -5.4702369-03	F(3) = -2.6118188+01
	D(4) = 2.4131044-01	F(4) = 1.3056651+02
	D(5) = -7.0338950-03	F(5) = 8.9609720-01
	D(6) = 2.6698290-03	F(6) = -8.5976113+00

Table 3-21. Summary of Forces and Deflections on Segments (continued)
Landing Condition

	DEFLECTION COLUMN	NODAL FORCES
SEGMENT 36	D(1) = 2.4131044-01	F(1) = -1.2967446+02
	D(2) = -7.0338950-03	F(2) = -8.9606942-01
	D(3) = 2.6698290-03	F(3) = 8.5976161+00
	D(4) = 2.4991925-01	F(4) = 1.2967446+02
	D(5) = -5.8786541-03	F(5) = -2.5438609-02
	D(6) = -1.3119097-03	F(6) = 4.2291656+00
SEGMENT 37	D(1) = 2.4991925-01	F(1) = -1.2849235+02
	D(2) = -5.8786541-03	F(2) = 2.5466226-02
	D(3) = -1.3119097-03	F(3) = -4.2291661+00
	D(4) = 2.5840453-01	F(4) = 1.2849235+02
	D(5) = -6.1237713-03	F(5) = 2.2748736-02
	D(6) = 6.6213508-04	F(6) = -2.0633996+00
SEGMENT 38	D(1) = 2.5840453-01	F(1) = -1.2760134+02
	D(2) = -6.1237713-03	F(2) = -2.2712302-02
	D(3) = 6.6213508-04	F(3) = 2.0634007+00
	D(4) = 2.6269916-01	F(4) = 1.2760134+02
	D(5) = -5.7777740-03	F(5) = 5.8034722-02
	D(6) = -5.4907997-04	F(6) = -5.4360346-01
SEGMENT 39	D(1) = 2.6269916-01	F(1) = -1.2714959+02
	D(2) = -5.7777740-03	F(2) = -5.7977924-02
	D(3) = -5.4907997-04	F(3) = 5.4360723-01
	D(4) = 2.6496805-01	F(4) = 1.2714959+02
	D(5) = -1.4996726-02	F(5) = -2.6808514+00
	D(6) = -1.3563443-03	F(6) = -2.9314843+00
SEGMENT 40	D(1) = 2.6496805-01	F(1) = -1.2598883+02
	D(2) = -1.4996726-02	F(2) = 2.6809017+00
	D(3) = -1.3563443-03	F(3) = 2.9315047+00
	D(4) = 2.6618375-01	F(4) = 1.2598883+02
	D(5) = -1.8235266-02	F(5) = -5.9929713+00
	D(6) = 3.2321118-04	F(6) = 1.7391721+01
SEGMENT 41	D(1) = 2.6618375-01	F(1) = -1.8278790+02
	D(2) = -1.8235266-02	F(2) = 7.4304272-01
	D(3) = 3.2321118-04	F(3) = 8.9507527+01
	D(4) = 2.7118650-01	F(4) = 1.8278790+02
	D(5) = -1.6687180-02	F(5) = -8.9933870+00
	D(6) = -8.1386858-05	F(6) = -1.0627556+01
SEGMENT 42	D(1) = 2.7118650-01	F(1) = -1.8125738+02
	D(2) = -1.6687180-02	F(2) = -6.7566007+00
	D(3) = -8.1386858-05	F(3) = 1.0627862+01
	D(4) = 2.8116854-01	F(4) = 1.8125738+02
	D(5) = -1.9330124-02	F(5) = -1.0892586+01
	D(6) = -7.5016208-05	F(6) = 1.1416203+01

Table 3-21. Summary of Forces and Deflections on Segments (continued)
Landing Condition

	DEFLECTION COLUMN	NODAL FORCES
SEGMENT 43	D(1) = 2.8116854-01	F(1) = -1.7819605+02
	D(2) = -1.9330124-02	F(2) = -2.0607364+01
	D(3) = -7.5016208-05	F(3) = -1.1416147+01
	D(4) = 3.0110516-01	F(4) = 1.7819605+02
	D(5) = -1.9641858-02	F(5) = -2.0704158+01
	D(6) = 3.5953065-05	F(6) = -4.5501230+00
SEGMENT 44	D(1) = 3.0110516-01	F(1) = -1.7386104+02
	D(2) = -1.9641858-02	F(2) = -2.3908902+01
	D(3) = 3.5953065-05	F(3) = 4.5501444+00
	D(4) = 3.2307024-01	F(4) = 1.7386104+02
	D(5) = -1.9333937-02	F(5) = -2.3398681+01
	D(6) = -1.3999490-05	F(6) = 1.8014600+00
SEGMENT 45	D(1) = 3.2307024-01	F(1) = -1.6927215+02
	D(2) = -1.9333937-02	F(2) = -2.3827909+01
	D(3) = -1.3999490-05	F(3) = -1.8014288+00
	D(4) = 3.4450809-01	F(4) = 1.6927215+02
	D(5) = -1.9147008-02	F(5) = -2.3345195+01
	D(6) = 1.5548836-05	F(6) = -1.7552240-01
SEGMENT 46	D(1) = 3.4450809-01	F(1) = -1.6465214+02
	D(2) = -1.9147008-02	F(2) = -2.4199437+01
	D(3) = 1.5548836-05	F(3) = 1.7554267-01
	D(4) = 3.6570715-01	F(4) = 1.6465214+02
	D(5) = -1.8946738-02	F(5) = -2.3705401+01
	D(6) = -1.2037511-05	F(6) = -1.3222466+00
SEGMENT 47	D(1) = 3.6570715-01	F(1) = -1.6000105+02
	D(2) = -1.8946738-02	F(2) = -2.4157040+01
	D(3) = -1.2037511-05	F(3) = 1.3222641+00
	D(4) = 3.8636355-01	F(4) = 1.6000105+02
	D(5) = -1.8637936-02	F(5) = -2.3593169+01
	D(6) = 3.1296930-05	F(6) = 3.6750899+00
SEGMENT 48	D(1) = 3.8636355-01	F(1) = -1.5591327+02
	D(2) = -1.8637936-02	F(2) = -1.7315479+01
	D(3) = 3.1296930-05	F(3) = -3.6750584+00
	D(4) = 4.0071014-01	F(4) = 1.5591327+02
	D(5) = -1.8963153-02	F(5) = -1.7167840+01
	D(6) = -6.3809392-05	F(6) = -1.2774316+01
SEGMENT 49	D(1) = 4.0071014-01	F(1) = -1.5238704+02
	D(2) = -1.8963153-02	F(2) = -1.6786654+01
	D(3) = -6.3809392-05	F(3) = 1.2774365+01
	D(4) = 4.1462151-01	F(4) = 1.5238704+02
	D(5) = -1.6215833-02	F(5) = -1.4558733+01
	D(6) = 2.4057800-04	F(6) = 4.1897105+01

Table 3-21. Summary of Forces and Deflections on Segments (continued)
Landing Condition

	DEFLECTION COLUMN		NODAL FORCES	
SEGMENT 50	D(1) =	4.1462151-01	F(1) =	-1.4953431+02
	D(2) =	-1.6215833-02	F(2) =	-1.2918331+01
	D(3) =	2.4057800-04	F(3) =	-4.1897034+01
	D(4) =	4.2277785-01	F(4) =	1.4953431+02
	D(5) =	-1.1713077-02	F(5) =	9.3096419-03
	D(6) =	-3.0724320-05	F(6) =	-8.3866487+01
SEGMENT 51	D(1) =	4.2277785-01	F(1) =	-1.4789899+02
	D(2) =	-1.1713077-02	F(2) =	-1.5759245+01
	D(3) =	-3.0724320-05	F(3) =	8.3866682+01
	D(4) =	4.2691498-01	F(4) =	1.4789899+02
	D(5) =	-2.0675453-02	F(5) =	7.1651905+00
	D(6) =	-1.2381838-03	F(6) =	-2.8971219+02
SEGMENT 52	D(1) =	4.2691498-01	F(1) =	3.6154386+01
	D(2) =	-2.0675453-02	F(2) =	-1.2415165+01
	D(3) =	-1.2381838-03	F(3) =	-2.1078662+01
	D(4) =	4.2653695-01	F(4) =	-3.6154386+01
	D(5) =	1.5648955-04	F(5) =	1.7613295+00
	D(6) =	3.0354257-03	F(6) =	-8.3145415+00
SEGMENT 53	D(1) =	4.2653695-01	F(1) =	3.7073040+01
	D(2) =	1.5648955-04	F(2) =	-1.7612908+00
	D(3) =	3.0354257-03	F(3) =	8.3145443+00
	D(4) =	4.2412451-01	F(4) =	-3.7073040+01
	D(5) =	1.8680163-03	F(5) =	-3.1919641-02
	D(6) =	-1.7665387-03	F(6) =	3.1467001+00
SEGMENT 54	D(1) =	4.2412451-01	F(1) =	3.8875205+01
	D(2) =	1.8680163-03	F(2) =	3.1981491-02
	D(3) =	-1.7665387-03	F(3) =	-3.1467001+00
	D(4) =	4.1974701-01	F(4) =	-3.8875205+01
	D(5) =	1.8250503-03	F(5) =	7.0739509-02
	D(6) =	9.8573569-04	F(6) =	-1.3734308+00
SEGMENT 55	D(1) =	4.1974701-01	F(1) =	4.0677042+01
	D(2) =	1.8250503-03	F(2) =	-7.0681043-02
	D(3) =	9.8573569-04	F(3) =	1.3734307+00
	D(4) =	4.1703040-01	F(4) =	-4.0677042+01
	D(5) =	1.5979081-03	F(5) =	-4.1071727-01
	D(6) =	-9.2589819-04	F(6) =	-6.8385781-01
SEGMENT 56	D(1) =	4.1703040-01	F(1) =	4.1594382+01
	D(2) =	1.5979081-03	F(2) =	4.1076932-01
	D(3) =	-9.2589819-04	F(3) =	6.8385801-01
	D(4) =	4.1598883-01	F(4) =	-4.1594382+01
	D(5) =	3.8482627-03	F(5) =	2.7905647-01
	D(6) =	1.5659148-03	F(6) =	8.1262323+00

Table 3-21. Summary of Forces and Deflections on Segments (continued)
Landing Condition

	DEFLECTION COLUMN		NODAL FORCES	
SEGMENT 57	D(1) =	-1.1523171-01	F(1) =	2.4566295+02
	D(2) =	8.8390096-02	F(2) =	6.2582397+01
	D(3) =	-1.2739522-03	F(3) =	9.2535989+02
	D(4) =	-1.1746681-01	F(4) =	-2.4566295+02
	D(5) =	6.5048665-02	F(5) =	-4.8804557+01
	D(6) =	-2.1006046-03	F(6) =	-1.8649020+02
SEGMENT 58	D(1) =	-1.1746681-01	F(1) =	2.4855926+02
	D(2) =	6.5048665-02	F(2) =	3.4597072+01
	D(3) =	-2.1006046-03	F(3) =	1.8649068+02
	D(4) =	-1.2117003-01	F(4) =	-2.4855926+02
	D(5) =	1.1597953-02	F(5) =	-2.3516888+01
	D(6) =	-1.7302962-03	F(6) =	4.3552393+02
SEGMENT 59	D(1) =	-1.2117003-01	F(1) =	2.5435366+02
	D(2) =	1.1597953-02	F(2) =	-5.0178704+00
	D(3) =	-1.7302962-03	F(3) =	-4.3552468+02
	D(4) =	-1.2665815-01	F(4) =	-2.5435366+02
	D(5) =	-3.3419178-02	F(5) =	-1.4852903+01
	D(6) =	-2.4505049-05	F(6) =	1.3804929+02
SEGMENT 60	D(1) =	-1.2665815-01	F(1) =	2.6330890+02
	D(2) =	-3.3419178-02	F(2) =	-2.9246065+01
	D(3) =	-2.4505049-05	F(3) =	-1.3804925+02
	D(4) =	-1.3319132-01	F(4) =	-2.6330890+02
	D(5) =	-2.3936292-02	F(5) =	-1.7318142+01
	D(6) =	1.9314514-04	F(6) =	-8.2528877+01
SEGMENT 61	D(1) =	-1.3319132-01	F(1) =	2.7681621+02
	D(2) =	-2.3936292-02	F(2) =	-3.2833400+01
	D(3) =	1.9314514-04	F(3) =	8.2529058+01
	D(4) =	-1.3645540-01	F(4) =	-2.7681621+02
	D(5) =	-1.6836948-02	F(5) =	-2.6737221+01
	D(6) =	2.3840604-05	F(6) =	-1.5427812-02
SEGMENT 62	D(1) =	-1.3645540-01	F(1) =	2.9161559+02
	D(2) =	-1.6836948-02	F(2) =	-1.7361782+01
	D(3) =	2.3840604-05	F(3) =	1.5637817-02
	D(4) =	-1.3940697-01	F(4) =	-2.9161559+02
	D(5) =	-9.6728458-03	F(5) =	-1.6677710+01
	D(6) =	2.6677638-04	F(6) =	1.5614380+02
SEGMENT 63	D(1) =	-1.3940697-01	F(1) =	3.0119300+02
	D(2) =	-9.6728458-03	F(2) =	-1.1857121+01
	D(3) =	2.6677638-04	F(3) =	-1.5614334+02
	D(4) =	-1.4111291-01	F(4) =	-3.0119300+02
	D(5) =	-2.8490330-04	F(5) =	1.4668098+00
	D(6) =	4.1342156-04	F(6) =	3.2346318+01

Table 3-21. Summary of Forces and Deflections on Segments (continued)
Landing Condition

	DEFLECTION COLUMN		NODAL FORCES	
SEGMENT 64	D(1) =	-1.4111291-01	F(1) =	3.0598297+02
	D(2) =	-2.8490330-04	F(2) =	-1.5734279+01
	D(3) =	4.1342156-04	F(3) =	-3.2345861+01
	D(4) =	-1.4205706-01	F(4) =	-3.0598297+02
	D(5) =	5.0557315-03	F(5) =	1.3527579+01
	D(6) =	3.6441861-04	F(6) =	-1.5831729+02
SEGMENT 65	D(1) =	-1.4205706-01	F(1) =	4.3652258+02
	D(2) =	5.0557315-03	F(2) =	-1.3573456+01
	D(3) =	3.6441861-04	F(3) =	-1.2822368+02
	D(4) =	-1.4890804-01	F(4) =	-4.3652258+02
	D(5) =	6.4042904-02	F(5) =	1.1888567+01
	D(6) =	7.2570601-03	F(6) =	-2.5457607+01
SEGMENT 66	D(1) =	-1.4890804-01	F(1) =	4.3728034+02
	D(2) =	6.4042904-02	F(2) =	-3.7884620-01
	D(3) =	7.2570601-03	F(3) =	2.5457445+01
	D(4) =	-1.5966604-01	F(4) =	-4.3728034+02
	D(5) =	1.4601944-01	F(5) =	6.2507030+00
	D(6) =	1.0368302-03	F(6) =	-3.8759706+01
SEGMENT 67	D(1) =	-1.5966604-01	F(1) =	4.3817647+02
	D(2) =	1.4601944-01	F(2) =	7.3468848+00
	D(3) =	1.0368302-03	F(3) =	3.8759612+01
	D(4) =	-1.7129709-01	F(4) =	-4.3817647+02
	D(5) =	1.2491377-01	F(5) =	2.1004587+00
	D(6) =	-2.8045473-03	F(6) =	-9.3186641-01
SEGMENT 68	D(1) =	-1.7129709-01	F(1) =	4.3893473+02
	D(2) =	1.2491377-01	F(2) =	9.4092721+00
	D(3) =	-2.8045473-03	F(3) =	9.3171689-01
	D(4) =	-1.7910101-01	F(4) =	-4.3893473+02
	D(5) =	1.2177761-01	F(5) =	-3.8624586+00
	D(6) =	2.9969441-03	F(6) =	8.7429248+01
SEGMENT 69	D(1) =	-1.7910101-01	F(1) =	5.7934840+02
	D(2) =	1.2177761-01	F(2) =	8.5724061+00
	D(3) =	2.9969441-03	F(3) =	8.5695685+01
	D(4) =	-1.9071872-01	F(4) =	-5.7934840+02
	D(5) =	1.1685563-01	F(5) =	-4.1294800+00
	D(6) =	-2.7494194-03	F(6) =	1.3046773+01
SEGMENT 70	D(1) =	-1.9071872-01	F(1) =	5.8045490+02
	D(2) =	1.1685563-01	F(2) =	4.1294779+00
	D(3) =	-2.7494194-03	F(3) =	-1.3046832+01
	D(4) =	-2.1368734-01	F(4) =	-5.8045490+02
	D(5) =	7.3621153-02	F(5) =	1.4054504-01
	D(6) =	-1.1294493-04	F(6) =	3.4152440+00

G

Table 3-21. Summary of Forces and Deflections on Segments (continued)
Landing Condition

	DEFLECTION COLUMN		NODAL FORCES	
SEGMENT 71	D(1) =	-2.1368734-01	F(1) =	5.8193696+02
	D(2) =	7.3621153-02	F(2) =	-1.4055762-01
	D(3) =	-1.1294493-04	F(3) =	-3.4152627+00
	D(4) =	-2.3623125-01	F(4) =	-5.8193696+02
	D(5) =	7.8085211-02	F(5) =	5.9126641-01
	D(6) =	3.1700474-04	F(6) =	-7.3075128-01
SEGMENT 72	D(1) =	-2.3623125-01	F(1) =	5.8341877+02
	D(2) =	7.8085211-02	F(2) =	-5.9127767-01
	D(3) =	3.1700474-04	F(3) =	7.3073027-01
	D(4) =	-2.5765431-01	F(4) =	-5.8341877+02
	D(5) =	-2.1492451-02	F(5) =	-8.2746799+00
	D(6) =	-7.3395729-03	F(6) =	-4.7076735+01
SEGMENT 73	D(1) =	-2.5765431-01	F(1) =	5.8452734+02
	D(2) =	-2.1492451-02	F(2) =	8.2746669+00
	D(3) =	-7.3395729-03	F(3) =	4.7076746+01
	D(4) =	-2.6726544-01	F(4) =	-5.8452734+02
	D(5) =	-8.4291283-02	F(5) =	-2.0491482+01
	D(6) =	1.2019570-03	F(6) =	1.5506365+02
SEGMENT 74	D(1) =	-3.0457265-01	F(1) =	2.5662203+00
	D(2) =	-8.9647423-02	F(2) =	7.8200874-05
	D(3) =	1.7840178-04	F(3) =	3.3514660-04
	D(4) =	-2.9886574-01	F(4) =	-2.7180330+00
	D(5) =	-8.9532548-02	F(5) =	-1.8232644+01
	D(6) =	2.3529616-04	F(6) =	1.4681575+02
SEGMENT 75	D(1) =	-2.9886574-01	F(1) =	7.8498248+00
	D(2) =	-8.9532548-02	F(2) =	1.8232579+01
	D(3) =	2.3529616-04	F(3) =	-1.4681172+02
	D(4) =	-2.8912030-01	F(4) =	-8.3473821+00
	D(5) =	-8.8544080-02	F(5) =	-4.0062692+01
	D(6) =	5.0543695-04	F(6) =	6.1065565+02
SEGMENT 76	D(1) =	-2.8912030-01	F(1) =	1.3477411+01
	D(2) =	-8.8544080-02	F(2) =	4.0061613+01
	D(3) =	5.0543695-04	F(3) =	-6.1067306+02
	D(4) =	-2.6726544-01	F(4) =	-1.4396370+01
	D(5) =	-8.4291283-02	F(5) =	-6.5891730+01
	D(6) =	1.2019570-03	F(6) =	1.4295310+03
SEGMENT 77	D(1) =	-2.6726544-01	F(1) =	-5.5966462+01
	D(2) =	-8.4291283-02	F(2) =	8.6384864+01
	D(3) =	1.2019570-03	F(3) =	-1.5845968+03
	D(4) =	-2.3120308-01	F(4) =	5.9531007+01
	D(5) =	-7.6790135-02	F(5) =	-1.1249923+02
	D(6) =	1.9625885-03	F(6) =	1.0145837+03

Table 3-21. Summary of Forces and Deflections on Segments (continued)
Landing Condition

Segment	Deflection	Column	Nodal	Forces
SEGMENT 78	D(1) =	-2.3120308-01	F(1) =	-5.5053546+01
	D(2) =	-7.6790135-02	F(2) =	1.1249924+02
	D(3) =	1.9625885-03	F(3) =	-1.0145210+03
	D(4) =	-1.8121806-01	F(4) =	5.8819930+01
	D(5) =	-6.6313125-02	F(5) =	-1.4109369+02
	D(6) =	2.4368464-03	F(6) =	5.6744057+02
SEGMENT 79	D(1) =	-1.8121806-01	F(1) =	-5.4341122+01
	D(2) =	-6.6313125-02	F(2) =	1.4109358+02
	D(3) =	2.4368464-03	F(3) =	-5.6738974+02
	D(4) =	-1.2270974-01	F(4) =	5.8353167+01
	D(5) =	-5.4746575-02	F(5) =	-1.7169607+02
	D(6) =	2.7058343-03	F(6) =	2.3117790+02
SEGMENT 80	D(1) =	-1.2270974-01	F(1) =	-5.3875141+01
	D(2) =	-5.4746575-02	F(2) =	1.7169561+02
	D(3) =	2.7058343-03	F(3) =	-2.3114169+02
	D(4) =	-5.9499369-02	F(4) =	5.8191314+01
	D(5) =	-4.3288693-02	F(5) =	-2.0404157+02
	D(6) =	2.8361025-03	F(6) =	-1.2478466+01
SEGMENT 81	D(1) =	-5.9499369-02	F(1) =	-5.3712842+01
	D(2) =	-4.3288693-02	F(2) =	2.0404148+02
	D(3) =	2.8361025-03	F(3) =	1.2501710+01
	D(4) =	5.8636190-03	F(4) =	5.8412495+01
	D(5) =	-3.2639534-02	F(5) =	-2.3803540+02
	D(6) =	2.8783432-03	F(6) =	-1.8725513+02
SEGMENT 82	D(1) =	5.8636190-03	F(1) =	-5.3934384+01
	D(2) =	-3.2639534-02	F(2) =	2.3803540+02
	D(3) =	2.8783432-03	F(3) =	1.8726437+02
	D(4) =	7.1763033-02	F(4) =	5.9127995+01
	D(5) =	-2.3165899-02	F(5) =	-2.7370410+02
	D(6) =	2.8668857-03	F(6) =	-3.2261400+02
SEGMENT 83	D(1) =	7.1763033-02	F(1) =	-5.4649968+01
	D(2) =	-2.3165899-02	F(2) =	2.7370385+02
	D(3) =	2.8668857-03	F(3) =	3.2259643+02
	D(4) =	1.3716347-01	F(4) =	6.0496091+01
	D(5) =	-1.5034496-02	F(5) =	-3.1115461+02
	D(6) =	2.8197712-03	F(6) =	-4.5513262+02
SEGMENT 84	D(1) =	1.3716347-01	F(1) =	-5.6018764+01
	D(2) =	-1.5034496-02	F(2) =	3.1115450+02
	D(3) =	2.8197712-03	F(3) =	4.5507875+02
	D(4) =	2.0125303-01	F(4) =	6.2753140+01
	D(5) =	-8.3102657-03	F(5) =	-3.5053588+02
	D(6) =	2.7390795-03	F(6) =	-6.3145421+02

Table 3-21. Summary of Forces and Deflections on Segments (continued)
Landing Condition

		DEFLECTION COLUMN		NODAL FORCES
SEGMENT 85	D(1) =	2.0125303-01	F(1) =	-5.8273868+01
	D(2) =	-8.3102657-03	F(2) =	3.5053585+02
	D(3) =	2.7390795-03	F(3) =	6.3138464+02
	D(4) =	2.6308395-01	F(4) =	6.6262312+01
	D(5) =	-3.0303794-03	F(5) =	-3.9196824+02
	D(6) =	2.6107554-03	F(6) =	-9.1369279+02
SEGMENT 86	D(1) =	2.6308395-01	F(1) =	-6.1785256+01
	D(2) =	-3.0303794-03	F(2) =	3.9196816+02
	D(3) =	2.6107554-03	F(3) =	9.1359986+02
	D(4) =	3.2121364-01	F(4) =	7.1628906+01
	D(5) =	7.7337369-04	F(5) =	-4.3558331+02
	D(6) =	2.4054298-03	F(6) =	-1.3895762+03
SEGMENT 87	D(1) =	3.2121364-01	F(1) =	-6.7148099+01
	D(2) =	7.7337369-04	F(2) =	4.3558337+02
	D(3) =	2.4054298-03	F(3) =	1.3894398+03
	D(4) =	3.7334929-01	F(4) =	7.9906068+01
	D(5) =	3.0661169-03	F(5) =	-4.8160270+02
	D(6) =	2.0775765-03	F(6) =	-2.1909738+03
SEGMENT 88	D(1) =	3.7334929-01	F(1) =	-7.5417769+01
	D(2) =	3.0661169-03	F(2) =	4.8160364+02
	D(3) =	2.0775765-03	F(3) =	2.1909383+03
	D(4) =	4.1598883-01	F(4) =	9.3147221+01
	D(5) =	3.8482627-03	F(5) =	-5.3088640+02
	D(6) =	1.5659148-03	F(6) =	-3.5318765+03
SEGMENT 89	D(1) =	4.1598883-01	F(1) =	-7.8658754+00
	D(2) =	3.8482627-03	F(2) =	5.3060625+02
	D(3) =	1.5659148-03	F(3) =	3.5237100+03
	D(4) =	4.3843189-01	F(4) =	9.4360820+00
	D(5) =	3.6068548-03	F(5) =	-5.6908222+02
	D(6) =	1.1577585-03	F(6) =	-3.4725113+03
SEGMENT 90	D(1) =	4.3843189-01	F(1) =	-6.2845728+00
	D(2) =	3.6068548-03	F(2) =	5.6908136+02
	D(3) =	1.1577585-03	F(3) =	3.4720852+03
	D(4) =	4.5470491-01	F(4) =	7.8536862+00
	D(5) =	2.9102504-03	F(5) =	-6.1343046+02
	D(6) =	8.1038432-04	F(6) =	-3.5786280+03
SEGMENT 91	D(1) =	4.5470491-01	F(1) =	-4.6638655+00
	D(2) =	2.9102504-03	F(2) =	6.1343138+02
	D(3) =	8.1038432-04	F(3) =	3.5780595+03
	D(4) =	4.6568385-01	F(4) =	6.2172338+00
	D(5) =	1.9932574-03	F(5) =	-6.6963621+02
	D(6) =	5.0925624-04	F(6) =	-3.9481779+03

Table 3-21. Summary of Forces and Deflections on Segments (continued)
Landing Condition

		DEFLECTION COLUMN		NODAL FORCES
SEGMENT 92	D(1) =	4.6508385-01	F(1) =	-3.0517237+00
	D(2) =	1.9932574-03	F(2) =	6.6963676+02
	D(3) =	5.0925624-04	F(3) =	3.9475682+03
	D(4) =	4.7201819-01	F(4) =	4.5769014+00
	D(5) =	1.0591342-03	F(5) =	-7.5379464+02
	D(6) =	2.3896959-04	F(6) =	-4.8067404+03
SEGMENT 93	D(1) =	4.7201819-01	F(1) =	-1.4132586+00
	D(2) =	1.0591342-03	F(2) =	7.5379630+02
	D(3) =	2.3896959-04	F(3) =	4.8057643+03
	D(4) =	4.7404427-01	F(4) =	2.8262145+00
	D(5) =	2.9993281-04	F(5) =	-9.4952660+02
	D(6) =	-3.2104189-05	F(6) =	-5.9891293+03
SEGMENT 94	D(1) =	4.7338437-01	F(1) =	5.3325080-01
	D(2) =	4.7404427-01	F(2) =	-5.3325080-01
	D(3) =	2.9993281-04	F(3) =	9.4951027+02
	D(4) =	-3.2104189-05	F(4) =	6.1523758+05
	D(5) =	0.0000000	F(5) =	0.0000000
	D(6) =	0.0000000	F(6) =	0.0000000
SEGMENT 95	D(1) =	-1.4969864-02	F(1) =	-2.9222751+00
	D(2) =	-5.6055569-02	F(2) =	-2.9290500+01
	D(3) =	-3.9283273-03	F(3) =	-2.9301412+01
	D(4) =	-5.1582954-02	F(4) =	2.9789990+00
	D(5) =	-5.6352734-02	F(5) =	-2.4247945-03
	D(6) =	-3.4480621-03	F(6) =	0.0000000
SEGMENT 96	D(1) =	-1.4969864-02	F(1) =	7.1377858+01
	D(2) =	-5.6055569-02	F(2) =	1.8913490+01
	D(3) =	-3.9283273-03	F(3) =	-2.3242291+02
	D(4) =	3.8249791-03	F(4) =	-7.0198361+01
	D(5) =	-8.3462303-02	F(5) =	-2.3688616+01
	D(6) =	-1.3849012-03	F(6) =	-1.2889893+02
SEGMENT 97	D(1) =	-1.4969864-02	F(1) =	-2.1442706+02
	D(2) =	-5.6055569-02	F(2) =	-6.1998301+01
	D(3) =	-3.9283273-03	F(3) =	-2.7691877+02
	D(4) =	-7.9163176-03	F(4) =	2.1359219+02
	D(5) =	-8.4011352-02	F(5) =	5.9138494+01
	D(6) =	-1.1639685-03	F(6) =	-1.5796894+02
SEGMENT 98	D(1) =	3.8249791-03	F(1) =	9.0377760+01
	D(2) =	-8.3462303-02	F(2) =	4.1862039+01
	D(3) =	-1.3849012-03	F(3) =	3.0772102+02
	D(4) =	-7.9163176-03	F(4) =	-9.1579961+01
	D(5) =	-8.4011352-02	F(5) =	-4.4749931+01
	D(6) =	-1.1639685-03	F(6) =	3.3012350+02

Table 3-21. Summary of Forces and Deflections on Segments (continued)
Landing Condition

	DEFLECTION COLUMN		NODAL FORCES	
SEGMENT 99	D(1) =	3.8249791-03	F(1) =	-1.7690608+01
	D(2) =	-8.3462303-02	F(2) =	-1.8173069+01
	D(3) =	-1.3849012-03	F(3) =	-1.7882212+02
	D(4) =	3.9942940-03	F(4) =	1.7508292+01
	D(5) =	-7.0603319-02	F(5) =	6.5371837+00
	D(6) =	-1.9526014-04	F(6) =	-1.5812593+02
SEGMENT 100	D(1) =	-7.9163176-03	F(1) =	-1.1964499+02
	D(2) =	-8.4011352-02	F(2) =	-1.4416024+01
	D(3) =	-1.6639685-03	F(3) =	-1.7208300+02
	D(4) =	-2.9464929-03	F(4) =	1.1964499+02
	D(5) =	-7.0861567-02	F(5) =	4.5454218+00
	D(6) =	-3.1022168-04	F(6) =	-1.5776283+02
SEGMENT 101	D(1) =	3.9942940-03	F(1) =	2.1332821+01
	D(2) =	-7.0603319-02	F(2) =	-2.3621753+01
	D(3) =	-1.9526014-04	F(3) =	1.3689137+02
	D(4) =	-2.9464929-03	F(4) =	-2.1839232+01
	D(5) =	-7.0861567-02	F(5) =	2.0292794+01
	D(6) =	-3.1022168-04	F(6) =	1.3308782+02
SEGMENT 102	D(1) =	3.9942940-03	F(1) =	-2.0309960+01
	D(2) =	-7.0603319-02	F(2) =	1.7083989+01
	D(3) =	-1.9526014-04	F(3) =	2.1252423+01
	D(4) =	0.0000000	F(4) =	2.0673995+01
	D(5) =	-7.6662532-02	F(5) =	-2.1691812+01
	D(6) =	-7.3847934-04	F(6) =	-1.5623838+00
SEGMENT 103	D(1) =	-2.9464929-03	F(1) =	-9.5364831+01
	D(2) =	-7.0861567-02	F(2) =	-2.4838400+01
	D(3) =	-3.1022168-04	F(3) =	2.4675100+01
	D(4) =	0.0000000	F(4) =	9.4823242+01
	D(5) =	-7.6662532-02	F(5) =	2.1691769+01
	D(6) =	-7.3847934-04	F(6) =	1.5625550+00

$$P_{n+1} = (F4) \cos \theta + (F5) \sin \theta$$

$$S_{n+1} = (F4) \sin \theta - (F5) \cos \theta$$

The algebraic signs of the loadings obtained from the above expressions are such that a positive "P" places the segment in compression and a positive "S" represents a shear load acting towards the interior of the component. The results of this transfer of loads are summarized in table 3-22 for the upper frustum and table 3-23 for the lower frustum. Because the segment orientation in the cylindrical bulkheads is parallel to the longitudinal centerline of the vehicle, the meridional and shear loadings are obtained directly from the computer printouts illustrated in tables 3-17 through 3-21, inclusive.

The unit area and section modulus (I/y) of the actual sandwich configurations were calculated in table 3-24 for subsequent use in determining the stresses in the face sheets. It should be noted that initially the data in this table were based on the sandwich overall thickness and face thickness shown in table 1-1. However, when the axial and discontinuity stresses were first calculated, some discontinuity stresses were found to exceed the limiting allowable stress. The face thicknesses were then increased as required to provide positive margins of safety. The segments where these changes were found necessary are indicated by an asterisk (*) in column (2) of table 3-24.

The final meridional and discontinuity stresses are calculated from the following equations based on the sign conventions established in figure 3-1 for moment, and previously in this paragraph for the meridional loading:

At node "n"

$$\text{Stress in inner face} = \sigma_{IF} = -\frac{P(n)}{A} - \frac{M(n)}{(I/y)}$$

$$\text{Stress in outer face} = \sigma_{OF} = -\frac{P(n)}{A} + \frac{M(n)}{(I/y)}$$

At node "n + 1"

$$\sigma_{IF} = +\frac{P(n+1)}{A} + \frac{M(n+1)}{(I/y)}$$

$$\sigma_{OF} = +\frac{P(n+1)}{A} + \frac{M(n+1)}{(I/y)}$$

Table 3-22. Summary of Meridional and Shear Loadings - Upper Frustum

①	②	③	④	⑤	⑥	⑦
SEGMENT No.	DESIGN COND. / LOAD COMP.	LIFT-OFF (T=0)	MAX DYNAMIC PRESSURE (T=77)	MAX. LONG. ACCELERATION (T=138)	MAX. REENTRY DYN. PRESS. (T_R=505)	LANDING
2	P(2)	1461.281	2004.466	2720.406	1320.891	624.991
	S(2)	-140.073	-192.222	-220.802	-91.833	-18.065
	P(3)	-1362.017	-1872.164	-2543.194	-1237.435	-590.127
	S(3)	121.377	170.778	203.530	83.327	20.211
3	P(3)	1362.484	1872.897	2544.364	1238.608	591.302
	S(3)	-120.904	-156.281	-195.042	-82.150	-19.034
	P(4)	-1188.571	-1648.389	-2240.305	-1095.926	-534.627
	S(4)	51.039	75.627	88.593	36.382	10.317
4	P(4)	1189.236	1649.179	2241.962	1097.578	536.276
	S(4)	-50.380	-55.595	-77.842	-34.734	-8.670
	P(5)	-1030.406	-1451.490	-1961.862	-961.066	-477.238
	S(5)	6.012	18.066	15.248	5.042	2.658
5	P(5)	1031.364	1452.631	1964.283	963.452	479.623
	S(5)	-5.058	11.145	0.415	-2.660	-0.275
	P(6)	-888.929	-1284.496	-1712.234	-836.005	-417.133
	S(6)	-0.499	15.944	9.592	3.423	1.717
6	P(6)	891.031	1285.866	1715.114	838.921	420.016
	S(6)	2.607	18.804	9.076	-0.505	1.166
	P(7)	-789.560	-1170.617	-1536.918	-747.181	-373.737
	S(7)	1.080	19.473	15.622	7.425	2.117
7	P(7)	789.559	1171.780	1539.296	749.562	376.118
	S(7)	-1.079	8.872	0.370	-5.042	0.266
	P(8)	-733.026	-1105.557	-1429.471	-686.341	-350.008
	S(8)	0.816	9.191	0.371	-5.045	0.486
8	P(8)	733.686	1106.344	1431.122	687.991	351.657
	S(8)	-0.158	10.552	10.244	6.693	1.163
	P(9)	-695.266	-1057.604	-1340.408	-627.229	-332.829
	S(9)	-0.994	-2.546	-27.728	-32.161	-2.068
9	P(9)	695.737	1058.243	1341.385	628.406	334.006
	S(9)	1.465	16.729	35.311	33.338	3.242
	P(10)	-671.583	-1025.556	-1275.333	-579.870	-321.581
	S(10)	-2.777	-14.050	-56.453	-60.194	-4.619
10	P(10)	633.871	907.178	863.197	138.499	285.022
	S(10)	-1.795	12.564	7.611	3.371	1.200
	P(11)	-595.705	-887.284	-781.070	-71.576	-265.133
	S(11)	-5.259	-17.188	-76.876	-82.326	-7.001
11	P(11)	596.457	858.160	752.946	73.455	267.010
	S(11)	-6.305	0.488	-44.032	-31.285	-3.438
	P(12)	-547.785	-793.909	-592.787	88.681	-241.065
	S(12)	-6.025	-11.877	-72.469	-79.457	-6.275
12	P(12)	548.860	793.190	598.472	-85.967	243.747
	S(12)	-10.884	-10.898	-100.182	-112.337	-8.721
	P(13)	-479.784	-709.040	-340.781	270.627	-206.986
	S(13)	-18.804	-9.660	-104.683	-116.556	-8.166

Table 3-22. Summary of Meridional and Shear Loadings - Upper Frustum (continued)

①	②	③	④	⑤	⑥	⑦
SEGMENT No.	DESIGN COND. / LOAD COMP.	LIFT-OFF (T=0)	MAX. DYNAMIC PRESSURE (T=77)	MAX. LONG. ACCELERATION (T=130)	MAX. REENTRY DYN. PRESS. (T_R = 505)	LANDING.
13	P(13)	480.309	711.133	353.140	-266.239	211.378
	S(13)	-15.625	-11.341	-173.330	-200.307	-16.687
	P(14)	-312.058	-615.270	30.250	625.098	-134.868
	S(14)	-32.806	4.622	-187.154	-217.914	-15.044
14	P(14)	375.081	617.918	-24.692	-619.440	160.425
	S(14)	-9.711	8.440	-139.240	-175.296	-15.631
	P(15)	-322.447	-617.637	247.627	871.674	-110.427
	S(15)	-1.637	62.051	-102.217	-166.648	-17.989
15	P(15)	324.203	619.729	-343.130	-867.206	114.816
	S(15)	-36.379	+12.019	-133.170	-138.856	-5.796
	P(16)	-340.747	-669.242	246.934	917.918	-88.325
	S(16)	70.603	97.674	105.832	26.414	-13.999
16	P(16)	341.819	670.319	-244.825	-913.256	91.008
	S(16)	-97.797	-43.903	-239.141	-214.918	-0.700
	P(17)	-374.378	-717.956	189.941	899.883	-75.060
	S(17)	137.138	115.994	274.983	185.800	-11.694
17	P(17)	375.331	718.850	-188.064	-898.011	76.938
	S(17)	-158.845	-64.514	-362.638	-318.231	1.364
	P(18)	-404.634	-754.219	110.895	869.360	-66.569
	S(18)	194.354	118.639	404.323	311.820	-9.489

Table 3-23. Summary of Meridional and Shear Loadings - Lower Frustum

①	②	③	④	⑤	⑥	⑦
SEGMENT No.	DESIGN COND. / LOAD COMP.	LIFT-OFF (T = 0)	MAX. DYNAMIC PRESSURE (T = 77)	MAX. LONG. ACCELERATION (T = 138)	MAX. REENTRY DYN. PRESS. (T_R = 508)	LANDING
19	P(18)	2863.294	3512.934	3565.407	402.368	-217.754
	S(18)	201.655	473.115	713.685	287.247	23.640
	P(20)	-2853.385	-3500.799	-3544.576	-522.897	218.374
	S(20)	-164.982	-426.026	-660.792	-275.664	-29.060
20	P(20)	2853.836	3501.334	3545.699	483.265	-217.239
	S(20)	152.517	351.569	530.311	212.816	16.909
	P(21)	-2838.621	-3479.598	-3522.776	-479.327	218.145
	S(21)	-114.789	-310.657	-408.931	-207.386	-23.912
21	P(21)	2839.809	3480.782	3525.256	481.802	-215.670
	S(21)	87.401	147.560	202.576	69.301	-2.793
	P(22)	-2772.954	-3359.663	-3371.538	-435.095	221.147
	S(22)	-34.723	-166.787	-287.798	-135.438	-24.005
22	P(22)	2774.520	3361.529	3375.452	439.005	-217.239
	S(22)	-8.290	-88.431	-161.505	-81.428	-17.929
	P(23)	-2672.308	-3157.538	-3096.727	-341.057	227.495
	S(23)	-8.314	-108.701	-199.386	-99.815	-21.039
23	P(23)	2674.033	3159.501	3100.847	345.980	-223.371
	S(23)	-36.936	-158.722	-273.241	-128.632	-23.132
	P(24)	-2560.977	-2938.072	-2791.268	-234.362	235.248
	S(24)	-18.348	-101.162	-186.049	-93.232	-19.414
24	P(24)	2562.741	2940.174	2793.676	238.769	-230.840
	S(24)	-46.581	-177.759	-308.739	-146.231	-26.855
	P(25)	-2424.266	-2695.038	-2445.609	-109.381	245.607
	S(25)	-61.920	-138.894	-250.339	-121.786	-23.781
25	P(25)	2426.208	2698.079	2450.671	114.248	-240.822
	S(25)	-64.164	-162.517	-285.194	-137.681	-26.321
	P(26)	-2261.247	-2458.617	-2107.434	13.101	155.796
	S(26)	-106.372	-150.542	-278.542	-134.088	-26.008
26	P(26)	2263.262	2461.017	2112.475	-8.061	-250.756
	S(26)	-100.908	-159.668	-275.097	-133.625	-25.839
	P(27)	-2075.036	-2237.141	-1793.402	127.416	265.242
	S(27)	-140.278	-146.030	-267.696	-130.827	-25.473
27	P(27)	2076.916	2239.382	1798.181	-122.719	-260.547
	S(27)	-115.681	-136.719	-237.954	-114.571	-21.877
	P(28)	-1887.614	-2039.632	-1524.437	227.980	274.253
	S(28)	-171.766	-164.062	-253.169	-124.752	-24.425
28	P(28)	1889.353	2041.704	1528.789	-223.639	-269.901
	S(28)	-121.628	-113.394	-206.513	-98.496	-18.622
	P(29)	-1690.912	-1840.186	-1277.698	320.230	282.461
	S(29)	-200.360	-203.997	-253.558	-127.259	-25.203
29	P(29)	1692.605	1842.200	1281.926	-316.002	-278.232
	S(29)	-136.450	-120.888	-192.450	-89.539	-16.599
	P(30)	-1519.244	-1664.863	-1065.946	307.894	286.543
	S(30)	-150.964	-166.897	-167.928	-86.104	-17.070

Table 3-23. Summary of Meridional and Shear Loadings - Lower Frustum (continued)

①	②	③	④	⑤	⑥	⑦
SEGMENT No.	DESIGN COND. / LOAD COMP.	LIFT-OFF (T = 0)	MAX. DYNAMIC PRESSURE (T = 77)	MAX. LONG. ACCELERATION (T = 138)	MAX. REENTRY DYN. PRESS. (T_R = 805)	LANDING
30	P (30)	1520.571	1666.446	1089.264	-384.877	-283.229
	S (30)	-145.428	-138.245	-180.687	-83.461	-16.622
	P (31)	-1432.879	-1574.458	-999.405	412.916	288.134
	S (31)	3.156	-7.825	19.069	7.902	1.887
31	P (31)	1433.834	1576.121	1001.926	-410.478	-282.694
	S (31)	-232.277	-238.113	-274.810	-126.958	-24.770
	P (32)	-1361.213	-1499.512	-933.107	427.422	282.265
	S (32)	110.933	111.986	148.593	77.296	-110.078
32	P (32)	1362.133	1500.610	935.406	-425.123	-279.967
	S (32)	-329.279	-351.793	-406.250	-183.581	-38.046
	P (33)	-1309.154	-1444.497	-890.044	428.713	276.755
	S (33)	245.632	264.666	327.156	162.861	37.302

Table 3-24. Calculation of Sandwich Unit Area and Section Modulus

①	②	③	④	⑤	⑥	⑦	⑧	⑨	⑩
COMP.	SEG. No.	t	t_F	A	$t^3 - t_c^3$	I	h	h/2	I/y
REF.		TABLE 1-1		2 ④	**	⑥/11.032	③-④	.5 ⑧	⑦/⑨
UPPER FRUSTUM	2-3 *	1.600	.026	.052	.386521	.035036	1.574	.787	.044518
	4-9 *	1.600	.018	.036	.270306	.024502	1.582	.791	.030976
	10-17	4.000	.020	.040	1.900864	.172303	3.980	1.990	.086816
LOWER FRUSTUM	19-20 *	2.700	.038	.076	1.618773	.146462	2.662	1.331	.110039
	21-23 *	2.700	.020	.040	.861904	.078128	2.680	1.340	.058304
	24-26	2.700	.018	.036	.776069	.070419	2.682	1.341	.052512
	27-30	2.700	.020	.040	.861904	.078128	2.680	1.340	.058304
	31-32	2.700	.027	.054	1.157518	.104922	2.673	1.336	.078534
INNER CYLINDRICAL BULKHEAD	33-34 *	.375	.030	.060	.021478	.001947	.345	.1725	.011286
	35-40	.375	.010	.020	.007995	.000725	.365	.182	.003984
	41-47	3.40	.010	.020	.689528	.062502	3.390	1.695	.036874
	48-51	3.80	.010	.020	.861848	.078122	3.790	1.895	.041225
	52 *	.375	.014	.028	.010952	.000993	.361	.1805	.005501
	53-56	.375	.010	.020	.007995	.000725	.365	.182	.003984
OUTER CYLINDRICAL BULKHEAD	57-60	4.000	.036	.072	3.394165	.307662	3.964	1.982	.155228
	61-64	4.000	.070	.140	6.407544	.580089	3.930	1.965	.299267
	65-68	.680	.014	.028	.037264	.003378	.666	.333	.010144
	69 *	.680	.016	.032	.042334	.003837	.664	.332	.011557
	70-73	.680	.014	.028	.037264	.003378	.666	.333	.010144

* Reflects final face thickness required to provide acceptable stress level. (refer to paragraph 3.6.1

** $t_c = t - 2t_F$

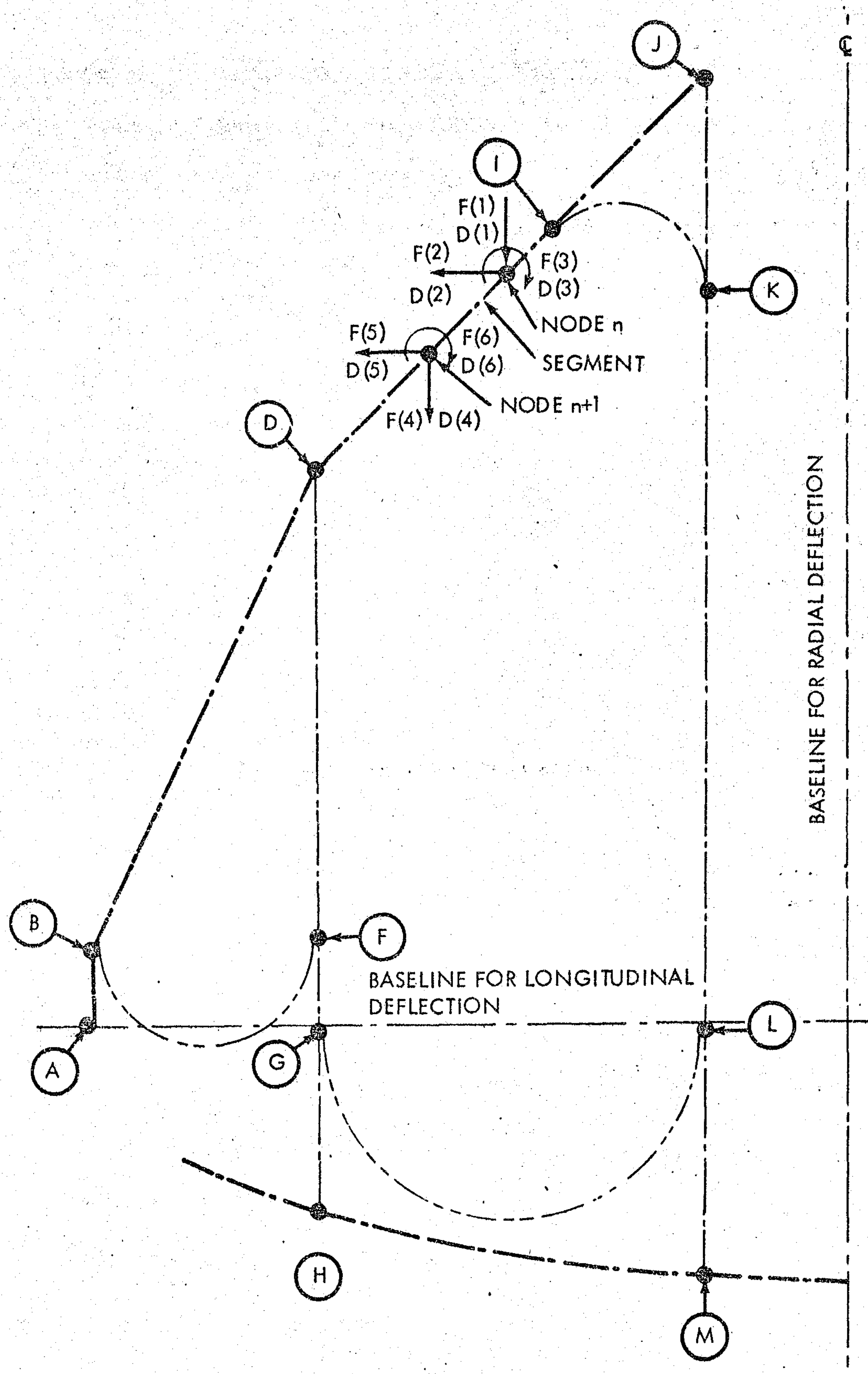

Figure 3-1. Positive Forces and Delections on Typical Segments

The meridional stress distributions are calculated in tables 3-25 through 3-28, inclusive. Distribution curves are plotted for the maximum longitudinal acceleration condition (T = 138 seconds) in figures 3-2 through 3-5, inclusive.

3.6.2 HOOP STRESS DISTRIBUTION

The hoop stress due to internal pressure acting on a structural component was computed from the expression:

$$\sigma_H = \frac{pRe}{2t_F}$$

where σ_H = hoop stress (positive when tension)

p = pressure

Re = equivalent cylindrical radius = $(R_1 + R_2)/2 \cos \theta$

R_1 = radius at small end of segment

R_2 = radius at large end of segment

θ = 1/2 cone angle = 0° for cylinder

t_F = face thickness

Note that the average pressure acting on a segment was used in the hoop stress computations because these values had been previously calculated for input data to the reference 1 computer program. To be rigorously correct, the maximum pressure value on a segment should have been used. However, in those segments where the peak pressures are found, the distance between nodes has been reduced in order to better define the distribution of the discontinuity bending moment. The error involved is therefore reduced in these cases and is not considered of a magnitude that will invalidate in any way the results of this feasibility study. Tables 3-29 through 3-32 were set up to calculate the hoop stress distribution in each major structural component for the various design conditions investigated. The results are plotted in figures 3-6 through 3-9, inclusive.

3.7 CALCULATION OF ALLOWABLE STRESSES

3.7.1 ALLOWABLE OVERALL BUCKLING STRESSES

The SERV primary structure has been broken down into basically two frustums and two cylindrical bulkheads. Note that the aft heat shield has been omitted from this portion of the analysis because due to its method of construction, sandwich panels supported by radial and cross beams, it is not subject to the same type of buckling failure discussed in this paragraph. The critical buckling stresses for the frustums and cylinders were calculated using the methods discussed previously in volume 3, appendix E. In all cases, that portion throughout which the sandwich configuration remained constant was isolated and the critical buckling stresses determined. When the length of the component appeared in any parameter,

Table 3-25. Calculation of Meridional Stresses - Upper Frustum

SEC. NO.	ROW NO.	ITEM	DESIGN COND. / REFERENCE	LIFT-OFF (T=0)	MAX. DYNAMIC PRESSURE (T=77)	MAX. LONG. ACCELERATION (T=138)	MAX. REENTRY DYN. PRESS. (T_R=508)	LANDING
2	①	P(2)	NOTE (1)	1461.281	2004.466	2720.406	1320.891	624.991
	②	M(2)	NOTE (2)	2716.187	3642.692	4491.768	1881.768	472.681
	③	A	TABLE 3-24	.052				
	④	I/y	TABLE 3-24	.044518				
	⑤	σ_{AXIAL}	- ①/③	-28102	-38548	-52316	-25402	-12019
	⑥	$\sigma_{BEND.}$	- ②/④	-61014	-81826	-100899	-42270	-10618
	⑦	σ_{IF}	⑤ + ⑥	-89116	-120374	-153215	-67672	-22637
	⑧	σ_{OF}	⑤ - ⑥	+32912	+43278	+48583	+16868	-1401
	①	P(3)	NOTE (1)	-1362.017	-1872.164	-2543.194	-1237.435	-590.127
	②	M(3)	NOTE (2)	-1194.801	-1561.131	-1976.404	-848.410	-233.244
	③	A	TABLE 3-24	.052				
	④	I/y	TABLE 3-24	.044518				
	⑤	σ_{AXIAL}	①/③	-26193	-36004	-48908	-23797	-11349
	⑥	$\sigma_{BEND.}$	②/④	-26839	-35068	-44396	-19058	-5239
	⑦	σ_{IF}	⑤ + ⑥	-53032	-71072	-93304	-42855	-16588
	⑧	σ_{OF}	⑤ - ⑥	+646	-936	-4512	-4739	-6110
3	①	P(3)	NOTE (1)	1362.484	1872.897	2544.364	1238.608	591.302
	②	M(3)	NOTE (2)	1194.801	1561.134	1976.406	848.408	233.243
	③	A	TABLE 3-24	.052				
	④	I/y	TABLE 3-24	.044518				
	⑤	σ_{AXIAL}	- ①/③	-26202	-36018	-40921	-23820	-11371
	⑥	$\sigma_{BEND.}$	- ②/④	-26839	-35068	-44396	-19058	-5239
	⑦	σ_{IF}	⑤ + ⑥	-53041	-71086	-93327	-42878	-16610
	⑧	σ_{OF}	⑤ - ⑥	+637	-950	-4535	-4762	-6132
	①	P(4)	NOTE (1)	-1188.571	-1648.389	-2240.305	-1095.926	-534.627
	②	M(4)	NOTE (2)	-10.322	12.017	-17.739	-20.738	-18.472
	③	A	TABLE 3-24	.052				
	④	I/y	TABLE 3-24	.044518				
	⑤	σ_{AXIAL}	①/③	-22857	-31700	-43083	-21076	-10281
	⑥	$\sigma_{BEND.}$	②/④	-232	+270	-398	-466	-415
	⑦	σ_{IF}	⑤ + ⑥	-23089	-31430	-43481	-21542	-10696
	⑧	σ_{OF}	⑤ - ⑥	-22625	-31970	-42685	-20610	-9866
4	①	P(4)	NOTE (1)	1189.236	1649.179	2241.962	1097.578	536.276
	②	M(4)	NOTE (2)	10.324	-12.017	17.741	20.738	18.472
	③	A	TABLE 3-24	.036				
	④	I/y	TABLE 3-24	.030976				
	⑤	σ_{AXIAL}	- ①/③	-33035	-45811	-62277	-30489	-14897
	⑥	$\sigma_{BEND.}$	- ②/④	-333	+388	-573	-669	-596
	⑦	σ_{IF}	⑤ + ⑥	-33368	-45423	-62850	-31158	-15493
	⑧	σ_{OF}	⑤ - ⑥	-32702	-46199	-61704	-29820	-14301
	①	P(5)	NOTE (1)	-1030.406	-1451.490	-1961.862	-961.066	-477.238
	②	M(5)	NOTE (2)	177.537	239.451	289.710	116.688	29.439
	③	A	TABLE 3-24	.036				
	④	I/y	TABLE 3-24	.030976				
	⑤	σ_{AXIAL}	①/③	-28623	-40319	-54497	-26696	-13257
	⑥	$\sigma_{BEND.}$	②/④	+5726	+7730	+9353	+3767	+950
	⑦	σ_{IF}	⑤ + ⑥	-22897	-32589	-45144	-22929	-12307
	⑧	σ_{OF}	⑤ - ⑥	-34349	-48049	-63850	-30463	-14207

Table 3-25. Calculation of Meridional Stresses - Upper Frustum (continued)

Sec. No.	Row No.	Item	Reference \ Design Cond.	Lift-off (T=0)	Max. Dynamic Pressure (T=77)	Max. Long. Acceleration (T=138)	Max. Reentry Dyn. Press. (T_R=508)	Landing
5	(1)	P(5)	Note (1)	1031.364	1452.361	1964.253	963.452	479.623
	(2)	M(5)	Note (2)	-177.536	-239.450	-289.709	-116.689	-29.439
	(3)	A	Table 3-24	.036				
	(4)	I/y	Table 3-24	.030976				
	(5)	σ_{AXIAL}	-(1)/(3)	-28649	-40351	-54563	-26763	-13323
	(6)	$\sigma_{BEND.}$	-(2)/(4)	+5726	+7730	+9353	+3767	+950
	(7)	σ_{IF}	(5)+(6)	-22923	-32621	-45210	-22996	-12373
	(8)	σ_{OF}	(5)-(6)	-34375	-48081	-63916	-30530	-14273
	(1)	P(6)	Note (1)	-888.929	-1284.496	-1712.234	-836.005	-417.133
	(2)	M(6)	Note (2)	-5.067	-21.433	-39.565	-30.954	-3.193
	(3)	A	Table 3-24	.036				
	(4)	I/y	Table 3-24	.030976				
	(5)	σ_{AXIAL}	(1)/(3)	-24693	-35681	-47562	-23223	-11587
	(6)	$\sigma_{BEND.}$	(2)/(4)	-164	-692	-1277	-999	-103
	(7)	σ_{IF}	(5)+(6)	-24857	-36373	-48839	-24222	-11690
	(8)	σ_{OF}	(5)-(6)	-24529	-34989	-46285	-22224	-11484
6	(1)	P(6)	Note (1)	891.031	1285.866	1715.114	838.921	420.016
	(2)	M(6)	Note (2)	5.068	21.434	39.565	30.954	3.193
	(3)	A	Table 3-24	.036				
	(4)	I/y	Table 3-24	.030976				
	(5)	σ_{AXIAL}	-(1)/(3)	-24751	-35719	-47642	-23304	-11667
	(6)	$\sigma_{BEND.}$	-(2)/(4)	-164	-692	-1277	-999	-103
	(7)	σ_{IF}	(5)+(6)	-24915	-36411	-48919	-24303	-11770
	(8)	σ_{OF}	(5)-(6)	-24587	-35027	-46365	-22305	-11564
	(1)	P(7)	Note (1)	-789.560	-1170.617	-1536.918	-747.181	-373.737
	(2)	M(7)	Note (2)	-7.345	31.814	123.438	136.102	9.609
	(3)	A	Table 3-24	.036				
	(4)	I/y	Table 3-24	.030976				
	(5)	σ_{AXIAL}	(1)/(3)	-21932	-32517	-42693	-20755	-10382
	(6)	$\sigma_{BEND.}$	(2)/(4)	-237	+1027	+3985	+4394	+310
	(7)	σ_{IF}	(5)+(6)	-22169	-31490	-38708	-16361	-10072
	(8)	σ_{OF}	(5)-(6)	-21695	-33544	-46678	-25149	-10692
7	(1)	P(7)	Note (1)	789.559	1171.750	1539.296	749.562	376.118
	(2)	M(7)	Note (2)	7.345	-31.813	-123.437	-136.102	-9.609
	(3)	A	Table 3-24	.036				
	(4)	I/y	Table 3-24	.030976				
	(5)	σ_{AXIAL}	-(1)/(3)	-21932	-32549	-42759	-20821	-10448
	(6)	$\sigma_{BEND.}$	-(2)/(4)	-237	+1027	+3985	+4394	+310
	(7)	σ_{IF}	(5)+(6)	-22169	-31522	-38774	-16427	-10138
	(8)	σ_{OF}	(5)-(6)	-21695	-33576	-46744	-25215	-10758
	(1)	P(8)	Note (1)	-733.026	-1105.557	-1429.471	-686.341	-350.008
	(2)	M(8)	Note (2)	11.794	64.721	228.209	239.502	18.493
	(3)	A	Table 3-24	.036				
	(4)	I/y	Table 3-24	.030976				
	(5)	σ_{AXIAL}	(1)/(3)	-20362	-30710	-39708	-19065	-9723
	(6)	$\sigma_{BEND.}$	(2)/(4)	+381	+2089	+7367	+7732	+597
	(7)	σ_{IF}	(5)+(6)	-19981	-28621	-32341	-11333	-9126
	(8)	σ_{OF}	(5)-(6)	-20743	-32799	-47075	-26797	-10320

Table 3-25. Calculation of Meridional Stresses - Upper Frustum (continued)

Sec. No.	Row No.	Item	Design Cond. / Reference	Lift-off (T=0)	Max. Dynamic Pressure (T=77)	Max. Long. Acceleration (T=138)	Max. Reentry Dyn. Press. (T_R=505)	Land...
8	①	P(8)	Note (1)	733.686	1106.344	1431.122	687.991	351.6[illegible]
	②	M(8)	Note (2)	-11.794	-64.719	-228.209	-239.503	-18.4[illegible]
	③	A	Table 3-24	.036				
	④	I/y		.030976				
	⑤	σ_{AXIAL}	-①/③	-20380	-30732	-39754	-19111	-9768
	⑥	$\sigma_{BEND.}$	-②/④	+381	+2089	+7367	+7732	+597
	⑦	σ_{IF}	⑤+⑥	-19999	-28643	-32387	-11379	-9171
	⑧	σ_{OF}	⑤-⑥	-20761	-32821	-47121	-26843	-10365
	①	P(9)	Note (1)	-695.266	-1057.604	-1340.408	-627.229	-332.829
	②	M(9)	Note (2)	7.599	-8.350	27.357	36.373	0.785
	③	A	Table 3-24	.036				
	④	I/y		.030976				
	⑤	σ_{AXIAL}	①/③	-19313	-29378	-37234	-17423	-9245
	⑥	$\sigma_{BEND.}$	②/④	+245	-270	+883	+1174	+25
	⑦	σ_{IF}	⑤+⑥	-19068	-29648	-36351	-16249	-9220
	⑧	σ_{OF}	⑤-⑥	-19558	-29108	-38117	-18597	-9270
9	①	P(9)	Note (1)	695.737	1058.243	1341.505	628.406	334.006
	②	M(9)	Note (2)	-7.594	8.355	-27.353	-36.373	-0.785
	③	A	Table 3-24	.036				
	④	I/y		.030976				
	⑤	σ_{AXIAL}	-①/③	-19326	-29396	-37267	-17456	-9278
	⑥	$\sigma_{BEND.}$	-②/④	+245	-270	+883	+1174	+25
	⑦	σ_{IF}	⑤+⑥	-19081	-29666	-36384	-16282	-9253
	⑧	σ_{OF}	⑤-⑥	-19571	-29126	-38150	-18630	-9303
	①	P(10)	Note (1)	-671.583	-1025.556	-1275.333	-579.870	-321.581
	②	M(10)	Note (2)	-11.638	-147.509	-385.089	-383.177	-34.733
	③	A	Table 3-24	.036				
	④	I/y		.030976				
	⑤	σ_{AXIAL}	①/③	-18655	-28488	-35426	-16108	-8933
	⑥	$\sigma_{BEND.}$	②/④	-376	-4762	-12432	-12370	-1121
	⑦	σ_{IF}	⑤+⑥	-19031	-33250	-47858	-28478	-10054
	⑧	σ_{OF}	⑤-⑥	-18279	-23726	+22994	-3738	-7812
10	①	P(10)	Note (1)	633.871	907.178	863.197	158.499	285.022
	②	M(10)	Note (2)	-64.788	-90.440	-441.712	-463.411	-40.927
	③	A	Table 3-24	.040				
	④	I/y		.088816				
	⑤	σ_{AXIAL}	-①/③	-15847	-22679	-21580	-3962	-7126
	⑥	$\sigma_{BEND.}$	-②/④	+729	+1018	+4973	+5218	+461
	⑦	σ_{IF}	⑤+⑥	-15118	-21661	-16607	+1256	-6665
	⑧	σ_{OF}	⑤-⑥	-16576	-23697	-26553	-9180	-7587
	①	P(11)	Note (1)	-595.705	-857.284	-751.070	-71.576	-265.133
	②	M(11)	Note (2)	43.202	-116.692	-125.784	-108.607	-15.505
	③	A	Table 3-24	.040				
	④	I/y		.088816				
	⑤	σ_{AXIAL}	①/③	-14893	-21432	-18777	-1789	-6628
	⑥	$\sigma_{BEND.}$	②/④	+486	-1314	-1416	-1223	-175
	⑦	σ_{IF}	⑤+⑥	-14407	-22746	-20193	-3012	-6803
	⑧	σ_{OF}	⑤-⑥	-15379	-20118	-17361	-566	-6453

Table 3-25. Calculation of Meridional Stresses - Upper Frustum (continued)

SEC. NO.	ROW NO.	ITEM	DESIGN COND. / REFERENCE	LIFT-OFF (T=0)	MAX. DYNAMIC PRESSURE (T=77)	MAX. LONG. ACCELERATION (T=138)	MAX. REENTRY DYN. PRESS. (T_R=505)	LANDING
	①	P(11)	NOTE (1)	594.457	838.180	752.946	73.455	267.010
	②	M(11)	NOTE (2)	-43.184	116.697	125.797	108.599	15.504
	③	A	TABLE 3-24	.040				
	④	I/y		.088816				
	⑤	σ_{AXIAL}	- ①/③	-14911	-21455	-18824	-1836	-6675
	⑥	$\sigma_{BEND.}$	- ②/④	+486	-1314	-1416	-1223	-175
	⑦	σ_{IF}	⑤ + ⑥	-14425	-22769	-20240	-3059	-6850
11	⑧	σ_{OF}	⑤ - ⑥	-15397	-20141	-17408	-613	-6500
	①	P(12)	NOTE (1)	-547.785	-793.909	-592.787	58.651	-241.065
	②	M(12)	NOTE (2)	58.669	-214.951	-284.024	-254.489	-34.334
	③	A	TABLE 3-24	.040				
	④	I/y		.088816				
	⑤	σ_{AXIAL}	①/③	-13695	-19848	-14820	+1466	-6027
	⑥	$\sigma_{BEND.}$	②/④	+661	-2420	-3198	-2865	-387
	⑦	σ_{IF}	⑤ + ⑥	-13034	-22268	-18018	-1399	-6414
	⑧	σ_{OF}	⑤ - ⑥	-14356	-17428	-11622	+4331	-5640
	①	P(12)	NOTE (1)	548.860	795.190	595.472	-55.967	243.747
	②	M(12)	NOTE (2)	-58.662	214.956	284.035	254.484	34.333
	③	A	TABLE 3-24	.040				
	④	I/y		.088816				
	⑤	σ_{AXIAL}	- ①/③	-13722	-19880	-14887	+1399	-6094
	⑥	$\sigma_{BEND.}$	- ②/④	+660	-2420	-3198	-2865	-387
	⑦	σ_{IF}	⑤ + ⑥	-13062	-22300	-18085	-1466	-6481
12	⑧	σ_{OF}	⑤ - ⑥	-14382	-17460	-11689	+4264	-5707
	①	P(13)	NOTE (1)	-479.754	-709.040	-348.751	270.627	-206.986
	②	M(13)	NOTE (2)	55.122	-223.535	-162.612	-95.933	-15.551
	③	A	TABLE 3-24	.040				
	④	I/y		.088816				
	⑤	σ_{AXIAL}	①/③	-11994	-17726	-8719	+6766	-5175
	⑥	$\sigma_{BEND.}$	②/④	+621	-2517	-1831	-1080	-175
	⑦	σ_{IF}	⑤ + ⑥	-11373	-20243	-10550	+5686	-5350
	⑧	σ_{OF}	⑤ - ⑥	-12615	-15209	-6888	+7846	-5000
	①	P(13)	NOTE (1)	480.509	711.133	353.140	-266.239	211.375
	②	M(13)	NOTE (2)	-55.120	223.537	162.614	95.929	15.551
	③	A	TABLE 3-24	.040				
	④	I/y		.088816				
	⑤	σ_{AXIAL}	- ①/③	-12013	-17778	-8829	+6656	-5284
	⑥	$\sigma_{BEND.}$	- ②/④	+621	-2517	-1831	-1080	-175
	⑦	σ_{IF}	⑤ + ⑥	-11392	-20295	-10660	+5576	-5459
13	⑧	σ_{OF}	⑤ - ⑥	-12634	-15261	-6998	+7736	-5109
	①	P(14)	NOTE (1)	-372.858	-615.270	30.250	625.098	-154.868
	②	M(14)	NOTE (2)	-405.027	-559.209	-969.745	-619.114	31.991
	③	A	TABLE 3-24	.040				
	④	I/y		.088816				
	⑤	σ_{AXIAL}	①/③	-9321	-15382	+756	+15627	-3872
	⑥	$\sigma_{BEND.}$	②/④	-4560	-6296	-10919	-6971	+360
	⑦	σ_{IF}	⑤ + ⑥	-13881	-21678	-10163	+8656	-3512
	⑧	σ_{IF}	⑤ - ⑥	-4761	-9086	+11675	+22598	-4232

Table 3-25. Calculation of Meridional Stresses - Upper Frustum (continued)

Seg. No.	Row No.	Item	Design Cond. / Reference	Lift-Off ($T=0$)	Max. Dynamic Pressure ($T=77$)	Max. Long. Acceleration ($T=138$)	Max. Reentry Dyn. Press. ($T_R=505$)	Landing
14	(1)	P(14)	Note (1)	375.081	617.918	-24.692	-619.440	160.425
	(2)	M(14)	Note (2)	405.029	559.210	969.743	619.110	-31.991
	(3)	A	Table 3-24	.040				
	(4)	I/y		.088816				
	(5)	σ_{AXIAL}	-(1)/(3)	-9377	-15448	+617	+15486	-4011
	(6)	$\sigma_{BEND.}$	-(2)/(4)	-4560	-6296	-10919	-6971	+360
	(7)	σ_{IF}	(5) + (6)	-13937	-21744	-10302	+8515	-3651
	(8)	σ_{OF}	(5) - (6)	-4817	-9152	+11536	+22457	-4371
	(1)	P(15)	Note (1)	-322.447	-617.637	247.627	871.674	-110.427
	(2)	M(15)	Note (2)	-1220.118	-619.259	-2915.159	-2473.706	-11.123
	(3)	A	Table 3-24	.040				
	(4)	I/y		.088816				
	(5)	σ_{AXIAL}	(1)/(3)	-8061	-15441	+6191	+21792	-2761
	(6)	$\sigma_{BEND.}$	(2)/(4)	-13738	-6972	-32822	-27852	-125
	(7)	σ_{IF}	(5) + (6)	-21799	-22413	-26631	-6060	-2886
	(8)	σ_{OF}	(5) - (6)	+5677	-8469	+39013	+49644	-2636
15	(1)	P(15)	Note (1)	324.203	619.729	-343.130	-867.286	114.816
	(2)	M(15)	Note (2)	1220.122	619.264	2907.978	2473.698	11.122
	(3)	A	Table 3-24	.040				
	(4)	I/y		.088816				
	(5)	σ_{AXIAL}	-(1)/(3)	-8105	-15493	+8578	+21682	-2870
	(6)	$\sigma_{BEND.}$	-(2)/(4)	-13738	-6972	-32742	-27852	-125
	(7)	σ_{IF}	(5) + (6)	-21843	-22465	-24164	-6170	-2995
	(8)	σ_{OF}	(5) - (6)	+5633	-8521	+41320	+49534	-2745
	(1)	P(16)	Note (1)	-340.747	-669.242	246.934	917.918	-88.325
	(2)	M(16)	Note (2)	38.895	767.361	-221.606	-714.522	-135.721
	(3)	A	Table 3-24	.040				
	(4)	I/y		.088816				
	(5)	σ_{AXIAL}	(1)/(3)	-8519	-16731	+6173	+22948	-2208
	(6)	$\sigma_{BEND.}$	(2)/(4)	+438	+8640	-2495	-8045	-1528
	(7)	σ_{IF}	(5) + (6)	-8081	-8091	+3678	+14903	-3736
	(8)	σ_{OF}	(5) - (6)	-8957	-25371	+8668	+30993	-680
16	(1)	P(16)	Note (1)	341.819	670.519	-244.825	-915.236	91.008
	(2)	M(16)	Note (2)	-38.878	-767.333	222.135	714.517	135.719
	(3)	A	Table 3-24	.040				
	(4)	I/y		.088816				
	(5)	σ_{AXIAL}	-(1)/(3)	-8545	-16763	+6121	+22881	-2275
	(6)	$\sigma_{BEND.}$	-(2)/(4)	+438	+8640	-2501	-8045	-1528
	(7)	σ_{IF}	(5) + (6)	-8107	-8123	+3620	+14836	-3803
	(8)	σ_{OF}	(5) - (6)	-8983	-25403	+8622	+30926	-747
	(1)	P(17)	Note (1)	-374.578	-717.956	189.941	899.888	-75.060
	(2)	M(17)	Note (2)	2281.932	2285.891	4618.602	3042.248	-247.691
	(3)	A	Table 3-24	.040				
	(4)	I/y		.088816				
	(5)	σ_{AXIAL}	(1)/(3)	-9364	-17949	+4749	+22497	-1877
	(6)	$\sigma_{BEND.}$	(2)/(4)	+25693	+25737	+52002	+34253	-2789
	(7)	σ_{IF}	(5) + (6)	+16329	+7788	+56751	+56750	-4666
	(8)	σ_{OF}	(5) - (6)	-35057	-43686	-47253	-11756	+912

Table 3-25. Calculation of Meridional Stresses - Upper Frustum (continued)

Sec. No.	Row No.	ITEM	DESIGN COND / REFERENCE	LIFT-OFF (T=0)	MAX. DYNAMIC PRESSURE (T=77)	MAX. LONG. ACCELERATION (T=138)	MAX. REENTRY DYN. PRESS. (T_R=508)	LANDING
17	①	P(17)	NOTE (1)	375.331	718.850	-188.064	-898.011	76.938
	②	M(17)	NOTE (2)	-2281.895	-2285.032	-4618.846	-3042.249	247.689
	③	A	TABLE 3-24	.040				
	④	I/y	TABLE 3-24	.088816				
	⑤	σ_{AXIAL}	-①/③	-9383	-17971	+4702	+22450	-1923
	⑥	$\sigma_{BEND.}$	-②/④	+25692	+25737	+52001	+34253	-2789
	⑦	σ_{IF}	⑤+⑥	+16309	+7766	+56703	+56703	-4712
	⑧	σ_{OF}	⑤-⑥	-35075	-43708	-47299	-11803	+866
	①	P(18)	NOTE (1)	-404.634	-754.219	110.595	869.560	-66.569
	②	M(18)	NOTE (2)	4857.771	3616.096	10193.200	7618.886	-329.317
	③	A	TABLE 3-24	.040				
	④	I/y	TABLE 3-24	.088816				
	⑤	σ_{AXIAL}	①/③	-10166	-18855	+2765	+21739	-1664
	⑥	$\sigma_{BEND.}$	②/④	+54695	+40714	+114768	+85783	-3708
	⑦	σ_{IF}	⑤+⑥	+44579	+21859	+117533	+107522	-5372
	⑧	σ_{OF}	⑤-⑥	-64811	-59569	-112003	-64044	+2044

NOTES: 1) The number in parentheses following the "P" or "M" in rows ① and ② identify the pertinent boundary node per figure 1-1. The meridional load "P" is from table 3-22.

2) The bending moment acting at the node is obtained from the pertinent design condition shown in tables 3-17 through 3-21 inclusive.

Table 3-26. Calculation of Meridional Stresses - Lower Frustum

Sec. No.	Load No.	Item	Reference / Design Cond.	Lift-off (T=0)	Max. Dynamic Pressure (T=77)	Max. Long. Acceleration (T=138)	Max. Reentry Dyn. Press. (TR=503)	Landing
	①	P(18)	Note (1)	2863.294	3512.934	3555.407	482.368	-217.754
	②	M(18)	Note (2)	-3186.110	-8045.648	-12631.193	-5304.588	-566.671
	③	A	Table 3-24	.076				
	④	I/y		.110039				
	⑤	σ_{AXIAL}	- ①/③	-37675	-46223	-46782	-6347	+2865
	⑥	$\sigma_{BEND.}$	- ②/④	+28955	+73119	+114792	+48208	+5150
	⑦	σ_{IF}	⑤ + ⑥	-8720	+26896	+68010	+41861	+8015
	⑧	σ_{OF}	⑤ - ⑥	-66630	-119342	-161574	-54555	-2285
19	①	P(20)	Note (1)	-2853.385	-3500.799	-3544.576	-522.097	218.374
	②	M(20)	Note (2)	1694.632	4383.966	7027.212	3006.766	350.086
	③	A	Table 3-24	.076				
	④	I/y		.110039				
	⑤	σ_{AXIAL}	①/③	-37545	-46064	-46640	-6880	+2873
	⑥	$\sigma_{BEND.}$	②/④	+15401	+39841	+63863	+27325	+3182
	⑦	σ_{IF}	⑤ + ⑥	-22144	-6223	+17223	+20445	+6055
	⑧	σ_{OF}	⑤ - ⑥	-52946	-85905	-110503	-34205	-309
	①	P(20)	Note (1)	2853.836	3501.334	3545.699	483.265	-217.239
	②	M(20)	Note (2)	-1694.617	-4383.940	-7027.176	-3006.760	-350.090
	③	A	Table 3-24	.076				
	④	I/y		.110039				
	⑤	σ_{AXIAL}	- ①/③	-37551	-46071	-46654	-6359	+2858
	⑥	$\sigma_{BEND.}$	- ②/④	+15401	+39841	+63863	+27325	+3182
	⑦	σ_{IF}	⑤ + ⑥	-22150	-6230	+17209	+20966	+6040
	⑧	σ_{OF}	⑤ - ⑥	-52952	-85912	-110517	-33684	-324
20	①	P(21)	Note (1)	-2838.821	-3479.598	-3522.776	-479.327	218.145
	②	M(21)	Note (2)	3764.218	1113.273	1984.626	924.468	145.932
	③	A	Table 3-24	.076				
	④	I/y		.110039				
	⑤	σ_{AXIAL}	①/③	-37353	-45785	-46353	-6307	+2870
	⑥	$\sigma_{BEND.}$	②/④	+34209	+10117	+18036	+8402	+1326
	⑦	σ_{IF}	⑤ + ⑥	-3144	-35668	-28317	+2095	+4196
	⑧	σ_{OF}	⑤ - ⑥	-71562	-55902	-64389	-14709	+1544
	①	P(21)	Note (1)	2839.809	3480.782	3525.256	481.802	-215.670
	②	M(21)	Note (2)	-3764.100	-1113.259	-1984.608	-924.465	-145.933
	③	A	Table 3-24	.040				
	④	I/y		.058304				
	⑤	σ_{AXIAL}	- ①/③	-70995	-87020	-88131	-12045	+5392
	⑥	$\sigma_{BEND.}$	- ②/④	+64558	+19094	+34038	+15855	+2503
	⑦	σ_{IF}	⑤ + ⑥	-6437	-67926	-54093	+3810	+7895
	⑧	σ_{OF}	⑤ - ⑥	-135553	-106122	-122169	-27900	+2889
21	①	P(22)	Note (1)	-2772.954	-3359.663	-3371.538	-435.095	221.147
	②	M(22)	Note (2)	-762.012	-1921.267	-2850.847	-1134.392	-90.313
	③	A	Table 3-24	.040				
	④	I/y		.058304				
	⑤	σ_{AXIAL}	①/③	-69324	-83992	-84288	-10877	+5529
	⑥	$\sigma_{BEND.}$	②/④	-13069	-32952	-48895	-19456	-1549
	⑦	σ_{IF}	⑤ + ⑥	-82393	-116944	-133183	-30333	+3980
	⑧	σ_{OF}	⑤ - ⑥	-56255	-51040	-35393	+8579	+7078

Table 3-26. Calculation of Meridional Stresses - Lower Frustum (continued)

SEC. NO.	ROW NO.	ITEM	REFERENCE \ DESIGN COND.	LIFT-OFF (T=0)	MAX. DYNAMIC PRESSURE (T=77)	MAX. LONG. ACCELERATION (T=138)	MAX. REENTRY DYN. PRESS. (T_R=508)	LANDING
22	①	P(22)	NOTE (1)	2774.520	3361.529	3375.452	439.005	-217.239
	②	M(22)	NOTE (2)	762.013	1921.267	2850.844	1134.391	90.313
	③	A	TABLE 3-24	.040				
	④	I/y	TABLE 3-24	.058304				
	⑤	σ_{AXIAL}	-①/③	-69363	-84038	-84386	-10975	+5431
	⑥	$\sigma_{BEND.}$	-②/④	-13069	-32952	-48895	-19456	-1549
	⑦	σ_{IF}	⑤+⑥	-82432	-116990	-133281	-30431	+3882
	⑧	σ_{OF}	⑤-⑥	-56294	-51086	-35491	+8481	+6980
	①	P(23)	NOTE (1)	-2672.388	-3157.538	-3096.727	-341.857	227.495
	②	M(23)	NOTE (2)	-284.828	-1187.463	-1820.003	-752.819	-78.053
	③	A	TABLE 3-24	.040				
	④	I/y	TABLE 3-24	.058304				
	⑤	σ_{AXIAL}	①/③	-66810	-78938	-77418	-8546	+5687
	⑥	$\sigma_{BEND.}$	②/④	-4885	-20366	-31215	-12912	-1339
	⑦	σ_{IF}	⑤+⑥	-71695	-99304	-108633	-21458	+4348
	⑧	σ_{OF}	⑤-⑥	-61925	-58572	-46203	+4366	+7026
23	①	P(23)	NOTE (1)	2674.033	3157.501	3100.847	345.980	-223.371
	②	M(23)	NOTE (2)	284.828	1187.458	1819.993	752.814	78.052
	③	A	TABLE 3-24	.040				
	④	I/y	TABLE 3-24	.058304				
	⑤	σ_{AXIAL}	-①/③	-66851	-78988	-77521	-8650	+5584
	⑥	$\sigma_{BEND.}$	-②/④	-4885	-20366	-31215	-12912	-1339
	⑦	σ_{IF}	⑤+⑥	-71736	-99354	-108736	-21562	+4245
	⑧	σ_{OF}	⑤-⑥	-61966	-58622	-46306	+4262	+6923
	①	P(24)	NOTE (1)	-2560.977	-2938.072	-2791.268	-234.362	235.248
	②	M(24)	NOTE (2)	208.713	-207.662	-301.810	-129.505	-14.965
	③	A	TABLE 3-24	.040				
	④	I/y	TABLE 3-24	.058304				
	⑤	σ_{AXIAL}	①/③	-64024	-73452	-69782	-5859	+5881
	⑥	$\sigma_{BEND.}$	②/④	+3580	-3562	-5176	-2221	-257
	⑦	σ_{IF}	⑤+⑥	-60444	-77014	-74958	-8080	+5624
	⑧	σ_{OF}	⑤-⑥	-67604	-69890	-64606	-3638	+6138
24	①	P(24)	NOTE (1)	2562.741	2940.174	2795.676	238.769	-238.840
	②	M(24)	NOTE (2)	-208.714	207.657	301.801	129.499	14.964
	③	A	TABLE 3-24	.036				
	④	I/y	TABLE 3-24	.052512				
	⑤	σ_{AXIAL}	-①/③	-71187	-81672	-77658	-6632	+6412
	⑥	$\sigma_{BEND.}$	-②/④	+3975	-3954	-5747	-2466	-285
	⑦	σ_{IF}	⑤+⑥	-67212	-85626	-83405	-9098	+6127
	⑧	σ_{OF}	⑤-⑥	-75612	-77718	-71911	-4166	+6697
	①	P(25)	NOTE (1)	-2424.266	-2695.035	-2445.809	-109.381	245.687
	②	M(25)	NOTE (2)	288.052	168.125	293.072	124.656	16.946
	③	A	TABLE 3-24	.036				
	④	I/y	TABLE 3-24	.052512				
	⑤	σ_{AXIAL}	①/③	-67341	-74862	-67939	-3038	+6825
	⑥	$\sigma_{BEND.}$	②/④	+5485	+3202	+5581	+2374	+323
	⑦	σ_{IF}	⑤+⑥	-61856	-71660	-62358	-664	+7148
	⑧	σ_{OF}	⑤-⑥	-72826	-78064	-73520	-5412	+6502

Table 3-26. Calculation of Meridional Stresses - Lower Frustum (continued)

Sec. No.	Row No.	Item	Reference \ Design Cond.	Lift-off (T=0)	Max. Dynamic Pressure (T=77)	Max. Long. Acceleration (T=138)	Max. Reentry Dyn. Press. (T_R=508)	Landing
25	①	P(25)	Note (1)	2426.208	2698.079	2450.671	114.245	-240.822
	②	M(25)	Note (2)	-288.054	-168.128	-293.082	-124.661	-16.946
	③	A	Table 3-24	.036				
	④	I/y		.052512				
	⑤	σ_{AXIAL}	-①/③	-67395	-74947	-68074	-3173	+6690
	⑥	$\sigma_{BEND.}$	-②/④	+5485	+3202	+5581	+2374	+323
	⑦	σ_{IF}	⑤+⑥	-61910	-71745	-62493	-799	+7013
	⑧	σ_{OF}	⑤-⑥	-72880	-78149	-73655	-5547	+6367
	①	P(26)	Note (1)	-2261.247	-2458.617	-2107.434	13.101	155.796
	②	M(26)	Note (2)	131.400	136.379	59.712	34.311	5.748
	③	A	Table 3-24	.036				
	④	I/y		.052512				
	⑤	σ_{AXIAL}	①/③	-62812	-68295	-58540	+364	+4328
	⑥	$\sigma_{BEND.}$	②/④	+2502	+2597	+1137	+653	+109
	⑦	σ_{IF}	⑤+⑥	-60310	-65698	-57403	+1017	+4437
	⑧	σ_{OF}	⑤-⑥	-65314	-70892	-59677	-289	+4219
26	①	P(26)	Note (1)	2263.262	2461.017	2112.475	-8.061	-250.756
	②	M(26)	Note (2)	-131.403	-136.382	-59.722	-34.317	-5.749
	③	A	Table 3-24	.036				
	④	I/y		.052512				
	⑤	σ_{AXIAL}	-①/③	-62868	-68362	-58680	+224	+6965
	⑥	$\sigma_{BEND.}$	-②/④	+2502	+2597	+1137	+653	+109
	⑦	σ_{IF}	⑤+⑥	-60366	-65765	-57543	+877	+7074
	⑧	σ_{OF}	⑤-⑥	-65370	-70959	-59817	-429	+6856
	①	P(27)	Note (1)	-2075.036	-2237.141	-1793.402	127.416	265.242
	②	M(27)	Note (2)	120.249	407.231	-0.894	19.760	6.699
	③	A	Table 3-24	.036				
	④	I/y		.052512				
	⑤	σ_{AXIAL}	①/③	-57640	-62143	-49817	+3539	+7368
	⑥	$\sigma_{BEND.}$	②/④	+2290	+7755	-17	+376	+128
	⑦	σ_{IF}	⑤+⑥	-55350	-54388	-49834	+3915	+7496
	⑧	σ_{OF}	⑤-⑥	-59930	-69898	-49800	+3163	+7240
27	①	P(27)	Note (1)	2076.916	2239.382	1798.101	-122.719	-260.547
	②	M(27)	Note (2)	-120.254	-407.235	0.879	-19.766	-6.700
	③	A	Table 3-24	.040				
	④	I/y		.058304				
	⑤	σ_{AXIAL}	-①/③	-51923	-55985	-44953	+3068	+6514
	⑥	$\sigma_{BEND.}$	-②/④	+2062	+6984	-15	+339	+115
	⑦	σ_{IF}	⑤+⑥	-49861	-49001	-44968	+3407	+6629
	⑧	σ_{OF}	⑤-⑥	-53985	-62969	-44938	+2729	+6399
	①	P(28)	Note (1)	-1807.614	-2039.632	-1524.457	227.988	274.253
	②	M(28)	Note (2)	-342.666	149.090	-398.330	-195.062	-39.926
	③	A	Table 3-24	.040				
	④	I/y		.058304				
	⑤	σ_{AXIAL}	①/③	-47190	-50991	-38111	+5700	+6856
	⑥	$\sigma_{BEND.}$	②/④	-5877	+2557	-6832	-3346	-685
	⑦	σ_{IF}	⑤+⑥	-53067	-48434	-44943	+2354	+6171
	⑧	σ_{OF}	⑤-⑥	-41313	-53548	-31279	+9046	+7541

Table 3-26. Calculation of Meridional Stresses - Lower Frustum (continued)

Sec. No.	Row No.	Item	Design Cond / Reference	Lift-Off (T=0)	Max. Dynamic Pressure (T=77)	Max. Long. Acceleration (T=138)	Max. Reentry Dyn. Press. (T_R=505)	Landing
28	①	P(28)	Note (1)	1889.353	2041.704	1528.789	-223.635	-269.901
	②	M(28)	Note (2)	342.659	-149.099	398.315	195.055	39.924
	③	A	Table 3-24	.040				
	④	I/y	Table 3-24	.058304				
	⑤	σ_{AXIAL}	-①/③	-47234	-51043	-38220	+5591	+6748
	⑥	$\sigma_{BEND.}$	-②/④	-5877	+2557	-6832	-3345	-685
	⑦	σ_{IF}	⑤+⑥	-53111	-48486	-45052	+2246	+6063
	⑧	σ_{OF}	⑤-⑥	-41357	-53600	-31388	+8936	+7433
	①	P(29)	Note (1)	-1690.912	-1840.186	-1277.698	320.230	282.461
	②	M(29)	Note (2)	-1460.122	-1221.520	-1571.847	-846.672	-180.702
	③	A	Table 3-24	.040				
	④	I/y	Table 3-24	.058304				
	⑤	σ_{AXIAL}	①/③	-42273	-46005	-31942	+8006	+7062
	⑥	$\sigma_{BEND.}$	②/④	-25043	-20950	-26959	-14521	-3099
	⑦	σ_{IF}	⑤+⑥	-67316	-66955	-58901	-6515	+3963
	⑧	σ_{OF}	⑤-⑥	-17230	-25055	-4983	+22527	+10161
29	①	P(29)	Note (1)	1692.603	1842.200	1281.926	-316.002	-278.232
	②	M(29)	Note (2)	1460.106	1221.503	1571.835	846.662	180.701
	③	A	Table 3-24	.040				
	④	I/y	Table 3-24	.058304				
	⑤	σ_{AXIAL}	-①/③	-42315	-46055	-32048	+7900	+6956
	⑥	$\sigma_{BEND.}$	-②/④	-25042	-20950	-26959	-14521	-3099
	⑦	σ_{IF}	⑤+⑥	-67357	-67005	-59007	-6621	+3857
	⑧	σ_{OF}	⑤-⑥	-17273	-25105	-5089	+22421	+10055
	①	P(30)	Note (1)	-1519.244	-1664.863	-1085.946	387.894	286.543
	②	M(30)	Note (2)	-2081.673	-2252.975	-2050.696	-1234.507	-278.728
	③	A	Table 3-24	.040				
	④	I/y	Table 3-24	.058304				
	⑤	σ_{AXIAL}	①/③	-37981	-41622	-27149	+9697	+7164
	⑥	$\sigma_{BEND.}$	②/④	-35703	-38641	-35171	-21173	-4780
	⑦	σ_{IF}	⑤+⑥	-73684	-80263	-62320	-11476	+2384
	⑧	σ_{OF}	⑤-⑥	-2278	-2981	+8022	+30870	+11944
30	①	P(30)	Note (1)	1520.571	1666.446	1089.264	-384.577	-283.227
	②	M(30)	Note (2)	2081.651	2252.962	2050.674	1234.492	278.726
	③	A	Table 3-24	.040				
	④	I/y	Table 3-24	.058304				
	⑤	σ_{AXIAL}	-①/③	-38014	-41661	-27232	+9614	+7081
	⑥	$\sigma_{BEND.}$	-②/④	-35702	-38641	-35171	-21173	-4780
	⑦	σ_{IF}	⑤+⑥	-73716	-80302	-62403	-11559	+2301
	⑧	σ_{OF}	⑤-⑥	-2312	-3020	+7939	+30787	+11861
	①	P(31)	Note (1)	-1432.079	-1574.958	-999.485	412.916	205.134
	②	M(31)	Note (2)	-889.833	-1215.833	-475.655	-540.308	-149.579
	③	A	Table 3-24	.040				
	④	I/y	Table 3-24	.058304				
	⑤	σ_{AXIAL}	①/③	-35822	-39374	-24987	+10323	+7128
	⑥	$\sigma_{BEND.}$	②/④	-15262	-20853	-8158	-9267	-2565
	⑦	σ_{IF}	⑤+⑥	-51084	-60227	-33145	+1056	+4563
	⑧	σ_{OF}	⑤-⑥	-20560	-18521	-16829	+19590	+9693

Table 3-26. Calculation of Meridional Stresses - Lower Frustum (continued)

Sec. No.	Row No.	Item	Reference \ Design Cond.	Lift-Off (T=0)	Max. Dynamic Pressure (T=77)	Max. Long. Acceleration (T=130)	Max. Reentry Dyn. Press. (T_R=505)	Landing
	(1)	P(31)	Note (1)	1433.854	1576.121	1001.926	-410.478	-282.694
	(2)	M(31)	Note (2)	889.800	1215.811	475.617	540.285	149.576
	(3)	A	Table 3-24	.054				
	(4)	I/y	Table 3-24	.078534				
	(5)	σ_{AXIAL}	-(1)/(3)	-26554	-29188	-18555	+7602	+5235
	(6)	$\sigma_{BEND.}$	-(2)/(4)	-11330	-15481	-6056	-6879	-1905
	(7)	σ_{IF}	(5)+(6)	-37884	-44669	-24611	+723	+3330
	(8)	σ_{OF}	(5)-(6)	-15224	-13707	-12499	+14481	+7140
31	(1)	P(32)	Note (1)	-1361.213	-1499.512	-933.107	427.422	282.265
	(2)	M(32)	Note (2)	1610.901	1338.090	2585.313	915.414	150.744
	(3)	A	Table 3-24	.054				
	(4)	I/y	Table 3-24	.078534				
	(5)	σ_{AXIAL}	(1)/(3)	-25208	-27769	-17280	+7915	+5227
	(6)	$\sigma_{BEND.}$	(2)/(4)	+20512	+17038	+32919	+11656	+1919
	(7)	σ_{IF}	(5)+(6)	-4696	-10731	+15639	+19571	+7146
	(8)	σ_{OF}	(5)-(6)	-45720	-44807	-50199	-3741	+3308
	(1)	P(32)	Note (1)	1362.133	1500.610	935.406	-425.123	-279.967
	(2)	M(32)	Note (2)	-1610.933	-1338.114	-2585.344	-915.432	-150.746
	(3)	A	Table 3-24	.054				
	(4)	I/y	Table 3-24	.078534				
	(5)	σ_{AXIAL}	-(1)/(3)	-25225	-27790	-17323	+7873	+5185
	(6)	$\sigma_{BEND.}$	-(2)/(4)	+20512	+17038	+32919	+11656	+1919
	(7)	σ_{IF}	(5)+(6)	-4713	-10752	+15596	+19529	+7104
	(8)	σ_{OF}	(5)-(6)	-45737	-44828	-50242	-3783	+3266
32	(1)	P(33)	Note (1)	-1309.154	-1444.497	-890.044	428.713	276.755
	(2)	M(33)	Note (2)	5779.449	5811.583	7907.037	3398.601	690.048
	(3)	A	Table 3-24	.054				
	(4)	I/y	Table 3-24	.078534				
	(5)	σ_{AXIAL}	(1)/(3)	-24244	-26751	-16483	+7939	+5125
	(6)	$\sigma_{BEND.}$	(2)/(4)	+73590	+73999	+100680	+43274	+8786
	(7)	σ_{IF}	(5)+(6)	+49346	+47248	+84197	+51213	+13911
	(8)	σ_{OF}	(5)-(6)	-97834	-100750	-117163	-35335	-3661

Notes: 1) The number in parentheses following the "P" or "M" in rows (1) and (2) identify the pertinent boundary node per figure 1-2. The meridional load "P" is from table 3-23

2.) The bending moment acting at the node is obtained from the pertinent design condition shown in tables 3-17 through 3-21 inclusive.

Table 3-27. Calculation of Meridional Stresses - Inner Cylindrical Bulkhead

Sec. No.	Row No.	Item	Design Cond. / Reference	Lift-off (T=0)	Max. Dynamic Pressure (T=77)	Max. Long. Acceleration (T=138)	Max. Reentry Dyn. Press. (T=805)	Landing
33	①	P(1)	Note (1)	-752.071	-1006.859	-1243.499	-521.370	-131.244
	②	M(1)	Note (2)	1175.208	1566.368	1944.011	819.412	210.878
	③	A	Table 3-24	.060				
	④	I/y	Table 3-24	.011286				
	⑤	σ_{AXIAL}	- ①/③	+12535	+16781	+20725	+8690	+2187
	⑥	$\sigma_{BEND.}$	- ②/④	-104129	-138806	-172249	-72604	-18685
	⑦	σ_{IF}	⑤ + ⑥	-91594	-122025	-151524	-63914	-16498
	⑧	σ_{OF}	⑤ - ⑥	+116664	+155587	+192974	+81294	+20872
	①	P(34)	Note (1)	752.071	1006.859	1243.499	521.370	131.844
	②	M(34)	Note (2)	-209.275	-278.856	-346.156	-145.947	-37.637
	③	A	Table 3-24	.060				
	④	I/y	Table 3-24	.011286				
	⑤	σ_{AXIAL}	①/③	+12535	+16781	+20725	+8690	+2187
	⑥	$\sigma_{BEND.}$	②/④	-18543	-24708	-30671	-12932	-3335
	⑦	σ_{IF}	⑤ + ⑥	-6008	-7927	-9946	-4242	-1148
	⑧	σ_{OF}	⑤ - ⑥	+31078	+41489	+51396	+21622	+5522
34	①	P(34)	Note (1)	-751.985	-1006.757	-1243.278	-521.145	-131.019
	②	M(34)	Note (2)	209.278	278.859	346.159	145.947	37.637
	③	A	Table 3-24	.060				
	④	I/y	Table 3-24	.011286				
	⑤	σ_{AXIAL}	- ①/③	+12533	+16780	+20722	+8686	+2184
	⑥	$\sigma_{BEND.}$	- ②/④	-18543	-24708	-30671	-12932	-3335
	⑦	σ_{IN}	⑤ + ⑥	-6010	-7928	-9949	-4246	-1151
	⑧	σ_{OF}	⑤ - ⑥	+31076	+41488	+51393	+21618	+5519
	①	P(35)	Note (1)	751.985	1006.757	1243.278	521.145	131.019
	②	M(35)	Note (2)	145.941	194.369	240.569	100.808	26.118
	③	A	Table 3-24	.060				
	④	I/y	Table 3-24	.011286				
	⑤	σ_{AXIAL}	①/③	+12533	+16780	+20722	+8686	+2184
	⑥	$\sigma_{BEND.}$	②/④	+12931	+17222	+21316	+8932	+2314
	⑦	σ_{IF}	⑤ + ⑥	+25464	+34002	+42038	+17618	+4498
	⑧	σ_{OF}	⑤ - ⑥	-398	-442	-594	-246	-130
35	①	P(35)	Note (1)	-751.799	-1006.537	-1242.822	-520.692	-130.567
	②	M(35)	Note (2)	-145.941	-194.369	-240.569	-100.808	-26.118
	③	A	Table 3-24	.020				
	④	I/y	Table 3-24	.003984				
	⑤	σ_{AXIAL}	- ①/③	+37590	+50327	+62141	+26035	+6528
	⑥	$\sigma_{BEND.}$	- ②/④	+36632	+48787	+60384	+25303	+6556
	⑦	σ_{IF}	⑤ + ⑥	+74222	+99114	+122525	+51338	+13084
	⑧	σ_{OF}	⑤ - ⑥	+958	+1540	+1757	+732	-28
	①	P(36)	Note (1)	751.799	1006.537	1242.822	520.692	130.567
	②	M(36)	Note (2)	-48.821	-64.714	-78.907	-31.951	-8.598
	③	A	Table 3-24	.020				
	④	I/y	Table 3-24	.003984				
	⑤	σ_{AXIAL}	①/③	+37590	+50327	+62141	+26035	+6528
	⑥	$\sigma_{BEND.}$	②/④	-12254	-16243	-19806	-8020	-2158
	⑦	σ_{IF}	⑤ + ⑥	+25336	+34084	+42335	+18015	+4370
	⑧	σ_{OF}	⑤ - ⑥	+49844	+66570	+81947	+34055	+8686

Table 3-27. Calculation of Meridional Stresses - Inner Cylindrical Bulkhead (continued)

Seg. No.	Row No.	Item	Design Cond. / Reference	Lift-off (T=0)	Max. Dynamic Pressure (T=77)	Max. Long. Acceleration (T=138)	Max. Reentry Dyn. Press. (T_R=503)	Landing
	①	P(36)	Note (1)	-751.438	-1006.110	-1241.926	-519.800	-129.674
	②	M(36)	Note (2)	48.821	64.714	78.907	31.951	8.598
	③	A	Table 3-24			.020		
	④	I/y	Table 3-24			.003984		
	⑤	σ_{AXIAL}	-①/③	+37572	+50306	+62096	+25990	+6484
	⑥	$\sigma_{BEND.}$	-②/④	-12254	-16243	-19806	-8020	-2158
	⑦	σ_{IF}	⑤+⑥	+25318	+34063	+42290	+17970	+4326
	⑧	σ_{OF}	⑤-⑥	+49826	+66549	+81902	+34010	+8642
36	①	P(37)	Note (1)	751.438	1006.110	1241.926	519.800	129.674
	②	M(37)	Note (2)	25.115	32.866	38.421	13.986	4.229
	③	A	Table 3-24			.020		
	④	I/y	Table 3-24			.003984		
	⑤	σ_{AXIAL}	①/③	+37572	+50306	+62096	+25990	+6484
	⑥	$\sigma_{BEND.}$	②/④	+6304	+8249	+9644	+3511	+1061
	⑦	σ_{IF}	⑤+⑥	+43876	+58555	+71740	+29501	+7545
	⑧	σ_{OF}	⑤-⑥	+31268	+42057	+52452	+22479	+5423
	①	P(37)	Note (1)	-750.965	-1005.551	-1240.744	-518.617	-128.492
	②	M(37)	Note (2)	-25.115	-32.866	-38.421	-13.986	-4.229
	③	A	Table 3-24			.020		
	④	I/y	Table 3-24			.003984		
	⑤	σ_{AXIAL}	-①/③	+37548	+50278	+62037	+25931	+6425
	⑥	$\sigma_{BEND.}$	-②/④	+6304	+8249	+9644	+3511	+1061
	⑦	σ_{IF}	⑤+⑥	+43852	+58527	+71681	+29442	+74866
	⑧	σ_{OF}	⑤-⑥	+31244	+42029	+52393	+22420	+5364
37	①	P(38)	Note (1)	750.965	1005.551	1240.744	518.617	128.492
	②	M(38)	Note (2)	-14.492	-18.136	-17.946	-3.302	-2.063
	③	A	Table 3-24			.020		
	④	I/y	Table 3-24			.003984		
	⑤	σ_{AXIAL}	①/③	+37548	+50278	+62037	+25931	+6425
	⑥	$\sigma_{BEND.}$	②/④	-3638	-4552	-4505	-829	-518
	⑦	σ_{IF}	⑤+⑥	+33910	+45726	+57532	+25102	+5907
	⑧	σ_{OF}	⑤-⑥	+41186	+54830	+66542	+26760	+6943
	①	P(38)	Note (1)	-750.612	-1005.127	-1239.855	-517.726	-127.601
	②	M(38)	Note (2)	14.492	18.136	17.946	3.302	2.063
	③	A	Table 3-24			.020		
	④	I/y	Table 3-24			.003984		
	⑤	σ_{AXIAL}	-①/③	+37531	+50256	+61993	+25886	+6380
	⑥	$\sigma_{BEND.}$	-②/④	-3638	-4552	-4505	-829	-518
	⑦	σ_{IF}	⑤+⑥	+33893	+45704	+57488	+25057	+5862
	⑧	σ_{OF}	⑤-⑥	+41169	+54808	+66498	+26715	+6898
38	①	P(39)	Note (1)	750.612	1005.127	1239.855	517.726	127.601
	②	M(39)	Note (2)	5.306	3.771	-8.023	-15.257	-0.544
	③	A	Table 3-24			.020		
	④	I/y	Table 3-24			.003984		
	⑤	σ_{AXIAL}	①/③	+37531	+50256	+61993	+25886	+6380
	⑥	$\sigma_{BEND.}$	②/④	+1332	+947	-2014	-3830	-137
	⑦	σ_{IF}	⑤+⑥	+38863	+51203	+59979	+22056	+6243
	⑧	σ_{OF}	⑤-⑥	+36199	+49309	+64007	+29716	+6517

Table 3-27. Calculation of Meridional Stresses - Inner Cylindrical Bulkhead (continued)

Seg. No.	Row No.	Item	Design Cond. / Reference	Lift-off (T=0)	Max. Dynamic Pressure (T=77)	Max. Long. Acceleration (T=138)	Max. Reentry Dyn. Press. (T=508)	Landing
39	①	P(39)	Note (1)	-750.439	-1004.922	-1239.411	-517.276	-127.150
	②	M(39)	Note (2)	-5.306	-3.771	8.023	15.257	0.544
	③	A	Table 3-24	.020				
	④	I/y	Table 3-24	.003984				
	⑤	σ_{AXIAL}	-①/③	+37522	+50246	+61971	+25864	+6358
	⑥	$\sigma_{BEND.}$	-②/④	+1332	+947	-2014	-3830	-137
	⑦	σ_{IF}	⑤+⑥	+38854	+51193	+59957	+22034	+6221
	⑧	σ_{OF}	⑤-⑥	+36190	+49299	+63985	+29694	+6495
	①	P(40)	Note (1)	750.439	1004.922	1239.411	517.276	127.150
	②	M(40)	Note (2)	-3.832	-9.733	-31.418	-31.326	-2.931
	③	A	Table 3-24	.020				
	④	I/y	Table 3-24	.003984				
	⑤	σ_{AXIAL}	①/③	+37522	+50246	+61971	+25864	+6358
	⑥	$\sigma_{BEND.}$	②/④	-962	-2443	-7886	-7863	-736
	⑦	σ_{IF}	⑤+⑥	+36560	+47803	+54085	+18001	+5622
	⑧	σ_{OF}	⑤-⑥	+38484	+52689	+69857	+33727	+7094
40	①	P(40)	Note (1)	-749.982	-1004.380	-1238.260	-516.118	-125.989
	②	M(40)	Note (2)	3.832	9.733	31.418	31.326	2.932
	③	A	Table 3-24	.020				
	④	I/y	Table 3-24	.003984				
	⑤	σ_{AXIAL}	-①/③	+37499	+50219	+61913	+25806	+6299
	⑥	$\sigma_{BEND.}$	-②/④	-962	-2443	-7886	-7863	-736
	⑦	σ_{IF}	⑤+⑥	+36537	+47776	+54027	+17943	+5563
	⑧	σ_{OF}	⑤-⑥	+38461	+52662	+69799	+33669	+7035
	①	P(41)	Note (1)	749.982	1004.380	1238.260	516.118	125.989
	②	M(41)	Note (2)	15.862	52.991	189.210	195.164	17.392
	③	A	Table 3-24	.020				
	④	I/y	Table 3-24	.003984				
	⑤	σ_{AXIAL}	①/③	+37499	+50219	+61913	+25806	+6299
	⑥	$\sigma_{BEND.}$	②/④	+3981	+13301	+47492	+48987	+4365
	⑦	σ_{IF}	⑤+⑥	+41480	+63520	+109405	+74793	+10664
	⑧	σ_{OF}	⑤-⑥	+33518	+36918	+14421	-23181	+1934
41	①	P(41)	Note (1)	-807.119	-1181.979	-1855.136	-1146.779	-182.788
	②	M(41)	Note (2)	91.974	282.494	976.269	996.346	89.508
	③	A	Table 3-24	.020				
	④	I/y	Table 3-24	.036874				
	⑤	σ_{AXIAL}	-①/③	+40356	+59099	+92757	+57339	+9139
	⑥	$\sigma_{BEND.}$	-②/④	-2494	-7661	-26475	-27020	-2427
	⑦	σ_{IF}	⑤+⑥	+37862	+51438	+66282	+30319	+6712
	⑧	σ_{OF}	⑤-⑥	+42850	+66760	+119232	+84359	+11566
	①	P(42)	Note (1)	807.119	1181.979	1855.136	1146.779	182.788
	②	M(42)	Note (2)	-12.875	-35.625	-118.712	-119.612	-10.628
	③	A	Table 3-24	.020				
	④	I/y	Table 3-24	.036874				
	⑤	σ_{AXIAL}	①/③	+40356	+59099	+92757	+57339	+9139
	⑥	$\sigma_{BEND.}$	②/④	-349	-966	-3219	-3244	-288
	⑦	σ_{IF}	⑤+⑥	+40007	+58133	+89538	+54095	+8851
	⑧	σ_{OF}	⑤-⑥	+40705	+60065	+95976	+60583	+9427

B

Table 3-27. Calculation of Meridional Stresses - Inner Cylindrical Bulkhead (continued)

Sec. No.	Row No.	Item	Reference \ Design Cond.	Lift-Off (T=0)	Max. Dynamic Pressure (T=77)	Max. Long. Acceleration (T=138)	Max. Reentry Dyn. Press. (T_R = 505)	Landing
42	①	P(42)	Note (1)	-806.502	-1181.244	-1853.600	-1145.249	-181.257
	②	M(42)	Note (2)	12.876	35.626	118.715	119.613	10.628
	③	A	Table 3-24			.020		
	④	I/y	Table 3-24			.036874		
	⑤	σ_{AXIAL}	- ①/③	+40325	+59062	+92680	+57262	+9063
	⑥	$\sigma_{BEND.}$	- ②/④	-349	-966	-3219	-3244	-288
	⑦	σ_{IF}	⑤ + ⑥	+39976	+58096	+89461	+54018	+8775
	⑧	σ_{OF}	⑤ - ⑥	+40674	+60028	+95899	+60506	+9351
	①	P(43)	Note (1)	806.502	1181.244	1853.600	1145.249	181.257
	②	M(43)	Note (2)	14.544	36.278	125.795	128.519	11.416
	③	A	Table 3-24			.020		
	④	I/y	Table 3-24			.036874		
	⑤	σ_{AXIAL}	①/③	+40325	+59062	+92680	+57262	+9063
	⑥	$\sigma_{BEND.}$	②/④	+394	+984	+3411	+3485	+310
	⑦	σ_{IF}	⑤ + ⑥	+40719	+60046	+96091	+60747	+9373
	⑧	σ_{OF}	⑤ - ⑥	+39931	+58078	+89269	+53777	+8753
43	①	P(43)	Note (1)	-805.275	-1179.782	-1850.536	-1142.187	-178.196
	②	M(43)	Note (2)	-14.544	-36.277	-125.794	-128.518	-11.416
	③	A	Table 3-24			.020		
	④	I/y	Table 3-24			.036874		
	⑤	σ_{AXIAL}	- ①/③	+40264	+58989	+92527	+57109	+8910
	⑥	$\sigma_{BEND.}$	- ②/④	+394	+984	+3411	+3485	+310
	⑦	σ_{IF}	⑤ + ⑥	+40658	+59973	+95938	+60594	+9220
	⑧	σ_{OF}	⑤ - ⑥	+39870	+58005	+89116	+53624	+8600
	①	P(44)	Note (1)	805.275	1179.782	1850.536	1142.187	178.196
	②	M(44)	Note (2)	-5.966	-14.133	-50.114	-51.608	-4.550
	③	A	Table 3-24			.020		
	④	I/y	Table 3-24			.036874		
	⑤	σ_{AXIAL}	①/③	+40264	+58989	+92527	+57109	+8910
	⑥	$\sigma_{BEND.}$	②/④	-162	-383	-1359	-1400	-123
	⑦	σ_{IF}	⑤ + ⑥	+40102	+58606	+91168	+55709	+8787
	⑧	σ_{OF}	⑤ - ⑥	+40426	+59372	+93886	+58509	+9033
44	①	P(44)	Note (1)	-803.541	-1177.715	-1846.201	-1137.852	-173.861
	②	M(44)	Note (2)	5.966	14.133	50.114	51.609	4.550
	③	A	Table 3-24			.020		
	④	I/y	Table 3-24			.036874		
	⑤	σ_{AXIAL}	- ①/③	+40177	+58886	+92310	+56893	+8693
	⑥	$\sigma_{BEND.}$	- ②/④	-162	-383	-1359	-1400	-123
	⑦	σ_{IF}	⑤ + ⑥	+40015	+58503	+90951	+55493	+8570
	⑧	σ_{OF}	⑤ - ⑥	+40339	+59269	+93669	+58293	+8816
	①	P(45)	Note (1)	803.541	1177.715	1846.201	1137.852	173.861
	②	M(45)	Note (2)	13.902	4.755	19.264	20.667	1.801
	③	A	Table 3-24			.020		
	④	I/y	Table 3-24			.036874		
	⑤	σ_{AXIAL}	①/③	+40177	+58886	+92310	+56893	+8693
	⑥	$\sigma_{BEND.}$	②/④	+377	+129	+522	+560	+49
	⑦	σ_{IF}	⑤ + ⑥	+40554	+59015	+92832	+57453	+8742
	⑧	σ_{OF}	⑤ - ⑥	+39800	+58757	+91788	+56333	+8644

Table 3-27. Calculation of Meridional Stresses - Inner Cylindrical Bulkhead (continued)

Sec. No.	No.	Item	Design Cond. / Reference	Lift-Off (T=0)	Max. Dynamic Pressure (T=77)	Max. Long. Acceleration (T=138)	Max. Reentry Dyn. Press. (T_R=508)	Landing
45	①	P(45)	Note (1)	-801.705	-1175.529	-1841.612	-1133.263	-169.272
	②	M(45)	Note (2)	-13.901	-4.755	-19.264	-20.666	-1.801
	③	A	Table 3-24	.020				
	④	I/y		.036874				
	⑤	σ Axial	-①/③	+40085	+58776	+92081	+56663	+8464
	⑥	σ Bend.	-②/④	+377	+129	+522	+560	+49
	⑦	σ IF	⑤+⑥	+40462	+58905	+92603	+57223	+8513
	⑧	σ OF	⑤-⑥	+39708	+58647	+91559	+56103	+8415
	①	P(46)	Note (1)	801.705	1175.529	1841.612	1133.263	169.272
	②	M(46)	Note (2)	1.702	-1.311	-0.690	-2.883	-0.176
	③	A	Table 3-24	.020				
	④	I/y		.036874				
	⑤	σ Axial	①/③	+40085	+58776	+92081	+56663	+8464
	⑥	σ Bend.	②/④	+46	-36	-19	-78	-5
	⑦	σ IF	⑤+⑥	+40131	+58740	+92062	+56585	+8459
	⑧	σ OF	⑤-⑥	+40039	+58812	+92100	+56741	+8469
46	①	P(46)	Note (1)	-799.856	-1173.326	-1836.995	-1128.643	-164.652
	②	M(46)	Note (2)	-1.701	1.311	0.690	2.884	0.176
	③	A	Table 3-24	.020				
	④	I/y		.036874				
	⑤	σ Axial	-①/③	+39993	+58666	+91850	+56432	+8233
	⑥	σ Bend.	-②/④	+46	-36	-19	-78	-5
	⑦	σ IF	⑤+⑥	+40039	+58630	+91831	+56354	+8228
	⑧	σ OF	⑤-⑥	+39947	+58702	+91869	+56510	+8238
	①	P(47)	Note (1)	799.856	1173.326	1836.995	1128.643	164.652
	②	M(47)	Note (2)	-5.659	-6.665	-17.220	-12.843	-1.322
	③	A	Table 3-24	.020				
	④	I/y		.036874				
	⑤	σ Axial	①/③	+39993	+58666	+91850	+56432	+8233
	⑥	σ Bend.	②/④	-153	-181	-467	-348	-36
	⑦	σ IF	⑤+⑥	+39840	+58485	+91383	+56084	+8197
	⑧	σ OF	⑤-⑥	+40146	+58847	+92317	+56780	+8269
47	①	P(47)	Note (1)	-797.998	-1171.710	-1832.343	-1123.992	-160.001
	②	M(47)	Note (2)	5.659	6.665	17.221	12.843	1.322
	③	A	Table 3-24	.020				
	④	I/y		.036874				
	⑤	σ Axial	-①/③	+39900	+58586	+91617	+56200	+8000
	⑥	σ Bend.	-②/④	-153	-181	-467	-348	-36
	⑦	σ IF	⑤+⑥	+39747	+58405	+91150	+55852	+7964
	⑧	σ OF	⑤-⑥	+40053	+58767	+92084	+56548	+8036
	①	P(48)	Note (1)	797.998	1171.710	1832.343	1123.992	160.001
	②	M(48)	Note (2)	14.773	18.090	43.615	37.400	3.675
	③	A	Table 3-24	.020				
	④	I/y		.036874				
	⑤	σ Axial	①/③	+39900	+58586	+91617	+56200	+8000
	⑥	σ Bend.	②/④	+400	+491	+1183	+1014	+100
	⑦	σ IF	⑤+⑥	+40300	+59077	+92800	+57214	+8100
	⑧	σ OF	⑤-⑥	+39500	+58095	+90434	+55186	+7900

Table 3-27. Calculation of Meridional Stresses - Inner Cylindrical Bulkhead (continued)

Sec. No.	Row No.	Item	Design Cond / Reference	Lift-off (T=0)	Max. Dynamic Pressure (T=77)	Max. Long. Acceleration (T=138)	Max. Reentry Dyn. Press. (T_R=503)	Landing
48	(1)	P(48)	Note (1)	-796.364	-1169.161	-1828.258	-1119.904	-155.913
	(2)	M(48)	Note (2)	-14.773	-18.090	-43.615	-37.399	-3.675
	(3)	A	Table 3-24	.020				
	(4)	I/y	Table 3-24	.041225				
	(5)	σ_{AXIAL}	-(1)/(3)	+39818	+58458	+91413	+55995	+7796
	(6)	$\sigma_{BEND.}$	-(2)/(4)	+358	+439	+1058	+907	+89
	(7)	σ_{IF}	(5)+(6)	+40176	+58897	+92471	+56902	+7885
	(8)	σ_{OF}	(5)-(6)	+39460	+58019	+90355	+55088	+7707
	(1)	P(49)	Note (1)	796.364	1169.161	1828.258	1119.904	155.913
	(2)	M(49)	Note (2)	-58.750	-72.842	-183.186	-134.449	-12.774
	(3)	A	Table 3-24	.020				
	(4)	I/y	Table 3-24	.041225				
	(5)	σ_{AXIAL}	(1)/(3)	+39818	+58458	+91413	+55995	+7796
	(6)	$\sigma_{BEND.}$	(2)/(4)	-1425	-1767	-4444	-3261	-310
	(7)	σ_{IF}	(5)+(6)	+38393	+56691	+86969	+52734	+7486
	(8)	σ_{OF}	(5)-(6)	+41243	+60225	+95857	+59256	+8106
49	(1)	P(49)	Note (1)	-794.952	-1167.480	-1824.730	-1116.378	-152.387
	(2)	M(49)	Note (2)	58.750	72.842	183.187	134.449	12.774
	(3)	A	Table 3-24	.020				
	(4)	I/y	Table 3-24	.041225				
	(5)	σ_{AXIAL}	-(1)/(3)	+39748	+58374	+91237	+55819	+7619
	(6)	$\sigma_{BEND.}$	-(2)/(4)	-1425	-1767	-4444	-3261	-310
	(7)	σ_{IF}	(5)+(6)	+38323	+56607	+86793	+52558	+7309
	(8)	σ_{OF}	(5)-(6)	+41173	+60141	+95681	+59080	+7929
	(1)	P(50)	Note (1)	794.952	1167.480	1824.730	1116.378	152.387
	(2)	M(50)	Note (2)	207.743	258.028	622.876	447.177	41.897
	(3)	A	Table 3-24	.020				
	(4)	I/y	Table 3-24	.041225				
	(5)	σ_{AXIAL}	(1)/(3)	+39748	+58374	+91237	+55819	+7619
	(6)	$\sigma_{BEND.}$	(2)/(4)	+5039	+6259	+15109	+10847	+1016
	(7)	σ_{IF}	(5)+(6)	+44787	+64633	+106346	+66666	+8635
	(8)	σ_{OF}	(5)-(6)	+34709	+52115	+76128	+44972	+6603
50	(1)	P(50)	Note (1)	-793.812	-1166.120	-1821.881	-1113.528	-149.534
	(2)	M(50)	Note (2)	-207.743	-258.027	-622.875	-447.176	-41.897
	(3)	A	Table 3-24	.020				
	(4)	I/y	Table 3-24	.041225				
	(5)	σ_{AXIAL}	-(1)/(3)	+39691	+58306	+91094	+55676	+7477
	(6)	$\sigma_{BEND.}$	-(2)/(4)	+5039	+6259	+15109	+10847	+1016
	(7)	σ_{IF}	(5)+(6)	+44730	+64565	+106203	+66523	+8493
	(8)	σ_{OF}	(5)-(6)	+34652	+52047	+75985	+44829	+6461
	(1)	P(51)	Note (1)	793.812	1166.120	1821.881	1113.528	149.534
	(2)	M(51)	Note (2)	-450.754	-559.147	-1337.278	-909.843	-83.866
	(3)	A	Table 3-24	.020				
	(4)	I/y	Table 3-24	.041225				
	(5)	σ_{AXIAL}	(1)/(3)	+39691	+58306	+91094	+55676	+7477
	(6)	$\sigma_{BEND.}$	(2)/(4)	-10934	-13563	-32438	-22070	-2034
	(7)	σ_{IF}	(5)+(6)	+28757	+44743	+58656	+33606	+5443
	(8)	σ_{OF}	(5)-(6)	+50625	+71869	+123532	+77746	+9511

Table 3-27. Calculation of Meridional Stresses - Inner Cylindrical Bulkhead (continued)

Sec. No.	Row No.	Item	Design Cond. / Reference	Lift-Off (T=0)	Max. Dynamic Pressure (T=77)	Max. Long. Acceleration (T=138)	Max. Reentry Dyn. Press. (T_R=503)	Landing
S1	①	P(S1)	Note (1)	-793.165	-1165.356	-1020.254	-1111.096	-147.899
	②	M(S1)	Note (2)	450.755	559.148	1337.281	909.845	83.067
	③	A	Table 3-24	.020				
	④	I/y	Table 3-24	.041225				
	⑤	σ_{AXIAL}	-①/③	+39658	+58268	+91013	+55595	+7395
	⑥	$\sigma_{BEND.}$	-②/④	-10934	-13563	-32438	-22070	-2034
	⑦	σ_{IF}	⑤+⑥	+28724	+44705	+58575	+33525	+5361
	⑧	σ_{OF}	⑤-⑥	+50592	+71831	+123451	+77665	+9429
	①	P(S2)	Note (1)	793.165	1165.356	1020.254	1111.096	147.899
	②	M(S2)	Note (2)	-1465.775	-1820.960	-4371.336	-3103.747	-289.712
	③	A	Table 3-24	.020				
	④	I/y	Table 3-24	.041225				
	⑤	σ_{AXIAL}	①/③	+39658	+58268	+91013	+55595	+7395
	⑥	$\sigma_{BEND.}$	②/④	-35555	-44171	-106035	-75288	-7028
	⑦	σ_{IF}	⑤+⑥	+4103	+14097	-15022	-19693	+367
	⑧	σ_{OF}	⑤-⑥	+75213	+102439	+197048	+130883	+14423
S2	①	P(S2)	Note (1)	45.852	-122.938	677.190	668.636	36.154
	②	M(S2)	Note (2)	-105.147	-131.554	-311.789	-224.381	-21.079
	③	A	Table 3-24	.028				
	④	I/y	Table 3-24	.005501				
	⑤	σ_{AXIAL}	-①/③	-1638	+4391	-24185	-23880	-1291
	⑥	$\sigma_{BEND.}$	-②/④	+19114	+23915	+56679	+40789	+3032
	⑦	σ_{IF}	⑤+⑥	+17476	+28306	+32494	+16909	+2541
	⑧	σ_{OF}	⑤-⑥	-20752	-19524	-80864	-64669	+5123
	①	P(S3)	Note (1)	-45.852	122.938	-677.190	-668.636	-36.154
	②	M(S3)	Note (2)	-41.973	-53.431	-122.021	-88.013	-8.315
	③	A	Table 3-24	.028				
	④	I/y	Table 3-24	.005501				
	⑤	σ_{AXIAL}	①/③	-1638	+4391	-24185	-23880	-1291
	⑥	$\sigma_{BEND.}$	②/④	-7630	-9713	-22182	-15999	-1512
	⑦	σ_{IF}	⑤+⑥	-9268	-5322	-46367	-39879	-2803
	⑧	σ_{OF}	⑤-⑥	+5992	+14104	-2003	-7881	+221
S3	①	P(S3)	Note (1)	46.226	-122.488	678.117	669.556	37.073
	②	M(S3)	Note (2)	41.973	53.431	122.021	88.013	8.315
	③	A	Table 3-24	.020				
	④	I/y	Table 3-24	.003984				
	⑤	σ_{AXIAL}	-①/③	-2311	+6124	-33906	-33478	-1854
	⑥	$\sigma_{BEND.}$	-②/④	-10535	-13411	-30628	-22092	-2087
	⑦	σ_{IF}	⑤+⑥	-12846	-7287	-64534	-55570	-3941
	⑧	σ_{OF}	⑤-⑥	+8224	+19535	-3278	-11386	+233
	①	P(S4)	Note (1)	-46.226	122.488	-678.117	-669.556	-37.073
	②	M(S4)	Note (2)	17.767	23.966	47.672	32.994	-3.147
	③	A	Table 3-24	.020				
	④	I/y	Table 3-24	.003984				
	⑤	σ_{AXIAL}	①/③	-2311	+6124	-33906	-33478	-1854
	⑥	$\sigma_{BEND.}$	②/④	+4460	+6016	+11966	+8282	+790
	⑦	σ_{IF}	⑤+⑥	+2149	+12144	-21940	-25196	-1064
	⑧	σ_{OF}	⑤-⑥	-6771	+108	-45872	-41760	-2644

Table 3-27. Calculation of Meridional Stresses - Inner Cylindrical Bulkhead (continued)

Sec. No.	Row No.	Item	Design Cond. / Reference	Lift-Off ($T=0$)	Max. Dynamic Pressure ($T=77$)	Max. Long. Acceleration ($T=138$)	Max. Reentry Dyn. Press. ($T_R=505$)	Landing
	①	P(54)	Note (1)	46,947	-121.623	679.922	671.361	38.875
	②	M(54)	Note (2)	-17.767	-23.966	-47.672	-32.994	-3.147
	③	A	Table 3-24	.020				
	④	I/y		.003984				
	⑤	σ_{AXIAL}	-①/③	-2347	+6081	-33996	-33568	-1948
	⑥	$\sigma_{BEND.}$	-②/④	+4460	+6016	+11966	+8282	+790
	⑦	σ_{IF}	⑤+⑥	+2113	+12097	-22030	-25286	-1158
54	⑧	σ_{OF}	⑤-⑥	-6807	+65	-45962	-41850	-2738
	①	P(55)	Note (1)	-46.947	121.623	-679.922	-671.361	-38.875
	②	M(55)	Note (2)	-10.689	-16.302	-23.127	-13.900	-1.373
	③	A	Table 3-24	.020				
	④	I/y		.003984				
	⑤	σ_{AXIAL}	①/③	-2347	+6081	-33996	-33568	-1948
	⑥	$\sigma_{BEND.}$	②/④	-2683	-4092	-5805	-3489	-345
	⑦	σ_{IF}	⑤+⑥	-5030	+1989	-39801	-37057	-2293
	⑧	σ_{OF}	⑤-⑥	+336	+10173	-28191	-30079	-1603
	①	P(55)	Note (1)	47.666	-120.770	681.719	673.162	40.677
	②	M(55)	Note (2)	10.689	16.302	23.127	13.900	1.373
	③	A	Table 3-24	.020				
	④	I/y		.003984				
	⑤	σ_{AXIAL}	-①/③	-2383	+6039	-34086	-33658	-2034
	⑥	$\sigma_{BEND.}$	-②/④	-2683	-4092	-5805	-3489	-345
	⑦	σ_{IF}	⑤+⑥	-5066	+1947	-39891	-37147	-2379
55	⑧	σ_{OF}	⑤-⑥	+300	+10131	-28281	-30169	-1689
	①	P(56)	Note (1)	-47.666	120.770	-681.719	-673.162	-40.677
	②	M(56)	Note (2)	6.066	14.551	-2.507	-8.857	-0.684
	③	A	Table 3-24	.020				
	④	I/y		.003984				
	⑤	σ_{AXIAL}	①/③	-2383	+6039	-34086	-33658	-2034
	⑥	$\sigma_{BEND.}$	②/④	+1523	+3652	-629	-2223	-172
	⑦	σ_{IF}	⑤+⑥	-860	+9691	-34715	-35881	-2206
	⑧	σ_{OF}	⑤-⑥	-3906	+2387	-33457	-31435	-1862
	①	P(56)	Note (1)	48.031	-120.342	682.632	674.078	41.594
	②	M(56)	Note (2)	-6.066	-14.510	2.507	8.857	0.684
	③	A	Table 3-24	.020				
	④	I/y		.003984				
	⑤	σ_{AXIAL}	-①/③	-2402	+6017	-34132	-33704	-2080
	⑥	$\sigma_{BEND.}$	-②/④	+1522	+3642	-629	-2223	-172
	⑦	σ_{IF}	⑤+⑥	-879	+9659	-34761	-35927	-2252
56	⑧	σ_{OF}	⑤-⑥	-3925	+2375	-33503	-31481	-1908
	①	P(57)	Note (1)	-48.031	120.342	-682.632	-674.078	-41.594
	②	M(57)	Note (2)	2.481	-16.710	65.822	68.399	8.126
	③	A	Table 3-24	.020				
	④	I/y		.003984				
	⑤	σ_{AXIAL}	①/③	-2402	+6017	-34132	-33704	-2080
	⑥	$\sigma_{BEND.}$	②/④	+623	-4194	+16522	+17168	+2040
	⑦	σ_{IF}	⑤+⑥	-1779	+1823	-17610	-16536	-40
	⑧	σ_{OF}	⑤-⑥	-3025	+10211	-50654	-50872	-4120

Table 3-27. Calculation of Meridional Stresses - Inner Cylindrical Bulkhead (continued)

1) and 2) The number in parenthesis following the "P" or "M" in columns (1) and (2) identify the pertinent boundary node per figure 1-3. The loadings are obtained from tables 3-17 through 3-21 depending upon the design condition under consideration.

Table 3-28. Calculation of Meridional Stresses - Outer Cylindrical Bulkhead

Seg. No.	Row No.	Item	Reference \ Design Cond.	Lift-off (T=0)	Max. Dynamic Pressure (T=77)	Max. Long. Acceleration (T=138)	Max. Reentry Dyn. Press. (T_R=503)	Landing
	①	P(18)	Note (1)	-2540.612	-2928.277	-3933.402	-1421.564	245.663
	②	M(18)	Note (2)	-1659.891	4443.615	2467.410	-2284.926	925.360
	③	A	Table 3-24	.072				
	④	I/y	Table 3-24	.155228				
	⑤	σ_{AXIAL}	-①/③	+35287	+40671	+54631	+19744	-3412
	⑥	$\sigma_{BEND.}$	-②/④	+10693	-28626	-15895	+14719	-5961
	⑦	σ_{IF}	⑤+⑥	+45980	+12045	+38736	+34463	-9373
	⑧	σ_{OF}	⑤-⑥	+24594	+69297	+70526	+5025	+2549
57	①	P(58)	Note (1)	2540.612	2928.277	3933.402	1421.564	-245.663
	②	M(58)	Note (2)	45.867	-2488.273	-1338.586	1041.984	-186.490
	③	A	Table 3-24	.072				
	④	I/y	Table 3-24	.155228				
	⑤	σ_{AXIAL}	①/③	+35287	+40671	+54631	+19744	-3412
	⑥	$\sigma_{BEND.}$	②/④	+295	-16029	-8623	+6712	-1201
	⑦	σ_{IF}	⑤+⑥	+35582	+24642	+46008	+26456	-4613
	⑧	σ_{OF}	⑤-⑥	+34992	+56700	+63254	+13032	-2211
	①	P(58)	Note (1)	-1877.101	-2539.889	-3930.504	-1418.668	248.559
	②	M(58)	Note (2)	-48.588	2488.278	1338.598	-1041.974	186.490
	③	A	Table 3-24	.072				
	④	I/y	Table 3-24	.155228				
	⑤	σ_{AXIAL}	-①/③	+35270	+40652	+54591	+19704	-3452
	⑥	$\sigma_{BEND.}$	-②/④	+313	-16029	-8623	+6712	-1201
	⑦	σ_{IF}	⑤+⑥	+35583	+24623	+45968	+26416	-4653
	⑧	σ_{OF}	⑤-⑥	+34957	+56681	+63214	+12992	-2251
58	①	P(59)	Note (1)	2539.448	2926.889	3930.504	1418.668	-248.559
	②	M(59)	Note (2)	-1296.379	88.975	129.852	-317.475	435.524
	③	A	Table 3-24	.072				
	④	I/y	Table 3-24	.155228				
	⑤	σ_{AXIAL}	①/③	+35270	+40652	+54591	+19704	-3452
	⑥	$\sigma_{BEND.}$	②/④	-8351	+573	+837	-2045	+2806
	⑦	σ_{IF}	⑤+⑥	+26919	+41225	+55428	+17659	-646
	⑧	σ_{OF}	⑤-⑥	+43621	+40079	+53754	+21749	-6258
	①	P(59)	Note (1)	-2537.120	-2924.116	-3924.692	-1412.870	254.354
	②	M(59)	Note (2)	1296.388	-88.959	-129.830	317.479	-435.525
	③	A	Table 3-24	.072				
	④	I/y	Table 3-24	.155228				
	⑤	σ_{AXIAL}	-①/③	+35238	+40613	+54510	+19623	-3533
	⑥	$\sigma_{BEND.}$	-②/④	-8351	+573	+836	-2045	+2806
	⑦	σ_{IF}	⑤+⑥	+26887	+41186	+55346	+17578	-727
	⑧	σ_{OF}	⑤-⑥	+43589	+40040	+53674	+21668	-6339
59	①	P(60)	Note (1)	2537.120	2924.116	3924.692	1412.870	-254.354
	②	M(60)	Note (2)	-169.326	1120.246	921.162	-225.405	138.049
	③	A	Table 3-24	.072				
	④	I/y	Table 3-24	.155228				
	⑤	σ_{AXIAL}	①/③	+35238	+40613	+54510	+19623	-3533
	⑥	$\sigma_{BEND.}$	②/④	-1091	+7217	+5934	-1452	+889
	⑦	σ_{IF}	⑤+⑥	+34147	+47830	+60444	+18171	-2644
	⑧	σ_{OF}	⑤-⑥	+36329	+33396	+48576	+21075	-4422

Table 3-28. Calculation of Meridional Stresses - Outer Cylindrical Bulkhead (continued)

Sec. No.	Row No.	Item	Design Cond. / Reference	Lift-Off (T=0)	Max. Dynamic Pressure (T=77)	Max. Long. Acceleration (T=138)	Max. Reentry Dyn. Press. (T_R=505)	Landing
	①	P(60)	Note (1)	-2533.538	-2919.847	-3915.736	-1403.915	263.309
	②	M(60)	Note (2)	169.328	-1120.342	-921.156	225.405	-138.049
	③	A	Table 3-24	.072				
	④	I/y	Table 3-24	.155228				
	⑤	σ_{AXIAL}	- ①/③	+35188	+40554	+54386	+19499	-3657
	⑥	$\sigma_{BEND.}$	- ②/④	-1091	+7217	+5934	-1452	+889
	⑦	σ_{IF}	⑤ + ⑥	+34097	+47771	+60320	+18047	-2768
	⑧	σ_{OF}	⑤ - ⑥	+36279	+33337	+48452	+20951	-4546
60	①	P(61)	Note (1)	2533.538	2919.847	3915.736	1403.915	-263.309
	②	M(61)	Note (2)	186.177	-644.548	-603.133	24.664	-82.529
	③	A	Table 3-24	.072				
	④	I/y	Table 3-24	.155228				
	⑤	σ_{AXIAL}	①/③	+35188	+40554	+54386	+19499	-3657
	⑥	$\sigma_{BEND.}$	②/④	+1199	-4152	-3885	+159	-532
	⑦	σ_{IF}	⑤ + ⑥	+36387	+36402	+50501	+19658	-4189
	⑧	σ_{OF}	⑤ - ⑥	+33989	+44706	+58271	+19340	-3125
	①	P(61)	Note (1)	-2528.139	-2913.418	-3902.234	-1390.409	276.816
	②	M(61)	Note (2)	-187.175	644.551	603.137	-24.664	82.529
	③	A	Table 3-24	.140				
	④	I/y	Table 3-24	.299267				
	⑤	σ_{AXIAL}	- ①/③	+18058	+20811	+27874	+9932	-1977
	⑥	$\sigma_{BEND.}$	- ②/④	+625	-2153	-2015	+82	-276
	⑦	σ_{IF}	⑤ + ⑥	+18683	+18658	+25859	+10014	-2253
	⑧	σ_{OF}	⑤ - ⑥	+17433	+22964	+29889	+9850	-1701
61	①	P(62)	Note (1)	2528.139	2913.418	3902.234	1390.409	276.816
	②	M(62)	Note (2)	-31.127	-413.941	33.766	33.434	-0.015
	③	A	Table 3-24	.140				
	④	I/y	Table 3-24	.299267				
	⑤	σ_{AXIAL}	①/③	+18058	+20811	+27874	+9932	-1977
	⑥	$\sigma_{BEND.}$	②/④	-104	-1383	+113	+112	0
	⑦	σ_{IF}	⑤ + ⑥	+17954	+19428	+27987	+10044	-1977
	⑧	σ_{OF}	⑤ - ⑥	+18162	+22194	+27761	+9820	-1977
	①	P(62)	Note (1)	-2522.232	-2906.369	-3887.444	-1375.613	291.616
	②	M(62)	Note (2)	31.133	413.946	-33.761	-33.433	0.016
	③	A	Table 3-24	.140				
	④	I/y	Table 3-24	.299267				
	⑤	σ_{AXIAL}	- ①/③	+18016	+20760	+27768	+9826	-2083
	⑥	$\sigma_{BEND.}$	- ②/④	-104	-1383	+113	+112	0
	⑦	σ_{IF}	⑤ + ⑥	+17912	+19377	+27881	+9938	-2083
	⑧	σ_{OF}	⑤ - ⑥	+1820	+22143	+27655	+9714	-2083
62	①	P(63)	Note (1)	2522.232	2906.369	3887.444	1375.613	291.616
	②	M(63)	Note (2)	-357.689	-687.609	-218.591	1178.000	156.144
	③	A	Table 3-24	.140				
	④	I/y	Table 3-24	.299267				
	⑤	σ_{AXIAL}	①/③	+18016	+20760	+27768	+9826	-2083
	⑥	$\sigma_{BEND.}$	②/④	-1195	-2297	-730	+3936	+522
	⑦	σ_{IF}	⑤ + ⑥	+16821	+18463	+27038	+13762	-1561
	⑧	σ_{OF}	⑤ - ⑥	+19211	+23057	+28498	+5890	-2605

Table 3-28. Calculation of Meridional Stresses - Outer Cylindrical Bulkhead (continued)

Sec. No.	Row No.	Item	Design Cond. / Reference	Lift-off (T=0)	Max. Dynamic Pressure (T=77)	Max. Long. Acceleration (T=138)	Max. Reentry Dyn. Press. (TR=508)	Landing
	①	P(63)	Note (1)	-2518.423	-2901.825	-3877.886	-1366.040	301.193
	②	M(63)	Note (2)	357.711	687.628	218.607	-1178.001	-156.143
	③	A	Table 3-24			.140		
	④	I/y	Table 3-24			.299267		
	⑤	σ_{AXIAL}	- ①/③	+17989	+20728	+27700	+9758	-2151
	⑥	$\sigma_{BEND.}$	- ②/④	-1195	-2297	-730	+3936	+522
	⑦	σ_{IF}	⑤ + ⑥	+16794	+18431	+26970	+13694	-1629
63	⑧	σ_{OF}	⑤ - ⑥	+19184	+23025	+28430	+5822	-2673
	①	P(64)	Note (1)	2518.423	2901.825	3877.886	1366.040	-301.193
	②	M(64)	Note (2)	-2131.838	-2222.760	-2687.677	619.526	32.346
	③	A	Table 3-24			.140		
	④	I/y	Table 3-24			.299267		
	⑤	σ_{AXIAL}	①/③	+17989	+20728	+27700	+9758	-2151
	⑥	$\sigma_{BEND.}$	②/④	-7122	-7426	-8980	+2070	+108
	⑦	σ_{IF}	⑤ + ⑥	+10867	+13302	+18720	+11828	-2043
	⑧	σ_{OF}	⑤ - ⑥	+25111	+28154	+36680	+7688	-2259
	①	P(64)	Note (1)	-2516.568	-2899.573	-3873.151	-1361.263	305.983
	②	M(64)	Note (2)	2131.912	2222.829	2687.748	-619.541	-32.346
	③	A	Table 3-24			.140		
	④	I/y	Table 3-24			.299267		
	⑤	σ_{AXIAL}	- ①/③	+17976	+20712	+27666	+9724	-2186
	⑥	$\sigma_{BEND.}$	- ②/④	-7123	-7426	-8980	+2070	+108
	⑦	σ_{IF}	⑤ + ⑥	+10853	+13286	+18686	+11794	-2078
64	⑧	σ_{OF}	③ - ⑥	+25099	+28138	+36646	+7654	-2294
	①	P(65)	Note (1)	2516.568	2899.573	3873.151	1361.263	-305.983
	②	M(65)	Note (2)	-3505.502	-3572.510	-4762.789	-536.846	-158.317
	③	A	Table 3-24			.140		
	④	I/y	Table 3-24			.299267		
	⑤	σ_{AXIAL}	①/③	+17976	+20712	+27666	+9724	-2186
	⑥	$\sigma_{BEND.}$	②/④	-11712	-11936	-15912	-1794	-529
	⑦	σ_{IF}	⑤ + ⑥	+6264	+8776	+11754	+7930	-2715
	⑧	σ_{OF}	⑤ - ⑥	+29688	+32648	+43578	+11518	-1657
	①	P(65)	Note (1)	-597.673	-944.299	-1155.750	-760.505	436.523
	②	M(65)	Note (2)	-809.331	-823.772	-1345.075	-807.650	-128.224
	③	A	Table 3-24			.028		
	④	I/y	Table 3-24			.010144		
	⑤	σ_{AXIAL}	- ①/③	+21345	+33725	+41276	+27161	-15590
	⑥	$\sigma_{BEND.}$	- ②/④	+79784	+81207	+132597	+79618	+12640
	⑦	σ_{IF}	⑤ + ⑥	+101129	+114932	+173873	+106779	-2950
65	⑧	σ_{OF}	⑤ - ⑥	-58439	-47482	-91321	-52457	-28230
	①	P(66)	Note (1)	597.673	944.299	1155.750	760.505	-436.525
	②	M(66)	Note (2)	-115.188	-118.107	-227.598	-173.635	-25.458
	③	A	Table 3-24			.028		
	④	I/y	Table 3-24			.010144		
	⑤	σ_{AXIAL}	①/③	+21345	+33725	+41276	+27161	-15590
	⑥	$\sigma_{BEND.}$	②/④	-11355	-11643	-22437	-17117	-2510
	⑦	σ_{IF}	⑤ + ⑥	+9990	+22082	+18839	+10044	-18100
	⑧	σ_{IF}	⑤ - ⑥	+32700	+45368	+63713	+44278	-13080

Table 3-28. Calculation of Meridional Stresses - Outer Cylindrical Bulkhead (continued)

Sec. No.	Row No.	Item	Design Cond. / Reference	Lift-Off ($T=0$)	Max. Dynamic Pressure ($T=77$)	Max. Long. Acceleration ($T=138$)	Max. Reentry Dyn. Press. ($T_R=505$)	Landing
66	(1)	P(66)	Note (1)	-597.363	-943.935	-1154.980	-759.747	437.280
	(2)	M(66)	Note (2)	115.188	118.108	227.598	173.634	25.457
	(3)	A	Table 3-24	.028				
	(4)	I/y		.010144				
	(5)	σ_{AXIAL}	-(1)/(3)	+21334	+33712	+41249	+27134	-15617
	(6)	$\sigma_{BEND.}$	-(2)/(4)	-11355	-11643	-22437	-17117	-2510
	(7)	σ_{IF}	(5)+(6)	+9979	+22069	+18812	+10017	-18127
	(8)	σ_{OF}	(5)-(6)	+32689	+45355	+63686	+44251	-13107
	(1)	P(67)	Note (1)	597.363	943.935	1154.980	759.747	-437.280
	(2)	M(67)	Note (2)	-213.033	-229.773	-441.350	-307.455	-38.760
	(3)	A	Table 3-24	.028				
	(4)	I/y		.010144				
	(5)	σ_{AXIAL}	(1)/(3)	+21334	+33712	+41249	+27134	-15617
	(6)	$\sigma_{BEND.}$	(2)/(4)	-21001	-22651	-43508	-30309	-3821
	(7)	σ_{IF}	(5)+(6)	+333	+11061	-2259	-3175	-19438
	(8)	σ_{OF}	(5)-(6)	+42335	+56363	+84757	+57443	-11796
67	(1)	P(67)	Note (1)	-597.010	-943.503	-1154.082	-748.850	438.176
	(2)	M(67)	Note (2)	213.033	229.773	441.350	307.455	38.760
	(3)	A	Table 3-24	.028				
	(4)	I/y		.010144				
	(5)	σ_{AXIAL}	-(1)/(3)	+21322	+33696	+41217	+26744	-15649
	(6)	$\sigma_{BEND.}$	-(2)/(4)	-21001	-22651	-43508	-30309	-3821
	(7)	σ_{IF}	(5)+(6)	+321	+11045	-2291	-3565	-19470
	(8)	σ_{OF}	(5)-(6)	+42323	+56347	+84725	+57053	-11828
	(1)	P(68)	Note (1)	597.010	943.503	1154.082	748.850	-438.176
	(2)	M(68)	Note (2)	-8.366	-5.660	0.350	-9.294	-0.932
	(3)	A	Table 3-24	.028				
	(4)	I/y		.010144				
	(5)	σ_{AXIAL}	(1)/(3)	+21322	+33696	+41217	+26744	-15649
	(6)	$\sigma_{BEND.}$	(2)/(4)	-825	-558	+35	-916	-92
	(7)	σ_{IF}	(5)+(6)	+20497	+33138	+41252	+25828	-15741
	(8)	σ_{OF}	(5)-(6)	+22147	+34254	+41182	+27660	-15557
68	(1)	P(68)	Note (1)	-596.707	-943.146	-1153.331	-748.095	438.935
	(2)	M(68)	Note (2)	8.365	5.659	-0.351	9.294	0.932
	(3)	A	Table 3-24	.028				
	(4)	I/y		.010144				
	(5)	σ_{AXIAL}	-(1)/(3)	+21311	+33684	+41190	+26717	-15676
	(6)	$\sigma_{BEND.}$	-(2)/(4)	-825	-558	+35	-916	-92
	(7)	σ_{IF}	(5)+(6)	+20486	+33126	+41225	+25801	-15768
	(8)	σ_{OF}	(5)-(6)	+22136	+34242	+41155	+27633	-15584
	(1)	P(69)	Note (1)	596.707	943.146	1153.331	748.095	-438.935
	(2)	M(69)	Note (2)	412.892	510.958	1236.851	948.482	87.429
	(3)	A	Table 3-24	.028				
	(4)	I/y		.010144				
	(5)	σ_{AXIAL}	(1)/(3)	+21311	+33684	+41190	+26717	-15767
	(6)	$\sigma_{BEND.}$	(2)/(4)	+40703	+50370	+121929	+93501	+8619
	(7)	σ_{IF}	(5)+(6)	+62014	+84054	+163119	+120218	-7057
	(8)	σ_{OF}	(5)-(6)	-19392	-16686	-80739	-66784	-24295

Table 3-28. Calculation of Meridional Stresses - Outer Cylindrical Bulkhead (continued)

Seg. No.	Row No.	Item	Reference \ Design Cond.	Lift-off (T=0)	Max. Dynamic Pressure (T=77)	Max. Long. Acceleration (T=138)	Max. Reentry Dyn. Press. (T_R=503)	Landing
69	(1)	P(69)	Note (1)	-206.705	-460.189	8.984	154.565	579.348
	(2)	M(69)	Note (2)	408.359	508.870	1238.165	939.689	85.696
	(3)	A	Table 3-24			.032		
	(4)	I/y				.011557		
	(5)	σ_{AXIAL}	-(1)/(3)	+6462	+14381	-281	-4830	-18105
	(6)	$\sigma_{BEND.}$	-(2)/(4)	-35334	-39819	-107136	-81309	-7415
	(7)	σ_{IF}	(5)+(6)	-28872	-25438	-107417	-86139	-25520
	(8)	σ_{OF}	(5)-(6)	+41796	+54200	+106855	+76479	-10690
	(1)	P(70)	Note (1)	206.705	406.189	-8.984	-154.565	-579.348
	(2)	M(70)	Note (2)	59,465	71.860	173.817	152,335	13,047
	(3)	A	Table 3-24			.032		
	(4)	I/y				.011557		
	(5)	σ_{AXIAL}	(1)/(3)	+6462	+14381	-281	-4830	-18105
	(6)	$\sigma_{BEND.}$	(2)/(4)	+5145	+6218	+15040	+13181	+1129
	(7)	σ_{IF}	(5)+(6)	+11607	+20599	+14759	+8351	-16976
	(8)	σ_{OF}	(5)-(6)	+1317	+8163	-15321	-18011	-19234
70	(1)	P(70)	Note (1)	-206.332	-459.655	10.099	155.674	580.455
	(2)	M(70)	Note (2)	-59.465	-71.860	-173.817	-152.335	-13.047
	(3)	A	Table 3-24			.028		
	(4)	I/y				.010144		
	(5)	σ_{AXIAL}	-(1)/(3)	+7369	+16416	-361	-5560	-20730
	(6)	$\sigma_{BEND.}$	-(2)/(4)	+5862	+7084	+17135	+15017	+1286
	(7)	σ_{IF}	(5)+(6)	+13231	+23500	+16774	+9457	-19444
	(8)	σ_{OF}	(5)-(6)	+1507	+9332	-17496	-20577	-22016
	(1)	P(71)	Note (1)	206.332	459.655	-10.099	-155.674	-580.455
	(2)	M(71)	Note (2)	14.182	18.610	43.027	27.904	3.415
	(3)	A	Table 3-24			.028		
	(4)	I/y				.010144		
	(5)	σ_{AXIAL}	(1)/(3)	+7369	+16416	-361	-5560	-20730
	(6)	$\sigma_{BEND.}$	(2)/(4)	+1398	+1835	+4242	+2751	+337
	(7)	σ_{IF}	(5)+(6)	+8767	+18251	+3881	-2809	-20393
	(8)	σ_{OF}	(5)-(6)	+5971	+14581	-4603	-8311	-21067
71	(1)	P(71)	Note (1)	-205.742	-458.948	11.579	157.156	581.937
	(2)	M(71)	Note (2)	-14.182	-18.610	-43.027	-27.904	-3.415
	(3)	A	Table 3-24			.028		
	(4)	I/y				.010144		
	(5)	σ_{AXIAL}	-(1)/(3)	+7348	+16391	-414	-5613	-20783
	(6)	$\sigma_{BEND.}$	-(2)/(4)	+1398	+1835	+4242	+2751	+337
	(7)	σ_{IF}	(5)+(6)	+8746	+18226	+3828	-2862	-20446
	(8)	σ_{OF}	(5)-(6)	+5950	+14556	-4656	-8364	-21120
	(1)	P(72)	Note (1)	205.742	458.948	-11.579	-157.156	-581.937
	(2)	M(72)	Note (2)	-5.509	-8.113	-13.442	-8.486	-0.731
	(3)	A	Table 3-24			.028		
	(4)	I/y				.010144		
	(5)	σ_{AXIAL}	(1)/(3)	+7348	+16391	-414	-5613	-20783
	(6)	$\sigma_{BEND.}$	(2)/(4)	-543	-800	-1325	-837	-72
	(7)	σ_{IF}	(5)+(6)	+6805	+15591	-1739	-6450	-20855
	(8)	σ_{OF}	(5)-(6)	+7891	+17191	+911	-4776	-20711

Table 3-28. Calculation of Meridional Stresses - Outer Cylindrical Bulkhead (continued)

Sec. No.	Row No.	Item	Design Cond. / Reference	Lift-Off (T=0)	Max. Dynamic Pressure (T=77)	Max. Long. Acceleration (T=138)	Max. Reentry Dyn. Press. (T_R=505)	Landing
72	①	P (72)	Note (1)	-205.146	-458.241	13.059	158.638	583.419
	②	M (72)	Note (2)	5.509	8.113	13.442	8.486	0.731
	③	A	Table 3-24	.028				
	④	I/y	Table 3-24	.010144				
	⑤	σ_{AXIAL}	-①/③	+7327	+16366	-466	-5666	-20836
	⑥	$\sigma_{BEND.}$	-②/④	-543	-800	-1325	-837	-72
	⑦	σ_{IF}	⑤+⑥	+6784	+15566	-1791	-6503	-20908
	⑧	σ_{OF}	⑤-⑥	+7870	+17166	+859	-4829	-20764
	①	P (73)	Note (1)	205.146	458.241	-13.059	-158.638	-583.419
	②	M (73)	Note (2)	-29.201	-48.104	-55.340	-30.776	-47.077
	③	A	Table 3-24	.028				
	④	I/y	Table 3-24	.010144				
	⑤	σ_{AXIAL}	①/③	+7327	+16366	-466	-5666	-20836
	⑥	$\sigma_{BEND.}$	②/④	-2879	-4742	-5455	-3034	-4641
	⑦	σ_{IF}	⑤+⑥	+4448	+11624	-5921	-8700	-25477
	⑧	σ_{OF}	⑤-⑥	+10206	+21108	+4989	-2632	-16195
73	①	P (73)	Note (1)	-204.712	-457.726	14.160	159.742	584.527
	②	M (73)	Note (2)	29.201	48.104	55.340	30.776	47.077
	③	A	Table 3-24	.028				
	④	I/y	Table 3-24	.010144				
	⑤	σ_{AXIAL}	-①/③	+7311	+16347	-506	-5705	-20876
	⑥	$\sigma_{BEND.}$	-②/④	-2879	-4742	-5455	-3034	-4641
	⑦	σ_{IF}	⑤+⑥	+4432	+11605	-5961	-8739	-25517
	⑧	σ_{OF}	⑤-⑥	+10190	+21089	+4949	-2671	-16235
	①	P (74)	Note (1)	204.712	457.726	-14.160	-159.742	-584.527
	②	M (74)	Note (2)	119.446	206.294	196.825	95.958	155.064
	③	A	Table 3-24	.028				
	④	I/y	Table 3-24	.010144				
	⑤	σ_{AXIAL}	①/③	+7311	+16347	-506	-5705	-20876
	⑥	$\sigma_{BEND.}$	②/④	+11775	+20336	+19403	+9460	+15286
	⑦	σ_{IF}	⑤+⑥	+19086	+36683	+18897	+3755	-5590
	⑧	σ_{OF}	⑤-⑥	-4464	-3989	-19909	-15165	-36162

Notes: 1) & 2) The number in parentheses following the "P" and "M" in Rows ① and ② identify the pertinent boundary node per figure 1-4. The loadings are obtained from tables 3-17 through 3-21 depending upon the design condition under consideration.

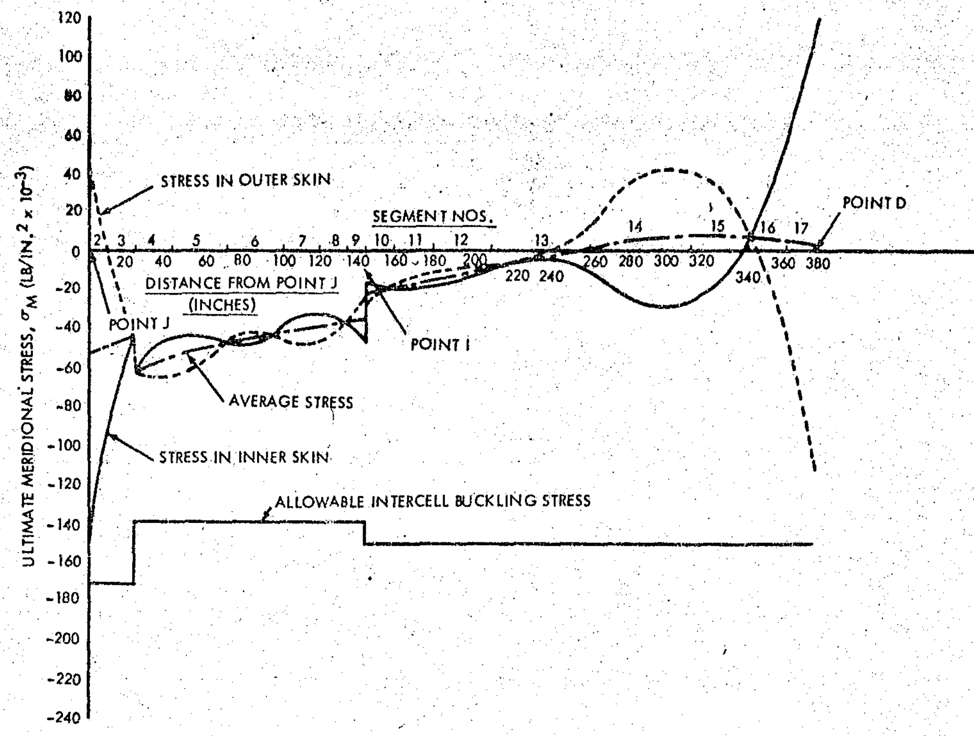

Figure 3-2. Ultimate Meridional Stress Distribution in Upper Frustum
Max. Longitudinal Acceleration Condition (T = 138 Seconds)

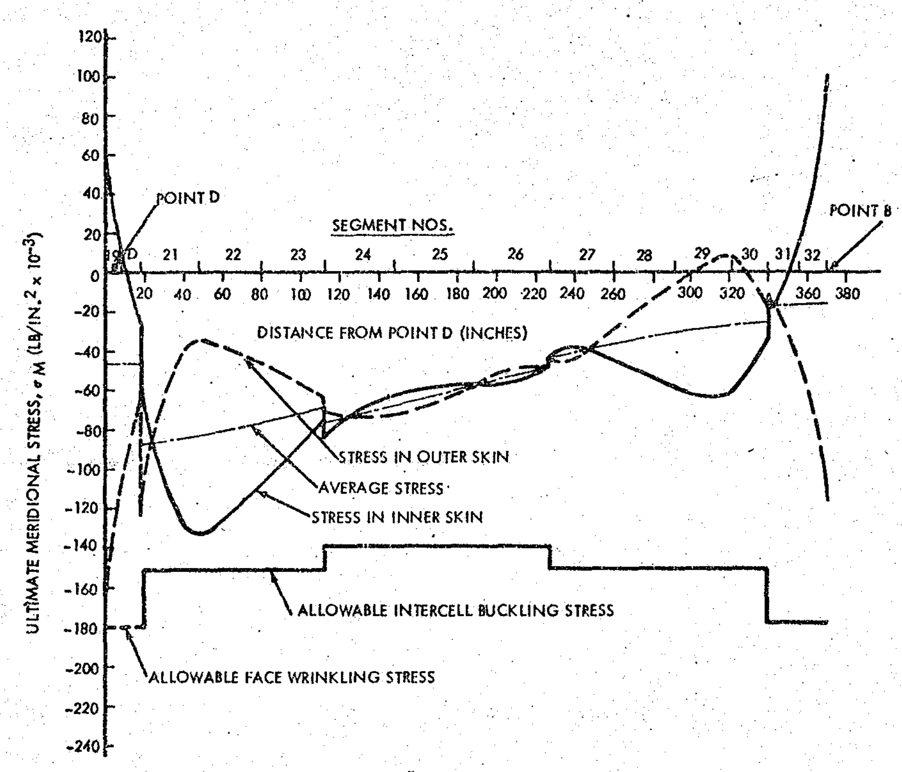

Figure 3-3. Ultimate Meridional Stress Distribution in Lower Frustum
Max. Longitudinal Acceleration Condition (T = 138 Seconds)

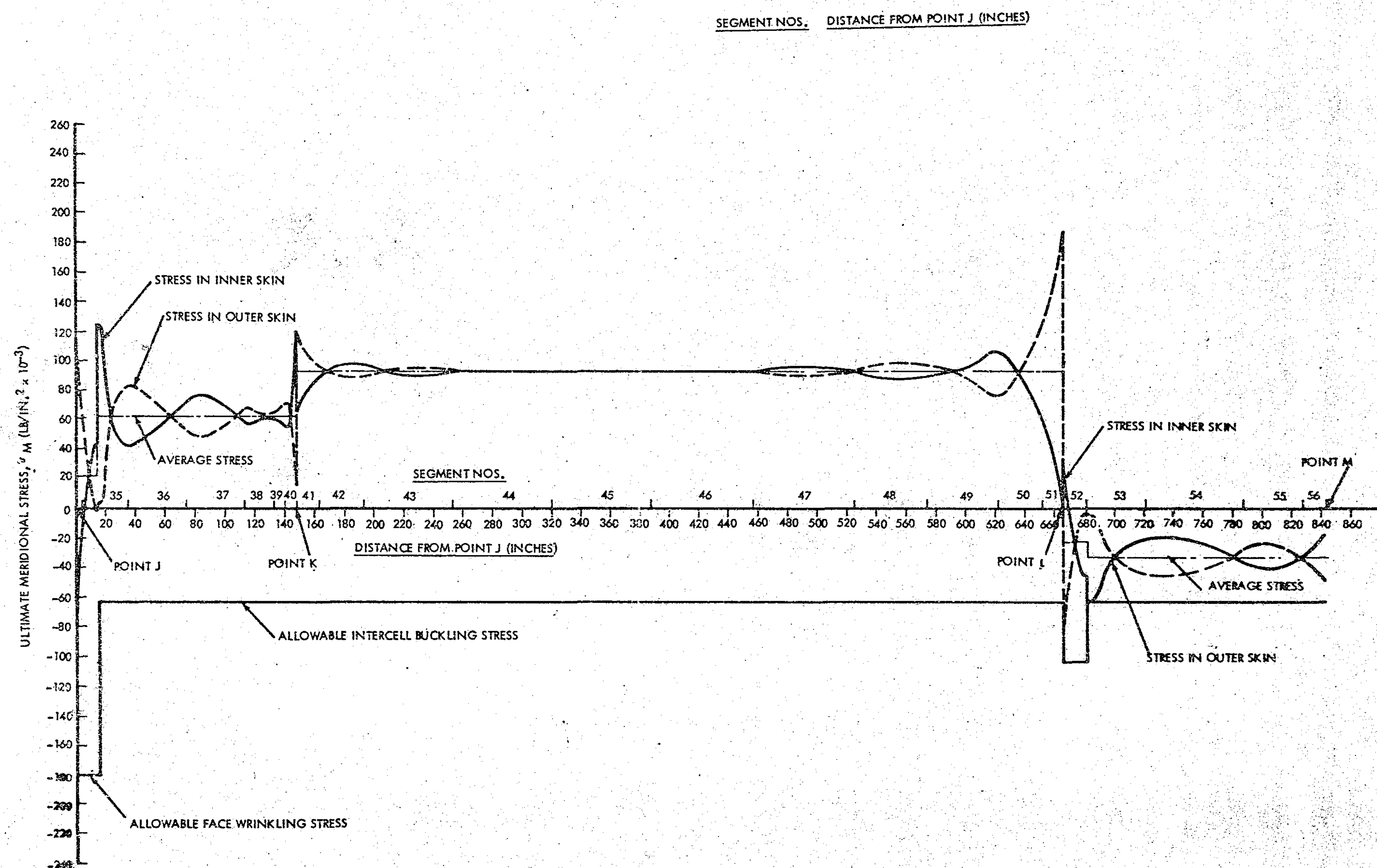

Figure 3-4. Ultimate Meridional Stress Distribution in Inner Cylindrical Bulkhead Max. Longitudinal Acceleration Condition (T = 138 Seconds)

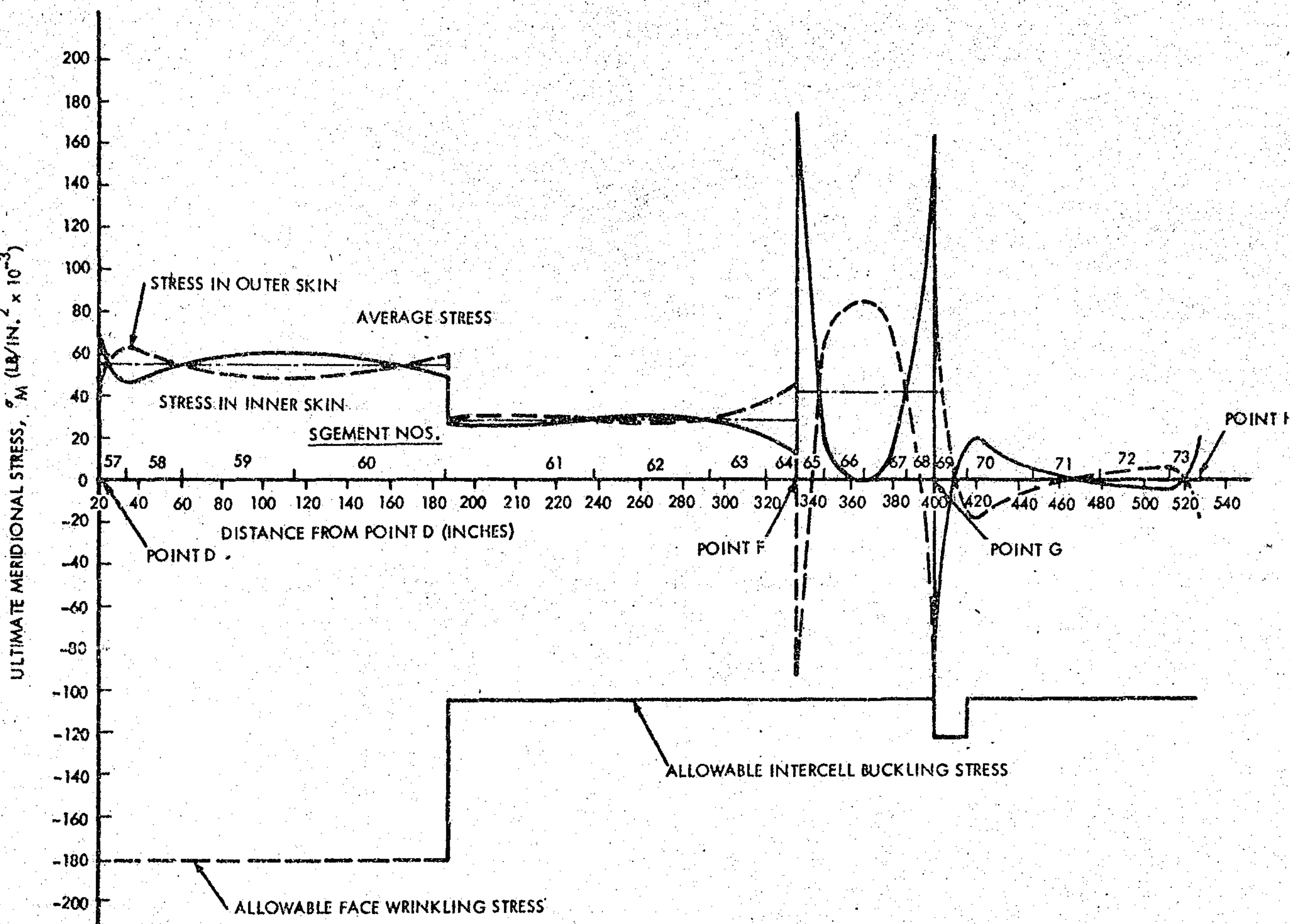

Figure 3-5. Ultimate Meridional Stress Distribution in Outer Cylindrical Bulkhead Max. Longitudinal Acceleration Condition (T = 138 Seconds)

Table 3-29. Calculation of Hoop Stress Distribution in Upper Frustum

(a) LIFT-OFF CONDITION (T = 0 SECONDS)

①	②	③	④	⑤	⑥	⑦	⑧	⑨	⑩
SEGMENT No.	R_i	R_j	R_{AV}	$\cos\theta$	R_e	p_n	$p_n R_e$	$2t_F$	σ_H
REF.	TABLE 3-7	TABLE 3-7	.5[② + ③]	FIGURE 1-1	④/⑤	TABLE 3-7	⑥ × ⑦	TABLE 3-24	⑧/⑨
2	103.365	110.078	106.722	.707107	150.928	0	0	.052	0
3	110.078	120.146	115.112		162.793			.052	
4	120.146	133.570	126.858		179.404			.036	
5	133.570	154.126	143.848		203.432				
6	154.126	174.682	164.404		232.502				
7	174.682	188.106	181.394		256.530				
8	188.106	198.174	193.140		273.141				
9	198.174	204.887	201.531		285.008	0	0	.036	0
10	204.887	215.494	210.191		297.255	0.700	208.079	.040	5202
11	215.494	229.636	222.565		314.755	0.700	220.329		5508
12	229.636	250.849	240.243		339.755	0.700	237.829		5946
13	250.849	287.469	269.159		380.648	.780	296.905		7423
14	287.469	324.089	305.779		432.437	.941	406.923		10173
15	324.089	345.302	334.696		473.332	1.065	504.099		12602
16	345.302	359.444	352.373		498.331	1.146	571.087		14277
17	359.444	370.050	364.747	.707107	515.630	1.200	618.996	.040	15475

Table 3-29. Calculation of Hoop Stress Distribution in Upper Frustum (continued)

(b) MAX. DYNAMIC PRESSURE CONDITION (T= 77 SECONDS)

①	②	③	④	⑤	⑥	⑦	⑧	⑨	⑩
SEGMENT No.	R_i	R_j	R_{AV}	$\cos\theta$	R_e	p_n	$p_n R_e$	$2t_F$	σ_H
REF.	TABLE 3-8	TABLE 3-8	.5[②+③]	FIGURE 1-1	④/⑤	TABLE 3-8	⑥×⑦	TABLE 3-24	⑧/⑨
2	103.365	110.078	106.722	.707107	150.928	-1.148	-173.265	.052	-3332
3	110.078	120.146	115.112	↑	162.793	↑	-186.886	.052	-3594
4	120.146	133.570	126.858		179.404		-205.956	.036	-5721
5	133.570	154.126	143.848		203.432		-233.540	↑	-6487
6	154.126	174.682	164.404		232.502		-266.912		-7414
7	174.682	188.106	181.394		256.530		-294.496		-8180
8	188.106	198.174	193.140		273.141	↓	-313.566	↓	-8710
9	198.174	204.887	201.531		285.008	-1.148	-327.189	.036	-9089
10	204.887	215.494	210.191		297.255	1.021	303.497	.040	7587
11	215.494	229.636	222.565		314.755	.985	310.034	↑	7751
12	229.636	250.849	240.243		339.755	.880	298.984		7475
13	250.849	287.469	269.159		380.648	.378	143.085		3597
14	287.469	324.089	305.779		432.437	-.733	-316.976		-7924
15	324.089	345.302	334.696		473.332	-1.880	-889.864		-22247
16	345.302	359.444	352.373	↓	498.331	-2.651	-1321.075	↓	-33020
17	359.444	370.050	364.747	.707107	515.830	-3.225	-1663.552	.040	-41588

Table 3-29. Calculation of Hoop Stress Distribution in Upper Frustum (continued)

(c) MAX. LONGITUDINAL ACCELERATION CONDITION (T = 138 SECONDS)

①	②	③	④	⑤	⑥	⑦	⑧	⑨	⑩
SEGMENT NO.	R_i	R_j	R_{AV}	$\cos\theta$	R_e	p_n	$p_n R_e$	$2t_f$	σ_H
REF.	TABLE 3-9	TABLE 3-9	.5[② + ③]	FIGURE 1-1	④/⑤	TABLE 3-9	⑥ × ⑦	TABLE 3-24	⑧/⑨
2	103.365	110.078	106.722	.707107	150.928	−.543	−81.954	.052	−1576
3	110.078	120.146	115.112		162.793		−88.397	.052	−1700
4	120.146	133.570	126.858		179.404		−97.416	.036	−2706
5	133.570	154.126	143.848		203.432		−110.464		−3068
6	154.126	174.682	164.404		232.502		−126.249		−3507
7	174.682	188.106	181.394		256.530		−139.296		−3869
8	188.106	198.174	193.140		273.141		−148.316		−4120
9	198.174	204.887	201.531		285.008	−.543	−154.759	.036	−4299
10	204.887	215.494	210.191		297.255	6.988	2077.008	.040	51925
11	215.494	229.636	222.565		314.755	6.971	2194.157		54853
12	229.636	250.849	240.243		339.755	6.922	2351.784		58795
13	250.849	287.469	269.159		380.648	6.684	2544.251		63606
14	287.469	324.089	305.779		432.437	6.158	2662.997		66574
15	324.089	345.302	334.696		473.332	5.616	2658.233		66456
16	345.302	359.444	352.373		498.331	5.251	2616.736		65418
17	359.444	370.050	364.747	.707107	515.630	4.979	2568.318	.040	64208

Table 3-29. Calculation of Hoop Stress Distribution in Upper Frustum (continued)

REENTRY CONDITION (T_R = 505 SECONDS)

①	②	③	④	⑤	⑥	⑦	⑧	⑨	⑩
SEGMENT No.	R_i	R_j	R_{AV}	$\cos\theta$	R_e	p_n	$p_n R_e$	$2t_F$	σ_H
REF.	TABLE 3-10	TABLE 3-10	.5[② + ③]	FIGURE 1-1	④/⑤	TABLE 3-10	⑥ × ⑦	TABLE 3-24	⑧/⑨
2	103.365	110.078	106.722	.707107	150.928	0	0	.052	0
3	110.078	120.146	115.112		162.793			.052	
4	120.146	133.570	126.858		179.404			.036	
5	133.570	154.126	143.848		203.432				
6	154.126	174.682	164.404		232.502				
7	174.682	188.106	181.394		256.530				
8	188.106	198.174	193.140		273.141				
9	198.174	204.887	201.531		285.008	0	0	.036	0
10	204.887	215.494	210.191		297.255	7.700	2288.633	.040	57216
11	215.494	229.636	222.565		314.755		2423.614		60590
12	229.636	250.849	240.243		339.755		2616.114		65403
13	250.849	287.469	269.159		380.648		2930.990		73275
14	287.469	324.089	305.779		432.437		3329.765		83244
15	324.089	345.302	334.696		473.332		3644.656		91116
16	345.302	359.444	352.373		498.381		3631.149		95929
17	359.444	370.050	364.747	.707107	515.830	7.700	3971.891	.040	99297

PRECEDING PAGE BLANK NOT FILMED

Table 3-30. Calculation of Hoop Stress Distribution in Lower Frustum

LIFT OFF CONDITION (T = 0 SECONDS)

①	②	③	④	⑤	⑥	⑦	⑧	⑨	⑩
SEGMENT NO.	R_i	R_t	R_{AV}	cos θ	R_c	p_n	$p_n R_c$	$2t_F$	σ_H
REF	TABLE 3-7	TABLE 3-7	.5[②+③]	FIGURE 1-2	④/⑤	TABLE 3-7	⑥ × ⑦	TABLE 3-24	⑧/⑨
19	37[illegible]	373.435	371.743	.908323	409.263	1.400	572.968	.076	7539
20	373.435	377.618	375.527		413.429		578.801	.076	7616
21	377.618	389.954	383.786		422.521		591.529	.040	14788
22	389.954	403.715	396.836		436.888		611.643		15291
23	403.716	417.492	410.600		452.041	1.400	632.857	[illegible]	15821
24	417.462	432.548	425.015		467.911	2.357	1102.866	.036	30635
25	432.548	448.731	440.640		485.113	4.341	2105.876		58497
26	448.731	464.914	456.823		502.930	6.397	3217.243	.036	89369
27	464.914	478.374	471.644		519.247	8.280	4299.365	.040	107484
28	476.874	491.834	485.104		534.065	9.989	5334.775		133369
29	491.8[illegible]	504.[illegible]	498.162		5[illegible]	11.651	6390.142		159754
30	504.529	512.346	508.438		559.754	12.953	7250.494	.040	181262
31	512.346	518.902	515.624		567.665	13.866	7871.243	.054	145768
32	518.902	525.176	522.039	.908323	574.728	14.681	8437.582	.054	1[illegible]256

Table 3-30. Calculation of Hoop Stress Distribution in Lower Frustum (continued)

MAX. DYNAMIC PRESSURE CONDITION (T = 77 SECONDS)

①	②	③	④	⑤	⑥	⑦	⑧	⑨	⑩
SEGMENT No.	R_i	R_j	R_{AV}	cos θ	R_e	P_n	$P_n R_e$	$2t_F$	σ_H
REF.	TABLE 3-8	TABLE 3-8	.5[②+③]	FIGURE 1-2	④/⑤	TABLE 3-8	⑥ × ⑦	TABLE 3-24	⑧/⑨
19	370.050	373.435	371.743	.908323	409.263	8.257	3379.285	.076	44464
20	373.435	377.618	375.527	↓	413.429	8.248	3409.962	.076	44868
21	377.618	389.954	383.786		422.521	8.221	3473.545	.040	86839
22	389.954	403.715	396.836		436.888	8.177	3572.433	↓	89311
23	403.715	417.482	410.600		452.041	8.132	3675.997	[illegible]	91900
24	417.482	432.548	425.015		467.911	8.096	3788.207	.036	105229
25	432.548	448.731	440.640		485.113	8.060	3910.011	↓	108612
26	448.731	464.914	456.823		502.930	8.033	4040.037	.036	112224
27	464.914	478.374	471.644		519.247	8.015	4161.765	.040	104044
28	478.374	491.834	485.104		534.065	9.277	4954.521	↓	123863
29	491.834	504.529	498.182		548.465	11.784	6446.634	↓	161166
30	504.529	512.346	508.438		559.754	13.700	7668.630	.040	191716
31	512.346	518.902	515.624	↓	567.665	15.068	8553.576	.054	158404
32	518.902	525.176	522.039	.908323	574.728	16.296	9365.767	.054	173[illegible]

C-199

Table 3-30. Calculation of Hoop Stress Distribution in Lower Frustum (continued)

MAX. LONGITUDINAL ACCELERATION CONDITION (T = 138 SECONDS)

①	②	③	④	⑤	⑥	⑦	⑧	⑨	⑩
SEGMENT NO.	R_i	R_{i+1}	R_{AV}	cos θ	R_c	p_n	$p_n R_c$	$2t_F$	σ_H
REF	TABLE 3-9	TABLE 3-9	.5[②+③]	FIGURE 1-2	④/⑤	TABLE 3-9	⑥ × ⑦	TABLE 3-24	⑧/⑨
19	370.050	373.435	371.743	.908323	409.263	14.469	5921.626	.076	77916
20	373.435	377.618	375.527	↓	413.429	14.464	5979.837	.076	78682
21	377.618	389.954	383.786	↓	422.521	14.452	6106.273	.040	152657
22	389.954	403.716	396.836	↓	436.885	14.431	6304.731	↓	157618
23	403.716	417.482	410.600	↓	452.041	14.410	6513.911	.040	162848
24	417.482	432.548	425.015	↓	467.911	14.393	6734.643	.036	187075
25	432.548	448.731	440.640	↓	485.113	14.376	6973.984	↓	193723
26	448.731	464.914	456.823	↓	502.930	14.363	7223.584	.036	200657
27	464.914	478.374	471.644	↓	519.247	14.354	7453.271	.040	186332
28	478.374	491.834	485.104	↓	534.065	14.341	7659.026	↓	191476
29	491.834	504.529	498.182	↓	548.463	14.329	7858.926	↓	196473
30	504.529	512.346	508.438	↓	559.754	14.320	8015.677	.040	200392
31	512.346	518.902	515.624	↓	567.665	15.619	8866.360	.034	164106
32	518.902	525.176	522.039	.908323	574.728	18.169	10442.233	.034	193380

Table 3-30. Calculation of Hoop Stress Distribution in Lower Frustum (continued)

REENTRY CONDITION (T_R = 505 SECONDS)

①	②	③	④	⑤	⑥	⑦	⑧	⑨	⑩
SEGMENT NO.	R_i	R_{γ}	R_{AV}	cos θ	R_e	p_n	$p_n R_e$	$2t_F$	σ_H
REF	TABLE 3-10	TABLE 3-10	.5[②+③]	FIGURE 1-2	④/⑤	TABLE 3-10	⑥×⑦	TABLE 3-24	⑧/⑨
19	370.050	373.435	371.743	.908323	409.263	7.000	2864.841	.076	37696
20	373.435	377.618	375.527	↕	413.429	↕	2899.003	.076	38099
21	377.618	389.954	383.786		422.521		2957.647	.040	73941
22	389.954	403.718	396.836		436.888		3058.216	↕	76455
23	403.718	417.402	410.600		452.041		3164.287	.040	79107
24	417.462	432.548	425.015		467.911		3275.377	.036	90983
25	432.548	448.731	440.640		485.113		3395.791	↕	94328
26	448.731	464.914	456.823		502.930		3520.510	.036	97793
27	464.914	478.374	471.644		519.247		3634.729	.040	90868
28	478.374	491.834	485.104		534.065		3738.455	↕	93461
29	491.834	504.529	498.182		548.463		3839.241		95981
30	504.529	512.346	508.438		559.754		3918.278	.040	97957
31	512.346	518.962	515.624		567.665		3973.655	.034	[illegible]
32	518.902	525.176	522.039	.908323	574.728	7.000	4023.096	.034	[illegible]

Table 3-30. Calculation of Hoop Stress Distribution in Lower Frustum (continued)

LANDING CONDITION

①	②	③	④	⑤	⑥	⑦	⑧	⑨	⑩
SEGMENT No.	R_i	R_j	R_{AV}	$\cos\theta$	R_e	p_n	$p_n R_e$	$2t_F$	σ_H
REF	TABLE 3-11	TABLE 3-11	.5[②+③]	FIGURE 1-2	④/⑤	TABLE 3-11	⑥ × ⑦	TABLE 3-24	⑧/⑨
19	370.050	373.435	371.743	.908323	409.263	1.400	572.968	.076	7441
20	373.435	377.618	375.527	↓	413.429	↑	578.801	.076	7616
21	377.618	389.954	383.786		422.521		591.529	.040	14788
22	389.954	403.718	396.836		436.888		610.323	↕	15263
23	403.718	417.482	410.600		452.041		632.857	.040	15821
24	417.482	432.548	425.015		467.911		655.075	.036	18197
25	432.548	448.731	440.640		485.113		679.158	↕	18866
26	448.731	464.914	456.823		502.930		704.102	.036	19559
27	464.914	478.374	471.644		519.247		726.946	.040	18174
28	478.374	491.834	485.104		534.065		747.691	↕	18692
29	491.834	504.529	498.182		548.463		767.848		19196
30	504.529	512.346	508.438		559.754		783.656	.040	19591
31	512.346	518.902	515.624	↓	567.665	↓	794.731	.054	14718
32	518.902	525.176	522.039	.908323	574.728	1.400	804.619	.054	14901

Table 3-31. Calculation of Hoop Stress Distribution in Inner Cylindrical Bulkhead

(a) Liftoff Condition (T = 0 Seconds)

①	②	③	④	⑤	⑥
SEGMENT NO.	R	p_n	$p_n R$	$2t_F$	σ_H
REF.	TABLE 3-7	TABLE 3-7	② x ③	TABLE 3-24	④/⑤
33	98.010	0	0	[illegible]	0
34	↑	↑	↑	.020	↑
35				.020	
36				↑	
37					
38					
39		↓	↓		↓
40		0	0		0
41		-.733	-71.841		-3592
42		-.832	-81.544		-4077
43		-1.029	-100.852		-5043
44		-1.309	-128.295		-6415
45		-1.606	-157.404		-7870
46		-1.904	-186.611		-9331
47		-2.205	-216.112		-10806
48		-2.461	-241.203		-12060
49		-2.674	-262.079		-13104
50		-2.847	-279.034		-13952
51		-2.946	-288.737		-14437
52		0	0		0
53		↑	↑		↑
54					
55	↓	↓	↓	↓	↓
56	98.010	0	0	.020	0

Table 3-31. Calculation of Hoop Stress Distribution in Inner Cylindrical Bulkhead (continued)

(b) Maximum Dynamic Pressure Condition (T = 77 Seconds)

①	②	③	④	⑤	⑥
SEGMENT No.	R	p_n	$p_n R$	$2t_f$	σ_H
REF.	TABLE 3-8	TABLE 3-8	② × ③	TABLE 3-24	④/⑤
33	96.010	0	0	.060	0
34	↑	↑	↑	.060	↑
35	│	│	│	.020	│
36	│	│	│	↑	│
37	│	│	│	│	│
38	│	│	│	│	│
39	│	↓	↓	│	↓
40	│	0	0	│	0
41	│	-2.170	-212.682	│	-10634
42	│	↑	↑	│	↑
43	│	│	│	│	│
44	│	↓	↓	│	↓
45	│	-2.170	-212.682	│	-10634
46	│	-2.389	-231.206	│	-11860
47	│	-2.736	-268.155	│	-13408
48	│	-3.059	-299.813	│	-14991
49	│	-3.326	-325.981	│	-16299
50	│	-3.543	-347.249	│	-17362
51	│	-3.667	-359.403	│	-17970
52	│	0	0	│	0
53	│	↑	↑	│	↑
54	│	│	│	│	│
55	↓	↓	↓	↓	↓
56	96.010	0	0	.020	0

Table 3-31. Calculation of Hoop Stress Distribution in Inner Cylindrical Bulkhead (continued)

(c) Maximum Longitudinal Acceleration Condition (T = 138 Seconds)

①	②	③	④	⑤	⑥
SEGMENT No.	R	P_n	$P_n R$	$2t_F$	σ_H
REF.	TABLE 3-9	TABLE 3-9	② × ③	TABLE 3-24	④/⑤
33	98.010	0	0	.068	0
34				.060	
35				.020	
36					
37					
38					
39					
40		0	0		0
41		-7.532	-738.211		-36911
42					
43					
44					
45					
46					
47		-7.532	-738.211		-36911
48		-7.810	-765.458		-38273
49		-8.366	-819.952		-40998
50		-8.816	-864.056		-43203
51		-9.074	-889.343		-44467
52		0	0		0
53					
54					
55					
56	98.010	0	0	.020	0

Table 3-31. Calculation of Hoop Stress Distribution in Inner Cylindrical Bulkhead (continued)

(d) Reentry Condition (T_R = 505 Seconds)

①	②	③	④	⑤	⑥
SEGMENT NO.	R	P_n	$P_n R$	$2t_F$	σ_H
REF.	TABLE 3-10	TABLE 3-10	② × ③	TABLE 3-24	④/⑤
33	98.010	0	0	.060	0
34	↑	↑	↑	.060	↑
35	│	│	│	.020	│
36	│	│	│	↑	│
37	│	│	│	│	│
38	│	│	│	│	│
39	│	↓	↓	│	↓
40	│	0	0	│	0
41	│	-7.700	-754.677	│	-37734
42	│	↑	↑	│	↑
43	│	│	│	│	│
44	│	│	│	│	│
45	│	│	│	│	│
46	│	│	│	│	│
47	│	│	│	│	│
48	│	│	│	│	│
49	│	│	│	│	│
50	│	↓	↓	│	↓
51	│	-7.700	-754.677	│	-37734
52	│	0	0	│	0
53	│	↑	↑	│	↑
54	│	│	│	│	│
55	↓	↓	↓	↓	↓
56	98.010	0	0	.020	0

Table 3-31. Calculation of Hoop Stress Distribution in Inner Cylindrical Bulkhead (continued)

(e) Landing Condition

①	②	③	④	⑤	⑥
SEGMENT NO.	R	p_n	$p_n R$	$2t_F$	σ_H
REF.	TABLE 3-11	TABLE 3-11	② × ③	TABLE 3-24	④/⑤
33	98.010	0	0	.060	0
34				.060	
35				.020	
36					
37					
38					
39					
40		0	0		0
41		-.700	-68.607		-3430
42					
43					
44					
45					
46					
47					
48					
49					
50					
51		-.700	-68.607		-3430
52		0	0		0
53					
54					
55					
56	98.010	0	0	.020	0

Table 3-32. Calculation of Hoop Stress Distribution in Outer Cylindrical Bulkhead

(a) Liftoff Condition (T = 0 Seconds)

(1)	(2)	(3)	(4)	(5)	(6)
SEGMENT No.	R	p_n	$p_n R$	$2t_r$	σ_H
REF.	TABLE 3-7	TABLE 3-7	(3) x (4)	TABLE 3-24	(4) / (5)
57	370.050	-.133	-49.217	.072	-684
58	↕	-.044	-16.282	↕	-226
59	↕	.135	49.957	↕	+694
60	↕	-2.219	-821.141	.072	-11405
61	↕	-6.933	-2565.557	.140	-18325
62	↕	-11.079	-4099.784	↕	-29284
63	↕	-13.762	-5092.628	↕	-36376
64	↕	-15.101	-5588.125	.140	-39915
65	↕	2.731	1010.607	.028	36093
66	↕	2.804	1037.620	↕	37058
67	↕	2.889	1069.074	↕	38181
68	↕	2.961	1095.718	.028	39132
69	↕	0	0	.032	0
70	↕	↕	↕	.028	↕
71	↕	↕	↕	↕	↕
72	↕	↕	↕	↕	↕
73	370.050	0	0	.028	0

Table 3-32. Calculation of Hoop Stress Distribution in Outer Cylindrical Bulkhead (continued)

(b) Maximum Dynamic Pressure Condition (T = 77 Seconds)

①	②	③	④	⑤	⑥
SEGMENT No.	R	p_n	$p_n R$	$2t_F$	σ_H
REF.	TABLE 3-8	TABLE 3-8	③ x ②	TABLE 3-24	④ / ⑤
57	370.050	-7.700	-2849.385	.072	-39575
58	↕	↕	↕	↕	↕
59	↕	-7.700	-2849.385	↕	-39575
60	↕	-7.643	-2828.292	.072	-39282
61	↕	-7.247	-2681.752	.140	-19155
62	↕	-8.546	-3162.447	↕	-22589
63	↕	-11.915	-4409.146	↕	-31499
64	↕	-13.600	-5032.680	.140	-35948
65	↕	3.383	1251.879	.028	44710
66	↕	3.474	1285.554	↕	45912
67	↕	3.581	1325.149	↕	47326
68	↕	3.672	1358.824	.028	48529
69	↕	0	0	.032	0
70	↕	↕	↕	.028	↕
71	↕	↕	↕	↕	↕
72	↕	↕	↕	↕	↕
73	370.050	0	0	.028	0

Table 3-32. Calculation of Hoop Stress Distribution in Outer Cylindrical Bulkhead (continued)

(c) Maximum Longitudinal Acceleration Condition (T = 138 Seconds)

①	②	③	④	⑤	⑥
SEGMENT No.	R	p_n	$p_n R$	$2t_F$	σ_H
REF.	TABLE 3-9	TABLE 3-9	③ x ②	TABLE 3-24	④ / ⑤
57	370.050	-7.700	-2849.385	.072	-39575
58	↕	↕	↕	↕	↕
59	↕	↕	↕	↕	↕
60	↕	↕	↕	.072	-39575
61	↕	-7.700	-2849.385	.140	-20353
62	↕	-7.605	-2814.230	↕	-20102
63	↕	-7.209	-2667.690	↕	-19055
64	↕	-10.706	-3961.755	.140	-28298
65	↕	8.483	3139.134	.028	112111
66	↕	8.671	3208.704	↕	114596
67	↕	8.984	3324.529	↕	118732
68	↕	9.083	3361.164	.028	120041
69	↕	0	0	.032	0
70	↕	↕	↕	.028	↕
71	↕	↕	↕	↕	↕
72	↕	↕	↕	↕	↕
73	370.050	0	0	.028	0

Table 3-32. Calculation of Hoop Stress Distribution in Outer Cylindrical Bulkhead (continued)

(d) Reentry Condition (T_R = 505 Seconds)

①	②	③	④	⑤	⑥
SEGMENT No.	R	p_n	$p_n R$	$2t_f$	σ_H
REF.	TABLE 3-10	TABLE 3-10	③ × ④	TABLE 3-24	④ / ⑤
57	370.050	0.700	259.035	.072	3598
58					
59					
60				.072	3598
61				.140	1850
62					
63					
64		0.700	259.035	.140	1850
65		7.700	2849.385	.028	101763
66					
67					
68		7.700	2849.385	.028	101763
69		0	0	.032	0
70				.028	
71					
72					
73	370.050	0	0	.028	0

Table 3-32. Calculation of Hoop Stress Distribution in Outer Cylindrical Bulkhead (continued)

(e) Landing Condition

①	②	③	④	⑤	⑥
SEGMENT No.	R	p_n	$p_n R$	$2t_r$	σ_H
REF.	TABLE 3-11	TABLE 3-11	③ × ④	TABLE 3-24	④ / ⑤
57	370.050	-0.700	-259.035	.072	-3598
58					
59					
60				.072	-3598
61				.140	-1850
62					
63					
64		-0.700	-259.035	.140	-1850
65		0.700	259.035	.028	9251
66					
67					
68		0.700	259.035	.028	9251
69		0	0	.032	0
70				.028	
71					
72					
73	370.050	0	0	.028	0

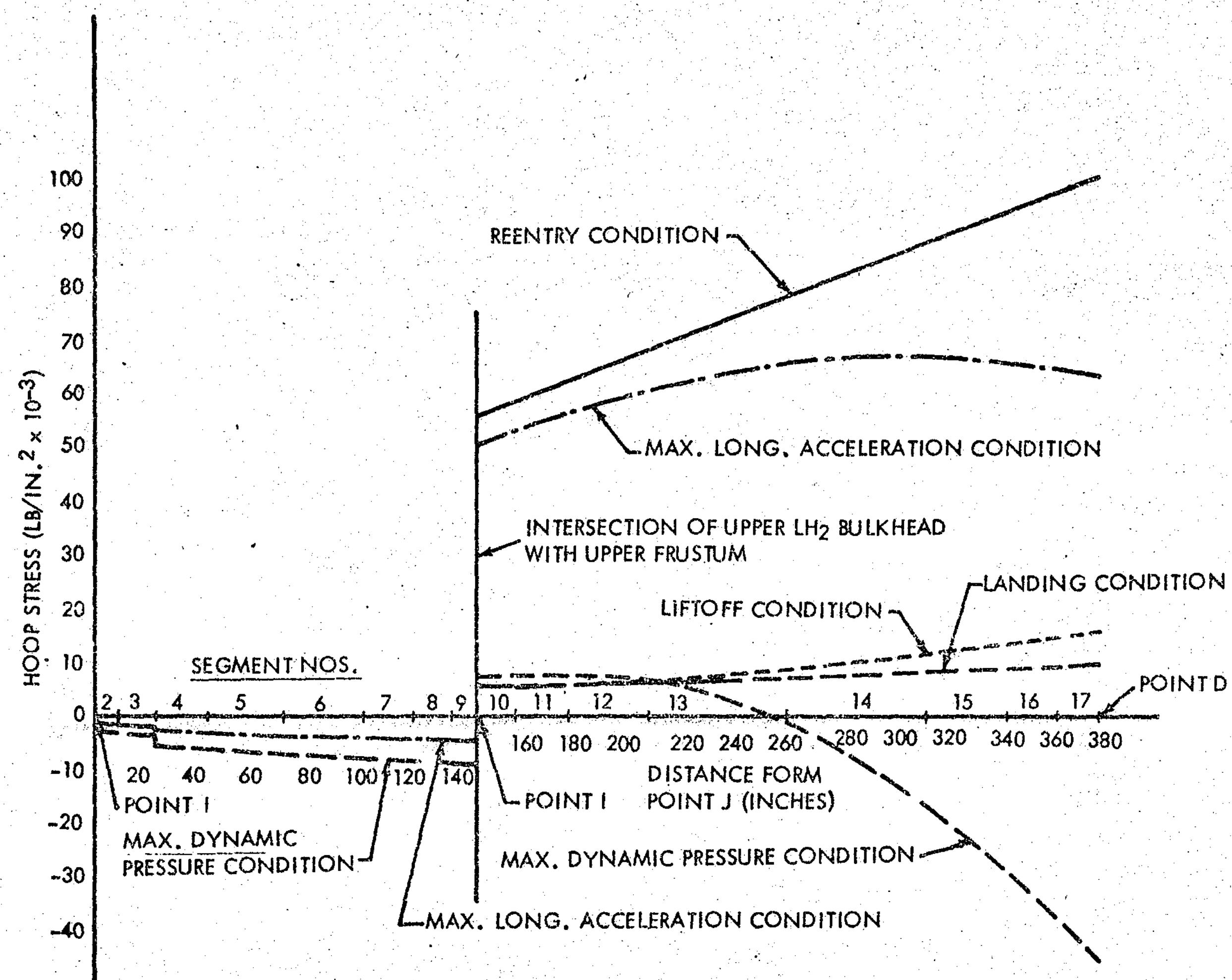

Figure 3-6. Hoop Stress Distribution in Upper Frustum

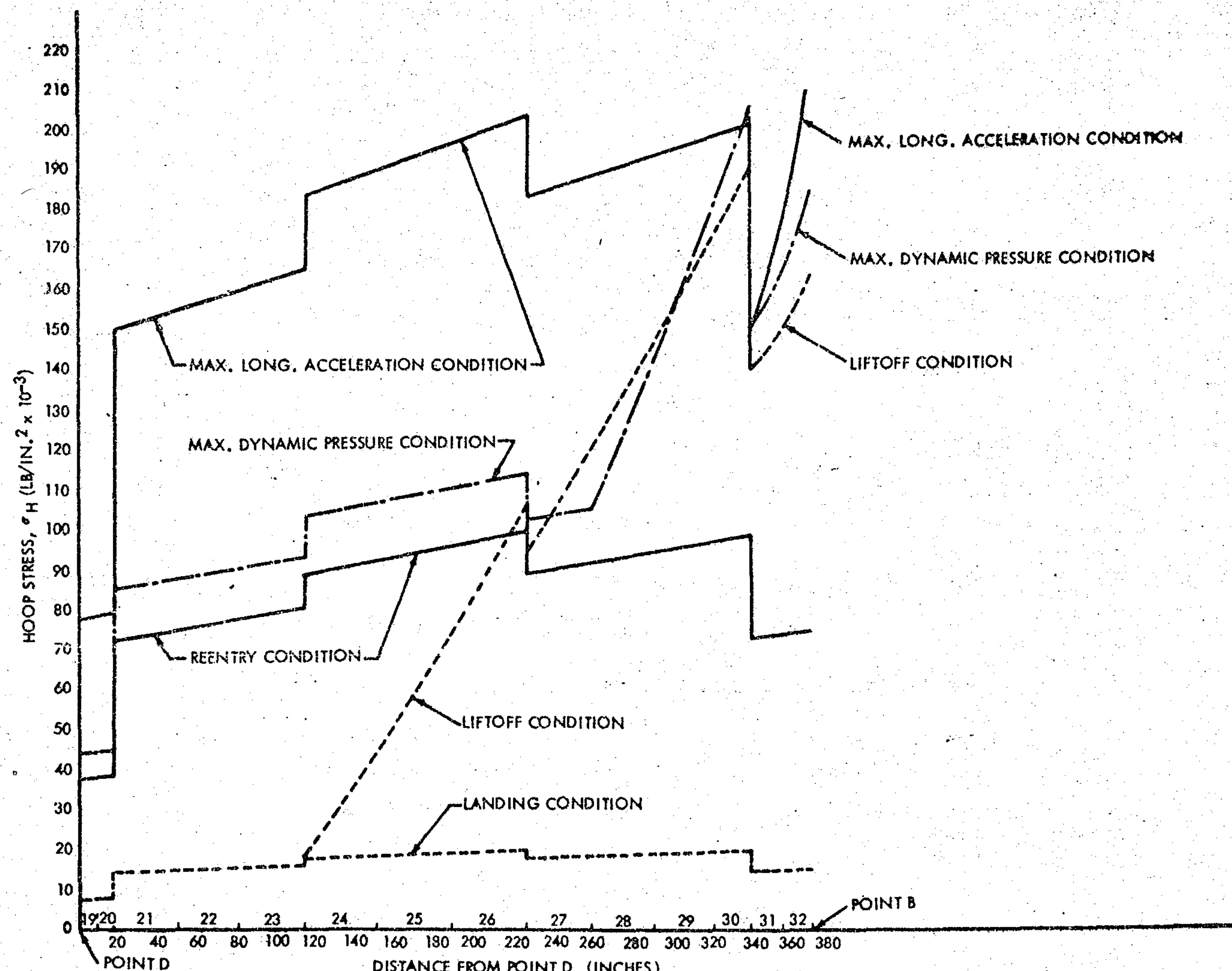

Figure 3-7. Hoop Stress Distribution in Lower Frustum

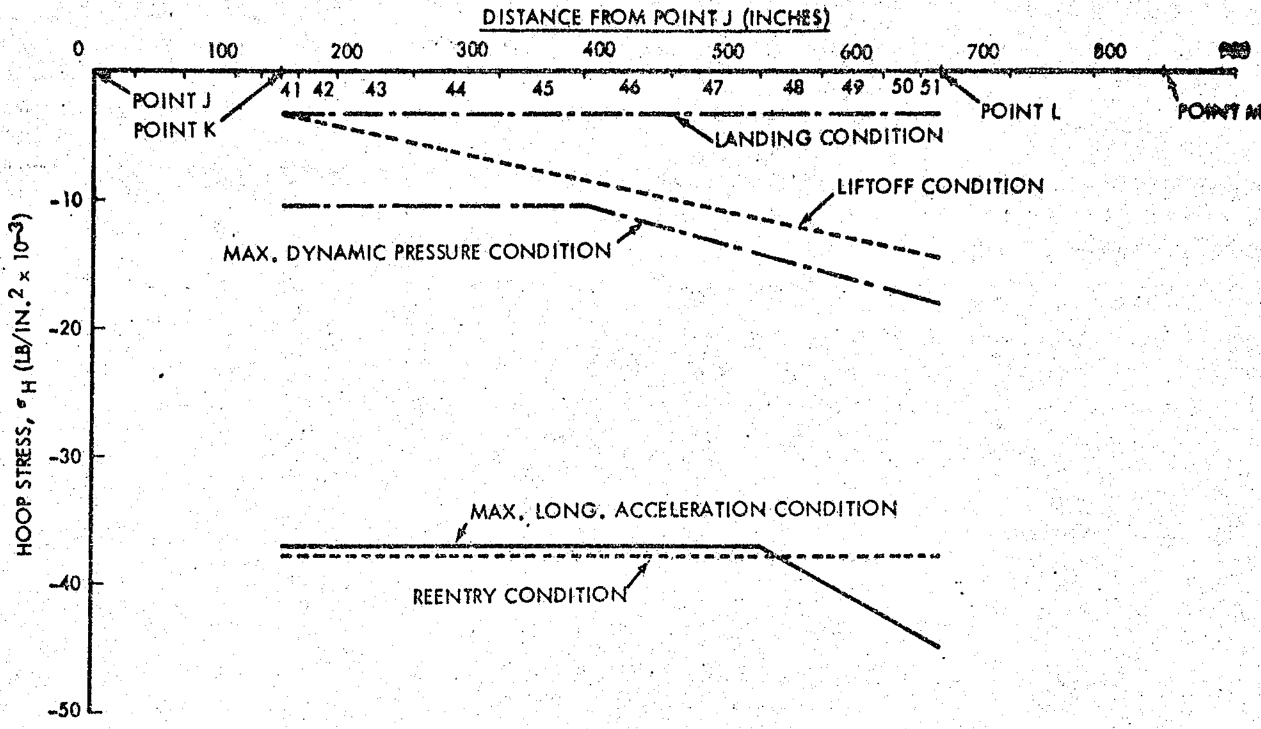

Figure 3-8. Hoop Stress Distribution in Inner Cylindrical Bulkhead

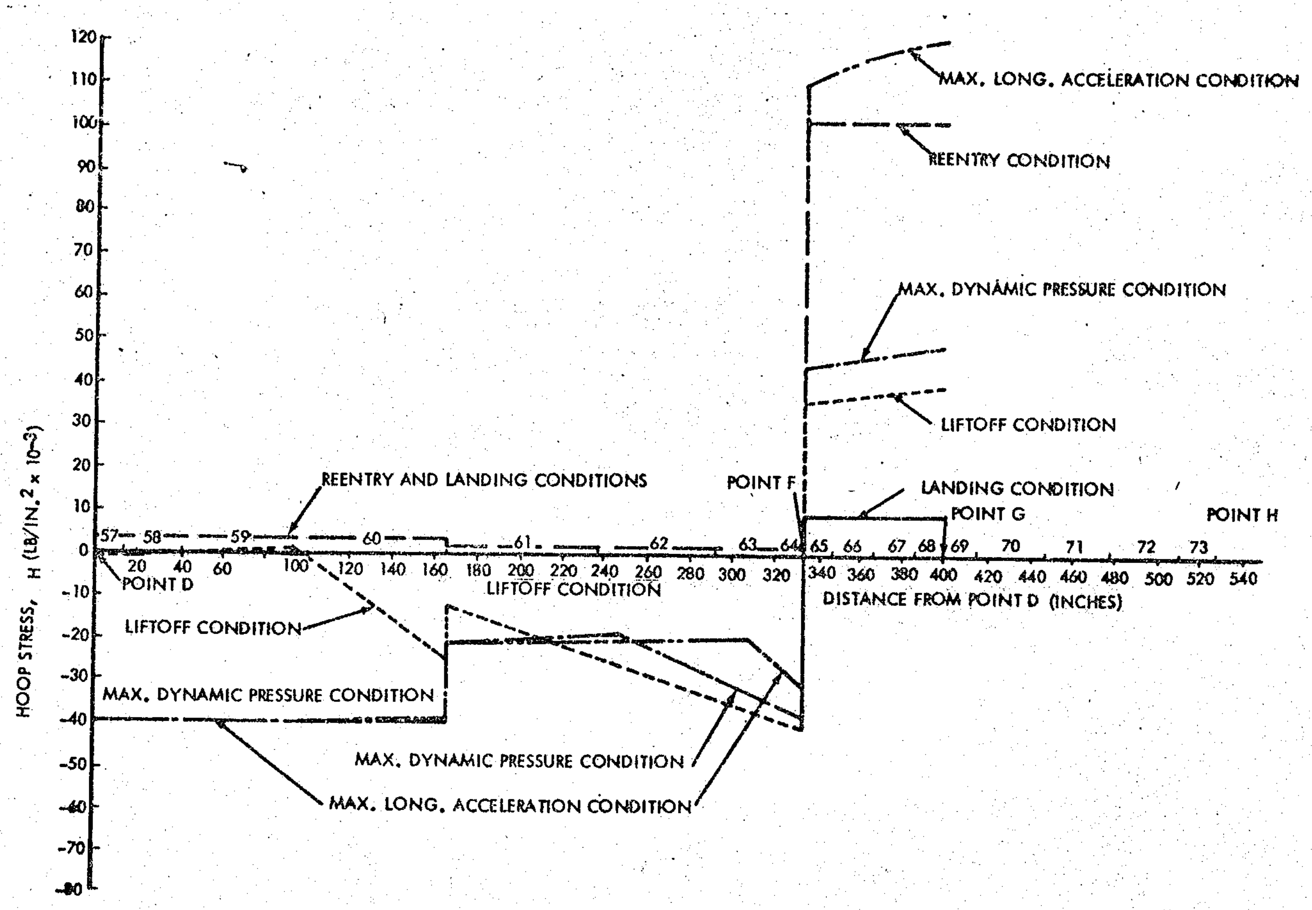

Figure 3-9. Hoop Stress Distribution in Outer Cylindrical Bulkhead

the total length of the component was used instead of the length of the isolated portion of the component, thereby resulting in somewhat conservative allowable stresses. Paragraph 9.3.1, volume 3, appendix E, gives the equation for the critical meridional buckling stress for a frustum (which is converted to an equivalent cylinder) subjected to compressive meridional loads only. When an internal pressure also exists, the equation for the critical meridional buckling stress is modified as shown in paragraph 9.6, volume 3, appendix E. When the frustum is subjected to an external lateral pressure, the critical hoop buckling stress is computed from the equation given in paragraph 9.3.2, volume 3, appendix E.

In all computations, the actual sandwich was replaced by an equivalent plate for which the thickness and modulus of elasticity were calculated using the equations presented in paragraph 9.2.3, volume 3, appendix E. These parameters were calculated in table 3-33 for all sandwich configurations. The critical hoop and meridional buckling stresses were calculated in table 3-34.

3.7.2 INTERCELL BUCKLING STRESS

The intercell buckling stress vs sandwich face thickness is calculated in table 3-35 using the method discussed in paragraph 9.2.3.1, volume 3, appendix E. The curves of intercell buckling parameters from this reference are reproduced here as figures 3-10 and 3-11.

3.7.3 FACE WRINKLING STRESS

The allowable face wrinkling stress versus sandwich cell size and foil thickness is calculated in table 3-36 using the method discussed in paragraph 9.2.3.2, volume 3, appendix E. The curves of face wrinkling parameters from this reference are reproduced here as figures 3-12 and 3-13.

3.7.4 ALLOWABLE SHEAR STRESS

The allowable shear stress was calculated from data presented in reference 5 which states that:

$$\sigma_S = 1.307 \left(\frac{\rho c^1}{\rho c}\right)^{1.34} \frac{\sigma_{SU}}{(tc)^{0.44}}$$

where σ_S = allowable shear stress

$\rho c^1/\rho c = 2t_{FOIL}/S$

σ_{SU} = material shear strength (assumed equal to 0.6 σ_{TU} = 129,000 lb/in.^{2})

tc = core thickness

t_{FOIL} = foil thickness

S = cell size = 0.50 in.

$(\rho c^1/\rho c) = 2(0.0020)/0.500 = 0.008$

$(0.008)^{1.34} = 0.001549$

therefore,

$$\sigma_S = 1.307\ (0.001549)(129,000)/(tc)^{0.44} = 261.166/(tc)^{0.44}$$

Table 3-33. Calculation of Effective Thickness and Modulus of Elasticity

①	②	③	④	⑤	⑥	⑦	⑧	⑨	⑩	⑪	⑫	⑬
COMP.	SEG. No.	t	t_F	$2t_F$	t_c	t^3	t_c^3	$t^3 - t_c^3$		t_e		E_e
REF.		TABLE 3 - 24		2 ④	③ - ⑤	③^3	⑥^3	⑦ - ⑧	⑨/⑤	⑩$^{1/2}$	⑤/⑪	(29.7×10⁶) ⑫
UPPER FRUSTUM	2-3	1.600	.026	.052	1.548	4.096	3.709479	.386521	7.433096	2.726370	.019073	566468
	4-9	1.600	.018	.036	1.564	4.096	3.825694	.270306	7.508500	2.740164	.013138	390199
	10-17	4.000	.020	.040	3.960	64.000	62.099136	1.900864	47.521600	6.893591	.005802	172319
LOWER FRUSTUM	19-20	2.700	.038	.076	2.624	19.683	18.067227	1.615773	21.260171	4.610875	.016483	489545
	21-23	↑	.020	.040	2.660	19.683	18.821096	.861094	21.547600	4.641939	.008617	255925
	24-26		.018	.036	2.664	19.683	18.906131	.776869	21.579694	4.645395	.007750	230175
	27-30	↓	.020	.040	2.660	19.683	18.821096	.861094	21.547600	4.641939	.008617	255925
	31-32	2.700	.027	.054	2.646	19.683	18.525482	1.157518	21.435518	4.629851	.011663	346391
INNER CYLIN. BLKD.	33-34	.375	.030	.060	.315	.052734	.031256	.021478	.357967	.598303	.100284	2978435
	35-40	.375	.010	.020	.355	.052734	.044739	.007995	.399750	.632258	.031633	939500
	41-47	3.400	↕	.020	3.380	39.304	38.614472	.689528	34.476400	5.871661	.003406	101158
	48-51	3.800	.010	.020	3.780	54.872	54.010152	.861848	43.092400	6.564480	.003047	90496
	52	.375	.014	.028	.347	.052734	.041782	.010952	.391143	.625414	.044770	1329669
	53-56	.375	.010	.020	.355	.052734	.044739	.007995	.399750	.632258	.031633	939500
OUTER CYLIN. BLKD.	57-60	4.000	.036	.072	3.928	64.000	60.605835	3.394165	47.141180	6.865943	.010487	311464
	61-64	4.000	.070	.140	3.860	64.000	57.512456	6.487544	46.339600	6.807320	.020566	610810
	65-68	.680	.014	.028	.652	.314432	.277168	.037264	1.330857	1.153628	.024271	720849
	69	↕	.016	.032	.648	.314432	.272098	.042334	1.322938	1.150190	.027821	826284
	70-73	.680	.014	.028	.652	.314432	.277168	.037264	1.330857	1.153628	.024271	720849

NOTES: 1) $t_e = 2\left[3\lambda_F D/H\right]^{1/2}$ where $\lambda_F = (1-\mu^2)$ $D = \frac{E_F}{12\lambda_F}(t^3 - t_c^3)$ $H = E_F(t - t_c) = E_F(2t_F)$

(refer to Paragraph 9.2.3, Volume 3, appendix E

Therefore $t_e = 2\left[3\lambda_F\left(\frac{E_F(t^3-t_c^3)}{12\lambda_F}\right)\left(\frac{1}{E_F(2t_F)}\right)\right]^{1/2}$

$= 2\left[\frac{(t^3-t_c^3)}{4(2t_F)}\right]^{1/2}$

$= \left[\frac{(t^3-t_c^3)}{(2t_F)}\right]^{1/2}$ which is solved in the above table.

Table 3-34. Calculation of Critical Hoop and Meridional Buckling Stresses

No.		Item	Component / Ref. (Seg. No.)	Upper Frustum 2-3	Upper Frustum 4-9	Upper Frustum 10-17	Lower Frustum 19-20	Lower Frustum 21-23	Lower Frustum 24-26	Lower Frustum 27-30	Lower Frustum 31-32	Inner Cylin. Blkd 33-34	Inner Cylin. Blkd 35-40
1	Given Data	t	Table 3-24	1.600	1.600	4.000	2.700	2.700	2.700	2.700	2.700	.375	.375
2		t_F	"	.026	.018	.020	.038	.020	.018	.020	.027	.030	.010
3		t_e	Table 3-33	2.726370	2.740164	6.893591	4.610875	4.641939	4.645395	4.641939	4.629851	.598303	.632258
4		E_e	"	566468	390199	172319	489545	255925	230175	255925	346391	2978435	939500
5		R_1	Table 3-7	103.365	120.146	204.887	370.050	377.618	417.482	464.914	512.346	98.010	98.010
6		R_2	"	120.146	204.887	370.050	377.618	417.482	464.914	512.346	525.176	98.010	98.010
7		μ	"	.284	.284	.284	.284	.284	.284	.284	.284	.284	.284
8		L	Note 1)	377.149	377.149	377.149	370.875	370.875	370.875	370.875	370.875	842.810	842.810
9		$\cos\theta$	"	.707107	.707107	.707107	.908323	.908323	.908323	.908323	.908323	1.000	1.000
10	Ext. Lateral Press.	R_e	Note 2)	158.046	229.833	406.542	411.565	437.675	485.728	537.947	571.120	98.010	98.010
11		Z	"	316.5	216.6	48.7	69.5	64.9	58.4	52.8	49.9	11614.6	10990.8
12		K_p	Fig. 3.23-7, Ref. 5	14.0	11.0	5.0	6.0	5.8	5.4	5.2	5.0	97.0	94.0
13		$(\sigma_{cr}/\eta)_e$	Note 2)	398.570	255.541	331.497	410.278	218.462	183.832	195.564	244.433	130.252	44.463
14		$t_e^2/2t_F$	(3) / 2(2)	52.430	76.116	172.340	60.669	116.048	129.039	116.048	85.738	9.972	31.613
15		(σ_{cr}/η)	(13) × (14)	20897	19450	57130	24890	25350	23720	22690	20960	1300	1400
16		$(\sigma_{cr})_m$	Note 4)	20897	19450	57130	24890	25350	23720	22690	20960	1300	1400
17	Comp. Meridion Load	R_e	Note 3)	146.150	169.912	289.753	407.397	415.730	459.618	511.837	564.057	98.010	98.010
18		Z	"	342.3	292.3	68.3	70.2	68.3	61.8	55.5	50.5	11614.6	10990.8
19		R_e/t_e	(17)/(3)	53.6	62.0	42.0	66.7	89.6	98.9	110.3	121.8	163.8	155.0
20		C_e	Fig. 3.24-1, Ref. 5	.234	.283	.235	.232	.228	.227	.226	.225	.219	.220
21		$(\sigma_{cr}/\eta)_e$	Note 3)	2473.022	1466.387	964.167	1702.758	651.238	528.311	524.378	639.885	3982.185	1338.483
22		(σ_{cr}/η)	(14) × (21)	129660	111610	166160	103300	75570	68170	60850	54860	39710	42150
23		$(\sigma_{cr})_m$	Note 4)	129660	111610	157000	103300	75570	68170	60850	54860	39710	42150

Table 3-34. Calculation of Critical Hoop and Meridional Buckling Stresses (continued)

No.		ITEM	COMPONENT REF. \ SEG. NO.	INNER CYLINDRICAL BULKHEAD 41-47	48-51	52	53-56	OUTER CYLINDRICAL BULKHEAD 57-60	61-64	65-68	69	70-73
(1)	GIVEN DATA	t	TABLE 3-24	3.400	3.800	.375	.375	4.000	4.000	.680	.680	.680
(2)		t_F	"	.010	.010	.014	.010	.036	.070	.014	.016	.014
(3)		t_e	TABLE 3-33	5.871661	6.564480	.625414	.632258	6.865943	6.807320	1.153628	1.150190	1.153628
(4)		E_e	"	101158	90496	1329669	939500	311464	610810	720849	826284	720849
(5)		R_1	TABLE 3-7	98.010	98.010	98.010	98.010	370.050	370.050	370.050	370.050	370.050
(6)		R_2	"	98.010	98.010	98.010	98.010	370.050	370.050	370.050	370.050	370.050
(7)		μ	"	.284	.284	.284	.284	.284	.284	.284	.284	.284
(8)		L	NOTE 1)	842.810	842.810	842.810	842.810	527.432	527.432	527.432	527.432	527.432
(9)		$\cos\theta$	"	1.000	1.000	1.000	1.000	1.000	1.000	1.000	1.000	1.000
(10)	EXT. LATERAL PRESS.	R_e	NOTE 2)	98.010	98.010	98.010	98.010 -	370.050	370.050	370.050	370.050	370.050
(11)		Z	"	1183.5	1058.6	11111.1	10990.3	105.0	105.9	624.8	626.7	624.8
(12)		K_p	FIG. 3.23-7, Ref. 5	29.9	29.7	95.0	94.0	9.4	9.4	23.0	23.0	23.0
(13)		$(\sigma_{cr}/\eta)_e$	NOTE 2)	131.357	145.507	62.228	44.463	445.802	858.873	70.948	80.974	111.088
(14)		$t_e/2t_F$	(3)/2(2)	293.583	328.224	22.336	31.613	95.360	48.624	41.201	35.943	41.201
(15)		(σ_{cr}/η)	(13) x (14)	38564	47758	1390	1400	42321	41762	2923	2910	2923
(16)		$(\sigma_{cr})_H$	NOTE 4)	38560	47760	1390	1400	42320	41760	2920	2910	2920
(17)	COMP. MERIDION LOAD	R_e	NOTE 3)	98.010	98.010	98.010	98.010	370.050	370.050	370.050	370.050	370.050
(18)		Z	"	1183.5	1058.6	11111.1	10990.8	105.0	105.9	624.8	626.7	624.8
(19)		R_e/t_e	(17)/(3)	16.7	14.9	156.7	155.0	53.9	54.4	320.8	321.7	320.8
(20)		C_e	FIG. 3.24-1 Ref 5	.238	.238	.219	.219	.233	.233	.198	.198	.198
(21)		$(\sigma_{cr}/\eta)_e$	NOTE 3)	1441.676	1445.503	1856.861	1327.718	1344.836	2619.257	444.742	507.969	444.742
(22)		(σ_{cr}/η)	(14) x (21)	423250	474450	41476	41974	125715	124640	18324	18258	18324
(23)		$(\sigma_{cr})_M$	NOTE 4)	192000	196000	41480	41970	125715	124640	18320	18260	18320

NOTES: 1) These parameters are from figures 1-1 through 1-4
2) These parameters are defined in Paragraph 9.3.2, Volume 3, appendix E
3.) These parameters are defined in Paragraph 9.3.1, Volume 3, appendix E
4.) Refer to figure 26, Volume 3, appendix E

Table 3-35. Calculation of Allowable Intercell Buckling Stress

Cell size = S = .500 ins. F_{cy} = 200000 lbs/in²

①	②	③	④	⑤	⑥
t_F	S/t_F	F_{ci}/η	$F_{cy}/(F_{ci}/\eta)$	F_{ci}/F_{cy}	F_{ci}
REF.	.500/①	FIGURE 3-10	200000/③	FIGURE 3-11	200000 ⑤
.010	50.0	63000	3.175	.316	63200
.014	35.7	105000	1.905	.523	104600
.016	31.3	127000	1.575	.618	123600
.018	27.8	152000	1.316	.697	139400
.020	25.0	180000	1.111	.757	151400
.026	19.3	260000	.768	.858	171600
.027	18.5	270000	.741	.869	173800
.030	16.7	325000	.615	.902	180400
.036	13.9	430000	.465	.950	190000
.038	13.2	460000	.435	.957	191400
.070	7.1	940000	.213	1.000	200000

E

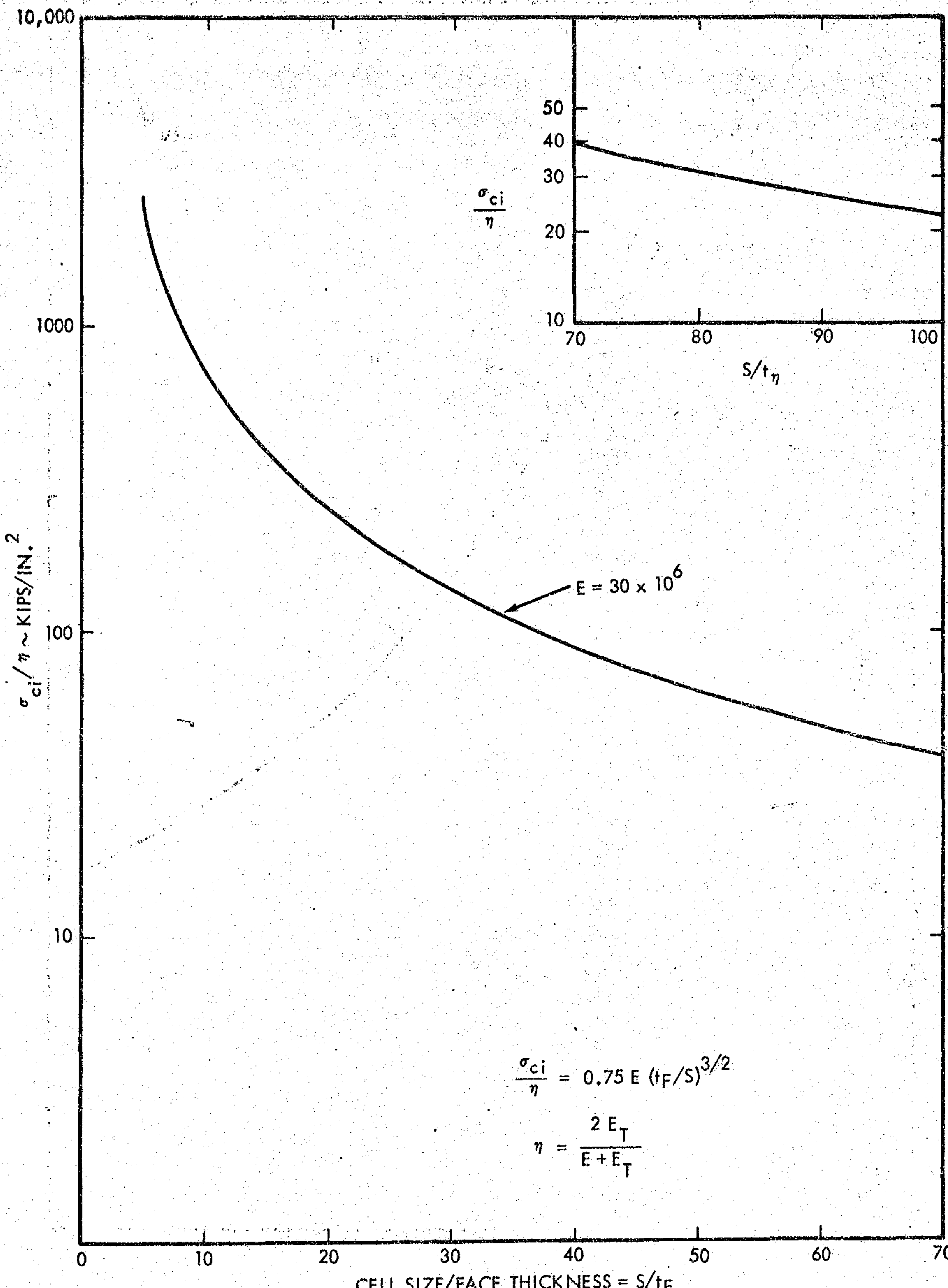

Figure 3-10. Intercell Buckling Stress versus Ratio of Cell Size to Face Thickness

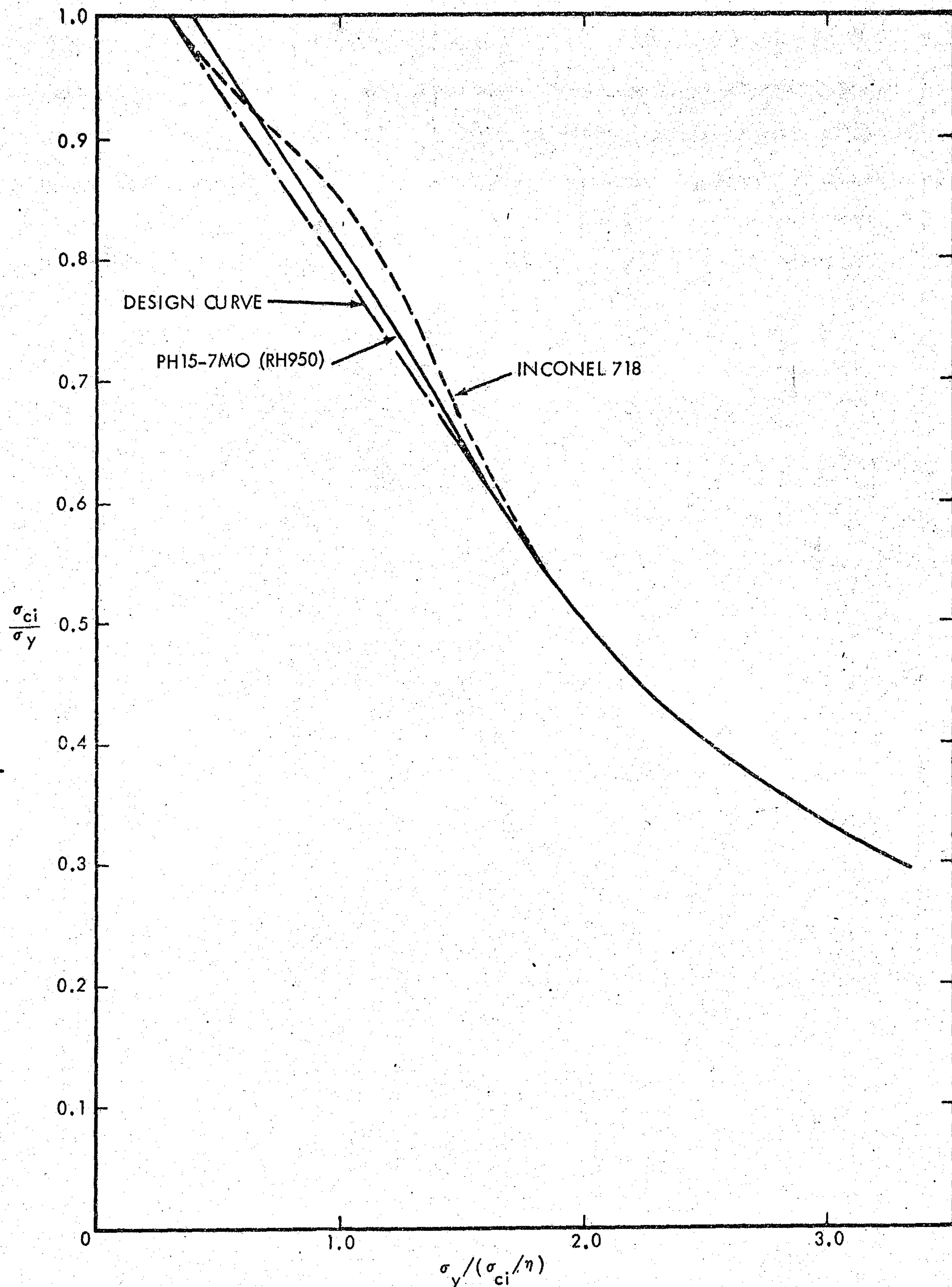

Figure 3-11. Intercell Buckling Stress

Table 3-36. Calculation of Allowable Face Wrinkling Stresses

(1)	(2)	(3)	(4)	(5)	(6)	(7)	(8)
CELL SIZE S	FOIL THICKNESS t_{FOIL}	S/t_{FOIL}	σ_{cw}/η	$\sigma_{cy}/(\sigma_{cw}/\eta)$	σ_{cw}/σ_{cy}	σ_{cw}	δ_c (LBS/FT^3)
REF.		(1)/(2)	FIGURE 3-12	200000/(4)	FIGURE 3-13	200000 (6)	NOTE 2)
.250	.0020	125.0	275000	.727	.982	196400	8.211
	.0025	100.0	342000	.585	1.000	200000	10.264
	.0030	83.3	410000	.488	1.000	↕	12.322
	.0035	71.4	475000	.421	1.000		14.376
	.0040	62.5	540000	.370	1.000	200000	16.423
.375	.0020	187.5	183000	1.093	.825	165000	5.474
	.0025	150.0	229000	.873	.923	184600	6.843
	.0030	125.0	275000	.727	.982	196400	8.211
	.0035	107.1	320000	.625	1.000	200000	9.584
	.0040	93.8	365000	.548	1.000	200000	10.943
.500	.0020	250.0	139000	1.439	.678	135600	4.106
	.0025	200.0	170000	1.176	.787	157400	5.132
	.0030	166.7	207000	.966	.882	176400	6.157
	.0035	142.9	240000	.833	.940	188000	7.183
	.0040	125.0	275000	.727	.982	196400	8.211

NOTES: 1) Compressive yield stress = σ_{cy} = 200 000 lbs/in^2 (refer to paragraph [illegible], Volume 3, appendix [illegible])

2) Core bulk density = $\delta'_c = (2t_{FOIL}/S)(.297)(1728) = 1026.432/(S/t_{FOIL})$ (refer to reference 5)

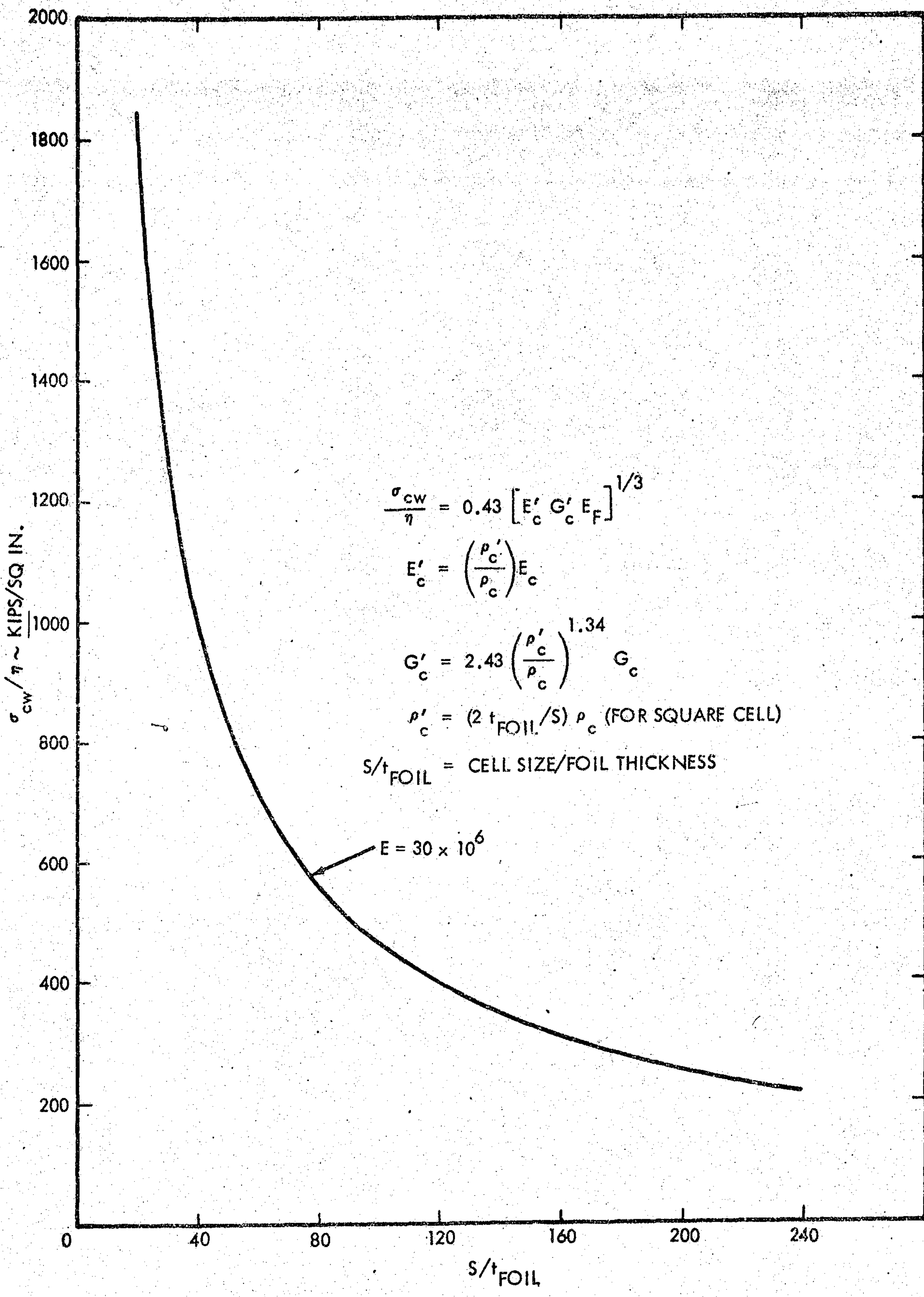

Figure 3-12. Wrinkling Stress Parameter

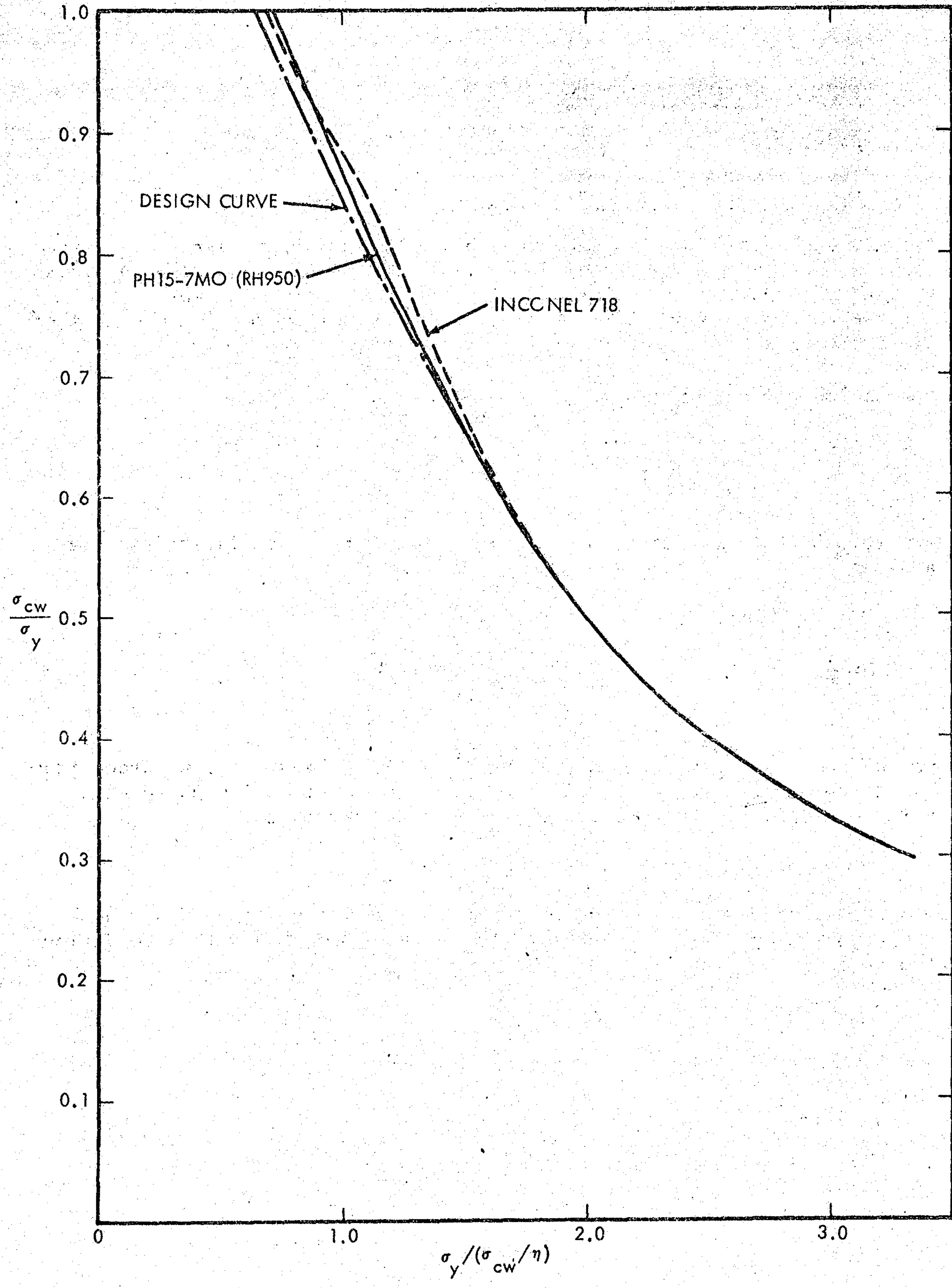

Figure 3-13. Sandwich Wrinkling Stress

The shear allowables for the various sandwich configurations are calculated in table 3-37.

3.8 CALCULATION OF MARGINS OF SAFETY

3.8.1 UPPER FRUSTUM

3.8.1.1 Portion From Node 2 to Node 4 (Segments 2 and 3)

With reference to table 3-24, the sandwich in this area has an overall thickness of 1.600 in. with a face thickness of 0.026 in. This portion of the upper frustum is checked for general stability as follows: examination of table 3-25 shows that the critical compressive axial stress occurs at node 2 in the maximum longitudinal acceleration condition (T = 138 seconds) and is:

$$\sigma_{AXIAL} = -52{,}316 \text{ lb/in.}^2$$

$$(\sigma_{CR})_M = 129{,}660 \text{ lb/in.}^2 \text{ (refer to table 3-34)}$$

$$R_M = 52{,}316/129{,}660 = 0.403$$

Table 3-29 reveals that the maximum compressive hoop stress is located in segment 3 and is:

$$\sigma_H = 1{,}700 \text{ lb/in.}^2$$

$$(\sigma_{CR})_H = 20{,}897 \text{ lb/in.}^2 \text{ (refer to table 3-34)}$$

$$R_H = 1{,}700/20{,}897 = 0.081$$

The above values of "R_H" and "R_M" are plotted in figure 3-14. A line drawn from the origin through their intersection, intersects the interaction curve at a value of $R_M^1 = 0.833$. The value of the margin of safety is then:

$$M.S. = (0.833/0.403) - 1 = +\underline{1.067}$$

Table 3-29 shows that the maximum dynamic pressure condition (T = 77 seconds) produces a higher hoop compression stress than that shown above; this condition is checked as follows:

$$\sigma_H = 3{,}594 \text{ lb/in.}^2 \text{ (table 3-29)}$$

$$(\sigma_{CR})_H = 20{,}897 \text{ lb/in.}^2 \text{ (refer to table 3-34)}$$

$$R_H = 3{,}594/20{,}897 = 0.172$$

$$\sigma_{AXIAL} = -38{,}548 \text{ lb/in.}^2 \text{ (refer to table 3-25)}$$

$$(\sigma_{CR})_M = 129{,}660 \text{ lb/in.}^2 \text{ (refer to table 3-24)}$$

$$R_M = 38{,}548/129{,}660 = 0.297$$

$$R_M^1 = 0.630 \text{ (determined from figure 3-14)}$$

$$M.S. = (0.630/0.297) - 1 = \underline{+1.121}$$

Table 3-37. Calculation of Allowable Shear Stresses

①	②	③	④	⑤
COMPONENT	SEGMENT No.	t_c	$(t_c)^{0.44}$	σ_s (lbs/in²)
REF.		TABLE 3-33	$③^{0.44}$	261.166/④
UPPER FRUSTUM	2-3	1.548	1.212	215
	4-9	1.564	1.217	214
	10-17	3.960	1.832	142
LOWER FRUSTUM	19-20	2.624	1.529	294 (1)
	21-23	2.660	1.538	169
	24-26	2.664	1.539	169
	27-30	2.660	1.538	169
	31-32	2.646	1.534	170
INNER CYLINDRICAL BULKHEAD	33-34	.315	.602	1098 (2)
	35-40	.355	.634	411
	41-47	3.380	1.709	152
	48-51	3.780	1.795	145
	52	.347	.628	881 (3)
	53-56	.355	.634	411
OUTER CYLINDRICAL BULKHEAD.	57-60	3.928	1.826	143
	61-64	3.860	1.812	144
	65-68	.652	.828	315
	69	.648	.826	316
	70-73	.652	.828	315

NOTES: 1) Core foil thickness changed to .0030 ins.

$$\sigma_s = 1.307\left(\frac{.0060}{.800}\right)^{1.34}(129000)/(t_c)^{0.44} = 449.823/(t_c)^{0.44} = 294 \text{ lbs/in}$$

2.) Core foil thickness changed to .0040 ins.

$$\sigma_s = 1.307\left(\frac{.0080}{.500}\right)^{1.34}(129000)/(t_c)^{0.44} = 661.254/(t_c)^{0.44} = 1098 \text{ lbs/in}^2$$

3.) Core foil thickness changed to .0035 ins.

$$\sigma_s = 1.307\left(\frac{.0070}{.500}\right)^{1.34}(129000)/(t_c)^{0.44} = 553.023/(t_c)^{0.44} = 881 \text{ lbs/in}^2$$

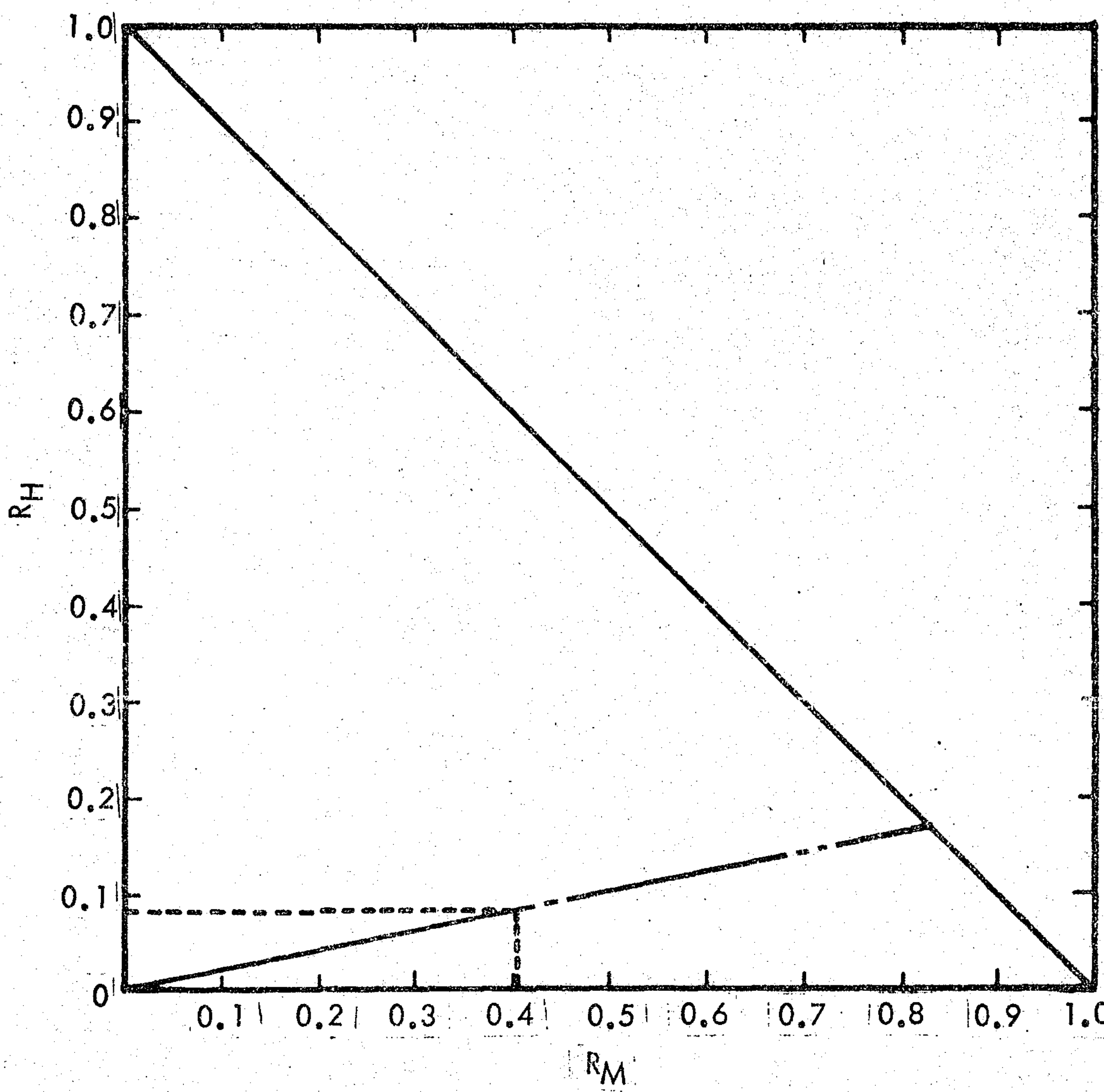

Figure 3-14. Assumed Interaction Curve

The intercell buckling characteristics of this portion of the upper frustum are checked as follows: table 3-25 shows that the maximum compressive stress in the face of the sandwich occurs at node 2 in the maximum longitudinal acceleration condition (T = 138 seconds) and is:

σ_{IF} = - 153,215 lb/in.^{2}

σ_{ci} = 171,600 lb/in.^{2} (refer to table 3-35 for t_F = 0.026 in)

M.S. = (171,600/153,215) - 1 = +0.120

The allowable face wrinkling stress is 157,400 lb/in.^{2} (refer to table 3-36 for S = 0.500 and t_{FOIL} = 0.0025)

M.S. = (157,400/153,215) - 1 = +0.027

The shear strength of this portion of the upper frustum is checked as follows: table 3-22 shows that the maximum transverse shear loading occurs at node 2 in the maximum longitudinal acceleration condition (T = 138 seconds) and is:

S(2) = 228.802 lb/in.

t_c = 1.548 in. (refer to table 3-33)

τ = 228.802/1.548 = 148 lb/in.^{2}

σ_S = 215 lb/in.^{2} (refer to table 3-37))

M.S. = (215/148) - 1 = +0.453

3.8.1.2 Portion From Node 4 to Node 10 (Segments 4 through 9)

With reference to table 3-24, the sandwich in this area has an overall thickness of 1.600 in. with a face thickness of 0.018 in. This portion of the upper frustum is checked for general stability as follows:

Examination of table 3-25 shows that the critical compressive axial stress occurs at node 4 in the maximum longitudinal acceleration condition (T = 138 seconds) and is:

σ_{AXIAL} = 62,277 lb/in.^{2}

$(\sigma_{CR})_M$ = 111,610 lb/in.^{2} (refer to table 3-34)

R_M = 62,277/111,610 = 0.558

Table 3-29 reveals that the maximum compressive hoop stress occurs in segment 9 and is:

σ_H = - 4,299 lb/in.^{2}

$(\sigma_{CR})_H$ = 19,450 lb/in.^{2} (refer to table 3-34)

R_H = 4,299/19,450 = 0.221

$R_M^1 = 0.717$ (refer to paragraph 3.8.1.1 for method)

$$M.S. = (.717/.558) - 1 = \underline{+0.285)}$$

The general stability under loads from the maximum dynamic pressure condition (T = 77 seconds) is checked as follows:

$\sigma_M = 45{,}811$ lb/in.^{2} (refer to table 3-25 at node 4)

$(\sigma CR)_M = 111{,}610$ lb/in.^{2} (refer to table 3-34)

$R_M = 0.410$

$\sigma_H = 9{,}089$ lb/in.^{2} (refer to table 3-29)

$(\sigma CR)_H = 19{,}450$ lb/in.^{2} (refer to table 3-34)

$R_H = 9{,}089/19{,}450 = 0.467$

$R_M^1 = 0.468$ (refer to paragraph 3.8.1.1 for method)

$$M.S. = (0.468/0.410) - 1 = \underline{+0.141}$$

The intercell buckling characteristics of this portion of the upper frustum are checked as follows: table 3-25 shows that the maximum compressive stress in the face of the sandwich occurs at node 5 of segment 5 in the maximum longitudinal acceleration condition (T = 138 seconds) and is:

$\sigma_{OF} = 63{,}916$ lb/in.^{2}

$\sigma_{ci} = 139{,}400$ lb/in.^{2} (refer to table 3-35 for $t_F = 0.018$ in.)

$$M.S. = (139{,}400/63{,}916) - 1 = \underline{+1.180}$$

The allowable face wrinkling stress is 135,600 lb/in.^{2} (refer to table 3-36 for S = .500 and $t_{FOIL} = .0020$) and is obviously not critical.

The shear strength of this portion of the upper frustum is checked as follows: table 3-22 shows that the maximum transverse shear loading occurs at node 4, segment 4, in the maximum longitudinal acceleration condition (T = 138 seconds) and is:

$S(4) = -77.842$ lb/in.

$t_c = 1.564$ in. (refer to table 3-33)

$\tau = 77.842/1.564 = 50$ lb/in.^{2}

$\sigma_S = 214$ lb/in.^{2} (refer to table 3-37)

$$M.S. = (214/50) - 1 = \underline{+3.280}$$

3.8.1.3 Portion From Node 10 to Node 18 (Segments 10 to 17)

With reference to table 3-24, the sandwich in this area has an overall thickness of 4.000 in. with a face thickness of 0.020 in. This portion of the upper frustum is checked for general stability as follows: examination of table 3-25 shows that the maximum compressive axial stress occurs at node 10 in segment 10 in the maximum dynamic pressure condition (T = 77 seconds) and is:

σ_{AXIAL} = - 22,679 lb/in.^{2}

$(\sigma\ CR)_M$ = 157,000 lb/in.^{2} (refer to table 3-34)

R_M = 22,679/157,000 = 0.144

Table 3-29 reveals that the maximum compressive hoop stress occurs in segment 17 and is:

σ_H = 41,588 lb/in.^{2}

$(\sigma\ CR)_H$ = 57,130 lb/in.^{2} (refer to table 3-34)

R_H = 41,588/57,130 = 0.728

$R_H{}^1$ = 0.835 (refer to paragraph 3.8.1.1 for method)

M.S. = (0.835/0.728) - 1 = +0.147

The maximum tensile stress in the sandwich faces occurs at node 18 of segment 17 in the maximum longitudinal acceleration condition (T = 138 seconds) and is:

σ_{IF} = + 117,533 lb/in.^{2} (refer to table 3-25)

σ_{UT} = 215,000 lb/in.^{2} (refer to paragraph 9.1, volume 3, appendix E)

M.S. = (215,000/117,533) - 1 = +0.829

The intercell buckling characteristics of this portion of the upper frustum are checked as follows: table 3-25 shows that the maximum compressive stress in the face of the sandwich occurs at node 18 of segment 17 and is:

σ_{OF} = - 112,003 lb/in.^{2}

σ_{ci} = 151,400 lb/in.^{2} (refer to table 3-35 for t_F = 0.020 in.)

M.S. = (151,400/112,003) - 1 = +0.352

The allowable face wrinkling stress is 135,600 lb/in.^{2} (refer to table 3-36 for S = .500 and t_{FOIL} = .0020)

M.S. = (135,600/112,003) - 1 = +0.210

The shear strength of this portion of the upper frustum is checked as follows: table 3-22 shows that the maximum transverse shear loading occurs at node 18 of segment 17 in the maximum longitudinal acceleration condtion (T = 138 seconds) and is:

$S(18) = 404.323$ lb/in.

$t_c = 3.960$ in. (refer to table 3-33)

$\tau = 404.323/3.960 = 102$ lb/in.^{2}

$\sigma_S = 142$ lb/in.^{2} (refer to table 3-37)

M.S. = (142/102) - 1 = <u>+0.392</u>

3.8.2 LOWER FRUSTUM

3.8.2.1 Portion From Node 18 to Node 21 (Segments 19 and 20)

With reference to table 3-24, the sandwich in this area has an overall thickness of 2.700 in. with a face thickness of 0.038 in. This portion of the lower frustum is checked for general stability as follows: examination of table 3-26 shows that the maximum compressive axial stress occurs at node 18 in segment 19 in the maximum longitudinal acceleration condition (T = 138 seconds) and is:

$\sigma_{AXIAL} = - 46{,}782$ lb/in.^{2}

Examination of table 3-30 reveals that the hoop stress throughout the lower frustum is always tension, indicating that the frustum is always subject to an internal pressure environment. The incremental increase in the meridional buckling stress coefficient due to the stabilizing effect of an internal pressure is now calculated using the method described in section 3.24.1B of reference 6, which states that ΔC_c is a function of the parameter $p(Re/t_e)^2/Ee$ (in terms of the equivalent plate) where:

ΔC_c = incremental buckling coefficient

p = internal pressure = 14.469 lb/in.^{2} (refer to table 3-30)

R_e = radius of equivalent cylinder = $R_1/\cos\theta$

R_1 = radius in plane normal to centerline of vehicle = 370.05 in. (refer to table 3-9)

$\cos\theta$ = cos (1/2 cone angle) = 0.908323 (refer to figure 1-2)

t_e = thickness of equivalent plate = 4.610875 (refer to table 3-33)

Ee = modulus of elasticity of equivalent plate = 489,545 (refer to table 3-33)

$p(Re/t_e)^2/Ee$ = (14.469) 370.050/(0.908323)(4.610875)^2/489,545 = 112,956/489,545 = 0.231

ΔCc = 0.140 (refer to figure 3.24-2, reference 6)

From table 3-34, the buckling coefficient and critical meridional buckling stress for a frustum without internal pressure was found to be:

$C_c = 0.232$ $(\sigma CR)_M = 103,300 \text{ lb/in.}^2$

Considering the stabilizing effect of the internal pressure, the new buckling coefficient is:

$$C_c^1 = (C_c + \Delta C_c) = 0.232 + 0.140 = 0.372$$

And the new critical meridional buckling stress is then:

$$(\sigma CR)_M^1 = (103,300)(0.372)/(0.232) = 165,630 \text{ lb/in.}^2$$

$$\text{M.S.} = (165,630/46,782) - 1 = \underline{+2.540}$$

The strength of the individual faces of the sandwich in this portion of the lower frustum is checked as follows: examination of table 3-26 shows that the maximum meridional tensile stress in the faces occurs in the maximum longitudinal acceleration condition (T = 138 seconds) at node 18 of segment 19 and is:

$$\sigma_{IF} = 68,010 \text{ lb/in.}^2$$

The hoop stress in segment 19 for the same design condition is:

$$\sigma_H = 77,916 \text{ lb/in.}^2 \text{ (refer to table 3-30)}$$

The maximum principal stress in the inner face is then:

$$\sigma_{t_{max}} = \left[(\sigma IF)^2 + (\sigma H)^2\right]^{1/2} = \left[(68,010)^2 + (77,916)^2\right]^{1/2} = 103,420 \text{ lb/in.}^2$$

$\sigma_{UT} = 215,000 \text{ lb/in.}^2$ (refer to paragraph 9.1, appendix E, volume 3)

$$\text{M.S.} = (215,000/103,420) - 1 = \underline{+1.079}$$

The intercell buckling strength is now checked. Table 3-26 shows that the maximum compressive stress in the sandwich faces occurs at node 18 of segment 19 in the maximum longitudinal acceleration condition (T = 138 seconds) and is:

$$\sigma_{OF} = 161,574 \text{ lb/in.}^2$$

$\sigma_{ci} = 191,400 \text{ lb/in.}^2$ (refer to table 3-35 for $t_F = .038$ in.)

$$\text{M.S.} = (191,400/161,574) - 1 = \underline{+0.185}$$

It should be noted that as a result of deficiency in shear strength, it was necessary to increase the foil thickness of the core from 0.0020 in. to 0.0030 in. The allowable face wrinkling stress is then 176,400 lb/in.^{2}(refer to table 3-36 for S = .500 and t_{FOIL} = .0030)

$$\text{M.S.} = (176,400/161,574) - 1 = \underline{+0.092}$$

The shear strength of this portion of the lower frustum is checked as follows: table 3-23 shows that the maximum transverse shear loading occurs at node 18 of segment 19 in the maximum longitudinal acceleration condition (T = 138 seconds) and is:

$S(18) = 713.685$ lb/in.

$t_c = 2.624$ in. (refer to table 3-33)

$\tau = 713.685/2.624 = 272$ lb/in.^{2}

$\sigma_S = 294$ lb/in.^{2} (refer to table 3-37)

M.S. = (294/272) - 1 = +0.081

3.8.2.2 Portion From Node 21 to Node 24 (Segments 21 to 23 Inclusive)

With reference to table 3-24, the sandwich in this area has an overall thickness of 2.700 in. with a face thickness of 0.020 in. This portion of the lower frustum is checked for general stability as follows: examination of table 3-26 shows that the maximum compressive axial stress occurs at node 21 of segment 21 in the maximum longitudinal acceleration condition (T = 138 seconds) and is:

$\sigma_{AXIAL} = - 88{,}131$ lb/in.^{2}

The incremental buckling coefficient due to internal pressure is evaluated in the same manner as discussed in paragraph 3.8.2.1.

$p = 14.452$ lb/in.^{2} (refer to table 3-30 at segment 21)

$R_1 = 377.618$ in. (refer to table 3-9 at node 21)

$\cos \theta = 0.908323$ (refer to figure 1-2)

$t_e = 4.641939$ (refer to table 3-33)

$E_e = 255925$ (refer to table 3-33)

$p\,(R_e/t_e)^2/E_e = (14.452)\ 377.618/(.908323)(4.641939)^2/255{,}925$
$= 115{,}917/255{,}925 = 0.453$

$\Delta C_c = 0.177$ (refer to figure 3.24-2, reference 6)

From table 3-34 the buckling coefficient and critical meridional buckling stress for a frustum without internal pressure was found to be:

$C_c = 0.228$ $(\sigma CR)_M = 75{,}570$ lb/in.^{2}

Considering the stabilizing effect of the internal pressure, the new buckling coefficient is:

$C_c{}^1 = (0.228 + 0.177) = 0.405$

And the new critical meridional buckling stress is:

$(\sigma CR)_M{}^1 = (75{,}570)(.405)/.228 = 134{,}230$ lb/in.^{2}

M.S. = (134,230/88,131) - 1 = +0.523

The strength of the individual faces of the sandwich in this portion of the lower frustum is checked as follows: examination of table 3-30 shows that the maximum hoop tension stress occurs in segment 23 in the maximum longitudinal acceleration condition (T = 138 seconds) and is:

σ_H = 162,848 lb/in.^{2}

σ_{UT} = 215,000 lb/in.^{2} (refer to paragraph 9.1, volume 3, appendix E)

M.S. = (215,000/162,848) - 1 = +0.320

The intercell buckling strength is now determined. Table 3-26 shows that the maximum compressive meridional stress occurs at node 21 of segment 21 in the liftoff condition (T = 0 seconds) and is:

σ_{OF} = 135,553 lb/in.^{2}

σ_{ci} = 151,400 lb/in.^{2} (refer to table 3-35 for t_F = 0.020 in.)

M.S. = (151,400/135,553) - 1 = +0.117

The allowable face wrinkling stress is 135,600 lb/in.^{2} (refer to table 3-36 for S = .500 and t_{FOIL} = .0020)

M.S. = (135,600/135,553) - 1 = +0

The shear strength of this portion of the lower frustum is checked as follows: table 3-23 shows that the maximum transverse shear loading occurs at node 22 of segment 21 in the maximum longitudinal acceleration condition (T = 138 seconds) and is:

S(24) = 287.798 lb/in.

t_c = 2.660 in. (refer to table 3-33)

τ = 287.798/2.660 = 108 lb/in.^{2}

σ_S = 169 lb/in.^{2} (refer to table 3-37)

M.S. = (169/108) - 1 = +0.565

3.8.2.3 Portion From Node 24 to Node 27 (Segment 24 to 26 Inclusive)

With reference to table 3-24, the sandwich in this area has an overall thickness of 2.700 in. with a face thickness of 0.018 in. This portion of the lower frustum is checked for general stability as follows: examination of table 3-26 shows that the maximum compressive axial stress occurs at node 25 of segment 25 in the maximum dynamic pressure condition (T = 77 seconds) and is:

σ_{AXIAL} = -74,947 lb/in.^{2}

The incremental buckling coefficient due to internal pressure is evaluated in the same manner as discussed in paragraph 3.8.2.1:

$p = 8.096$ lb/in.^{2} (refer to table 3-30 at segment 24)

$R_1 = 417.482$ in. (refer to table 3-9 at node 24)

$\cos \theta = 0.908323$ (refer to figure 1-2)

$t_e = 4.645395$ (refer to table 3-33)

$E_e = 230,175$ (refer to table 3-33)

$$p\ (R_e/t_e)^2/E_e = (8.096)(417.482)/(.908323)(4.645395)^2/230,175$$
$$= 78,955/230,175 = 0.345$$

$\Delta C_c = 0.160$ (refer to figure 3.24-2, reference 6)

From table 3-34 the buckling coefficient and critical meridional buckling stress for a frustum without internal pressure was found to be:

$C_c = 0.227$ $\qquad$ $(\sigma CR)_M = 68,170$ lb/in.^{2}

Considering the stabilizing effect of the internal pressure, the new buckling coefficient is:

$$C_c^{\ 1} = (0.227 + 0.160) = 0.387$$

Ane the new critical meridional buckling stress is:

$$(\sigma CR)_M^{\ 1} = (68,170)(0.387)/0.227 = 116,220 \text{ lb/in.}^2$$

M.S. = (116,220/74,947) - 1 = <u>+0.551</u>

The strength of the individual faces of the sandwich in this portion of the lower frustum is checked as follows: examiniation of table 3-30 shows that the maximum hoop tension stress occurs in segment 26 in the maximum longitudinal acceleration condition (T = 138 seconds) and is:

$\sigma_H = 200,657$ lb/in.^{2}

$\sigma_{UT} = 215,000$ lb/in.^{2} (refer to paragraph 9.1, volume 3, appendix E)

M.S. = (215,000/200,657) - 1 = <u>+0.071</u>

The intercell buckling strength is now checked. Table 3-26 shows that the maximum compressive meridional stress occurs at node 25 of segment 25 in the maximum dynamic pressure condition (T = 77 seconds) and is:

$\sigma_{OF} = 78,149$ lb/in.^{2}

$\sigma_{ci} = 139,400$ lb/in.^{2} (refer to table 3-35 for $t_F = 0.018$ in.)

M.S. = (139,400/78,149) - 1 = <u>+0.784</u>

The allowable face wrinkling stress is 135,600 lb/in.^{2} (refer to table 3-36 for S = .500 and t_{FOIL} = .0020)

$$M.S. = (135,600/78,149) - 1 = \underline{+.735}$$

The shear strength of this portion of the lower frustum is checked as follows: table 3-23 shows that the maximum transverse shear loading occurs at node 24 of segment 24 in the maximum longitudinal acceleration condition (T = 138 seconds) and is:

$S(24) = -308.739$ lb/in.

$t_c = 2.664$ in. (refer to table 3-33)

$\tau = 308.739/2.664 = 116$ lb/in.^{2}

$\sigma_S = 169$ lb/in.^{2} (refer to table 3-37)

$$M.S. = (169/116) - 1 = \underline{+0.457}$$

3.8.2.4 Portion From Node 27 to Node 31 (Segments 27 to 30 Inclusive)

With reference to table 3-24, the sandwich in this area has an overall thickness of 2.700 in. with a face thickness of 0.020 in. This portion of the lower frustum is checked for general stability as follows: examination of table 3-26 shows that the maximum compressive axial stress occurs at node 27 of segment 27 in the maximum dynamic pressure condition (T = 77 seconds) and is:

$\sigma_{AXIAL} = 55,985$ lb/in.^{2}

The incremental buckling coeffiecient due to internal pressure is evaluated in the same manner as discussed in paragraph 3.8.2.1:

$p = 8.015$ lb/in.^{2} (refer to table 3-30 for segment 27)

$R_1 = 464.914$ in. (refer to table 3-9 at node 27)

$\cos\theta = 0.908323$ (refer to figure 1-2)

$t_e = 4.641939$ (refer to figure 3-33)

$E_e = 255,925$ (refer to figure 3-33)

$$p(R_e/t_e)^2/E_e = (8.015)\left[464.914/(.908323)(4.641939)\right]^2/255,925 = 97,446/255,925 = 0.381$$

$\Delta C_c = 0.167$

From table 3-34 the buckling coefficient and critical meridional buckling stress for a frustum without internal pressure was found to be:

$C_c = 0.226$ $(\sigma_{CR})_M = 60,850$ lb/in.^{2}

Considering the stabilizing effect of the internal pressure, the new buckling coefficient is:

$$C_c^{1} = (0.226 + 0.67) = 0.393$$

And the new critical meridional buckling stress is:

$$(\sigma_{CR})_M^{1} = (60{,}850)(.393)/.226 = 105{,}810 \text{ lb/in.}^2$$

$$\text{M.S.} = (105{,}810/55{,}985) - 1 = \underline{+0.890}$$

The strength of the individual faces of the sandwich in this portion of the lower frustum is checked as follows: examination of table 3-30 shows that the maximum hoop tension stress occurs in segment 30 in the maximum longitudinal acceleration condtion (T = 138 seconds) and is:

$$\sigma_H = 200{,}392 \text{ lb/in.}^2$$

$\sigma_{UT} = 215{,}000 \text{ lb/in.}^2$ (refer to paragraph 9.1, volume 3, appendix E)

$$\text{M.S.} = (215{,}000/200{,}392) - 1 = \underline{+0.073}$$

The intercell buckling strength is now checked. Table 3-26 shows that the maximum compressive meridional stress occurs at node 30 of segment 30 in the maximum dynamic pressure condition (T = 77 seconds) and is:

$$\sigma_{IF} = 80{,}302 \text{ lb/in.}^2$$

$\sigma_{ci} = 151{,}400 \text{ lb/in.}^2$ (refer to table 3-35 for $t_F = 0.020$ in.)

$$\text{M.S.} = (151{,}400/80{,}302) - 1 = \underline{+0.885}$$

The allowable face wrinkling stress is 135,600 lb/in.^{2} (refer to table 3-36 for S = .500 and $t_{FOIL} = .0020$)

$$\text{M.S.} = (135{,}600/80{,}302) - 1 = \underline{+0.688}$$

The shear strength of this portion of the lower frustum is checked as follows: table 3-23 shows that the maximum transverse shear loading occurs at node 29 of segment 28 in the maximum longitudinal acceleration condtion (T = 138 seconds) and is:

$$S(29) = 253.558 \text{ lb/in.}$$

$t_c = 2.660$ in. (refer to table 3-33)

$$\tau = 253.558/2.660 = 95 \text{ lb/in.}^2$$

$\sigma_S = 169 \text{ lb/in.}^2$ (refer to table 3-37)

$$\text{M.S.} = (169/95) - 1 = \underline{+0.779}$$

3.8.2.5 Portion from Node 31 to Node 33 (Segments 31 and 32)

With reference to table 3-24, the sandwich in this area has an overall thickness of 2.700 in. with a face thickness of 0.027 in. This portion of the lower frustum is checked for general stability as follows: examination of table 3-26 shows that the maximum compressive axial stress occurs at node 31 of segment 31 in the maximum dynamic pressure condition (T = 77 seconds) and is:

$$\sigma_{AXIAL} = -29,188 \text{ lb/in.}^2$$

The incremental buckling coefficient due to internal pressure is evaluated in the same manner as discussed in paragraph 3.8.2.1:

$p = 15.068 \text{ lb/in.}^2$ (refer to table 3-30 for segment 31)

$R_1 = 512.346 \text{ lb/in.}^2$ (refer to table 3-30 for node 31)

$\cos\theta = 0.908323$ (refer to table 1-2)

$t_e = 4.4629851$ (refer to table 3-33)

$E_e = 346,391$ (refer to table 3-33)

$$p(R_e/t_e)^2/E_e = (15.068)(512.346)/(0.908323)(4.629851)^2/346,391$$
$$= 223,648/346,391 = 0.646$$

$\Delta C_c = 0.193$

From table 3-34 the buckling coefficient and critical meridional buckling stress for a frustum without internal pressure was found to be:

$C_c = 0.225$ $(\sigma CR)_M = 54,860 \text{ lb/in.}^2$

Considering the stabilizing effect of the internal pressure, the new buckling coefficient is:

$$C_c^1 = (0.225 + 0.193) = 0.418$$

And the new critical meridional buckling stress is:

$$(\sigma CR)_M^1 = (54,860)(0.418)/(0.225) = 101,920 \text{ lb/in.}^2$$

$$\text{M.S.} = (101,920/29,188) - 1 = \underline{+2.492}$$

The strength of the individual faces in this portion of the lower frustum is checked as follows: examination of table 3-30 shows that the maximum hoop tension occurs in segment 32 in the maximum longitudinal acceleration condition (T = 138 seconds) and is:

$$\sigma_H = 193,380 \text{ lb/in.}^2$$

From table 3-26 the meridional tension stress at node 33 of segment 32 at this same time point is:

σ_M = 84,197 lb/in.^{2}

The vector sum of these stresses is:

$$\sigma_t = \left[(193,380)^2 + (84,197)^2\right]^{1/2} = 210,910 \text{ lb/in.}^2$$

σ_{ut} = 215,000 lb/in.^{2} (refer to paragraph 9.1, volume 3, appendix E)

M.S. = (215,000/210,910) - 1 = +0.019

The intercell buckling strength is now checked. Table 3-26 shows that the maximum compressive meridional stress occurs at node 33 of segment 32 in the maximum longitudinal acceleration condition (T = 138 seconds) and is:

σ_{OF} = - 117,163 lb/in.^{2}

σ_{ci} = 173,800 lb/in.^{2} (refer to table 3-35 for t_F = 0.027 in.)

M.S. = (173,800/117,163) - 1 = +0.483

The allowable face wrinkling stress is 135,600 lb/in.^{2} (refer to table 3-36 for S = .500 and t_{FOIL} = .0020)

M.S. = (135,600/117,163) - 1 = +0.157

The shear strength of this portion of the lower frustum is checked as follows: table 3-23 shows that the maximum transverse shear loading occurs at node 32 of segment 32 in the maximum longitudinal acceleration condition (T = 138 seconds) and is:

S(32) = - 406.250 lb/in.

t_c = 2.646 in. (refer to table 3-33)

τ = 406.250/2.646 = 154 lb/in.^{2}

σ_S = 170 lb/in.^{2} (refer to table 3-37)

M.S. = (170/154) - 1 = +0.104

3.8.3 INNER CYLINDRICAL BULKHEAD

3.8.3.1 Portion From Node 1 to Node 35 (Segments 33 and 34)

With reference to table 3-24, the sandwich in this area has an overall thickness of 0.375 in. with a face thickness of 0.030 in. This portion of the inner cylindrical bulkhead is checked for general stability as follows: examination of table 3-27 shows that the axial stresses in this region of the bulkhead are tension, so that buckling in the meridional direction cannot be a failure mode. Examination of table 3-31 shows no hoop stresses in this region of the bulkhead.

The strength of the individual sandwich faces is then checked as follows:: table 3-27 shows that the maximum meridional tension stress occurs at node 1 of segment 33 in the maximum longitudinal acceleration condition (T = 138 seconds) and is:

σ_{OF} = 192,974 lb/in.^{2}

σ_{ut} = 215,000 lb/in.^{2} (refer to paragraph 9.1, volume 3, appendix E)

M.S. = (215,000/192,974) - 1 = <u>+0.114</u>

The intercell buckling strength is now checked. Table 3-27 shows that the maximum compressive meridional stress occurs at node 1 of segment 33 in the maximum longitudinal acceleration condition (T = 138 seconds) and is:

σ_{IF} = 151,524 lb/in.^{2}

σ_{ci} = 180,400 lb/in.^{2} (refer to table 3-35 for t_F = 0.030 in.)

M.S. = (180,400/151,524) - 1 = <u>+0.191</u>

Because of a deficiency in shear strength, it was necessary to change the foil thickness of the core from 0.0020 in. to 0.0040 in. The allowable face wrinkling stress is then 196,400 lb/in.^{2} (refer to table 3-36 for S = .500 and t_{FOIL} = 0.0040).

M.S. (196,400/151,524) - 1 = <u>+0.296</u>

The shear strength of this portion of the inner cylindrical bulkhead is checked as follows: it should be noted that the transverse shear loadings are obtained directly from tables 3-17 through 3-21 as the F(2) and F(5) loadings with the algebraic sign changed. Examination of these tables shows that the maximum transverse shear loading occurs at node 1 of segment 33 in the maximum longitudinal acceleration condition (T = 138 seconds) and is:

S(1) = 325.298 lb/in.

t_c = 0.315 in. (refer to table 3-33)

τ = 325.298/.315 = 1033 lb/in.^{2}

σ_S = 1098 lb/in.^{2} (refer to table 3-37)

M.S. = (1098/1033) - 1 = <u>+0.063</u>

3.8.3.2 <u>Portion From Node 35 to Node 41 (Segments 35 to 40 Inclusive)</u>

With reference to table 3-24, the sandwich in this area has an overall thickness of 0.375 in. with a face thickness of 0.010 in. Examination of tables 3-27 and 3-21 reveals that the meridional loading is tension and there is no hoop stress. General stability is, therefore, not a problem.

The strength of the individual sandwich faces is then checked as follows: table 3-27 shows that the maximum tensile meridional stress occurs at node 35 of segment 35 in the maximum longitudinal acceleration condition (T = 138 seconds) and is:

σ_{IF} = 122,525 lb/in.^{2}

σ_{ut} = 215,000 lb/in.^{2} (refer to paragraph 9.1, volume 3, appendix E)

M.S. = (215,000/122,525) - 1 = +0.755

The intercell buckling strength is checked as follows: table 3-27 shows that the maximum compressive meridional stress occurs at node 41 of segment 40 in the maximum reentry dynamic pressure condition (T_R = 505 seconds) and is:

σ_{OF} = - 23,181 lb/in.^{2}

σ_{ci} = 63,200 lb/in.^{2} (refer to table 3-35 for t_F = 0.010 in.)

M.S. = (63200/23181) - 1 = +1.726

The allowable face wrinkling stress is 135,600 lb/in.^{2} (refer to table 3-36 for S = .500 and t_{FOIL} = .0020) which is obviously not critical.

The shear strength of this portion of the inner cylindrical bulkhead is checked as follows: examination of tables 3-17 through 3-21 shows that the maximum transverse shear loading occurs in segment 40 in the maximum reentry dynamic pressure condition (T_R = 505 seconds) and is:

S(41) = 66.554 lb/in.

t_c = 0.355 in. (refer to table 3-33)

τ = 66.554/0.355 = 187 lb/in.^{2}

σ_S = 411 lb/in.^{2} (refer to table 3-37)

M.S. = (411/187) - 1 = +1.198

3.8.3.3 Portion From Node 41 to Node 48 (Segments 41 to 47 Inclusive)

With reference to table 3-24, the sandwich in this area has an overall thickness of 3.400 in. with a face thickness of 0.010 in. Examination of table 3-27 reveals that the meridional loading is tension; however, table 3-31 shows that the maximum compressive hoop stress occurs in segments 41 through 47 in the maximum reentry dynamic pressure condition (T_R = 505 seconds) and is:

σ_H = -37,734 lb/in.^{2}

$(\sigma_{cR})_H$ = 38,560 lb/in.^{2} (refer to table 3-34)

M.S. = (38,560/37,734) - 1 = +0.022

The strength of the individual sandwich faces is then checked as follows: table 3-27 shows that the maximum tensile meridional stress occurs at node 41 of segment 41 in the maximum longitudinal acceleration condition (T = 138 seconds) and is:

σ_{OF} = 119,232 lb/in.^{2}

σ_{ut} = 215,000 lb/in.^{2} (refer to paragraph 9.1, volume 3, appendix E)

M.S. = (215,000/119,232) - 1 = +0.803

The intercell buckling strength is checked as follows: table 3-31 shows that the maximum compressive hoop stress is a constant value in segments 41 to 47 in the maximum reentry dynamic pressure condition (T_R = 505 seconds) and is:

σ_{IF} = σ_{OF} = -37,734 lb/in.^{2}

σ_{ci} = 63,200 lb/in.^{2} (refer to table 3-35 for t_F = 0.010 in.)

M.S. = (63,200/37,734) - 1 = +0.675

The allowable face wrinkling stress is 135,600 lb/in.^{2} (refer to table 3-36 for S = .500 and t_{FOIL} = .0020) and is obviously not critical.

The shear strength of this portion of the inner cylindrical bulkhead is checked as follows: examination of tables 3-17 through 3-21 shows that the maximum transverse shear loading occurs in segment 46 in the maximum reentry dynamic pressure condition (T_R = 505 seconds) and is:

S(46) = -263.717 lb/in.

t_c = 3.380 in. (refer to table 3-33)

τ = 263.717/3.380 = 78 lb/in.^{2}

σ_S = 152 lb/in.^{2} (refer to table 3-37)

M.S. = (152/78) - 1 = +0.949

3.8.3.4 Portion From Node 48 to Node 52 (Segments 48 to 51 Inclusive)

With reference to table 3-24, the sandwich in this portion has an overall thickness of 3.800 in. with a face thickness of .010 in. Examination of table 3-27 reveals that the meridional loading is tension; however, table 3-31 shows that the maximum compressive hoop stress occurs in segment 51 in the maximum longitudinal acceleration condition (T = 138 seconds) and is:

σ_H = - 44,467 lb/in.^{2}

$(\sigma_{CR})_H$ = 47,760 lb/in.^{2} (refer to table 3-34)

M.S. = (47,760/44,467) - 1 = +0.074

The strength of the individual sandwich faces is then checked as follows: table 3-27 shows that the maximum tensile meridional stress occurs at node 52 of segment 51 in the maximum longitudinal acceleration condition (T = 138 seconds) and is:

σ_{OF} = 197,048 lb/in.^{2}

σ_{ut} = 215,000 lb/in.^{2} (refer to paragraph 9.1, volume 3, appendix E)

M.S. = (215,000/197,048) - 1 = <u>+0.091</u>

The intercell buckling strength is checked as follows: table 3-31 shows that the maximum compressive hoop stress occurs in segment 51 in the maximum longitudinal acceleration condition (T = 138 seconds) and is:

σ_H = - 44,467 lb/in.^{2}

σ_{ci} = 63,200 lb/in.^{2} (refer to table 3-35 for t_F = 0.010 in.)

M.S. = (63,200/44,467) - 1 = <u>+0.421</u>

The allowable face wrinkling stress is 135,600 lb/in.^{2} (refer to table 3-36 for S = .500 and t_{FOIL} = .0020) which is obviously not critical.

The shear strength of this portion of the inner cylindrical bulkhead is checked as follows: examination of tables 3-17 through 3-21 shows that the maximum transverse shear loading occurs in segment 51 in the maximum longitudinal acceleration condition (T = 138 seconds) and is:

S(51) = 222.156 lb/in.

t_c = 3.780 in. (refer to table 3-33)

τ = 222.156/3.780 = 59 lb/in.^{2}

σ_S = 145 lb/in.^{2} (refer to table 3-37)

M.S. = (145/59) - 1 = <u>+1.458</u>

3.8.3.5 <u>Portion From Node 52 to Node 53 (Segment 52)</u>

With reference to table 3-24, the sandwich in this area has an overall thickness of 0.375 in. with a face thickness of 0.014 in. Table 3-27 shows the maximum compressive axial stress to occur in the maximum longitudinal acceleration condition (T = 138 seconds) and is:

σ_{AXIAL} = 24,185 lb/in.^{2}

$(\sigma CR)_M$ = 41,480 lb/in.^{2} (refer to table 3-34)

M.S. = (41,480/24,185) - 1 = <u>+0.715</u>

The strength of the individual sandwich faces is then checked as follows: table 3-27 shows that the maximum tensile meridional stress occurs at node 52 of segment 52 in the maximum longitudinal acceleration condition (T = 138 seconds) and is:

σ_{IF} = 32,494 lb/in.^{2}

σ_{ut} = 215,000 lb/in.^{2} (refer to paragraph 9.1, volume 3, appendix E)

$$M.S. = (215{,}000/32{,}494) - 1 = \underline{+5.62}$$

The intercell buckling strength is checked as follows: table 3-27 shows that the maximum compressive meridional stress occurs at node 52 of segment 52 in the maximum longitudinal acceleration condition (T = 138 seconds) and is:

$$\sigma_{OF} = 80{,}864 \text{ lb/in.}^2$$

$$\sigma_{ci} = 104{,}600 \text{ lb/in.}^2 \text{ (refer to table 3-35 for } t_F = 0.14 \text{ in)}$$

$$M.S. = (104{,}600/80{,}864) - 1 = \underline{+0.294}$$

The allowable face wrinkling stress is 135,600 lb/in.^{2} (refer to table 3-36 for S = .500 and t_{FOIL} = .0020) which is obviously not critical.

The shear strength of this portion of the inner cylindrical bulkhead is checked as follows: examination of tables 3-17 through 3-21 shows that the maximum transverse shear loading occurs in segment 52 in the maximum longitudinal acceleration condition (T = 138 seconds) and is:

$$S(52) = 255.507 \text{ lb/in.}$$

$$t_c = 0.347 \text{ in. (refer to table 3-33)}$$

$$\tau = 255.507/0.347 = 736 \text{ lb/in.}^2$$

$$\sigma_S = 881 \text{ lb/in.}^2 \text{ (refer to table 3-37)}$$

$$M.S. + (881/736) - 1 = \underline{+0.197}$$

3.8.3.6 <u>Portion From Node 53 to Node 57 (Segments 53 to 56 Inclusive)</u>

With reference to table 3-24, the sandwich in this area has an overall thickness of 0.375 in. with a face thickness of 0.010 in. Table 3-27 shows that the maximum compressive axial stress occurs in segment 56 in the maximum longitudinal acceleration condition (T = 138 seconds) and is:

$$\sigma_{AXIAL} = -34{,}132 \text{ lb/in.}^2$$

$$(\sigma_{CR})_M = 41{,}970 \text{ lb/in.}^2 \text{ (refer to table 3-34)}$$

$$M.S. = (41{,}970/34{,}132) - 1 = \underline{+0.230}$$

The strength of the individual sandwich faces is then checked as follows: table 3-27 shows that the maximum meridional tensile stress occurs at node 53 of segment 53 in the maximum dynamic pressure condition (T = 77 seconds) and is:

$$\sigma_{OF} = 19{,}535 \text{ lb/in.}^2$$

Because the allowable stress is 215,000 lb/in.^{2} (refer to paragraph 9.1, volume 3, appendix E) the margin of safety is large.

The intercell buckling strength is checked as follows: table 3-27 shows that the maximum compressive meridional stress occurs at node 53 of segment 53 in the maximum longitudinal acceleration condition (T = 138 seconds) and is:

$\sigma_F = - 64,534$ lb/in.^{2}

$\sigma_{ci} = 63,200$ lb/in.^{2}

This situation indicates that if the change in face thickness from 0.014 in. in segment 53 is allowed to remain at node 53, a small negative margin would exist. This can be eliminated by moving the station at which the thickness changes to a few inches below node 53. It has been arbitrarily decided to move this transition point a distance of 6.0 in. From table 3-27, the bending moment at node 53 (segment 53) is 122.021-in. lb/in.; at node 54 (segment 53) the moment is 47.672-in. lb/in. Conservatively assuming a linear variation in moment between nodes, the bending moment at the transition point becomes:

$$M = (40-6)(122.021 + 47.672)/40 - 47.672 = 144.239 - 47.672 = 96.567 \text{ in.lb/in.}$$

$I/y = 0.003984$ in.^{3} (refer to table 3-24)

Bending stress = 96.567/.003984 = 24,239 lb/in.^{2}

Axial stress = - 33,906 lb/in.^{2} (refer to table 3/27 at segment 53)

$\sigma_{IF} = - 33,906 - 24,239 = - 58,145$ lb/in.^{2}

$\sigma_{OF} = - 33,906 + 24,239 = - 9,667$ lb/in.^{2}

By moving the transition point a distance of 6.0 in., the margin of safety becomes:

$$M.S. = (63,200/58,145) - 1 = \underline{+0.087}$$

The allowable face wrinkling stress is 135,600 lb./in.^{2} (refer to table 3-36 for S = .500 and t_{FOIL} = 0.0020) which is obviously not critical.

The shear strength of this portion of the inner cylindrical bulkhead is checked as follows: examination of tables 3-17 through 3-21 shows that the maximum transverse shear loading occurs at segment 53 in the maximum longitudinal acceleration condition (T = 138 seconds) and is:

S(53) = 25.550 lb/in.

t_c = 0.355 in. (refer to table 3-33)

$\tau = 25.550/0.355 = 72$ lb/in.^{2}

$\sigma_S = 411$ lb/in.^{2} (refer to table 3-37)

$$M.S. + (411/72) - 1 = \underline{+4.708}$$

3.8.4 OUTER CYLINDRICAL BULKHEAD

3.8.4.1 <u>Portion From Node 18 to Node 61 (Segments 57 to 60 Inclusive)</u>

With reference to table 3-24, the sandwich in this area has an overall thickness of 4.000 in. with a face thickness of 0.036 in. Table 3-28 shows that the primary axial loading is in tension. Table 3-32 shows that the maximum compression hoop stress occurs in segment 57 in both the maximum dynamic pressure condition (T = 77 seconds) and the maximum longitudinal acceleration condition (T = 138 seconds) and is:

$\sigma_H = 39,575 \text{ lb/in.}^2$

$(\sigma_{CR})_H = 42,320 \text{ lb/in.}^2$ (refer to table 3-34)

M.S. = (42,320/39,575) - 1 = +0.069

The strength of the individual sandwich faces is then checked as follows: table 3-28 shows that the maximum meridional tensile stress occurs at node 57 of segment 57 in the maximum longitudinal acceleration condition (T = 138 seconds) and is:

$\sigma_{OF} = 70,256 \text{ lb/in.}^2$

$\sigma_{ut} = 215,000 \text{ lb/in.}^2$ (refer to paragraph 9.1, volume 3, appendix E)

M.S. = (215,000/70,256) - 1 = +2.048

The intercell buckling strength is checked as follows: table 3-32 shows that the maximum compressive hoop stress occurs in segments 57 to 59 in the maximum dynamic pressure condition (T = 77 seconds) and is:

$\sigma_H = - 39,575 \text{ lb/in.}^2$

$\sigma_{ci} = 104,600 \text{ lb/in.}^2$ (refer to table 3-35 for $t_F = 0.140$ in.)

M.S. = (104,600/39,575) - 1 = +1.643

The allowable face wrinkling stress is 135,600 lb/in.^{2} (refer to table 3-36 for S = .500 and $t_{FOIL} = 0.0020$) which is obviously not critical.

The shear strength of this portion of the outer cylindrical bulkhead is checked as follows: examination of tables 3-17 through 3-21 shows that the maximum transverse shear loading occurs in segment 60 in the maximum longitudinal acceleration condition (T = 138 seconds) and is:

S(60) = 278.342 lb/in.

$t_c = 3.928$ in. (refer to table 3-33)

$\tau = 278.342/3.928 = 71 \text{ lb/in.}^2$

$\sigma_S = 143 \text{ lb/in.}^2$ (refer to table 3-37)

M.S. = (143/71) - 1 = +1.014

3.8.4.2 Portion From Node 61 to Node 65 (Segments 61 to 64 Inclusive)

With reference to table 3-24, the sandwich in this area has an overall thickness of 4.000 in. with a face thickness of 0.070 in. Table 3-28 shows that the primary axial loading is in tension. Table 3-32 shows the maximum compressive hoop stress occurs in segment 64 in the liftoff condition (T = 0 seconds) and is:

$\sigma_H = -39{,}915$ lb/in.^{2}

$(\sigma_{CR})_H = 41{,}760$ lb/in.^{2} (refer to table 3-34)

M.S. = (41,760/39,915) - 1 = +0.046

The strength of the individual sandwich faces is checked as follows: table 3-28 shows that the maximum meridional tensile stress occurs at node 65 of segment 64 in the maximum longitudinal acceleration condition (T = 138 seconds) and is:

$\sigma_{OF} = 43{,}578$ lb/in.^{2}

$\sigma_{ut} = 215{,}000$ lb/in.^{2} (refer to paragraph 9.1, volume 3, appendix E)

M.S. = (215,000/43,578) - 1 = +3.934

The intercell buckling strength is checked as follows: table 3-32 shows that the maximum compressive hoop stress occurs in segment 64 in the liftoff condition (T = 0 seconds) and is:

$\sigma_H = -39{,}915$ lb/in.^{2}

$\sigma_{ci} = 63{,}200$ lb/in.^{2} (refer to table 3-35)

M.S. = (63,200/39,915) - 1 = +0.583

The allowable face wrinkling stress is 135,600 lb/in.^{2} (refer to paragraph 3-36 for S = .500 and t_{FOIL} = 0.0020) which is obviously not critical.

The shear strength of this portion of the outer cylindrical bulkhead is checked as follows: examination of tables 3-17 through 3-21 shows that the maximum transverse shear loading occurs at node 61 of segment 61 in the maximum longitudinal acceleration condition (T = 138 seconds) and is:

S(61) = 414.833 lb/in.

t_c = 3.860 in. (refer to table 3-33)

$\tau = 414.833/3.860 = 107$ lb/in.^{2}

$\sigma_S = 144$ lb/in.^{2} (refer to table 3-37)

M.S. = (144/107) - 1 = +0.346

3.8.4.3 Portion From Node 65 to Node 69 (Segments 65 to 68 Inclusive)

With reference to table 3-24, the sandwich in this area has an overall thickness of 0.680 in. with a face thickness of 0.014 in. Table 3-32 shows that the maximum hoop tension stress occurs in segment 68 in the maximum longitudinal acceleration condition (T = 138 seconds) and is 120,041 lb/in.^{2}. Table 3-28 shows the meridional stress at node 69 of segment 68 at this same time point to be 163,119 lb/in.^{2}. The vector sum of these stresses is:

G

$$\sigma_{IF} = \left[(120{,}041)^2 + (163{,}119)^2\right]^{1/2} = 202{,}530 \text{ lb/in.}^2$$

σ_{ut} = 215,000 lb/in.^{2} (refer to paragraph 9.1, volume 3, appendix E)

M.S. = (215,000/202,530) - 1 = <u>+0.062</u>

The intercell buckling strength is checked as follows: table 3-28 shows that the maximum compressive meridional loading occurs at node 65 of segment 65 in the maximum longitudinal acceleration condition (T = 138 seconds) and is:

σ_{OF} = - 91,321 lb/in.^{2}

σ_{ci} = 104,600 lb/in.^{2} (refer to table 3-35 for t_F = 0.014 in.)

M.S. = (104,600/91,321) - 1 = <u>+0.145</u>

The shear strength of this portion of the outer cylindrical bulkhead is checked as follows: examination of tables 3-17 through 3-21 shows that the maximum transverse shear loading occurs at node 66 of segment 65 in the maximum longitudinal acceleration condition (T = 138 seconds) and is:

S(66) = - 132.749 lb/in.

t_c = 0.652 in. (refer to table 3-33)

τ = 132.749/0.652 = 204 lb/in.^{2}

σ_S = 315 lb/in.^{2} (refer to table 3=37)

M.S. = (315/204) - 1 = <u>+0.544</u>

3.8.4.4 <u>Portion From Node 69 to Node 70 (Segment 69)</u>

With reference to table 3-24, the sandwich in this area has an overall thickness of 0.680 in. with a face thickness of 0.016 in. Table 3-28 shows that the maximum compressive axial stress occurs in the landing condition and is:

σ_{AXIAL} = - 18,105 lb/in.^{2}

$(\sigma_{CR})_M$ = 18,260 lb/in.^{2} (refer to table 3-34)

M.S. = (18,260/18,105) - 1 = <u>+0.009</u>

Table 3-28 shows the maximum tensile meridional stress occurs at node 69 of segment 69 in the maximum longitudinal acceleration condition (T = 138 seconds) and is:

σ_{OF} = 106,855 lb/in.^{2}

σ_{ut} = 215,000 lb/in.^{2} (refer to paragraph 9.1, volume 3, appendix E)

M.S. = (215,000/106,855) - 1 = <u>+1.012</u>

Table 3-28 shows the maximum compressive meridional stress occurs at node 69 of segment 69 in the maximum acceleration condition (T - 138 seconds) and is:

σ_{IF} = - 107,417 lb/in.^{2}

The allowable intercell buckling stress is:

σ_{ci} = 123,600 lb/in.^{2} (refer to table 3-35 for t_F = .016)

M.S. = (123,600/107,417) - 1 = <u>+0.151</u>

The allowable face wrinkling stress is 135,600 lb/in.^{2} (refer to table 3-36 for S = .500 and t_{FOIL} = .0020) which is obviously not critical.

The shear strength of this portion of the outer cylindrical bulkhead is checked as follows: examination of tables 3-17 through 3-21 shows that the maximum transverse shear loading occurs in the maximum longitudinal acceleration condition (T = 138 seconds) and is:

S(69) = - 120.398 lb/in.^{2}

t_c = 0.648 in. (refer to table 3-33)

τ = 120.398/0.648 = 186 lb/in.^{2}

σ_S = 316 lb/in.^{2} (refer to table 3-37)

M.S. = (316/186) - 1 = +0.699

3.8.4.5 Portion From Node 70 to Node 74 (Segments 70 to 73 Inclusive)

With reference to table 3-24, the sandwich in this area has an overall thickness of 0.680 in. with a face thickness of 0.014 in. Table 3-28 shows that the maximum compressive axial stress occurs in segment 73 in the landing condition and is:

σ_{AXIAL} = 20,876 lb/in.^{2}

$(\sigma\ CR)_M$ = 18,320 lb/in.^{2} (refer to table 3-34)

The above represents a negative margin of safety of 12.2 percent, however, it is based on a limit acceleration during landing of 3.0g. Reference 7 indicates that a decision had been made to reduce the landing acceleration to a limit value of 2 g. Because the major portion of this analysis had been completed when this change was made, no attempt was made towards its incorporation. Now, in order to prevent an unnecessary weight increase, the critical axial stress in this portion of the structure will be made to conform to the new criteria. Therefore:

σ_{AXIAL} = - (20,876)(2/3) = - 13,920 lb/in.^{2}

M.S. = (18,320/13,920) - 1 = +0.316

The maximum tensile meridional stress occurs at node 74 of segment 73 in the maximum dynamic pressure condition (T = 77 seconds) and is:

σ_{IF} = 36,683 lb/in.^{2} (refer to table 3-28)

Because the allowable tensile strength is 215,000 lb/in.^{2} (refer to paragraph 9.1, volume 3, appendix E) the resulting margin of safety is large.

The maximum meridional compressive stress occurs at node 74 of segment 73 in the landing condition and is (reduced per the above discussion):

$$\sigma_{OF} = -(36,162)(2/3) = -24,110 \text{ lb/in.}^2 \text{ (refer to table 3-28)}$$

$$\sigma_{ci} = 104,600 \text{ lb/in.}^2 \text{ (refer to table 3-35)}$$

$$\text{M.S.} = (104,600/36,162) - 1 = \underline{+3.338}$$

The shear strength of this portion of the outer cylindrical bulkhead is checked as follows: Examination of tables 3-17 through 3-21 shows that the maximum transverse shear loading occurs at node 70 of segment 70 in the maximum longitudinal acceleration condition (T = 138 seconds) and is:

$$S(70) = 59.126 \text{ lb/in.}$$

$$t_c = 0.652 \text{ in. (refer to table 3-33)}$$

$$T = 59.126/0.652 = 91 \text{ lb/in.}^2$$

$$\sigma_S = 315 \text{ lb/in.}^2 \text{ (refer to table 3-37)}$$

$$\text{M.S.} = (315/91) - 1 = \underline{+2.461}$$

3.8.4.6 Result of Weight Reduction Review

In the course of this analysis, it was generally apparent that in sizing the sandwich for any primary structural component that is critical in a compressive buckling mode, the minimum weight was achieved when the face thickness was minimized and the overall thickness was allowed to grow until stability resulted. In the case of the outer cylindrical bulkhead, this optimization was not realized because a maximum overall sandwich thickness of 4.00 in. was imposed by existing manufacturing equipment. However, discussions with the sandwich manufacturer has indicated that the 4.00-in. manufacturing limit could be increased to 5.00 in. with modification of the manufacturing tooling and core cell size and material thickness.

The decision was then made to reexamine the sizing of the outer cylindrical bulkhead using a 5.00-in. overall thickness. Examination of paragraphs 3.8.4.1 and 3.8.4.2 shows that the portion of the bulkhead from segment 57 to 64, inclusive (refer to figure 1-4), was designed by the external pressure distributions from the maximum dynamic pressure condition (T = 77 seconds) and the maximum longitudinal acceleration condition (T = 138 seconds). The intensity of the external pressure acting at the mid-point of the individual segments is found in column (6) of table 3-8 and 3-9. The hoop stress in each face of the sandwich is given by the equation:

$$(\sigma_{CR})_H = \frac{P_{CR} R}{2 t_F}$$

where,

$(\sigma_{CR})_H$ = critical hoop buckling stress

P_{CR} = critical external pressure

R = radius of cylinder

t_F = individual face thickness of sandwich

Because the computer runs described in paragraph 9.4.2, volume 3, appendix E, provided the critical bulking stress for a family of 5.00-in.-thick sandwiches with variable face thicknesses, the above equation is used to evaluate the critical external pressure as follows:

$$P_{CR} = \frac{(\sigma_{CR})_H \, (2t)_F}{R}$$

Because R = 370.050 ins. (refer to table 1-1), the equation becomes

$$P_{CR} = \frac{2(\sigma_{CR})_H \, (t_F)}{370.050} = 0.005404 \, (\sigma_{CR})_H \, (t_F)$$

Table 3-38 was set up to calculate the critical external pressure versus face thickness for a 5.00-in.-thick sandwich.

Table 3-38. Critical External Pressure versus Face Thickness for t = 5.00 Ins. - Outer Cylindrical Bulkhead

①	②	③	④
t_F	$(\sigma_{cr})_H$	$(\sigma_{cr})_H (t_F)$	p_{cr}
REF.	NOTE 1)	① × ②	.005404 ③
.010	59960	599.600	3.240
.012	59926	719.112	3.886
.014	59892	838.488	4.531
.016	59859	957.744	5.176
.018	59825	1076.850	5.819
.020	59791	1195.820	6.462
.022	59758	1314.676	7.105
.024	59724	1433.376	7.746
.026	59690	1551.940	8.387
.028	59657	1670.396	9.027
.030	59623	1788.690	9.666
.032	59589	1906.848	10.305
.034	59556	2024.904	10.943
.036	59522	2142.792	11.580
.038	59489	2260.582	12.216
.040	59456	2378.240	12.852
.042	59422	2495.724	13.487
.044	59388	2613.072	14.121
.046	59355	2730.330	14.755
.048	59321	2847.408	15.387
.050	59288	2964.400	16.020

Notes: 1) Data from computer runs are described in paragraph 9.4.2, appendix E, volume 3.

Examination of table 3-9 shows that the maximum external pressure acting on the outer cylindrical bulkhead remains constant from the forward end of the bulkhead to the midpoint of segment 61, and is 7.700 lb/in.^{2}. The required face thickness for a 5.00-in. sandwich to withstand this pressure is found to be 0.024 in. (table 3-38) with a critical pressure of 7.746 lb/in.^{2}. The strength of this portion of the bulkhead is then

$$M.S. = (7.746/7.700) - 1 = \underline{+.006}$$

The length of this portion of the bulkhead is the sum of the L_s values for segments 57 through 60 plus $L_s/2$ for segment 61 and is:

$$L = (13.588 + 27.176 + 54.352 + 71.645 + \frac{71.645}{2}) = 202.584 \text{ in.}$$

(values of L_s are from table 1-1)

The next transition point in the sandwich configuration was arbitrarily established as the midpoint of segment 62. The intensity of the maximum external pressure at this station is obtained from table 3-7 (liftoff condition, T = 0 seconds) and is 11.079 lb/in.^{2}. The required face thickness for a 5.0-in. sandwich to withstand this pressure is found to be 0.036 in. from table 3-38, with a critical pressure of 11.580 lb/in.^{2}. The strength of this portion of the bulkhead is then:

$$M.S. = (11.580/11.079) - 1 = \underline{+.045}$$

The length of this portion of the bulkhead is one-half of segment 61 plus one-half of segment 62 or:

$$L = 0.5\ (71.645 + 54.352) = 63.0 \text{ in.}$$

The remaining portion of the bulkhead down to, and including segment 64, was sized as follows: the maximum external pressures acting at the midpoint of segments 63 and 64 in the liftoff condition (T = 0 seconds) are 13.762 lb/in.^{2} and 15.101 lb/in.^{2}, respectively (refer to table 3-7). From table 1-1 the lengths of segments 63 and 64 are 27.176 in. and 13.588 in., respectively. Because the pressure variation is linear, it can be shown that the pressure intensity at the lower end of segment 64 (node 65) is 15.547 lb/in.^{2}. The required face thickness for a 5.0 in. sandwich to withstand this pressure is found to be 0.050 in. from table 3-38, with a critical pressure of 16.020 lb/in.^{2}. The strength of this portion of the bulkhead is then:

$$M.S. = (16.020/15/547) - 1 = \underline{+.030}$$

In order to check the other possible failure modes of the sandwich, the assumption has to be made that the internal loads in the new configuration remain unchanged. This is not rigorously correct because the change in sandwich sizing affects the stiffness of the outer cylindrical bulkhead, which in turn will affect the discontinuity loads (bending moment and transverse shear loading).

In the region where the sandwich has a face thickness of 0.024 in., the maximum meridional tensile stress occurs in the maximum longitudinal acceleration condition (T = 138 seconds) and is calculated as follows:

$P(57) = -3933.402$ lb/in.

$M(57) = +2467.410$ in-lb/in.

(refer to table 3-28)

$A = 2t_F = 2(.024) = .048$ in.^{2}/in.

$I/y = (t^3 - t_c^3)/12(1 - u^2)(h/2)$

$= 2 \left[(5.000)^3 - (4.952)^3\right] /(11.032)(5.000 - 0.024)$

$= 7.134/54.895 = 0.129957$ in.^{3}/in. (refer to table 3-34)

$\sigma_{OF} = -(-3933.402/.048) + (2467.410/0.129957)$

$= +81{,}946 + 18{,}986 = +100{,}932$ lb/in.^{2}

$\sigma_{ut} = 215{,}000$ lb/in.^{2} (refer to paragraph 9.1, volume 3, appendix E)

M.S. = (215,000/100,932) - 1 = <u>+1.130</u>

The maximum compressive stress occurs in the hoop direction in both the maximum dynamic pressure condition (T = 77 seconds) and the maximum longitudinal acceleration condition (T = 138 seconds) and is:

$\sigma_H = pR/2t_F = (7.70)(370.050)/2(.024) = 59{,}362$ lb/in.^{2}

The intercell buckling allowable is calculated as follows:

$S/t_F = 0.500/0.24 = 20.8$

$\sigma_{ci}/\eta = 235{,}000$ lb/in.^{2} (refer to figure 3-10)

$\sigma_{cy}/(\sigma_{ci}/\eta) = 200{,}000/235{,}000 = 0.851$

$\sigma_{ci}/\sigma_{cy} = 0.835$ (refer to figure 3-11)

$\sigma_{ci} = 0.835\ (200{,}000) = 167{,}000$ lb/in.^{2}

M.S. = (167,000/59,362) - 1 = <u>+1.813</u>

The allowable face wrinkling stress is 135,600 lb/in.^{2} (refer to table 3-36 for S = 0.500 and t_{FOIL} = 0.0020)

M.S. = (135,600/59,362) - 1 = <u>+1.284</u>

The shear strength of this portion of the outer cylindrical bulkhead is checked as follows: examination of tables 3-17 through 3-21 shows that the maximum transverse shear loading occurs in segment 61 in the maximum longitudinal acceleration condition (T = 138 seconds) and is:

$$S(61) = 414.833 \text{ lb/in.}$$

$$t_c = 5.00 - 0.048 = 4.952 \text{ in.}$$

$$\tau = 414.833/4.952 = 84 \text{ lb/in.}^2$$

$$\sigma_S = 1.307\ (\rho_{c1}/\rho_c)^{1.34}\ (\sigma_{SU})/(t_c)^{0.44} \text{ (from paragraph 3.7.4)}$$

$$= 261.166/(4.952)^{0.44} = 261.166/2.022 = 129 \text{ lb/in.}^2$$

$$M.S. = (129/84) - 1 = \underline{+.535}$$

In the region of the bulkhead where the face thickness is 0.036 ins., the maximum meridional tensile stress occurs at segment 61 in the maximum longitudinal acceleration condition (T = 138 seconds) and is determined as follows:

$$\left.\begin{array}{l} P(61) = -3902.234 \text{ lb/in.} \\ M(61) = 603.317 \text{ in-lb/in.} \end{array}\right\} \text{refer to table 3-28}$$

$$A = 2(0.036) = 0.072 \text{ in.}^2\text{/in.}$$

$$I/y = 2\left[(5.000)^3 - (4.928)^3\right]/(11.032)(5.000 - 0.036)$$

$$= 10.648/54.763 = 0.94437 \text{ in.}^3\text{/in.}$$

$$\sigma_{OF} = -(-3902.234/.072) + (603.137/.194437)$$

$$= +54{,}198 + 3102 = 57{,}300 \text{ lb/in.}^2$$

$$\sigma_{ut} = 215{,}000 \text{ lb/in.}^2 \text{ (refer to paragraph 9.1, volume 3, appendix E)}$$

$$M.S. = (215{,}000/57{,}300) - 1 = \underline{+2.752}$$

The maximum compressive stress occurs in the hoop direction in the liftoff condition (T = 0 seconds) in segment 62 and is:

$$\sigma_H = (11.079)(370.050)/2(0.036) = 56{,}941 \text{ lb/in.}^2$$

$$\sigma_{ci} = 190{,}000 \text{ lb/in.}^2 \text{ (refer to table 3-35)}$$

$$M.S. = (190{,}000/56{,}941) - 1 = \underline{+2.336}$$

The allowable face wrinkling stress is 135,600 lb/in.^{2} (refer to table 3-36 for S = 0.500 and $t_{FOIL} = 0.0020$).

$$M.S. = (135{,}600/56{,}941) - 1 = \underline{+1.380}$$

The shear strength of this portion of the outer cylindrical bulkhead is checked as follows: examination of tables 3-17 through 3-21 shows that the maximum transverse shear loading occurs in segment 61 in the maximum longitudinal acceleration condition (T = 138 seconds) and is:

$$S(61) = -414.833 \text{ lb/in.}$$

$$t_c = 5.000 - 0.072 = 4.928 \text{ in.}$$

$$\tau = 414.833/4.928 = 84 \text{ lbs/in.}^2$$

$$\sigma_s = 261.166/(4/928)^{0.44} = 261.166/2.017 = 129 \text{ lb/in.}^2$$

$$\text{M.S.} = (129/84) - 1 = \underline{+.535}$$

In the region of the bulkhead where the face thickness is 0.050 in., the maximum tensile meridional stress occurs at segment 64 in the maximum longitudinal acceleration condition (T = 138 seconds) and is determined as follows:

$$\left.\begin{aligned} P(64) &= 3873.151 \text{ lb/in.} \\ M(64) &= -4762.789 \text{ in.-lb/in.} \end{aligned}\right\} \text{refer to table 3-28}$$

$$A = 2(0.050) = 0.100 \text{ in.}^2\text{/in.}$$

$$I/y = 2\left[(5.000)^3 - (4.900)^3\right]/(11.032)(5.000 - 0.050)$$

$$= 14.702/54.608 = 0.269227 \text{ in.}^3\text{/in.}$$

$$\sigma_{OF} = (3873.151/.100) - (-4762.789/0.269227)$$

$$= +38{,}732 + 17{,}691 = +56{,}423 \text{ lb/in.}^2$$

$$\sigma_{ut} = 215{,}000 \text{ lb/in.}^2 \text{ (refer to paragraph 9.1, volume 3, appendix E)}$$

$$\text{M.S.} = (215{,}000/56{,}423) - 1 = \underline{+2.810}$$

The maximum compressive stress occurs in the hoop direction in segment 64 in the liftoff condition and is:

$$\sigma_H = (15.547)(370.050)/2(.050) = 57{,}532 \text{ lb/in.}^2$$

The allowable face wrinkling stress is 135,600 lb/in.^{2} (refer to table 3-36 for S = 0.500 and t_{FOIL} = 0.0020).

$$\text{M.S.} = (135{,}600/57{,}532 - 1 = \underline{+1.356}$$

The shear strength of this portion of the outer cylindrical bulkhead is checked as follows: examination of tables 3-17 through 3-21 shows that the maximum transverse shear loading occurs in segment 62 in the liftoff condition (T = 0 seconds) and is

$$S(63) = 281.329 \text{ lb/in.}$$

$$t_c = 5.000 - 0.100 = 4.900 \text{ in.}$$

$$\tau = 281.329/4.900 = 57 \text{ lb/in.}^2$$

$$\sigma_s = 261.166/(4.950)^{0.44} = 261.166/2.022 = 129 \text{ lb/in.}^2$$

$$\text{M.S.} = (129/57) - 1 = \underline{+1.263}$$

3.9 SUMMARY OF RESULTS

The results of the preceding determination and justification of the primary structural sizes (less the aft heat shield bulkhead) are summarized in figure 3-15. A summary of the margins of safety is given in table 3-39.

3.10 HEAT SHIELD

The heat shield configuration is depicted in figure 3-16 and serves as geometry and nomenclature reference for the beam and panel configuration. The method of analysis utilized is referenced to section 9.8 of volume 3, appendix E. The revised heat shield design criteria are as shown below:

1) Load factor equals 1.1, see table 3.2-1, section 3.2.2 of volume 4

2) Maximum dynamic pressure equals 180 psf, reference 8

3) Configuration geometry as in figure 3-16

4) Panel ΔT equals 200° F and panel operating temperature equals 500° F, reference 9

5) Beam operating temperature equals 150° F, reference 9

The material selection for the heat shield structure was PH15-7MO steel. The material was assumed to exhibit the following properties at room temperature:

$$F_{cy} = 200{,}000 \text{ psi}$$

$$E = 30 \times 10^6 \text{ psi}$$

$$\mu = 0.282$$

Table 3-39. Summary of Minimum Margins of Safety in Shell Structure (Sheet 1 of 3)

Component	Segment Range	Margin of Safety	Failure Mode	Critical Design Condition
Upper Frustum	2- 3	0.027	Face Wrinkling (Meridional and Bending)	Max Longitudinal Acceleration (T = 138 sec)
	4- 9	0.141	General Stability (Hoop and Meridional)	Max Dynamic Pressure (T = 77 sec)
	10-17	0.147	General Stability (Hoop and Meridional)	Max Dynamic Pressure (T = 77 sec)
Lower Frustum	19-20	0.081	Transverse Shear	Max Longitudinal Acceleration (T = 138 sec)
	21-24	0	Face Wrinkling (Meridional and Bending)	Liftoff (T = 0 sec)
	24-26	0.071	Tension (Hoop)	Max Longitudinal Acceleration (T = 138 sec)
	27-30	0.073	Tension (Hoop)	Max Longitudinal Acceleration (T = 138 sec)
	31-33	0.019	Tension (Meridional and Hoop)	Max Longitudinal Acceleration (T = 138 sec)

Table 3-39. Summary of Minimum Margins of Safety in Shell Structure (Sheet 2 of 3)

Component	Segment Range	Margin of Safety	Failure Mode	Critical Design Condition
Inner Cylindrical Bulkhead	33-34	0.063	Transverse Shear	Max Longitudinal Acceleration (T = 138 sec)
	35-40	0.755	Tension (Meridional and Bending)	Max Longitudinal Acceleration (T = 138 sec)
	41-47	0.022	General Stability (Hoop)	Max Re-entry Dynamic Pressure (T_R = 505 sec)
	48-51	0.074	General Stability (Hoop)	Max Longitudinal Acceleration (T = 138 sec)
	52	0.197	Transverse Shear	Max Longitudinal Acceleration (T = 138 sec)
	53-56	0.087	Intercell Buckling (Meridional and Bending)	Max Longitudinal Acceleration (T = 138 sec)
Outer Cylindrical Bulkhead	57-61	0.006	General Stability (Hoop)	(1)
	61-62	0.045	General Stability (Hoop)	Liftoff (T = 0 sec)
	62-64	0.030	General Stability (Hoop)	Liftoff (T = 0 sec)

Table 3-39. Summary of Minimum Margins of Safety in Shell Structure (Sheet 3 of 3)

Component	Segment Range	Margin of Safety	Failure Mode	Critical Design Condition
Outer Cylindrical Bulkhead (Continued)	65-68	0.062	Tension (Meridional and (Hoop)	Max Longitudinal Acceleration (T = 138 sec)
	69	0.009 (2)	General Stability (Meridional)	Landing
	70-73	0.316	General Stability (Meridional)	Landing

NOTES: (1) This margin of safety applies to the maximum dynamic pressure condition (T = 77 seconds) and the maximum longitudional acceleration condition (T = 138 seconds).

(2) This margin of safety is conservative (subsection 3.1).

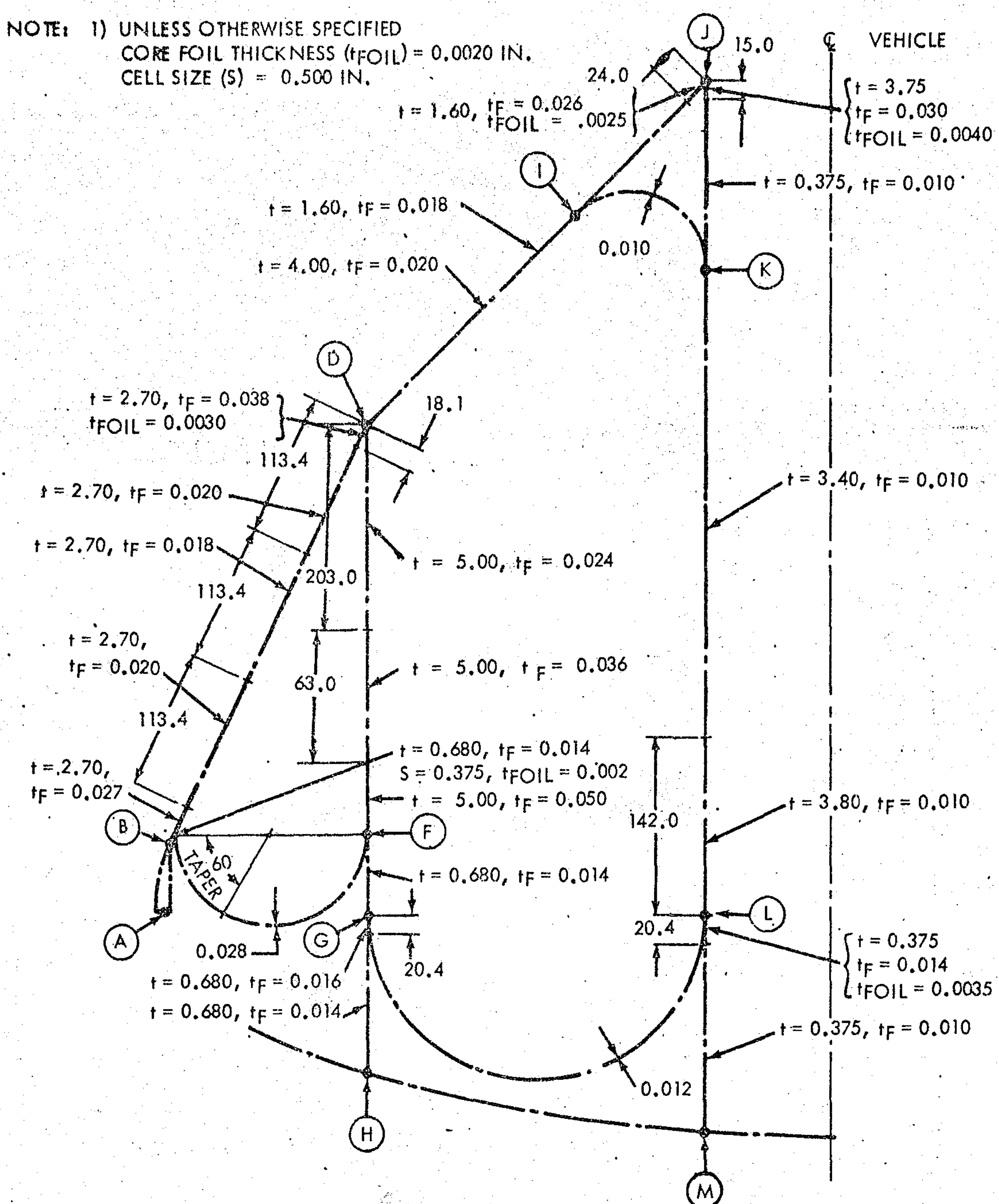

Figure 3-15. Preliminary Structural Sizing - Task 4

C 4

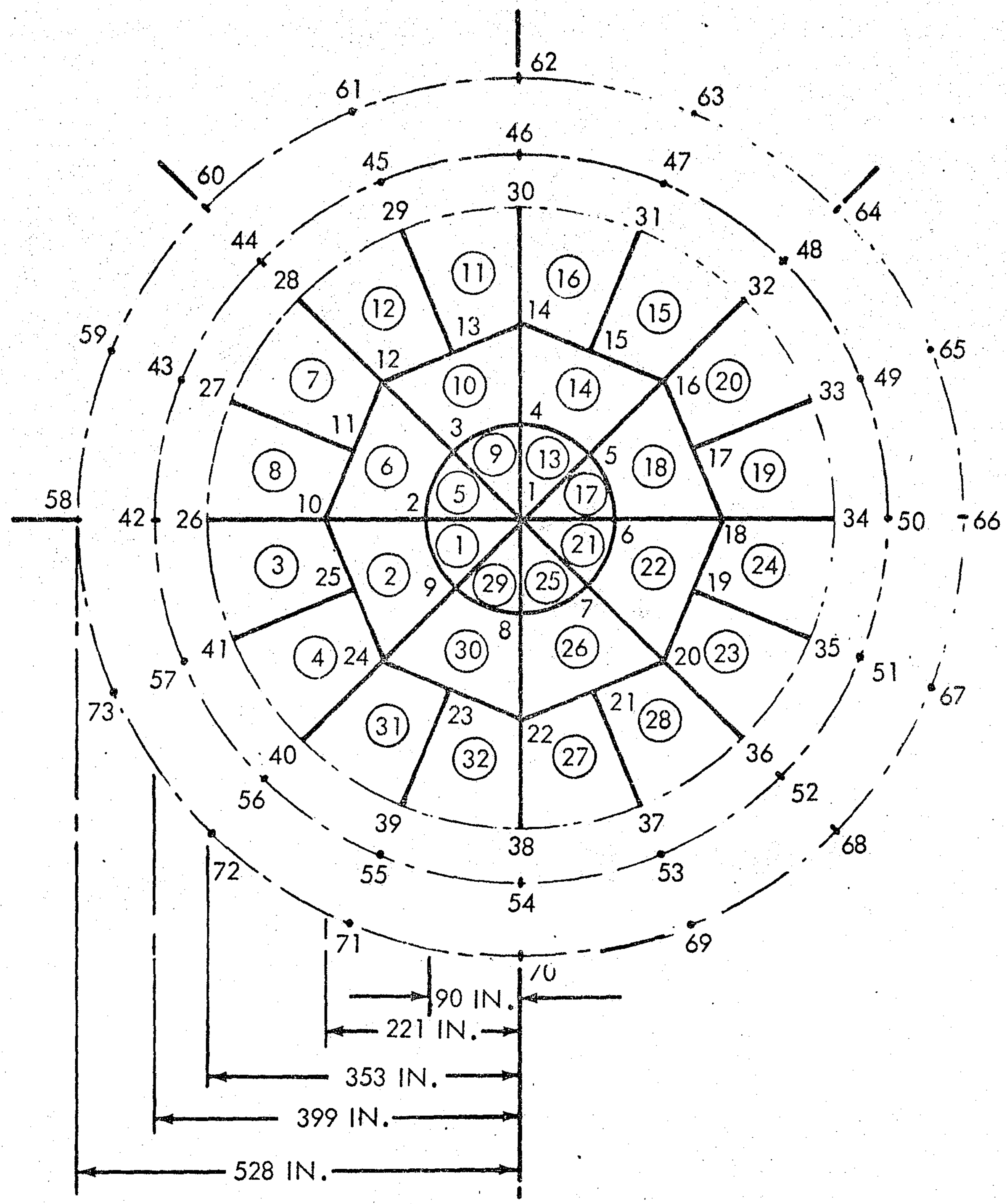

Figure 3-16. Bulkhead Configuration

The 500° F operating temperature of the panels would reduce the compression yield and modulus of elasticity values to:

$$F_{cy} = 200{,}000 \times 0.89 = 178{,}000 \text{ psi}$$

$$E = 30 \times 10^6 \times .93 = 27.99 \times 10^6 \text{ psi}$$

The reduction values were obtained from reference 10 on page 161, figure 2.7.3.2.2(a), and page 162, figure 2.7.3.2.4.

The 150° F operating temperature of the beams reduces the compression yield and modulus of elasticity values to:

$$F_{cy} = 200{,}000 \times 0.98 = 196{,}000 \text{ psi}$$

$$E = 30 \times 10^6 \times 0.99 = 29.7 \times 10^6 \text{ psi}$$

The reduction values were obtained from reference 10 on page 161, figure 2.7.3.2.2(2), and page 162, figure 2.7.3.2.4.

3.10.1 LOADS ANALYSIS

The pressure loads for the heat shield panels were calculated by ratioing the revised design criteria, i.e., panel design pressures in tables 31, 32 and 33 of volume 3, appendix E, multiplied by (1.1/1.5) (180/165). These pressures are shown in tables 3-40, 3-41, and 3-42. The pressure coefficients were assumed to be the same as utilized in figure 32, 33 and 34, volume 3, appendix E.

3.10.2 HEAT SHIELD PANELS

The geometry of a typical section (45°) of heat shield is shown in figure 3-17. These panels receive the maximum pressure loading. The idealized panel geometry is shown in figure 3-18. Using the revised design criteria and the new configuration geometry, the operating stress levels for the panel configurations were calculated. Tables 3-40, 3-41, and 3-42 present the design calculations for the outboard rectangular panels, inboard rectangular panels, and circular sector panels, respectively. Tables 3-43, 3-44, and 3-45 describe the selected designs for the panel configurations.

3.10.3 HEAT SHIELD BEAMS

The beam configuration is depicted in figure 3-16. Because the method of analysis would be the same as presented in subsection 9.8.4, volume 3, the beam designs were obtained by ratio. The required areas itemized in tables 44, 45 and 46 of volume 3, appendix E, were multiplied by the ratio of the load factors, beam lengths, allowable compressive stresses, and maximum dynamic pressures in order to obtain the new required areas. The required area and/or section modulus for a given beam varies directly with its loading, length and allowable stress. The beam loading would have the same shape, but

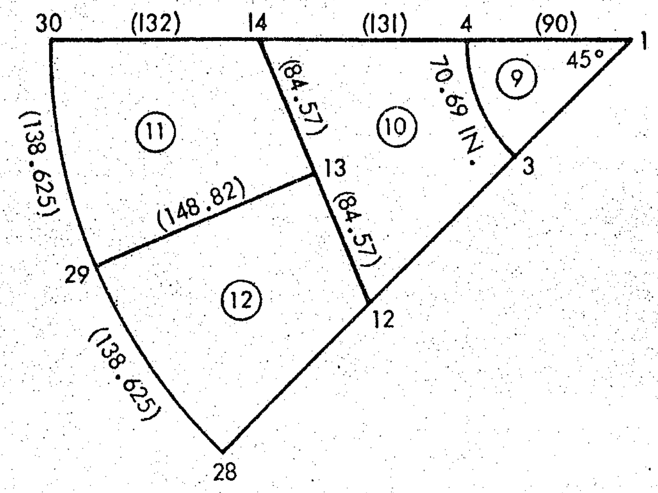

Figure 3-17. Geometry - Typical 45° Section

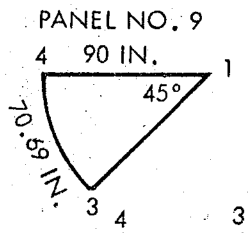

PANEL WILL BE ANALYZED AS SHOWN.

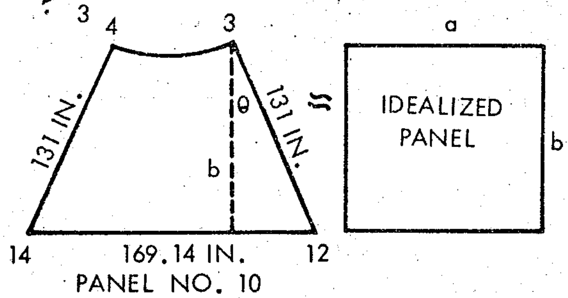

AREA 4-3-12-14 = 15,509.10 IN^2
LET IDEALIZED PANEL AREA = 15,509.10
θ = 22.5°, ∴ b = Cos 22.5° (131) = 121.03 IN.
AREA = a x b
15,509.10 = 121.03 x a
∴ a = 128.14 IN. a/b = 1.06, ∴ β = 0.3136

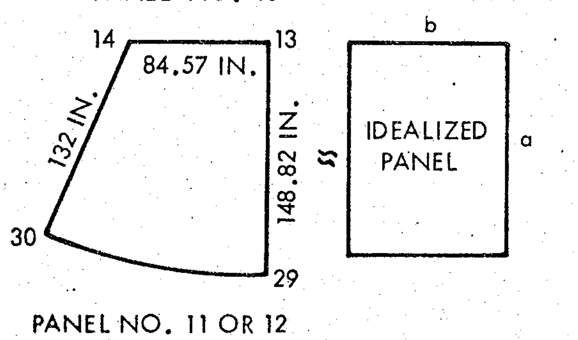

AREA 13-14-30-29 = 15,121.92 $IN.^2$
LET IDEALIZED PANEL AREA = 15,121.92
LET a = (132 + 148.82)/2 = 140.41 IN.
AREA = a x b
15,121.92 = 140.41 x b
∴ b = 107.7 IN. a/b = 1.303, β = 0.4192

Figure 3-18. Idealized Panel Geometry

Table 3-40. Outboard Rectangular Panels - Design Calculations

PANEL	t	t_c	t_F	β PANEL COEFF.	w ULT. DESIGN PRES.	b PANEL DIM'NS	t_e	σ_e $= \frac{\beta w b^2}{t_e^2}$	M $= \sigma_e \frac{t_c^2}{6}$	σ $= \frac{M c E}{D \lambda_F}$	K_L $= \frac{1.259 \sigma \lambda_F}{E}$	t_F/s REF. NASA SHELL MANUAL	s $s = \frac{t_F}{t_F/s}$	M.S.
11	2.73	2.70	.015	0.4192	3.20	107.7	4.7014	703.965	2893.407	63630	.00264	.030	.500	0
16	2.73	2.70	.015	0.4192	3.20	107.7	4.7014	703.965	2893.407	63630	.00264	↑	↑	↑
15	2.46	2.43	.015	0.4192	2.89	107.7	[illegible]	782.777	2342.069	63890	.00265			
12	2.46	2.43	.015	0.4192	2.89	107.7	4.257	782.777	2342.069	63890	.00265			
20	2.19	2.16	.015	0.4192	2.57	107.7	3.765	881.574	2083.159	63990	.00266			
7	2.19	2.16	.015	0.4192	2.57	107.7	3.765	881.574	2083.159	63990	.00266			
19	[illegible]	1.89	.015	0.4192	2.25	107.7	3.303	1002.791	1823.074	63790	.00265			
8	1.92	1.89	.015	0.4192	2.25	107.7	3.303	1002.791	1823.074	63790	.00265			
24	1.72	1.67	.015	0.4192	2.02	107.7	2.9502	1128.457	1637.391	64200	.00267			
3	1.72	1.69	.015	0.4192	2.02	107.7	2.9502	1128.457	1637.391	64200	.00267			
23	1.63	1.60	.015	[illegible]	1.91	107.7	2.8005	1184.143	1547.675	63870	.00265			
4	1.63	1.60	.015	[illegible]	1.91	107.7	2.8005	1184.143	1547.675	63870	.00265			
28	1.58	1.55	.015	[illegible]	1.86	107.7	2.7117	1229.988	1507.965	64330	.00267			
31	1.58	1.55	.015	[illegible]	1.86	107.7	2.7117	1229.988	1507.965	64330	.00267			
27	1.58	1.55	.015	0.4192	1.84	107.7	2.7117	1216.763	1491.751	63640	.00264	↓	↓	↓
32	1.58	1.55	.015	0.4192	1.84	107.7	2.7117	1216.763	1491.751	63640	.00264	.030	.500	0

Table 3-41. Inboard Rectangular Panels - Design Calculations

Data / Panel Design: Panel	t	t_c	t_F	β Panel Coeff.	w Ult. Design Pres.	b Panel Dim'ns	t_e	σ_e $\frac{\beta w b^2}{t_e^2}$	M $\sigma_e \frac{t_e^2}{6}$	σ $\frac{McE}{D \lambda_F}$	K_L $\frac{1.259 \sigma \lambda_F}{E}$	t_F/s Ref. NASA Shell Manual	s $s = \frac{t_F}{t_F/s}$	Margin of Safety
(10)	2.85	2.82	.015	0.3136	3.420	121.03	4.909	651.941	2618.195	61500	.00255	.0294	.5102	+.020
(14)	2.85	2.82	.015	0.3136	3.420	121.03	4.909	651.941	2618.195	61500	.00255	.0294	.5102	+.020
(6)	2.49	2.46	.015	0.3136	2.955	121.03	4.285	739.306	2262.276	60860	.00253	.0293	.5119	+.024
(18)	2.49	2.46	.015	0.3136	2.955	121.03	4.285	739.306	2262.276	60860	.00253	.0293	.5119	+.024
(2)	2.12	2.09	.015	0.3136	2.490	121.03	3.647	859.959	1906.529	60270	.00250	.0290	.5172	+.034
(22)	2.12	2.09	.015	0.3136	2.490	121.03	3.647	859.959	1906.529	60270	.00250	.0290	.5172	+.034
(26)	1.98	1.95	.015	0.3136	2.340	121.03	3.404	927.698	1791.385	60680	.00252	.0292	.5137	+.027
(30)	1.98	1.95	.015	0.3136	2.340	121.03	3.404	927.698	1791.385	60680	.00252	.0292	.5137	+.027

Table 3-42. Circular Sector Panels - Design Calculations

PANEL DESIGN \ DATA				β	w	a	t_e	σ_e	M	σ	K_L	t_F/s	s	MARGIN OF SAFETY
				PANEL COEFF.	ULT DESIGN PRES.	PANEL DIM'NS		$\frac{\beta w a^2}{t_e^2}$	$\sigma_e \frac{t_e^2}{6}$	$\frac{MCE}{D \lambda_F}$	$\frac{1.259 \sigma \lambda_F}{E}$	REF. NASA SHELL MANUAL	$s = \frac{t_F}{t_F/s}$	
PANEL	t	t_c	t_F											
⑬	1.77	1.75	.010	0.114	3.43	94	3.051	371.153	576.029	32620	.00135	.0199	.5025	+.005
⑨	1.77	1.75	.010	0.114	3.43	94	3.051	371.153	576.029	32620	.00135	.0199	.5025	+.005
⑰	1.69	1.67	.010	0.114	3.27	94	2.9165	387.243	549.111	32510	.00135	.0199	.5025	+.005
⑤	1.69	1.67	.010	0.114	3.27	94	2.9165	387.243	549.111	32510	.00135	.0199	.5025	+.005
㉑	1.55	1.53	.010	0.114	3.015	94	2.6634	428.112	506.028	32900	.00137	.0200	.5000	0
①	1.55	1.53	.010	0.114	3.015	94	2.6634	428.112	506.028	32900	.00137	.0200	.5000	0
㉕	1.47	1.45	.010	0.114	2.85	94	2.5316	447.935	478.395	32670	.00136	.0200	.5000	0
㉙	1.47	1.45	.010	0.114	2.85	94	2.5316	447.935	478.395	32670	.00136	.0200	.5000	0

Table 3-43. Panel Design Configurations

Panel \ Design	Selected Design Configuration					
	Panel Thickness	Core Thickness	Face Thickness	Foil Gage	Cell Size	Weight lb.
(16) – (14-15-31-30) (11) – (13-14-30-29)	2.73"	2.70"	0.015"	0.0020	0.500	217
(15) – (15-16-32-31) (12) – (12-13-29-28)	2.46"	2.43"	0.015"	0.0020	0.500	208
(20) – (16-17-33-32) (7) – (11-12-28-27)	2.19"	2.16"	0.015"	0.0020	0.500	199
(19) – (17-18-34-33) (8) – (10-11-27-26)	1.92"	1.89"	0.015"	0.0020	0.500	190
(24) – (18-19-35-34) (3) – (10-25-41-26)	1.72"	1.69"	0.015"	0.0020	0.500	183
(23) – (19-20-36-35) (4) – (24-25-41-40)	1.63"	1.60"	0.015"	0.0020	0.500	180
(28) – (20-21-37-36) (31) – (23-24-40-39)	1.58"	1.55"	0.015"	0.0020	0.500	179
(27) – (21-22-38-37) (32) – (22-23-39-38)	1.58"	1.54"	0.015"	0.0020	0.500	178

Table 3-44. Panel Design Configurations

Panel \ Design	Selected Design Configuration: Panel Thickness	Core Thickness	Face Thickness	Foil Gage	Cell Size	Weight lb.
(10) - (4-3-12-13-14)	2.85"	2.82"	0.015"	0.0020	0.500	226
(14) - (5-4-14-15-16)	2.85"	2.82"	0.015"	0.0020	0.500	226
(6) - (3-2-10-11-12)	2.49"	2.46"	0.015"	0.0020	0.500	214
(18) - (6-5-16-17-18)	2.49"	2.46"	0.015"	0.0020	0.500	214
(2) - (2-9-24-25-10)	2.12"	2.09"	0.015"	0.0020	0.500	201
(22) - (7-6-18-19-20)	2.12"	2.09"	0.015"	0.0020	0.500	201
(26) - (8-7-20-21-22)	1.98"	1.95"	0.015"	0.0020	0.500	196
(30) - (9-8-22-23-24)	1.98"	1.95"	0.015"	0.0020	0.500	196

Table 3-45. Panel Design Configurations

Panel \ Design	Selected Design Configuration					
	Panel Thickness	Core Thickness	Face Thickness	Foil Gage	Cell Size	Weight lb.
⑬ - (1-4-5)	1.77"	1.75"	0.010	0.0020	0.500	34
⑨ - (1-3-4)	1.77"	1.75"	0.010	0.0020	0.500	34
⑰ - (1-5-6)	1.69"	1.67"	0.010	0.0020	0.500	33.4
⑤ - (1-2-3)	1.69"	1.67"	0.010	0.0020	0.500	33.4
㉑ - (1-6-7)	1.55"	1.53"	0.010	0.0020	0.500	32.3
① - (1-2-9)	1.55"	1.53"	0.010	0.0020	0.500	32.3
㉕ - (1-7-8)	1.47"	1.45"	0.010	0.0020	0.500	31.6
㉙ - (1-8-9)	1.47"	1.45"	0.010	0.0020	0.500	31.6

the magnitude would be lower in value which would reduce the required area and/or section modulus ($S_{REQ'D} = M/F$). The ratios applied to the particular beam segments are defined as:

$$A_{REQ'D} = (\text{Task 3 Area}) \frac{(\text{Task 4 Load Factor})(\text{Task 4 } q_{MAX})}{(\text{Task 3 Load Factor})(\text{Task 3 } q_{MAX})}$$

$$\times \left[\frac{\text{Task 4 Length}}{\text{Task 3 Length}}\right] \left[\frac{\text{Task 3 Fcy}}{\text{Task 4 Fcy}}\right]$$

Short radial beam:

$$A_{REQ'D} = (\text{Task 3 Area})(0.795)$$

Cross beams:

$$A_{REQ'D} = \text{Task 3 Area } (0.765)$$

Major radial beams:

Inside segments -

$$A_{REQ'D} = \text{Task 3 Area } (0.74)$$

Where:

Task 3 Areas:	reference tables 44, 45, 46 of volume 3, appendix E
Task 4 Load Factors:	reference table 3.2-1, section 3.2.2 of volume 4
Task 3 Load Factor:	reference section 9.8, volume 3, appendix E
Task 4 q_{MAX}:	see reference 8
Task 3 q_{MAX}:	reference table 30A in section 9.8, volume 3, appendix E
Task 4 Length:	reference figure 3-16 in subsection 3.10
Task 3 Length:	reference figure 31 in subsection 9.8, volume 3, appendix E
Task 3 Fcy:	reference subsection 9.8, volume 3, appendix E
Task 4 Fcy:	reference section 3-10

Utilizing these ratios, the new beams were defined. It should be noted that sample analyses were made on individual beam segments to ensure the accuracy of the ratios. A design summary of the beam configuration is presented in table 3-46.

Table 3-46. Beam Design Summary

Beam Segment \ Design Data	Area in²	Length in	Weight lb.
Short Radial			(566)
13-29	2.27	148	93
15-31	2.27	148	93
11-27	1.79	148	74
17-33	1.79	148	74
25-41	1.46	148	60
19-35	1.46	148	60
23-29	1.37	148	56
21-37	1.37	148	56
Cross Beam			(878)
12-14	2.98	169.14	140
14-16	2.98	169.14	140
10-12	2.45	169.14	115
16-18	2.45	169.14	115
10-24	2.03	169.14	95
18-20	2.03	169.14	95
22-24	1.904	169.14	89
20-22	1.904	169.14	89
Major Radial			(3957)
4-1-8	2.67	188	139
3-1-7	2.67	188	139
2-1-6	2.67	188	139
9-1-5	2.67	188	139
30-14-4	7.41	261.475	537
28-12-3	6.50	261.475	471
32-16-5	6.50	261.475	471
26-10-2	5.96	261.475	432
34-18-6	5.96	261.475	432
40-24-9	5.15	261.475	373
36-20-7	5.15	261.475	373
38-22-8	4.33	261.475	314

3.11 THERMAL PROTECTION SYSTEM SELECTION FOR UPPER AND LOWER FRUSTUMS

The rigid body analysis discussed in sections 3.0 to 3.9 assumed a room temperature environment. However, thermal protection analyses of the upper and lower frustums, see section 3.3 volume 3, and section 2.3 volume 4, identified the need for external thermal protection to ensure that the thermal gradients across the primary structure do not become unacceptable. Because the ratio between weight of thermal protection and increase in primary structure weight due to strength degradation caused by thermal gradient has an important bearing on total system weight, a selection trade was performed to:

1) determine the optimum proportions of the frustum thermal protection in terms of insulation weight vs. increased load bearing structural weight

2) to establish the resulting TPS sizes for the point design of the frustums

3) to estimate the resulting total protection weight as an input for the SERV task 4 baseline weight report

The TPS trade studies for the upper and lower structural frustums, see section 3.3 volume 3, conclude with one recommended insulation system (double honeycomb, reference 11) and one variation (double honeycomb-perforated, reference 11) which, to be complete, must be integrated with the load bearing frustum sandwich structure from a thermal stress and optimum weight point of view. The load bearing structural sandwich weight and sizes were, and still are, reported on the basis of a room temperature environment. Such additional structural weight and/or thermal insulation required to enable the load bearing structure to sustain the flight thermal environemtn are the subject of the TPS selection reported below.

Figures 3-19 and 3-20 show the weight increase for sustaining a range of thermal gradients in the load bearing sandwich frustums, in terms of percent of the frustum structural weights given on figure 3-21(a) for a room temperature environment. The facing thicknesses required to sustain the combined thermal, inertial, and pressure stresses (including thermal stress and reduction of E and F_t) were calculated and the percentage increase in unit structural sandwich weight per square foot, was determined and plotted. The thermal stress calculations were in accordance with reference 13.

Figures 3-22 through 3-26 combine the structural weight increases shown in figures 3-19 and 3-20 with the range of insulation thickness recommended in section 3.3 volume 3, using the approximate weight relationship of figure 3-21(b). They show a resulting total percent of weight increase attributable to frustum thermal protection. This increase is shown parametrically in terms of a percentage of the frustum structural weights for room temperature environment cited in figure 3-21(a), and for a range of thermal gradients in the load bearing sandwich. On figures 3-22 through 3-26, the curves labeled "insulation only" are re-plots of the structural gradient vs. insulation thickness data in terms of percentage of room temperature load bearing sandwich weight, also using the approximate weight relationships of figures 3-21(a) and (b).

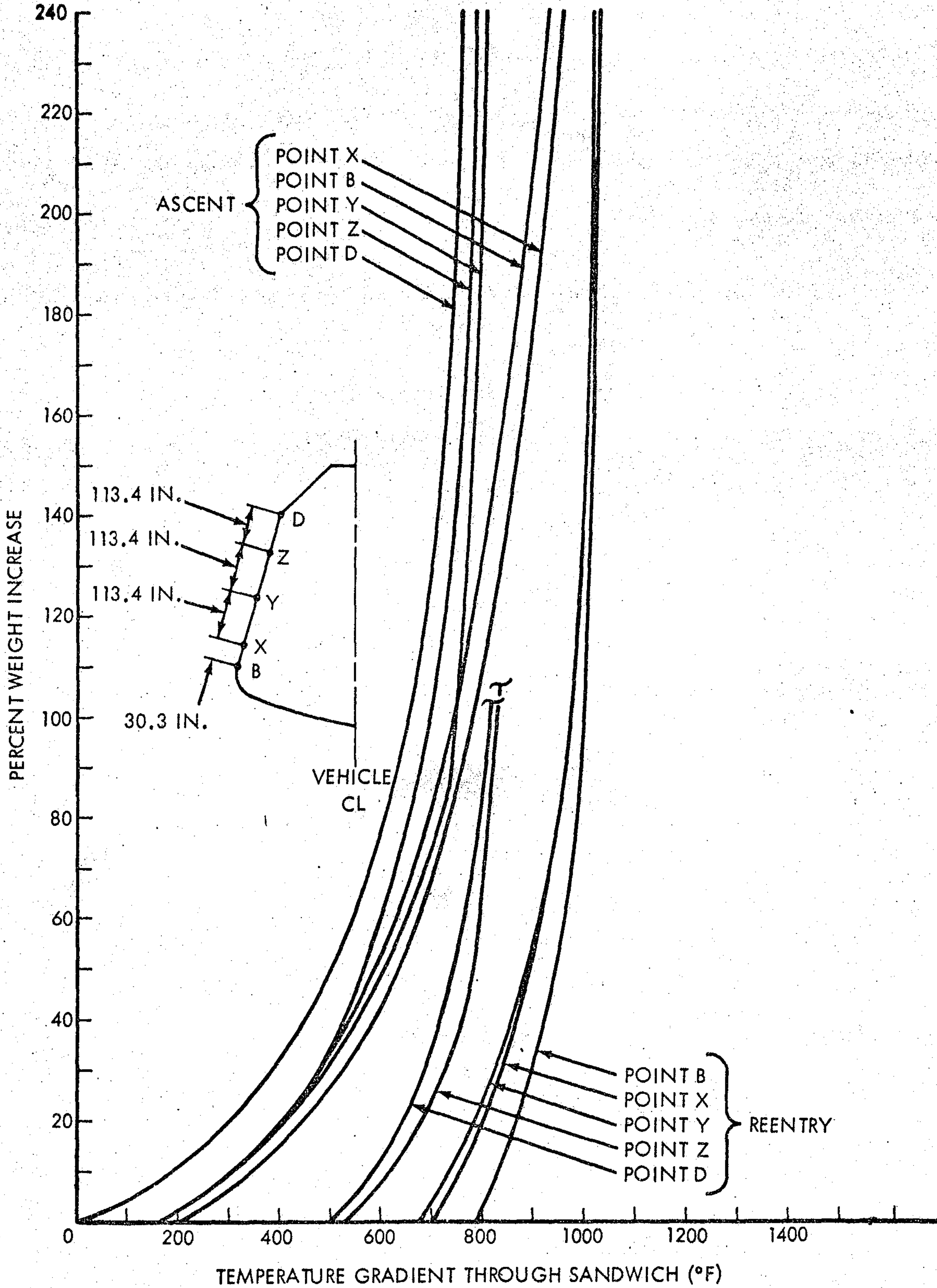

Figure 3-19. Weight Penalty Versus ΔT at Various Points on Lower Frustum (Inner Skin Temperature = 200°F)

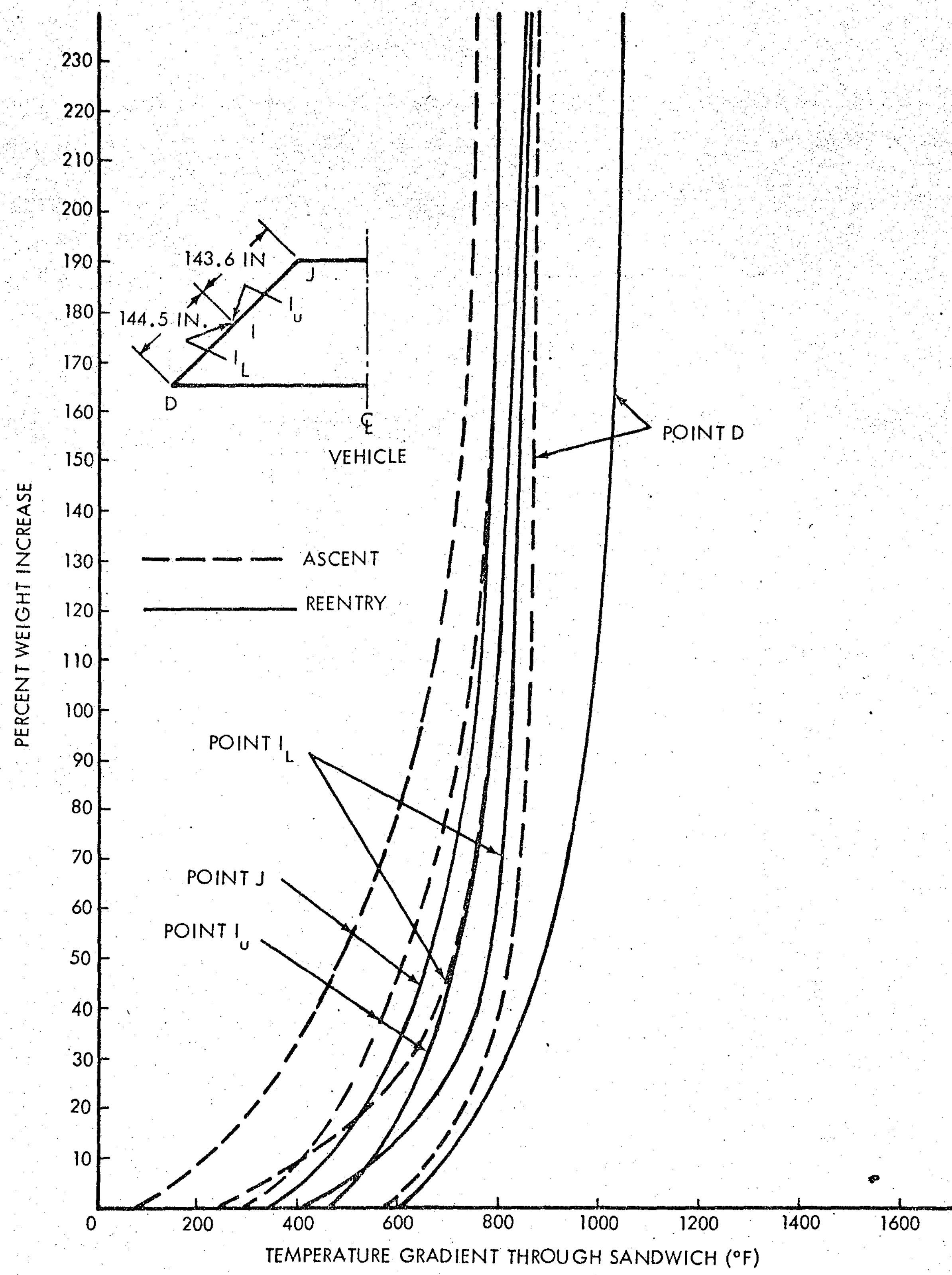

Figure 3-20. Weight Penalty Versus ΔT at Various Points on Upper Frustum (Inner Skin Temperature = $200^{o}F$)

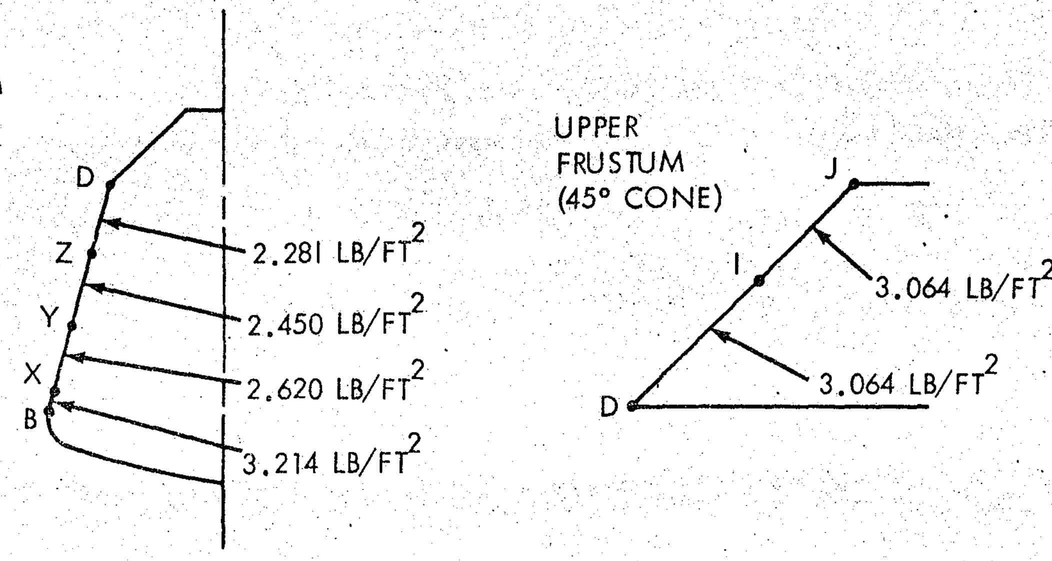

(a) UNIT WEIGHT (LB/FT^2) FOR BASIC LOAD BEARING SANDWICH STRUCTURE (CORE + FACES) AT ROOM TEMPERATURE

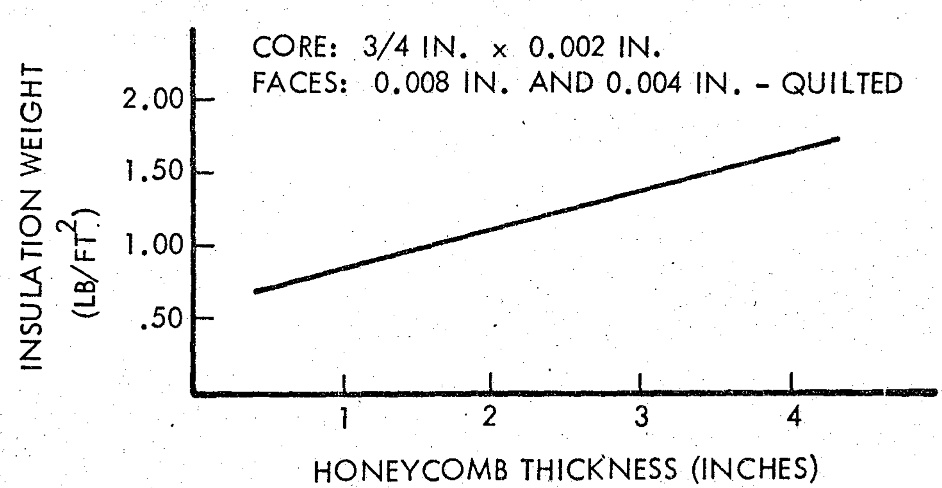

(b) HONEYCOMB INSULATION WEIGHT VERSUS THICKNESS

Figure 3-21. Frustum and Insulation Weight Relationships

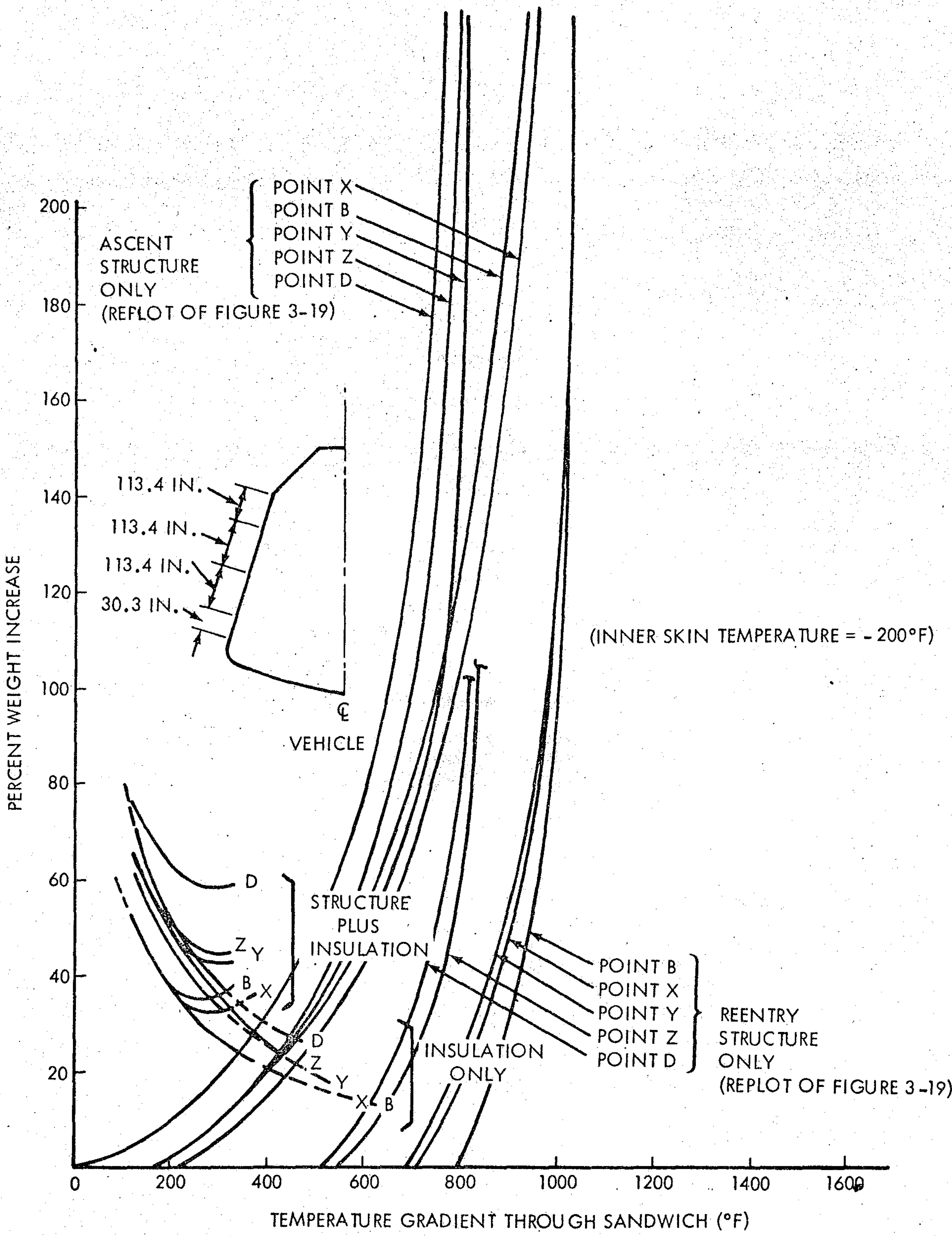

Figure 3-22. Weight Penalty Versus ΔT - Ascent - Perforated Double Honeycomb, Lower Frustum

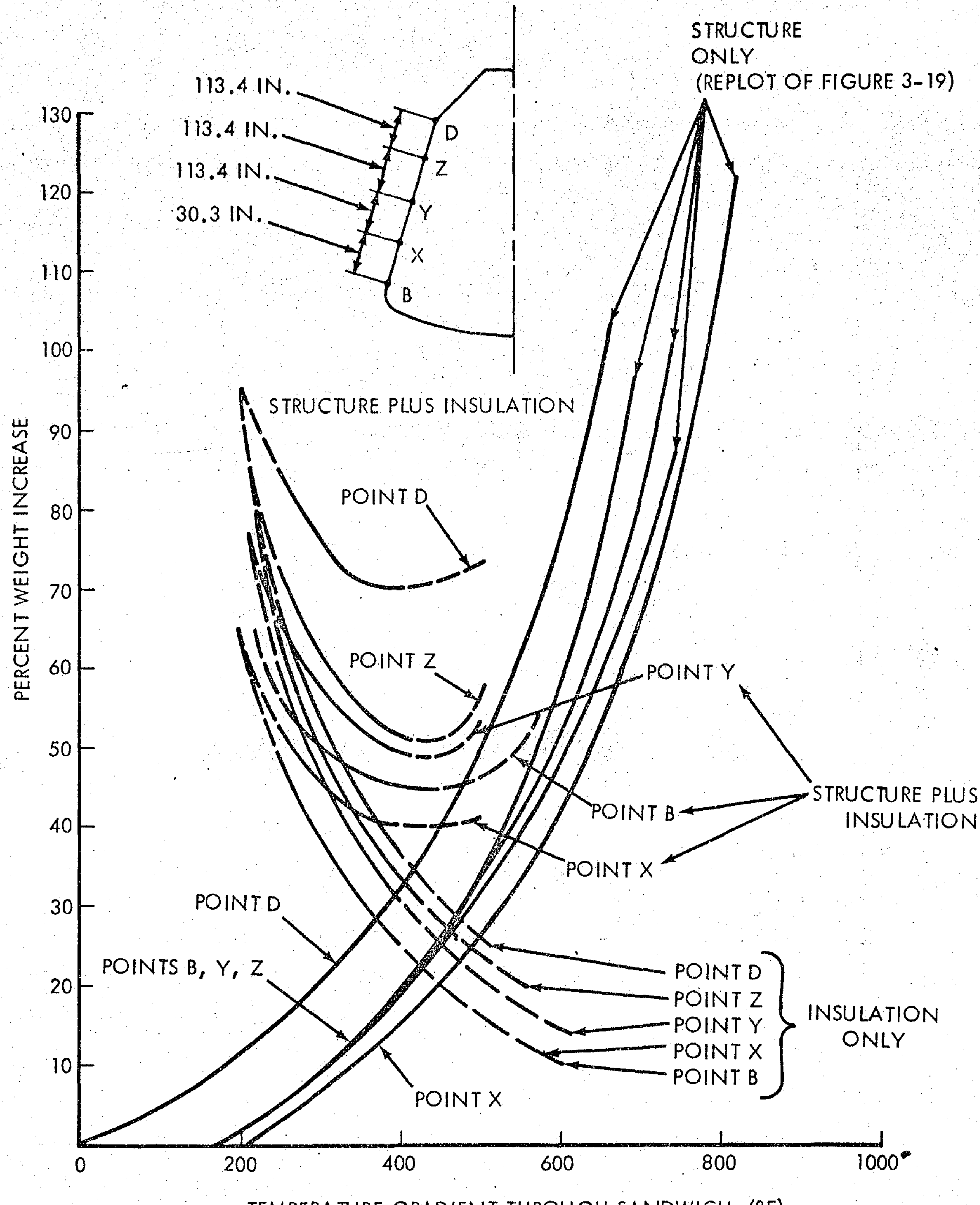

Figure 3-23. Weight Penalty Versus ΔT - Ascent - Nonperforated Double Honeycomb, Lower Frustum

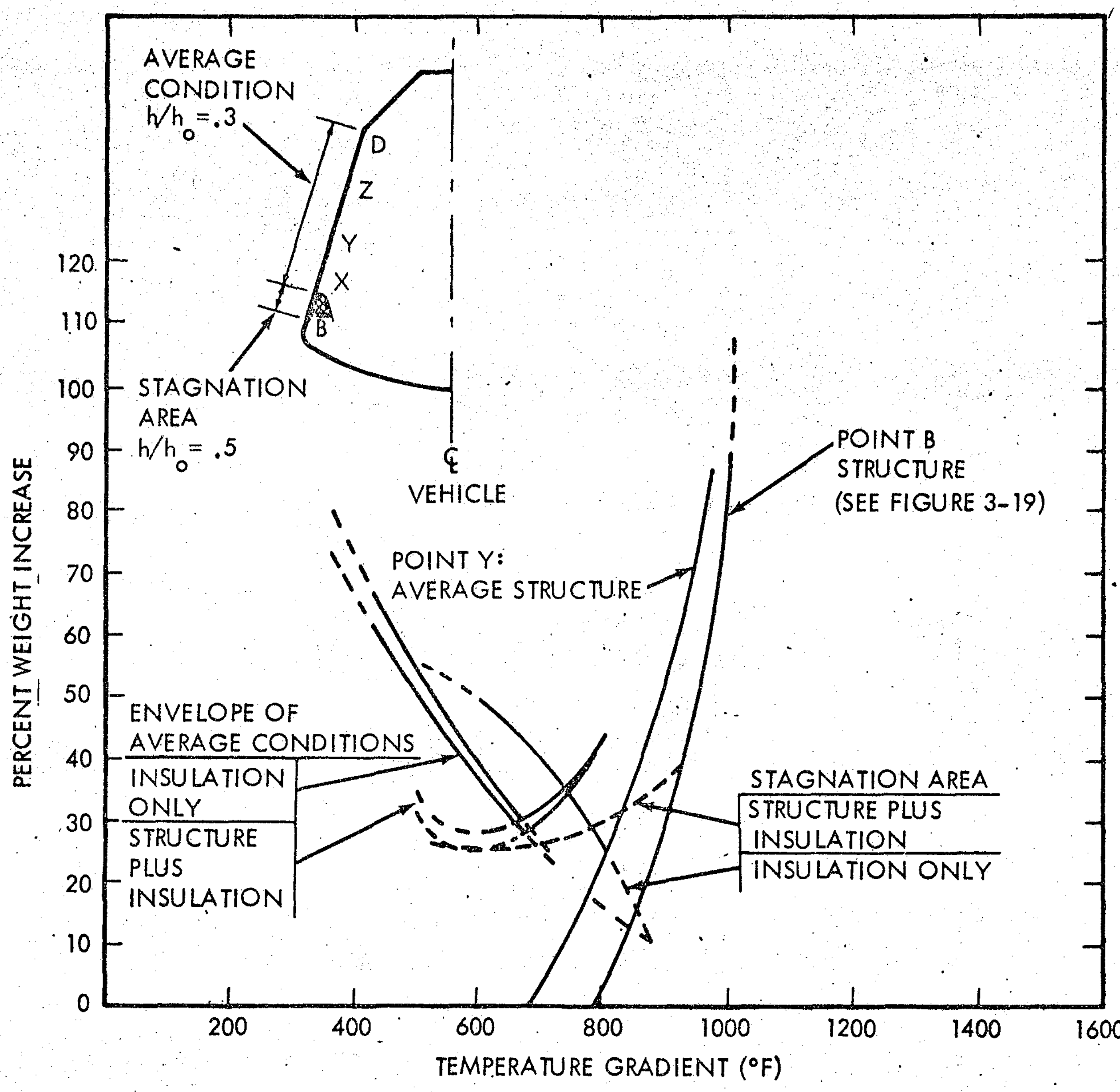

Figure 3-24. Weight Penalty Versus ΔT - Reentry - Lower Frustum

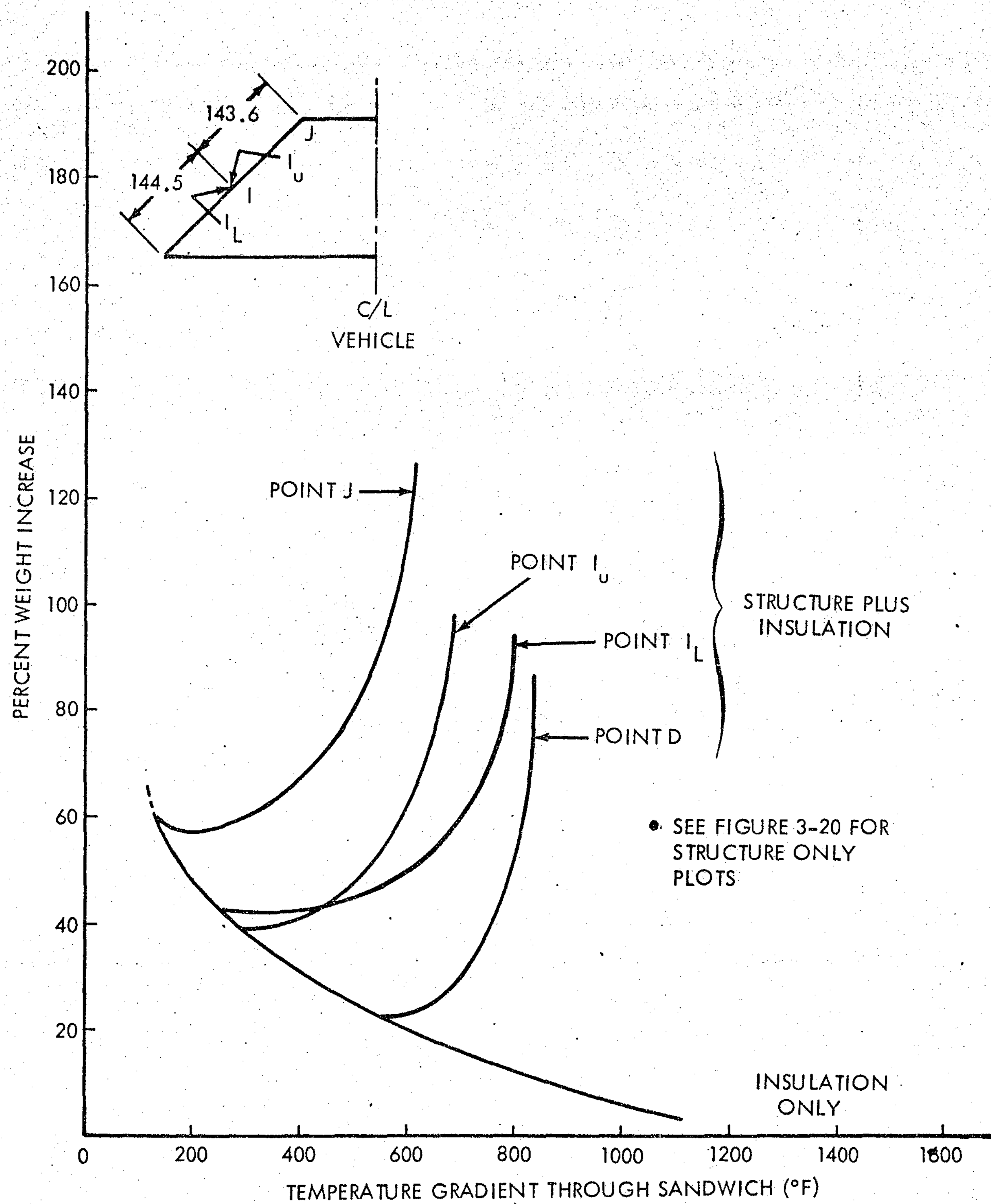

Figure 3-25. Weight Penalty Versus ΔT - Ascent - Perforated Double Honeycomb, Upper Frustum

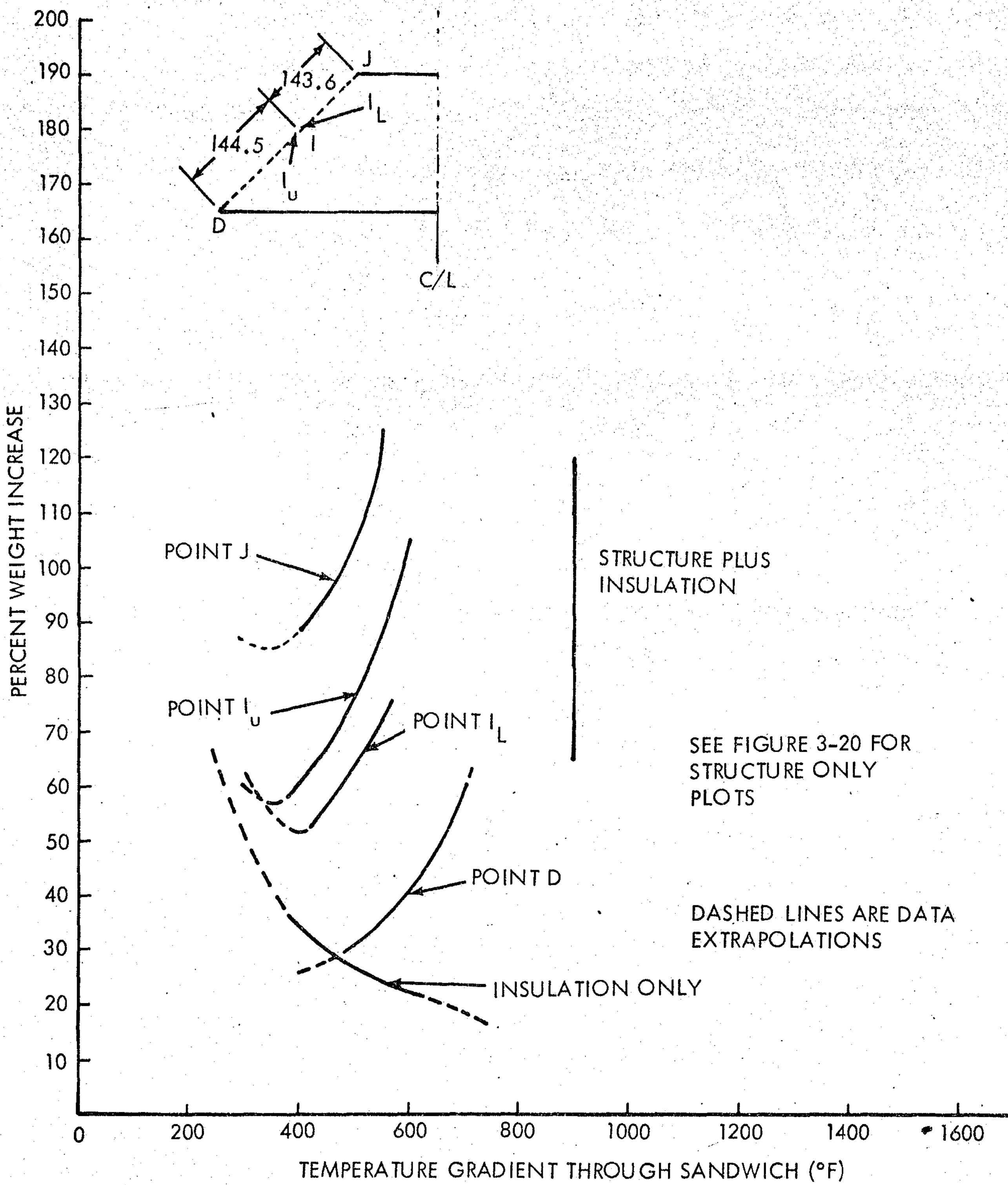

Figure 3-26. Weight Penalty Versus ΔT - Ascent - Nonperforated Double Honeycomb, Upper Frustum

The fish-hook shaped curves of figures 3-22 through 3-26 labeled "structure plus insulation", are the sum of the "insulation only" and "structures only" values. The low point of these fish-hook curves determines: 1) the minimum percent weight increase required for thermal protection; and 2) the accompanying "optimum" thermal gradient in the load bearing frustum sandwich.

No combined curves were shown for the reentry condition of the upper frustum because the upper frustum TPS selected for ascent will be more than adequate for reentry. A review of the fish-hook low points on figures 3-22, 3-23, and 3-24 shows that the lower frustum also will be adequately protected in reentry by the TPS selected for ascent. Thus, it is concluded that the ascent flight conditions are critical for the frustum TPS.

Comparing the fish-hook low points of figure 3-22 to those of figure 3-23 reveals that from 8 percent to 11 percent of the lower frustum room temperature load bearing structural weight might be saved by using the perforated double honeycomb discussed in section 3.3, volume 3. Comparing figure 3-25 to 3-26 shows a similar saving potential of from 7 percent to 8 percent for the upper frustum. However, as discussed in section 4.3, volume 3, the perforated double honeycomb was discarded for practical reasons and the nonperforated double honeycomb insulation was selected as the frustum thermal protection system.

The optimum thermal gradients in the load bearing frustum sandwich defined by the low points of the fish-hook curves of figures 3-23 and 3-26 are listed in table 3-47 as ΔT. The required thickness of exterior honeycomb insulation to ensure the tabulated ΔTs is also given. These are the insulation thicknesses used in the final baseline definition of SERV.

The percent weight increase due to the insulation thickness listed in table 3-47 is read from the "insulation only" curves of figures 3-23 and 3-26 for the tabulated ΔTs and also entered in table 3-47 The percent weight increase of load bearing structure to sustain the tabulated ΔTs is read from the ascent curves of figures 3-19 and 3-20 and entered in table 3-47. The sum of these two percent weight increases is listed in table 3-47 as total percent weight increase for TPS and checks as identical with the low point of each of the fish-hook curves of figures 3-23 and 3-26.

Using the average percentage of the point-to-point weight increase listed in table 3-47, the unit weight of the room temperature load bearing structure per figure 3-21, and the SERV Task 4 baseline frustum surface dimensions, the required weight of insulation and additional load bearing structure is calculated and totaled in table 3-48. The values are entered in the SERV final baseline weight report as Frustum Thermal Protection, and used as input to the vehicle sizing analysis.

4.0 CONCENTRATED LOAD ANALYSIS

In the analysis of the inner and outer cylinders described in section 3.0 all loads and their induced stresses were assumed uniformly distributed around the circumference of the vehicle. This assumption was dictated by the characteristics of the computer program, reference 1, used to calculate the internal load distributions within the primary structural components. There are known concentrated loads applied to these shell structures from the landing gear, lift engines, and major radial beams in the heat shield bulkhead which are of

Table 3-47. Thermal Protection System - Selection Criteria

STRUCTURAL LOCATION	ΔT (DEGREES)	REQUIRED THICKNESS (INCHES)	WEIGHT INCREASE (%)		
			INSULATION	STRUCTURE	TOTAL
UPPER FRUSTUM - D	570	1.6	29	0	29
UPPER FRUSTUM - I_L	500	2.1	35	16	51
UPPER FRUSTUM - I_U	460	2.5	40	17	57
UPPER FRUSTUM - J	450	2.6	42	43	85
LOWER FRUSTUM - D	400	1.0	37	33	70
LOWER FRUSTUM - Z	430	.8	33	19	52
LOWER FRUSTUM - Y	430	.8	28	20	48
LOWER FRUSTUM - X	430	.8	22	18	40
LOWER FRUSTUM - B	440	.8	27	18	45

Table 3-48. SERV Thermal Gradient Weight Penalties

UPPER FRUSTUM	UNIT WT. LB/FT^2	STRUCTURE %	STRUCTURE UNIT WT.	INSULATION %	INSULATION UNIT WT.	DIMENSION LENGTH	DIMENSION S.A. (FT^2)	WT. PENALTY STRUCTURE	WT. PENALTY INSULATION
SECTION J-I	3.064	.30	.919	.41	1.256	145.7	924.396	850	1,160
SECTION I-D	3.064	.08	.245	.32	.980 1.018*	216.4	2,581.368	632	2,530 2,630*
TOTALS:								1,482	3,690 3,790*
LOWER FRUSTUM									
SECTION D-Z	2.281	.33	.753	.37	.844	115.8	1,968.715	1,482	1,660
SECTION ZY	2.450	.19	.462	.33	.802	115.8	2,202.833	1,018	1,767
SECTION YX	2.620	.20	.524	.28	.734	115.8	2,436.632	1,277	1,788
SECTION XB	3.214	.18	.579	.245	.787	36.3	694.389	402	546
* (1.8 INCH THICKNESS AVERAGE)									
TOTALS:								4,179	5,761
SUBTOTAL: BOTH FRUSTUMS								5,661	9,551
TOTAL PENALTY (THERMAL GRADIENT)									15,212

of appreciable magnitude. In assuming these concentrated loads to be applied as distributed loads, one obtains unconservative weights for that portion of the structure between the point of application of the load, and that point at which the shear lag effect results in a truly uniformly distributed load. The following paragraphs are, therefore, included to describe the work performed to more exactly define the weight impact resulting from the concentrated loads introduced by the landing gear, lift engines, and heat shield support beams.

4.1 CONCENTRATED LOADS ON OUTER CYLINDRICAL BULKHEAD FROM LANDING GEAR

The geometry of the outer cylindrical bulkhead to which the landing gear loads are transferred is shown in figure 4-1. This figure also serves as a nomenclature reference for the development of the shear lag geometry. The shear geometry is shown in figure 4-2. The shaded area (area inside lag lines) is the effective area in reacting the concentrated axial loads. The panel designs for the uniformly distributed loading are superimposed on the shear lag geometry in figure 4-3. These panels are redesigned to accommodate the concentrated loading.

The concentrated moment applied at the housing interface was assumed to be reacted by the heat shield beams through two rings at the lower end, see figure 4-4 and a further ring at the LH_2 tank interface on the upper end. The moment is distributed to the ring and heat shield beam by the housing and a longeron, see figure 4-4. The shear and axial loads applied at the housing interface were assumed to be reacted by the effective area inside the lag lines. The axial load was transferred to the skin at such a rate that it would not exceed the general instability allowable of the configuration. The honeycomb configuration in the effective area of the outer cylindrical bulkhead was considered to be 4-in. by 0.0225-in. face sheets with a core of 1/2-in. cell by 0.0020-in. foil gage. This configuration has a general instability allowable of 79,000 plus psi, reference figure 4-5 for analysis. Utilizing the shear lag geometry, figure 4-2, the allowable loads in the skin are:

P_{H_1} allowable = 0

P_Q allowable = 80 x 0.045 x 79,000 = 284,000 lb

P_G allowable = 170 x 0.045 x 79,000 = 604,000 lb

Therefore, the net axial load in the housing and longeron is:

P_{H_1} = 588,000 lb

P_Q = 588,000 - 284,000 = 304,000 lb

P_G = 0

Therefore, the axial load is sheared into the skin at the rates:

between H_1 and Q q = 284,000/57 x 4 = 1248 lb/in

between Q and G q = 304,000/44.96 x 4 = 1693 lb/in

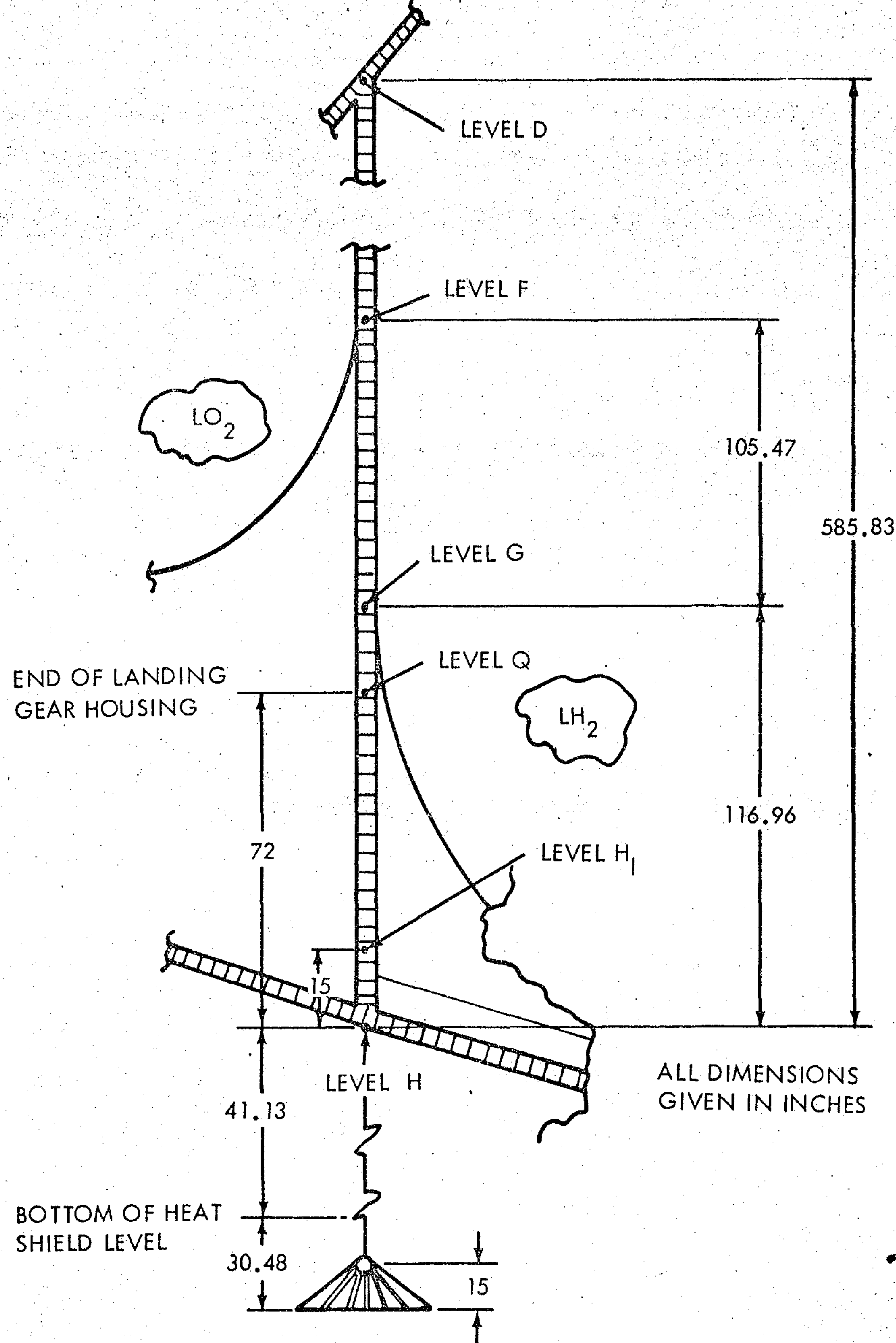

Figure 4-1. Geometry - Outer Cylindrical Bulkhead

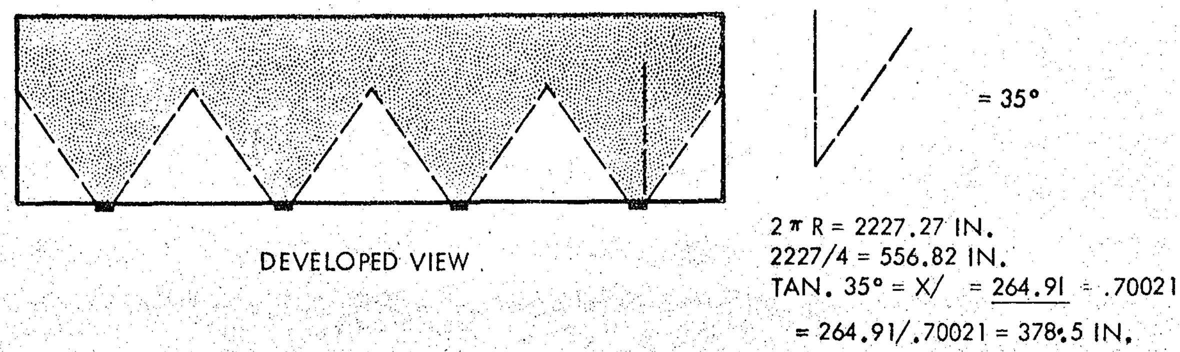

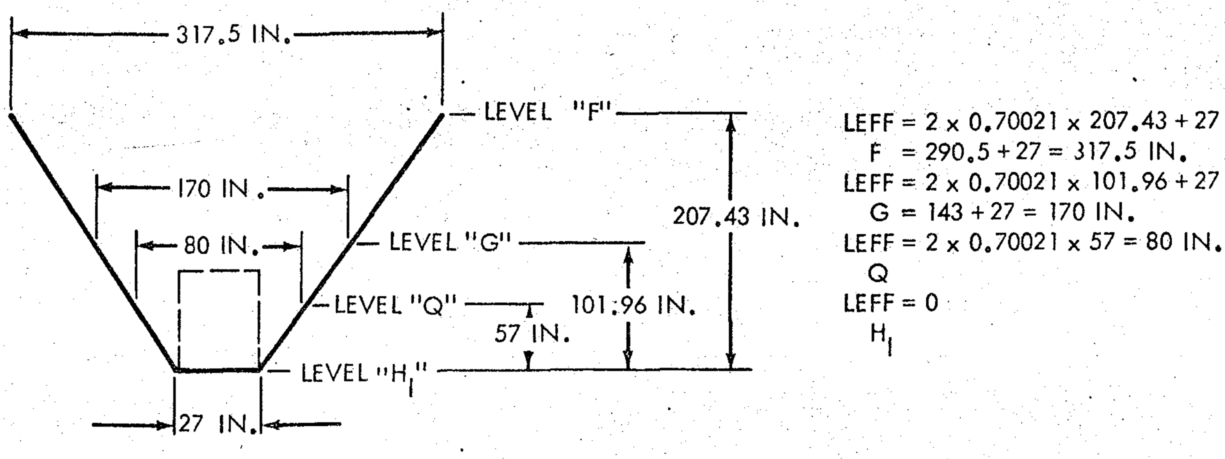

Figure 4-2. Shear Lag Geometry

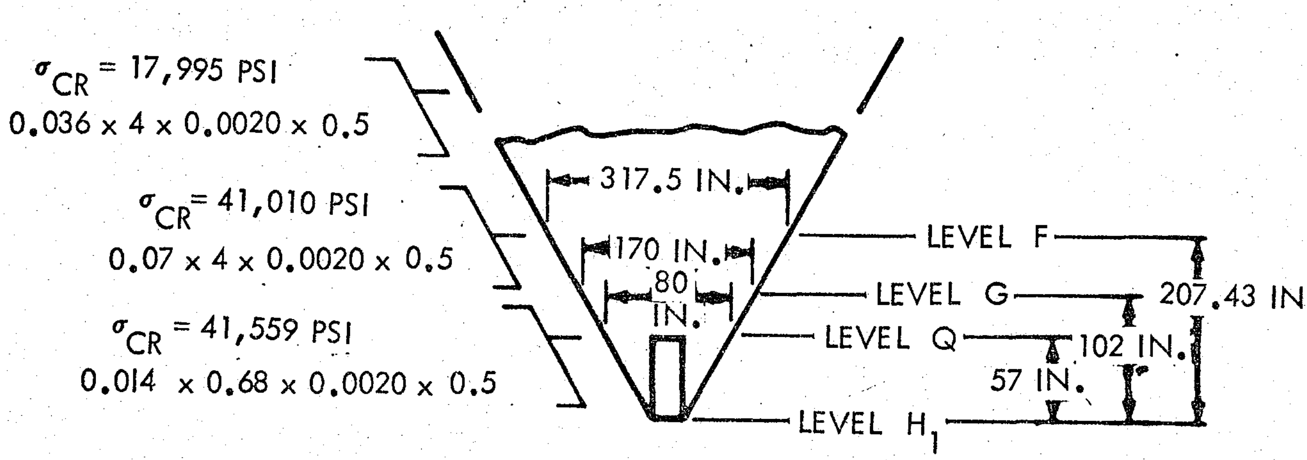

Figure 4-3. Panel Designs for Uniform Load

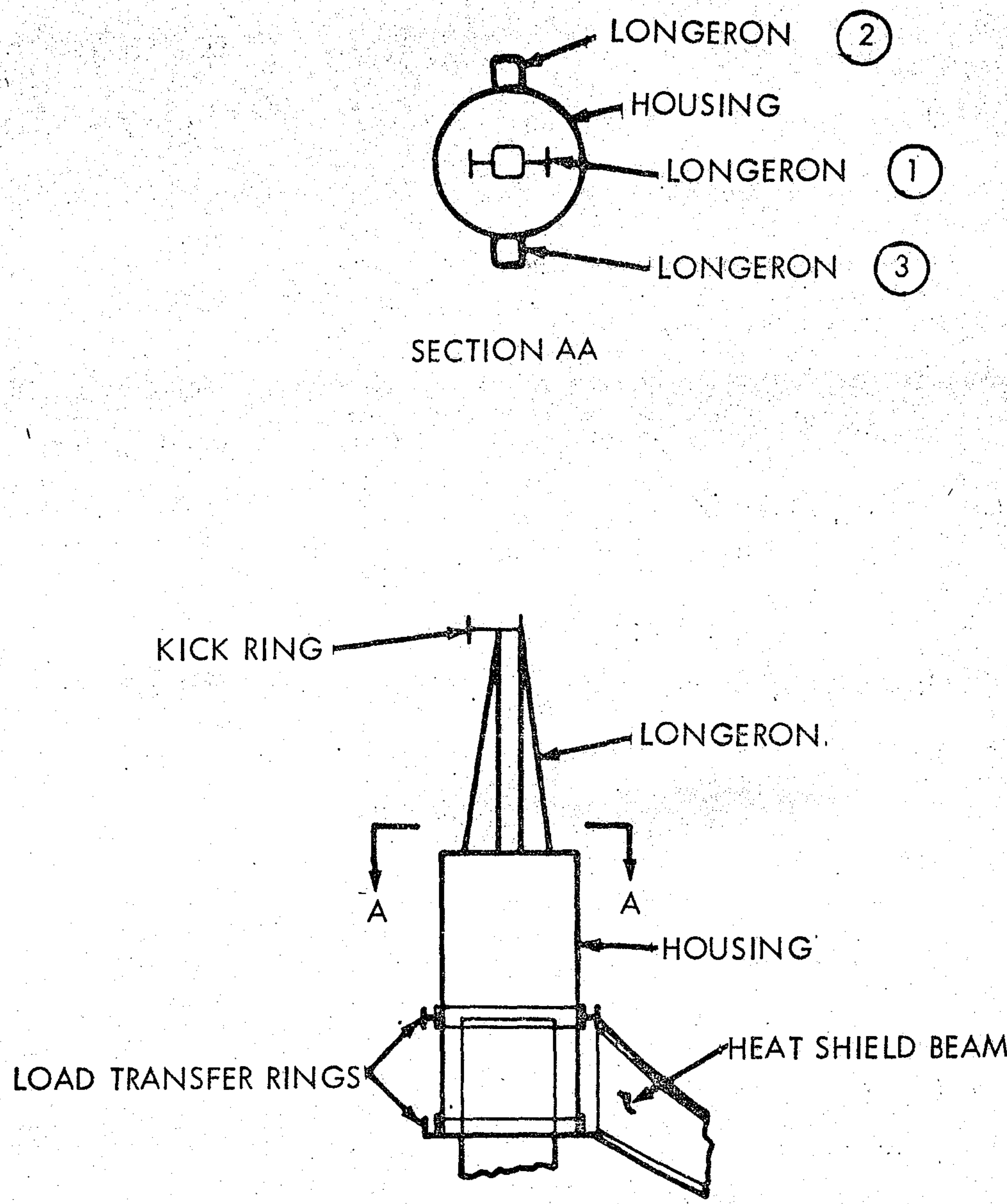

Figure 4-4. Detail - Longeron and Rings

These rates of load introduction yield shear stresses of:

between H_1 and Q σ_s = 1248/0.0225 = 55,400 psi

between Q and G σ_s = 1692/0.0225 = 75,300 psi

The analysis of the reinforcement panel configuration is presented in figure 4-5. Utilizing the results of the lag analysis, shear, moment and axial load diagrams were generated for the housing and longeron, and are presented in figure 4-6. Longeron (1) (reference figure 4-4) consists of a square tube insert with a structural tee which tapers from an effective area of 5.75 in.^{2} at level "Q", to an effective area of 0 at level "G". The taper was calculated in accordance with the shape of the axial and moment load diagrams shown in figure 4-6. Because the moment load could be in either plane, a longeron was added to the system in the other plane as shown in figure 4-4. This longeron would distribute the moment load if applied in the other plane (rotate moment 90°). The longeron analysis is shown in figure 4-7.

The ring at the hydrogen tank bulkhead interface was idealized and analyzed per the loading shown in figure 4-8. The combined loading is a superimposition of case 1 and case7 loads in the ring archives. The ring loads at various locations are shown in table 4-1. Using this loading, the analysis was generated and is presented in figure 4-9.

A summary of the reinforcement configuration design is presented in figure 4-10. The concentrated load penalty weight for the honeycomb was calculated using the method presented in figure 4-11.

The total penalty weight for introducing the concentrated loads is presented in table 4-2.

4.2 CONCENTRATED LOADS ON OUTER CYLINDRICAL BULKHEAD FROM LIFT ENGINES

In the SERV configuration studied, there are 36 lift engines installed in 4 clusters of 9 engines each. The typical arrangement within one cluster is illustrated in figure 4-12. The analysis of the lift engine installation assumed that the thrust and inertia loads were reacted in their entirety by the outer cylindrical bulkhead. This portion of the analysis deals only with the effect of the lift engines on the local design of the outer cylindrical bulkhead. Examination of figure 4-12 reveals that the outer cylindrical bulkhead receives loads from the longerons shown in detail A and from the lift engine support fitting attached to the bulkhead midway between webs, as shown in detail B.

In order to distribute the loads from the shear webs in the lift engine support system to the outer cylindrical bulkhead, longerons are provided as shown in detail A, figure 4-12. The longeron extends from the lower heat shield to the kick ring, a distance of 117.0 in., as shown in section A-A, figure 4-12. The averaged moment introduced by the shear plate to the longeron is 523,300 in-lb (refer to paragraph 5.2). The maximum bending moment in the longeron occurs at the forward edge of the shear plate and can be shown to be:

$$M = (523,000/117.0)(117.0 - 26.0) = 407,040 \text{ in-lb}$$

CONSIDER 4" x .0225' x 1/2" x .0020 CONFIGURATION

$t = 4"$ (METHOD REF – NASA MSC "SHELL ANALYSIS MANUAL", PARA. 3.24.1)

$t_c = 3.955"$

$t^3 = 64$

$t_c^3 = 61.864$

$t^3 - t_c^3 = 2.136$

$D = \frac{30 \times 10^6}{12 \times (1 - .284^2)} [2.136] = 5.807 \times 10^6$

$t - t_c = .045$

$H = E(t - t_c) = 1.35 \times 10^6$

$D/H = 4.302$

$(D/H)^{1/2} = 2.074$

$t_e = 2\left[3\lambda_F \frac{D}{H}\right]^{1/2} = 6.8898"$

$R/t = 353/6.8898 = 51.235, \therefore C_c = 0.235$

$\left.\frac{\sigma_{cr}}{\eta}\right]_e = C_c E_a t_e / R_e = 0.235 \times \left(\frac{1.35 \times 10^6}{6.8898}\right)(6.8898)/353$

$= 898.72$

$\left.\frac{\sigma_{cr}}{\eta}\right] = \left[\frac{\sigma_{cr}}{\eta}\right]_e \times \left[\frac{t}{t - t_c}\right] = 898.72\left(\frac{4}{4 - 3.955}\right) = \underline{79,886 \text{ psi}}$

CHECK INTRACELL BUCKLING:

(METHOD REF – NASA MSC "SHELL ANALYSIS MANUAL", PARA. 3.52.1)

USING 79,886 AS WORKING STRESS,

$K_L = 1.259 \sigma \lambda_F / E = .003082$

$\therefore t_F/s = .03325$

$\therefore s$ REQ'D $= .0225/.03325 = 0.677 \therefore$ O.K.

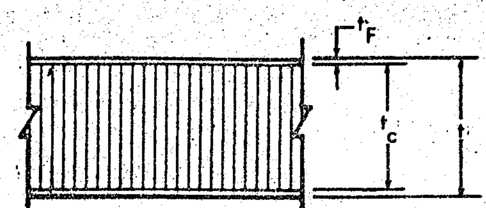

Figure 4-5. Reinforcement Panel Analysis

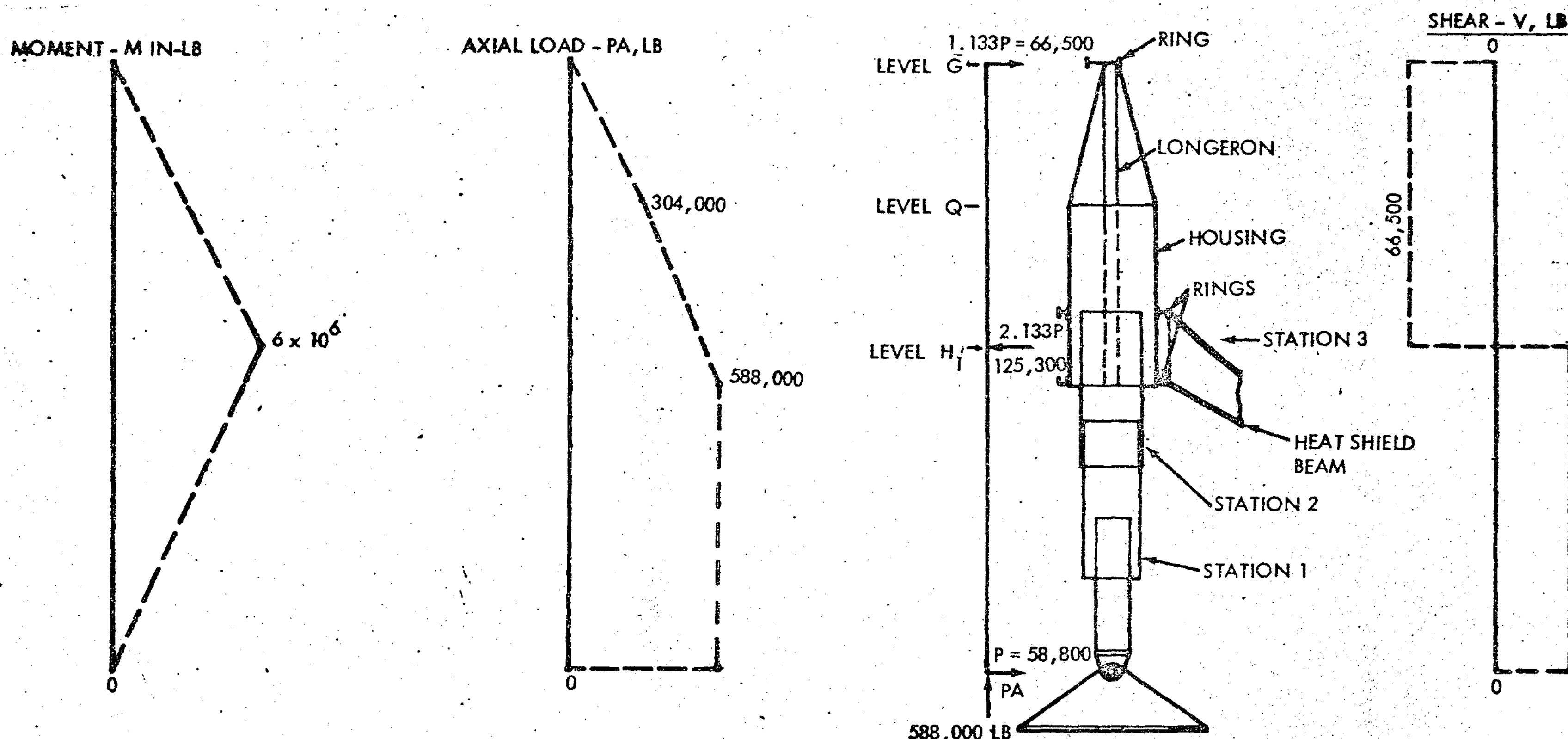

Figure 4-6. Landing Gear Loading

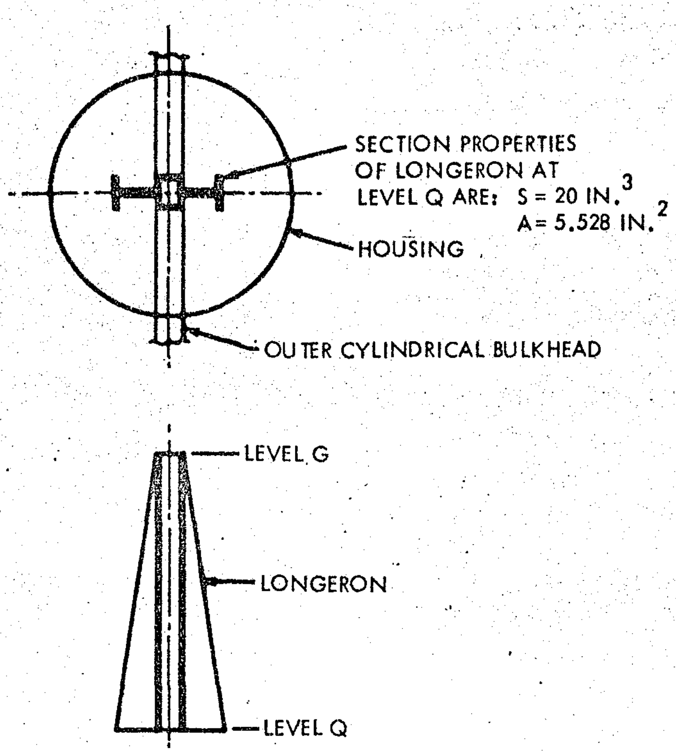

* - LONGERON (2) AREA = 4.168 IN.^{2}
FOR SECTION, SEE FIGURE 4-4.

1. LOADS: (SEE FIGURE 4-6)

   $M = 3 \times 10^6$ IN-LB, $P = 304{,}000$ LB — AT LEVEL Q

   $$fc = P/A + M/S = \frac{304{,}000}{5.528} + \frac{3 \times 10^6}{20}$$

   $$= 55{,}000 + 150{,}000 = 205{,}000 \text{ psi}$$

2. MATERIAL PROPERTIES

   INCONEL 718 - Foy = 200,000 psi

3. MARGIN OF SAFETY

   THE OPERATING STRESS LEVEL SHOWN ABOVE WOULD YIELD A NEGATIVE MARGIN, BUT THE AREA OF LONGERON (2)* WAS NOT CONSIDERED IN ABOVE CALCULATION. THEREFORE, THE DESIGN WOULD SHOW A POSITIVE MARGIN.

   $$fc = \frac{304{,}000}{9.696} + 150{,}000 = 181{,}400 \text{ psi}$$ (CONSERVATIVE)

   $$M.S. = \frac{200{,}000}{181{,}400} - 1 = \underline{+0.10}$$

4. WEIGHT OF LONGERONS

   $$WT. = \frac{9.696}{2} \times 44.96 \times 0.297 = 65 \text{ LB}$$

   TOTAL = WT. x 4 (4 LOCATIONS)
   = 65 x 4 = 260 LB

Figure 4-7. Longeron Analysis

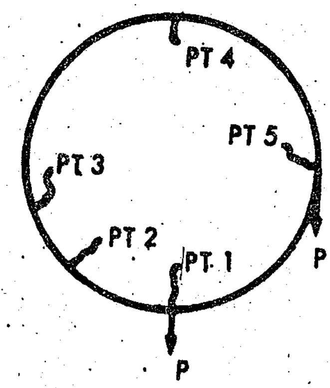

Figure 4-8. Ring Loading - LH_2 Tank Interface

Table 4-1.

LOCATION	KM TOTAL	KQ TOTAL	KW TOTAL	P *	R	M	Q	N
PT 1	-0.230	+0.60	+0.315	55,000	354.48	-4.47×10^6	+33,000	+17,300
PT 2	+0.095	+0.225	+0.580		354.48			
PT 3	+0.120	-0.08	+0.42		354.48			
PT 4	-0.093	+0.09	-0.350		354.48			
PT 5	+0.115	-0.155	-0.250		354.48			

* P LOAD FOR KICK RING WAS DERIVED AS FOLLOWS:
MAXIMUM LATERAL LOAD OCCURS ON GEAR AT BOTTOM OF SHOCK STROKE, THEREFORE, KICK LOAD FOR RING = (84 x 58,800/90) = 55,000 LB

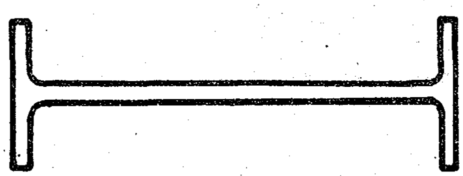

12 x 4 B LIGHT BEAM

$S = 22.9 \text{ IN.}^3$, $A = 6.08 \text{ IN.}^2$

VALUES INTERPOLATE IN TABLE ON PAGE 1-23 IN AISC STEEL HANDBOOK

1. LOADS (REF. TABLE 4-1)

   $M = 4.47 \times 10^6$ IN-LB

   $N = 17,300$ LB

   $f_c = N/A + M/S$

   $= 17,300/6.08 + 4.47 \times 10^6/22.9$

   $= 2845 + 195,250$

   $= 198,095$ psi

2. MATERIAL PROPERTIES

   INCONEL 718 - $F_{OY} = 200,000$ psi

3. MARGIN OF SAFETY

   $M.S. = \frac{200,000}{198,095} - 1 = +0.01$

4. RING WEIGHT

   $WT = 2227 \times 6.08 \times 0.297 = 4015$ LB

Figure 4-9. LH_2 Bulkhead Interface Ring

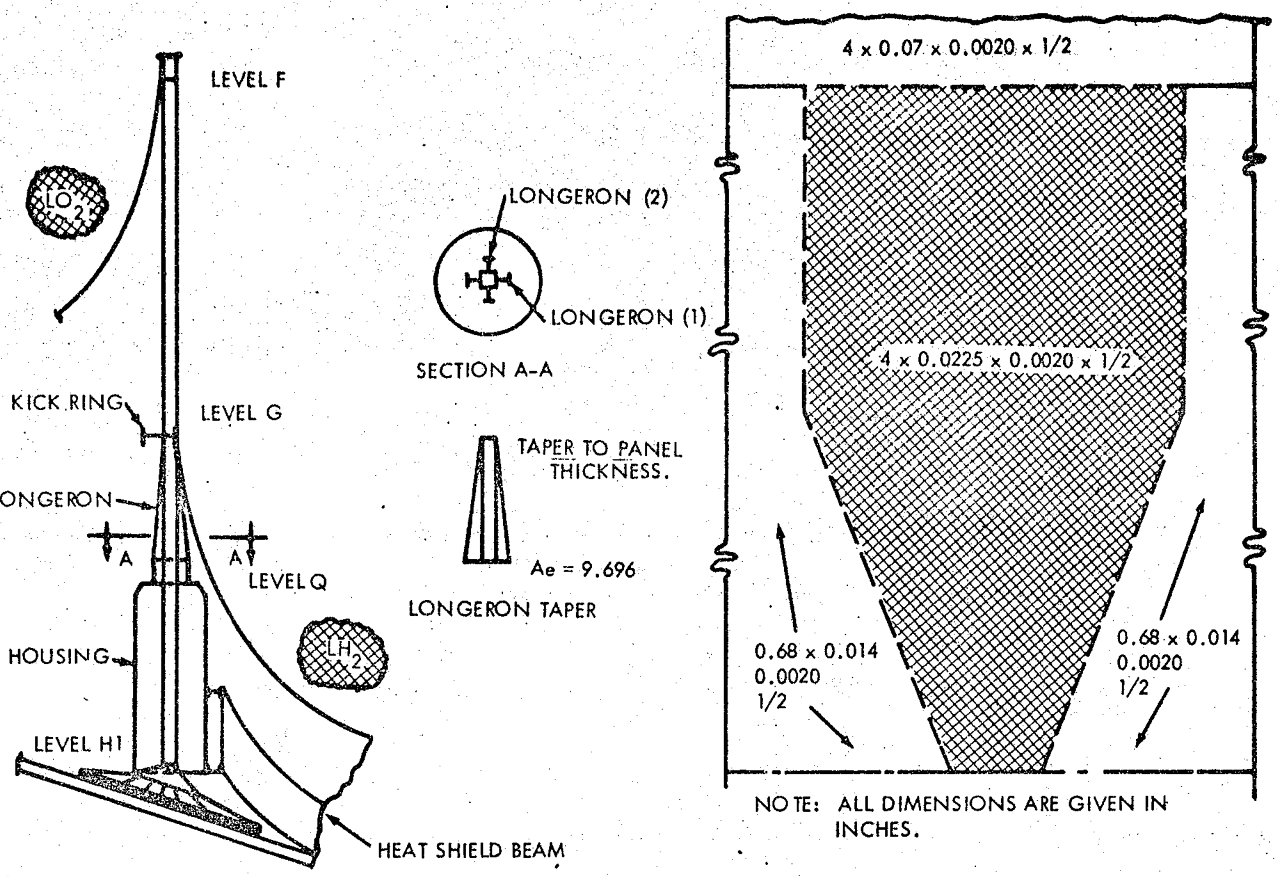

Figure 4-10. Reinforcement Configuration Design

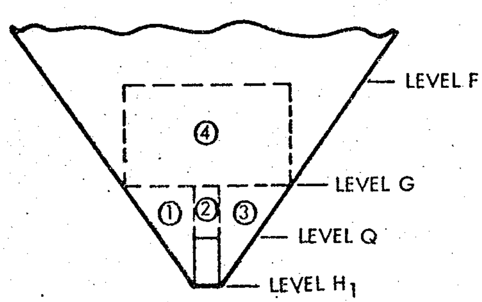

AT LEVEL G, THE REINFORCEMENT PANEL CONFIGURATION CAN CARRY THE AXIAL LOAD WHICH DICTATES THE SHAPE OF PANEL ④ IN ABOVE SKETCH.

REINFORCEMENT PANEL SURFACE AREA = 21,300 $IN.^2$
(PANELS ①, ②, ③, ④)

ADDED SKIN WT. = 21,300 x (0.045 - 0.028) x 4 x 0.297 = 430 LB

ADDED CORE WT. = $\frac{21,300 \times 4 \times (3.955 - 0.652)}{1728} \times 4.1 = 667$ LB

TOTAL PENALTY = 667 + 430 = 1,097 LB

Figure 4-11. Honeycomb Penalty Weight Calculations

Table 4-2. Penalty Weight Summary

Reinforcement Item	Weight Penalty (lb.)
Panel Configuration	1097
Longeron	260
Kick Ring	4015
Total	5372

C-290

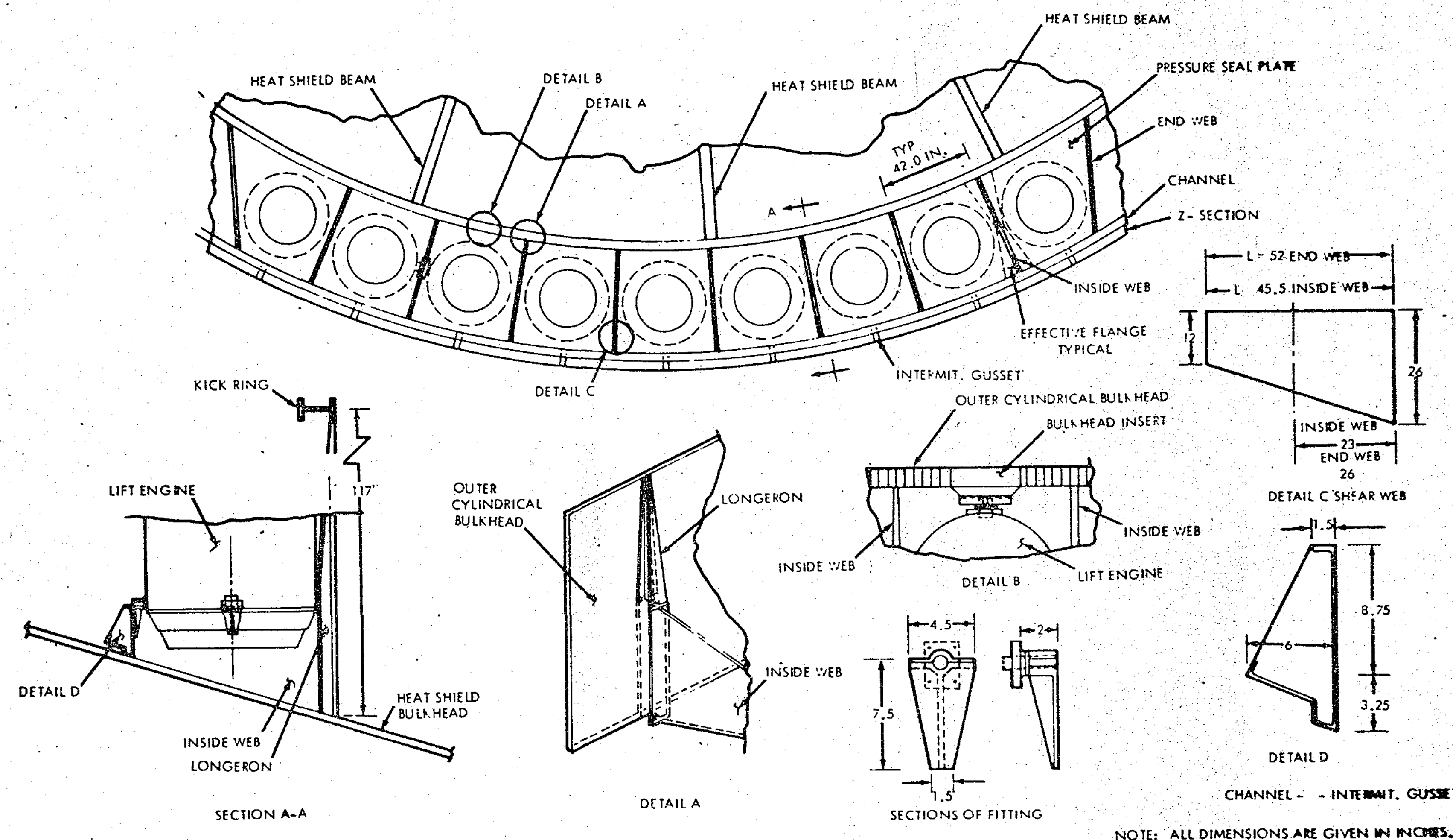

Figure 4-12. Lift Engine Support Structure

Assuming the longeron cross-section to be proportioned so that the allowable crippling stress is equal to the compressive yield stress:

cy = 200,000 lb/in.^{2} (refer to paragraph 9.1 volume 3, appendix E)

The required section modulus is then:

$$(I/y) = 407{,}040/200{,}000 = 2.035 \text{ in.}^3$$

From reference 14, the standard I-beam shape that most closely meets the requirements is a 3.00-in. section with a cross-sectional area of 2.17 in.^{2} and a section modulus of 1.900 in.^{3}. Although the section modulus of this shape is slightly less than that required, it is considered satisfactory because, in the determination of loads, the relieving effect of lift engine inertia has not been included.

The weight increment to be added to the outer cylindrical bulkhead caused by the requirement for longerons in the lift engine support system is then:

$$W_L = (40)(2.17)(117.0/2)(.297) = 1500 \text{ lb}$$

The ability of the outer cylindrical bulkhead to carry the loads introduced by the longerons is investigated as follows:

T = ultimate thrust per engine = 23,652 lb (refer to paragraph 5.2).

With reference to paragraph 5.2, and figure 5-5, the uniformly distributed loading in the longeron is:

$$q_L = (3T/4)/L$$

where T = 23,652 lb

L = 117 in. (refer to figure 4-12)

then $q_L = (0.75)(23652)/117 = 152$ lb/in.

Assuming this running load on the longerons to be divided equally to the portions of the outer cylindrical bulkhead, and equally between the faces of the bulkhead sandwich, the shear stress in the face skins of the outer cylindrical sandwich is:

$$\gamma = q_L/4(t_F)$$

where $t_F = 0.014$ in. (refer to figure 3-15)

$$\gamma = 152/4(0.014) = 2710 \text{ lb/in.}^2$$

The allowable shear buckling stress in the outer cylindrical buckhead, for which t = 0.680 in., t_F = 0.014 in., S = 0.500 in. and t_{FOIL} = 0.0020 in. (refer to figure 3-15) is calculated by the method discussed in reference 5. The intercell buckling stress for this sandwich configuration is:

$$\sigma_{ci} = \sigma_{ci}/\eta = 105{,}000 \text{ lb/in.}^2$$ (refer to table 3-35)

$$\sigma_{si}/\eta = 0.8 \; (\sigma_{ci}/\eta) = 0.8(105{,}000) = 84{,}000 \text{ lb/in.}^2$$

$$\gamma_i = (3)^{\frac{1}{2}} = 1.732$$

$$\sigma_i/\eta = \gamma_i \; (\sigma_{si}/\eta) = (1.732)\;(84{,}000) = 145{,}500 \text{ lb/in.}^2$$

σ_{cy} = 200,000 lb/in.^{2} (refer to paragraph 9.1, volume 3, appendix E)

$$\sigma_{cy}/(\sigma_i/\eta) = 200{,}000/145{,}500 = 1.375$$

σ_i/σ_{cy} = 0.680 (refer to figure 3-11)

$$\sigma_i = (200{,}000)\;(0.680) = 136{,}000 \text{ lb/in.}^2$$

$$\sigma_{si} = \sigma_i/(3)^{\frac{1}{2}} = 136{,}000/1.732 = 78{,}500 \text{ lb/in.}^2$$

Because the ultimate shear stress is only 2,710 lb/in.^{2}, the resulting margin of safety is large.

The longeron spacing on the outer cylindrical bulkhead is 42.0 in. (refer to figure 4-12). Assuming the longeron load to be completely difused to a uniformly distributed compressive loading at the forward end of the longeron, the stress in each face of the outer cylindrical bulkhead is then:

$$\sigma_c = (0.75)(23652)/(42.0)(2)(0.014) = 17{,}739/1.176 = 15{,}080 \text{ lb/in.}^2$$

The allowable intercell buckling stress (see above) is:

$$\sigma_{ci} = 105{,}000 \text{ lb/in.}^2$$

M.S. = (105,000/15,080) - 1 = + <u>5.96</u>

The critical buckling stress for this region of the outer cylindrical bulkhead is:

$(\sigma_{CR})_M$ = 18,320 lb/in.^{2} (refer to table 3-34)

M.S. = (18,320/15,080)-1 = + <u>.214</u>

This margin of safety is very conservative because it has been assumed that the buckling stress is determined on the basis of the outer cylindrical bulkhead acting as a pure monocoque cylinder. Actually, the presence of the longerons will prevent the cylinder from buckling as a monocoque, and will instead break the surface of the cylinder into numerous long, relatively narrow rectangular panels which will inherently possess a considerably higher buckling stress.

The strength of the kick ring located at the juncture of the lower toroidal LH_2 tank bulkhead with the outer cylindrical bulkhead is investigated as follows:

The load induced on the kick ring by the longeron is:

P_L = (T/4) (52) + (T/2) 23/117.0 (refer to detail C, figure 4-12)

$P_L = (23,652)\ (52/4) + (23,652)\ (23/2)/117.0$

$P_L = 307,480 + 272,000 \quad /117.0 = 4,950$ lb (acting radially inward).

Because it is believed that the kick ring is not critically loaded in this mode, the conservative assumption is made that the longerons (ten per engine cluster) apply their loads at single concentrated points, 90 in. apart. Total load per cluster is then:

$P = 10(4950) = 49,500$ lb

With reference to Case 5, section B6, reference 15, the maximum bending moment and axial load in the ring occur at stations midway between the assumed loading points and are:

$M = K_M PR$; and $N = K_N P$

where M = bending moment

N = axial load

K_M and K_N are loading coefficients from the referenced manual.

P = load applied at four diametrically opposite points

R = radius of ring = 354.48 in. (refer to paragraph 4.1)

$M = (0.071)\ (49,500)\ (354.48) = 1,245,800$ in-lb

$N = (0.71)\ (49,500) = 35,150$ lb (compression)

In paragraph 4.1, the ring shape selected had an area of 6.08 $in.^2$ and a section modulus of 22.9 $in.^3$ with $\sigma cy = 200,000\ lb/in^2$. The maximum compressive stress in the ring is then:

$f_c = (1,245,800/22.9) + (35,150/6.08)$

$= 54,400 + 5,780 = 60/180\ lb/in^2$.

M.S. = (200,000/60,180) - 1 = + <u>2.32</u>

The kick ring is obviously more critically loaded by landing gear loads (refer to paragraph 4.1).

The strength of the outer cylindrical bulkhead at the point of application of the loads from the inboard attachment point for a lift engine is checked as follows:

The ultimate load at the fitting is:

$P = T/4 = 23,652/4 = 5,913$ lb (refer to paragraph 5.2)

The moment due to the transfer of this loading to the centerline of the outer cylindrical bulkhead sandwich is:

$$M = (5913)\left(2.00 + \frac{.680}{2}\right) = 13{,}840 \text{ in-lb}$$ (refer to figure 4-12 for moment arm of fitting)

Assuming the insert to have a rectangular shape with dimensions of 4.50 in. by 7.5 in. (see sections of fitting details on figure 4-12), and considering the shear stresses induced in the sandwich core to have the same characteristics as a bending stress, the equivalent moment of inertia of the shear area is:

$$I_s = 2(0.680 - 0.028)(4.50)\frac{(7.50)^2}{2} + \frac{2(7.50)(0.680 - 0.028)(7.50)^3}{12}$$

$$= 82.519 + 343.828 = 426.347$$

The maximum intensity of the transverse shear stress is then:

$$\tau = (13{,}840)(7.50/2)/426.347 = 122 \text{ lb/in.}^2$$

$$\sigma_S = 315 \text{ lb/in.}^2$$ (refer to table 3-37)

M.S. = (315/122) - 1 = <u>+1.581</u>

The maximum local compressive stress developed in the face skin of the bulkhead sandwich (at the forward end of the insert) is:

$$\sigma_c = 5913/(4.50)(2)(0.014) = 5913/0.126 = 46{,}930 \text{ lb/in}^2.$$

The intercell buckling stress for this sandwich configuration is:

$$\sigma_{ci} = 105{,}000 \text{ lb/in}^2$$ (refer to table 3-35)

M.S. = (105,000/46.930) - 1 = <u>+1.237</u>

The allowable buckling stress for a curved panel with a length of 117 - 26 = 91 in., a width of 42 in. and a radius of curvature of 354.48 in. (refer to figure 4-12 for these dimensions) is calculated from the equation given in reference 16 which is (in terms of sandwich design parameters):

$$(\sigma_{CR}/\eta) = k_c \pi^2 E_e (t_e/b)^2/12(1 - \mu^2),$$

$$Z = L^2 (1 - \mu^2)^{\frac{1}{2}}/Rt_e$$

where

σ_{CR} = allowable buckling stress

η = plasticity reduction factor

E_e = equivalent modulus of elasticity = 720,800 } refer to table 3-33

t_e = equivalent plate thickness = 1.154 } refer to table 3-33

b = 42.0 in.

L = 91.0 in.

$R = 354.48$ in.

$\mu = 0.281$ (refer to paragraph 9.1, volume 3, appendix E)

then $Z = (91.0)^2 \left[1 - (0.281)^2\right]^{\frac{1}{2}} / (354.48)(1.154) = 19$

$kc = 6.5$ (refer to figure 38 (b) of reference 16)

$$(\sigma CR/\eta)_e = (6.5)\,(3.142)^2\,(720{,}800)/12\left[1 - (0.281)^2\right]\,(42/1.154)^2$$

$$= 3{,}160 \text{ lb/in.}^2$$

This is converted to actual sandwich stresses by multiplying by $t_e/2t_f =$ 41.201 (refer to table 3-34) so that:

$$(\sigma CR/\eta) = 3{,}160\ (41.201) = 130{,}200 \text{ lb/in.}^2$$

$\sigma CR = 130{,}200$ lb/in.^{2} (refer to figure 26, volume 3, appendix E)

M.S. = (130,200/46,930) - 1 = +1.774

4.3 CONCENTRATED LOADS ON INNER CYLINDRICAL BULKHEAD FROM HEAT SHIELD RADIAL BEAMS

The inner cylindrical bulkhead reinforcement configuration consists of tapered longerons running from the radial beam intersection at the heat shield to the intersection with the toroidal lower LH_2 tank bulkhead. The longeron was designed to introduce the radial beam load into the inner cylindrical bulkhead at a rate such that the compressive allowable stress in the sandwich face skins would not be exceeded. The geometry involved in this analysis is shown in figure 4-13. The maximum concentrated load used in this analysis was conservatively taken from paragraph 9.8, volume 3, appendix E,and is 78,090 lb. This conservative value was selected in order to avoid the necessity for the time consuming reanalysis of the point design heat shield configuration in which both loads and geometry changed. With reference to paragraph 3.10.3, this load could legitimately have been reduced by the factor, (0.734)(1.095) = 0.801.

In this vehicle configuration, the radius of the inner cylindrical bulkhead was assumed to be 94.0 in. The sandwich configuration in this portion of the bulkhead specified an overall thickness of 0.375 in., face thickness of 0.010 in., cell size of 0.500 in. and foil thickness of 0.0020 in. (refer to figure 3-15).

The maximum uniformly distributed stress in the face skins, assuming the shear lag effect fully accomplished is:

$$\sigma c = 78{,}090/(2)(3.142)(94.00)(2)(.010) = 78{,}090/11.814 = 6{,}610 \text{ lb/in.}^2$$

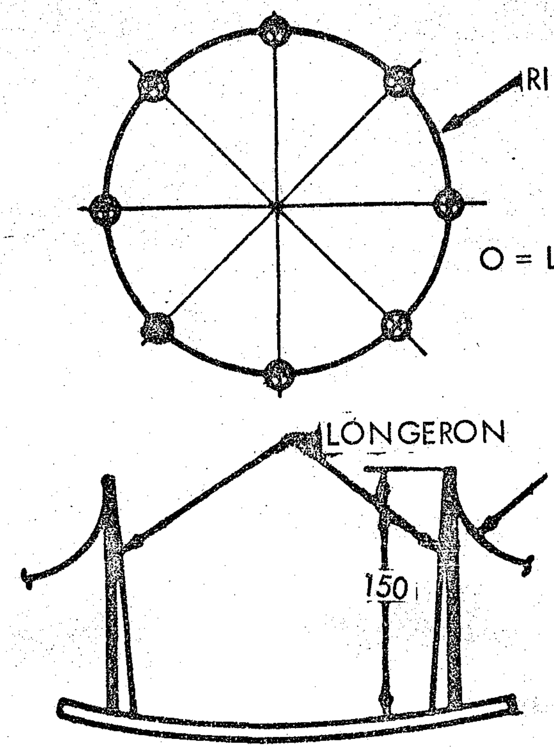

Figure 4-13. Inner Cylindrical Bulkhead Reinforcement

The critical meridional buckling stress for this part of the cylinder is:

$(\sigma CR)_M = 41,970\ lb/in^2$ (refer to table 3-34)

M. S. = (41,970/6,610 - 1 = + 5.34

The allowable intercell buckling stress is:

$\sigma ci = 63,200\ lb/in.^2$ (refer to table 3-35) which is not critical.

From reference 14, a 5.0-in. channel with an area of 1.97 $in.^2$ and a radius of gyration of 1.95 in. was selected as the section at the aft end of the longeron.

The maximum stress = $\sigma c = 78,000/1.97 = 39,594\ lb/in.^2$

The allowable column stress is then:

$$\sigma AC = \pi^2 E/(KL/p)^2$$

where E = $29.7 \times 10^6\ lb/in.^2$ (refer to paragraph 9.1, volume 3, appendix E)

K = fixity coefficient = 1.0

L = 150.0 in. (refer to figure 4-13)

p = 1.95 in. (see above)

$$\sigma AC = (3.141)^2 (29.7 \times 10^6)/(150/1.95)^2 = 49,517\ lb/in.^2$$

M.S. = (49,517/39,594)-1 = <u>+ 0.250</u>

Because the longeron effectively feeds the concentrated load acting at its aft end into the sandwich as a uniformly distributed shear loading, its area can be varied along its length. Assuming the longeron to taper from an area of 1.97 $in.^2$ at the aft end to 0.25 $in.^2$ at the forward end, the total longeron weight becomes

$$W_L = (8)\ (0.297)(150)(1.97 + 0.25)/2 = 396\ lb$$

A developed view of the inner cylindrical bulkhead including the longerons is given in figure 4-14.

5.0 MISCELLANEOUS STRESS ANALYSES

The stress analysis associated with the landing gear assembly and the lift engine support structure is presented in the following paragraphs.

5.1 LANDING GEAR ASSEMBLY

The landing gear assembly consists of a housing, housing extension tube, hydraulic actuator and shock assembly, and a piston rod. The lower end of the piston rod has a lug attachment which acts as the structural tie to the land-

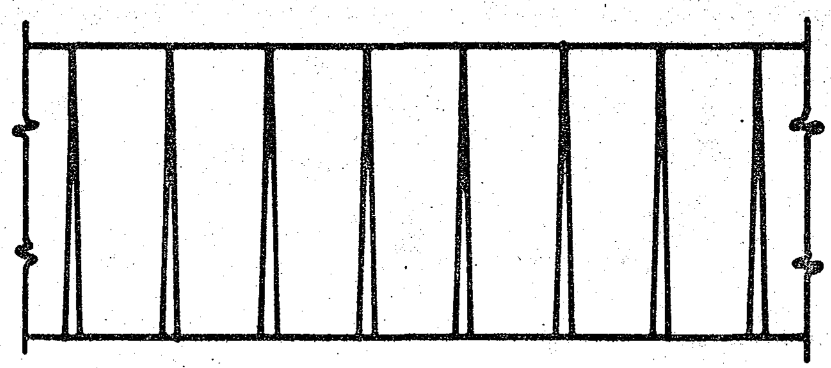

Figure 4-14. Developed View - Inner Cylindrical Bulkhead

ing pad. The landing gear assembly is depicted in figure 5-1 in a fully extended position. The geometry of the individual segments and the bearing pad-ring structure used to transfer the moment load between segments is also shown in figure 5-1. The gear structure is extended using hydraulic and mechanical actuation. On attaining full extension, the various segments are locked into position by shear pins that transfer the axial load between segments. The geometry of the outer cylindrical bulkhead in the landing gear area is shown in figure 4-1. This figure serves as a nomenclature reference for the development of the shear lag geometry. The shear lag geometry is shown in figure 4-2.

The design criteria utilized in the analysis of the landing gear structure are as follows:

1) Landing impact, 2G limit, 12 fps sink speed, at 2 degrees attitude

2) 1/2 of landing weight of 1 gear

3) friction factor, μ , between pad and gear 0.1 maximum

4) 1.4 factor of safety

5) vehicle landing weight 420,000 pounds

The ultimate axial load to the gear was then calculated to be:

$$P_{ult} = \frac{420,000 \times 1.4 \times 2}{2} = 588,000 \text{ lb}$$

The maximum lateral load to the gear was then calculated to be:

$$P_{lateral} = \mu\, P_{ult} = 0.1 \times 588,000 = 58,800 \text{ lb}$$

The gear was designed to withstand the combined maximum azial and lateral loads which were calculated at the fully extended gear position.

The gear structure was idealized as a cantilevered beam column. The shear, moment and axial loads applied at the housing interface were assumed to be reacted by the heat shield beams through two rings at the lower end, and a further ring at the hydrogen tank interface on the upper end. The housing and an added longeron (see figure 4-6) distribute the moment to the rings and the heat shield beams. The shear, moment and axial load diagrams are also depicted in figure 4-6 was calculated using the results of the shear lag analysis on the outer cylindrical bulkhead structure. The outer cylindrical bulkhead honeycomb configuration in the landing gear region was considered to be a 4-in. by 0.0225-in. face sheet with a core of 1/2-in. cell size by 0.0020-in. foil gage. This configuration yielded a general instability allowable of 79,000 psi. The axial load in the housing and lingeron was sheared into the skin at a rate not to exceed the general instability allowable at any section. Utilizing the shear lag geometry (see figure 4-2) the allowable loads in the skin are:

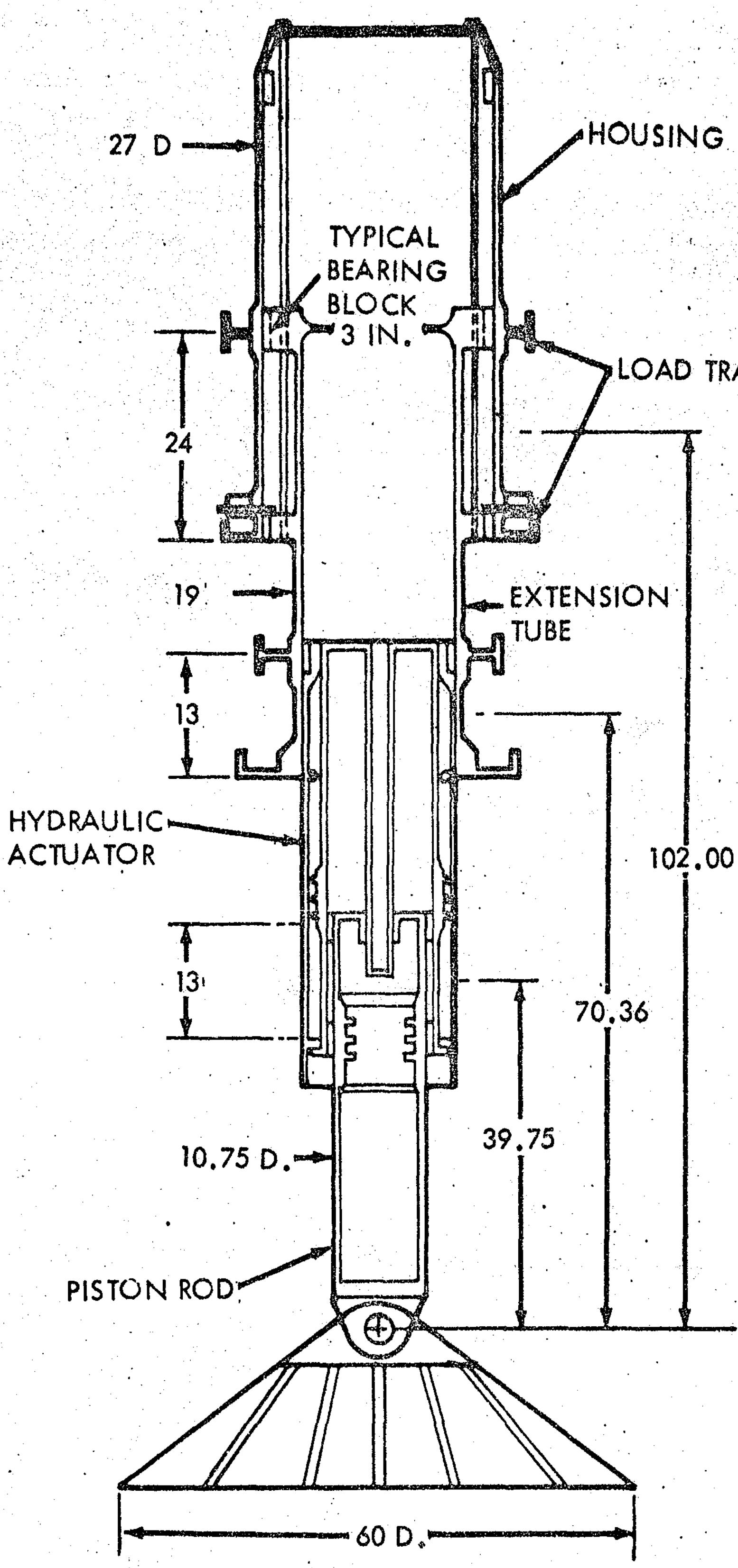

NOTE: ALL DIMENSIONS ARE GIVEN IN INCHES.

Figure 5-1. Landing Gear Assembly

P_{H1} Allowable = 0

P_Q Allowable = 80 x 0.045 x 79,000 = 284,000 lb

P_G Allowable = 170 x 0.045 x 79,000 = 604,000 lb

Therefore, the net axial load in the housing and longeron is:

P_{H1} = 588,000 lb

P_Q = 588,000 - 284,000 = 304,000 lb

P_G = 0

The reinforcement panel configuration was also checked for intracell buckling in accordance with methods outlined in reference 6. The panel was not critical.

The gear segments were designed to accept the loads itemized in table 5-1. The section properties of the gear segments are defined by the equations:

$$\text{Area} = 0.7854\ (Do^2 - Di^2)$$

$$\text{Moment of Inertia} = 0.04908\ (Do^4 - Di^4)$$

$$\text{Section Modulus} = \frac{0.09816\ (Do^4 - Di^4)}{Do}$$

$$\text{Radius of Gyration} = 0.25\ \sqrt{Do^2 + Di^2}$$

The allowable column load was calculated assuming an effective column length of 84 in. (length minus shock stroke = 102 - 18 = 84). The section properties of the gear segments are shown in table 5-2. A weighted ρ value for the column was calculated as shown in table 5-3. The allowable stress calculations for the column sections are shown in table 5-4. The actual stress levels and margins of safety are shown in table 5-5.

The rings and bearing pads at station 1 (see figure 4-6) were designed to accept the loading shown in figure 5-2. The rings were idealized as a case 18 ring, and analyzed per the ring archived in reference 15. The loads for three locations on the ring are shown in table 5-6. Using the loading in table 5-6, the actual stress levels may be calculated:

$$fc\ max = \frac{P}{A} + \frac{M}{S} = \frac{28,651}{A} + \frac{71,201}{S}$$

$$ft\ max = \frac{P}{A} + \frac{M}{S} = \frac{85,952}{A} + \frac{71,201}{S}$$

By selecting a standard section from reference 14 (ensuring against local crippling):

Table 5-1. Design Loads

Data	V	Marm	M	Pa
Station	Shear (lb)	Moment Arm (in.)	Moment	Axial Load (in.)
1	58,800	39.75	2.34×10^6	588,000
2	58,800	70.36	4.14×10^6	588,000
3	66,500	102.00	6×10^6	530,000
Q	66,500		3×10^6	304,000

Table 5-2. Gear Segment - Section Properties

Gear Segment	Section Properties	Area p.7854 $(Do^2 - D_i)^2$	Moment of Inertia $0.04908\ (Do^4 - Di^4)$	Section Modulus $\frac{0.09816\ (Do^4 - Di^4)}{Do}$	Radius of Gyration $0.25 \sqrt{Do^2 + Di^2}$
Piston Rod Do = 10.75 in.	Aft t = .185	6.14	85.71	15.95	3.74
	Sta. 1 t = .325	10.64	144.72	26.92	3.69
Hydraulic Act. and Shock Assy. Do = 19 in.	Sta. 1 t = .250	14.73	647.17	68.12	6.63
	Sta. 2 t = .285	16.76	733.75	77.24	6.62
Housing Extension Tube Do = 19 in.	Sta. 2 t = .285	16.76	733.75	77.24	6.62
	Sta. 3 t = .325	19.07	831.42	87.52	6.61
Landing Gear Housing Do = 27 in.	Sta. 3 t = .285	23.92	2,133.95	158.07	9.45
	Pt. "B" t = .175	14.75	1,326.49	98.26	4.48

Table 5-3. Gear Radius of Gyration

Gear Segment	Length L	Radius of Gyration ρ	$L\rho$
Piston Rod	15.75	3.715	58.51
Hydraulic Actuator and Shock Assy.	37.00	6.625	245.13
Extension Tube	31.25	6.615	206.72
Σ	34.00		510.36

$$\text{Eff. } \rho = \frac{510.36}{84.00}$$

$$= 6.08$$

Table 5-4. Gear Allowable Stress

Gear Segment		Radius R	Thickness t	R/t	Fcc Ref 1 KSI	R / ρ	Fcol KSI
Piston Rod	Aft.	5.375	0.185	29.05	105	27.62	98.00
	Sta 1	5.375	0.325	16.52	151	27.62	133.00
	Sta 1	9.500	0.250	38.00	82	27.62	77.50
Hyd. Actuator and Shock Assy.	Sta 2	9.500	0.285	33.33	94	27.62	87.00
	Sta 2	9.500	0.285	33.33	94	27.62	87.00
Extension Tube	Sta 3	9.500	0.325	29.25	103	27.62	87.00
	Sta 3	13.500	0.285	47.40	62		
Landing Gear Housing	Pt. "B"	b_e=16	0.175	be_t=91.5	52		

Reference 1 - CCMD Structures Manual

Table 5-5. Actual Stress Levels

Gear Segment	Area A	Section Modulus S	Axial Load Pa k	Moment M in-k	P/A ksi	M/S ksi	c P/A+M/S ksi	Allowable Stress FA ksi	Margin of Safety $\frac{FA}{fc} - 1$
Piston Rod	Aft 6.14	15.95	588	0	94.2	0	94.2	98	+0.040
	Sta 1 10.64	26.92	588	2.34×10^3	53.6	79.4	133	133	0
Hyd. Actu & Shock Assy	Sta 1 14.73	68.12	588	2.34×10^3	39.4	33.0	72.4	77.5	+0.070
	Sta 2 16.76	77.24	588	4.14×10^3	34.6	51.2	85.8	87	+0.013
Extension Tube	Sta 2 16.76	77.24	588	4.14×10^3	34.6	51.2	85.8	87	+0.013
	Sta 3 19.07	87.52	588	6×10^3	30.3	65.0	95.3	97	+0.018
Landing Gear Housing	Sta 3 23.92	158.07	588	6×10^3	24.35	36.85	61.2	62	+0.012
	Pt"B" 14.75	98.26	304	3×10^3	20.50	30.00	50.5	52	+0.030

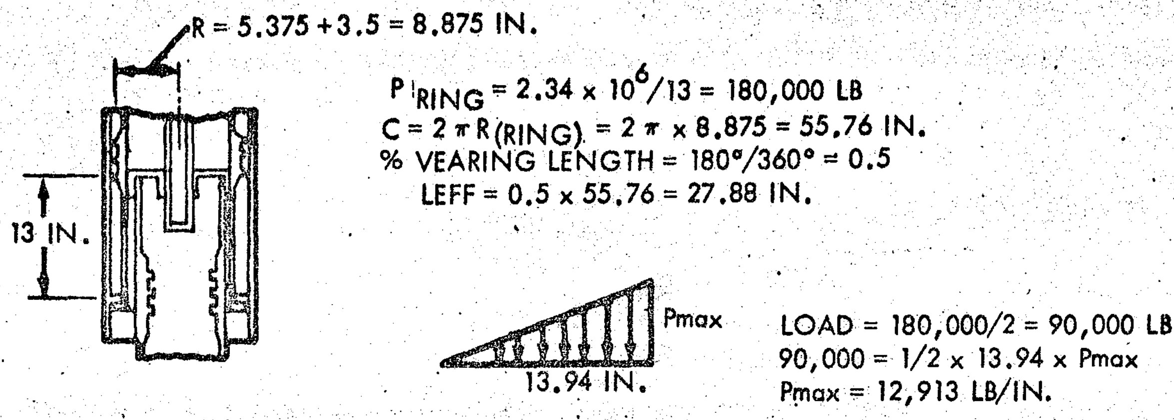

Figure 5-2. Ring Loading - Station 1

Table 5-6.

LOCATION	Km	Kq	Kn	Pmax	R	R^2	M	Q	N
0°	-0.07	0	+0.75	12,913	8.875	78.77	-71,201	0	+85,952
90°	+0.07	0	+0.40	12,913	8.875	78.77	+71,201	0	+45,841
180°	-0.07	0	-0.25	12,913	8.875	78.77	-71,201	0	-28,651

ASSUMED CASE 18 RING:

$M = Km\ Pmax\ R^2$

$Q = Kq\ Pmax\ R$

$N = Kn\ Pmax\ R$

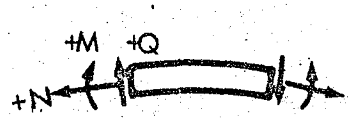

POSITIVE SIGN CONVENTION

Select ST4JR, $A = 0.96$ in.^{2}, $S = 0.56$ in.^{3}

$$fc = 29{,}900 + 127{,}100 = 157{,}000 \text{ psi}$$

$$ft = 89{,}500 + 127{,}100 = 216{,}600 \text{ psi}$$

The margin of safety for the tension stress is then:

$$M.S. = \frac{220{,}000}{216{,}600} - 1 = \underline{+ 0.015}$$

The rings and bearing pads at station 2 (see figure 4-6) were designed to transfer the loading shown in figure 5-3. The method of analysis utilized is referenced to the station 1 ring analysis. The loads for three locations on the ring are shown in table 5-7. Using this loading, the actual stress levels were calculated to be:

assuming a standard section from reference 14:

3 x 1 1/2 x 6 standard channel, $A = 1.75$, $S = 1.4$

$$ft = 208{,}000 \text{ psi}$$

$$M.S. = \frac{220{,}000}{208{,}000} - 1 = + \underline{0.058}$$

The inside rings would be checked in the same manner. The design weights were calculated by ratio of the geometry.

The rings at station 3 (see figure 4-6) were designed to transfer the loading shown in figure 5-4. The loads for three locations on the ring are shown in table 5-8. Using this loading and selecting a standard section from reference 14 (3 x 1 1/2 x 6 standard channel, $A = 1.75$, $S = 1.4$), the actual stress levels were calculated to be:

$$ft = \frac{178{,}250}{1.4} + \frac{119{,}500}{1.75} = 127{,}500 + 68{,}500 = 196{,}000 \text{ psi}$$

$$M.S. = \frac{220{,}000}{196{,}000} - 1 - + \underline{0.121}$$

The inside rings were checked in the same manner, considering a hollow rectangle shape and the geometry. The analysis yielded a cross section of 1 in.^{2} for weight calculations which yielded a high positive margin of safety.

5.2 LIFT ENGINE SUPPORT STRUCTURE

The lift engine support structure was designed by deflection criteria. The structural assembly consists of shear webs stabilized laterally at the outboard edge by a continuous channel and Z segment with intermittent gussets for stiffness and load introduction. The webs are also stabilized at the top by the pressure seal plate. The lift engine support structure assembly is depicted in figure 4-12. The analysis was generated assuming the structure was cantilevered from the outer cylindrical bulkhead. The structure was then

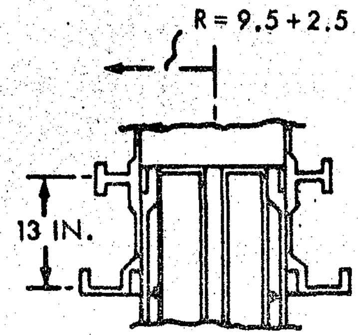

$P_{RING} = 4.14 \times 10^6/13 = 317,500$ LB
$C = 2\pi R_{(RING)} = 2\pi \times 12 = 75.40$ IN.
% BEARING LENGTH = 180°/360° = 0.5
$\therefore L_{eff.} = 0.5 \times 75.40 = 37.70$ IN.

LOAD = 317,500/2 = 158,750 LB.
$158,750 = 1/2 \times 18.85 \times P_{max}$
$P_{max} = 16,850$ LB/IN.

Figure 5-3. Ring Loading - Station 2

Table 5-7.

LOCATION	Km	Kq	Kn	Pmax	R	R^2	M	Q	N
0°	-0.07	0	+0.75	16,850	12	144	-170,000	0	+151,750
90°	+0.07	0	+0.40	16,850	12	144	+170,000	0	+80,900
180°	-0.07	0	-0.25	16,850	12	144	-170,000	0	-50,500

ASSUMED CASE 18 RING:

$M = K_m P_{max} R^2$

$Q = K_q P_{max} R$

$N = K_n P_{max} R$

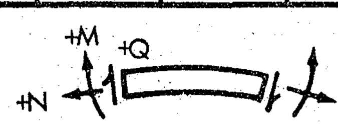

POSITIVE SIGN CONVENTION

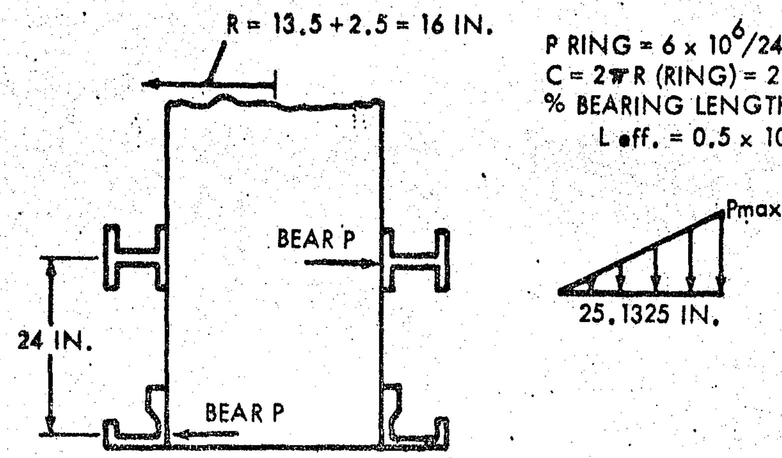

P RING = $6 \times 10^6/24$ = 250,000 LB
C = 2πR (RING) = 2π × 16 = 100.53 IN.
% BEARING LENGTH = 180°/360° = 0.5
L eff. = 0.5 × 100.53 = 50.265 IN.

LOAD = 250,000/2 = 125,000
125,000 = 1/2 × 25.1325 × Pmax
Pmax = 9950 LB/IN.

Figure 5-4. Ring Loading - Station 2

Table 5-8.

LOCATION	Km	Kq	Kn	Pmax	R	R^2	M	Q	N
0°	-0.07	0	+0.75	9,950	16	256	-178,250	0	+119,500
90°	+0.07	0	+0.40	9,950	16	256	+178,250	0	+63,600
180°	-0.07	0	-0.25	9,950	16	256	-178,250	0	-39,800

ASSUMED CASE 18 RING:

$M = K_m P_{max} R^2$

$Q = K_q P_{max} R$

$N = K_n P_{max} R$

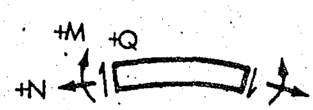

POSITIVE SIGN CONVENTION

sized to give the required stiffness for the limiting deflection criteria. The limiting deflection was assumed to be 0.1 in. vertical. The bending moment and axial load transferred to the outer cylindrical bulkhead are distributed to the rings (at LH_2 bulkhead - forward, and heat shield interface aft) by the longeron depicted in figure 4-12. The longeron is tapered aft-to-forward to transfer the axial load into the skin at a rate which will not exceed the compressive buckling allowable of the skin. An insert, see figure 4-12, is used at the inside engine fitting at the outer cylindrical bulkhead in order to distribute the load to the honeycomb panel. The analysis of the reinforcement configuration is presented in paragraph 4.2.

The load distribution from the engines is depicted in figure 5-5. The ultimate thrust load utilized in the analysis was 23,652 lb. Shear and moment diagrams for the channel segments are shown in figures 5-6 and 5-7. Shear and moments for the shear webs are shown in figures 5-8, 5-9, and 5-10. The engine fitting and door seat loads are depicted in figures 5-11 and 5-12, respectively. The analysis of the channel segment is referenced to figure 5-13. The analysis of the shear webs is shown in figure 5-14 through 5-16. The engine fitting weight calculations are shown in figure 5-17. The door seat analysis is shown in figure 5-18, while the seal plate weight calculations are presented in figure 5-19.

In summary, the web structure sized for the deflection criteria in stable for the applied shear and compression loads. The summary weight statement for the structure is shown in table 5-9.

6.0 SCAR WEIGHTS FOR ALTERNATE PAYLOADS

The primary objective of this task was to define the "scar weights" for the expendable and reusable SERV vehicles for a due-east launch of large-diameter payloads. The analysis was generated with the following assumptions:

1) Geometry of vehicle from reference 60SKC0195

2) Payloads interface at present 15.65-ft-diameter kick ring

3) Pressure loading is the same as in the baseline analysis

4) Expendable SERV payload equals 250,000 lb

5) Reusable SERV payload equals 119,652 lb

6) Component analyses methods are the same as for baseline vehicle.

The method of analysis is as herein defined. The existing design allowable stress level (baseline vehicle design) will not be exceeded in the upper frustum. The face thickness of the skins will be increased in order to carry the added compression load at the same working stress. A second iteration will determine the increased allowable of the honeycomb configuration caused by the increased skin thickness. If such changes in configuration geometry alter the critical design loading condition, a correction will be made to the previously calculated weights. If changing the configuration by only increasing the skin

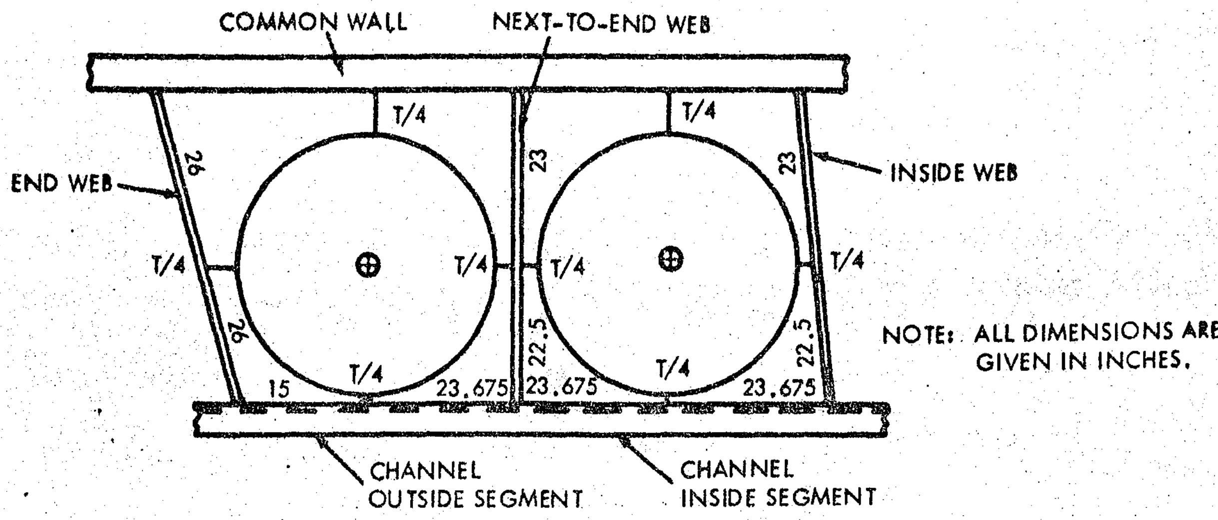

Figure 5-5. Load Distribution

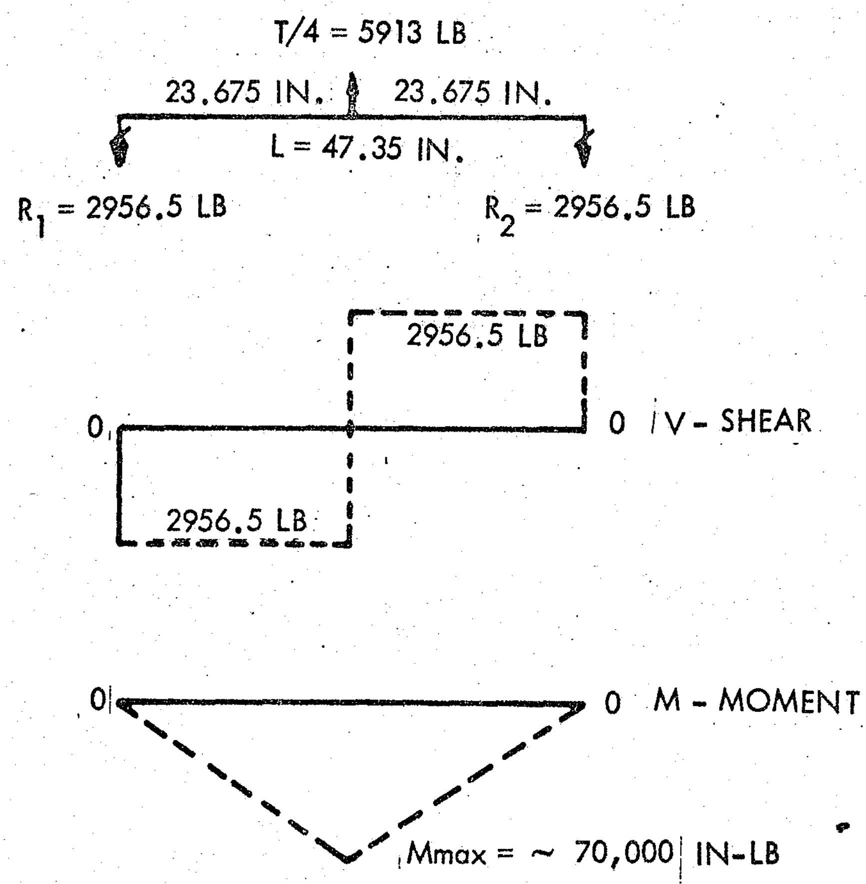

Figure 5-6. Loading - Inside Channel Segment

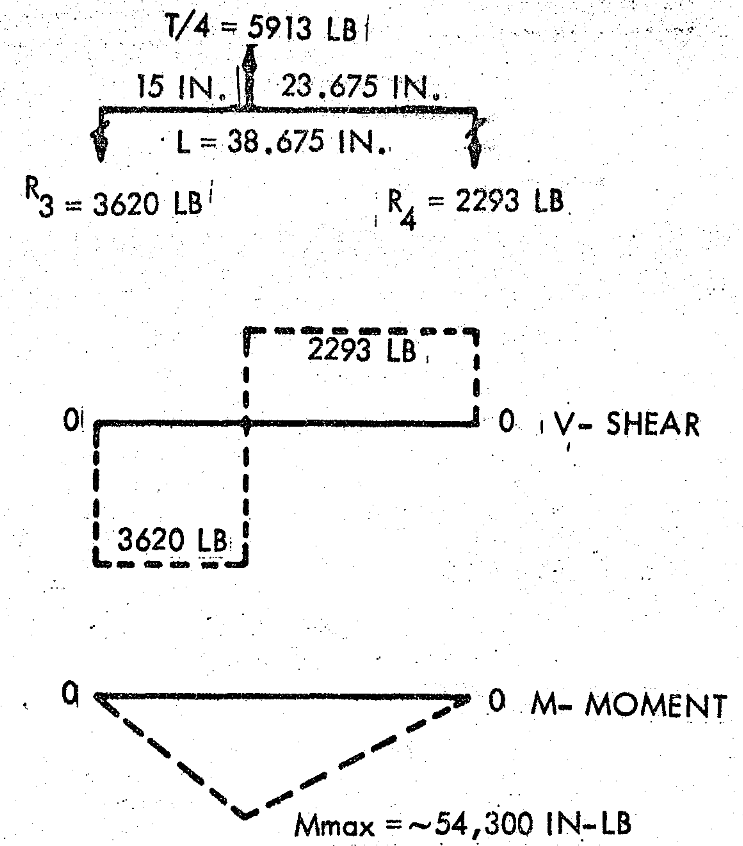

Figure 5-7. Loading - Outside Channel Segment

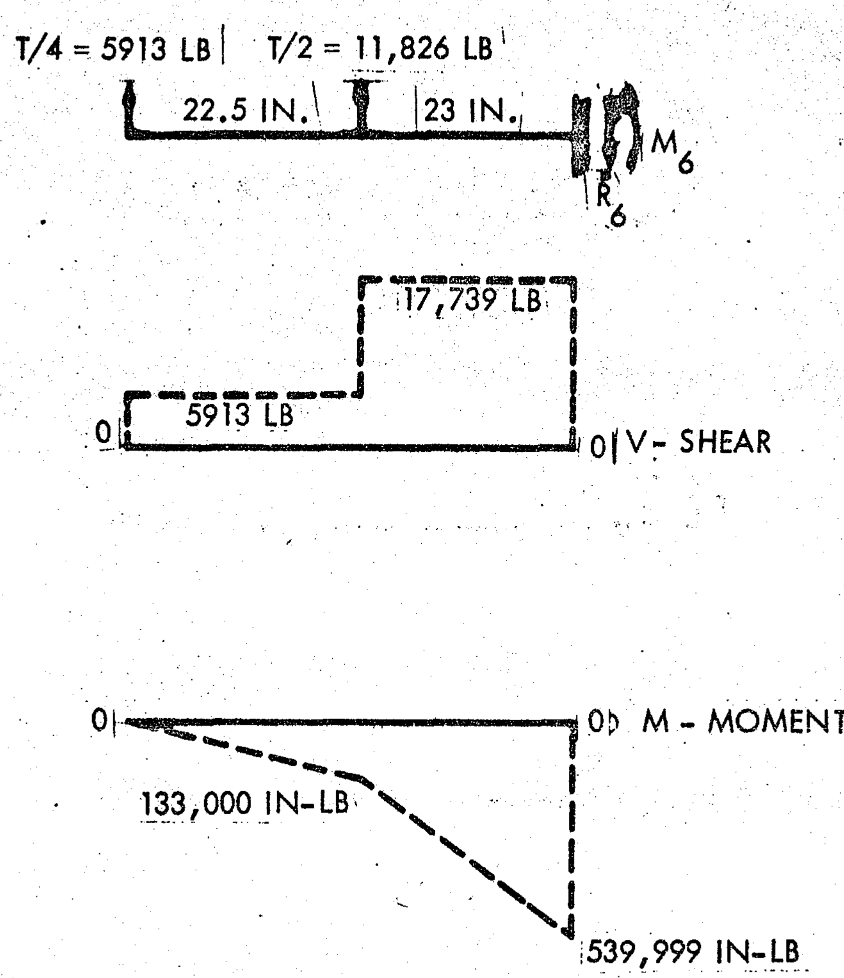

Figure 5-8. Loading - Inside Web

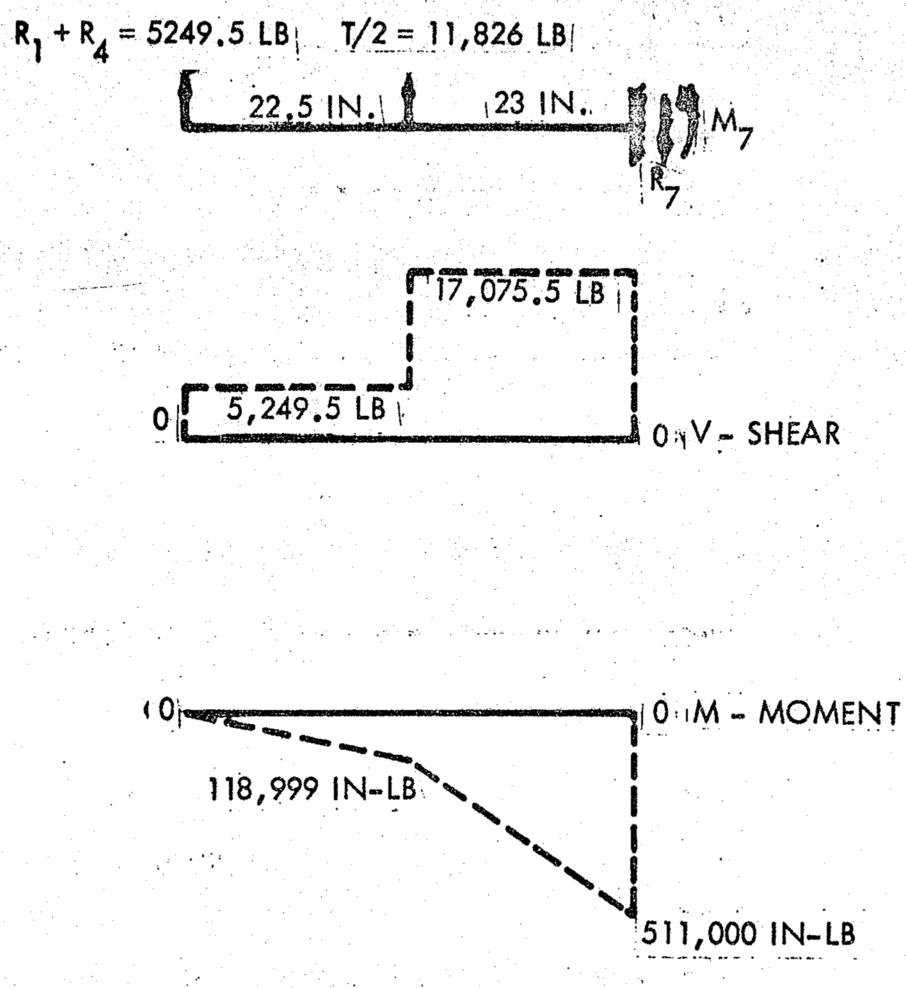

Figure 5-9. Loading - Next-to-End Web

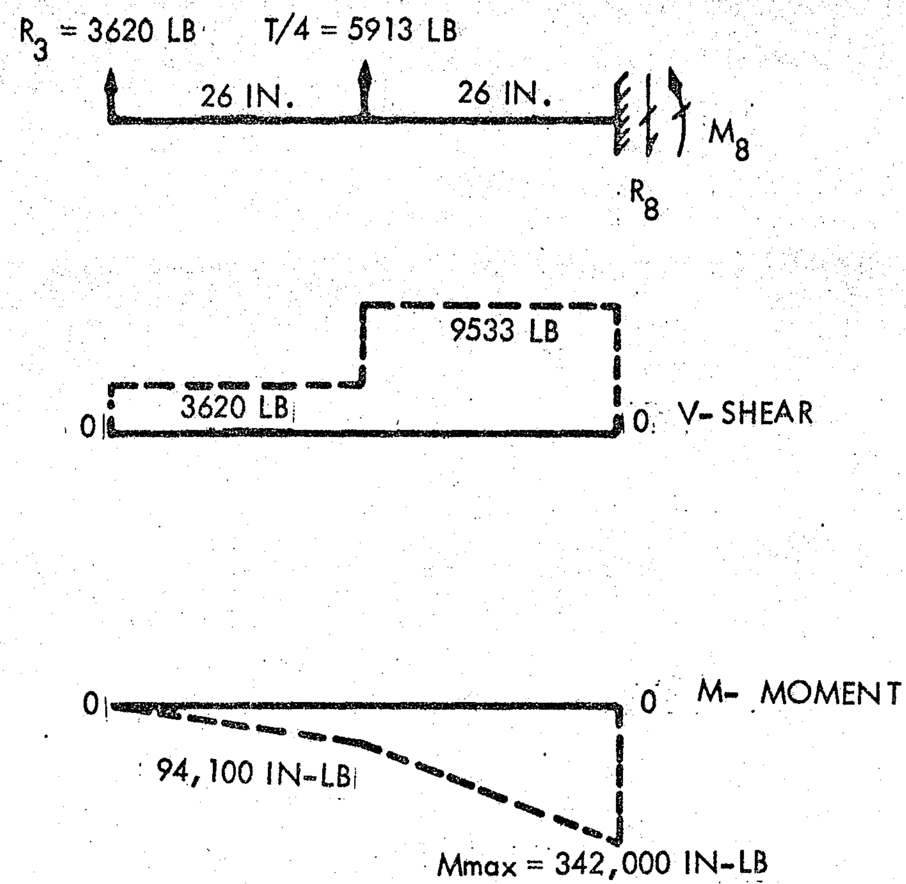

Figure 5-10. Loading - End Web

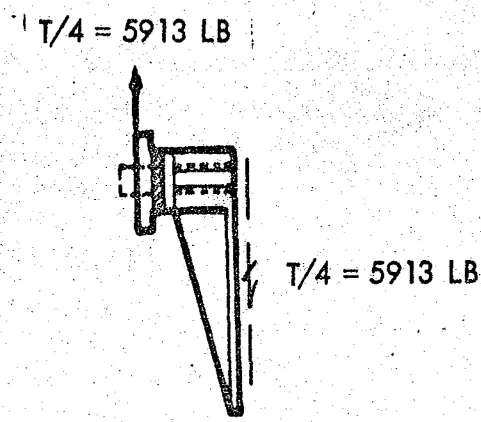

Figure 5-11. Engine Fitting Loading

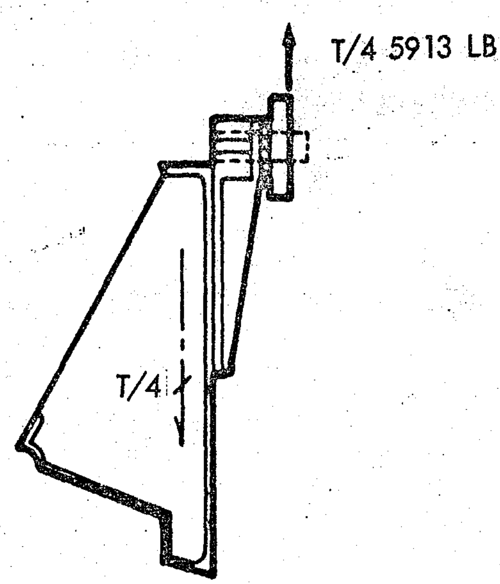

Figure 5-12. Door Seat - Gusset Loading

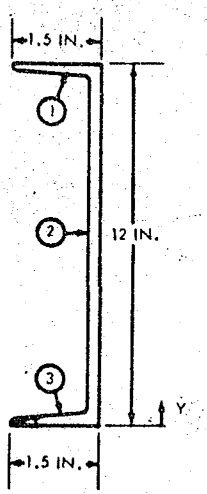

ELE.	t	Area	Y	AY	AY^2	I_0
1	0.125	0.1875	11.937	2.238	26.715	-
2	0.125	1.5000	6	9.000	54.000	18.000
3	0.125	0.1875	0.625	0.012	0.001	-
		1.8750		11.250	80.716	18.000

$\bar{Y} \quad \frac{\Sigma(AY)}{(A)} \quad 11\ 25/1\ 875 \quad 6 \text{ IN.}$

$I \quad \Sigma(AY^2) \cdot I_0 - A\bar{Y}^2$

$80.716 \cdot 18 - 1.875 \times 6^2$

$98.716 - 67.500$

31.216 IN.^4

ELE.	b	t	b/t	Fccn	Area	Pccn
1	1.5	0.125	12	115.0	0.1875	21.55
2	12.0	0.125	96	54.4	1.5000	81.60
3	1.5	0.125	12	115.0	0.1875	21.55
					1.875	124.70

$Fcc_{Avg} \quad 124.70/1.875 \quad 66.5 \text{ KSI}$

1. MATERIAL PROPERTIES

   SELECT PH 15-7 MO -

   Ftu 215,000 psi   E 29.7×10^6 psi
   Fty 211,000 psi   W 0.277 LB-IN^3
   Fcy 200,000 psi   Fsu 140,000 (RATIO NUMBER)

2. MAX LOADS (REF. FIGURE 5-6 - INSIDE CHANNEL SEGMENT)

   V 2956.5 LB   M 70,000 IN-LB

3. ANALYSIS

   ASSUME DEFLECTION CONTROLS THE DESIGN (δ_{max} 0.1 IN.)

   $\delta_{max} \quad \frac{PL^3}{48EI}, \quad \therefore I_{Req'd} \quad \frac{PL^3}{48E\delta_{max}}$

   $I_{Req'd} \quad 5913 \times 47.35^3/48 \times 29.7 \times 10^6 \times 0.1 \quad 4.41 \text{ IN.}^4$

   USE SECTION SHOWN ON LEFT -
   CHECK BENDING STRESS:

   $f_b \quad 70,000 \times 6/31.216 \quad 13.43 \text{ KSI}$

   CRIPPLING ALLOWABLE 66.5 KSI, ∴ HIGH MARGIN

4. WEIGHT IN CHANNEL

   $C \quad \pi D \quad \pi \times 804.95 \quad 2525$

   WT. $1.875 \times 2525 \times 0.277 \quad 1310$ LB

Figure 5-13. Typical Channel Analysis

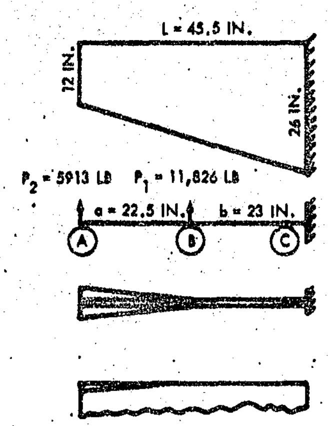

DESIGN:
CONSIDER THE SECTION AT Ⓐ TO BE A 12 x 3 x 20.7 STD. CHANNEL EQUIVALENT WHICH YIELDS THE PROPERTIES (I = 128.1, A = 6.03, S = 21.4 - REF AISC HANDBOOK). THE FLANGES ARE CONSIDERED TAPERED TO 0 AREA AT Ⓑ WHILE KEEPING THE WEB THICKNESS AT 0.28 IN. THE WEB IS THEN TAPERED IN THICKNESS TO 0.14 IN. AT Ⓒ.

1. MATERIAL PROPERTIES:
   SELECT PH15-7MO - $F_{tu} = 215{,}000$ psi $E = 29.7 \times 10^6$ psi
   $F_{ty} = 211{,}000$ psi $W = 0.277$ LB/IN.^{3}
   $F_{cy} = 200{,}000$ psi $F_{su} = 140{,}000$ (RATIO NUMBER)
2. LOADS (REF. FIGURE 5-8 - LOADING INSIDE WEB)
   AT Ⓐ - V = 5913 LB, M = 0, δ max = 0.1 IN.
   AT Ⓑ - V = 17,739 LB, M = 133,000 IN.-LB, δ max = 0.0506 IN.
   AT Ⓒ - V = 17,739 LB, M = 539,000 IN.-LB, δ max = 0
3. ANALYSIS: (ASSUME DEFLECTION CONTROLS THE DESIGN)

δ max at Ⓐ = 0.1 IN. = 1

$$\delta \text{ max at Ⓐ} = 0.1 \text{ IN.} = \frac{P_1 b^2}{6EI}(3L - b) + \frac{P_2 L^3}{3EI}$$

$$= \frac{11{,}826 \times 23^2}{6 \times 29.7 \times 10^6 I}(3 \times 45.5 - 23) + \frac{5913 \times 45.5^3}{3 \times 29.7 \times 10^6 I} = \frac{10.26}{I}$$

$$\therefore I_{REQ'D} = 10.26/0.1 = 102.6 \text{ IN.}^4$$

$$\delta \text{ max at Ⓑ} = 0.0506 = \frac{P_2}{6EI}(2L^3 - 3L^2 X + X^3) + \frac{P_1 b^3}{3EI}$$

$$= \frac{5913}{6 \times 29.7 \times 10^6 \times I}(2 \times 45.5^3 - 3 \times 45.5^2 \times 22.5 + 22.5^3) + \frac{11{,}826 \times 23^3}{3 \times 29.7 \times 10^6 \times I}$$

$$= 3.62/I$$

$$\therefore I_{REQ'D} = 3.62/0.0506 = 71.5 \text{ IN.}^4$$

<u>CHECK DESIGN AT Ⓐ :</u>

$I_{REQ'D} = 102.6$ IN.^{4}, $I = 128.1$ IN.^{4}, $\therefore$ DEFLECTION O.K.

<u>CHECK DESIGN AT Ⓑ :</u> $A = 18.93 \times 0.28 = 5.3$ IN.^{2}

$I_{REQ'D} = 71.5$ IN.^{4}, $I = bh^3/12 = 0.28 \times 18.93^3/12 = \sim 158$ IN.^{4} $\therefore$ O.K.

$f_b = MC/I = 133{,}000 \times 9.465/158 = 7975$ psi

$b/t = 20.75/0.28 = \sim 74$, $b/t \sqrt{F_{cy}/E} = 6.15$, $\therefore F_{ccn} = 26{,}600$ $\therefore$ O.K.

<u>CHECK DESIGN AT Ⓒ :</u> $A = 26 \times 0.14 = 3.64$ IN.^{2}

$I = bh^3/12 = 0.14 \times 26^3/12 = 205$ IN.^{4}

$f_b = MC/I = 539{,}000 \times 13/205 = 34{,}200$ psi

$b/t = 20.75/0.14 = \sim 148$, $b/t \sqrt{F_{cy}/E} = 13.3$, $\therefore F_{ccn} = 35{,}600$ $\therefore$ O.K.

WEIGHT:

$(6.03 + 5.3)/2 \times 22.5 \times 0.277 + (5.3 + 3.64)/2 \times 23 \times 0.277 = 35.3$ LB + 28.5 LB. = 63.8 LB

TOTAL INSIDE WEB WEIGHT = 63.8 x 24 = 1531 LB

Figure 5-14. Inside Web Analysis

C-319

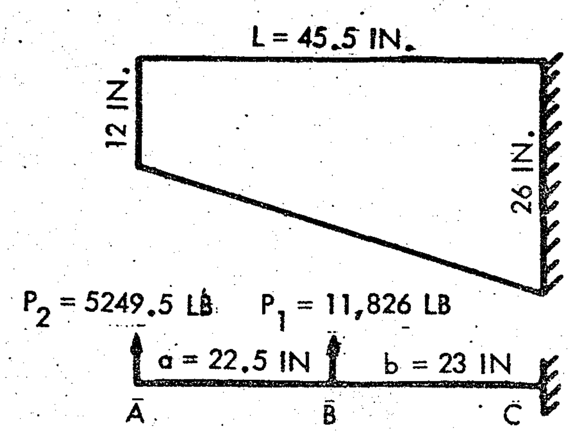

DESIGN :

CONSIDER THE SECTION AT Ⓐ TO BE A 12 x 8½ 20.7 STD. CHANNEL EQUIVALENT WHICH YIELDS THE PROPERTIES ($I = 128.1$, $A = 6.03$, $S = 21.4$ – REF. AISC HDBK). THE FLANGES ARE CONSIDERED TAPERED TO 0 AREA AT Ⓑ WHILE KEEPING THE WEB THICKNESS @ 0.28". THE WEB IS THEN TAPERED IN THICKNESS TO 0.14" AT Ⓒ.

1. MATERIAL PROPERTIES :

SELECT PH15-7 MO – $F_{tu} = 215{,}000$ PSI $E = 29.7 \times 10^6$ PSI
$F_{ty} = 211{,}000$ $w = 0.277$ LB/IN³
$F_{cy} = 200{,}000$ $F_{su} = 140{,}000$

2. LOADS (REF. FIGURE 5-4 LOADING NEXT TO END WEB)

AT Ⓐ – $V = 5249.5$ LB AT Ⓑ – $V = 17{,}075.5$ LB AT Ⓒ – $V = 17{,}075.5$ LB
$M = 0$ $M = 118{,}000$ IN-LB. $M = 511{,}000$ IN-LB.
$\delta_{MAX} = 0.1"$ $\delta_{MAX} = 0.0506"$ $\delta_{MAX} = 0$

3. ANALYSIS : (ASSUME DEFLECTION CONTROLS THE DESIGN)

$$\delta_{MAX} \text{ AT Ⓐ} = 0.1" = \frac{P_1 b^2}{6EI}(3L - b) + \frac{P_2 L^3}{3EI} = 9.55/I$$

$\therefore I_{REQ'D} = 9.55/0.1 = 95.5$ IN⁴

$$\delta_{MAX} \text{ AT Ⓑ} = 0.0506" = \frac{P_2}{6EI}(2L^3 - 3L^2x + x^3) + \frac{P_1 b^3}{3EI} = 3.39/I$$

$\therefore I_{REQ'D} = 3.39/.0506 = 67$ IN⁴

CHECK DESIGN AT Ⓐ :

$I_{REQ'D} = 95.5$ IN⁴, $I = 128.1$ IN⁴ ∴ DEFLECTION O.K.

CHECK DESIGN AT Ⓑ :

$I_{REQ'D} = 67$ IN⁴, $I = bh^3/12 = .28 \times 18.93^3/12 = 158$ IN⁴ ∴ O.K.
$f_b = MC/I = 118{,}000 \times 9.465/158 = 7075$ PSI
$b/t = 20.75/.28 = \sim 74$, $b/t \sqrt{F_{cy}/E} = 6.15$; ∴ $F_{ccr} = 25{,}600$ ∴ O.K.

CHECK DESIGN AT Ⓒ :

$I = bh^3/12 = .14 \times 26^3/12 = 205$ IN⁴
$f_b = MC/I = 511{,}000 \times 13/205 = 32{,}500$ PSI
$b/t = 20.75/.14 = 148$, $b/t \sqrt{F_{cy}/E} = 13.3$; ∴ $F_{ccr} = 35{,}600$
∴ O.K.

WEIGHT :

WT. = 63.8 LB (REF. FIGURE).
TOTAL NEXT TO END WEB WEIGHT = 63.8 x 8 = 510.4 LB

Figure 5-15. Next-to-End Web Analysis

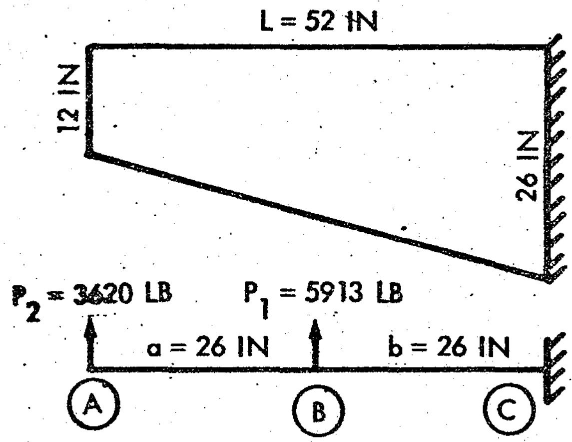

DESIGN:

CONSIDER THE SECTION AT Ⓐ TO BE A 12 x 3 x 20.7 STD. CHANNEL EQUIVALENT WHICH YIELDS THE PROPERTIES (I = 128.1, A = 6.03, S = 21.4 – REF. AISC HDBK). THE FLANGES ARE CONSIDERED TAPERED TO 0 AREA AT Ⓑ WHILE TAPERING THE WEB TO 0.15" THICKNESS. THE WEB IS THEN TAPERED IN THICKNESS TO 0.11" AT Ⓒ.

1. MATERIAL PROPERTIES:

SELECT PH15-7MO – F_{tu} = 215,000 PSI $E = 29.7 \times 10^6$ PSI
F_{ty} = 211,000 W = 0.277 #/IN³
F_{cy} = 200,000 F_{su} = 140,000

2. LOADS (REF. FIGURE 5-15 LOADING END WEB)

AT Ⓐ – V = 3620# M = 0 δ_{MAX} = 0.1"
AT Ⓑ – V = 9533# M = 94,100 IN-LB. δ_{MAX} = 0.05"
AT Ⓒ – V = 9533# M = 342,000 IN-LB. δ_{MAX} = 0

3. ANALYSIS: (ASSUME DEFLECTION CONTROLS THE DESIGN)

$$\delta_{MAX} \text{ AT } Ⓐ = 0.1'' = \frac{P_1 b^2}{6EI}(3L-b) + \frac{P_2 L^3}{3EI}$$

$$= \frac{5913 \times 26^2}{6 \times 29.7 \times 10^6 I}(3 \times 52 - 26) + \frac{3620 \times 52^3}{3 \times 29.7 \times 10^6 I} = \frac{8.625}{I}$$

$\therefore I_{REQ'D} = 8.625 / 0.1 = 86.25 \text{ IN}^4$

$$\delta_{MAX} \text{ AT } Ⓑ = 0.05'' = \frac{P_2}{6EI}(2L^3 - 3L^2x + x^3) + \frac{P_1 b^3}{3EI}$$

$$= \frac{3620}{6 \times 29.7 \times 10^6 I}(2 \times 52^3 - 3 \times 52^2 \times 26 + 26^3) + \frac{5913 \times 26^3}{3 \times 29.7 \times 10^6 I} = \frac{2.955}{I}$$

$\therefore I_{REQ'D} = 2.955 / 0.05 = 59.10 \text{ IN}^4$

CHECK DESIGN AT Ⓐ:

$I_{REQ'D} = 86.25 \text{ IN}^4$, $I = 128.1 \text{ IN}^4$ ∴ DEFLECTION O.K.

CHECK DESIGN AT Ⓑ: $A = 19 \times .15 = 2.85 \text{ IN}^2$

$I_{REQ'D} = 59.10 \text{ IN}^4$, $I = bh^3/12 = .15 \times 19^3/12 = \sim 86 \text{ IN}^4$ ∴ O.K.

$f_b = Mc/I = 94,100 \times 9.5 / 86 = 10,400$ PSI

$b/t = 23.75/.15 = \sim 158$, $b/t \sqrt{F_{cy}/E} = 13.12$, ∴ $F_{CCN} = \sim 35,000$ ∴ O.K.

CHECK DESIGN AT Ⓒ: $A = 26 \times 0.11 = 2.86 \text{ IN}^2$

$I = bh^3/12 = .11 \times 26^3/12 = 161.0 \text{ IN}^4$

$f_b = Mc/I = 342,000 \times 13 / 161.0 = 27,620$ PSI

$b/t = 23.75/.11 = 216$, $b/t \sqrt{F_{cy}/E} = 17.9$, ∴ $F_{CCN} = 28,500$ ∴ O.K.

WEIGHT:

$(6.03 + 2.85)/2 \times 26 \times .277 + (2.85 + 2.86)/2 \times 26 \times .277 = 32^{\#} + 20.55^{\#} = 52.55^{\#}$

TOTAL END WEB WEIGHT = 52.55 × 8 = 420.4#

Figure 5-16. End Web Analysis

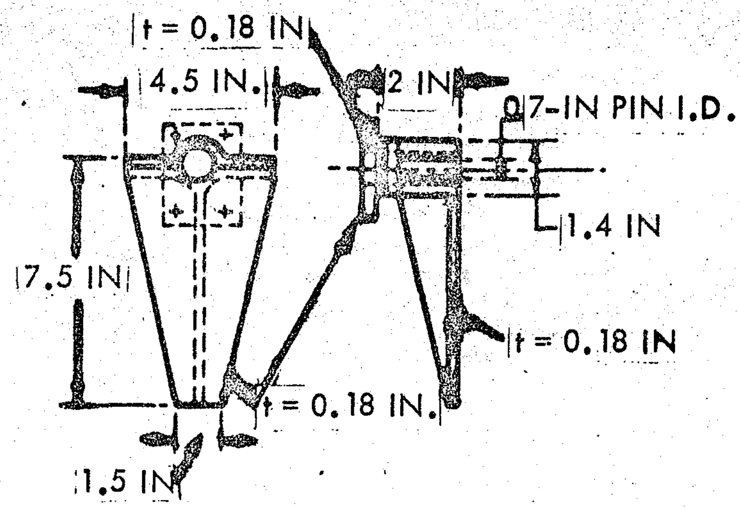

PIN & LUG WEIGHT:

$WT. = \pi(.7^2 - .35^2) \times 2 \times .277 = 0.64^{\#}$

FITTING WEIGHT:

$A_S = (1.5 \times 7.5 + 3 \times 7.5) + (\frac{1}{2} \times 6.5 \times 2)$

$= 11.25 + 22.5 + 6.5$

$= 40.25 \, IN^2$

$WT. = 40.25 \times 0.18 \times 0.277 = 2.005^{\#}$

PLATE WEIGHT:

$A_S = 2.375 \times 3 = 7.125 \, IN^2$

$WT. = 7.125 \times 0.18 \times 0.277 = 0.355^{\#}$

TOTAL WEIGHT = $3^{\#}$

TOTAL FITTINGS = $3^{\#} \times 4 \times 36 = 432^{\#}$

Figure 5-17. Engine Fitting Weights

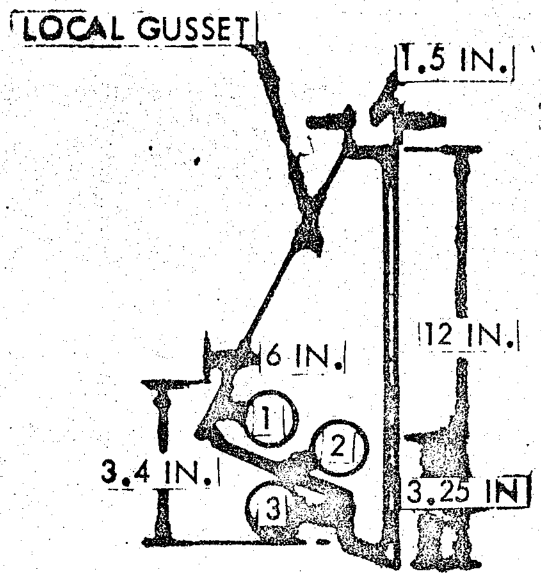

DISTANCE BETWEEN GUSSETS = 47.35 IN.

W = 160 LB/IN. (REF. PRES. DIST. TO SEAT)

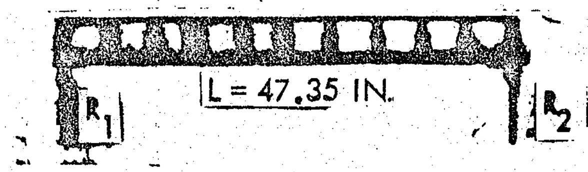

$\bar{W} = 160 \times 47.35 = 7580^{\#}$

$R_1 = R_2 = 7580/2 = 3790^{\#}$

$M_{MAX} = WL^2/8 = 44,800$ IN-lb.

CONSIDERING Z-SECTION ONLY:

FLANGES: $t = 0.1875''$, $b = 1.00''$

WEB: $t = 0.1000''$, $b = 5.00''$

SECTION PROPERTIES – $I = 2.55$ IN^4

$S = 1.5$ IN^3

$A = 0.875$

CHECK CRIPPLING:

ELE	b/t	$b/t\sqrt{F_{cy}/E}$	Fcc	AREA	Pcc
1	5.33	0.442	200	0.1875	37.5
2	50	4.150	90	0.5000	45.0
3	5.33	0.442	200	0.1875	37.5
Σ				0.8750	120.0

$$F_{cc\,AVG.} = \frac{120}{0.875} = 137.2 \text{ KSI}$$

$f_b = Mc/I = 44,800 \times 1.7/2.55 = 29,900$ PSI

∴ HAVE HIGH MARGIN, BUT HAVE NOT CONSIDERED TORSION LOAD OR THERMAL ENVIRONMENT.

CONSIDER GUSSET: GUSSET STABLIZES AREA AND IS USED TO INTRODUCE THE CONCENTRATED LOADS (REF. FIGURE 5-12). GUSSET THICKNESS EQUALS 0.125"

WEIGHTS:

CIRCUMFERENCE OF Z-SECTION EQUALS 2525".

$WT. = 2525 \times 0.875 \times 0.277 = 612^{\#}$

SURFACE AREA OF GUSSET $= \frac{1}{2} \times 6 \times 3.25 + \frac{1}{2} \times 6 \times 8.75 = 36$ IN^2

$WT. = 36 \times 0.125 \times 36 \times 0.277 = 45^{\#}$

Figure 5-18. Door Seat (F and Gusset) Analysis

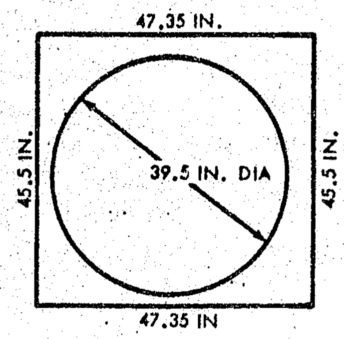

ASSUMED DIMENSIONS SHOWN:

NET SEAL AREA = $(47.35 \times 45.5 - \pi \times 39.5^2/4)\ 36 - 1750$

$= 31{,}600\ IN.^2$

ASSUMING $t_{SEAL} = 0.038$ IN.

WT. = 31,600 X 0.038 X 0.277 = 333 LB

Figure 5-19. Seal Plate Weight

Table 5-9. Summary Weight Statement

STRUCTURAL ITEM	WEIGHT (LB)
CHANNEL ASSY. (REF. FIG. 5-13)	1310
WEB ASSY. (REF. FIGS. 5-14, 5-16)	2480
ENGINE FITTINGS (REF. FIG. 5-17)	432
DOOR SEAT ASSY. (REF. FIG. 5-18)	662
SEAL PLATE ASSY. (REF. FIG. 5-19)	333
TOTAL WEIGHT	5217

thickness serves to yield an excessive weight penalty in a given area, a new honeycomb configuration that is more efficient will be defined for the calculation of "scar weights". The upper and center kick rings will be redesigned and sized to accommodate the new loading. The summation of the weight penalty on SERV will include the increased weight of the upper frustum and the increased weight of the kick rings.

The enveloping geometry utilized in the analysis is depicted in figure 6-1. Figure 6-1 also defines the existing honeycomb panel designs as well as the critical stress condition. Section JI was critical in intracell buckling at a design stress level of 104,638 psi. Section ID was critical for general instability at a design stress level of 25,000 psi.

Section JI of the baseline vehicle received its critical loading at the Max g condition during ascent (t = 150 seconds). The Max g loading summary is presented in figure 6-2. Section ID received its critical loading at the Max q condition during ascent (t = 90 seconds). The Max q loading summary is presented in figure 6-3.

The calculation of the new meridional loading proceed is:

$$\begin{aligned} \text{added payload} &= \text{expendable SERV} - \text{Baseline} \\ &= 250{,}000 - 85{,}125 \\ &= 164{,}875 \text{ lb} \end{aligned}$$

Considering section JI:

$$\begin{aligned} \text{new loading at J} &= 3{,}349 \text{ (reference figure 6-2)} + \frac{164{,}875 \times 3 \times 1.4}{2 \times \pi \times 103.365 \times .707} \\ &= 3{,}349 + 1{,}508 \\ &= 4{,}857 \text{ lb/in.} \end{aligned}$$

Then the new required face thickness is:

working stress = 104,638 psi (reference figure 6-1)

$$\sigma = \frac{\bar{P}}{2t_F} \qquad t_{FREQ'D} = \frac{4857}{2 \times 104{,}638} = 0.0232 \text{ in.}$$

Therefore, the penalty weight may be calculated as:

$$\text{penalty weight} = \frac{\pi D_J + \pi D_I}{2} \times (t_{FNEW} - t_{FOLD}) \times (R_I - R_J) \times \rho\ 2$$

$$= \frac{649.46 + 1287.35}{2} \times (0.0232 - 0.0160) \times (204.887 - 103.365) \times 0.297 \times 2 = 421 \text{ lb}$$

F

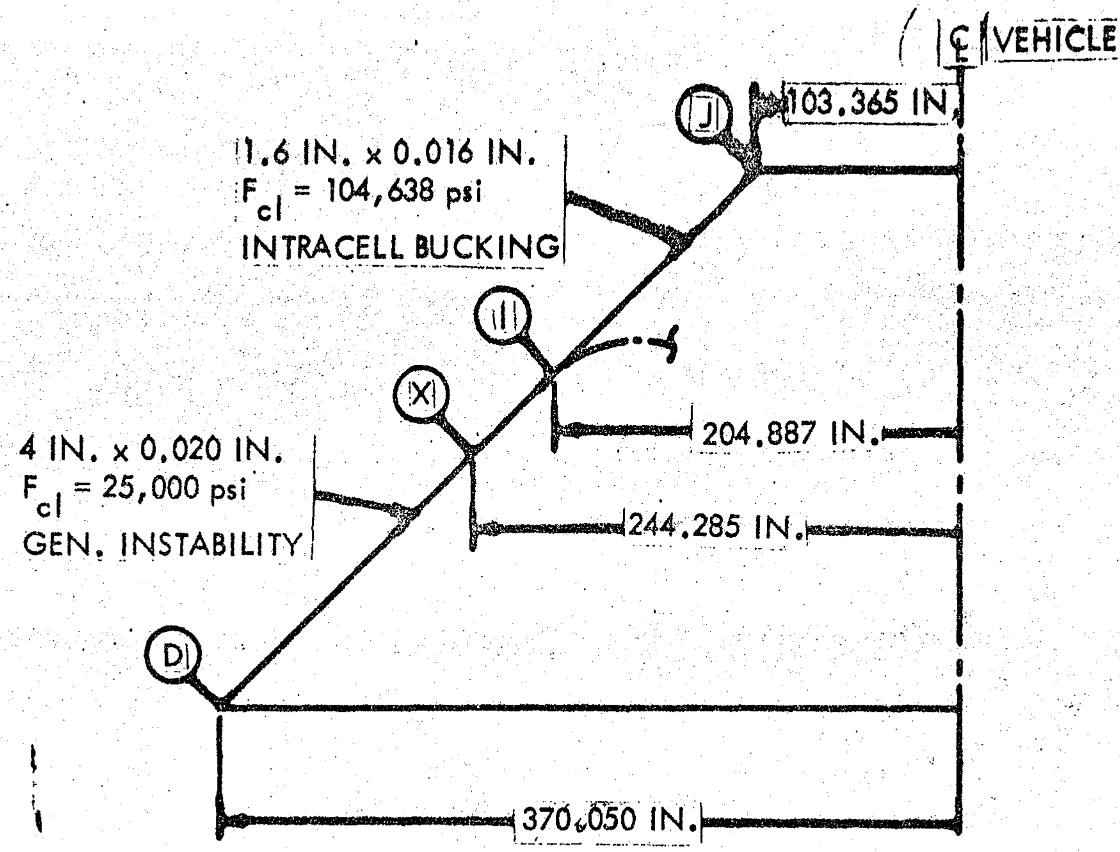

Figure 6-1. Honeycomb Design Geometry

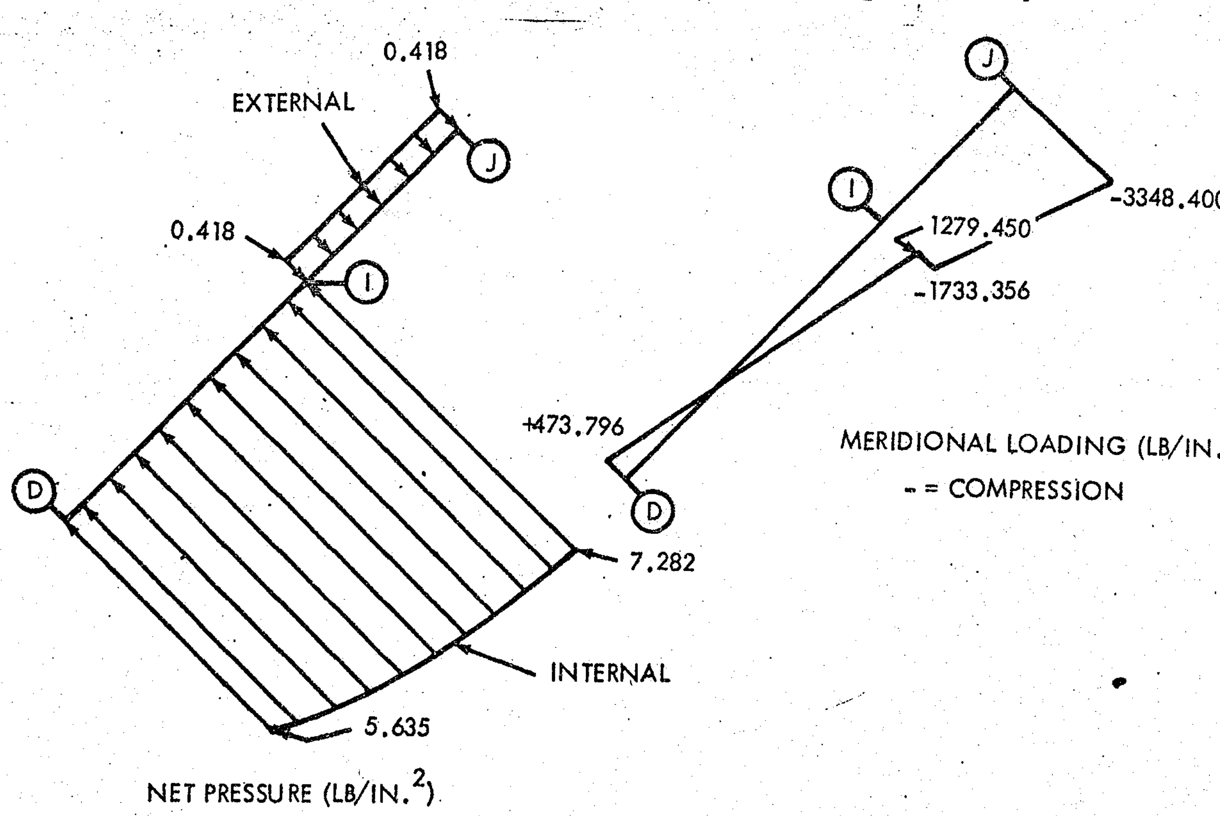

Figure 6-2. Max g Loading Condition (t = 150 Seconds)

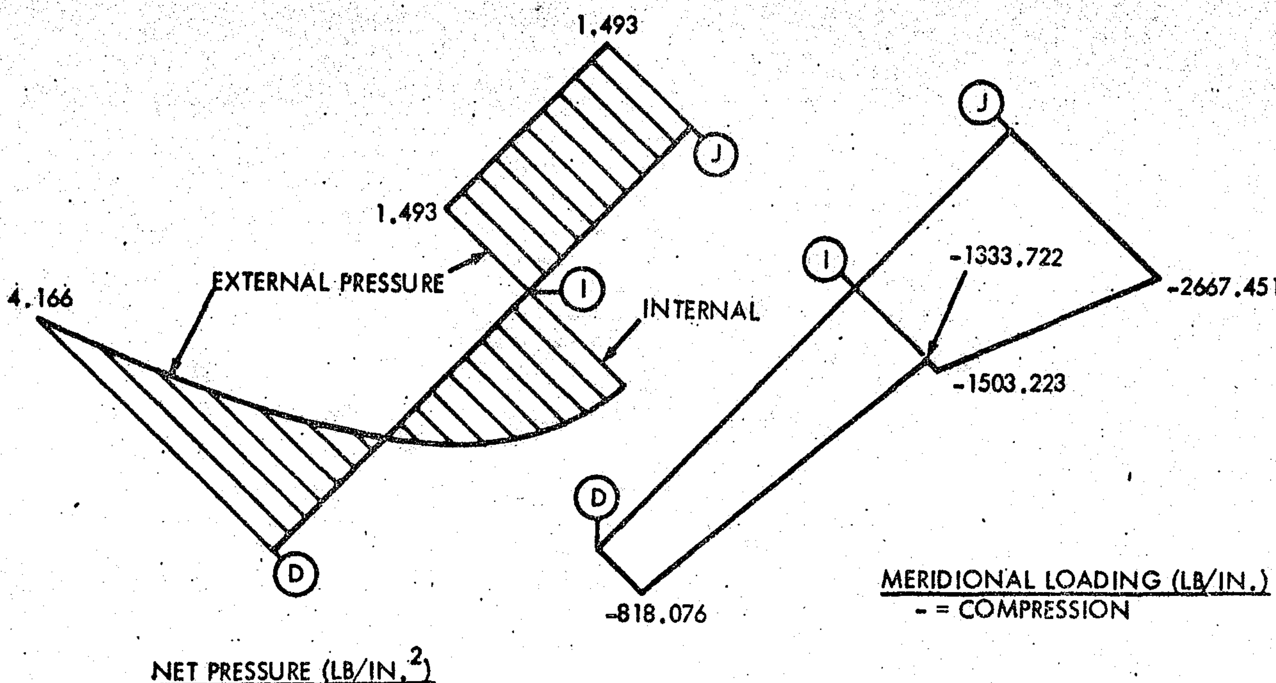

Figure 6-3. Max g Loading Condition (t = 90 Seconds)

Considering Section ID:

new loading at I = 1503 (reference figure 6-3) + $\frac{164,875 \times 3 \times 1.4}{2 \times \pi \times 204.887 \times .707}$

$= 1,503 + 761$
$= 2,264$ lb/in.

new loading at D = 818 (reference figure 6-3) + $\frac{164,875 \times 5 \times 1.4}{2 \times \pi \times 370.05 \times .707}$

$= 818 + 421$
$= 1,239$ lb/in.

Now checking the section at D;

The new required thickness is:

assume working stress equals 25,000 psi (reference figure 6-1)

$$\sigma = \frac{\bar{P}}{2t} \qquad t_{DREQ'D} = \frac{1239}{2 \times 25,000} = 0.0248 \text{ in.}$$

Now checking the section at I;

The new required thickness is:

assume working stress equals 25,000 psi (reference figure 6-1)

$$\sigma = \frac{\bar{P}}{2t} \qquad T_{IREQ'D} = \frac{2264}{2 \times 25,000} = 0.0454 \text{ in.}$$

The weight penalty would then be calculated as:

$$\text{penalty weight} = \frac{1,287.35 + 2,325.10}{2} \times (0.0454 - 0.02) \times (370.05 - 204.887) \times 0.297 \times 2 = 4,500 \text{ lb}$$

Because this is a large penalty, consider a sandwich configuration of 4-in. x 0.04 in. faces and define the stress levels:

$$\lambda F = (1 - u_F^2) = 1 - 0.282^2) = 0.9205$$

$$D = \frac{EF}{12 \lambda F} (t^3 - t_c^3) = \frac{29.7 \times 10^6}{12 \times 0.9205} (4^3 - 3.92^2) = 10.215 \times 10^6$$

$$H = EF (t - t_c) = 29.7 \times 10^6 (4 - 3.92) = 2.375 \times 10^6$$

$$t_e = 2 \left[3 \lambda F \frac{D}{H} \right]^{\frac{1}{2}} = 2 \left[3 \times 0.9205 \times \frac{10.215 \times 106}{2.375 \times 10^6} \right]^{\frac{1}{2}} = 6.89 \text{ in.}$$

$$E_e = H/t_e = \frac{2.375 \times 10^6}{6.89} = 0.3445 \times 10^6$$

The hoop stress analysis is:

$$Re = \frac{R_1 + R_2}{2 \cos} = \frac{204.887 + 370.05}{2 \times 0.707} = 406.603 \text{ in.}$$

$$Z = \frac{L^2(1 - u_F^2)^{\frac{1}{2}}}{} = \frac{377^2(1 - 0.282^2)^{\frac{1}{2}}}{406.603 \times 6.89} = \sim 49 \quad \therefore KP = 5$$

$$\left.\frac{\sigma CR}{\eta}\right]_e = \frac{Rp\ \pi^2 Ee}{12(1-\mu F^2)} \left(\frac{te}{L}\right)^2 \frac{R2}{Re \cos\alpha}$$

$$\left.\frac{\sigma CR}{\eta}\right]_e = \frac{5 \times \pi^2 \times 0.3445 \times 10^6}{12 \times 0.9205} \left(\frac{6.89}{377}\right)^2 \frac{370.05}{406.603 \times 0.707} = 659$$

$$\left.\frac{\sigma CR}{\eta}\right] = 659 \left(\frac{t}{t - tc}\right) = 659 \frac{4}{4 - 3.92} = 32{,}950 \text{ psi}$$

$$\sigma = \frac{PR2}{2t_F \cos\alpha} = \frac{4.166 \times 370.05}{2 \times 0.04 \times 0.707} = 27{,}300 \text{ psi}$$

therefore $Rp = \frac{27{,}300}{32{,}950} = 0.83$

The meridional stress analysis is:

$$Re = \frac{R_1}{\cos\alpha} = \frac{204.887}{0.707} = 290$$

$$Re/te = \frac{290}{6.89} = 42.1 \qquad \therefore Cc = 0.235$$

$$\left.\frac{\sigma CR}{\eta}\right]_e = \frac{CcEete}{Re} = \frac{0.235 \times 0.3445 \times 10^6 \times 6.89}{290} = 1{,}925$$

$$\left.\frac{\sigma CR}{\eta}\right] = 1{,}925 \times \frac{4}{0.08} = 96{,}250 \text{ psi}$$

$$\sigma = \frac{818 + 421}{2 \times 0.04} = \frac{1{,}239}{0.08} = 15{,}490 \text{ psi}$$

$$Rc = \frac{15{,}490}{96{,}250} = 0.161$$

$$Rp + R_C \leq 1.0$$

$$0.83 + 0.161 \leq 1.0$$

$0.991 < 1.0$ Configuration satisfactory

The penalty weight is then:

$$\text{penalty weight} = \frac{0.02}{0.0254} (4{,}500) = 3{,}540 \text{ lb}$$

The added loading on the upper kick ring is calculated as:

$$P^1 = 1{,}503 \times 0.707 = 1{,}066 \text{ lb/in.}$$

Therefore the new design loading is

$$\overline{P} = 2{,}034 \text{ lb/in. (see table 18, volume 3, appendix E)} + 1{,}066 = 3{,}100 \text{ lb/in.}$$

The area required is calculated as:

$$A_{REQ'D} = \frac{R}{F} = \frac{3{,}100 \times 103.365}{200{,}000} = 1.602 \text{ in.}^2 \text{ (assuming F = 200,000 psi)}$$

This area corresponds to a weight of:

$$\text{Weight} = 653 \times 1.602 \times 0.297 = 311 \text{ lb}$$

The existing ring weight was calculated to be 205 lb which would yield a penalty weight of 106 lb.

The added loading on the center kick ring is calculated as:

$$P^1 = 421 \text{ lb/in.} \times 0.707 = 298 \text{ lb/in}$$

Therefore, the new design loading is:

$$\overline{P} = 1{,}309 \text{ lb/in. tension (see table 18, volume 3, appendix E)} + 298 = 1{,}607 \text{ lb/in.}$$

Therefore, the area required is:

$$A_{REQ'D} = \frac{R}{F} = \frac{1{,}607 \times 370.05}{211{,}000} = 2.81 \text{ in.}^2 \text{ (where F = 211,000 psi)}$$

$$\text{Weight} = 2{,}325 \times 2.81 \times .297 = 1{,}940 \text{ lb}$$

The penalty weight would be:

penalty weight = new weight - reference weight
= 1,940 - 1,585 = 355 lb

In summary, the total penalty weight (i.e. scar weight) for the expendable SERV is:

section JI	421 lb	
section ID	3,540 lb	
upper kick ring	106 lb	
center kick ring	355 lb	
Total Penalty		4,422 lb

The scar weight for the reusable SERV configuration for a due-east launch can be obtained by rationing the payload changes to the above weights because the loading change is strictly meridional. The payload for the reusable SERV is 119,652 lb. The ratio is:

$$\text{Ratio} = \frac{119{,}652 - 85{,}125}{164{,}875} = 0.21$$

In summary, the total penalty weight for the reusable SERV in a due-east launch is:

section JI	0.210 x	421 =	88 lb	
section ID	0.210 x	3,540 =	742 lb	
upper kick ring	0.210 x	106 =	22 lb	
center kick ring	0.210 x	335 =	74 lb	
	Total Penalty			926 lb

REFERENCES

1. Moellering, E., Discontinuity Stress in Axisymmetric Shell by Direct Stiffness Method - Program Number CR0033, CCSD Report TN-SE-67-126, April 1967

2. ICC, J. E. Harris to C. E. Tharratt, "SERV Task 4 Baseline Vehicle", 8 February 1971

3. ICC, B. L. Seider to J. H. Wood, "SERV Task 4 Design Reference Trajectory and Performance Weight Summaries", 15 February 1971

4. ICC, J. M. Landon to C. E. Tharratt, "SERV Dry Weight = 90 x 16 Reference Vehicle Structure", 18 January 1971

5. Bruhn, E. F., Analysis and Design of Flight Vehicle Structures, 1965

6. Shell Analysis Manual, MSC, June 1966

7. ICC, J. D. Magness to J. M. Landon, "SERV Landing Gear Assembly Weights", 12 March 1971

8. ICC, R. C. Pocklington to J. H. Wood, 2780/1/2/55, "Reference Reentry Trajectories for the SERV Task 4 Baseline Vehicle", 22 February 1971

9. ICC, B. Widofsky to J. Wood, 2780/1/3/110, "Comparison of a Silicone Elastomer and Avcoat 5026-39 Ablator for SERV", 26 March 1971

10. Metallic Materials and Elements for Aerospace Vehicle Structure MIL-HDBK-5A, 8 February 1966

11. Chrysler ICC, D. W. Wolsefer to J. H. Wood, "Thermal Protection Concepts for SERV Conical Honeycomb Structures", 22 March 1971

12. Chrysler ICC, R. C. Smith to J. H. Wood, "Effect of Temperature Gradients on SERV Structural Weight", 28 January 1971

13. Gallatly, R. A. and Gallagher, R. H., "Stresses in Sandwich Cylinders" Machine Design, 26 March 1964

14. AISC Steel Handbook, sixth edition, copyright 1965

15. NASA Astronautics Structures Manual

16. Gerard, G and Becker, H., Handbook of Structural Stability Part III - Buckling of Curved Plates and Shells, NACA TN 3783, August 1957

APPENDIX D

METEOROID PROTECTION ANALYSIS

APPENDIX D
METEOROID PROTECTION ANALYSIS

D.0 GENERAL

Space vehicles are subjected to encounters with meteoroids that could cause considerable damage to vital components of the vehicle. To ensure adequate mission reliability, it is necessary to provide protection against this hazard. The most promising technique for protecting vital components and structures is to erect a thin bumper shield a short distance from the item to be protected. The shield serves to disintegrate the incoming meteoroid, allowing only a relatively diffuse cloud of debris to strike the component. With the bumper shield, the rear wall need only withstand the impact of a cloud instead of a solid incoming meteoroid. The meteoroid environment and shield models used, the method of analysis, and results obtained are described in this appendix.

D.1 METEOROID ENVIRONMENT

Meteoroid flux varies considerably during the course of a year, and the total activity comprises two components: 1) a fairly constant although sporadic component associated with meteoroid streams, and 2) the stream flux that has well defined recurring peaks associated with the individual meteoroid streams. The intensity of the individual streams can vary up to 20 times that of the background, or sporadic flux.

It is a simple matter to use a sporadic environment model, which is time-invariant, to determine the shielding requirements. However, computation of the meteoroid design mass for the stream fluxes is more difficult since they vary from day to day and stream to stream. Since the exact mission times (day or month) were not known, the stream flux parameters were time-averaged.

The meteoroid environment selected for this analysis was the average accumulative total meteoroid flux-mass model proposed by B. G. Cour-Palais, et al (reference D-1). Mathematically the meteoroid flux-mass relationship can be expressed as follows:

$$\log_{10}N_t = -14.339 - 1.584(\log_{10}M) - 0.063(\log_{10}M)^2, \text{ for } 10^{-12} \leq M \leq 10^{-6} \text{ and}$$

$$\log_{10}N_t = -14.37 - 1.213(\log_{10}M), \text{ for } 10^{-6} \leq M \leq 10^{0}$$

where:

N_t is the average unshielded focused accumulative total flux (number of particles of mass, M, or greater per square meter per second), and

M is the meteoroid design mass (gm).

Figure D-1 depicts this meteoroid flux-mass relationship graphically. Other pertinent data used in conjunction with this model are listed below:

1) Average velocity of 20km/sec.
2) Average density of $0.50 gm/cm^3$.
3) Spherical shape.

The actual number of meteoroid impacts received by a vehicle in cislunar space depends upon the vehicle altitude above the Earth or moon. This dependence on altitude results from two phenomena, gravity focusing and body shielding. The gravitational attraction of the earth or moon will tend to enhance the meteoroid flux near the surface, and the gravitational focusing will decrease with distance from the surface. To correct for this phenomenon, the average cumulative total meteoroid flux given in figure D-1 must be corrected by multiplying by a defocusing factor, G_e. The defocusing factor used in the analysis is illustrated in figure D-2 (reference D-2). These data assume the gravitational effect influences only the lower-velocity sporadic meteoroids, and hence the effect on the flux of the stream meteoroids has been omitted.

The other altitude correction that must be applied to the flux accounts for shielding provided by the Earth or moon. This occurs not only when the planet shields the vehicle from the impacts of sporadic meteoroids but also when the spacecraft, planet, and meteoroid stream are aligned so as to block the impacts of the stream meteoroids. The shielding factor (ζ) used in this analysis was computed from the following: (reference D-3)

$$\zeta = \frac{1 + \cos \theta}{2}$$

where

$$\sin\theta = \frac{R}{R + H},$$

R is the radius of the shielding body,

H is the altitude of the spacecraft above the surface.

In developing these equations it was assumed that the space vehicle was spherical and randomly oriented. The shielding factor for the Earth is presented as a function of altitude in figure D-3. This shielding factor will yield only a small error in the total flux impacting on any shaped, randomly oriented space vehicle, when multiplied by the unshielded defocused flux. Hence the total corrected flux can be found by multiplying the unshielded focused flux by the defocusing factor (G_e) and the body shielding factor (ζ); that is:

$$N_{TC} = G_e \cdot \zeta \cdot N_T$$

where

N_{TC} is the average corrected accumulative total flux (number of particles of mass, M, or greater per square meter per second).

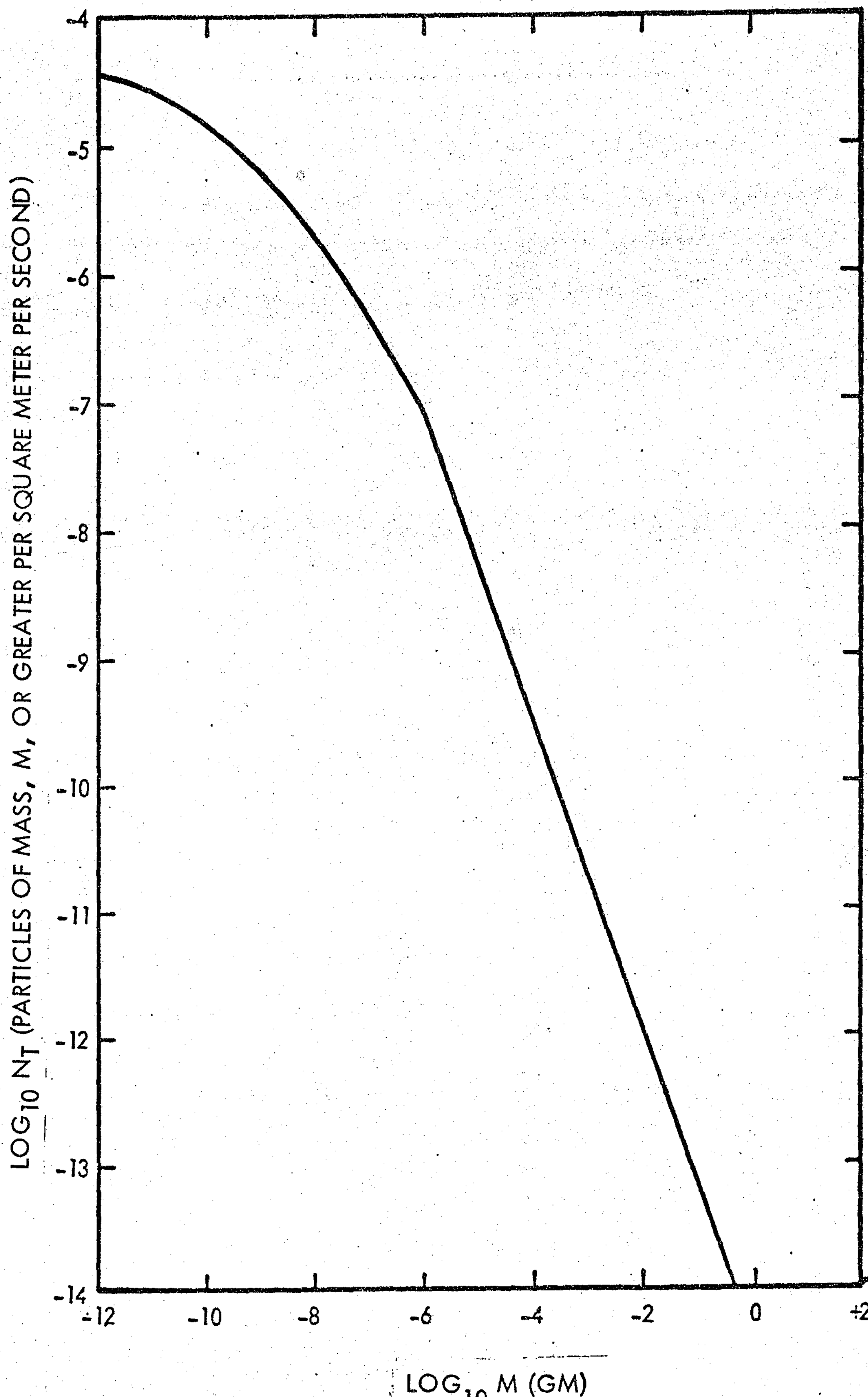

Figure D-1. Average Unshielded, Focused Cumulative Total Meteoroid Flux-Mass Model for 1 au

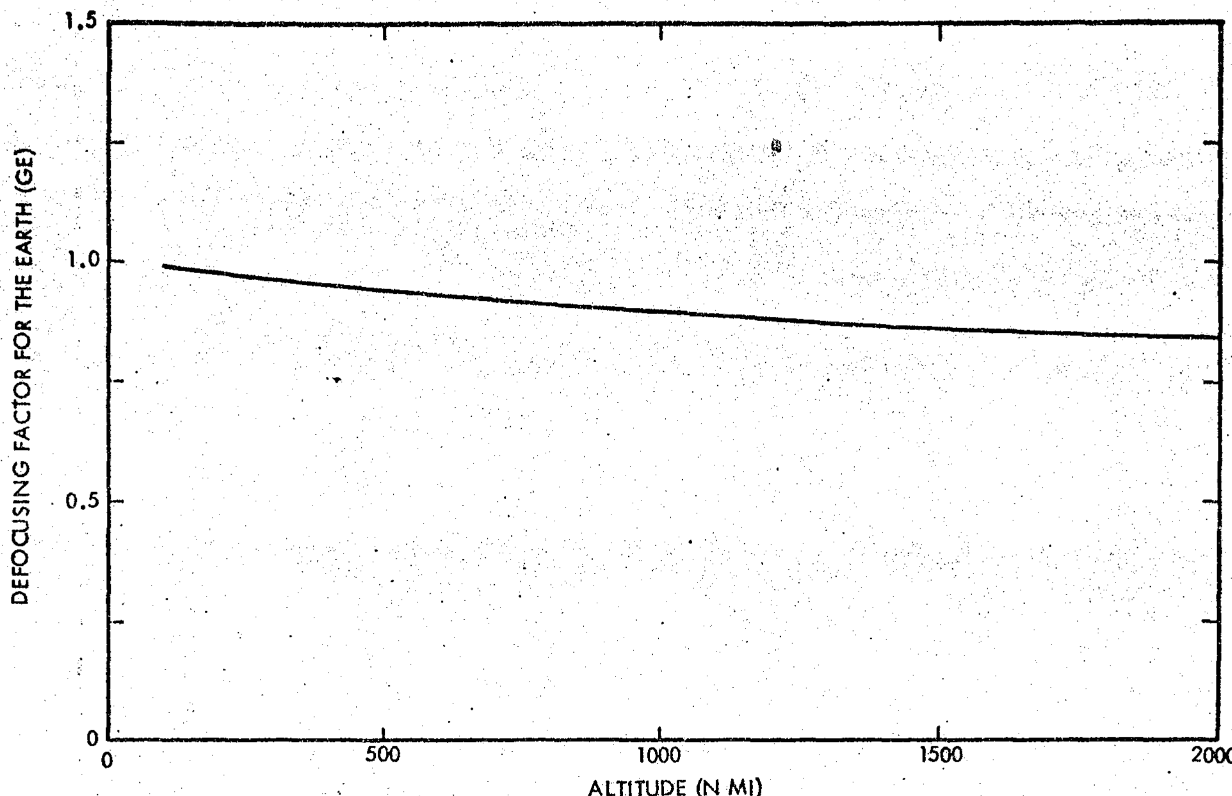

Figure D-2. Defocusing Factor for the Earth

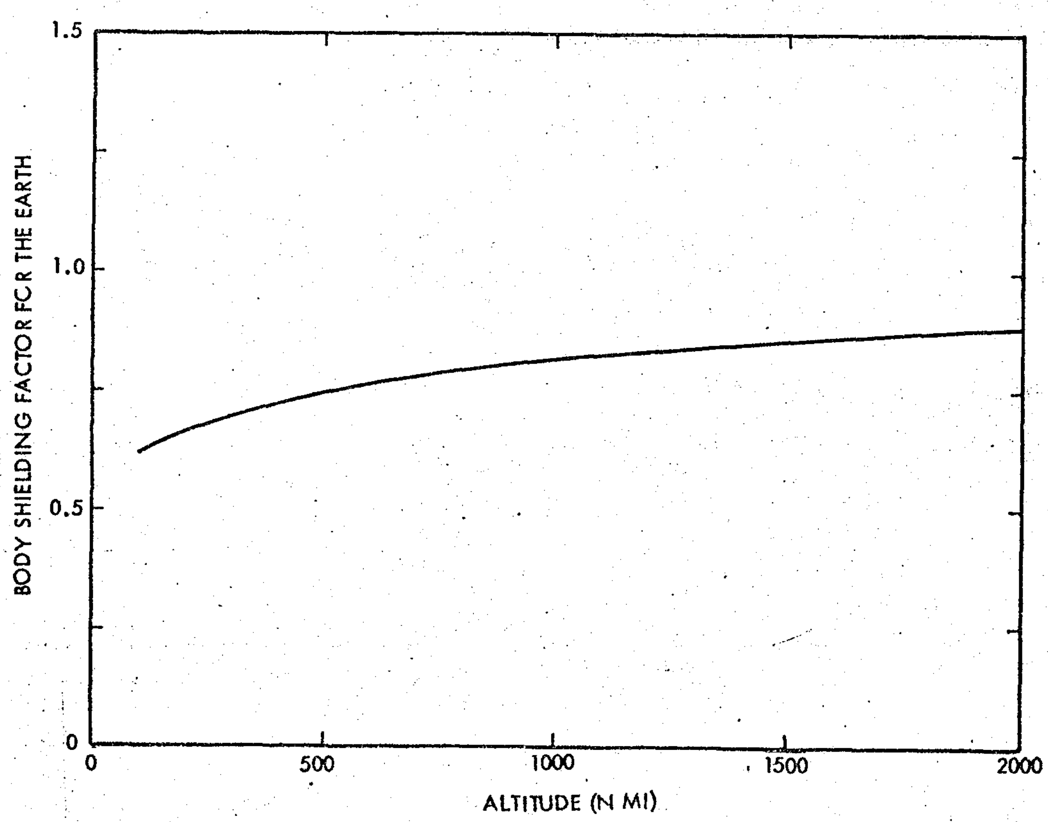

Figure D-3. Shielding Factor for the Earth

D.2 METEOROID DESIGN MASS

The present method of protecting a space vehicle from meteoroid damage is to ensure that the meteoroids do not impact directly on vital components. This is accomplished by designing the protective shield so that the largest meteoroid likely to be encountered during the mission will not penetrate the shield. The probablity of encountering a meteoroid having a specific design mass is a function of the meteoroid flux, the area exposed and the time spent in the environment. Mathematically this can be expressed as:

$$P_o = \exp(-N_{TC}AT)$$

where

P_o is the probability of not being hit,

A is the area exposed (m^2), and

T is the exposure time (sec.).

Substituting for the corrected flux, and then solving for the focused-unshield total average accumulated flux,

$$N_T = \frac{\log_e P_o}{-\zeta G_e AT}$$

it is possible to determine the corresponding meteoroid design mass from the environment (see figure D-1).

D.3 METEOROID SHIELD MODEL

Whipple's bumper shield concept was used as a means of protecting the vehicle from meteoroid damage since this is the most promising technique. Basically, the concept consists of a thin outer shield and a primary or backup structure. The thin shield which surrounds the space vehicle (see figure D-4) fragments the incoming meteoroid into a relatively diffuse cloud of smaller particles. The debris then impinges on a second backup wall or sheet. Since the backup wall is impacted by the diffuse debris cloud, the damage done to the spacecraft itself is much less than if it had been struck directly by the meteoroid.

The most important element in this type of meteoroid protection system is the shield or bumper, since it controls the physical state of the debris in the cloud. The cloud consists not only of the disintegrated meteoroid, but a significant amount of shield material. The debris, from both the shield and the meteoroid, can take the form of solid particles, liquid droplets, vapors, or some combination. Since it is evident that an all-gaseous debris cloud would produce the least damage to the back-up sheet, it is desirable to design the shield to vaporize the debris. In order to accomplish this it is necessary to look at the phenomena through which it can be achieved.

B. G. Cour-Palais (reference D-4) reasons that the impact of a hypervelocity meteoroid on a shield produces intense compressive shock waves which travel

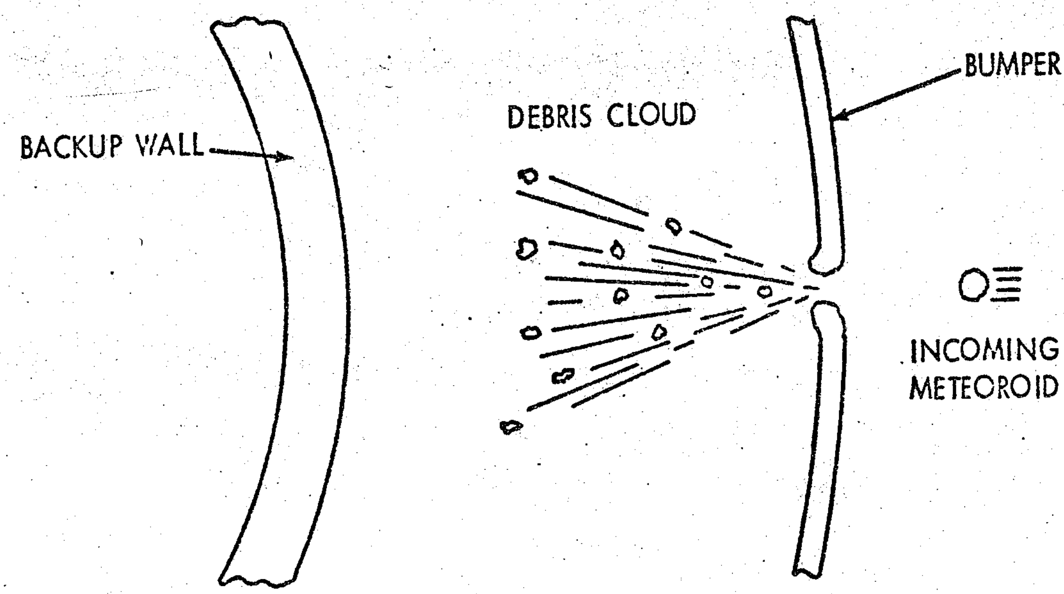

Figure D-4. Whipple's "Bumper Shield" Concept

G

forward in the bumper and rearward in the particle. Since the shock waves are not isentropic, they increase the internal energy of both the shield and meteoroid. When the internal energy of debris exceeds its fusion energy or sublimation energy, the debris either becomes molten or vaporizes.

The maximum internal energy increase will occur when the unloading wave, which is reflected from the rear surface of the shield, overtakes the compressive wave in the meteoroid as the latter reaches the rear end of the particle. Therefore, the shield should be designed to a thickness which is proportional to the particle diameter. According to Cour-Palais (reference D-4), the optimum product of the bumper thickness and density falls between 0.1 and 0.2 of the product of the meteoroid diameter and density. However, he states that because there are more small particles in the meteoroid population than the size corresponding to this optimum ratio, a shield thickness-density product of the order of 0.3 of the meteoroid diameter-density product should be used. Mathematically, this can be expressed as:

$$t_s \simeq 0.3D(P_m/P_s)$$

where

t_s is the thickness of the bumper or shield (cm),

D is the diameter of the meteoroid (cm),

P_m is the meteoroid density (gm/cm^3), and

P_s is the shield density (gm/cm^3).

When the bumper thickness falls outside the optimum region ($0.1 \leq P_s t_s/P_m D \leq 0.2$), the design of the backup sheet is governed by solid fragments in the meteoroid and the shield debris cloud. The Manned Space Center's emperical formula for the nonoptimum regions, which was used to calculate the backup wall requirements, is given by the following (reference D-4):

$$t_b = \frac{0.055\,(P_s P_m)^{1/6}\, M^{1/3}\, V}{S^{1/2}} \left(\frac{7000}{\sigma}\right)^{1/2},$$

where

t_b is the thickness of the backup wall (cm),

m is the meteoroid mass (gm),

V is the meteoroid velocity (km/sec),

S is the spacing between the shield and backup wall (cm),

σ is the 0.2 percent yield stress for the backup wall material (lb/in^2),

P_s is the density of the shield material (gm/cm^3), and

P_m is the density of the meteoroid (gm/cm^3).

Although the validity of the above expression has not been completely established, preliminary evidence suggests that it is valid for bumper-backup wall spacings between 10 and 30 particle diameters (reference D-5).

D.4 METEOROID SHIELD RESULTS

Whipple's bumper shield concept previously discussed was used as a model for the SERV meteoroid shield. As illustrated in figure D-5, the front sheet of the TPS honeycomb panel was utilized as the bumper. The combined thicknesses of the rear sheet of the TPS honeycomb panel and front sheet of the structural honeycomb panel was used as the backup wall. The Task 4 baseline vehicle was analyzed in three sections due to the various sizes of honeycomb used, and figure D-6 depicts the general configuration. Table D-1 gives the thicknesses of the honeycomb panels and the resulting meteoroid shields required for each portion of the vehicle. Each of the four honeycomb face sheets were assumed to have a density of 505 lb/ft^3 and a 2 percent yield stress of 200,000 psi.

A computer program was used to determine the shielding requirements necessary to afford the desired protection of 0.995 probability of no hits by meteoroids having a design mass or larger. The required bumper thickness-density product was assumed to be 0.30 times the product of the diameter and density of the design meteoroid. Although this did not give the optimum thickness, it yielded results that are accurate enough for preliminary designs. The reasons for this are twofold. First as discussed in paragraph D.3, even though the optimum bumper product range is between 0.10 and 0.20 particle diameters, the bumper is usually designed to a slightly higher value; and second, even at a ratio of 0.30, the bumper thicknesses were found to fall below the minimum allowable skin gauges for manufacturing. As shown in figure D-7, the latter was found to be the case on all three frustums.

The spacing between the bumper and backup sheet used was equal to the core thickness of the TPS honeycomb panel. The spacing in all cases was found to be greater than the minimum ratio of ten times the meteoroid diameter.

The backup wall thickness requirements were computed using MSC's empirical relation (section D.3). Figures D-8, D-9, and D-10 depict the required backup sheet thicknesses for the upper, middle and lower frustums, respectively. In cases where the spacing between the backup wall and bumper exceeded 30 meteoroid diameters the program sized the backup sheet on the basis of 30 diameters, although the spacing was actually larger. This condition occurred in several instances. The spacing in the upper frustum has a spacing-diameter ratio greater than 30 up to 7 days, while the lower frustum drops below a ratio of 30 at approximately 6 hours. Figure D-9 shows that the spacing-diameter ratio of the middle frustum falls below the 30 at 2.6 days, where the slope of the required thickness curve changes abruptly.

The computer program determined the additional thickness required to provide the necessary meteoroid protection in cases where the required thickness exceeded the actual thickness and computed weight associated with this delta thickness. Figure D-11 shows that additional weight is required to provide the necessary meteoroid protection at approximately 4½ days into the mission. This weight is due of the added thickness required in the backup wall in the lower frustum, caused by the small bumper-backup wall spacing, which is close to minimum (S/D=10). From figure D-10 it can be seen that only 0.001 or 0.002 inches of additional

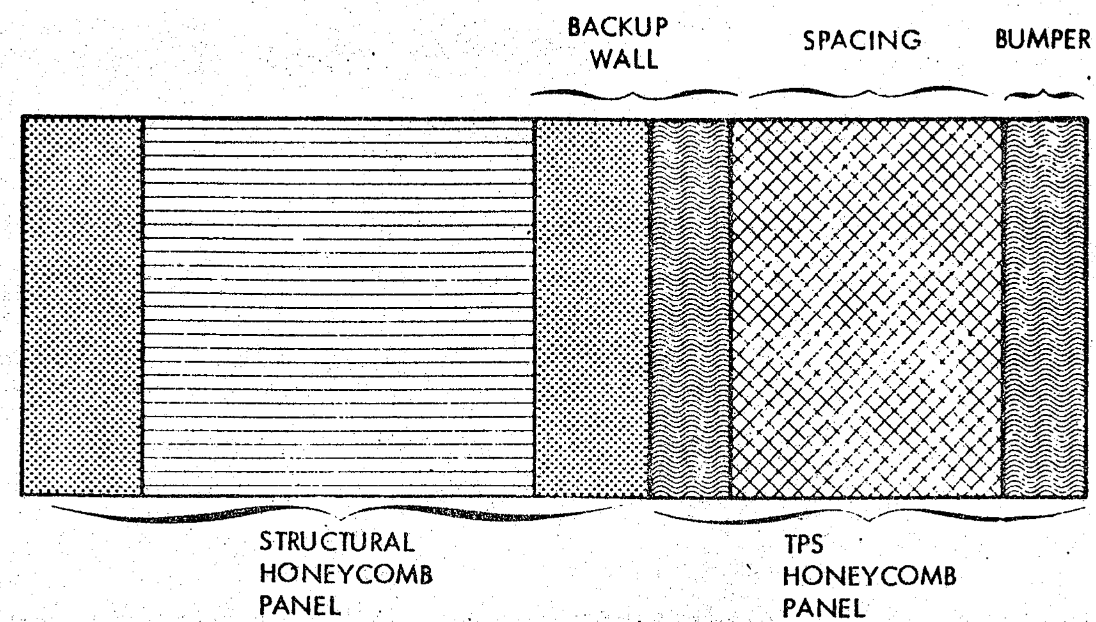

Figure D-5. Meteoroid Shield Model for SERV

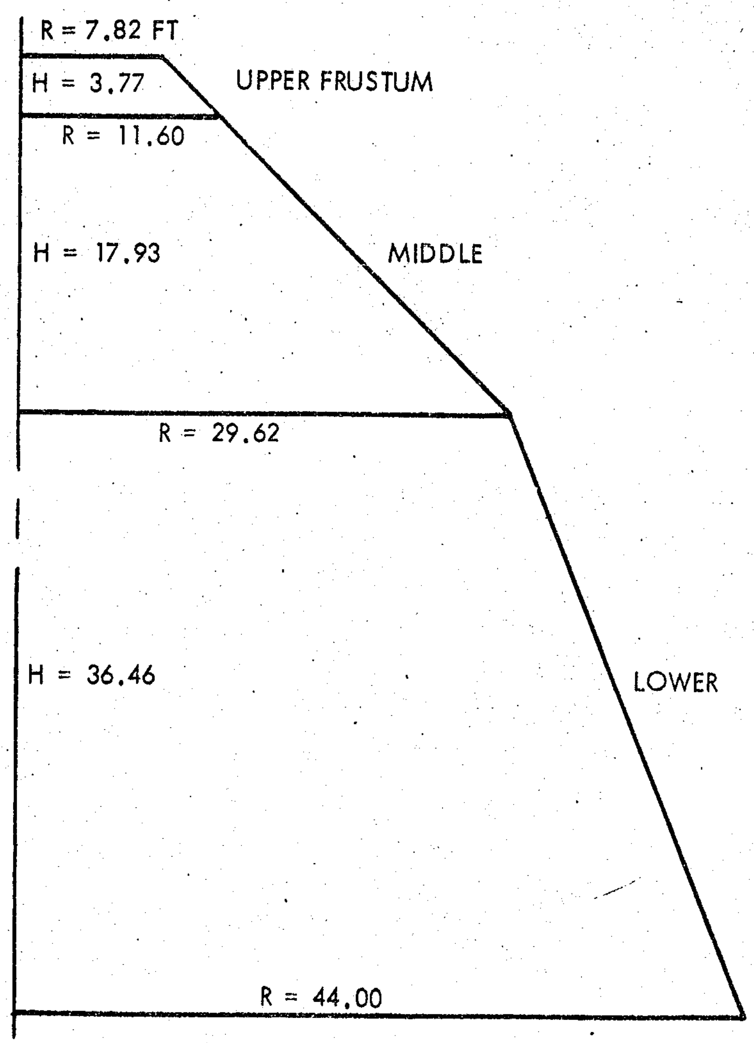

Figure D-6. SERV Geometry Used for Meteoroid Protection Analysis

Table D-1. Honeycomb Panel and Meteoroid Shield Thicknesses

Thicknesses (inches) \ Location	Frustum		
	Upper	Middle	Lower
<u>TPS Honeycomb Panel</u>			
Front Sheet	0.008	0.008	0.008
Core	2.500	1.600	0.800
Rear Sheet	0.004	0.004	0.004
<u>Structural Honeycomb Panel</u>			
Front Sheet	0.026	0.020	0.020
Core	1.600	4.000	2.700
Rear Sheet	0.026	0.020	0.020
<u>Required Meteoroid Shield</u>			
Bumper	0.008	0.008	0.008
Spacing	2.500	1.600	0.800
Backup Wall	0.030	0.024	0.024

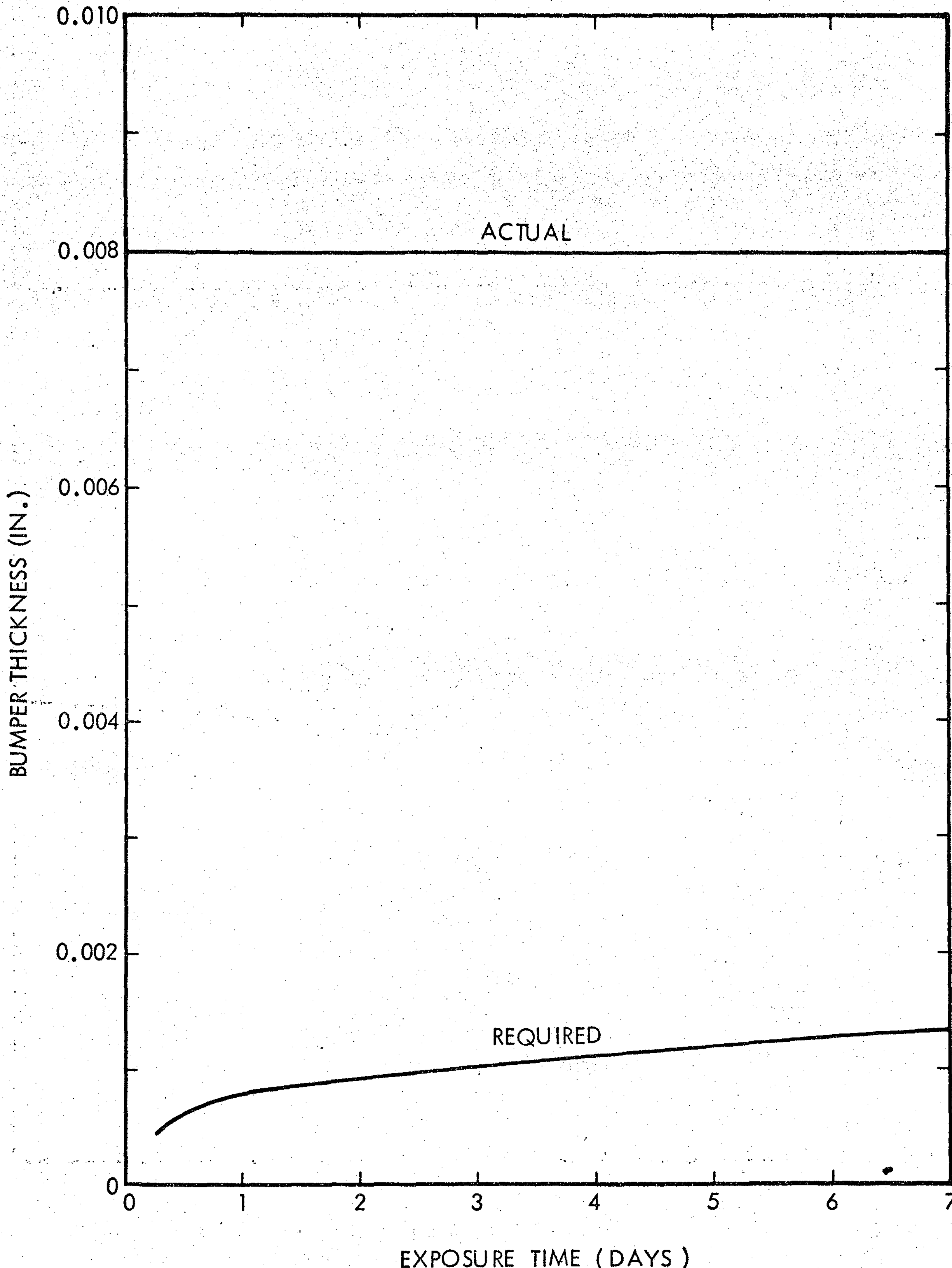

Figure D-7. Comparison of Actual and Required Bumper Thickness for SERV Frustum Sections

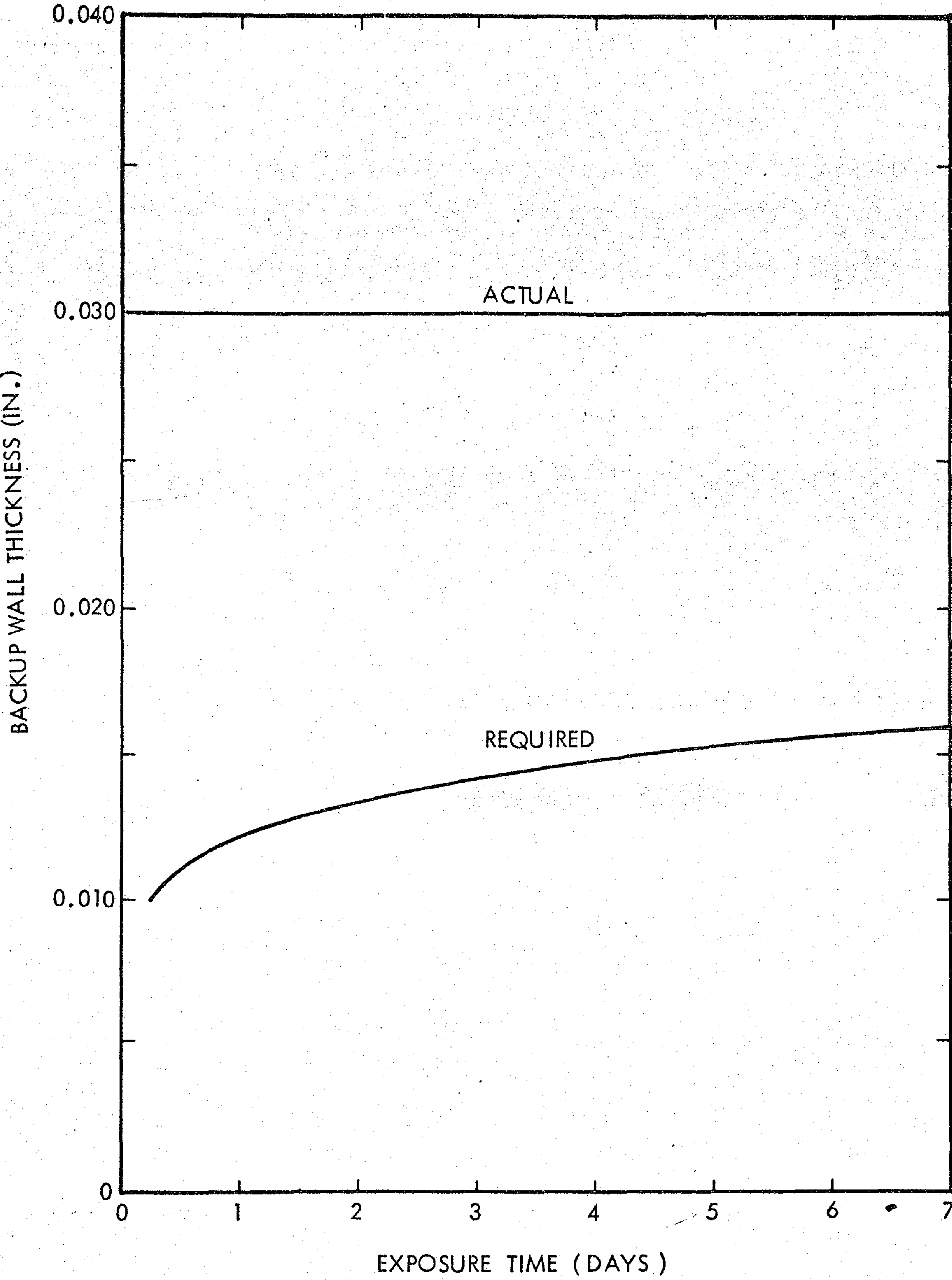

Figure D-8. Comparison of Actual and Required Backup Wall Thickness for Upper Frustum

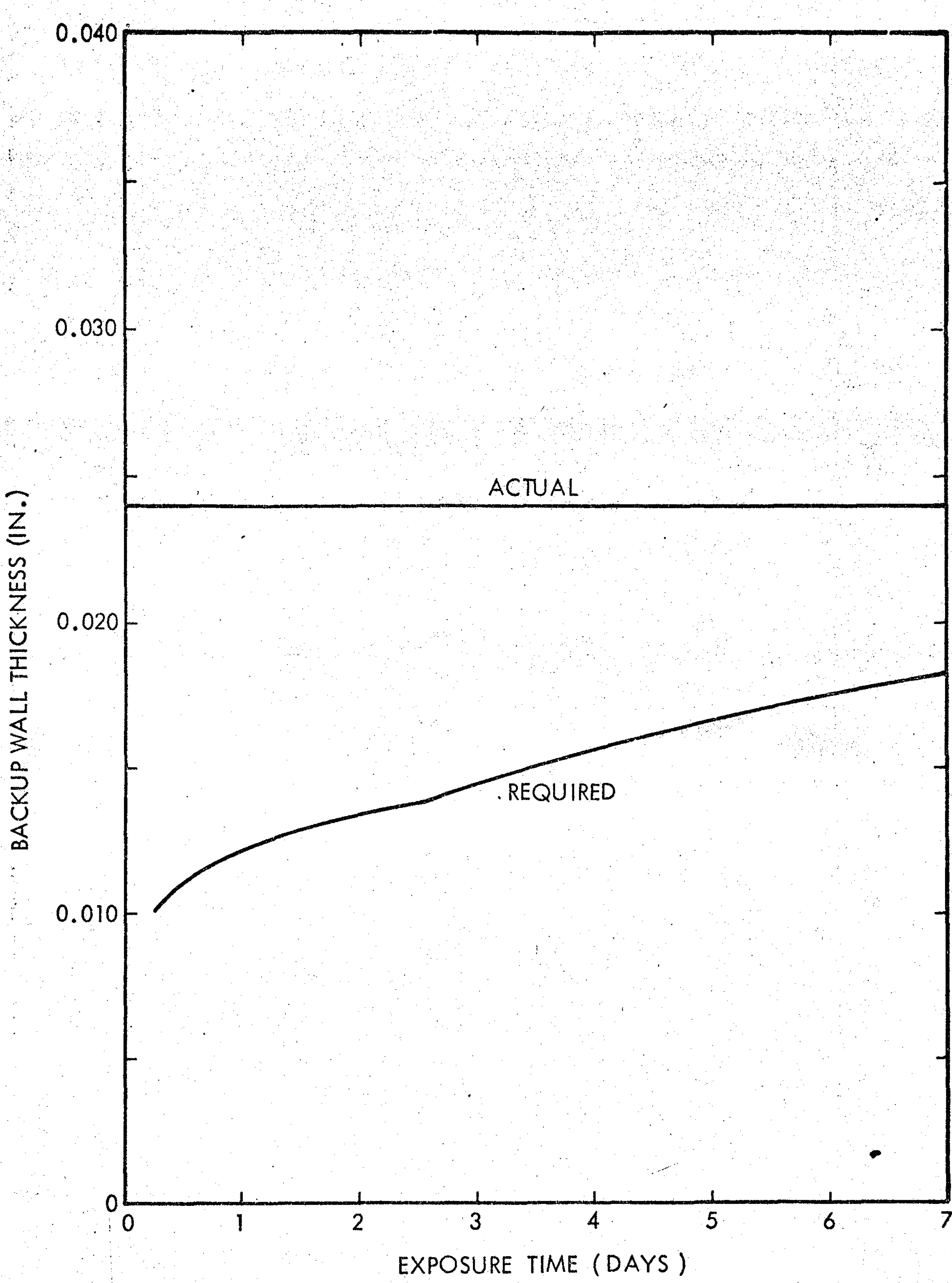

Figure D-9. Comparison of Actual and Required Backup Wall Thickness for Middle Frustum

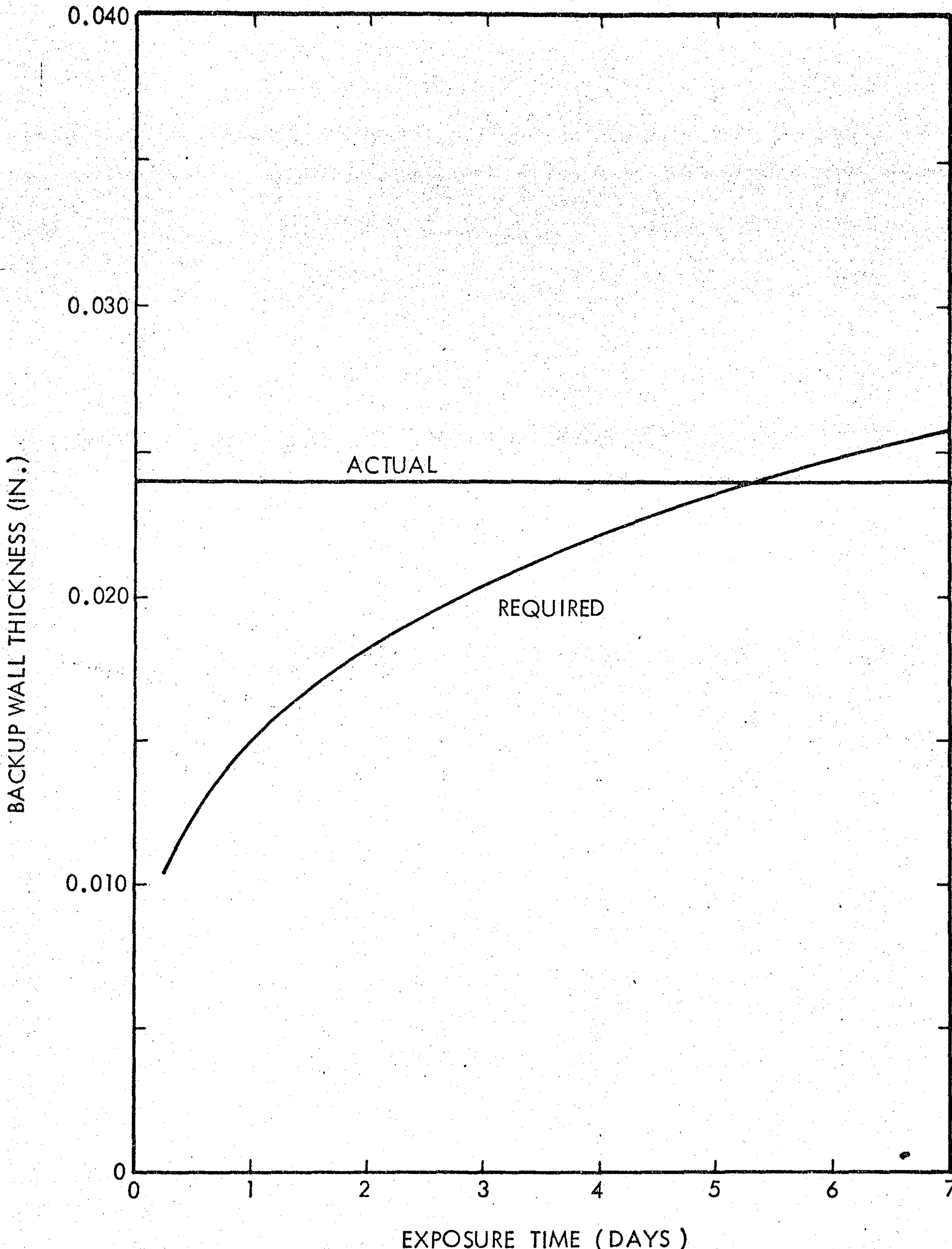

Figure D-10. Comparison of Actual and Required Backup Wall Thickness for Lower Frustum

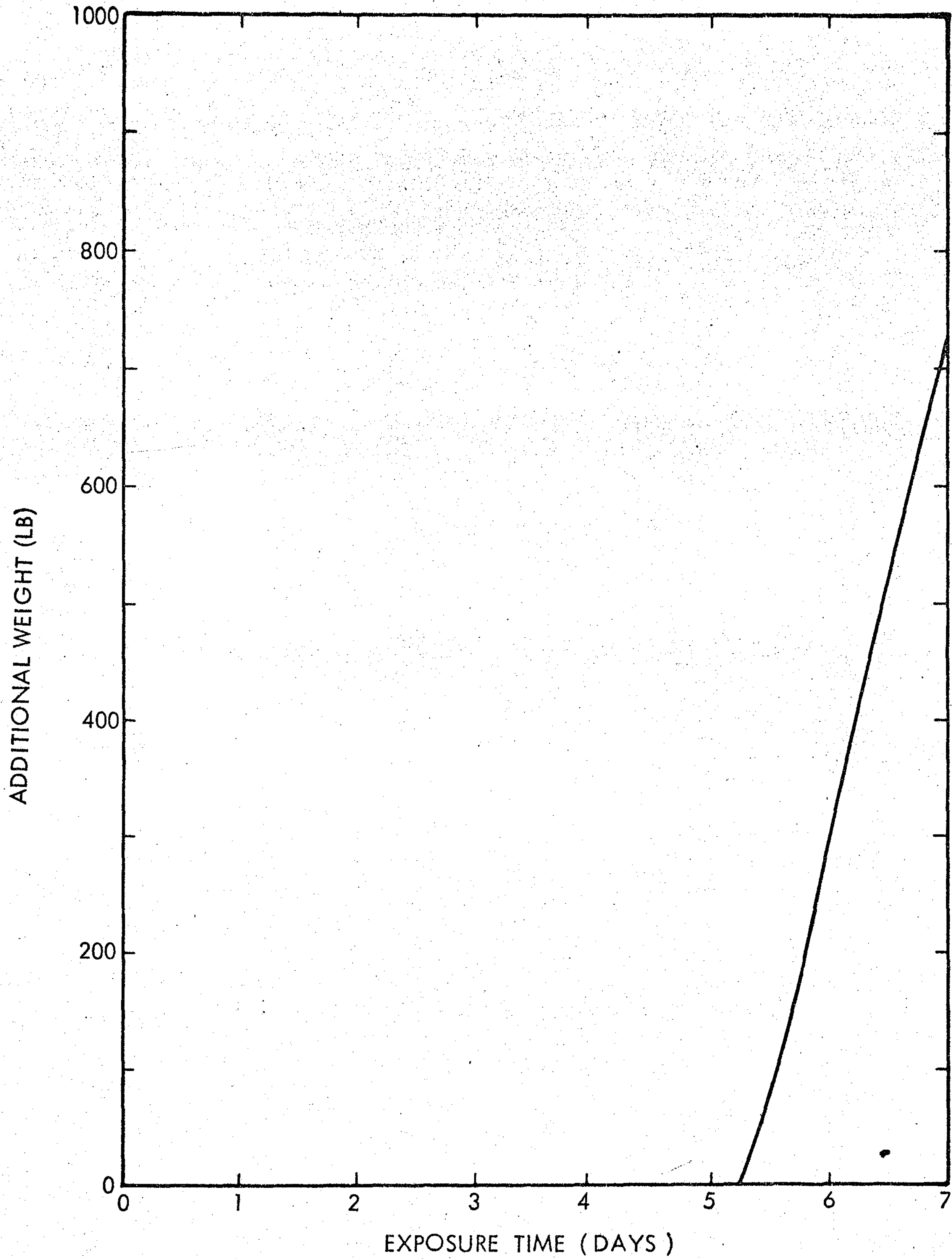

Figure D-11. Additional Weight Required for Meteoroid Protection material is required to provide the desired protection. This slight increase might be eliminated in either of two ways. First, any additional structural strength requirements for the vehicle would probably cause the face sheet thickness of the structural honeycomb panels to increase by more than 1 or 2 mils; and second, it might be possible in future design efforts to decrease the rear sheet of the structural honeycomb panel and increase the front sheet.

Although no consideration was given in this preliminary analysis to the use of the rear sheet of the structural honeycomb panel as a second backup wall, the use of multiple backup barriers tend to reduce the thicknesses required for first. This approach to the meteoroid shield might not require any additional shielding. However, the actual protection afforded by honeycomb for any type of meteoroid shield, must be verified in laboratory test. This is because there is no analytical technique for predicting the extent of the damage to the sandwich core by the expanding debris cloud. Thus, before any honeycomb meteoroid shield can be designed, its worth must be substantiated in the laboratory.

References

D-1 B. G. Cour-Palais, et al, "Meteoroid Environment Model - 1969 (Near Earth to Lunar Surface), NASA Space Vehicle Design Criteria (Environment)", NASA SP-8013 - March 1969, p. 18.

D-2 ibid., p.19.

D-3 ibid., p. 21.

D-4 Cour-Palais, B. G., "Meteoroid Protection by Multiwall Structures", AIAA Paper No. 69-372, AIAA Hypervelocity Impact Conference, Cincinnati, Ohio, April 30 - May 2, 1969, American Institute of Aeronautics and Astionics, New York.

D-5 Private communication, P. D. Thompson with G. B. Cour-Palais, March 11, 1971.

APPENDIX E

SERV ENGINE POINT DESIGN

ASR 71-86

INFORMAL REPORT
TASK IV
SERV POINT DESIGN

Advanced Programs
Canoga Park, California

H. G. Diem
Program Manager
Advanced Technology Programs

30 March 1971

72

Rocketdyne
North American Rockwell

6633 Canoga Avenue
Canoga Park California 91304

ABSTRACT

The Rocketdyne subcontract to Chrysler Corporation had four principal task areas:

- Task I - The fabrication of a 2-1/2% scale SERV model with aerospike engine for slipstream and still-air testing,
- Task II - Model design and testing support,
- Task III - Propulsion analysis and design, and
- Task IV - Engine design description for the point design.

This report presents the results of the Task IV effort.

INTRODUCTION AND SUMMARY

The SERV (Single-Stage, Earth-Orbital Reusable Vehicle) proposed by the Chrysler Corporation is designed to incorporate an aerospike engine, integrated into the base of the vehicle and having a diameter of approximately 89 feet. The engine design provides a short length engine assembly integrated into the vehicle base to minimize the combined engine weight, thrust structure weight, and vehicle structure weight. The engine has a very high nozzle area ratio and thus a high vacuum specific impulse.

The Rocketdyne subcontract to the Chrysler Corporation has provided data on engine design, performance, and operational characteristics for the SERV aerospike engine. This information was gathered in four tasks.

In Tasks I and II preliminary nozzle performance calculations were made, areas of uncertainty were identified, a cold-flow test program was formulated, a model was designed and built, tests were run, data were evaluated, and analytical procedures were updated, based upon the newly-available test data. This work was documented in Ref. 1.

Task III provided baseline (preliminary) design information for the engine system, as well as parametric data for trade studies. In addition, related studies on base pressure ground effects, base heating, reentry nozzle cooling, reliability, and the dual combustor aerospike were presented, Task III was documented in Ref. 2.

The purpose of the Task IV effort was to formulate a point design aerospike engine for SERV. This work built logically upon the results of the preceding tasks. The Task IV effort presented here covers engine description, module layout, engine layout, engine-vehicle interface, structural aspects, engine weight, combustor heat transfer, engine performance, and engine balance for the SERV Point Design Engine.

C5

POINT DESIGN ENGINE DESCRIPTION

The propulsion system for the SERV is an integrated aerospike-nozzle engine comprised of twelve modules, each having a sea level thrust of 475,000 pounds. A module is defined as the smallest basic operating unit of the engine, i.e., it is comprised of an assembly of combustor segments jointed together with the nozzle and operated using one turbopump set. The total engine generates 5.7 million pounds of thrust at sea level operating with LOX/H_2 propellants at a chamber pressure of 2000 psia and an engine mixture ratio of 6.0

The engine is designed to provide a high performance, reusable propulsion system having short length and a minimum propulsion installation weight. Altitude compensation (i.e., the ability to deliver high performance at both sea level and vacuum) is achieved with the aerospike nozzle design. The engine is designed to provide maximum integration benefits by matching the engine gometry and the vehicle configuration. The aerospike-nozzle engine is tailored in diameter (and in length) to the base of the SERV vehicle. This provides a large diameter engine and hence, a high area ratio. With integration of the engine and its nozzle into the structure of the vehicle the combined engine, engine thrust structure, and vehicle structure weight are minimized. The inherent capability of the aerospike-nozzle to efficiently perform with very short nozzle lengths permits the overall vehicle length to be minimized.

The integrated, aerospike-nozzle engine is designed, developed and fabricated in independent sections (or arcs) of the complete circular engine system. These sections are defined as engine modules. Each module is an independent engine-system with its own turbopumps, propellant inlet ducts, start system, controls, etc. These modules are assembled to provide the complete engine much in the same manner that bell-nozzle engines are clustered to provide a stage propulsion system.

The annular combustor for the aerospike-nozzle engine is assembled from essentially independent combustor segments. Segmenting of the combustor permits combustor development, testing and fabrication to be conducted on a unit having approximately 1/288th the thrust of the engine system and approximately 1/24th the thrust of the engine module (SERV baseline design utilizes 12 engine modules each comprised of 24 combustor segments). High performance, combustion stability and production cost benefit from this design. Each combustor is an isolated unit from the injector to an area ratio of approximately 6:1. Efficient combustor development can therefore occur using research-type test stands which reduces cost compared to testing the complete combustor in all tests.

ENGINE POWER CYCLE

In the SERV configuration, high-pressure and low-pressure (inducer type) pumps driven by individual turbines are used for the fuel and oxidizer circuits as shown in the schematic of Fig. 1 . The turbine drive gases are provided by a separate turbine drive combustor (i.e., a low-mixture-ratio gas generator). This cycle allows the pump discharge pressures to be minimized in relation to the chamber pressure. The pump components are not an integral part of the combustion chamber. They function independently of the thrust chamber and are readily accessible. On the fuel side, the high-pressure pump is a two-stage centrifugal pump. The oxidizer side has a single stage, high-pressure pump. The fuel and oxidizer low speed inducer-type pumps allow operation at a low NPSH value.

The turbine drive gas, after expanding through the turbines, provides the secondary flow to the base region of the nozzle which increases the base pressure and thrust. This efficient use of the turbine drive gas results in high nozzle performance and a very high overall engine efficiency. To furnish the required power of the system, a gas generator flowrate of

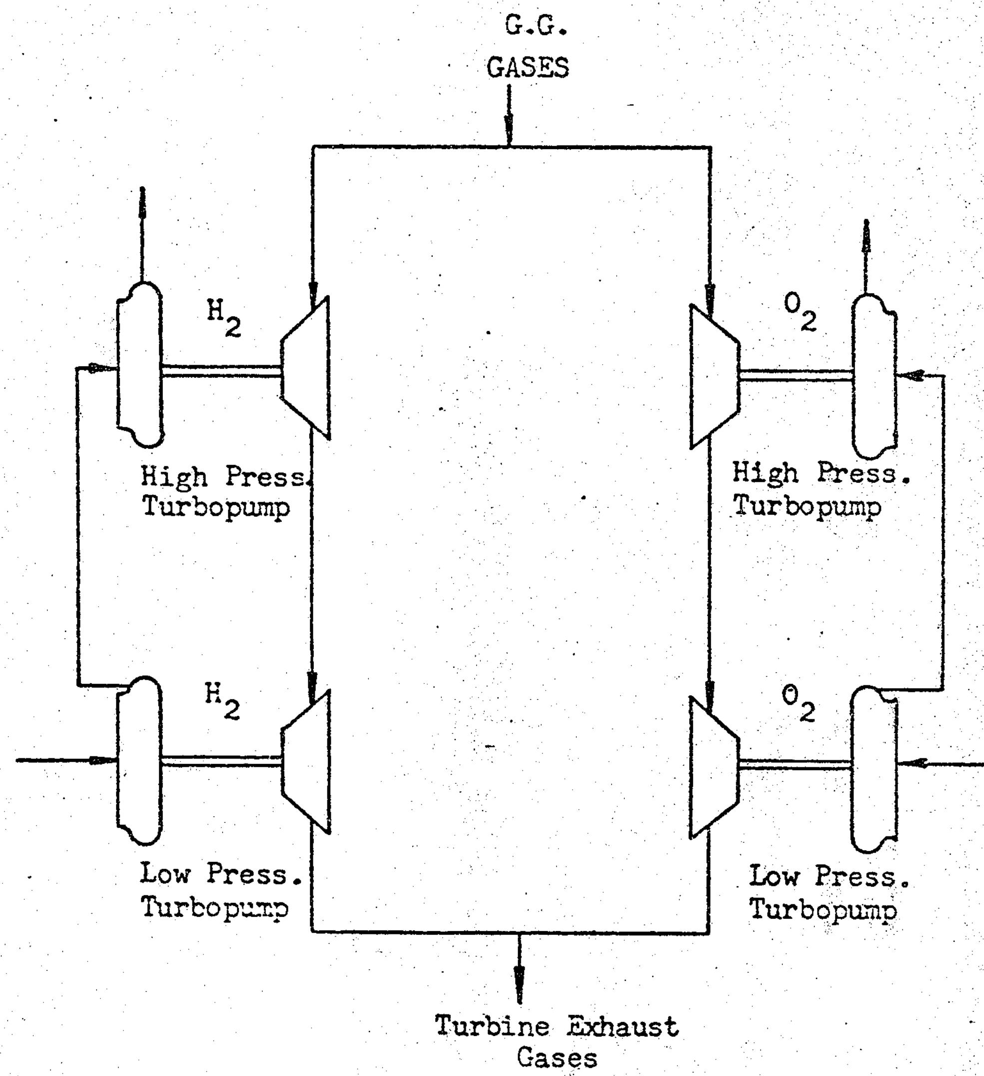

FIG. 1. SERV ENGINE TURBINE DRIVE SCHEMATIC

36.2 lb per second for each pump system is needed, operating with O_2/H_2 propellants at a pressure of approximately 1050 psia and a mixture ratio of 1.12. The total gas generator flow required to operate twelve pump systems is 419.1 lb per second. This flow results in a mixture ratio (O/F) shift from the 6:1 tanked conditions to a value of 6.45 in the main combustor.

Engine start, to full mainstage thrust or intermediate throttled thrust levels, is initiated by opening of the main fuel valve which permits chilling of the thrust chamber cooling passages to begin. Controlled sequencing of the main oxidizer and turbine inlet valves allows main combustor ignition and engine power buildup to occur in accordance with the dynamic operating envelope of the engine start components. Engine start controls can be provided so that starting NPSH requirements never exceed the mainstage pump NPSH requirements. A pump inlet pressure in excess of ambient is required, however, to accelerate the flow in the pump inlet line. Minimum possible start time is a function of this pressure.

For a tank head start, enough energy must be available to "breakaway" the turbopumps. In the case of the SERV engine, gas generator conditions under tank head must be sufficient for this task. With breakaway accomplished necessary engine operating point servo controls can be provided to permit mainstage to be achieved. Should there be insufficient energy for turbopump breakaway, an auxiliary power source such as the pressurized hydrogen bottle of the J-2, the solid propellant spinner of the J-2S, or the propellant start tanks of the Thor may be provided. In either case the start may be controlled so that starting NPSH requirements do not exceed those of mainstage provided that pump inlet static pressure, due to tank pressure or static head exceeds ambient pressure. This is necessary to accelerate the fluid in the pump inlet duct.

The start transient is then limited by the fluid accelerating force acting on the fluid in the inlet ducts. For the SERV vehicle, for example, if a 2 psig head is available on the fuel side with a 13 inch diameter duct 50 inches in length; approximately 0.1 second is required to accelerate the fluid to the mainstage flowrate. If 6 psig is available on the oxidizer side for a similar duct, 0.2 second is required to accelerate the oxidizer to the mainstage flowrate. Thus, a start transient of less than 0.2 second could not be attempted without at least a momentary dip in NPSH. It is likely, however, that other component restrictions would limit the start time before the 0.2 second oxidizer acceleration limit was encountered. Maintenance of a high fuel pump flow coefficient to avoid sudden head loss will undoubtedly dictate a slower start.

The same conditions would apply to an orbital restart with the additional stipulation that good quality propellant be provided at the pump inlet. Settling the propellants and providing good propellant quality are the major problems associated with orbital restart. In the case of the J-2 engine on the Saturn S-IVB stage, small settling rockets, and a propellant recirculation system are provided.

In addition, the engine start control system must be designed to detect and adapt to a wide range of hardware temperatures. This is because hardware conditioning has an effect on component operating conditions during start. Further, hardware temperatures are difficult to control during orbital coast periods.

One additional consideration is that the number of starts must be predetermined if any system such as the solid propellant spinner is adopted. The number of starts required determines the number of spinners. Should a large number of restarts be required, some replenishable energy source such as the J-2 start bottle or tank head would be favored.

The engine cutoff sequence may be initiated from any engine thrust level. Engine propellant volumes downstream of the main valves are minimized to reduce cutoff impulse levels. Engine cutoff is initiated by closure of the turbine drive combustor valves allowing turbine power to decay. The sequence is followed by closure of the main oxidizer valve and finally the main fuel valve. Main oxidizer valve closure and, therefore, cutoff time must, however, be accomplished within the limitations for maximum vehicle duct surge pressure associated to vehicle duct lengths. For a specified duct geometry and maximum surge pressure, engine shutdown will be accomplished by either first throttling down to a low thrust level and then fully closing the main oxidizer valve, or by controlling the closure of the valve from full thrust shutdown to limit surge pressure below safe limits.

TURBOMACHINERY DESCRIPTION

The designs for the high pressure pumps are based on technology and experience obtained from the development of many past rocket engine turbopumps. The oxidizer pump is a one-stage, shrouded centrifugal impeller design without an inducer. The head developed by the low pressure pump prevents cavitation of this pump. The fuel pump is a two-stage, shrouded centrifugal-impeller design also without an inducer. Shrouds are utilized to improve the pump efficiency and to permit labyrinth seals to be incorporated with the impeller. Pump efficiencies of 81 and 77 percent are based on actual experimental data obtained from the developed rocket engine pumps. The high pressure pumps develop discharge pressures of 3653 psia and 3050 psia for the oxidizer and fuel pumps, respectively. The critical design parameters were maintained well under the present state-of-the-art for rocket engine pumps to obtain the necessary long-life for an economically reusable system.

Both the hydrogen and oxygen low-pressure pump designs are based on current high suction performance inducer technology. These pumps are designed for low NPSH operation with the oxygen and hydrogen pumps capable of operation down to 12 and zero feet respectively. These values of NPSH reflect current design capability.

The zero-NPSH capability of the hydrogen pump is based on considerable experience in the design of hydrogen pump for two-phase flow, such as in the J-2 Mark 15 and the NERVA March 25 hydrogen pumps. The required pump inlet diameter increases with decreasing pump inlet total pressure. In the SERV application, an inlet diameter of 13.25 inches is required to operate at an inlet total pressure of 14.7 psia. The corresponding inlet vapor friction is 50 percent by volume and the inlet static pressure is 11.7 psia.

For an NPSH of 12 feet for oxygen, the oxidizer low-speed inducer diameter will be 12.70 inches. This latter specification is based on the capability of inducers to pump at suction heads (or NPSH) of two inlet velocity heads in liquid oxygen.

Sufficient head is developed by these pumps to avoid cavitation in the high preesure pumps. The experience gained in the development of various inducer types have led to low pressure pumps that are capable of both high suction performance and high efficiency operation. The recently completed hydrogen inducer program (NAS 8-25069) has also provided the technology for the design of low pressure pumps for two-phase flow. The inlet geometry of these low pressure pumps are similar to the two-phase flow hydrogen inducer which was designed, fabricated, and tested. Vapor volume pumping capabilities in excess of 35 percent were demonstrated.

The turbines for the SERV turbopumps were designed for minimum flowrate and high efficiency to maximize engine performance. To minimize flowrate, the turbines for the low-pressure and high-pressure pumps are arranged in series on both fuel and oxidizer turbopumps. The main fuel turbine is a 4-stage impulse turbine, designed for a stage velocity ratio of 0.40 and has an efficiency of 74 percent. The 4-stage design reduces the stress of the last rotor at the turbine discharge. The turbine for the low-pressure fuel pump is a single stage impulse, designed for a velocity ratio of 0.35, and an efficiency of 70 percent. The aerothermodynamic design of these turbines is based on Rocketdyne's extensive experience in developing these turbine types.

The main oxidizer turbine is a 3-row, impulse turbine designed for a stage velocity ratio of 0.35, and has an efficiency of 70 percent. The turbine for the low-pressure oxidizer pump is a 2-row, impulse turbine with a velocity ratio of 0.12 and has an efficiency of 50 percent.

SERV ENGINE THROTTLING

The SERV engine throttling requirements during the primary mission result from a restriction on the maximum vehicle acceleration level experienced and maintenance of an effective gimbal angle. The throttle range for limiting vehicle acceleration above 100,000 ft in the baseline mission is from full thrust to 18 percent nominal thrust (throttle ratio of 5.55:1). In addition the engine is capable of differential throttling of 15 percent within the thrust range (total throttle ratio of 6.5:1). The modular concept employed in the SERV engine is extremely versatile when it comes to the throttling requirement. The modules may be throttled either together or separately.

Generally, the type of engine control depends greatly upon the system response requirements. For example, the engine throttling response may need to be sufficiently fast so that the engine system will fit a projected mission profile without requiring pulse mode operation. Liquid propellant control elements generally provide superior dynamic response, but require high valve pressure drops at design conditions and subsequently higher pump discharge pressures. Turbine-drive gas controllers allow lower pump discharge pressures at the expense of system response time, which increases due to the lag in turbomachinery response. Both types of controls would be used in the SERV engine. Additionally, pump recirculation for propellant utilization and prevention of pump stall at deep throttled conditions may become necessary.

Control of engine thrust and mixture ratio during the start transient can be accomplished by means of the mainstage control system (Fig. 2), but special consideration must be given to other aspects such as system preconditioning requirements, pump stall effects, and initial turbine power provided to initiate mainstage engine operation.

The main propellant valves and turbine drive combustor valves would be variable position and function as throttle control valves as well as on-off valves. The hot gas valves also function as on-off and throttle control valves. Position indicators are provided for proper system sequencing and to facilitate operational evaluation by the engine in-flight monitoring system. Throttled operation will be obtained by operation of the main oxidizer valve in conjunction with the turbine supply valves. These valves are controlled in a closed loop manner. The system is capable of throttling from full thrust to 18 percent thrust including differential throttling of 15 percent within the thrust range, and of varying the engine MR to $\pm.5$ mixture ratio units about a nominal of 6:1 during mainstage operation.

Investigation results of the previous NASA-Advanced Engine Aerospike (AEA) program indicate that, for stringent throttling ramp rates (45%/sec), a combined liquid valve-hot gas valve control system gave preferred response characteristics. This same combination of valving for throttle control would be used for SERV engine even though the ramp rate is less severe estimated to be about (25%/sec).

Fuel Thrust MR Excursions:	1 and 2 (Closed Loop); 5, 6, 7 (Scheduled)
Throttling:	1 and 2 (Closed Loop); 3 and 4 (Scheduled)
Acceleration:	1 and 2 (Closed Loop), 3 and 4 (Scheduled) 5, 6 (Sequenced)
Module-Out	8, 9, 10, 11

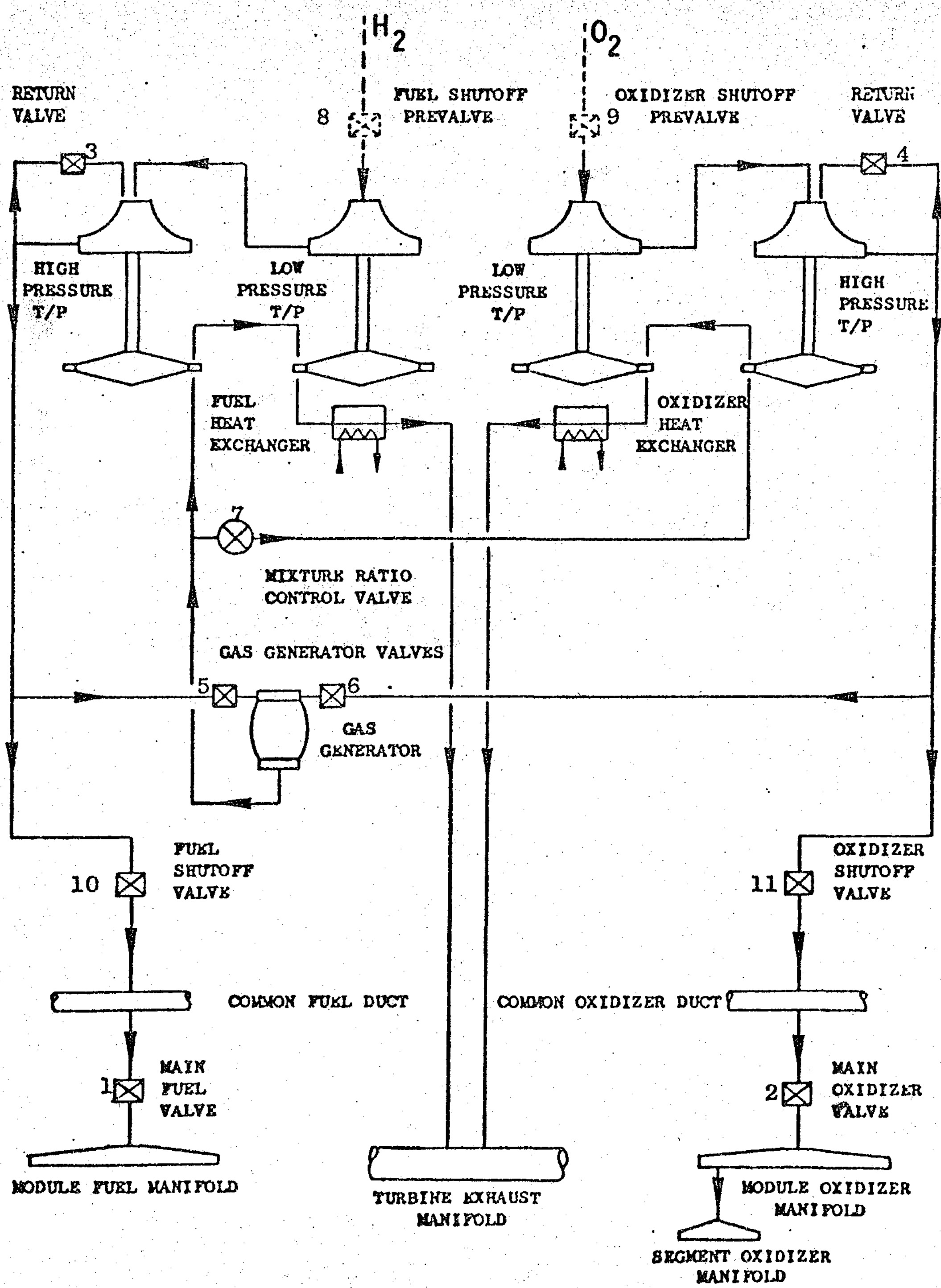

Fig. 2. SERV Engine Control System

The impact of SERV engine throttling on specific impulse has been investigated. The data (Fig. 3 and 4) provide performance trends for altitudes equal to or above 100,000 ft and for throttling down to 10 percent of nominal thrust (basis: original baseline design). The combustion efficiency trend with throttle level is provided on Fig. 5 . The combustion efficiency is 0.995 for the full chamber pressure conditions. This efficiency value has been achieved in extensive aerospike nozzle segment testing conducted under the Air-Force-ADP and NASA-AEA programs. During the latter program, high combustion efficiencies were measured with both triplet and coaxial type injectors. As chamber pressure decreases in the throttling mode, the combustion efficiency is affected.

The SERV engine performance data were generated including assumptions relative to the method of throttle control. For example, an oxidizer injector pressure drop of 1330 lb/in^2 (conservative) was allowed to provide stability at the 6.5:1 throttle level. Nominally, the oxidizer injector pressure drop at full thrust for a non-throttling engine would be 500 lb/in^2 for the SERV engine.

Investigation during the NASA-Advanced Engine Aerospike program at Rocketdyne concerning main engine throttling capability to 3 percent nominal thrust has shown that the injector pressure drop (P_{inj}) must remain large to maintain control stability and performance at low thrust levels. Data presented on Fig. 6 show P_{inj}/P_c vs throttle ratio for O_2/H_2 propellants in the regeneratively cooled AEA application. The GH_2 injection curve (AEA-1 curve) indicates acceptable throttling characteristics. The P_{inj}/P_c values in the LO_2 curve (AEA-2) decreases sharply as the throttle ratio exceeds 5:1 and falls below a minimum stability limit line established by stability and control criteria. It is noted that GO_2 was used as injectant for the AEA system (AEA-3 curve) and so eliminated the problem of stability and injector pressure drop increase.

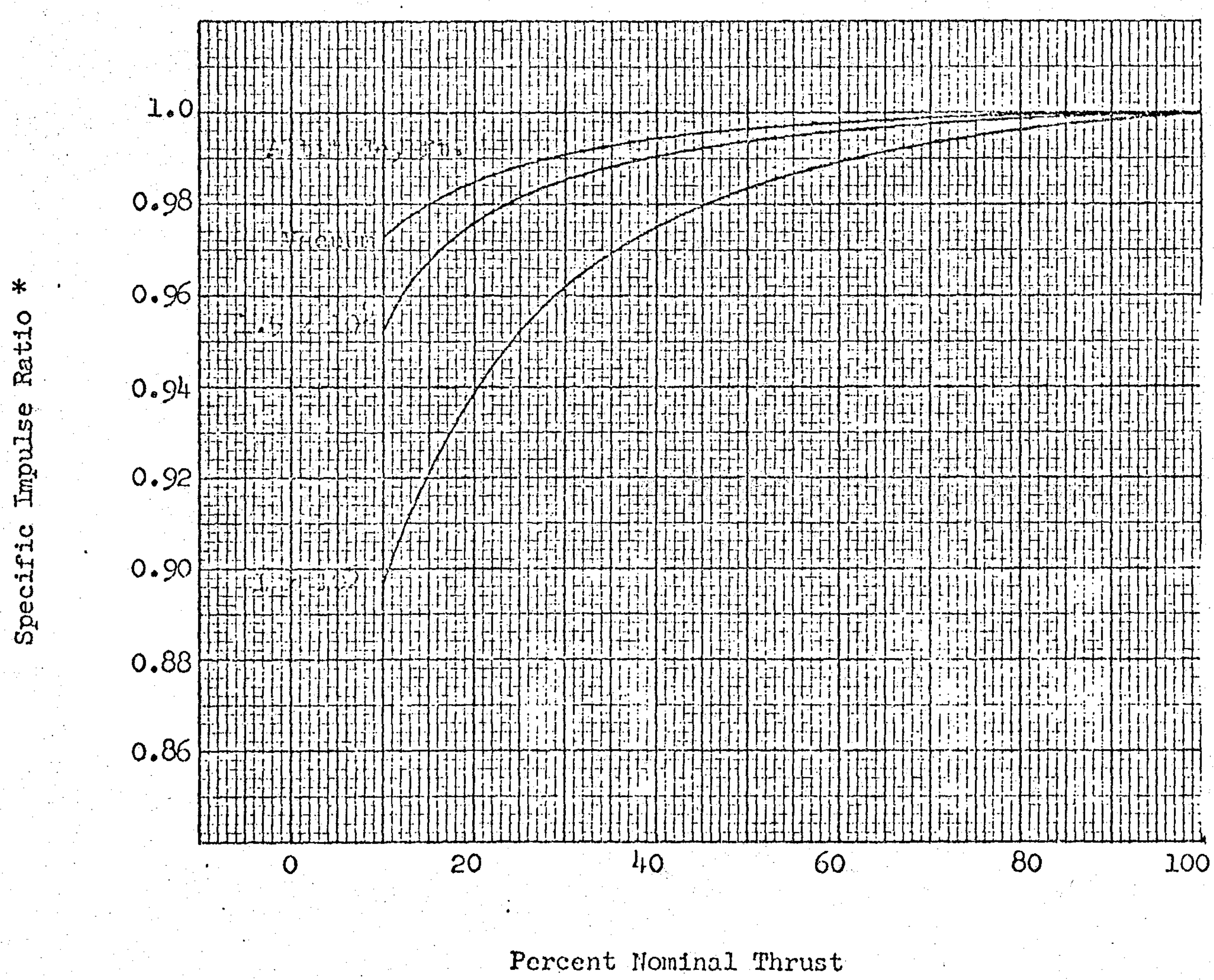

*Referred to full thrust I_s at given altitude.

Fig. 3 SERV Engine Throttling Performance.

Figure 4 SERV ENGINE THROTTLING PERFORMANCE

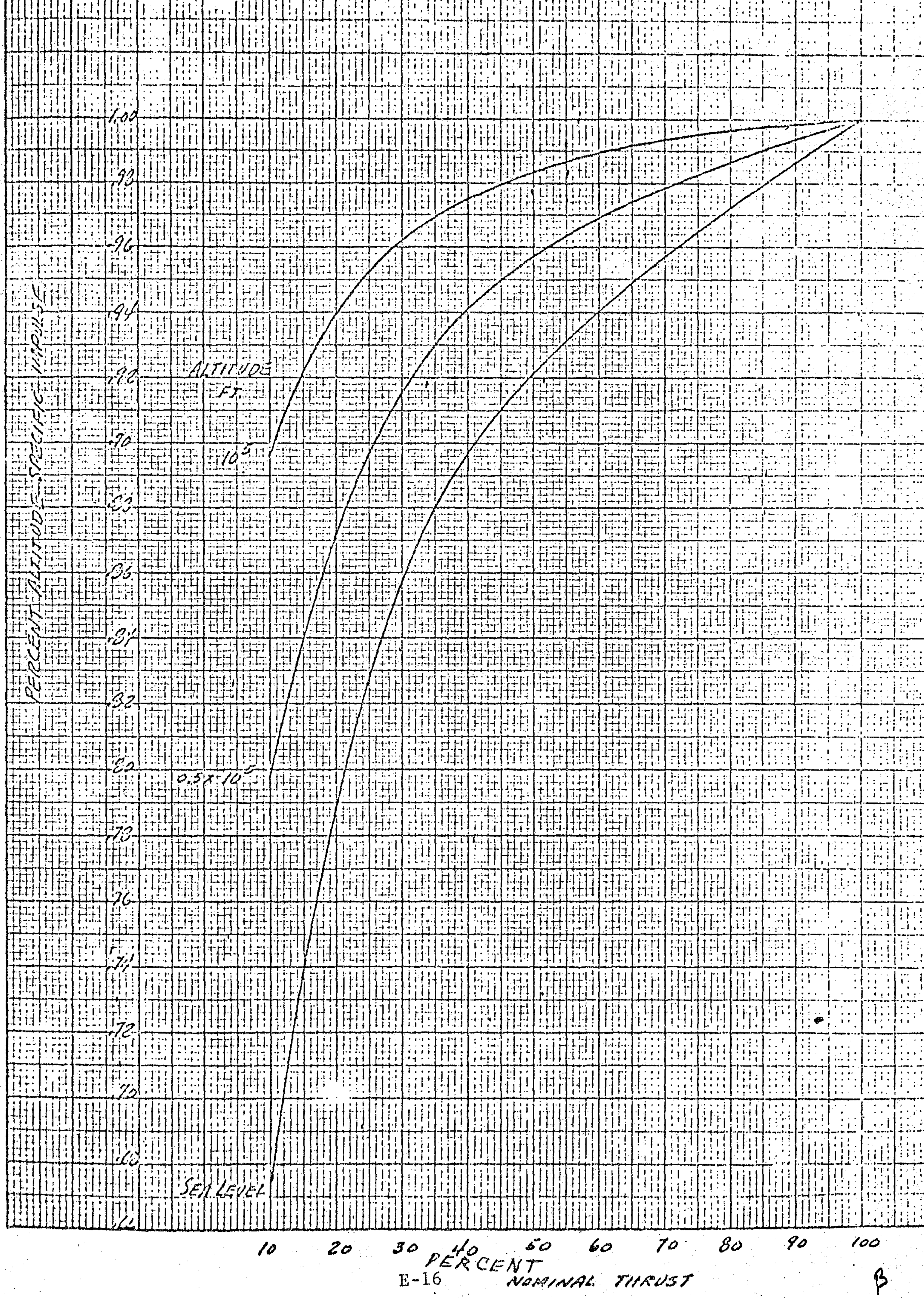

B

15

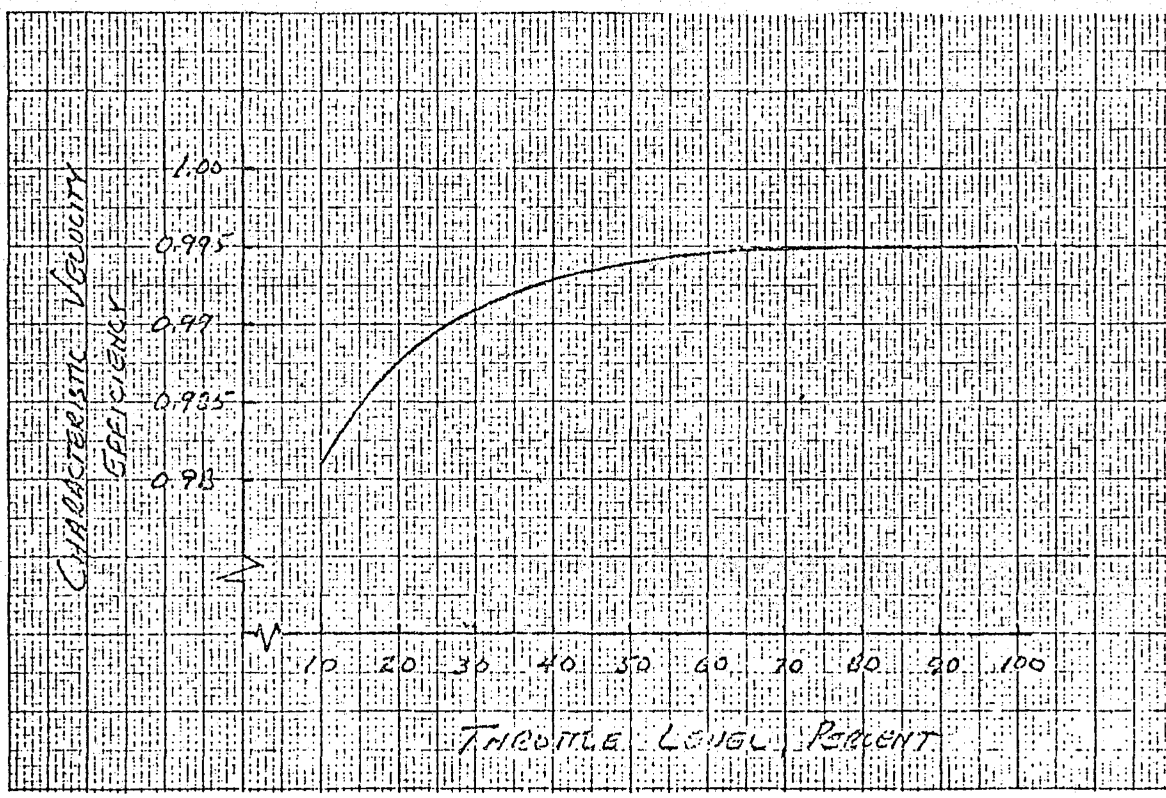

FIGURE 5 CHARACTERISTIC VELOCITY EFFICIENCY TREND

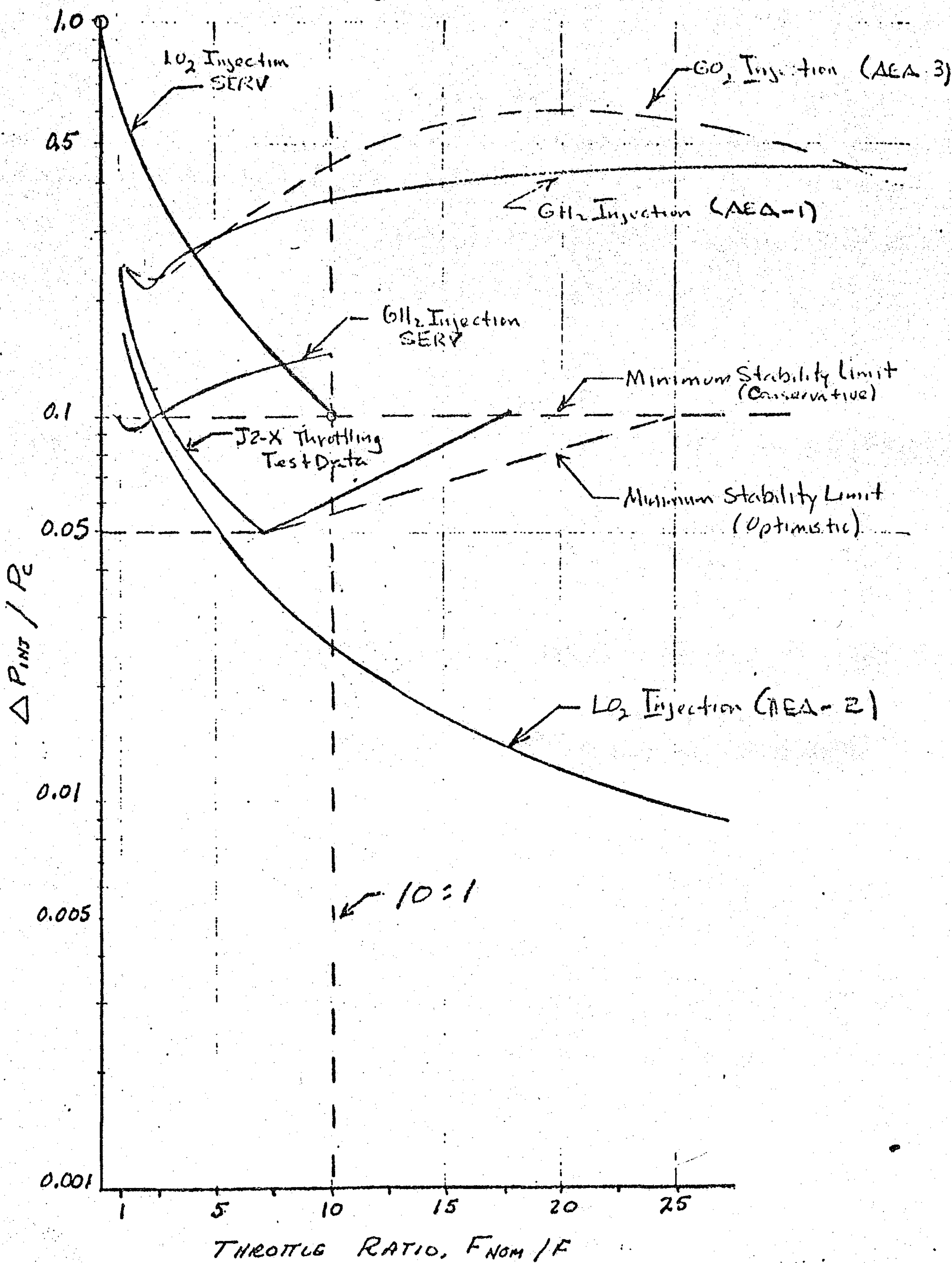

Figure 6. INJECTOR PRESSURE DROP CHARACTERISTIC WITH THROTTLE RATIO

Also, during the AF-ADP program, an injector was successfully operated at a throttle ratio of 5:1 and experienced a value of P_{inj}/P_c of 0.05. Further, the J-2X test data shown on Fig. 6 reflects stable operation to a value of 0.05. Therefore, the minimum level of 0.10 can be considered a conservative throttle level value as the throttle ratio approaches 10:1. The SERV engine data are based on this value.

An experimental data line from J-2X testing is shown on Fig. 6 which indicates the concentric element injector with LO_2/GH_2 propellants follows a P_{inj}/P_c curve for LO_2 injection down to about 7:1 throttle ratio (14% F_{nom}) beyond which gasification of the oxygen occurs. The J-2X data indicate the concentric element injector follows a P_{inj}/P_c curve for LO_2 injection down to about 7:1 throttling and then apparently gasifies the oxygen to follow the GO_2 curve. This characteristic can be attributed to the inherent heat exchange injector capability of the J-2X system. It is not expected that the SERV injector configuration would have sufficient heat exchange characteristics (enthalpy exchange to incoming oxygen) with throttling to gasify the oxygen.

DIFFERENTIAL THROTTLING TVC

Because of the unique geometry of the SERV vehicle, thrust vector control (TVC) can be achieved efficiently by differential throttling of engine quadrants. Large effective gimbal angles are obtained with only moderate throttling ratios, which results in small specific impulse losses. Mission requirements can be easily balanced by using the engine upthrust capability to keep the engine total thrust at the required level. An alternative thrust vector control system for a fixed engine uses secondary gas injected at a point near the end of the nozzle to produce an unbalanced side thrust. Design and analysis capability for secondary injection TVC with aerospike nozzles is well established, and this method has proven attractive in several previous applications. However, vectoring demands for the SERV vehicle are such that secondary flow requirements and attendant specific impulse losses (on the order of 1 to 2 percent) may be excessive.

The SERV aerospike engine is readily amenable to differential throttling TVC, because it must undergo at least 5:1 throttling to satisfy baseline mission requirements regardless of the TVC method. It should be relatively easy to combine these functions. Because each module is separate, individual controls can be employed to provide independent throttling. Previous studies have shown that several control systems are capable of 10:1 throttle levels, and that the choice of one over the other depends on a tradeoff between response, performance, and complexity. Moderate throttling rates are obtained with systems that employ hot gas valves in the lines upstream of the turbines. Faster response can be obtained by providing additional valves in the liquid lines. The present SERV control system includes liquid line control and turbine drive gas control.

Results of a recent study conducted for a representative aerospike engine are summarized in Fig. 7 . Characteristic relationships and transfer functions for all system components and controls were combined in this study to evaluate transient response characteristics of each control technique; hence, these data represent the effect of all major time lags in each system. The curves indicate upper bounds of regions for which the controlled response was smooth and stable at all levels. It is readily seen that several methods are capable of throttling rates around 10 percent per second to levels much lower than that needed to TVC. This is equivalent to gimbaling the engine at a rate of about 10 degrees per second, which should be more than sufficient. The present combination liquid/gas control system will allow much faster TVC response rates; approaching 50 percent change/second (i.e., a change in thrust will occur about two seconds after command is given).

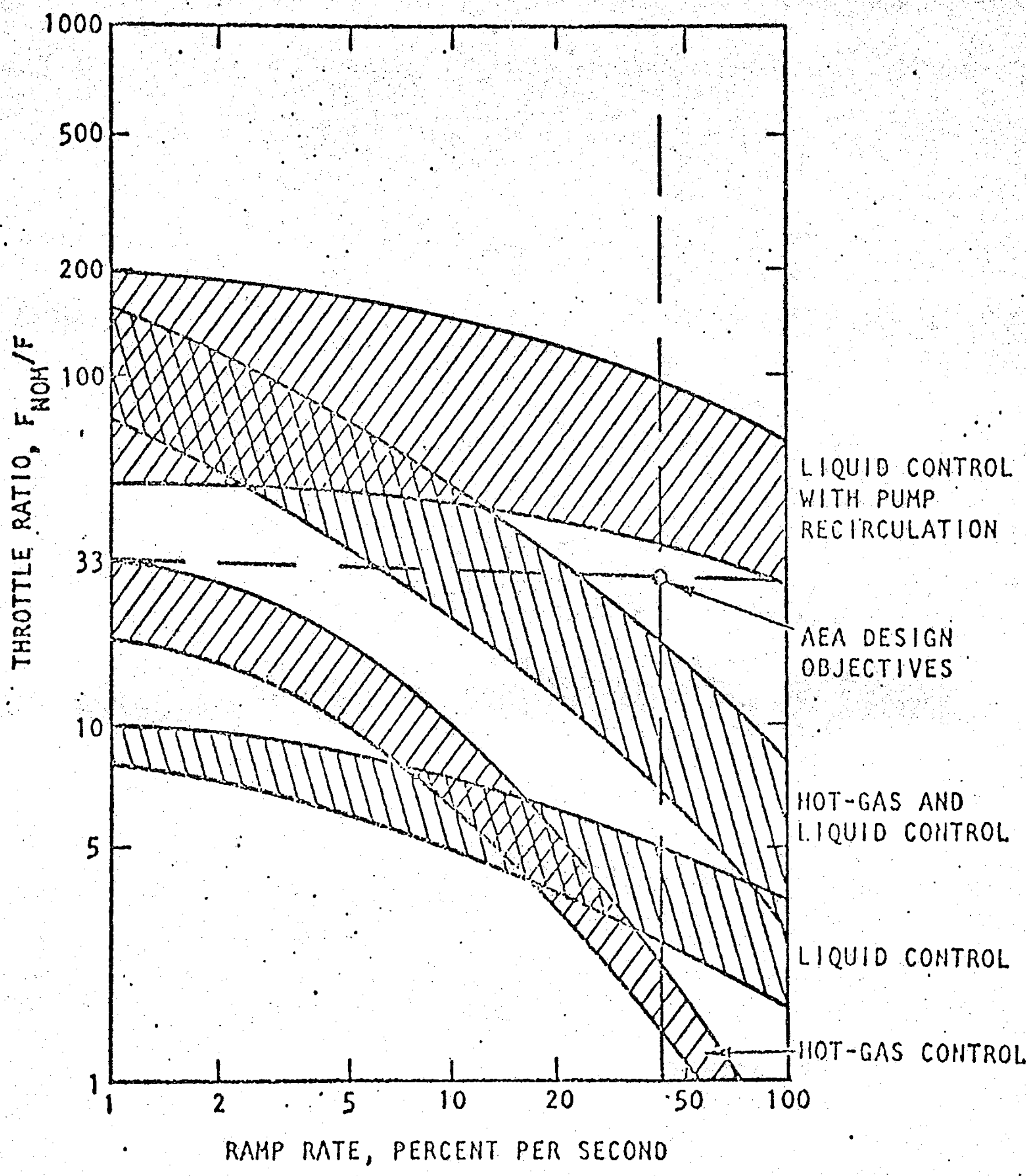

Fig. 7 Comparison of Control Methods Throttle Ratio vs Ramp Rates (Constant Mixture Ratio)

Figure 8. SERV GIMBAL ANGLE CAPABILITY FOR DIFFERENTIAL THROTTLING OF ONE QUADRANT (3 MODULES)

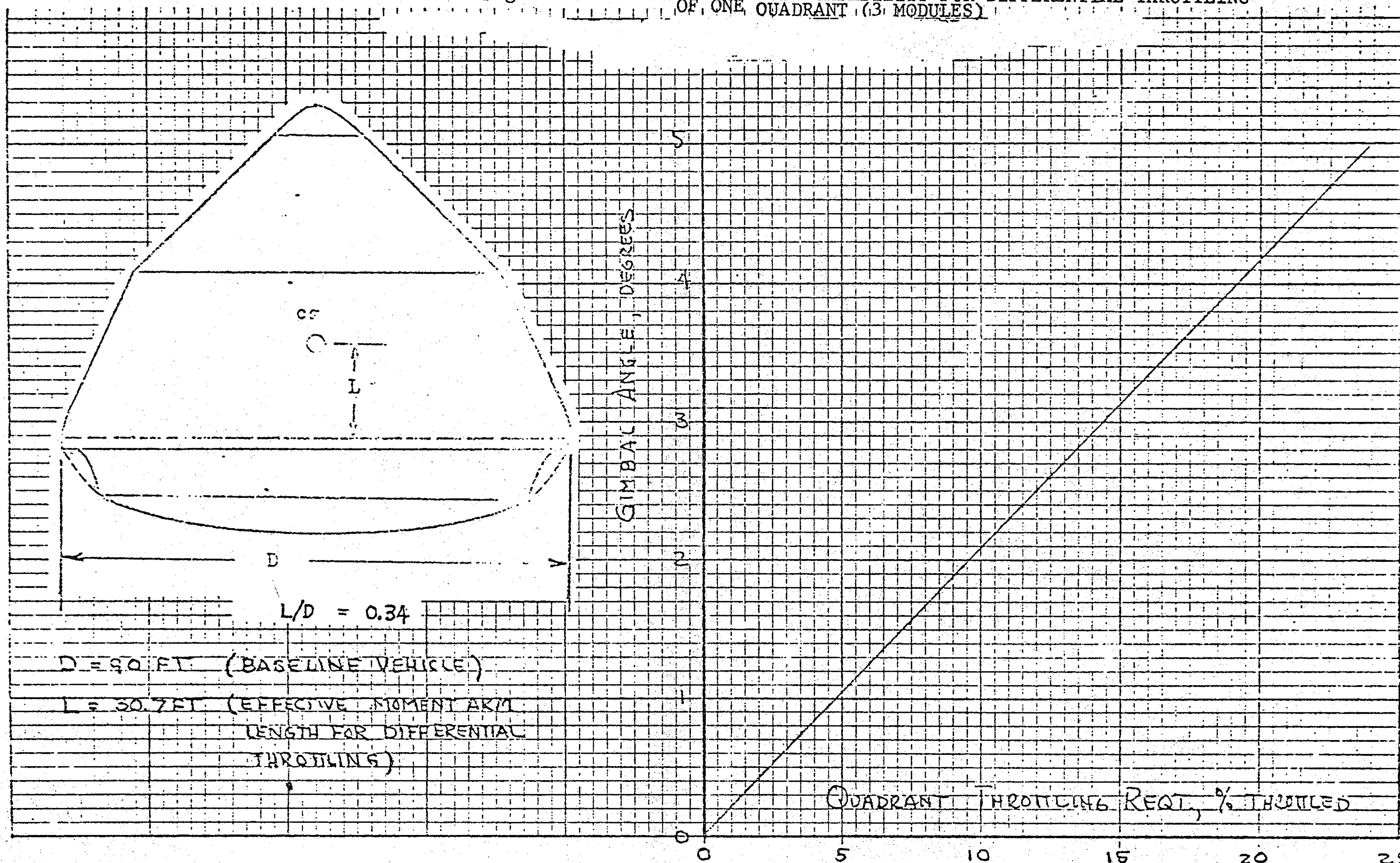

Figure 9. SERV ENGINE THRUST VECTOR CONTROL CAPABILITIES

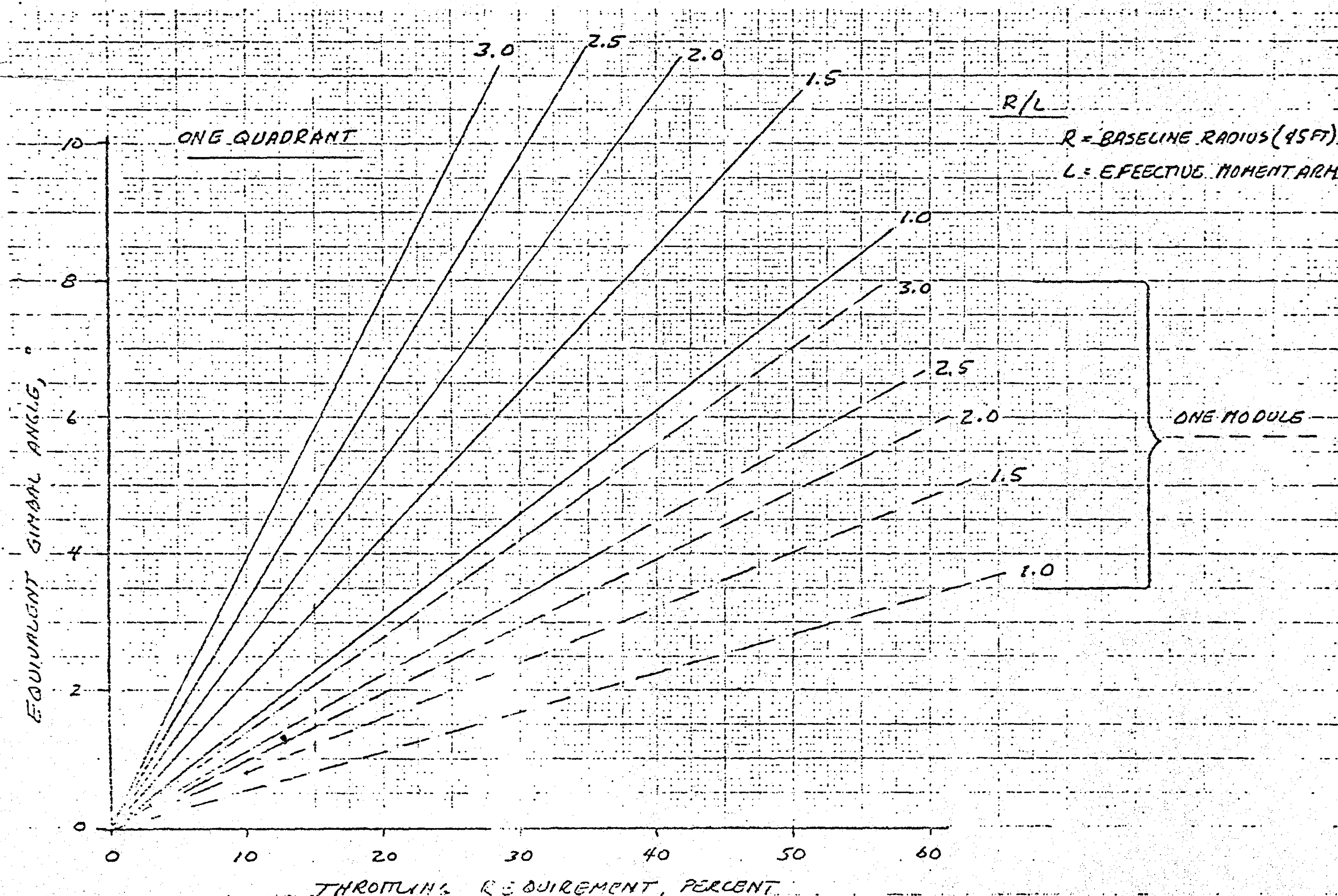

Analysis for the SERV differential throttling TVC system indicates that the attitude control force required can be supplied by throttling one quadrant of the engine (three modules/quadrant). For example, a quadrant throttling requirement of 23.9 percent is required for a gimbal angle of 5 degrees (Fig. 8). The data presented on Fig. 9 resulted from a parametric study of relative moment arm length and degree of throttling required. Figure 9 presents these results for a single module and for a quadrant of modules with variable R/L values (R = Baseline vehicle radius (45 ft), and L = Effective moment arm length). The SERV R/L value corresponding to the data of Fig. 8 is 1.5.

MODULE OUT

One of the features of the SERV engine is that compensation for malfunction or premature shutdown of a pump set can be provided. This is accomplished by the use of pump-out valves as shown in Fig. 2 . The turbomachinery overspeed capabilities allow the remaining 11 pumps to provide the additional flow to compensate for one module pump set shutdown. When required, the disabled pump is isolated, and the propellants supplied to the common manifolds by the remaining pumps, thereby maintaining the required flows over the entire engine. In this manner, thrust misalignment is prevented without additional control system or vectoring requirements. The effect on engine performance is a decrease of 0.2 seconds in engine specific impulse caused by an increase in turbine flow required by the higher pump discharge pressures.

Detailed dynamic analysis is necessary to define the operational modes, response requirements, and operating performance with this approach. For such an investigation, a computer dynamic module of the engine modules and the entire engine system need be developed. Such an undertaking was beyond the scope of the present contractual effort.

ENGINE DESIGN AND WEIGHT

MODULE LAYOUT (AP 71-044) Figure 10.

Each engine module can be defined by 1) thrust chamber (combustion chamber, injector, nozzle and base injection section), 2) interconnects/supports (lines, valves and supports), 3) turbomachinery (low pressure rise turbopumps, high pressure rise turbopumps and turbine drive gas generator), and 4) controls (including pogo suppression and ignition).

THRUST CHAMBER

Combustion Chamber

The combustor assembly for each engine module is comprised of 24 combustor segments. The core for each combustor segment is fabricated as a casting. Coolant flow passages in the casting are defined by coolant velocity, heat transfer and pressure drop requirements. The coolant passages are cast channels with an electroformed closeout for the cold wall.

The distance from the injector end of the combustor to the nozzle throat has been selected to ensure high combustion efficiency and stable combustion. The side walls of the combustor act as baffles between segments further assuring combustion stability. The combustor walls are tapered and contoured from the injector face to the throat. This allows the correct boundary layer formation and prevents unfavorable pressure gradients from developing in the combustion gas stream.

Wall radii upstream and downstream of the throat are selected to develop maximum performance.

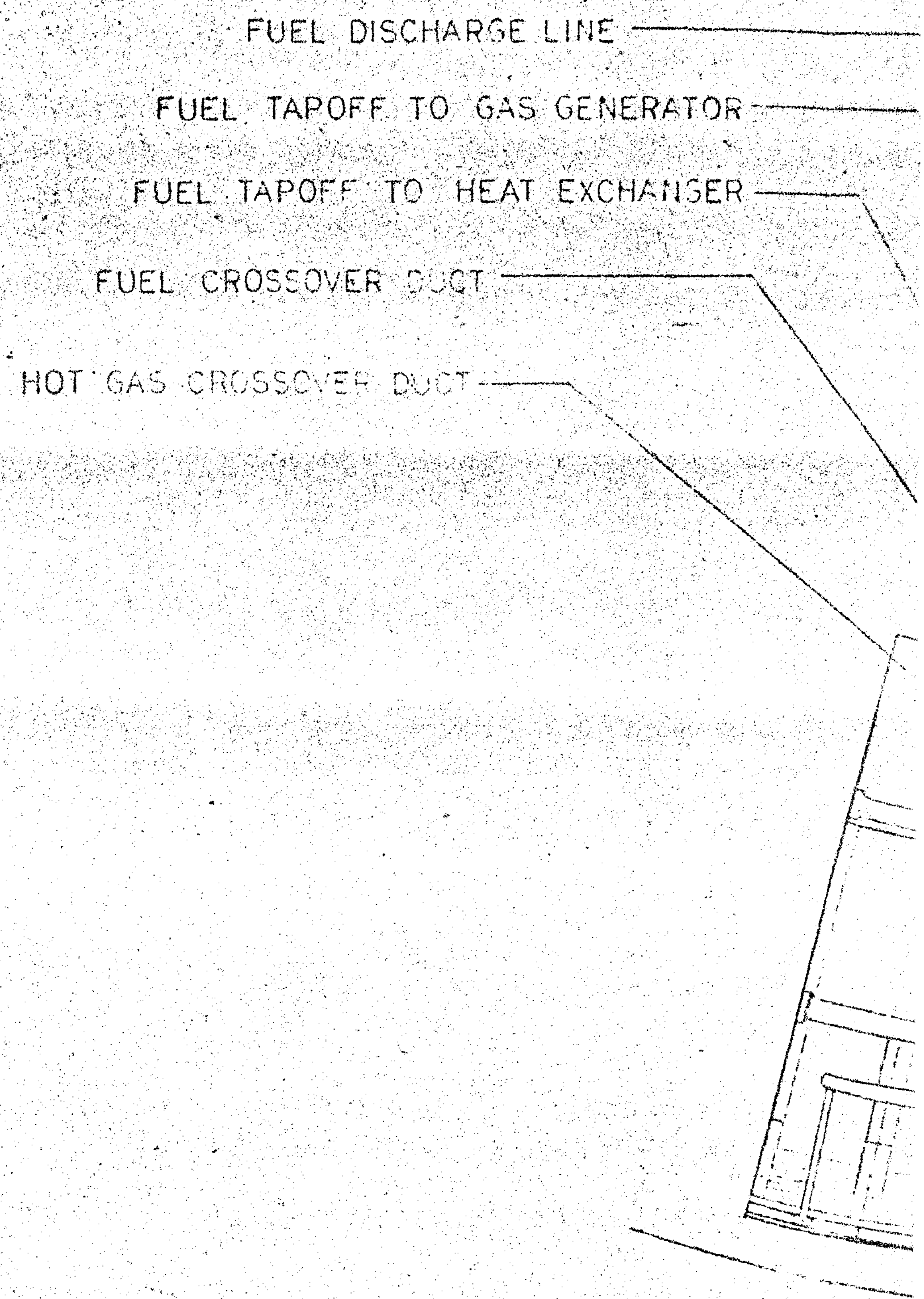
FUEL DISCHARGE LINE
FUEL TAPOFF TO GAS GENERATOR
FUEL TAPOFF TO HEAT EXCHANGER
FUEL CROSSOVER DUCT
HOT GAS CROSSOVER DUCT

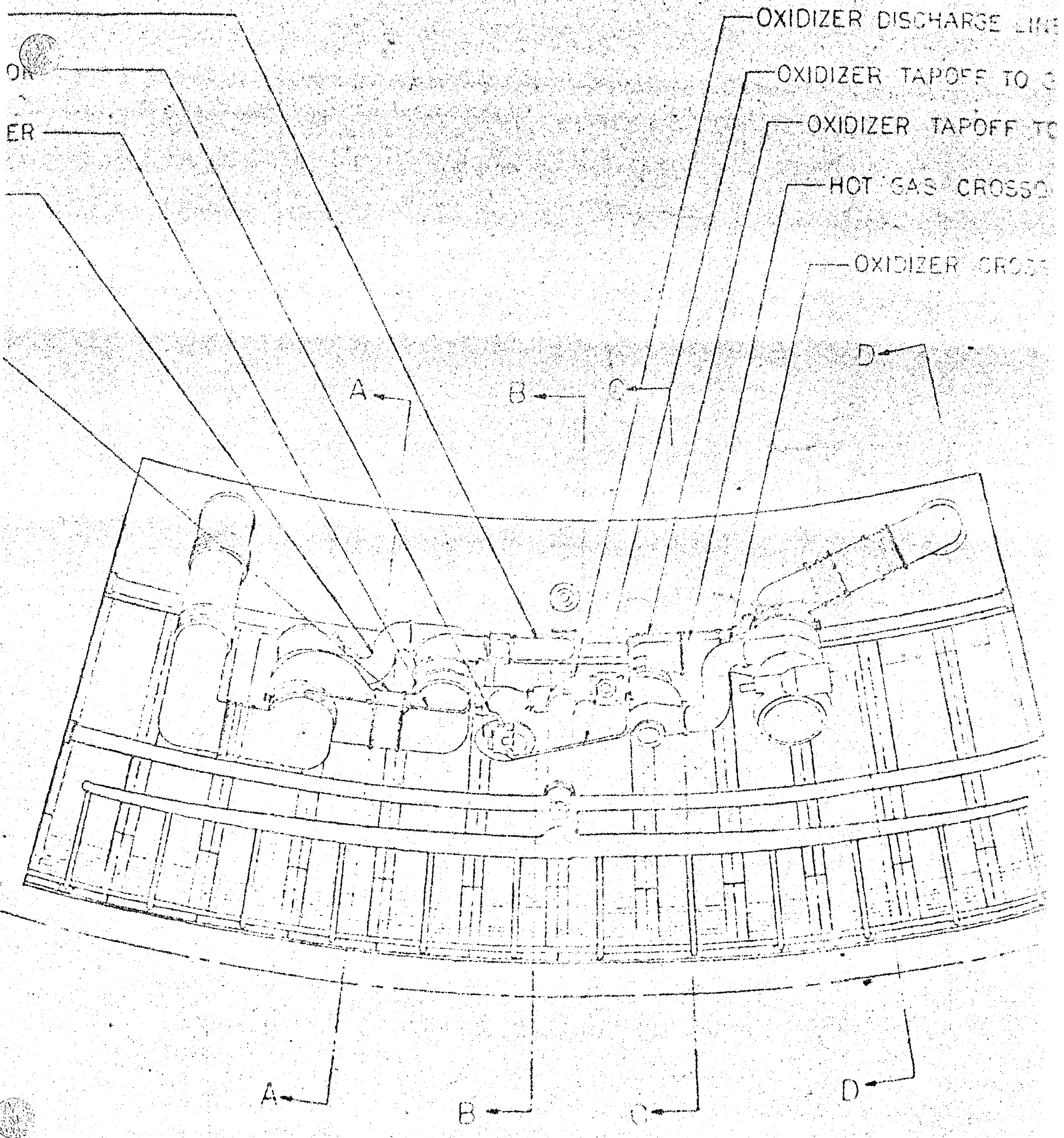

SERV ENGINE MODULE

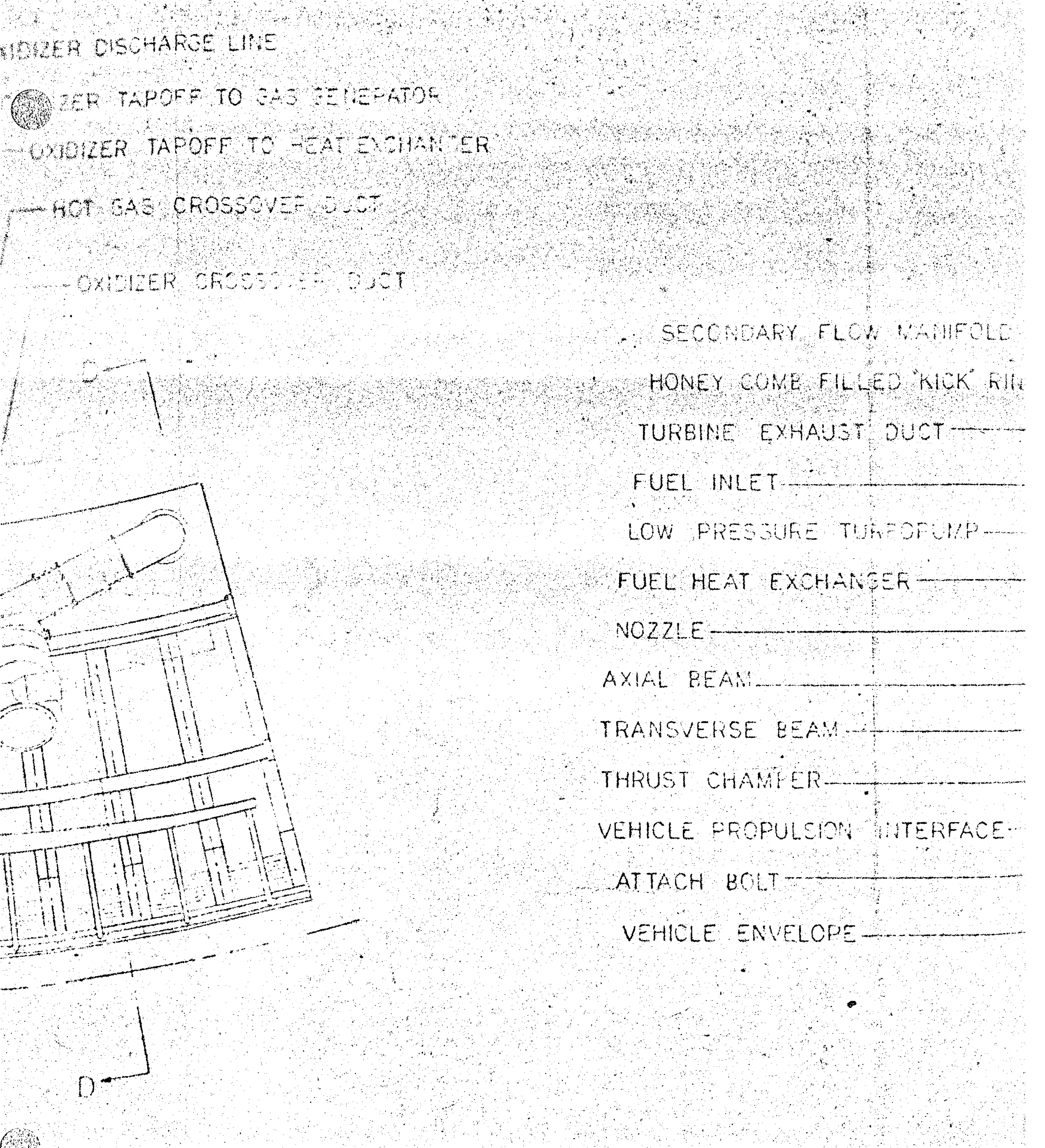

IDIZER DISCHARGE LINE
ZER TAPOFF TO GAS GENERATOR
OXIDIZER TAPOFF TO HEAT EXCHANGER
HOT GAS CROSSOVER DUCT
OXIDIZER CROSSOVER DUCT
D
D
SECONDARY FLOW MANIFOLD
HONEY COMB FILLED "KICK" RI
TURBINE EXHAUST DUCT
FUEL INLET
LOW PRESSURE TURBOPUMP
FUEL HEAT EXCHANGER
NOZZLE
AXIAL BEAM
TRANSVERSE BEAM
THRUST CHAMBER
VEHICLE PROPULSION INTERFACE
ATTACH BOLT
VEHICLE ENVELOPE

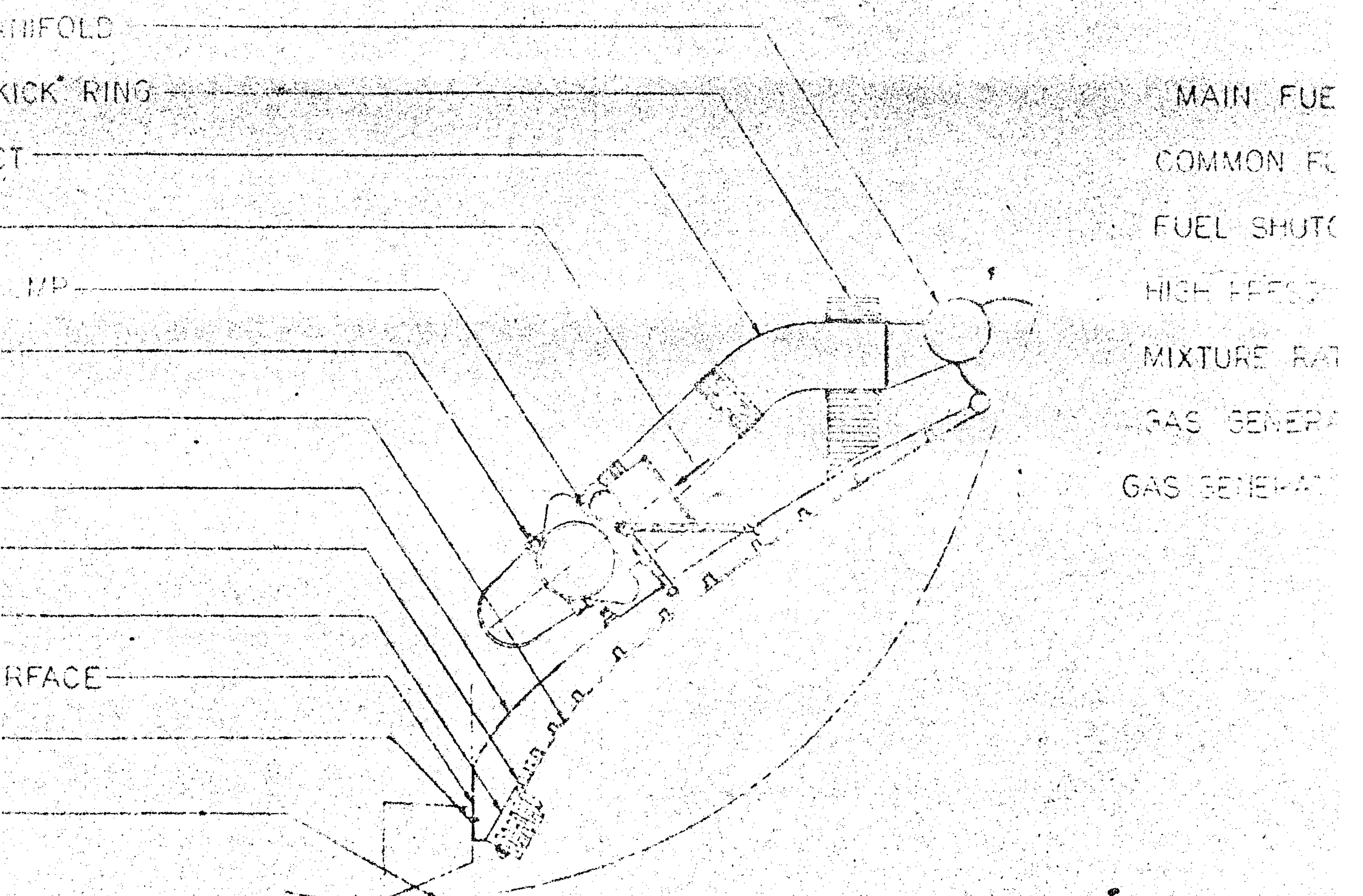

SECTION A-A
LOW PRESSURE FUEL FEED SYSTEM

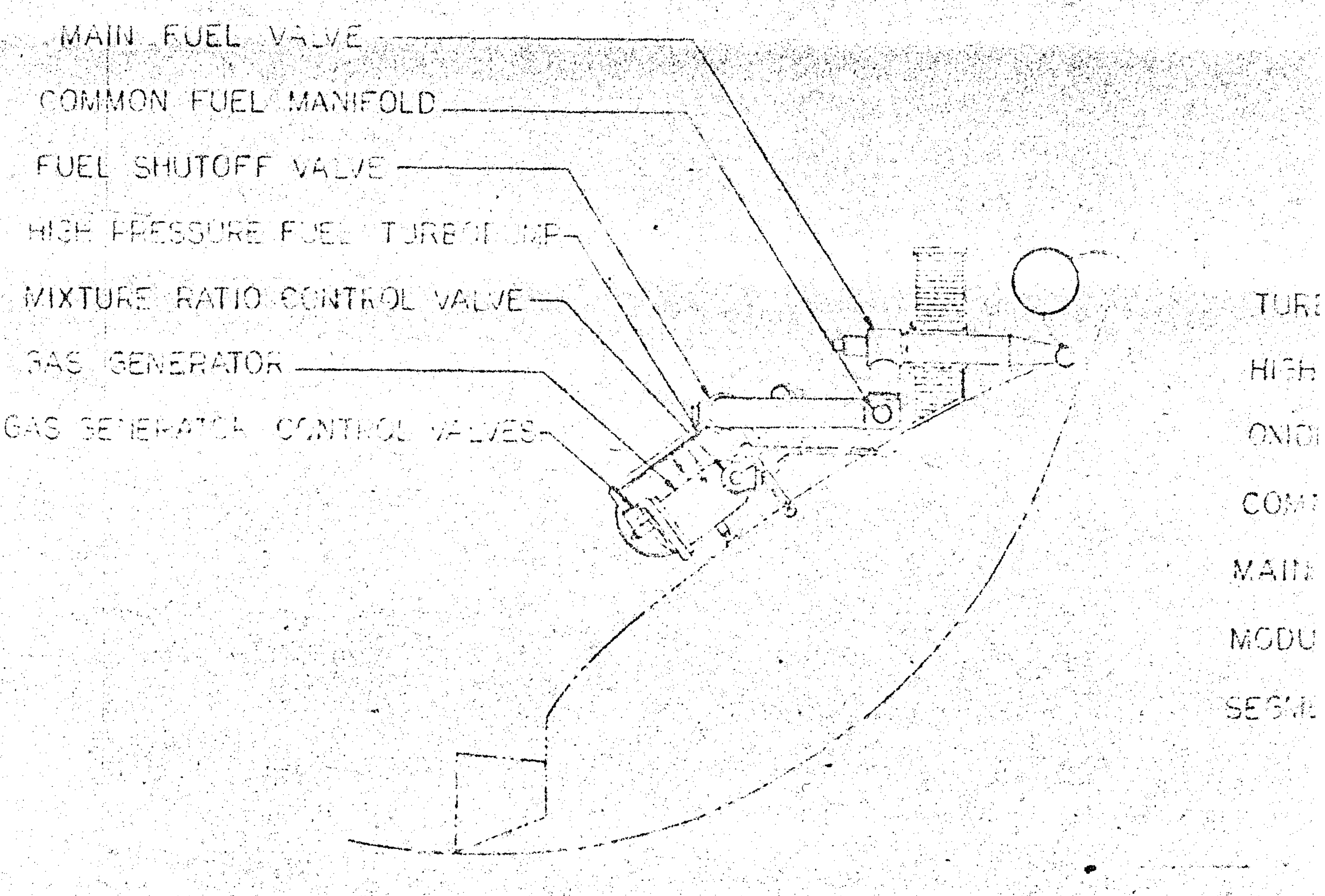

SECTION B-B
HIGH PRESSURE FUEL FEED SYSTEM

C

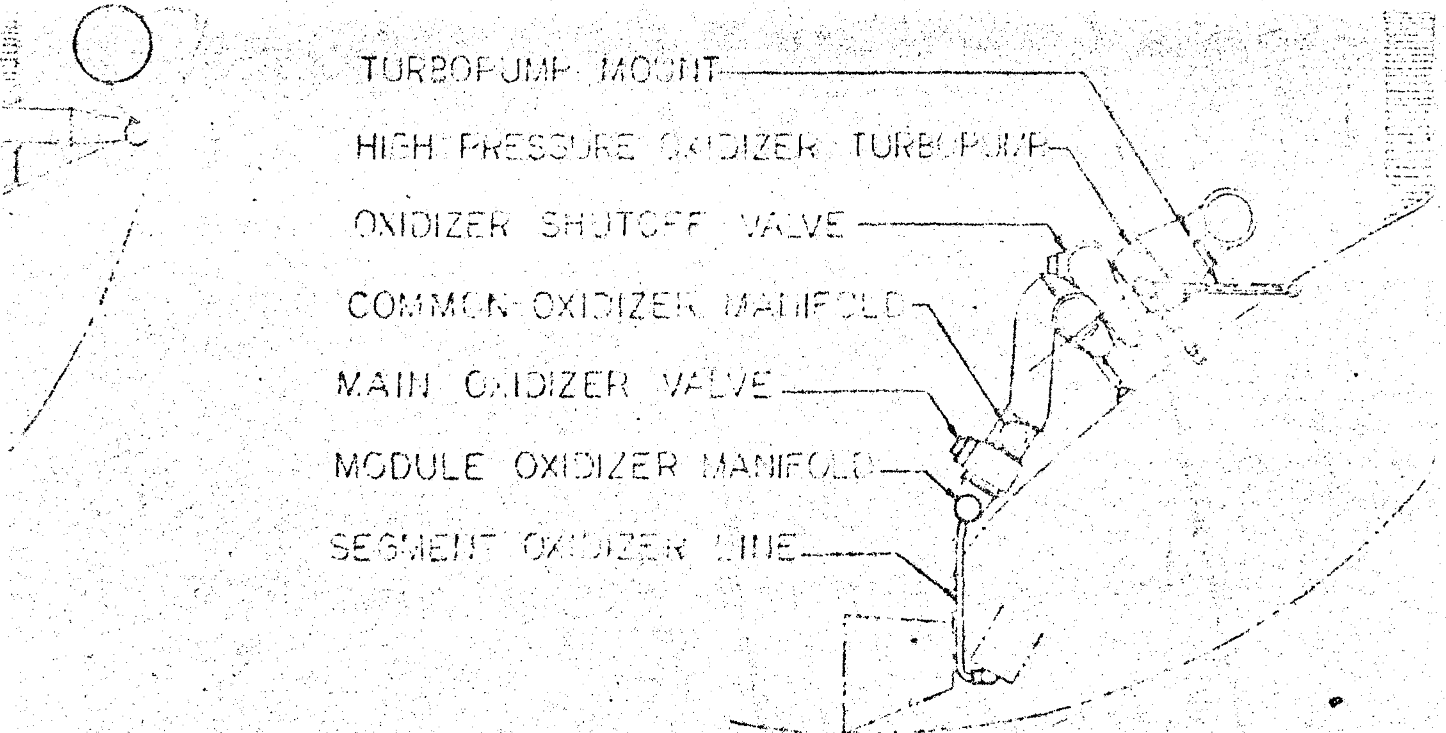

SECTION C-C

HIGH PRESSURE OXIDIZER FEED

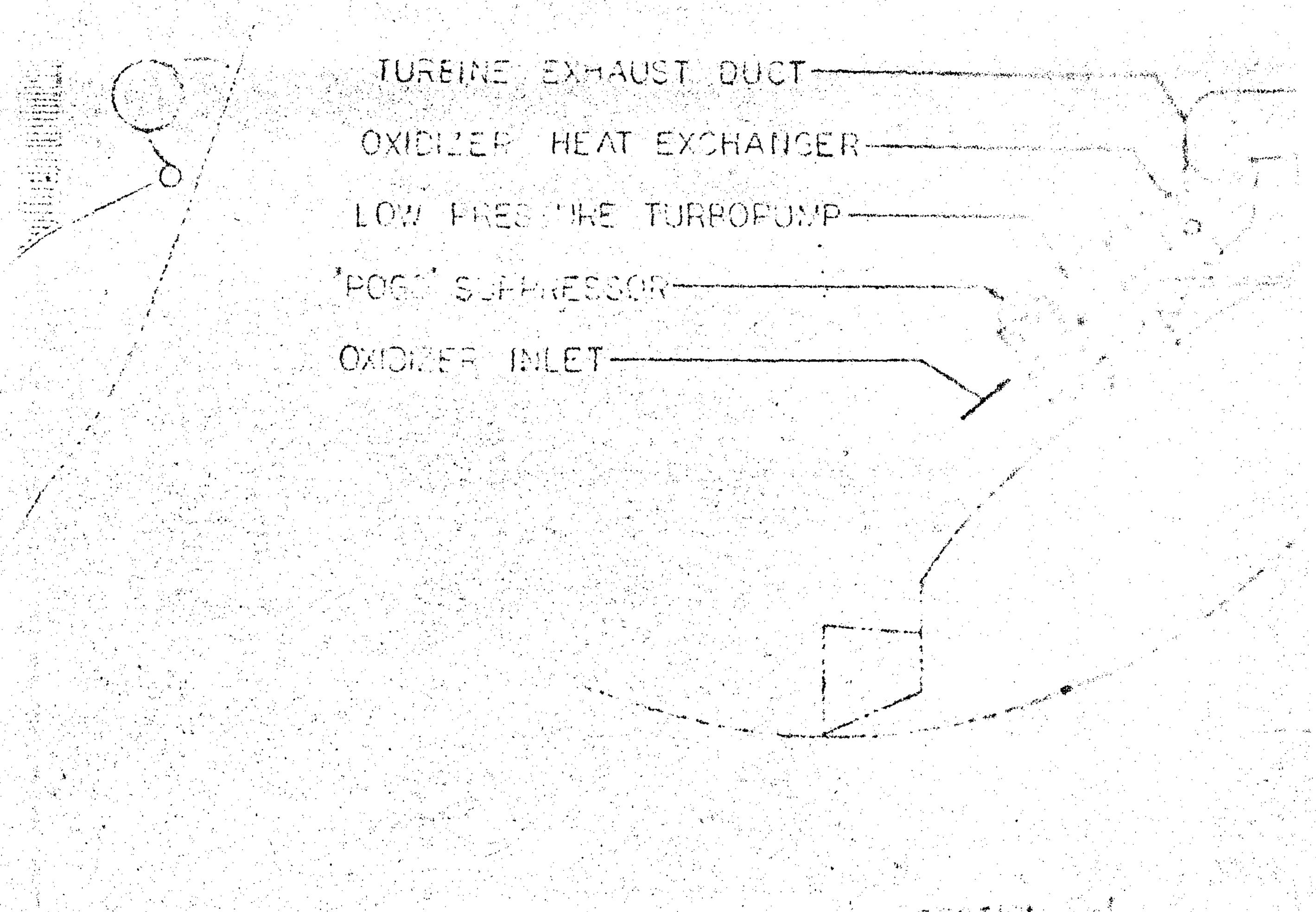
TURBINE EXHAUST DUCT
OXIDIZER HEAT EXCHANGER
LOW PRESSURE TURBOPUMP
"POGO" SUPPRESSOR
OXIDIZER INLET

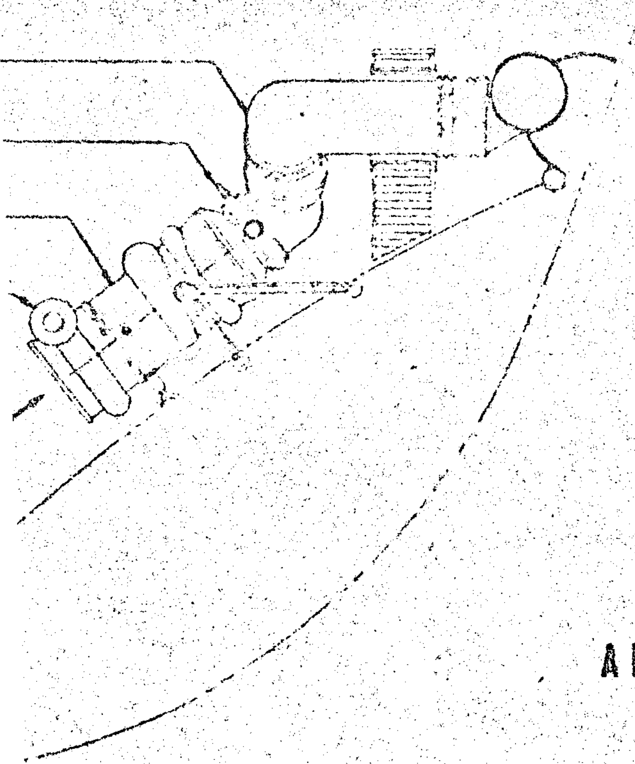

…ION D-D

…OXIDIZER FEED SYSTEM

ADVANCED DESIGN

Rocketdyne
North American Rockwell
Canoga Park, California

SERV POINT DESIGN
MODULE LAYOUT

L KAITH		CODE IDENT NO 02602
SCALE	DATE 8 MAR 71	

AP-71-044

Structural inner and outer rings, assembled about the combustors and joined by bolts between combustor segments, provide restraint against pressure and thermal loads. The inner structural ring is welded to the nozzle axial beams.

Injector

The injector face for each combustor segment is rectangular with a length to width ratio of approximately 6.7. The injector element is a coaxial type with hydrogen injected into an annular passage concentric with a tube through which liquid oxygen is injected. Proper recessing of the central tube controls the expansion of the hydrogen and provides for proper atomization and mixing of the propellants before combustion. The injector face is porous and transpiration cooled with hydrogen thereby maintaining the injector face at a low operating temperature. The injector body is an investment casting with fuel manifolding and oxidizer posts cast integrally with the body. The oxidizer manifold is welded to the body and the latter is welded to the combustion chamber.

Nozzle

The thrust chamber nozzle is formed in two parts. Downstream of the throat of the combustion chamber, the combustor body forms a two-dimensional shrouded spike nozzle. The module combustor assembly (composed of 24 segments) is attached to a one-piece tubular nozzle to complete the module nozzle (with a two-dimensional nozzle contour joined to a truncated ideal spike nozzle contour). The nozzle has a length from throat to end of section equal to 5.175 percent of that of a 15-degree cone of identical area ratio. The external flow field generated by the nozzle is essentially identical to that of a point-expansion truncated ideal spike nozzle. The nozzle tubular wall is backed by a shear skin and axial and transverse beams. The inner structural combustor ring is welded to the axial beams which in turn are welded to the shear panel which is attached to the inner (cold) surface of the tubular nozzle wall.

Base Injection Section

Secondary gas flow is introduced into the engine base through a porous annular injection section. The design of a high base performance, injection section is based on data from cold flow tests.

The secondary flow system (turbine exhaust base injection) consists of turbine exhaust ducts, a continuous toroidal duct and a flexible coupling. The toroidal duct serves as both turbine exhaust manifold and secondary flow injector. The injector is formed by holes punched in the aft segment of the duct. The toroidal duct is supported both outboard and inboard by a sealed flexible coupling assembly.

The flexible coupling permits radial translation of both the toroidal duct and thrust chamber skirt under action of thermal and thrust loading. Simply supported ends are provided at attach points (to the module nozzle and the vehicle structure) by piano hinges sealed against base pressure. Tangential stresses which would produce buckling failure and excessive rigidity of the structure are relieved by circumferential slots in the coupling wall. The voids thus formed are also sealed against base pressure.

INTERCONNECTS AND SUPPORTS

Lines and Valves

Rigid high-pressure propellant and hot gas lines are used to achieve a lightweight engine with simplicity of design and ease of component packaging. The main propellant valves and turbine drive gas generator propellant valves are variable position valves which function as control valves as well as on-off valves. Recirculation valves are provided on the high pressure rise pumps to facilitate engine throttling. Propellant valves are also provided to isolate the module turbopump set from the common propellant feed lines. This provides the engine system with pump set out/fail safe capability.

The hot gas valve functions as a mixture ratio control valve. Position indicators are provided for proper system sequencing and to facilitate operational evaluation by the engine inflight monitoring system.

Supports

Each turbopump is supported from the nozzle axial beams by the conventional 1-2-3 suspension system, i.e., one support has one attachment point to the axial beams, one support has two attachment points to the axial beams and one support has three attachment points to the axial beams. The turbine drive gas generator is attached to the high pressure rise fuel turbopump (the fuel pumping system consuming approximately twice the gas generator flow compared to the oxidizer pumping system).

TURBOMACHINERY

Low Pressure Rise Turbopumps

The low pressure rise fuel and oxidizer turbopumps have the capability of operating with minimum mainstage NPSH (e.g., a minimum of 0 ft and 12 ft for fuel and oxidizer, respectively), high efficiency, reliability, and maintainability. Minimum engine NPSH requirements are desirable in order to minimize tank pressure.

High Pressure Rise Turbopumps

The fuel pump is a two-stage centrifugal pump. The oxidizer pump is a single stage centrifugal pump. An accessory drive is provided on the oxidizer turbopump. Turbopump bearings, seals, and tip speeds were selected based on previous experience and long life considerations.

Turbine Drive Gas Generator

The gas generator produces low-mixture-ratio combustion gases to power the turbines. The gas generator can operate on gaseous, liquid, or two-phase propellants. During mainstage, the gas generator will operate on liquid propellants. Propellant valves located in the feed lines control the propellant flowrates and mixture ratio during operation.

CONTROLS

The control system is discussed elsewhere in this report. Two control items can be discussed here as part of the engine design since they effect the control of the engine system although they do not appear in the conventional controls section.

Pogo Suppression

Each engine module is equipped with a Pogo suppression device at the oxidizer pump inlet to prevent the oscillations experienced in previous launch vehicles. These oscillations are due to the inherent resonance in the vehicle structure and propellant feed system. The suppressor consists of an active control system utilizing a servo-controlled flow absorber. On command from the control system which senses vehicle acceleration, a quantity of fluid is displayed in such a way that the oscillations are cancelled. The fuel feed system does not require such a device because of the lower flowrate and the compressibility of the fuel, which tends to damp the oscillations.

Ignition

The gas generator and each combustion chamber segment will be equipped with resonance ignitors. This will provide a lightweight multistart ignition system.

ENGINE LAYOUT (AP 71-045) Figure 11.

The propulsion system for the SERV is an integrated aerospike-nozzle engine. The engine generates 5.7 million pounds of thrust at sea level at a chamber pressure of 2000 psia and an engine mixture ratio of 6.0.

The aerospike nozzle, which integrates into the vehicle base, has an area ratio of 433.7 and a length equal to 5.175 percent of an equivalent 15 degree conical nozzle.

The engine system is comprised of twelve modules, each module having a sea level thrust of 475,000 pounds. A module is the smallest basic operating unit of the engine and is an assembly of 24 combustor segments, a nozzle segment and one turbopump set. The modules are bolted together to form the complete 1040 inch O.D. engine system. The inlets to the low pressure rise pumps have been orientated for maximum accessibility to the propellant tanks.

The integrated engine operates on an open-flow power cycle, with the pumps driven by individual turbines powered by low-mixture-ratio combustion gases provided by the turbine drive gas generator. The engine system has common propellant feed ducts for the combustion chamber injectors. These common ducts and associated valves allows one turbopump set to shut down while still operating the attendant thrust chamber, i.e., pump set out/fail safe operation.

The engine system is equipped with heat exchangers capable of heating liquid propellants tapped from the engine for use in pressurizing the vehicle propellant tanks during mainstage operation.

Thrust vector control is provided by differential throttling of the engine quadrants.

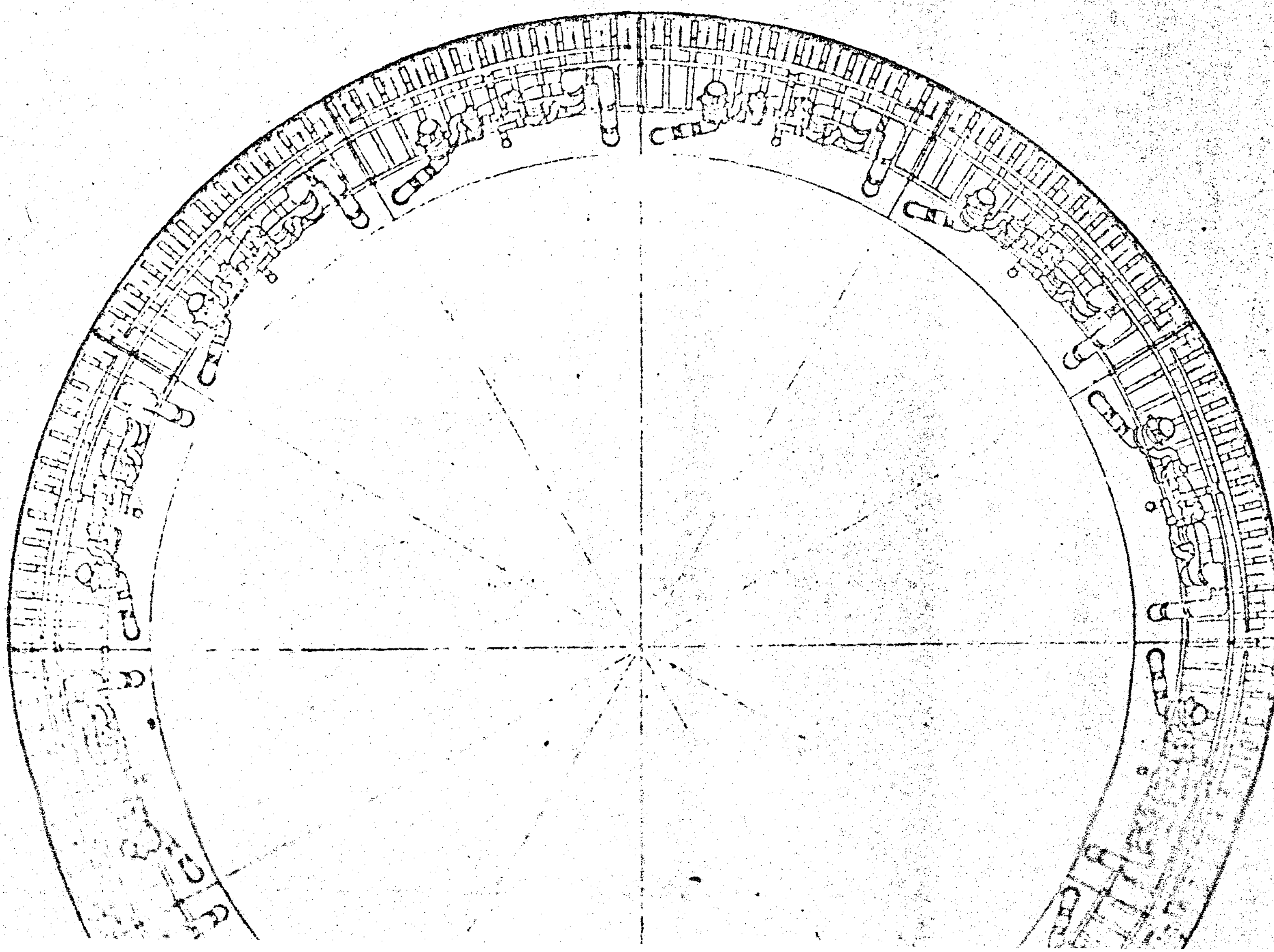

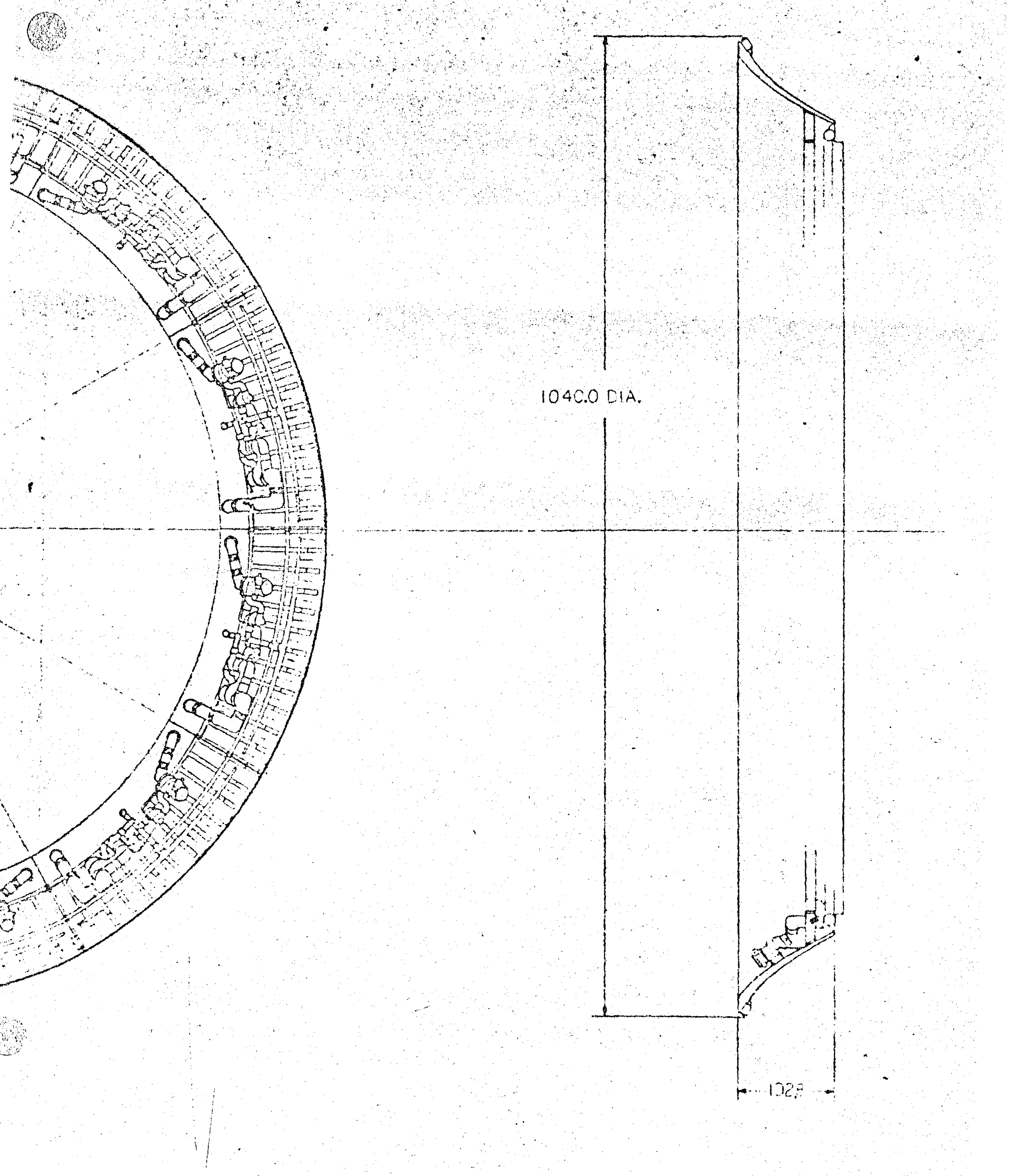

104C.0 DIA.
1028

THE STRUCTURAL ASPECTS OF ENGINE THRUST

The total thrust of the aerospike nozzle is generated by the combination of the peripherial combustion chamber load, the nozzle pressure profile and the base pressure (Fig.12). The principal nozzle structural element is the axial beam (I-sections made of titanium). These beams are supported at the forward end by the vehicle thrust structure and at the aft end by the kick ring. The aft "kick ring" is fabricated of titanium sheet formed in a box section with honeycomb as the core. The ring is bolted to the axial beams and to the transverse beams. Engine thrust loads are transmitted to the axial beams in the manner described below.

The magnitude and direction of the peripherial combustion chamber load is such that it tends to counterbalance the nozzle loading. Thus, the net side load from the system is small in comparison to the vertical thrust load. The combustion chamber load is transmitted to the axial beams by bending and shear of the combustion chamber structure. The line of action of the combustion chamber load is offset from the axial beam centroid and, therefore, provides a reverse (or reacting) moment to the moment generated by the nozzle pressure profile. The nozzle pressure load is reacted first by the nozzle tubes and transmits the loading to the transverse beams in bending. The transverse beams transmit these loads to the axial beams in bending.

The forward mount reacts both vertical (thrust) and horizontal loading. The kick ring reacts horizontal loading only and therefore, is sized structurally to resist hoop buckling under the influence of this loading. When a quadrant (3 engine modules) is throttled, the reduced loading on the ring has the same effect as imposing a distributed load in the opposite direction to the hoop loading that is already present (Fig. 13). The unbalanced loading imposes bending on the ring and in addition, the resulting

ADVANCED DESIGN

Rocketdyne
North American Rockwell
Canoga Park, California

SERV POINT DESIGN ENGINE LAYOUT		
[illegible]		CODE IDENT NO 02602
SCALE	DATE [illegible]	

AP-71-[illegible]

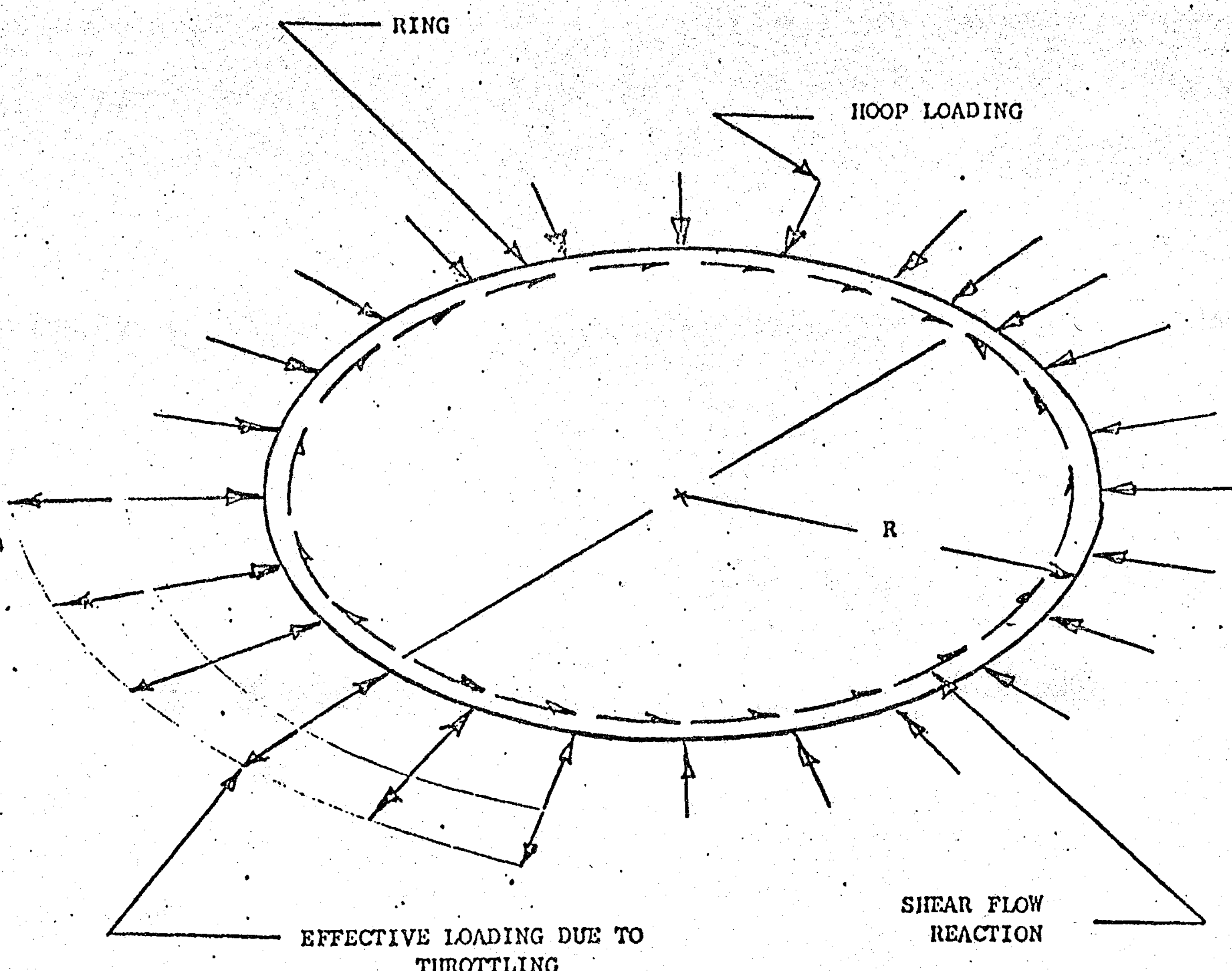

Figure 13.

AFT KICK RING LOADING

unbalanced side load must be reacted in shear flow. A shear skin is provided (bonded to the nozzle tubes for stability) to transmit this shear flow to the forward mount. The transverse beams are increased in height in the area of the aft kick ring to provide the required shear tie between the ring and this skin.

The bending imposed on the aft kick ring by differential throttling was reviewed in some detail during the previous report period. For the same effective gimbal angle, quadrant throttling results in a maximum ring bending moment of approximately 62 percent of the maximum moment obtained for module throttling. It was also apparent that a large reduction of maximum bending moments could be obtained if opposing quadrants (or modules) are throttled. However, this was not pursued since, in all cases, the ring size was governed by hoop buckling and the stress from ring bending was relatively small.

In summary, the propulsion system generates three peripheral loads that must be reacted by the vehicle thrust structure. This loading is summarized in Fig. 14 . It consists of the vertical (thrust) load, R_v, a horizontal load, R_h, and the shear flow that arises as a result of differential throttling for thrust vector control. During throttling, the vertical and horizontal loading can be calculated using the percent of module thrust for the given condition. The shear flow is then calculated from the resulting unbalanced side load. The loads shown are the maximum values that occur at altitude and include a limit load factor of five percent.

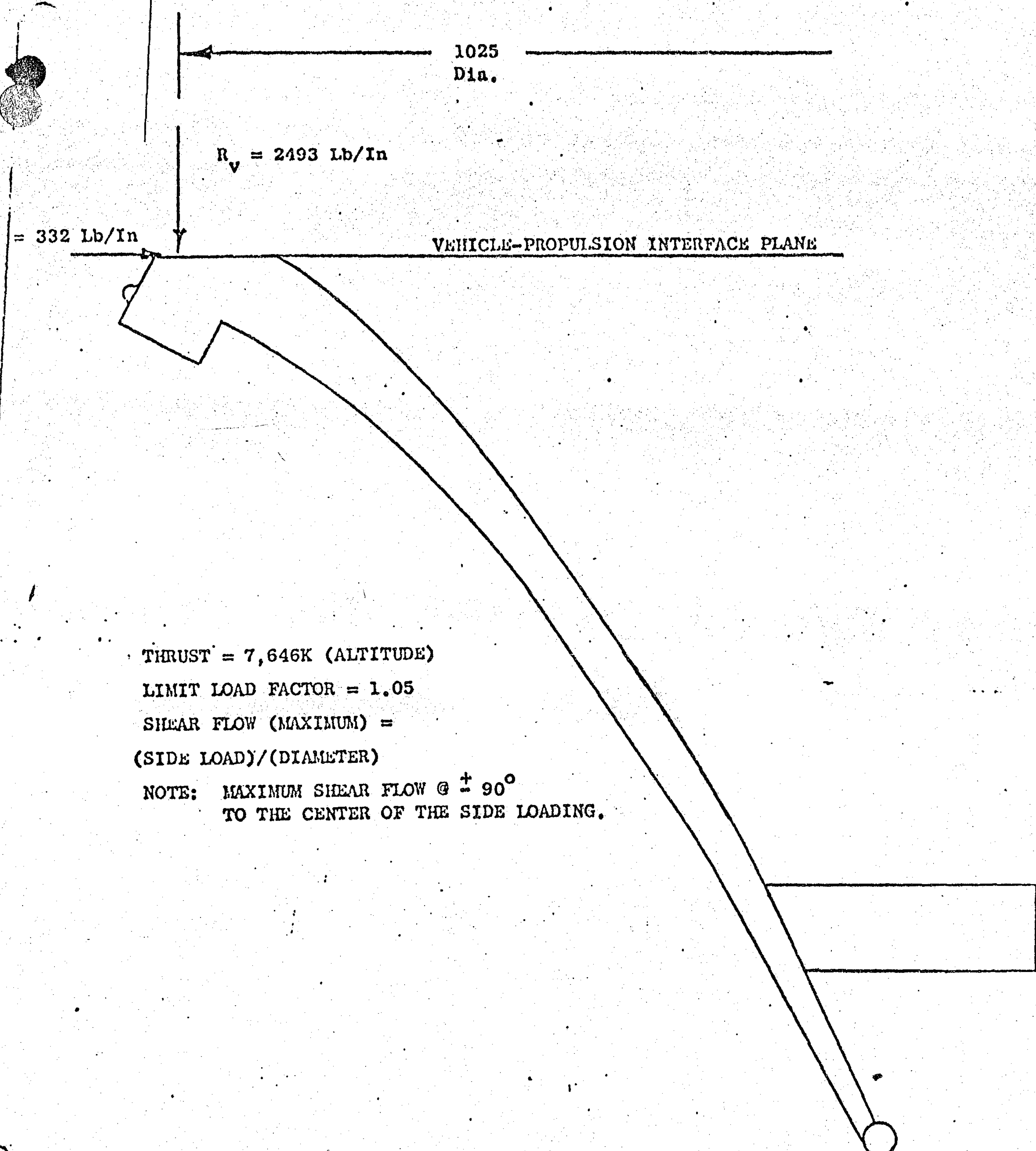

LIMIT LOADING AT ALTITUDE

ENGINE VEHICLE INTERFACE (AP 71-046) Figure 15.

The primary interface between the engine and the vehicle is the structural attachments and the propellant feed ducts. The secondary interface is the flow of propellant tank pressurant and control signals and actuation power.

Since the engine system is not gimbaled, many design requirements usually associated with an engine vehicle interface have been eliminated, i.e., the great variety of flexible and/or gimbaling lines is not required. Also, location restrictions imposed by gimbaling requirements as to where the lines may be routed have been eliminated.

The structural interface is the conical thrust structure attachment to the vehicle and the base injection section attachment to the structure. The thrust structure is attached using two bolts at each axial beam location (144 beams located 2^{o} 30' apart). The base injection section is attached by a simple supported seal.

The propellant feed ducts must have enough flexibility to allow for installation alignment and thermal changes brought about by the propellants.

ENGINE WEIGHT AND MASS PROPERTIES

The point design engine weights are summarized in Table 1 . Dry, wet and burnout weights are presented for both the engine and the engine module. A more detailed breakdown of these weights was used in conjunction with the engine design drawing to calculate the system mass properties. These properties are summarized in Table 2 . They include dry, wet and burnout center of gravity locations and the calculated mass moments of inertia about the center of gravity. The coordinate axis system used has its origin at the

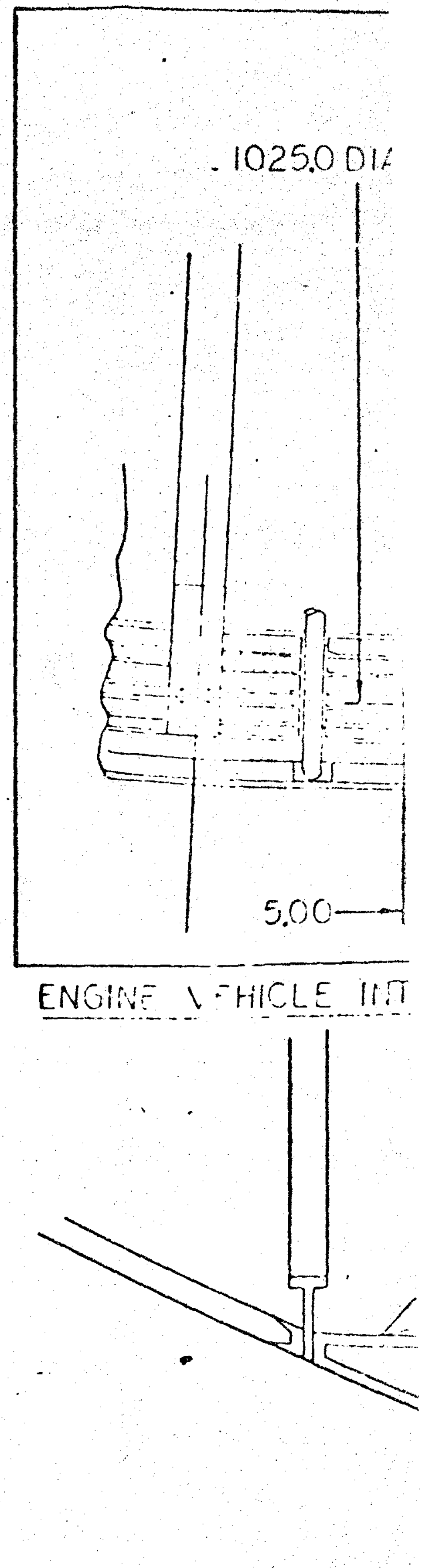
1025.0 DI/
5.00
ENGINE V:HICLE INT

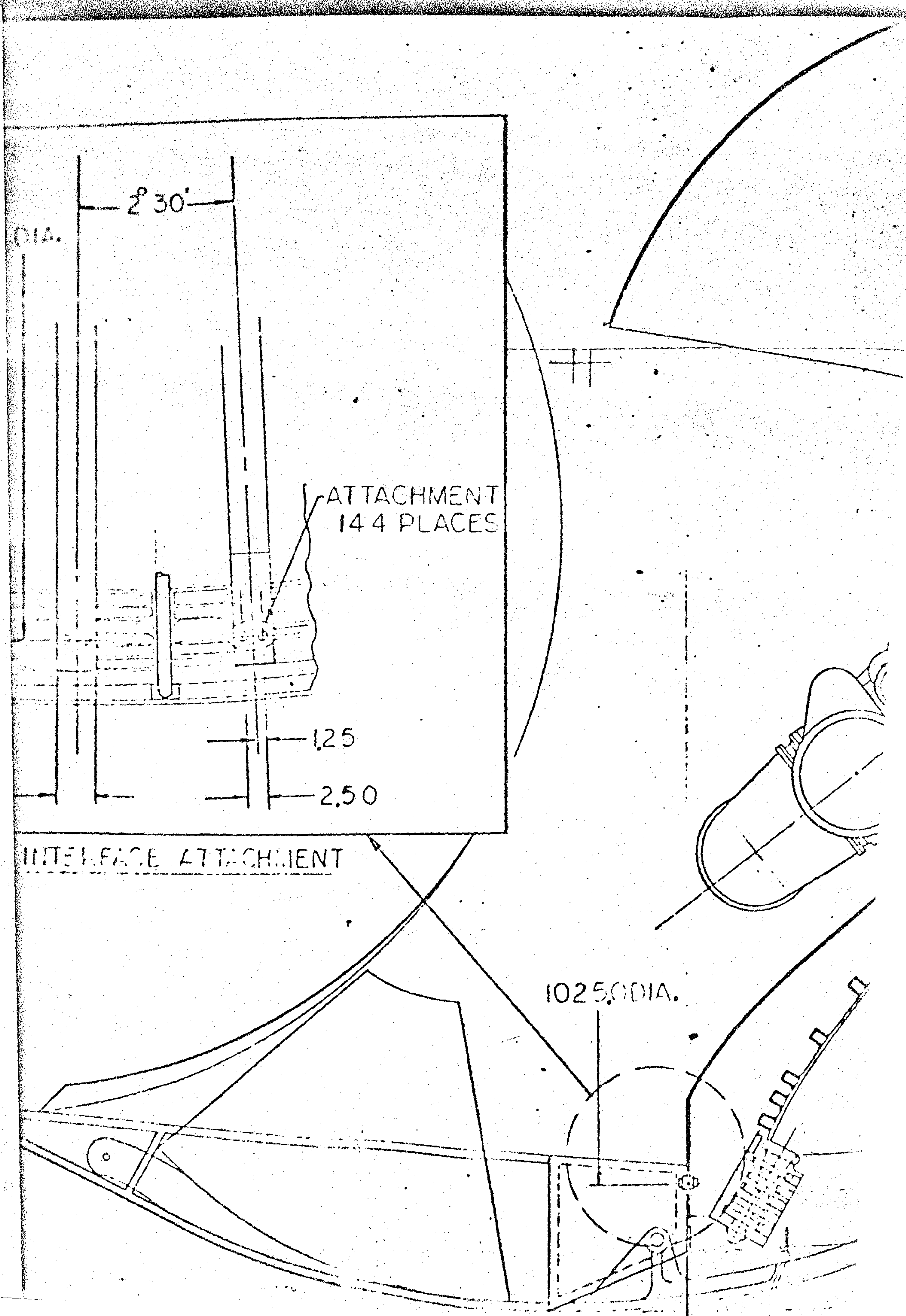

DIA.
2° 30'
ATTACHMENT
144 PLACES
1.25
2.50
INTERFACE ATTACHMENT
102.500 DIA.

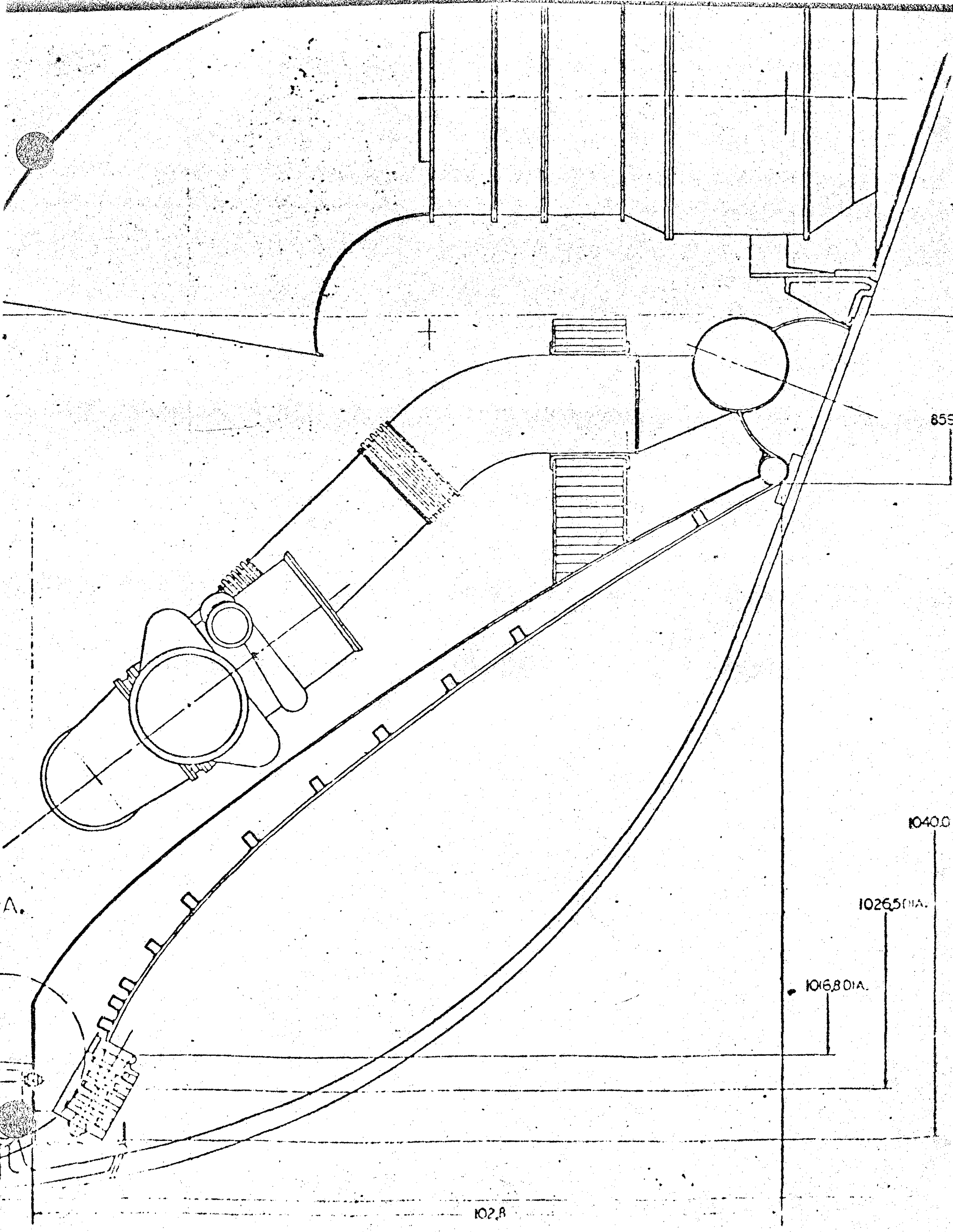

859
1040,0
1026,5 DIA.
1016,8 DIA.
102,8

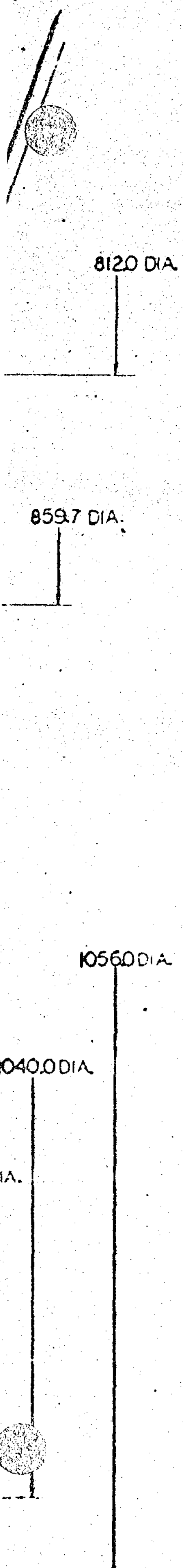

ADVANCED DESIGN

Rocketdyne
North American Rockwell
Canoga Park, California

SERV POINT DESIGN
ENGINE VEHICLE INTERFACE

T. KAITH		CODE IDENT NO 02602
SCALE	DATE 8 MAR 71	

AP-71-046

TABLE 1

ENGINE WEIGHT BREAKDOWN

- F = 5700 K (SEA LEVEL
- P_c = 2000 psia
- MIXTURE RATIO = 6
- OUTSIDE DIAMETER = 1040 in. (86.67 ft)
- THRUST VECTOR CONTROL: DIFFERENTIAL THROTTLING
- NOZZLE PERCENT LENGTH = 5.175

	WEIGHT, LBS.	
	ENGINE	MODULE
	(65,448)	(5,454)
COMBUSTION CHAMBER	9,965	830
NOZZLE	16,214	1,351
TURBOPUMPS AND MOUNTS	14,195	1,183
LOW PRESSURE TURBOPUMPS AND MOUNTS	4,911	409
PROPELLANT DUCTING AND VALVES	11,635	970
HOT GAS/IGNITION SYSTEM	5,179	432
CONTROLS AND MISCELLANEOUS	3,349	279
	(18,482)	
AFT KICK RING	16,222	
BASE FLOW INJECTION SYSTEM	1,972	
MODULE ATTACH PARTS	288	
FLUIDS, WET	2,704	225
FLUIDS, BURNOUT	870	73
SYSTEM WEIGHT, DRY	83,930	5,454
SYSTEM WEIGHT, WET	86,634	5,679
SYSTEM WEIGHT, BURNOUT	84,800	4,527

TABLE 2

BASELINE ENGINE MASS PROPERTIES

Weight, lbs.		Center of Gravity, in.			Mass Moments of Inertia (Slug-Ft^2)		
		x	y	z	Ix	Iy	Iz
83,930	Dry	-40	0	0	3,831,800	1,932,600	1,932,600
86,634	Wet	-39	0	0	3,959,500	1,997,000	1,997,000
84,800	Burnout	-39	0	0	3,871,500	1,952,500	1,952,500

engine (and vehicle) centerline in the vehicle-propulsion interface plane (Ref. 183.32 dimension, Chrysler drawing number 60SK-193, "SERV - Revised Baseline Vehicle, 88 feet Diameter", 2/12/71). The positive x-axis is directed forward (away from the propulsion system) and the y and z axis are in the interface plane. Since the propulsion system is symmetrical, the y and z axis can be assigned any compatible directions that may be desired.

SERV THRUST CHAMBER COOLING ANALYSIS

The SERV engine consists of an annular combustor expansing hot combustion gases on a truncated aerospike nozzle. The combustor, Fig.16 , is about 5 inches in length from the injector face to throat plane with a throat gap (neglecting baffles) of 0.5806 inches and injector end height of 1.5 inches. The combustor axis is canted radially outward 62.3 degrees with respect to the engine centerbody axis of symmetry. The combustor shroud extends about 4.8 inches below the throat to an area ratio of about 5.5.

The combustor including the shroud will be fabricated from a NARloy casting or billet with coolant passages machined on the outer contour. The coolant passages are closed out with an elecrodeposited nickel backwall which also provides structural rigidity for the contour.

Coolant passages for the combustor throat should be about 0.050 inches square with a 0.060 inch land. The gas-side wall thickness for the expected heat flux at 2000 P_c is about 0.035 inches, which should also meet other requirements. If constant land thickness is maintained throughout the combustor length, passage width will be about 0.052 inches at the injector and about 0.051 at the shroud exit. An engine combustor segment will contain about 100 passages.

The spike nozzle is truncated to 5.175 percent length of a 15 degree conical nozzle of the same area ratio. This results in a nozzle length of about 93 inches along the centerbody axis from the combustor throat, Fig.17 . The nozzle will be cooled with a tubular wall of about 50 stainless steel tubes per segment. A heat flux of 10 Btu/in^2-sec at the attach point requires a coolant mass velocity of 4.0 lb/in^2-sec with a

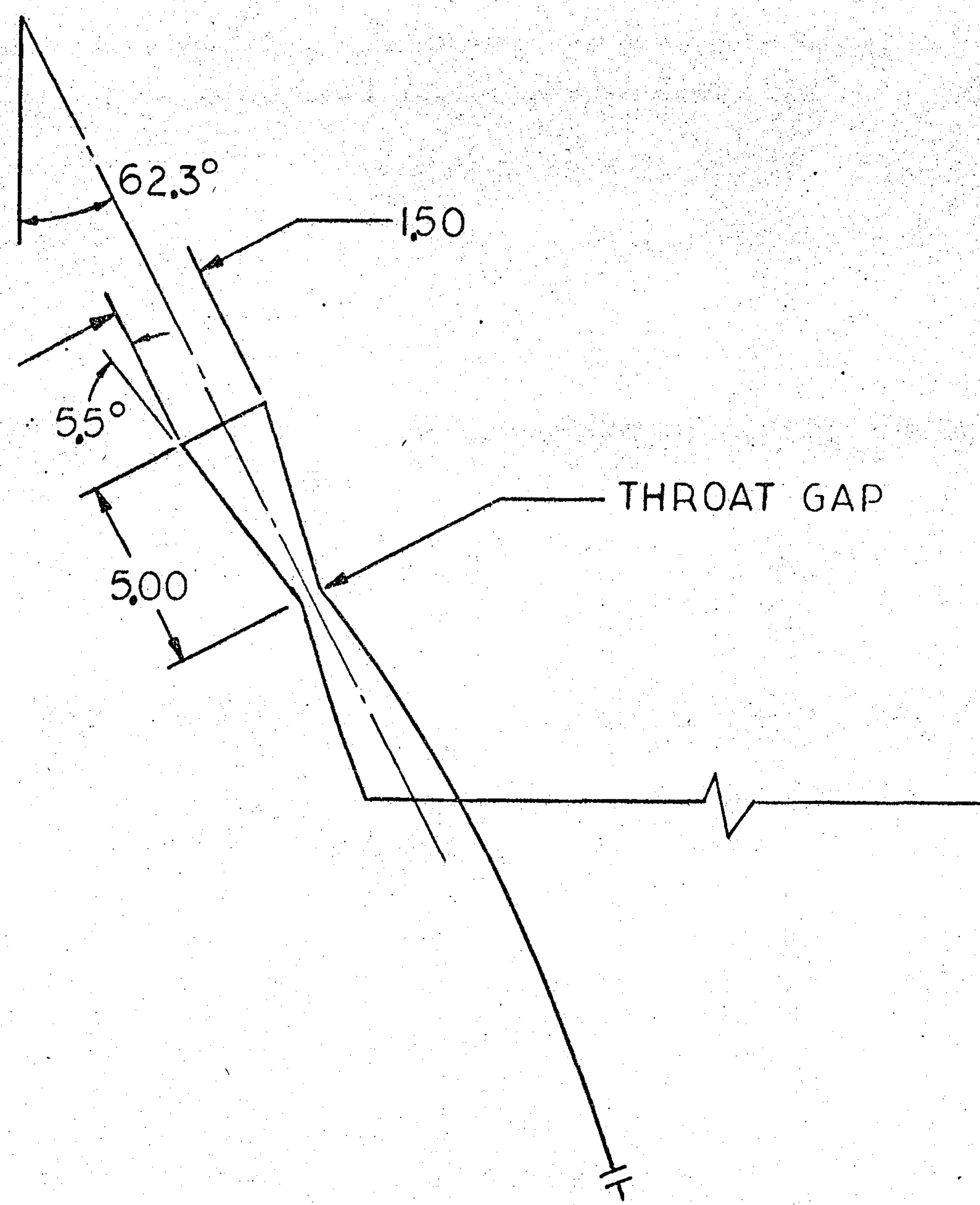

Figure 16 . SERV Engine Combustor Geometry

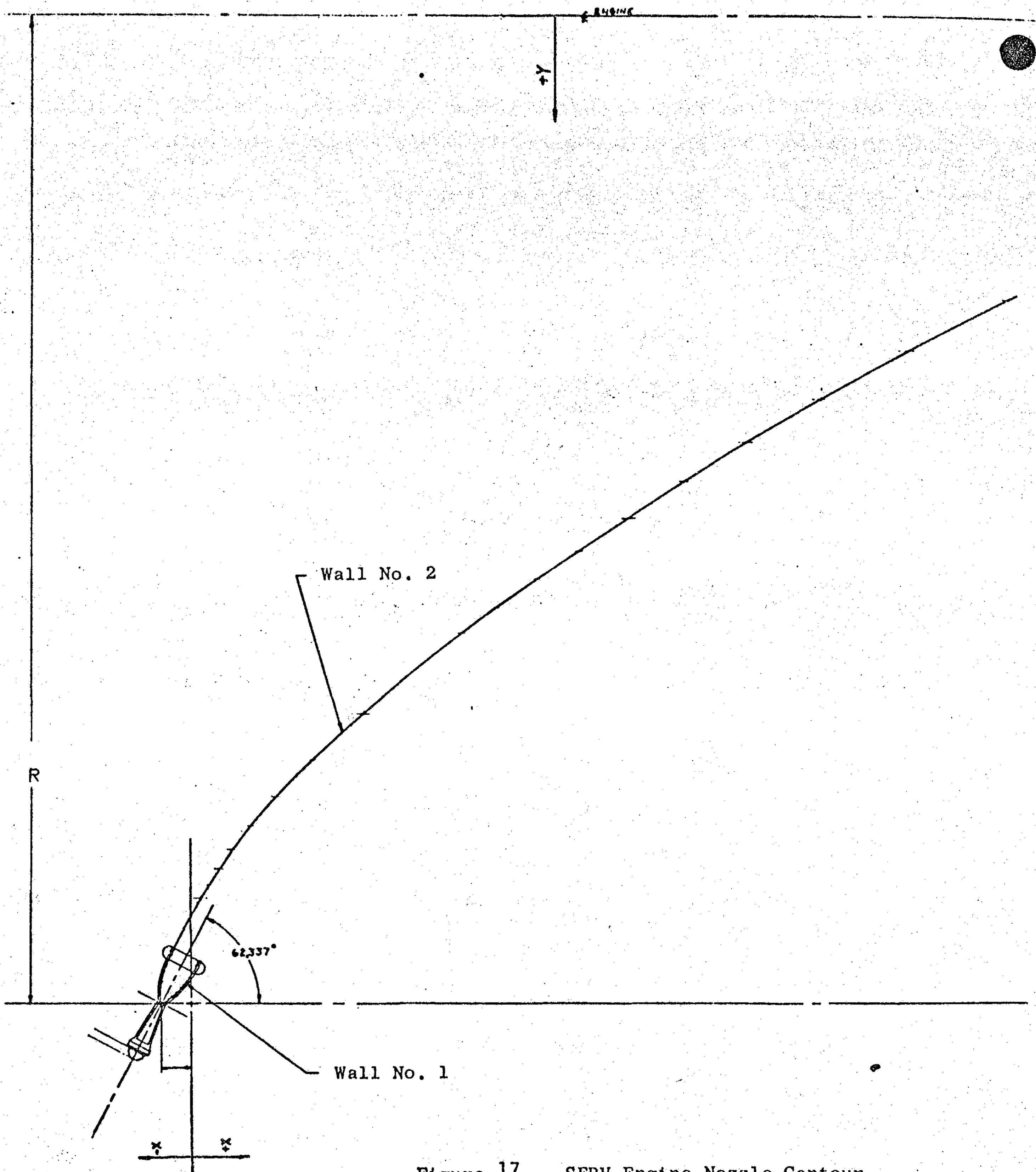

Figure 17 . SERV Engine Nozzle Contour

0.015 inch tube wall thickness. This may be achieved with a 0.20 inch inside tube diameter. The heat flux at the nozzle exit plane is about 0.9 Btu/in^2-sec requiring a coolant mass velocity of 0.5 lb/in^2-sec. The tube width at the exit is 0.150 inches requiring a flat length of about 0.9 inches to achieve the 0.5 mass velocity.

Proper design would retain an L/D ratio of about 3 resulting in a flat length of about 0.4 inches. This effects a substantial reduction in tube wall weight and simplifies fabrication. The result is usually a small increase in coolant pressure drop since the over-cooled wall is in a low heat flux region near the spike exit.

The SERV combustor is very similar to the linear engine cast NARloy segment recently designed and tested under NASA contract NAS8-30182. The operating conditions for the cast segment are similar to those for the SERV combustor as shown in Table 3. The SERV combustor heat load may be predicted from the experimental data taken on the linear engine cast segment. The composite heat loads to an area ratio of 3.87 for the four 11.25 inch side panels are plotted versus chamber pressure in Fig.18. Extrapolating this data to 2000 psia and summing the result yields a total combustor heat load of 630 Btu/sec per inch of combustor width.

A throat mean diameter for the SERV engine of 1026.5 inches yields a total heat load of 2.03 x 10^6 Btu/sec to an area ratio of 3.87. The heat load for the balance of the SERV shroud is derived from a boundary layer analysis of the contour from ϵ = 3.87 to the exit at ϵ = 5.53. This resulted in an additional 112,530 Btu/sec per side, assuming the inner and outer bodies are identical to the shroud exit. A theoretical analysis of the spike nozzle surface indicates an additional contribution of 991,000 Btu/sec. The total engine heat load to be absorbed by fuel coolant is then 3.25 x 10^{-6} Btu/sec. If the entire fuel flow is available to cool the thrust chamber walls, a bulk temperature rise of 430 degrees F is predicted. "Film coefficients for SERV are shown in Figures 19 and 20."

E

TABLE 3

COMBUSTOR OPERATING CONDITIONS

	SERV	LINEAR ENGINE
P_c, psia	2000	1200
Throat Gap, in.	0.5806 (No Baffles)	0.456
Propellants	LOX/H_2	LOX/H_2
Mixture Ratio	6.45	6.0
Material	NARloy	Cast NARloy
Length, in.	5.0	5.0
Convergence, degrees	5.5	6.0
Injector Height, in.	1.5	1.5
ϵ_c	2.59	3.29
ϵ_{exit}	5.53	3.87
Cooling Circuit	--	All sides in parallel

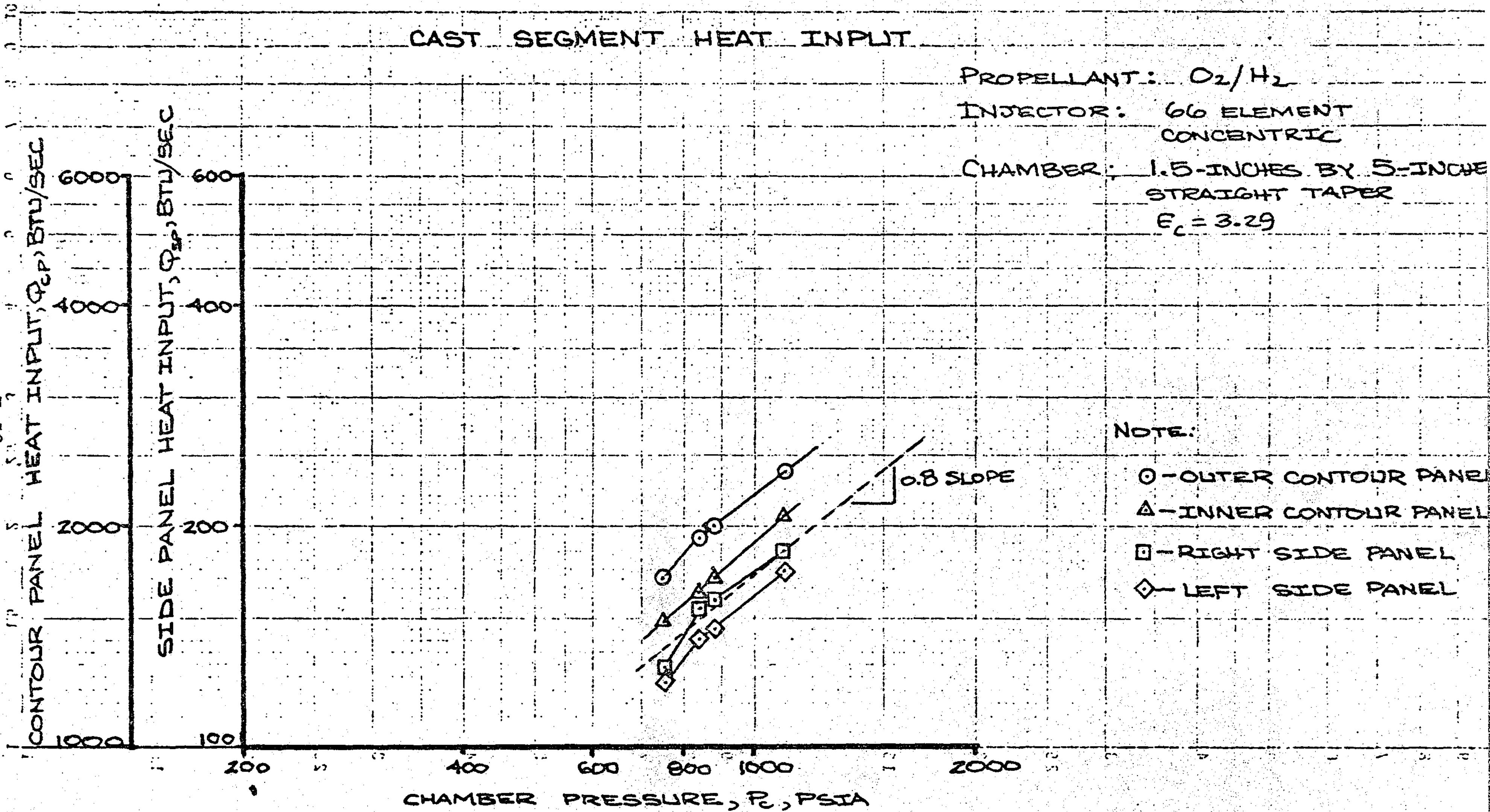

CAST SEGMENT HEAT INPUT
PROPELLANT: O_2/H_2
INJECTOR: 66 ELEMENT CONCENTRIC
CHAMBER: 1.5-INCHES BY 5-INCHE
STRAIGHT TAPER
$\epsilon_c = 3.29$
CONTOUR PANEL HEAT INPUT, Q_{CP}, BTU/SEC
SIDE PANEL HEAT INPUT, Q_{SP}, BTU/SEC
6000
4000
2000
1000
600
400
200
100
200
400
600
800
1000
2000
CHAMBER PRESSURE, P_c, PSIA
0.8 SLOPE
NOTE:
⊙ - OUTER CONTOUR PANEL
△ - INNER CONTOUR PANEL
⊡ - RIGHT SIDE PANEL
◇ - LEFT SIDE PANEL

Figure 18

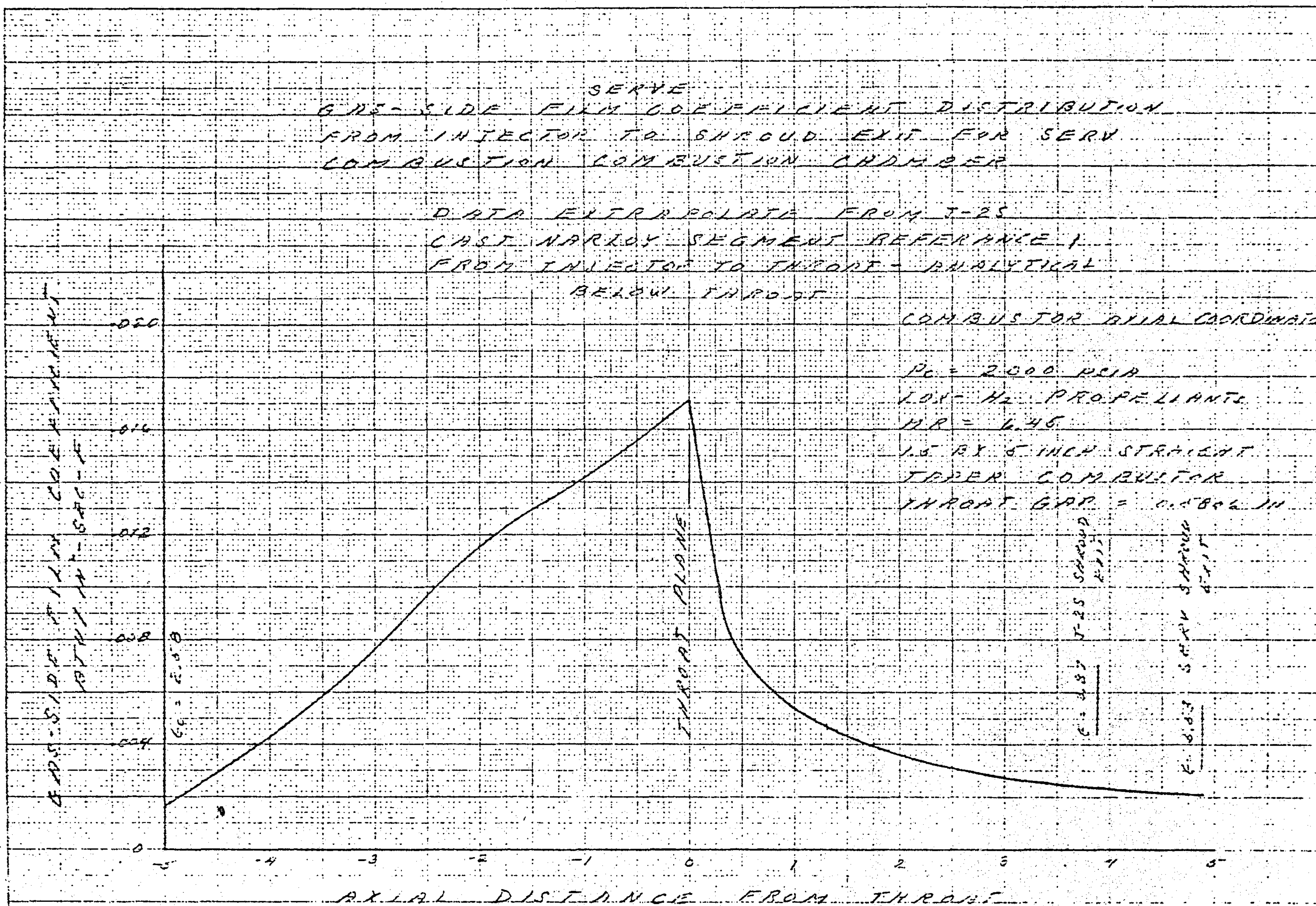
SERVE
GAS-SIDE FILM COEFFICIENT DISTRIBUTION
FROM INJECTOR TO SHROUD EXIT FOR SERV
COMBUSTION COMBUSTION CHAMBER
DATA EXTRAPOLATE FROM J-2S
CAST NARLOY SEGMENT REFERANCE 1
FROM INJECTOR TO THROAT - ANALYTICAL
BELOW THROAT
COMBUSTOR AXIAL COORDINATE
Pc = 2000 PSIA
LOX - H2 PROPELLANTS
MR = 6.45
1.5 BY 5 INCH STRAIGHT
TAPER COMBUSTOR
THROAT PLANE
AXIAL DISTANCE FROM THROAT
.020
.016
.012
.008
.004
0
-5
-4
-3
-2
-1
0
1
2
3
4
5

Figure 19

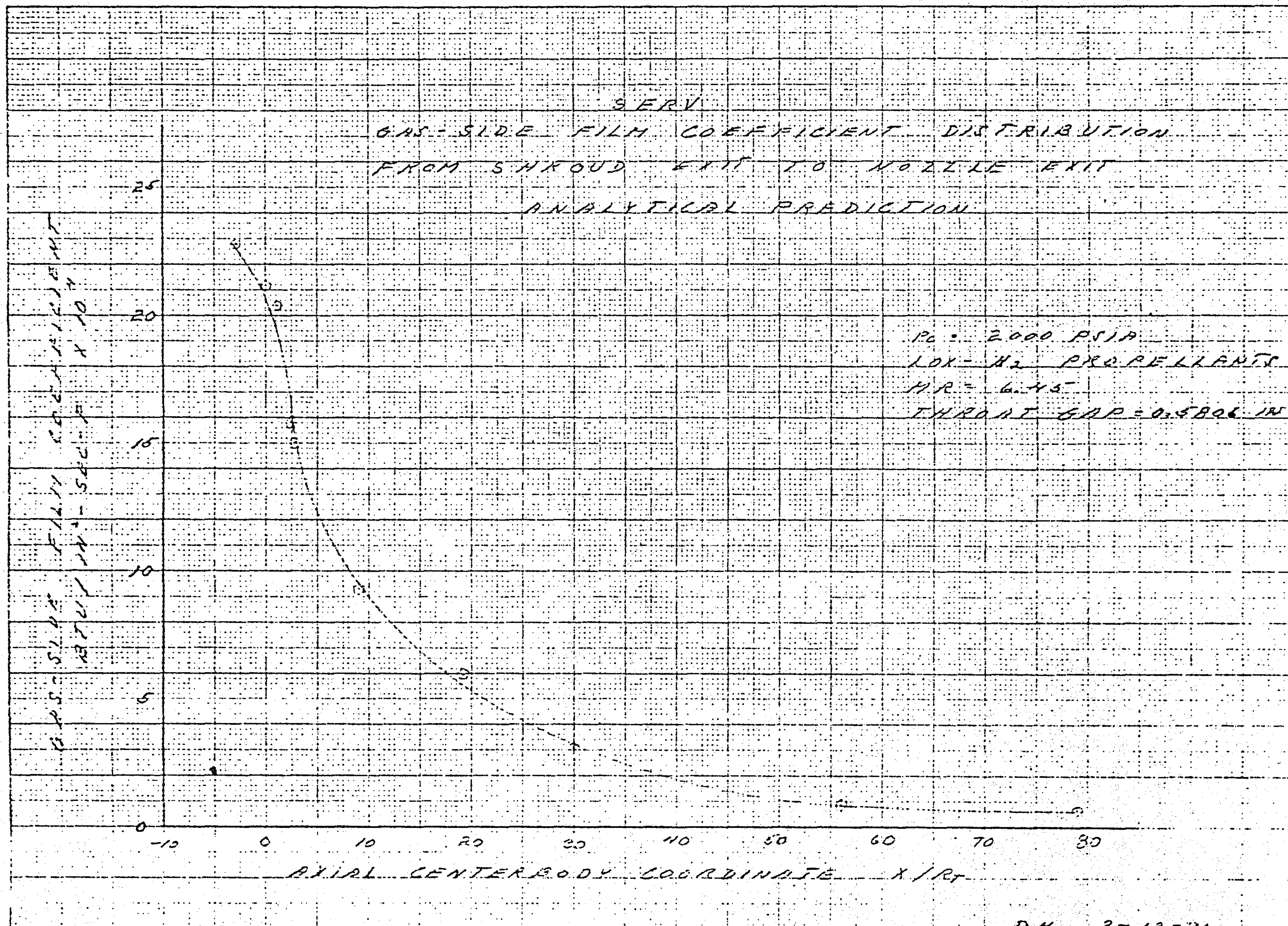

SERV
GAS-SIDE FILM COEFFICIENT DISTRIBUTION
FROM SHROUD EXIT TO NOZZLE EXIT
ANALYTICAL PREDICTION
Pc = 2000 PSIA
LOX-H2 PROPELLANTS
MR = 6.45
THROAT GAP = 0.5806 IN
GAS-SIDE FILM COEFFICIENT
BTU/IN²-SEC-°F x 10⁴
AXIAL CENTERBODY COORDINATE X/RT
DH 3-12-71

Figure 20

POINT DESIGN ENGINE PERFORMANCE

The SERV vehicle aerospike nozzle engine is tailored in diameter (and in length) to the base of the vehicle. This provides a large diameter engine and hence, a high area ratio. The SERV point design engine resulted in a nozzle area ratio of 433.7 and a nozzle percent length of 5.18 percent.

ENGINE PERFORMANCE

The complete description of the SERV point design, engine balance, and component efficiency parameters is shown in Table 4. This information is shown for an engine with an overall throttling capability of 6.53:1. In this table, values are furnished for the various process efficiencies whose combined effect determine the engine specific impulse. System geometry and flowrates as well as temperature and pressure schedules are presented.

In the following sections, a review of the various engine efficiencies is provided together with additional descriptive information on the engine performance calculations.

OVERALL ENGINE PERFORMANCE EQUATIONS

All the nozzle performance parameters and the turbomachinery performance parameters are combined in this section to develop the engine specific impulse.

TABLE 4

POINT DESIGN ENGINE PERFORMANCE SURVEY

	NPL POINT DESIGN GEOMETRY 6.53:1 THROTTLING	
CONFIGURATION		
ENGINE DIAMETER, IN.	1040	
COMBUSTOR	SINGLE	
CYCLE	GAS GENERATOR	
TURBINE ARRANGEMENT	PARALLEL	
ENGINE		
SEA LEVEL THRUST, LB	5.7×10^6	
SEA LEVEL SPECIFIC IMPULSE, SEC	345.8	
VACUUM THRUST, LB	7.65×10^6	
VACUUM SPECIFIC IMPULSE, SEC	467.5	
MIXTURE RATIO, O/F	6.0	
OXIDIZER FLOWRATE, LB/SEC	14,018	
FUEL FLOWRATE, LB/SEC	2336	
EFFICIENCY AT VACUUM	0.9463*	(0.9612**)
COMBUSTOR		
MIXTURE RATIO, O/F	6.45	
CHAMBER PRESSURE, PSIA	2000	
OXIDIZER FLOWRATE, LB/SEC	13,797	
FUEL FLOWRATE, LB/SEC	2,139	
FUEL INJECTION TEMPERATURE, R	474	
CHARACTERISTIC VELOCITY, FT/SEC	7561	
COMBUSTION EFFICIENCY (REF. TO INJECTION CONDITIONS)	0.995	

* REFERENCED TO PROPELLANT INJECTION CONDITIONS
** REFERENCED TO PROPELLANT TANK CONDITIONS

NPL POINT DESIGN GEOMETRY
6.53:1 THROTTLING

PRIMARY NOZZLE	
AREA RATIO	433.7
NOZZLE THRUST COEFFICIENT	1.871
DIVERGENCE EFFICIENCY	0.9096
DRAG EFFICIENCY	0.9865
KINETICS EFFICIENCY	0.9996
BAFFLE EFFICIENCY	0.999
BASE	
SECONDARY FLOW RATIO, $\dot{W}_S/\dot{W}_P$	0.0263
SECONDARY CHARACTERISTIC VELOCITY, FT/SEC	5500
BASE PRESSURE AT VACUUM, PSIA	1.099
GAS GENERATOR	
MIXTURE RATIO, O/F	1.12
OXIDIZER FLOWRATE	221.4
FUEL FLOWRATE, LB/SEC	197.7
TEMPERATURE, R	1960
SPECIFIC HEAT, BTU/LB-R	1.8
GAMMA	1.348
MOLECULAR WEIGHT	4.272
CHARACTERISTIC VELOCITY, FT/SEC	7045
GEOMETRY	
ENGINE DIAMETER, IN.	1040
NOZZLE EXIT DIAMETER, IN.	1016.8
THROAT CENTERLINE DIAMETER, IN.	1026.5
BASE AREA RATIO	310
BASE DIAMETER, IN.	859.7
NOZZLE PERCENT LENGTH	5.175
NOZZLE LENGTH, IN.	93.47
COMBUSTOR THROAT AREA, IN.	1872.4
COMBUSTOR THROAT GAP, IN.	0.6277**

** BASED ON 0.075 BLOCKAGE DUE TO BAFFLES

NPL POINT DESIGN GEOMETRY
6.53:1 THROTTLING

	OXIDIZER		FUEL
PRESSURE SCHEDULE			
CHAMBER PRESSURE, PSIA		2000	
INJECTOR END PRESSURE, PSIA		2030	
ΔP INJECTOR, PSI	2000		200
ΔP COOLING JACKET, PSI	--		700
ΔP LINES, VALVES, MANIFOLDS, PSI	290		120
GG SOURCE PRESSURE, PSIA	2820		3050
TURBINE INLET PRESSURE, PSIA	825		900
TURBINE EXIT PRESSURE - STATIC, PSIA	60		60

SERV TURBINES
(NORMAL POWER LEVEL)

FUEL

- MAIN TURBOPUMP; TURBINE

Inlet T	=	1960 R
Inlet Pressure	=	900 psia
Pressure Ratio	=	11.25
Speed	=	22,700 rpm
Diameter (D_m)	=	12 in.
Efficiency	=	0.74
Flowrate	=	25 lb/sec
Horsepower	=	43,000

- LOW PRESSURE PUMP; TURBINE

Inlet T	=	1050 R
Inlet Pressure	=	78 psia
Pressure Ratio	=	1.3
Speed	=	13,100 rpm
Diameter (D_m)	=	15 in.
Efficiency	=	0.70
Flowrate	=	25 lb/sec
Horsepower	=	3,130

OXIDIZER

- MAIN TURBOPUMP; TURBINE

Inlet T	=	1960 R
Inlet Pressure	=	825 psia
Pressure Ratio	=	7.5
Speed	=	21,700 rpm
Diameter (D_m)	=	12.0 in.
Efficiency	=	0.70
Flowrate	=	11.2 lb/sec
Horsepower	=	16,650

- LOW PRESSURE PUMP; TURBINE

Inlet T	=	1110 R
Inlet Pressure	=	85 psia
Pressure Ratio	=	2.22
Speed	=	4,330 rpm
Diameter (D_m)	=	20 in.
Efficiency	=	0.46
Flowrate	=	11.2 lb/sec
Horsepower	=	2,565

SERV TURBINES
(EMERGENCY POWER LEVEL)

FUEL

• MAIN TURBOPUMP; TURBINE

Inlet T	=	1960 R
Inlet Pressure	=	900 psia
Pressure Ratio	=	11.25
Speed	=	24,800 rpm
Diameter (D_m)	=	12 in.
Efficiency	=	0.74
Flowrate	=	29.9 lb/sec
Horsepower	=	50,600

• LOW PRESSURE PUMP; TURBINE

Inlet T	=	1050 R
Inlet Pressure	=	78 psia
Pressure Ratio	=	1.3
Speed	=	13,100 rpm
Diameter (D_m)	=	15 in.
Efficiency	=	0.70
Flowrate	=	25 lb/sec 4.9 lb/sec bypass
Horsepower	=	3,130

OXIDIZER

• MAIN TURBOPUMP; TURBINE

Inlet T	=	1960 R
Inlet Pressure	=	825 psia
Pressure Ratio	=	7.5
Speed	=	23,700 rpm
Diameter	=	12 in.
Efficiency	=	0.70
Flowrate	=	13.7 lb/sec
Horsepower	=	20,300

• LOW PRESSURE PUMP: TURBINE

Inlet T	=	1110 R
Inlet Pressure	=	85 psia
Pressure Ratio	=	2.22
Speed	=	4,330 rpm
Diameter (D_m)	=	20 in.
Efficiency	=	0.46
Flowrate	=	11.2 lb/sec 2.5 lb/sec bypass
Horsepower	=	2,565

SERV TURBOPUMPS

HIGH PRESSURE PUMPS

	OXIDIZER (O_2) *NPL/EPL	FUEL (H_2) *NPL/EPL
Speed, rpm	21,700/23,700	22,700/24,8000
Delta Head, ft	6,270/7,450	90,900/108,000
Specific Speed, N_s	2710	1030
Efficiency, %	81/80	77/77
Horsepower, HP	16,650/20,300	42,200/50,600
Discharge Pressure, psia	3,653/4,340	3,050/3,560
Inlet Pressure, psia	451/413	217/199
Bearing DN x 10^{-6}MM rpm	1.3/1.45	1.68/1.89

LOW PRESSURE PUMPS

Speed, rpm	4,330	13,100
Delta Head, ft	912/836	7,160/6,480
Specific Speed, N_s	2,320/2,600	2,340/2,670
Efficiency, %	80/80	80/80
Horsepower, HP	2,565	3,130
Discharge Pressure, psia	451/413	217/199
Inlet NPSH, ft	16 ft	64 ft
Flow Coefficient, ϕ	.07/.0763	.07/.0763
Head Coefficient, ψ	.436/.4	.436/.4
Suction Specific Speed, S_s	51,000/50,000	88,000/85,000
Inlet Diameter, in.	15.8	14.5

* NPL - Normal Power Level
EPL - Emergency (Module-Out) Power Level

COMBUSTOR INJECTOR GEOMETRY AND COMBUSTION EFFICIENCY, η_{C*}

A combustion efficiency value of 0.995 has been used in the performance investigations. This efficiency has been achieved in the aerospike nozzle segment testing conducted under the ADP and AEA programs. Under the latter program, high combustion efficiencies were measured with both triplet and coaxial type injectors. In particular, a coaxial injector tested at 2000 psia in a combustion chamber of geometry similar to that of the SERV yielded a combustion efficiency of 0.996.

NOZZLE OPTIMUM THRUST COEFFICIENT RATIO ($C_{F_{OPT}}$)

At a given altitude, the maximum thrust coefficient occurs when the nozzle exit pressure equals the prevailing ambient pressure. A nozzle whose area ratio can be adjusted at each altitude to match the ambient pressure, will generate an optimum thrust coefficient. The thrust coefficient of this ideal nozzle is obtained using the propellant combination and temperature, mixture ratio, and chamber pressure, and is based on a shifting equilibrium, ideal expansion to the ambient pressure. It is used as a reference for nozzle thrust coefficient efficiency, C_T.

At design pressure ratio for the nozzle, the C_F which results is the $C_{F_{OPT_d}}$.

NOZZLE GEOMETRY AND EXPANSION EFFICIENCY, η_G

Past the throat of the thrust chamber the gases expand internally in a two-dimensional nozzle contour, i.e., the shrouded portion of the spike nozzle. The expansion area ratio at the exit of the shroud is 6.2:1. The two-

At design pressure ratio (which is in the closed wake regime):

$$I_s = \frac{\eta_{c^*} \; C^*_{ideal} \; C_{T_d} \; C_{F_{OPT_d}}}{g}$$

$$\text{where } C_{T_d} = \frac{C_{F_{vac\,ideal}} \left(\eta_g + \eta_B + \eta_d \eta_K - 3\right) - \frac{P_A}{P_C} \epsilon + \frac{P_B}{P_C} \epsilon_B}{C_{F_{OPT_d}} \quad (1 + \dot{w}_s/\dot{w}_p)}$$

C_{T_d} = nozzle thrust efficiency at design P.R.

$C_{F_{OPT_d}}$ = nozzle optimum thrust coefficient at design P.R.

The term $\dot{w}_s/\dot{w}_p$ reflects all the turbomachinery efficiencies and secondary flow energy level. The terms P_B and ϵ_B reflect the contribution of the base toward engine thrust. The term P_A/P_C reflects the ambient back pressure term.

At sea level pressure ratio (which is in the open-wake regime):

$$I_s = \frac{\eta_{c^*} \; C^*_{ideal} \; \Phi \; C_{T_d} \; C_{F_{OPT_{SL}}}}{g}$$

$\Phi = \frac{C_T}{C_{T_d}}$ from normalized C_T plot

$C_{F_{OPT_{SL}}}$ = optimum thrust coefficient at sea level dimensional nozzle contour is joined to the truncated ideal spike contour. This nozzle has a length from throat to end of the spike section equal to 5.18 percent that of a 15 degree cone of identical area ratio. The external flowfield generated by the nozzle is essentially identical to that of a point-expansion truncated ideal spike nozzle.

Nozzle expansion losses (i.e., a divergence loss) results from the truncation of the ideal spike contour. Truncation yields a nozzle lighter in weight, whose contour discharges the gases at an angle from the vehicle longitudinal axis. The divergence of the gases from this axis leads to the divergence loss in the nozzle thrust coefficient. The nozzle geometric and expansion efficiency applies to the primary nozzle, C_F, it is used in the engine performance analysis to adjust the overall nozzle performance to account for the geometric and expansion efficiencies. This loss is partly made up in the base pressure and by the addition of secondary flow.

A computer program employing a high accuracy method of characteristics procedure evaluates this nozzle expansion loss at any altitude of operation. For the nozzle contour chosen the value of the nozzle divergence loss calculated was 9.04 percent of the ideal thrust coefficient, yielding thus a nozzle divergence (or geometric) efficiency (η_G) of 0.9096.

BAFFLE EFFICIENCY (η_B)

Baffles are used in the combustion chamber to assure combustion stability. A baffle width of approximately 0.84 inches is utilized. The baffles would be tapered and contoured to a width of approximately 0.17 inches; the baffles produce a loss in nozzle expansion efficiency of only 0.1 percent.

F

NOZZLE KINETIC LOSSES, η_K

In chemical equilibrium nozzle flow the various species undergo continuous reactions as the flow expands in the nozzle. The reactions are considered to be in chemical equilibrium when they are able to proceed at a faster rate than that imposed by the nozzle rate of expansion. When these two rates are equal, the composition of the gas flow remains constant. The freezing process occurs in each streamline, so that the overall nozzle flow will consist of an upstream region where the species will be in chemical equilibrium and a downstream region where the flow is considered frozen. The larger the region of equilibrium flow the higher the performance of the nozzle.

The calculation of reaction kinetic effects in the nozzle is performed by dividing the nozzle flow into a large number of streamtubes derived from the aerodynamic analysis. The one-dimensional reaction kinetic analysis is then applied to the flow in each streamtube. The reaction kinetic loss for the nozzle is calculated by integrating the impulse function across the streamtubes at the nozzle exit for both equilibrium flow and for flow calculated using the kinetic model. For O_2/H_2 propellants at high thrusts and high chamber pressures the reaction kinetic effects are very small.

NOZZLE DRAG LOSS, η_D

Friction in the boundary layer along the combustion chamber and nozzle walls dissipates part of the energy available in the combustion products. The nozzle boundary layer drag losses are applicable to the primary nozzle, C_F. A computer program is used to solve the boundary layer equations along the thrust chamber walls (from the injector, through the combustor to the nozzle exit). This program uses as input the inviscid flowfield generated in the computer program which evaluates the nozzle divergence efficiency. The friction loss is then evaluated as a loss in thrust coefficient (ΔC_F), and converted to a loss in the nozzle efficiency ($\Delta C_F/C_{Fi_v}$). A drag loss in nozzle expansion efficiency (η_D) of 0.0135 was calculated for the combustor/nozzle geometry for this engine.

REGENERATIVE COOLING GAIN

Heat gained by the hydrogen during the regenerative cooling of the thrust chamber increases its temperature. Therefore upon injection into the combustion chamber a greater amount of energy results than would be generated by the hydrogen at tank conditions. To properly incorporate this effect a correction is made to the heat of formation of hydrogen from which the ideal specific impulse is calculated at the mixture ratio of the combustion chamber.

BASE PRESSURE (P_B)

The aerospike nozzle has two basic thrust components. The primary nozzle and the thrust resulting from this flow (as a result of combustor and primary nozzle wall pressures) is the major thrust component. The pressure acting on the nozzle base time the area of the base is the secondary thrust contribution.

For the closed wake condition, extensive past results have provided good correlation methods. A set of empirical equations for the closed wake regime were developed These equations have been obtained from data generated in extensive cold flow and hot-firing testing of the aerospike nozzle and are directly applicable to nozzles with expansion ratios of 8:1 to 150:1, nozzle lengths from 10 to 30 percent, and gas specific heat ratios of 1.23 to 1.67. For the SERV engine configuration, the empirical relationship and values developed from these test data points have been employed.

In the empirical relationship employed, the base pressure is primarily a function of the primary divergence efficiency, η_G, the primary and secondary characteristic velocities (C*), the amount of secondary flow and the nozzle base area ratio (ϵ_B). The relationship of base pressure to nozzle area ratio and length comes from the η_G calculation.

The closed-wake base pressure calculated for the SERV point design was 1.099 psia. Figure 21 presents the SERV point-design base pressure as a function of altitude and Mach number.

NORMALIZED THRUST EFFICIENCY, Φ

The Φ term is based on the normalized C_T vs normalized pressure ratio, formulated from previous test data. It is used with the engine design C_T to obtain intermediate altitude still-air performance. Recent SERV cold-flow test data were used to revise the normalized thrust efficiency factor O obtained from previous test data at sea level conditions. At other pressure ratios the previous correlation was found to apply.

NOZZLE PERFORMANCE (C_T)

For the SERV engine point design, the predicted still-air nozzle C_T, I_s and thrust vs pressure ratio are shown in Table 5 . The effects of module-out conditions on the same parameters are shown in Table 6 . This relationship has been derived from the calculated C_T vs normalized pressure ratio (recently verified with SERV cold-flow model data). Figure 22 presents the SERV point design engine I_s as a function of altitude and Mach number.

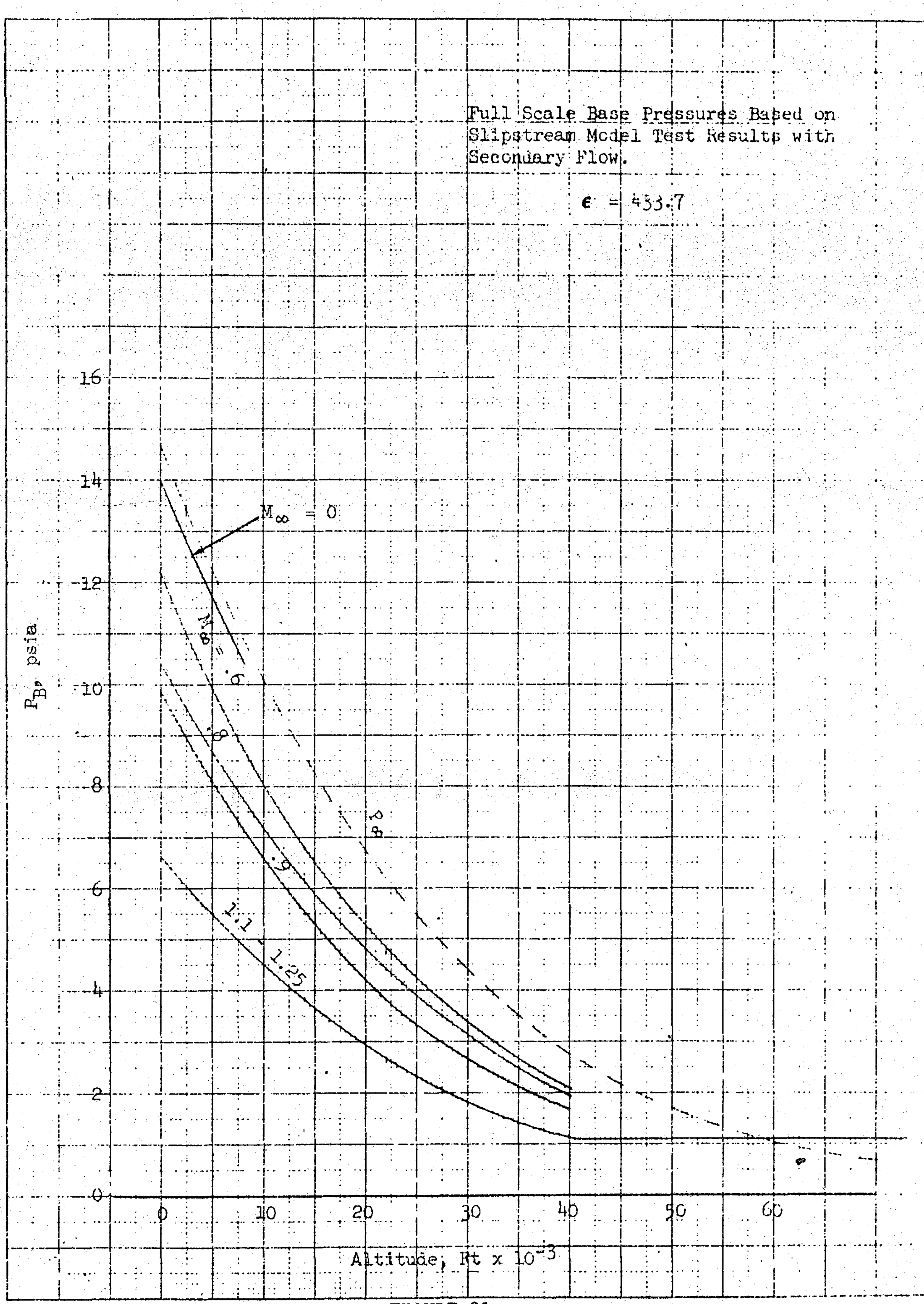

Full Scale Base Pressures Based on Slipstream Model Test Results with Secondary Flow.
ε = 433.7
M_∞ = 0
M_∞ = .6
.8
.9
1.1
1.25
P_∞
P_B, psia
Altitude, Ft x 10^{-3}

FIGURE 21

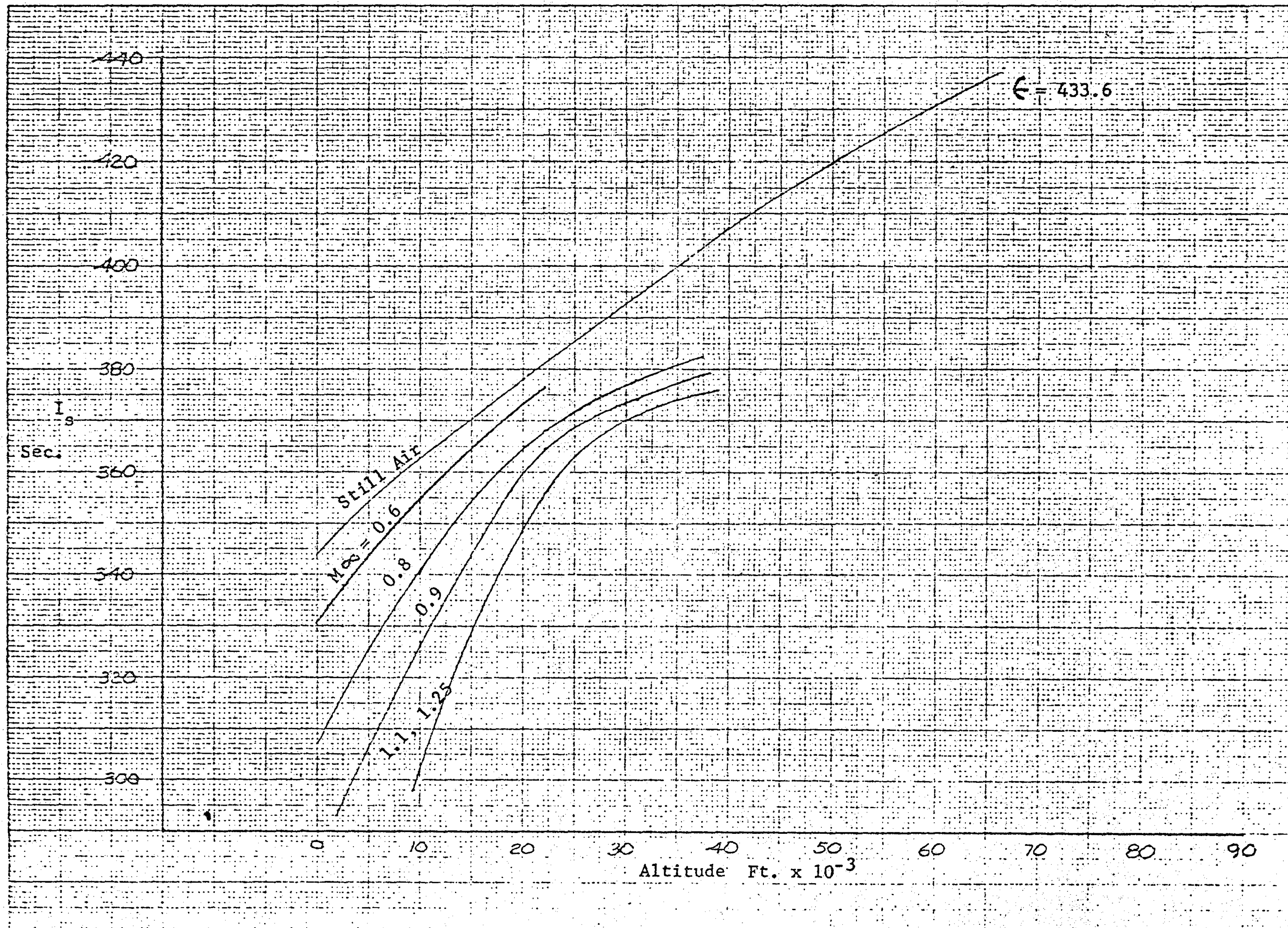

Figure 22. SERV Point Design Engine Performance vs. Altitude and Mach Number

TABLE 5

SERV Still-Air Engine Performance vs Altitude

Performance-Altitude Data

Design Point Data

Pressure Ratio	0.976806E 04
Engine Thrust	0.747962E 07
Engine Specific Impulse	0.457341E 03
C Sub T	0.950590E 00

ALTITUDE	PRESSURE RATIO	ENGINE THRUST	ENGINE SPECIFIC IMPULSE	C SUB T
0.0	0.136091E 03	0.569997E 07	0.345800E 03	0.855100E 00
0.100000E 04	0.141113E 03	0.572375E 07	0.348200E 03	0.858800E 00
0.300000E 04	0.151837E 03	0.577097E 07	0.352100E 03	0.864100E 00
0.500000E 04	0.163559E 03	0.581853E 07	0.355774E 03	0.868785E 00
0.700000E 04	0.176367E 03	0.586641E 07	0.358701E 03	0.871582E 00
0.100000E 05	0.197883E 03	0.593791E 07	0.363073E 03	0.875796E 00
0.130000E 05	0.222618E 03	0.601026E 07	0.367497E 03	0.880037E 00
0.160000E 05	0.251089E 03	0.608283E 07	0.371934E 03	0.884296E 00
0.200000E 05	0.296112E 03	0.618024E 07	0.377890E 03	0.890015E 00
0.250000E 05	0.366737E 03	0.630164E 07	0.385313E 03	0.897140E 00
0.300000E 05	0.458232E 03	0.642220E 07	0.392685E 03	0.903964E 00
0.350000E 05	0.578319E 03	0.653433E 07	0.399541E 03	0.909583E 00
0.400000E 05	0.735078E 03	0.665712E 07	0.407049E 03	0.916810E 00
0.500000E 05	0.118913E 04	0.686743E 07	0.419908E 03	0.927580E 00
0.600000E 05	0.190858E 04	0.704508E 07	0.430771E 03	0.935768E 00
0.800000E 05	0.496524E 04	0.733676E 07	0.448605E 03	0.947400E 00
0.100000E 06	0.129116E 05	0.752010E 07	0.459816E 03	0.950714E 00
0.150000E 06	0.959233E 05	0.762895E 07	0.466471E 03	0.951043E 00
0.200000E 06	0.432901E 06	0.764213E 07	0.467277E 03	0.951083E 00
0.100000E 07	0.200000E 10	0.764588E 07	0.467507E 03	0.951094E 00

TABLE 6

SERV Still-Air Engine Performance During Pump-out ondition (Overspeed Capability)

Performance-Altitude Data

Design Point Data

Pressure Ratio	0.970981E 04
Engint Thrust	0.749483E 07
Engine Specific Impulse	0.457081E 03
C Sub T	0.950328E 00

ALTITUDE	PRESSURE RATIO	ENGINE THRUST	ENGINE SPECIFIC IMPULSE	C SUB T
0.0	0.136091E 03	0.571123E 07	0.345600E 03	0.855100E 00
0.100000E 04	0.141113E 03	0.573508E 07	0.348000E 03	0.858800E 00
0.300000E 04	0.151837E 03	0.578242E 07	0.351900E 03	0.864100E 00
0.500000E 04	0.163559E 03	0.583012E 07	0.333337E 03	0.868769E 00
0.700000E 04	0.176367E 03	0.587812E 07	0.358484E 03	0.871563E 00
0.100000E 05	0.197883E 03	0.594982E 07	0.362857E 03	0.875772E 00
0.130000E 05	0.222618E 03	0.602239E 07	0.367283E 03	0.880008E 00
0.160000E 05	0.251089E 03	0.609516E 07	0.371720E 03	0.884263E 00
0.200000E 05	0.296112E 03	0.619288E 07	0.377680E 03	0.889976E 00
0.250000E 05	0.366737E 03	0.631459E 07	0.385103E 03	0.897086E 00
0.300000E 05	0.458232E 03	0.643537E 07	0.392469E 03	0.903884E 00
0.350000E 05	0.578319E 03	0.654775E 07	0.399322E 03	0.909476E 00
0.400000E 05	0.735078E 03	0.667098E 07	0.406837E 03	0.916706E 00
0.500000E 05	0.118913E 04	0.688181E 07	0.419695E 03	0.927440E 00
0.600000E 05	0.190858E 04	0.706003E 07	0.430564E 03	0.935607E 00
0.800000E 05	0.496524E 04	0.735262E 07	0.448408E 03	0.947189E 00
0.100000E 06	0.129116E 05	0.753631E 07	0.459610E 03	0.950449E 00
0.150000E 06	0.959233E 05	0.764516E 07	0.466249E 03	0.950761E 00
0.200000E 06	0.432901E 06	0.765833E 07	0.467052E 03	0.950798E 00
0.100000E 07	0.200000E 10	0.766209E 07	0.457281E 03	0.950809E 00

REFERENCES

1. Rocketdyne Report ASR 71-67, "SERV 2½% Scale Model", 10 March 1971

2. Rocketdyne Report ASR 70-459, "Informal Report, Task 3, Preliminary Design and Parametric Analysis," 31 October 1970.

APPENDIX A

CAST SEGMENT EVALUATION

FINAL REPORT

February 1971

Contract No. NAS8-30182

SUMMARY

The Cast Segment Evaluation Program has successfully met the objective of establishing the feasibility of segmented thrust chamber fabrication using castings for low cost and light weight. Four segments were built using the simplified procedure, with successive improvements. One segment underwent a series of 110 hot-firing tests and successfully demonstrated design suitability, good performance, and long life. Three segments were assembled together into a linear multisegment and will be test fired under the continuing multisegment effort of contract NAS8-25068. In addition, the technology developed has been successfully transferred to a separate and expanded program to demonstrate a 20-segment thrust chamber using the basic segment design.*

The cast segment design depended on the development of the thin-walled liner casting of the high (thermal) conductivity alloy designated as NARloy, a North American Rockwell trademark (Fig. 1). In developing this investment casting, the state of the art was extended in the casting size, complexity, and the ability to provide thin sections and narrow, deep cooling channels. The casting development efforts included trial castings at two vendors, tooling fabrication and a total of 30 experimental castings made under various conditions by the

---

*Breadboard Test Bed Engine, NAS8-25156

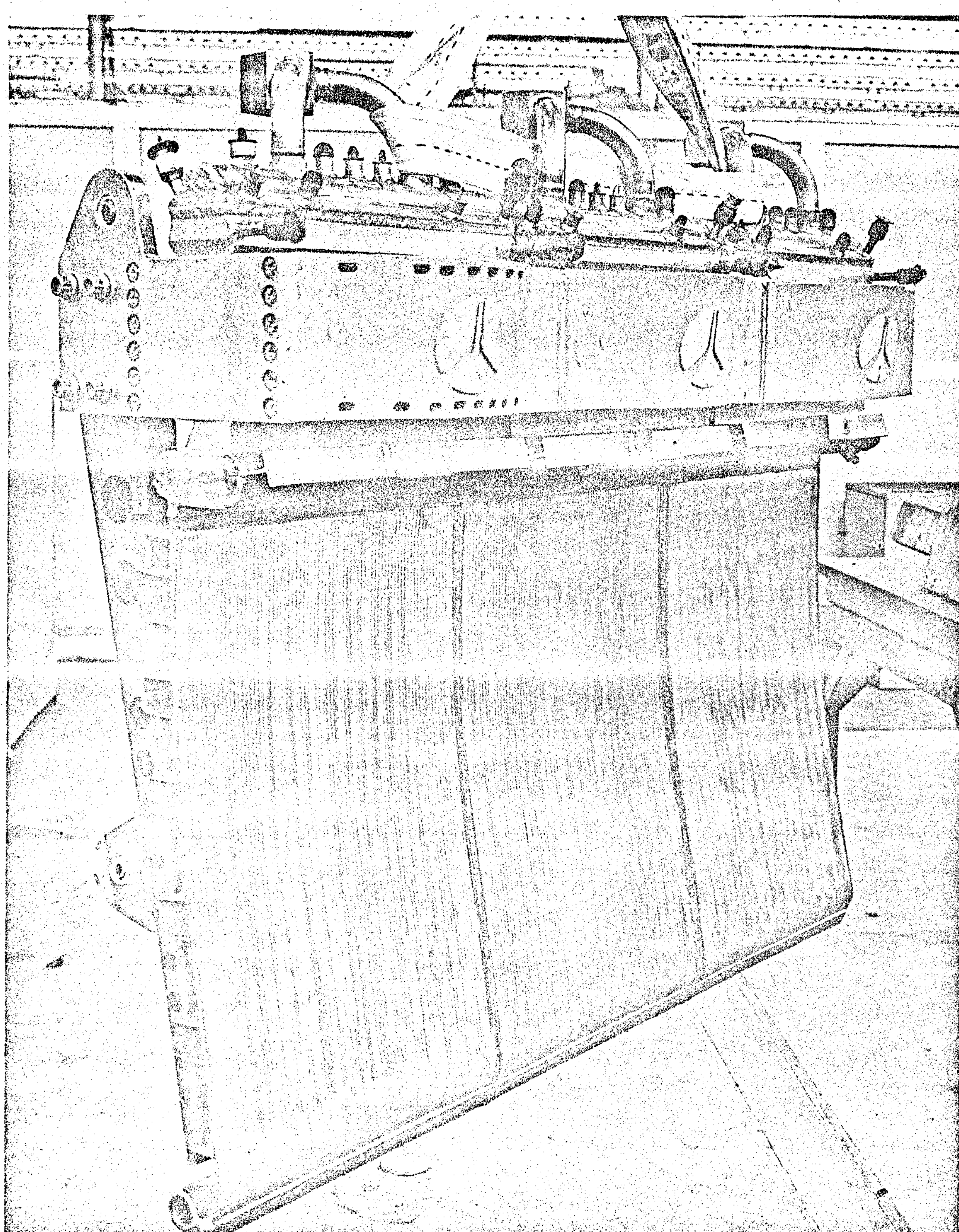

1XZ32-11/10/70-C1A*

Frontispiece. Multisegment Assembly of Cast Segments 2, 3, and 4 selected vendor, Hitchiner Manufacturing Company. Problems were encountered and solved in casting areas of shell strength, shell dewaxing, wax cracks, and clen cleanup procedure. Six acceptable castings were made under this technology program. The casting process was developed so that larger orders were successfully filled under a subsequent program.*

The relatively inexpensive cast liner was the basis of the low-cost segment design. Other design innovations included the extensive use of electroformed nickel to close out the coolant passages and to form manifold joints. The segment design was a 100-percent welded or brazed assembly with no joints or seals. During the course of fabrication of the four segments, the learning (together with design simplification) resulted in reduced time and cost. Actual segment weight was 92 pounds, with design provision included for further reduction to flight weight.

A development problem was uncovered when it was found that electroformed nickel is subject to environmental hydrogen embrittlement. The cast segments were strengthened to function with this material, and work was undertaken to provide a complete solution. This work is continuing under other related programs.

The tubular nozzle extension for each segment was made as an inexpensive braze assembly of plain, round nickel tubes, brazed flat and formed to contour on simple tooling.

---

*Breadboard Test Bed Engine, NAS8-25156

The hot-fire test program exceeded expectations in many areas. Performance of the relatively inexpensive injector and small combustion chamber was good; η_{I_s} averaged 96.8 percent, and η_{c*} averaged 97.4 percent. Durability was excellent; 110 hot-firing tests were accomplished on one segment assembly, some at more severe conditions than normal. Although fatigue cracks eventually developed in the NARloy liner, performance was not affected and the segment was still suitable for use when retired for examination. Following the test series, the chamber was thoroughly examined and found to fulfill the design intent in all respects.

The segments were stable in mainstage with regard to both acoustic vibration modes and feed system-coupled oscillations. Characteristic vibrations during start were self-damping under all conditions, including tests designed to explore the low chamber pressure/mixture ratio region.

With the satisfactory development of the technology for this particular useful segment size, additional technology effort should be undertaken to extend the range of chamber pressure (higher P_c) and to provide approaches for ignition improvement and thrust vector control. Further development of the geometry of miltisegment shapes, such as for linear thrust chamber assemblies with rounded ends, is an important technical challenge, and would include the optimization and parametric study of chord length, combustion chamber length, thrust/inch, and all aspects of throttling. This continuation of the technology program is recommended to provide the engineering basis for new or enlarged future engine programs.

APPENDIX F

AERODYNAMIC CHARACTERISTICS

APPENDIX F
AERODYNAMIC CHARACTERISTICS

F.0 GENERAL

This appendix presents vehicle longitudinal distributions of aerodynamic normal forces, axial forces, meridian pressures, and local flow properties for the three SERV ascent payload configurations of the task 4 baseline. The reference configuration for each figure is illustrated as a silhouette sketch at the bottom of the graph. These aerodynamic characteristics are defined for the ascent flight region of maximum dynamic pressure (MACH = 0.8-1.46). Table F.0-1 presents an index of the appendix figures.

F.1 LOCAL NORMAL AND AXIAL FORCE COEFFICIENTS

The local aerodynamic normal and axial force coefficients (C_N' and C_A') are presented for the wind angle of attack condition of $\alpha = 10^o$ (figures F.1-1 through F.1-24). Total normal and forebody pressure axial forces are determined by the integrations:

$$C_N = \int_0^{L/D} C_N' \, d\,(X/D)$$

$$C_{A_{\text{FOREBODY PRESSURE}}} = \int_0^{L/D} C_A' \, d\,(X/D)$$

F.2 LOCAL PRESSURE COEFFICIENTS

Vehicle longitudinal pressure coefficient ($C_{P_{LOCAL}}$) distributions are presented for wind angles of attack of $\alpha = 0^o$ and 10^o (see figures F.2-1 through F.2-24). The longitudinal meridian distribution for $\alpha = 0^o$ is assumed constant for all radial meridians through 360°. At $\alpha = 10^o$, only the vehicle lower surface windward meridian and the top surface leeward meridian are presented. Other radial meridians from windward to leeward are not presented here; however, they are available as working data.

F.3 LOCAL FLOW PROPERTY RATIOS

Vehicle longitudinal distributions of local flow property ratios (P_{O_L}/P_{O_∞}, P_L/P_∞, M_L/M_∞, T_L/T_∞, ρ_L/ρ_∞ are presented for zero wind angle of attack (see figures F.3-1 through F.3-24). These are assumed constant for all radial meridians through 360° for this angle of attack condition.

6

Table F.0-1. Index of Aerodynamic Characteristics Presented in Appendix F

Payload Configuration	Figure No.	Aerodynamic Parameter	Mach No.	Wind Angle of Attack (deg)
Retracted PM	F.1-1 thru F.1-4	Local Normal Force Coefficient C_N' vs. X/D	0.8, 1.0, 1.2, 1.46	10
Winged Payload	F.1-5 thru F.1-8			
Large Payload	F.1-9 thru F.1-12			
Retracted PM	F.1-13 thru F.1-16	Local Axial Force Coefficient C_A' vs. X/D	0.8, 1.0, 1.2, 1.46	10
Winged Payload	F.1-17 thru F.1-20			
Large Payload	F.1-21 thru F.1-24			
Retracted PM	F.2-1 thru F.2-8	Local Pressure Coefficient $C_{P_{LOCAL}}$ vs. $^X/_D$	0.8, 1.0, 1.2, 1.46	0,10
Winged Payload	F.2-9 thru F.2-16			
Large Payload	F.2-17 thru F.2-24			
Retracted PM	F.3-1 thru F.3-8	Local Flow Property Ratios $\frac{P_{O_L}}{P_{O_\infty}}$, $\frac{P_L}{P_\infty}$, $\frac{M_L}{M_\infty}$, $\frac{T_L}{T_\infty}$, $\frac{\rho_L}{\rho_\infty}$	0.8, 1.0, 1.2, 1.46	0
Winged Payload	F.3-9 thru F.3-16			
Large Payload	F.3-17 thru F.3-24			

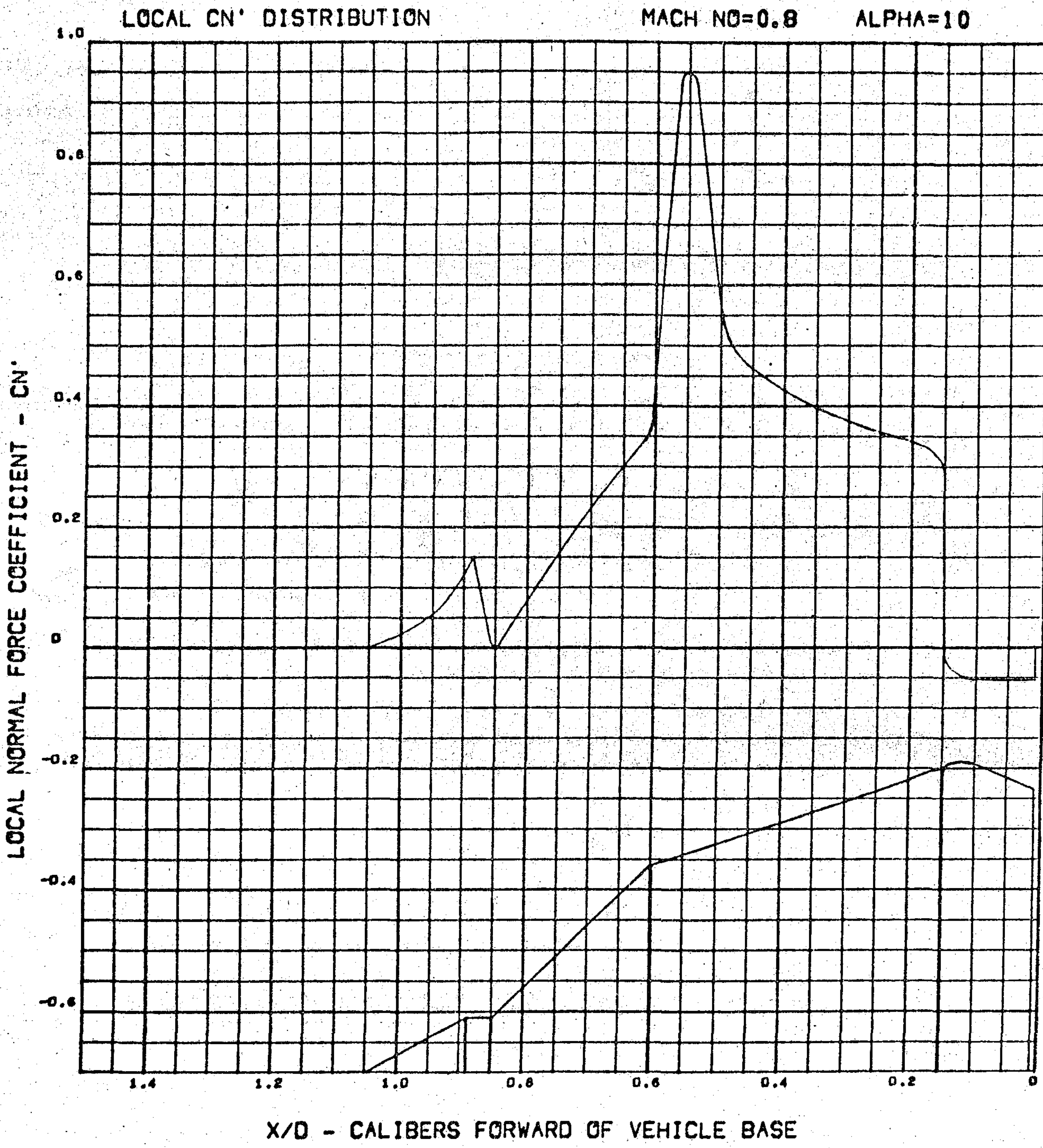

LOCAL CN' DISTRIBUTION
MACH NO=0.8
ALPHA=10
LOCAL NORMAL FORCE COEFFICIENT - CN'
1.0
0.8
0.6
0.4
0.2
0
-0.2
-0.4
-0.6
1.4
1.2
1.0
0.8
0.6
0.4
0.2
0
X/D - CALIBERS FORWARD OF VEHICLE BASE

Figure F.1-1

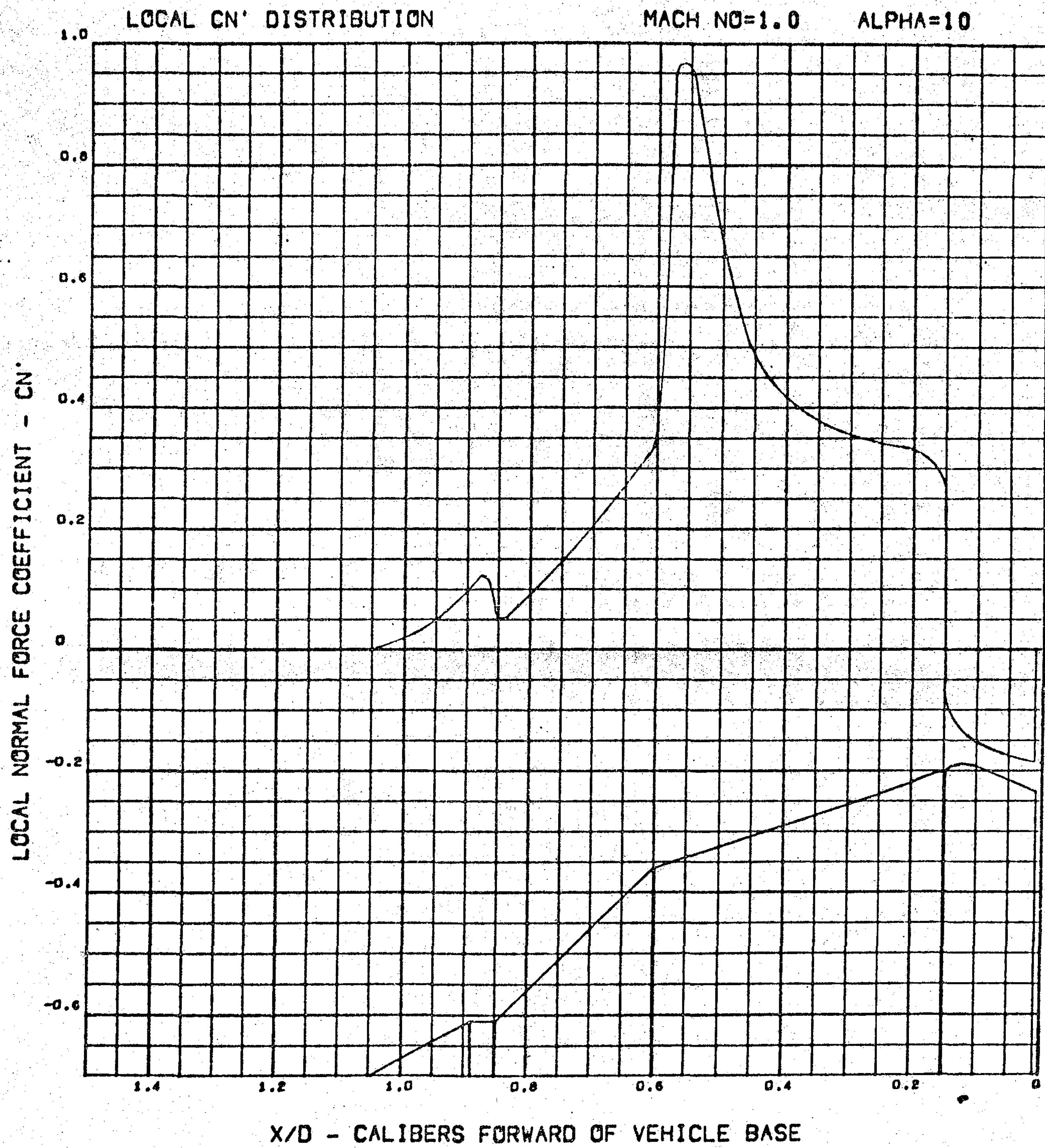

LOCAL CN' DISTRIBUTION
MACH NO=1.0
ALPHA=10
1.0
0.8
0.6
0.4
0.2
0
-0.2
-0.4
-0.6
LOCAL NORMAL FORCE COEFFICIENT - CN'
1.4
1.2
1.0
0.8
0.6
0.4
0.2
0
X/D - CALIBERS FORWARD OF VEHICLE BASE

Figure F.1-2

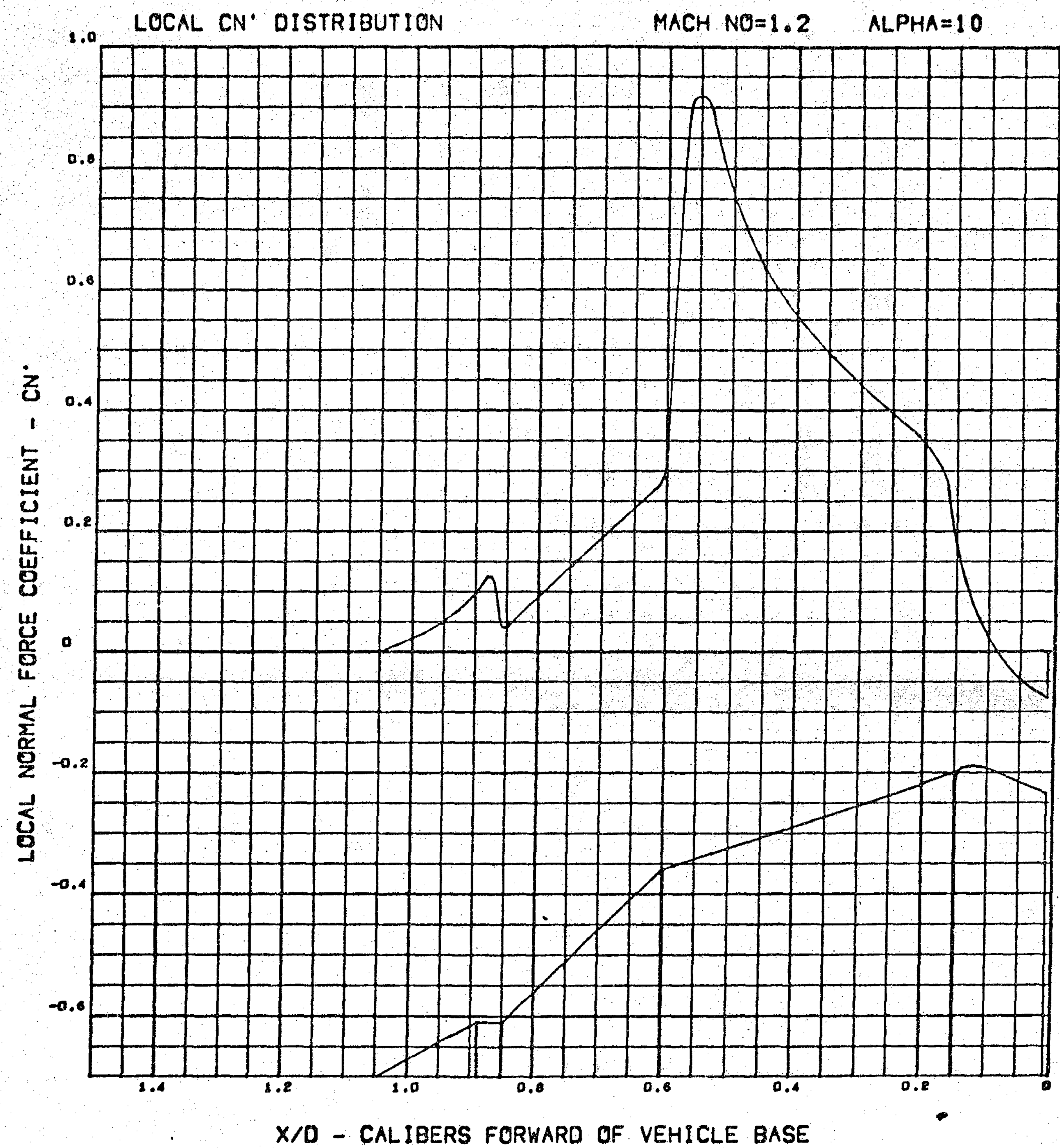
LOCAL CN' DISTRIBUTION
MACH NO=1.2
ALPHA=10
LOCAL NORMAL FORCE COEFFICIENT - CN'
1.0
0.8
0.6
0.4
0.2
0
-0.2
-0.4
-0.6
1.4
1.2
1.0
0.8
0.6
0.4
0.2
0
X/D - CALIBERS FORWARD OF VEHICLE BASE

Figure F.1-3

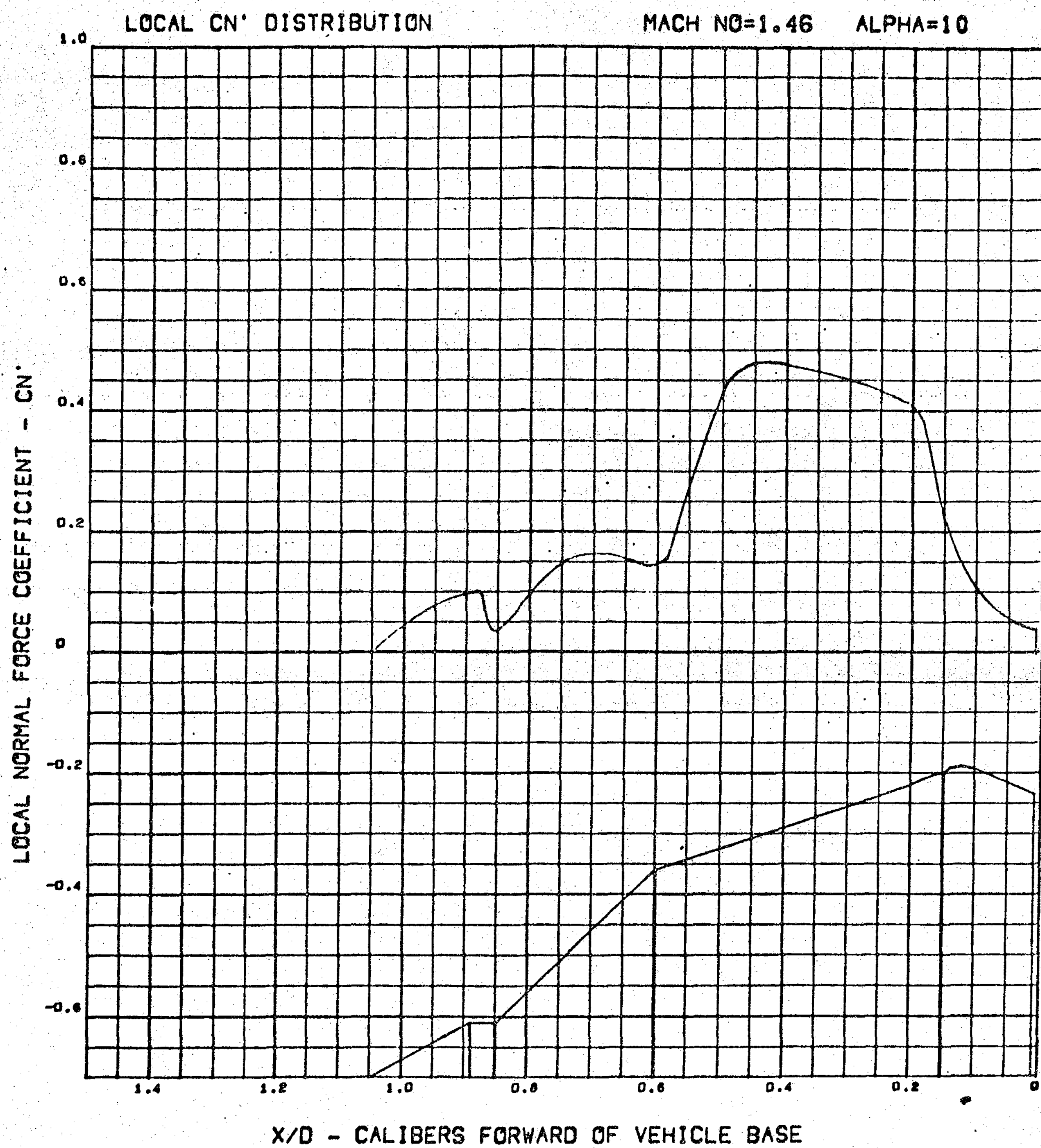
LOCAL CN' DISTRIBUTION
MACH NO=1.46 ALPHA=10
1.0
0.8
0.6
0.4
0.2
0
-0.2
-0.4
-0.6
LOCAL NORMAL FORCE COEFFICIENT - CN'
1.4
1.2
1.0
0.8
0.6
0.4
0.2
0
X/D - CALIBERS FORWARD OF VEHICLE BASE

Figure F.1-4

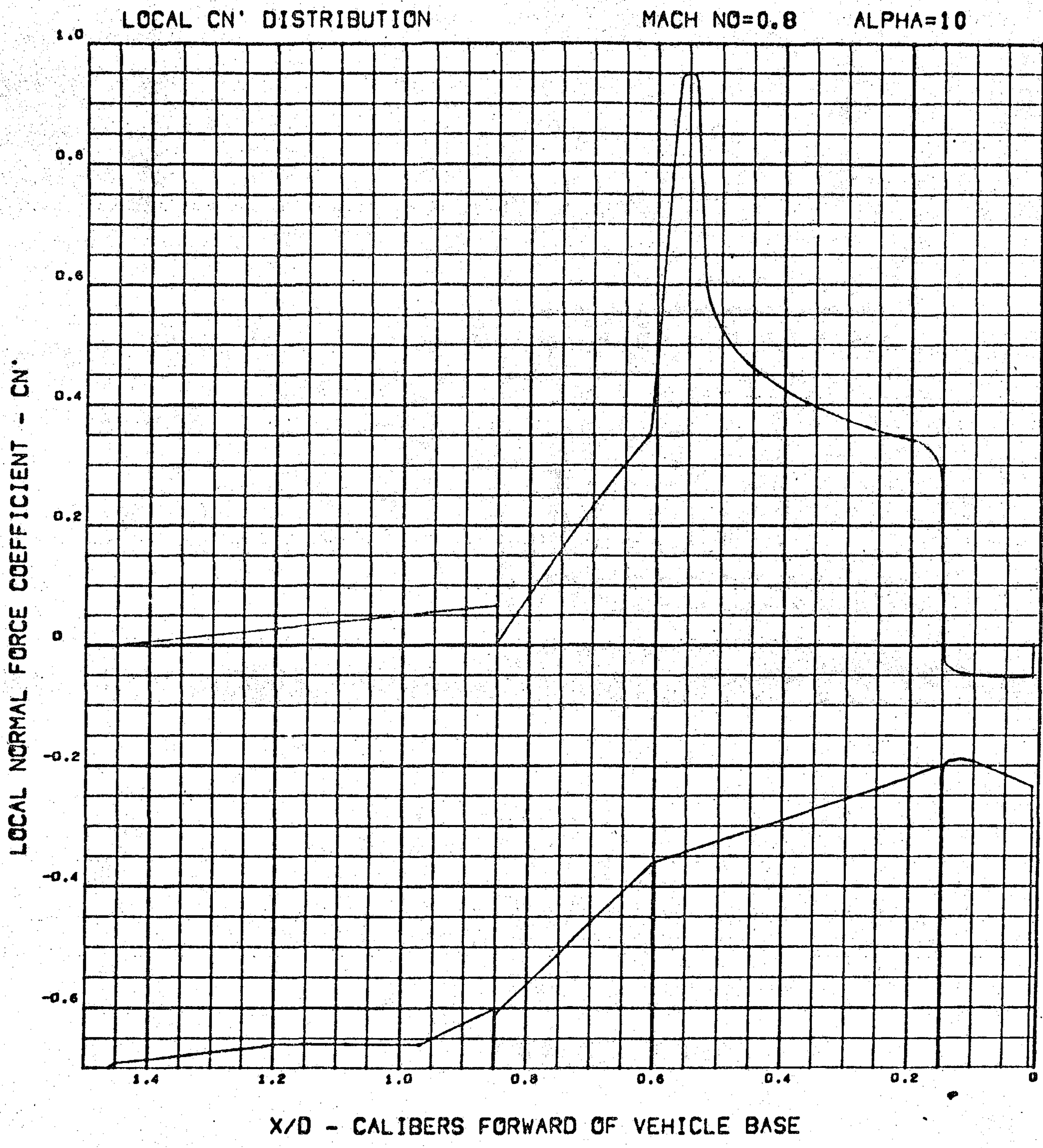
LOCAL CN' DISTRIBUTION
MACH NO=0.8
ALPHA=10
LOCAL NORMAL FORCE COEFFICIENT - CN'
1.0
0.8
0.6
0.4
0.2
0
-0.2
-0.4
-0.6
1.4
1.2
1.0
0.8
0.6
0.4
0.2
0
X/D - CALIBERS FORWARD OF VEHICLE BASE

Figure F.1-5

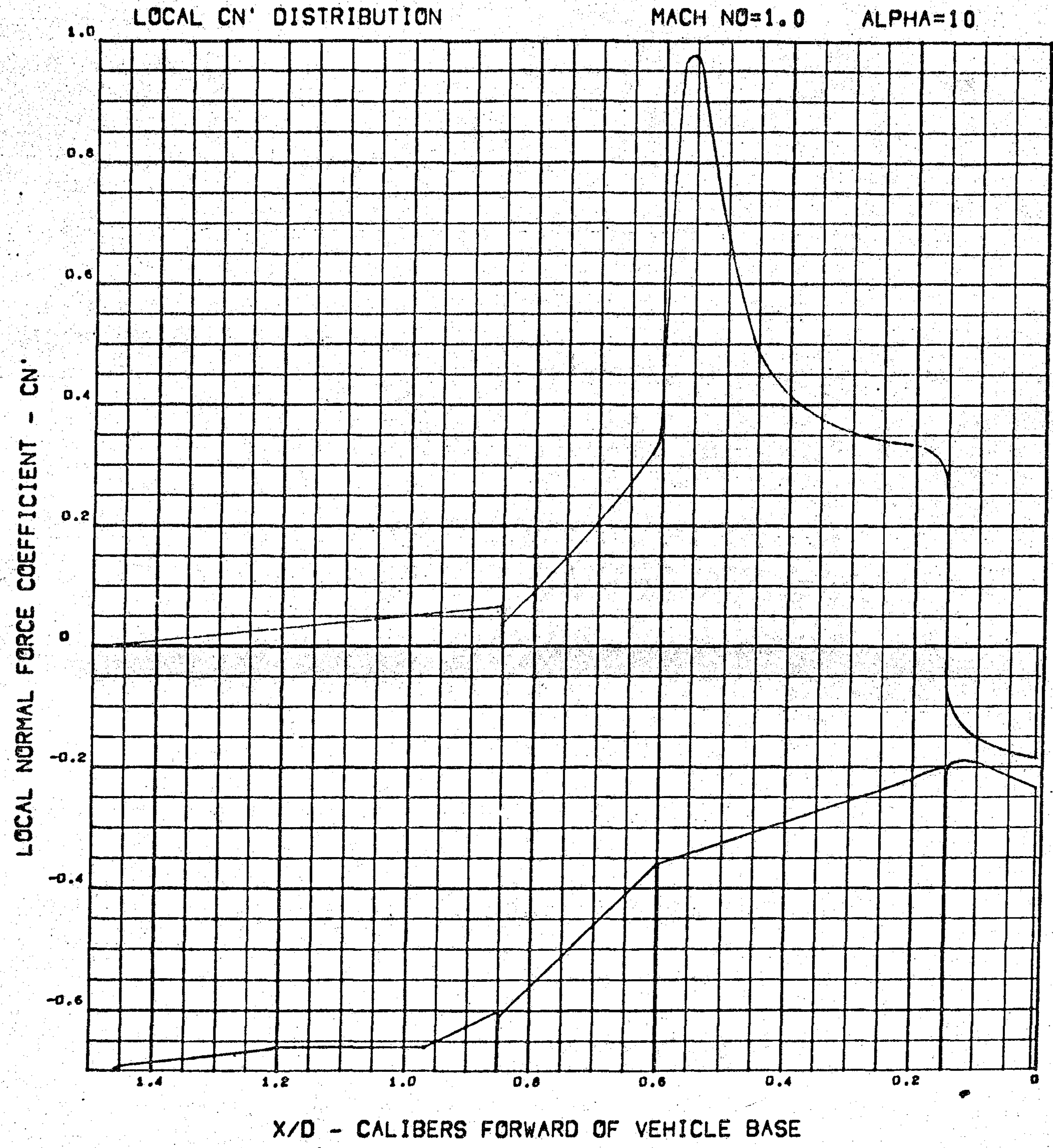
LOCAL CN' DISTRIBUTION
MACH NO=1.0
ALPHA=10
LOCAL NORMAL FORCE COEFFICIENT - CN'
1.0
0.8
0.6
0.4
0.2
0
-0.2
-0.4
-0.6
1.4
1.2
1.0
0.8
0.6
0.4
0.2
0
X/D - CALIBERS FORWARD OF VEHICLE BASE

Figure F.1-6

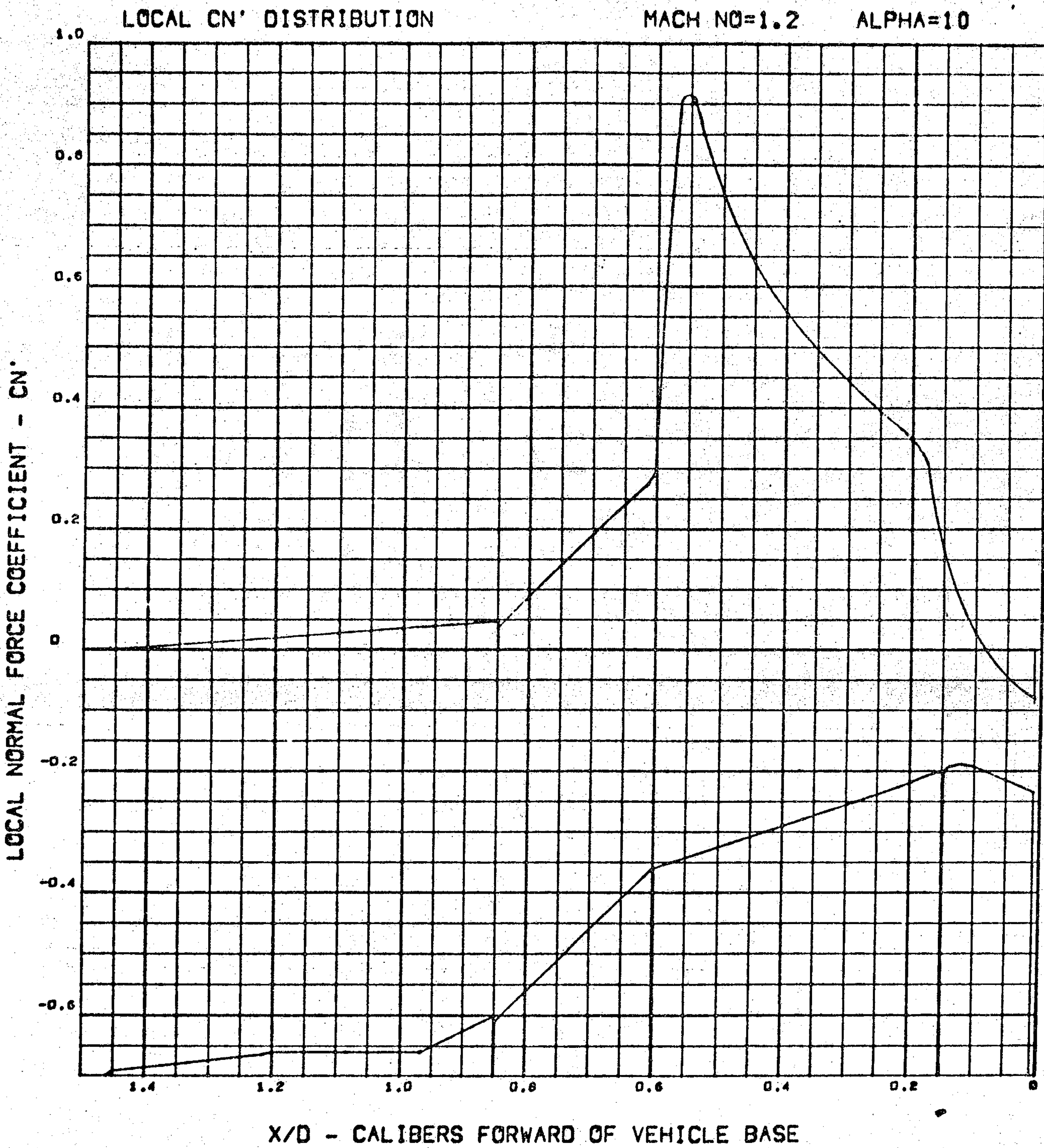
LOCAL CN' DISTRIBUTION
MACH NO=1.2
ALPHA=10
LOCAL NORMAL FORCE COEFFICIENT - CN'
1.0
0.8
0.6
0.4
0.2
0
-0.2
-0.4
-0.6
1.4
1.2
1.0
0.8
0.6
0.4
0.2
0
X/D - CALIBERS FORWARD OF VEHICLE BASE

Figure F.1-7

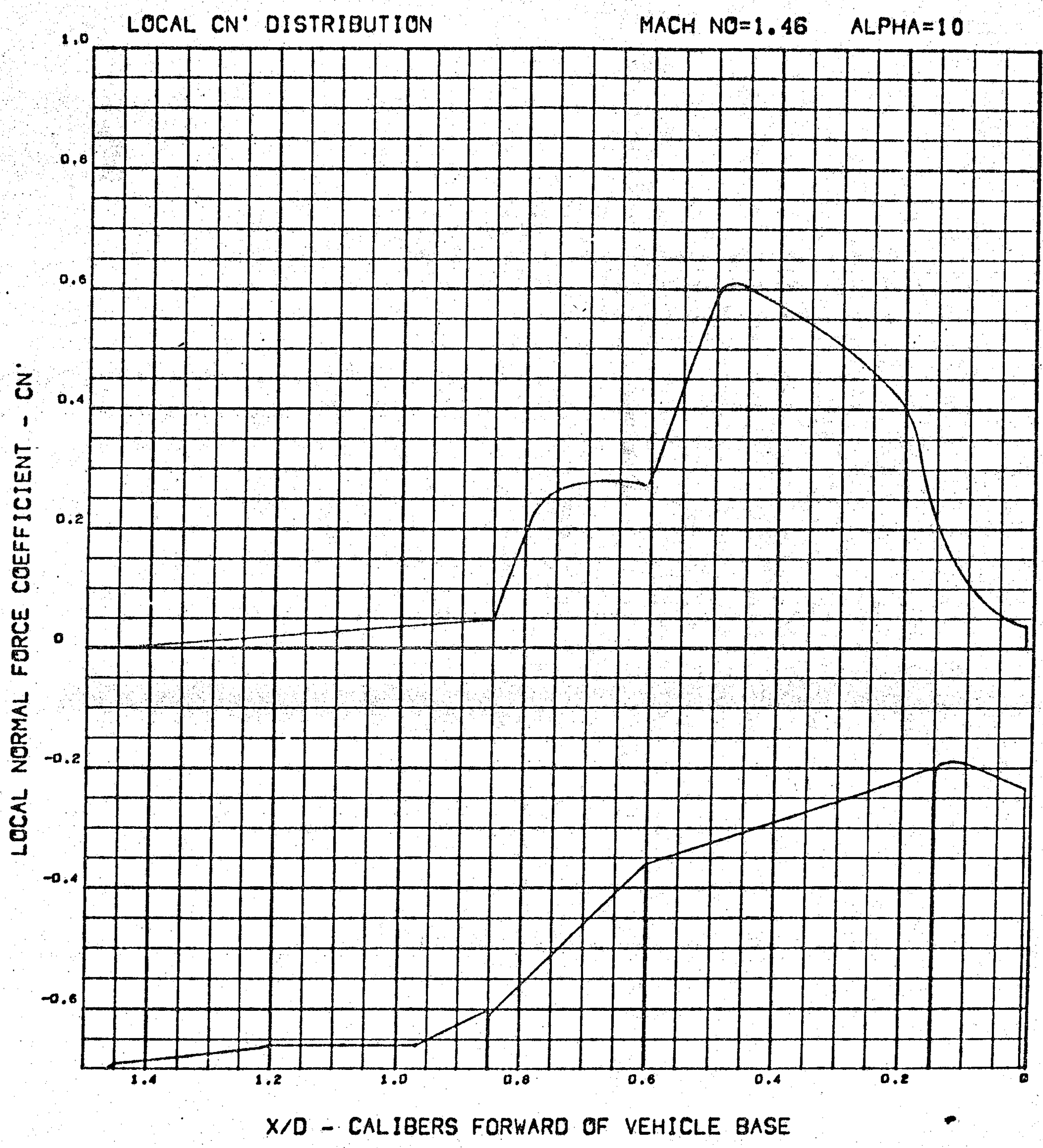

LOCAL CN' DISTRIBUTION
MACH NO=1.46
ALPHA=10
1.0
0.8
0.6
0.4
0.2
0
-0.2
-0.4
-0.6
LOCAL NORMAL FORCE COEFFICIENT - CN'
1.4
1.2
1.0
0.8
0.6
0.4
0.2
0
X/D - CALIBERS FORWARD OF VEHICLE BASE

Figure F.1-8

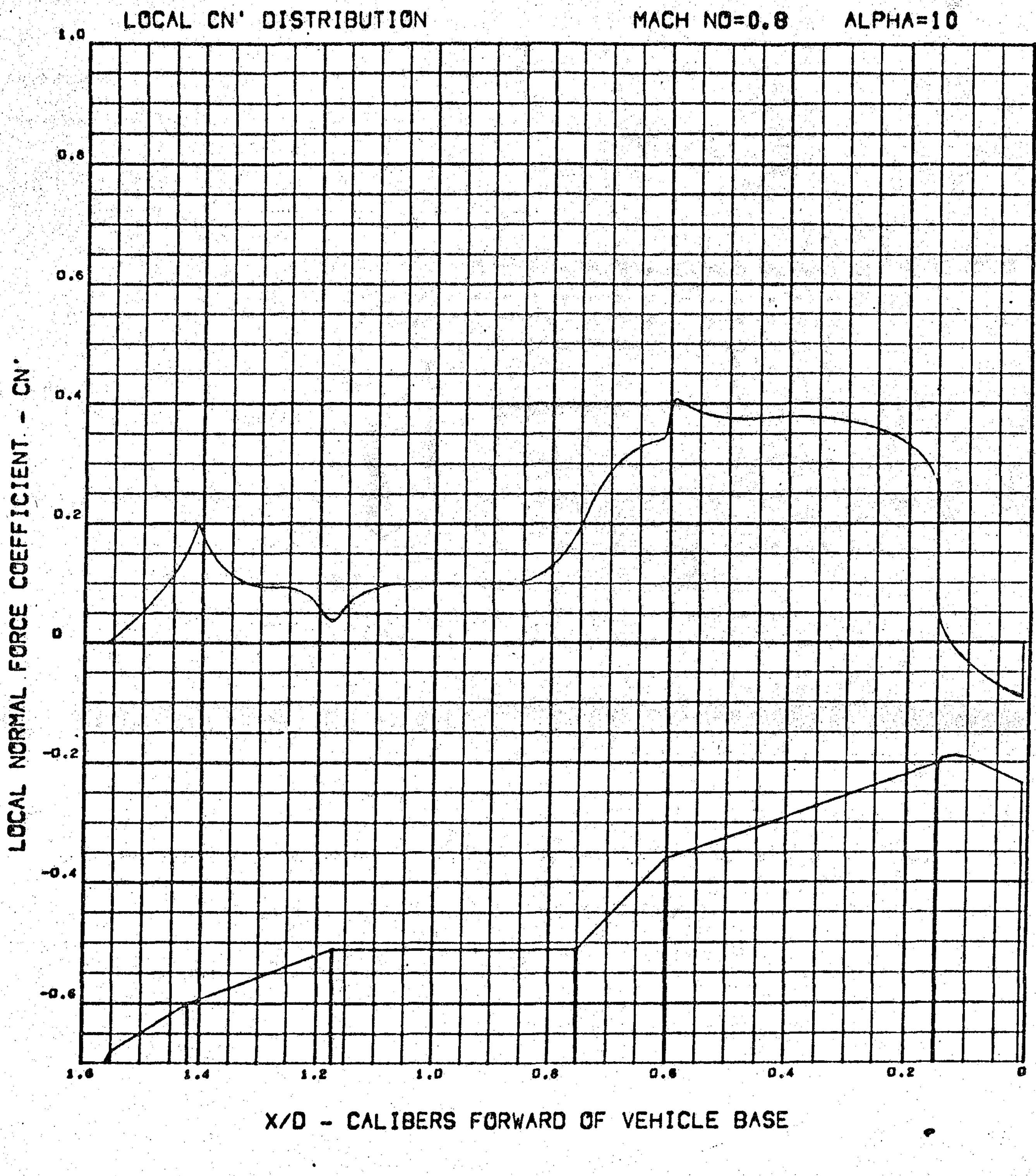
LOCAL CN' DISTRIBUTION
MACH NO=0.8
ALPHA=10
LOCAL NORMAL FORCE COEFFICIENT - CN'
1.0
0.8
0.6
0.4
0.2
0
-0.2
-0.4
-0.6
1.6
1.4
1.2
1.0
0.8
0.6
0.4
0.2
0
X/D - CALIBERS FORWARD OF VEHICLE BASE

Figure F.1-9

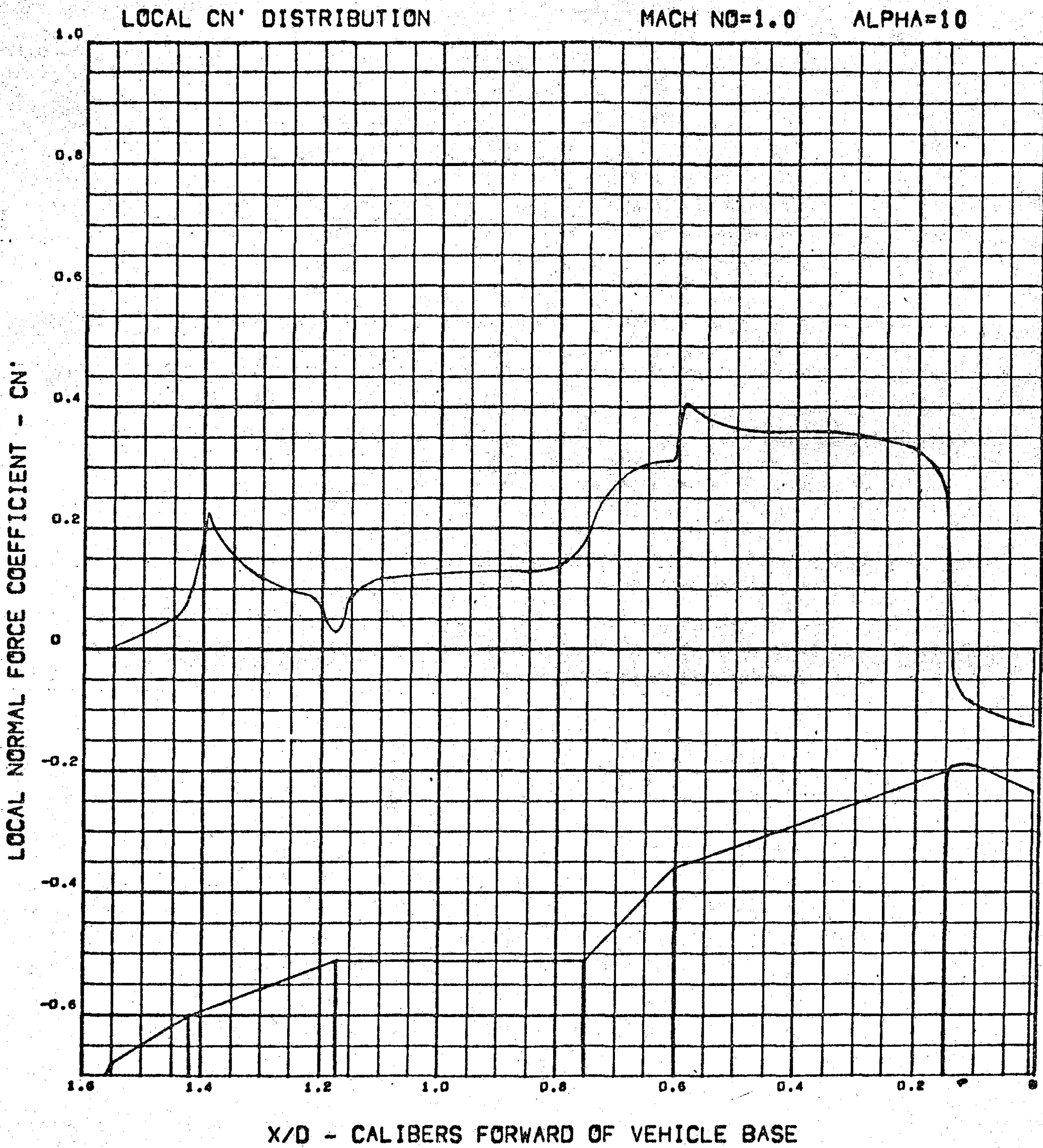

LOCAL CN' DISTRIBUTION
MACH NO=1.0
ALPHA=10
LOCAL NORMAL FORCE COEFFICIENT - CN'
1.0
0.8
0.6
0.4
0.2
0
-0.2
-0.4
-0.6
1.6
1.4
1.2
1.0
0.8
0.6
0.4
0.2
0
X/D - CALIBERS FORWARD OF VEHICLE BASE

Figure F.1-10

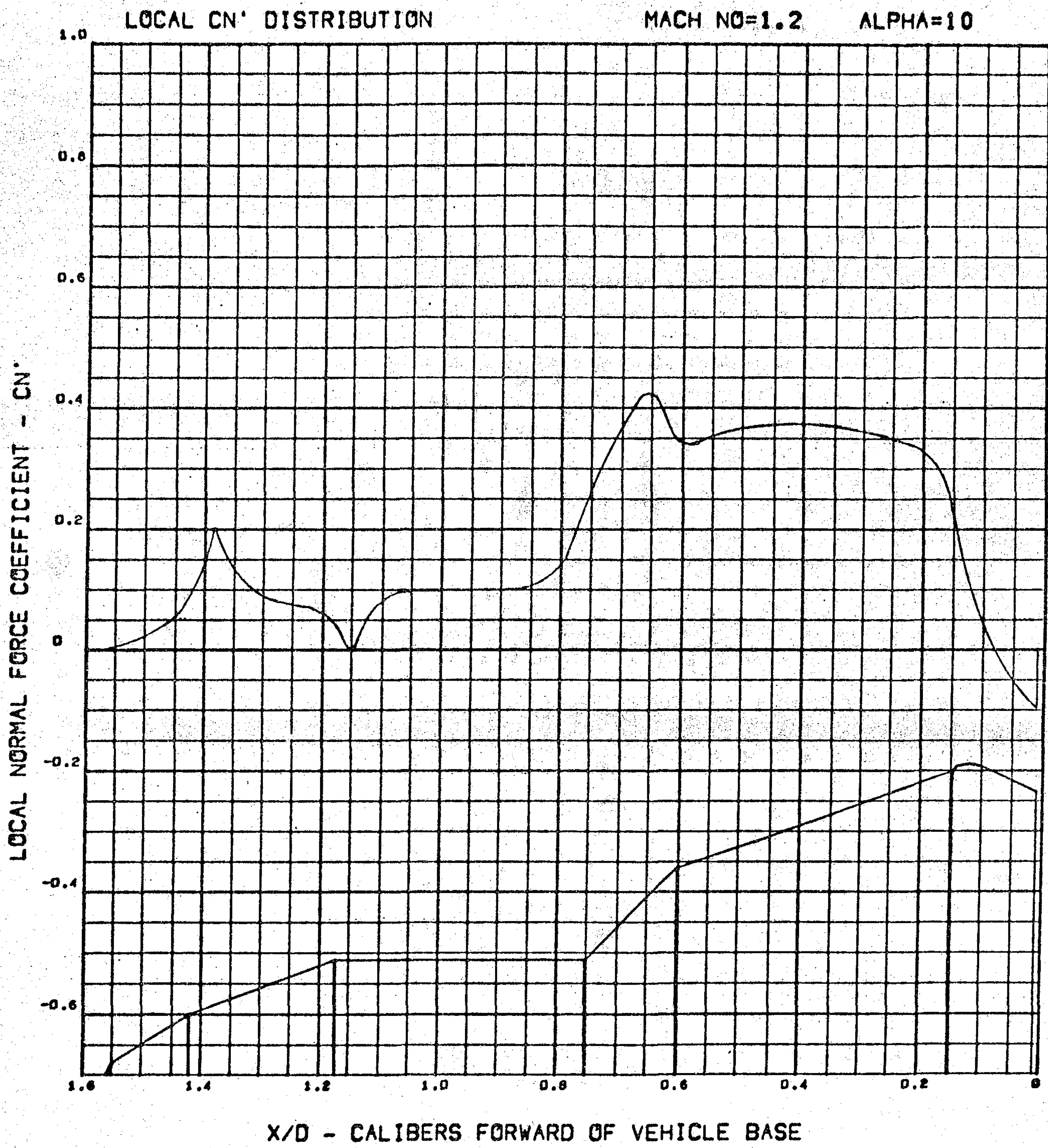
LOCAL CN' DISTRIBUTION
MACH NO=1.2
ALPHA=10
LOCAL NORMAL FORCE COEFFICIENT - CN'
1.0
0.8
0.6
0.4
0.2
0
-0.2
-0.4
-0.6
1.6
1.4
1.2
1.0
0.8
0.6
0.4
0.2
0
X/D - CALIBERS FORWARD OF VEHICLE BASE

Figure F.1-11

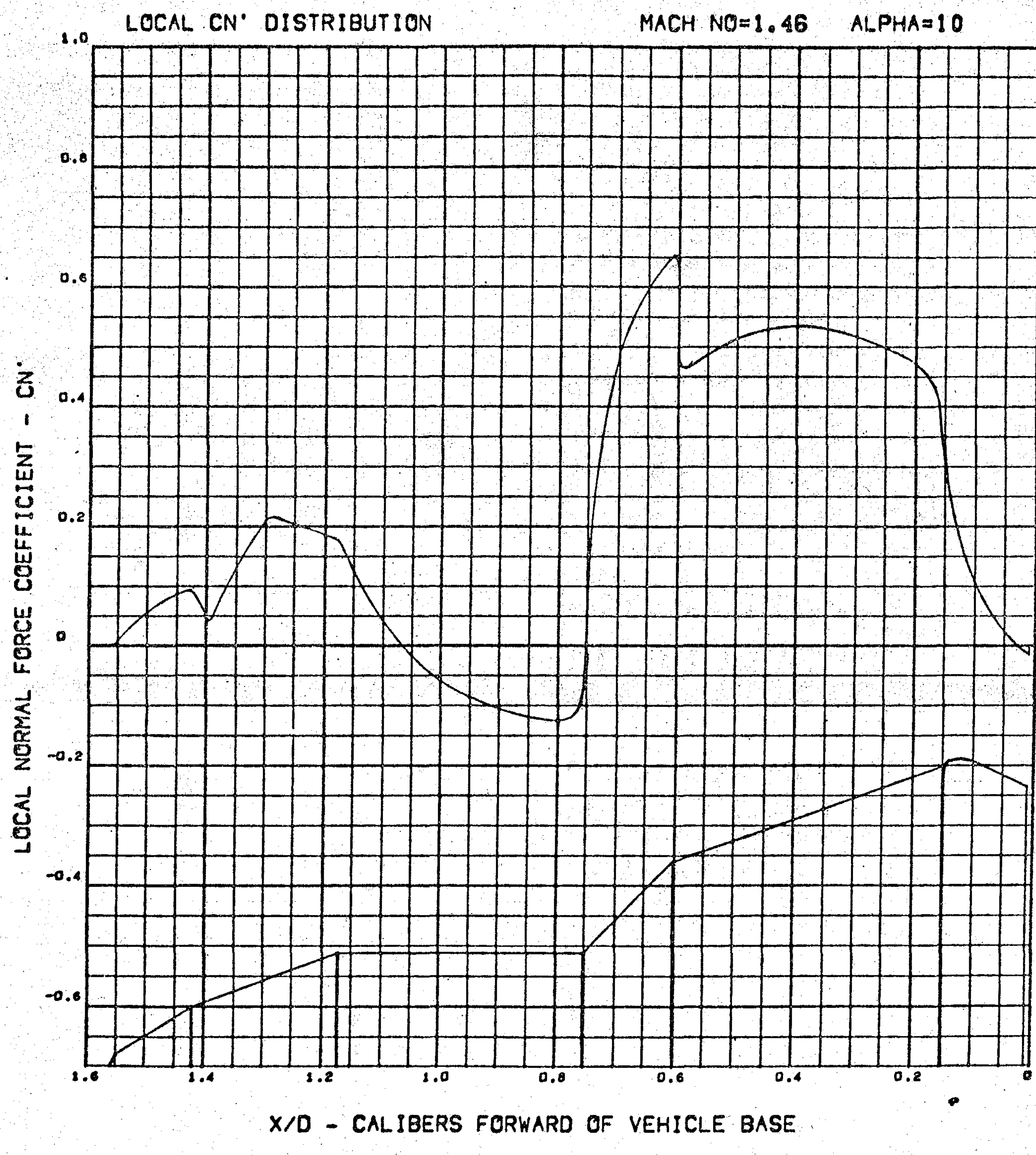
LOCAL CN' DISTRIBUTION
MACH NO=1.46
ALPHA=10
1.0
0.8
0.6
0.4
0.2
0
-0.2
-0.4
-0.6
LOCAL NORMAL FORCE COEFFICIENT - CN'
1.6
1.4
1.2
1.0
0.8
0.6
0.4
0.2
0
X/D - CALIBERS FORWARD OF VEHICLE BASE

Figure F.1-12

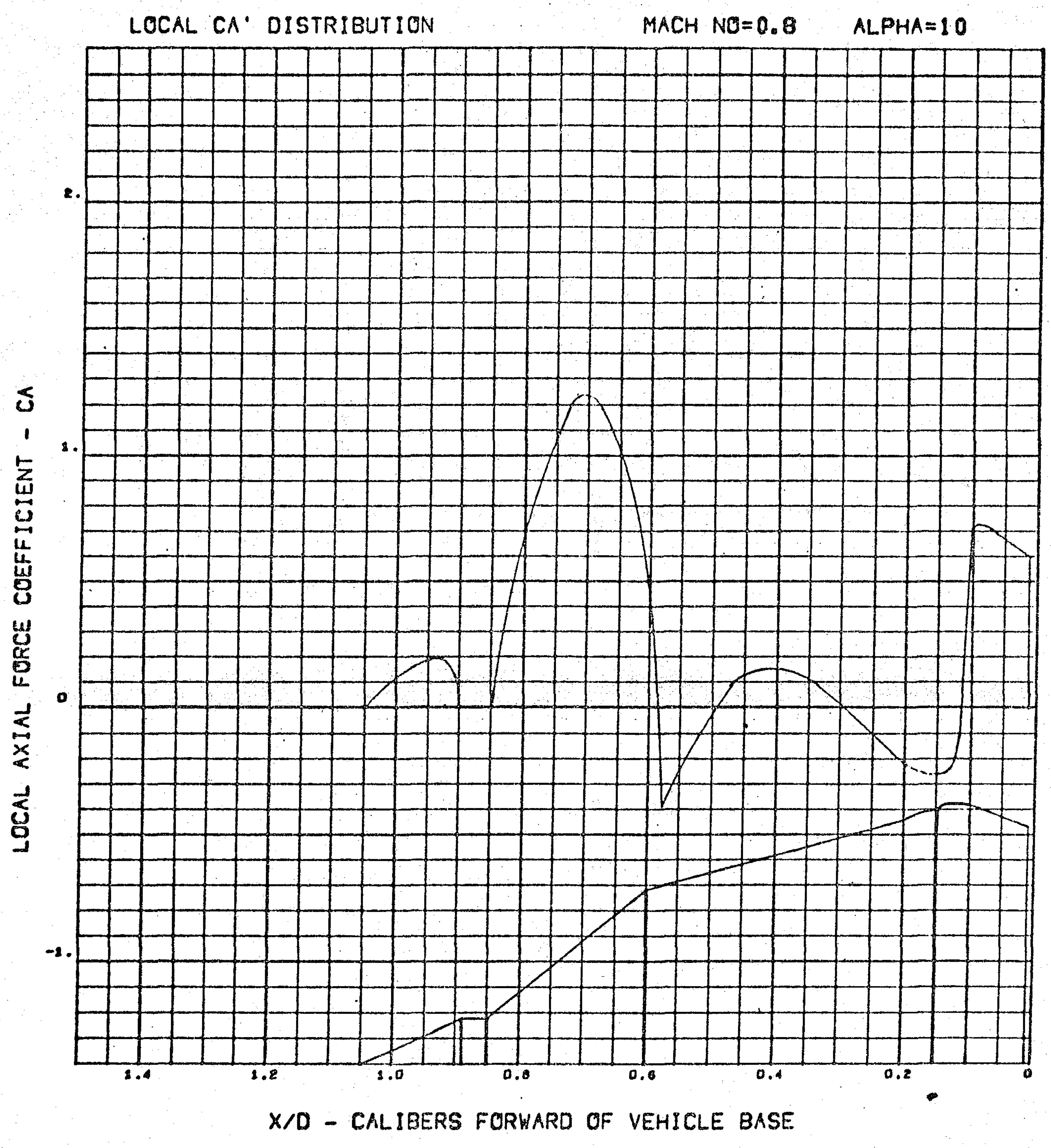

Figure F.1-13

C6

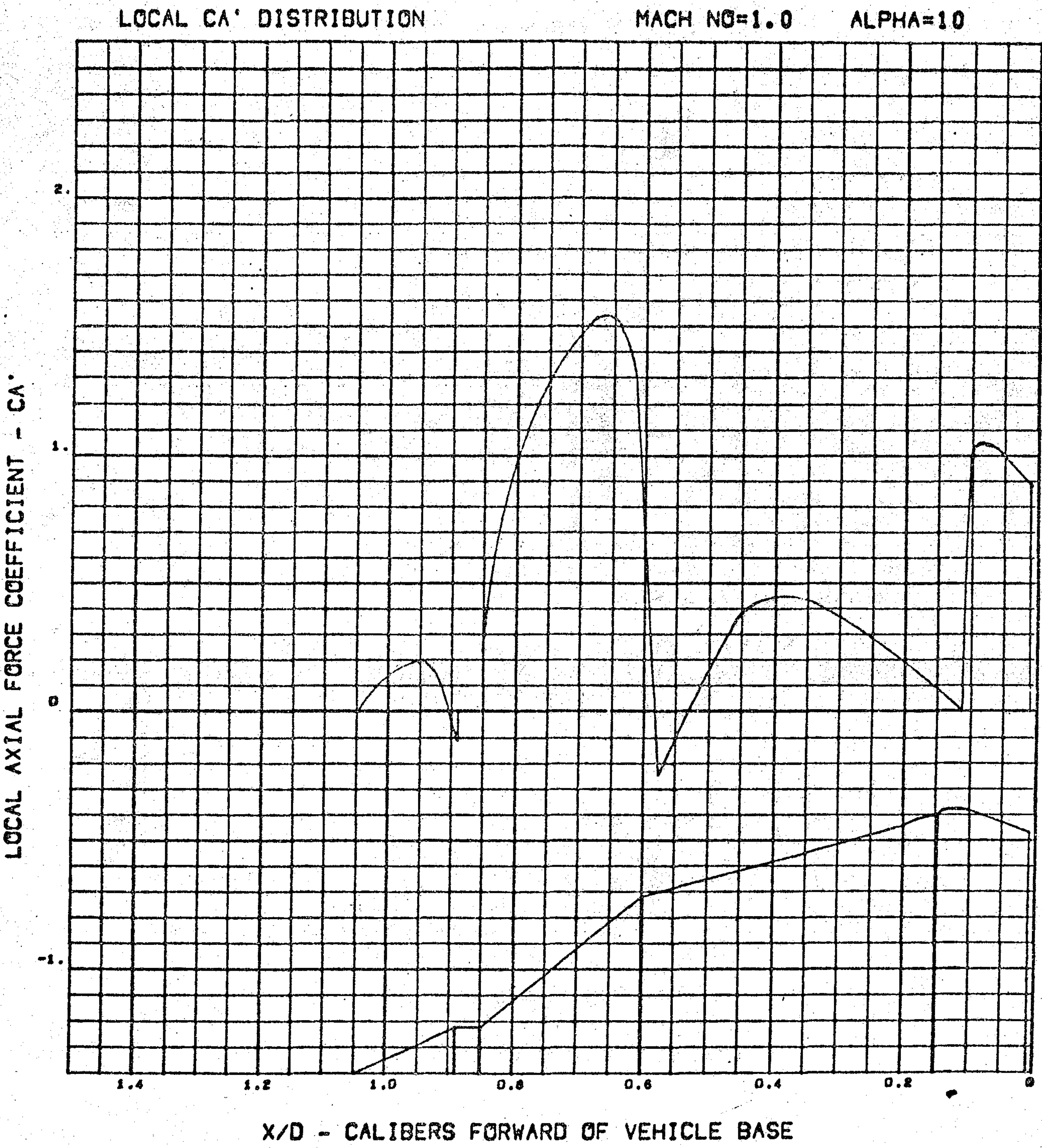

LOCAL CA' DISTRIBUTION
MACH NO=1.0
ALPHA=10
LOCAL AXIAL FORCE COEFFICIENT - CA'
2.
1.
0
-1.
1.4
1.2
1.0
0.8
0.6
0.4
0.2
0
X/D - CALIBERS FORWARD OF VEHICLE BASE

Figure F.1-14

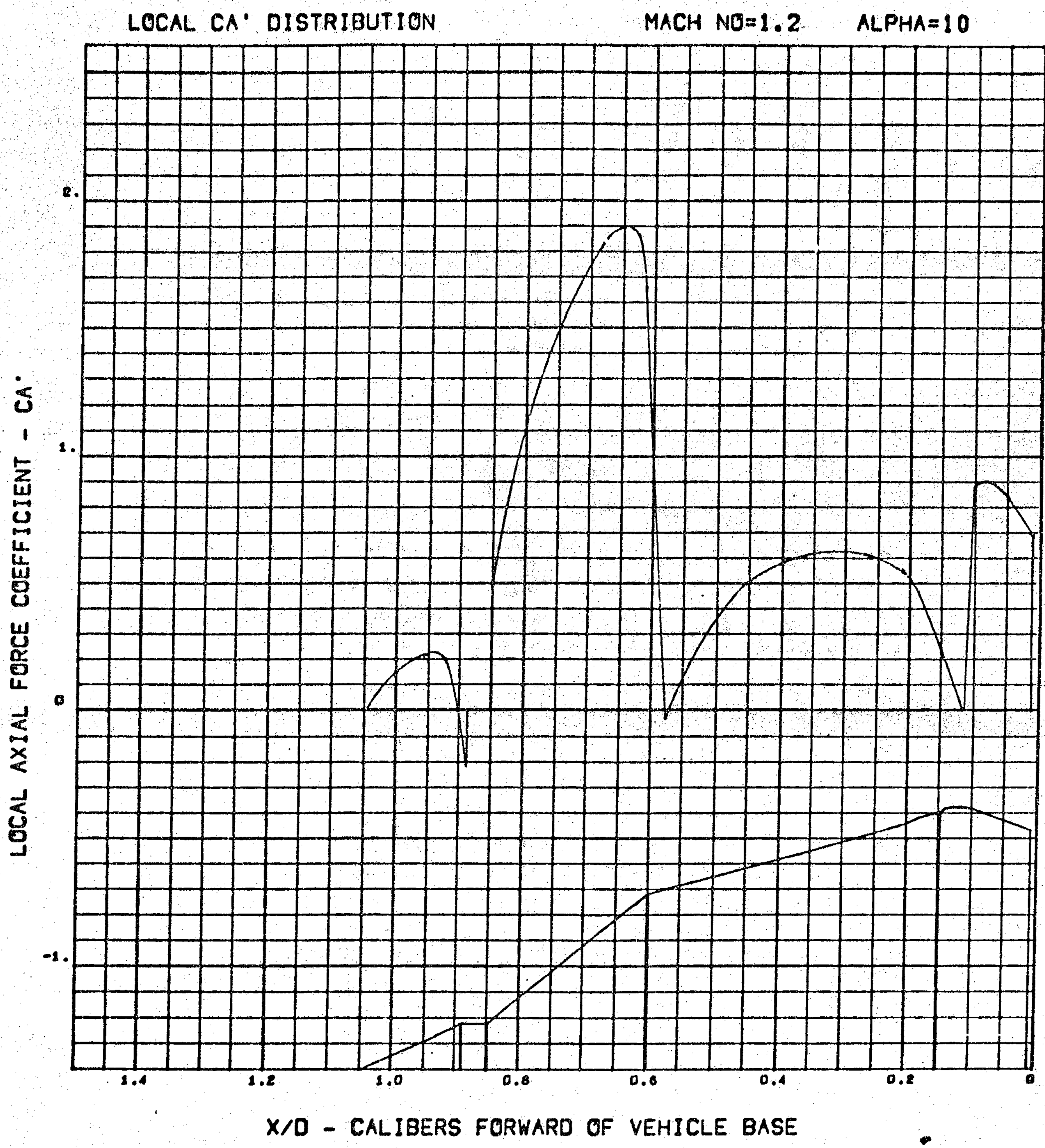
LOCAL CA' DISTRIBUTION
MACH NO=1.2
ALPHA=10
LOCAL AXIAL FORCE COEFFICIENT - CA'
2.
1.
0
-1.
1.4
1.2
1.0
0.8
0.6
0.4
0.2
0
X/D - CALIBERS FORWARD OF VEHICLE BASE

Figure F.1-15

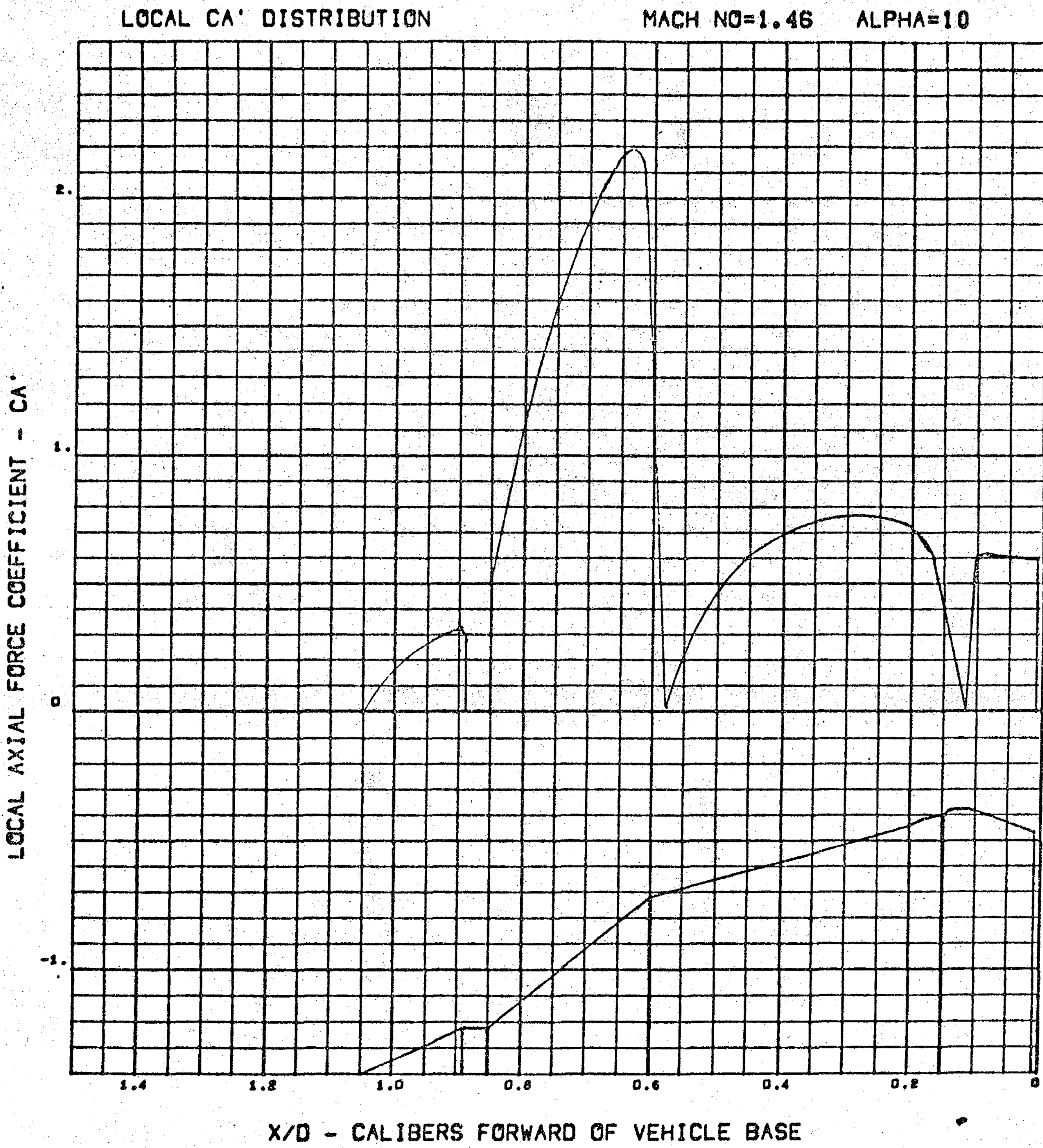
LOCAL CA' DISTRIBUTION
MACH NO=1.46 ALPHA=10
LOCAL AXIAL FORCE COEFFICIENT - CA'
2.
1.
0
-1.
1.4
1.2
1.0
0.8
0.6
0.4
0.2
0
X/D - CALIBERS FORWARD OF VEHICLE BASE

Figure F.1-16

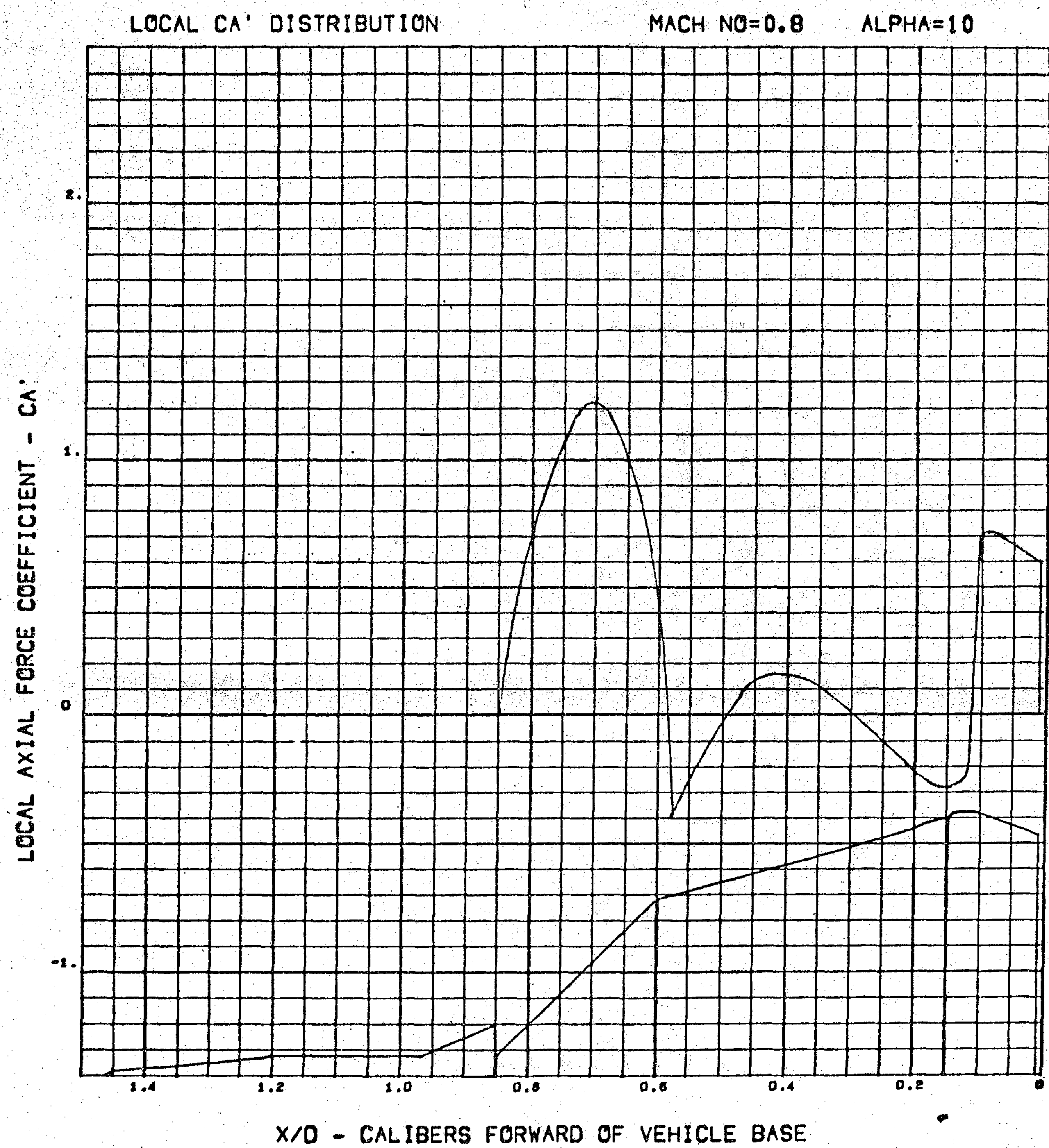
LOCAL CA' DISTRIBUTION
MACH NO=0.8
ALPHA=10
LOCAL AXIAL FORCE COEFFICIENT - CA'
2.
1.
0
-1.
1.4
1.2
1.0
0.8
0.6
0.4
0.2
0
X/D - CALIBERS FORWARD OF VEHICLE BASE

Figure F.1-17

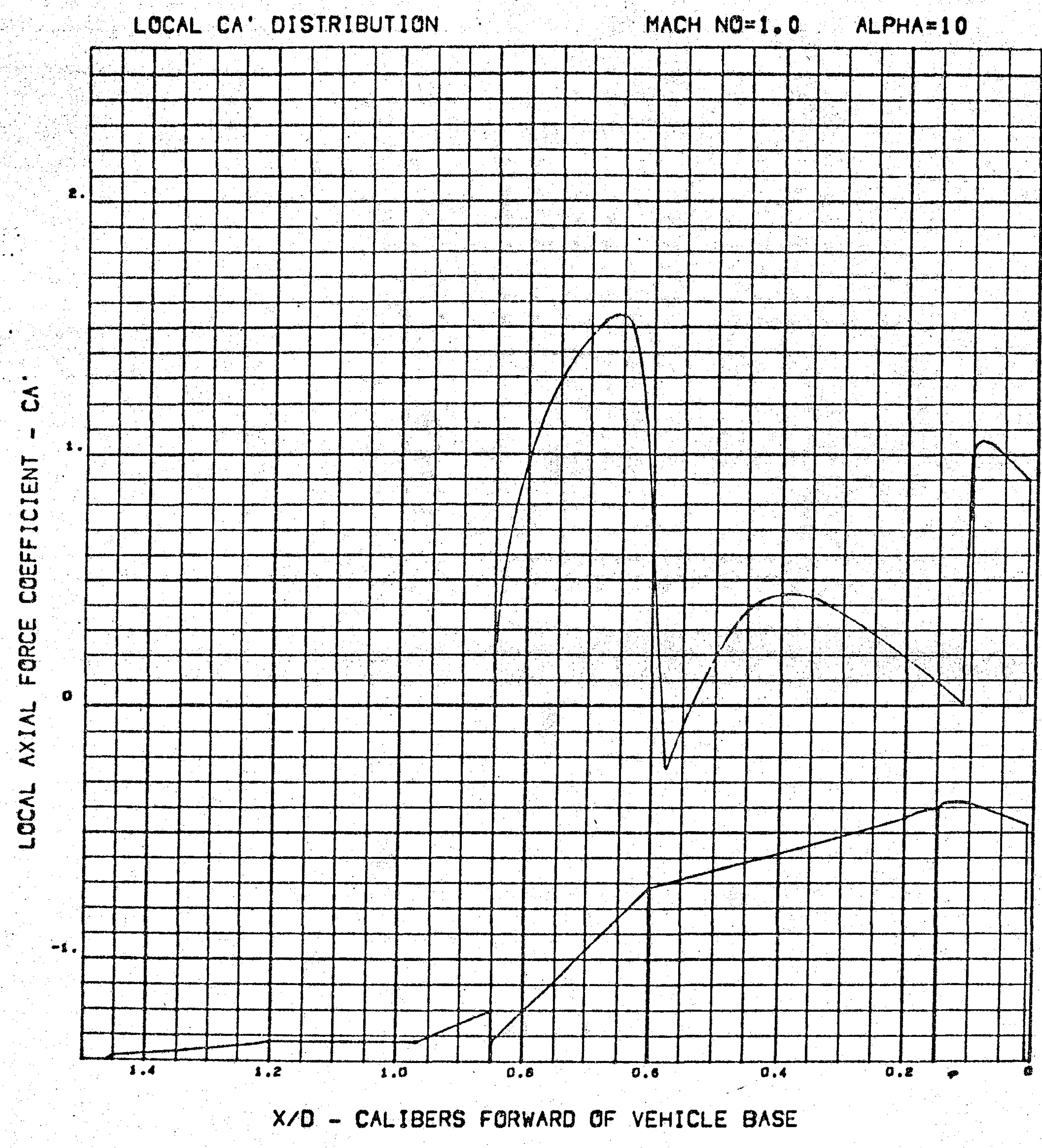
LOCAL CA' DISTRIBUTION
MACH NO=1.0
ALPHA=10
LOCAL AXIAL FORCE COEFFICIENT - CA'
2.
1.
0
-1.
1.4
1.2
1.0
0.8
0.6
0.4
0.2
0
X/D - CALIBERS FORWARD OF VEHICLE BASE

Figure F.1-18

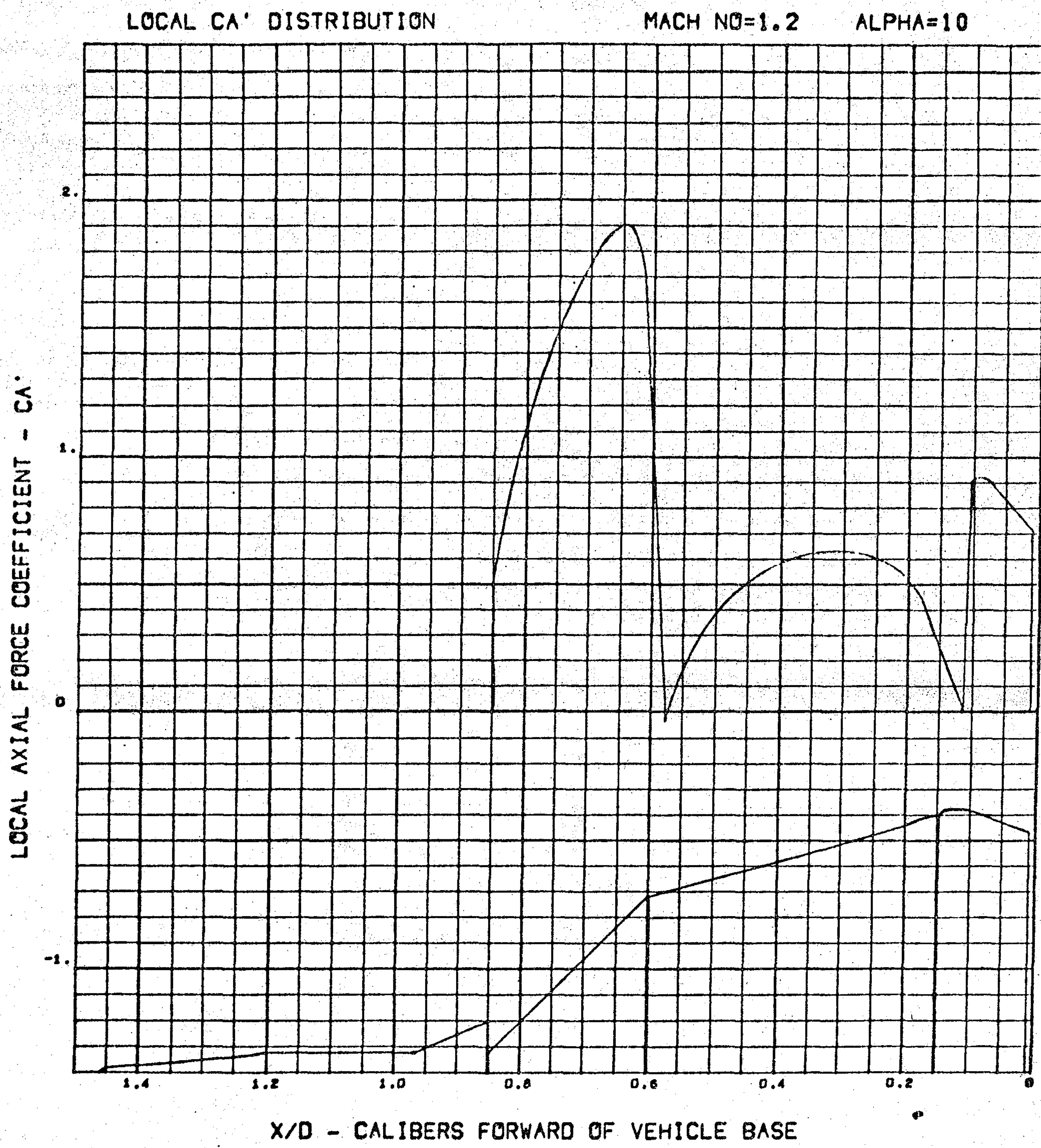
LOCAL CA' DISTRIBUTION
MACH NO=1.2
ALPHA=10
LOCAL AXIAL FORCE COEFFICIENT - CA'
2.
1.
0
-1.
1.4
1.2
1.0
0.8
0.6
0.4
0.2
0
X/D - CALIBERS FORWARD OF VEHICLE BASE

Figure F.1-19

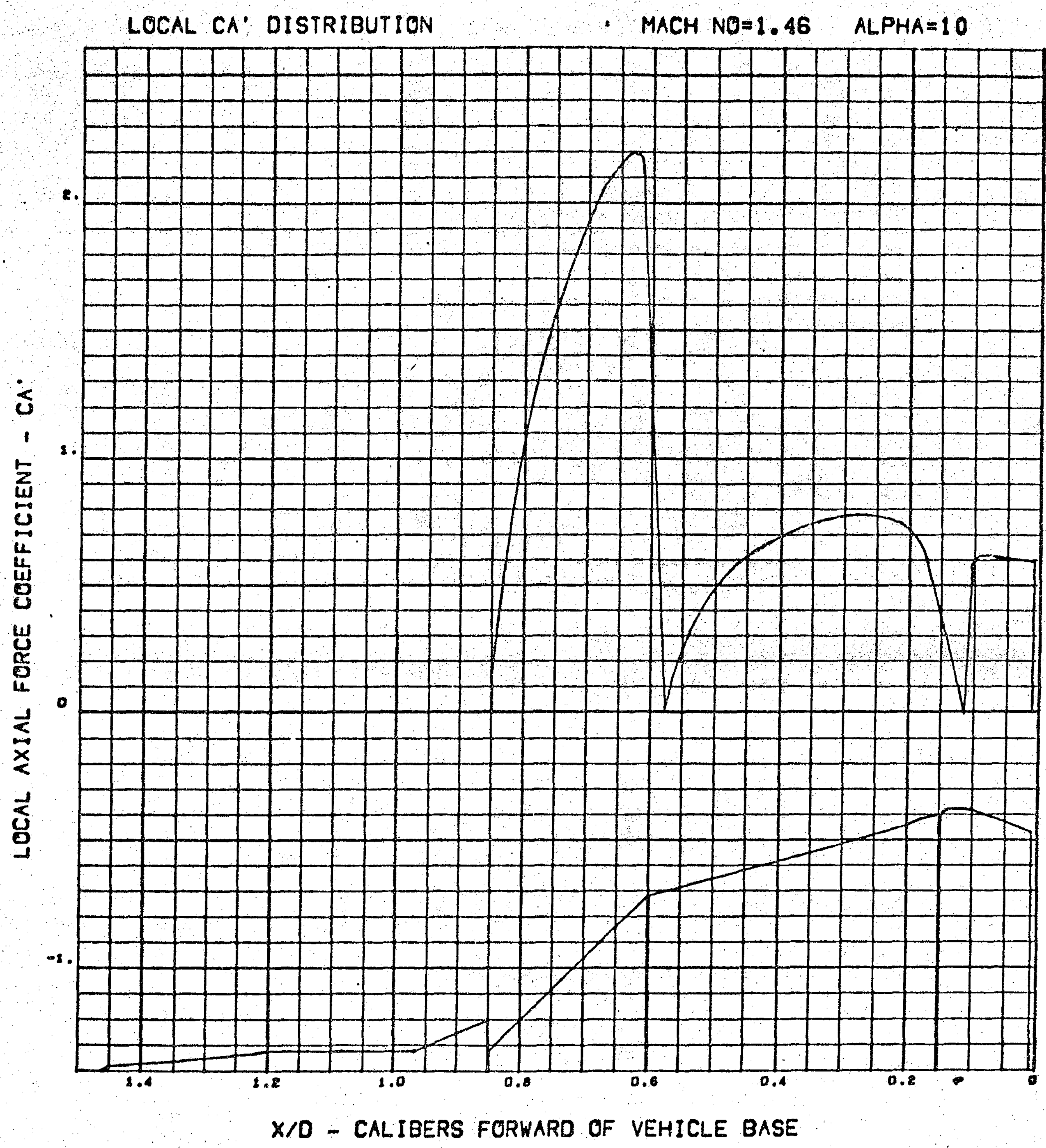
LOCAL CA' DISTRIBUTION
MACH NO=1.46 ALPHA=10
LOCAL AXIAL FORCE COEFFICIENT - CA'
2.
1.
0
-1.
1.4
1.2
1.0
0.8
0.6
0.4
0.2
0
X/D - CALIBERS FORWARD OF VEHICLE BASE

Figure F.1-20

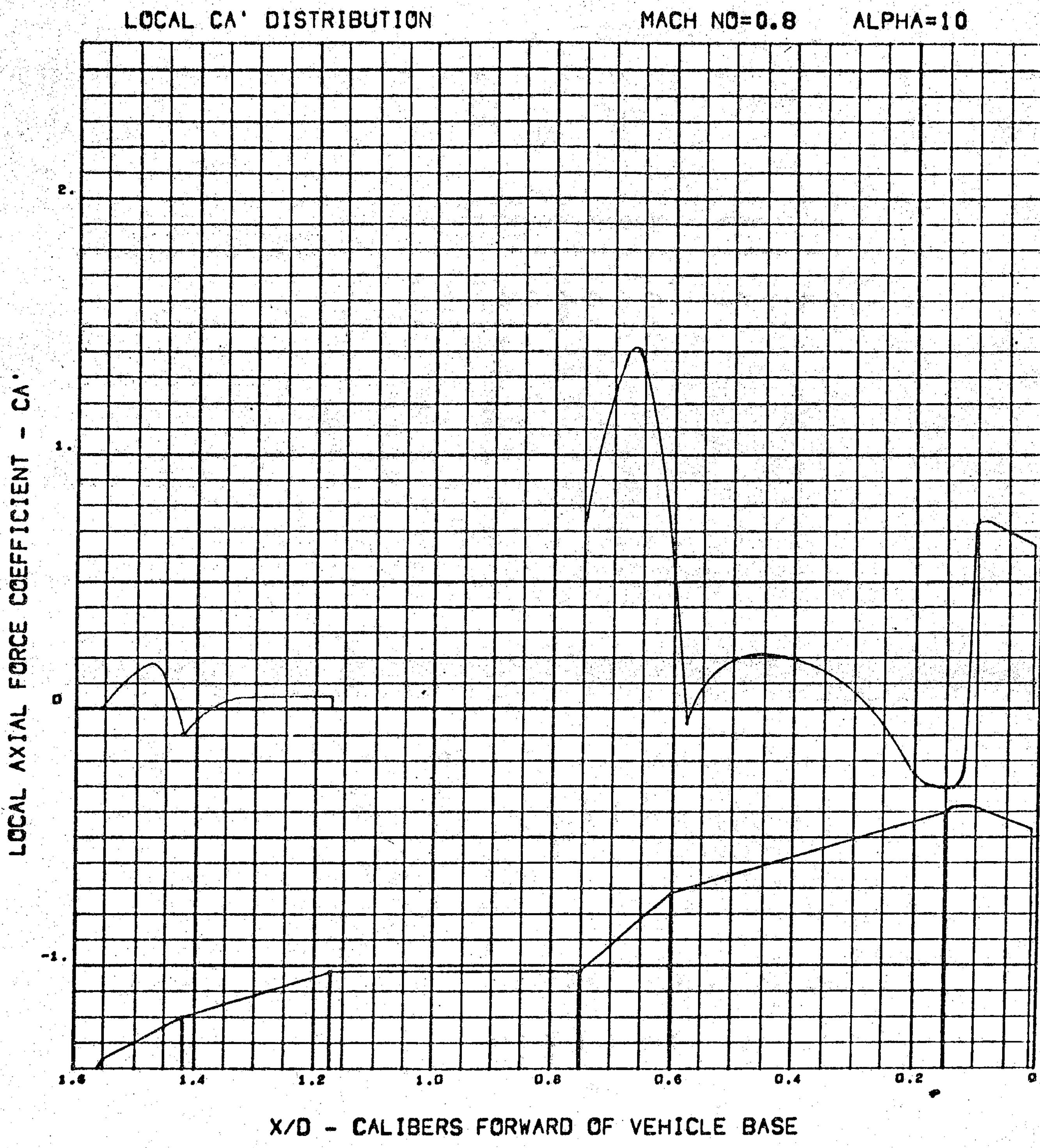
LOCAL CA' DISTRIBUTION
MACH NO=0.8
ALPHA=10
LOCAL AXIAL FORCE COEFFICIENT - CA'
2.
1.
0
-1.
1.6
1.4
1.2
1.0
0.8
0.6
0.4
0.2
0
X/D - CALIBERS FORWARD OF VEHICLE BASE

Figure F.1-21

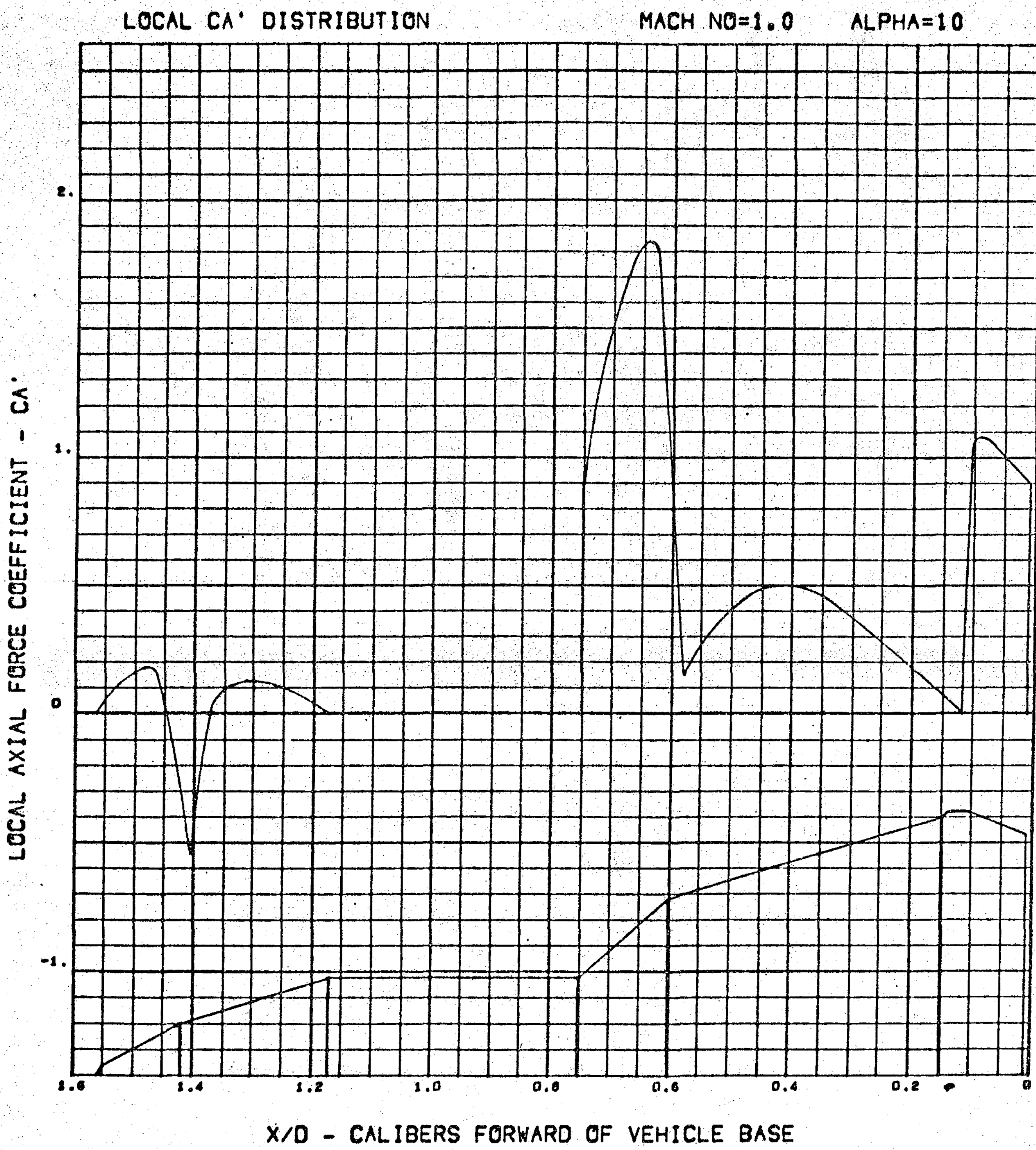
LOCAL CA' DISTRIBUTION
MACH NO=1.0
ALPHA=10
LOCAL AXIAL FORCE COEFFICIENT - CA'
2.
1.
0
-1.
1.6
1.4
1.2
1.0
0.8
0.6
0.4
0.2
0
X/D - CALIBERS FORWARD OF VEHICLE BASE

Figure F.1-22

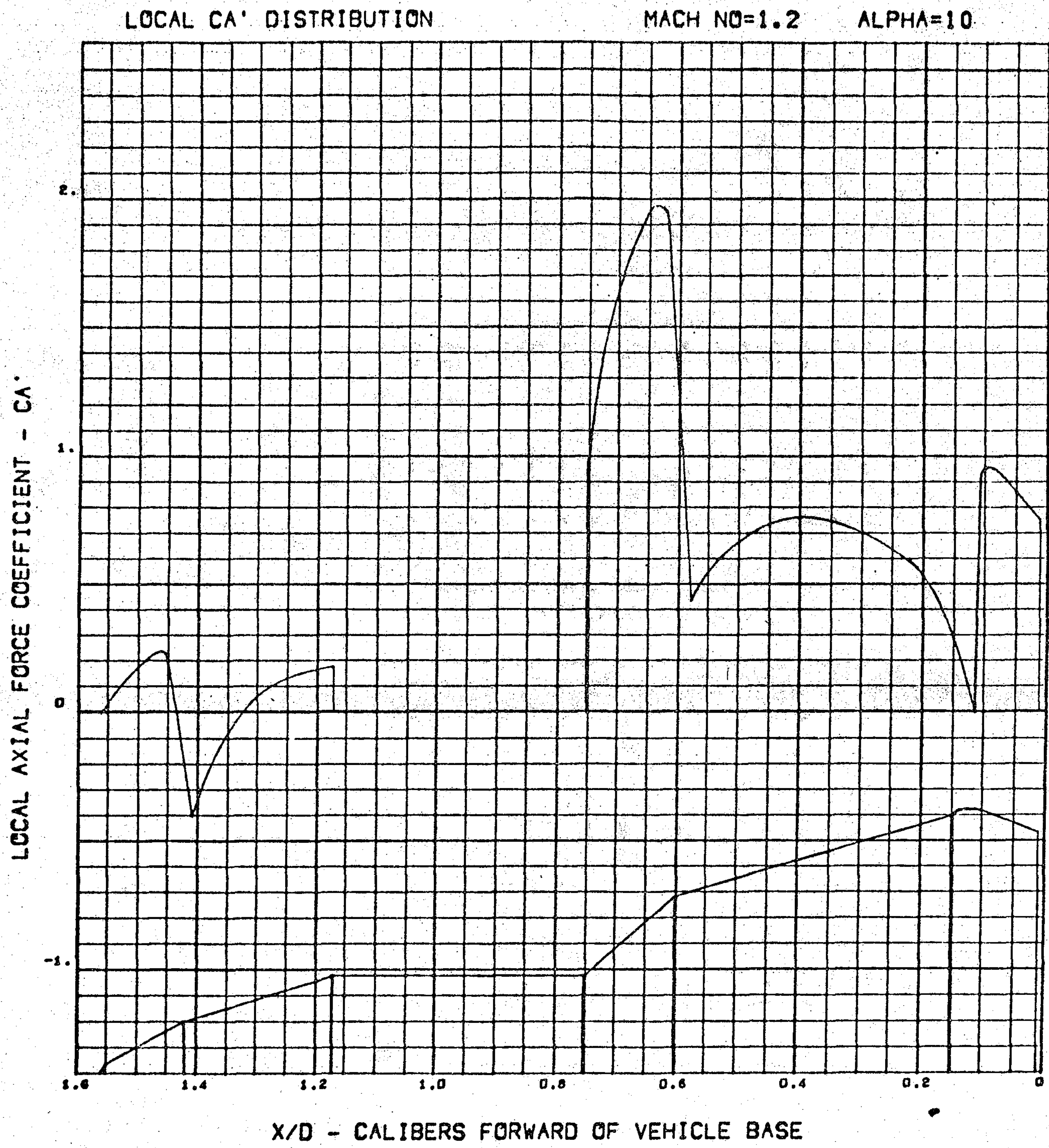

LOCAL CA' DISTRIBUTION
MACH NO=1.2
ALPHA=10
LOCAL AXIAL FORCE COEFFICIENT - CA'
2.
1.
0
-1.
1.6
1.4
1.2
1.0
0.8
0.6
0.4
0.2
0
X/D - CALIBERS FORWARD OF VEHICLE BASE

Figure F.1-23

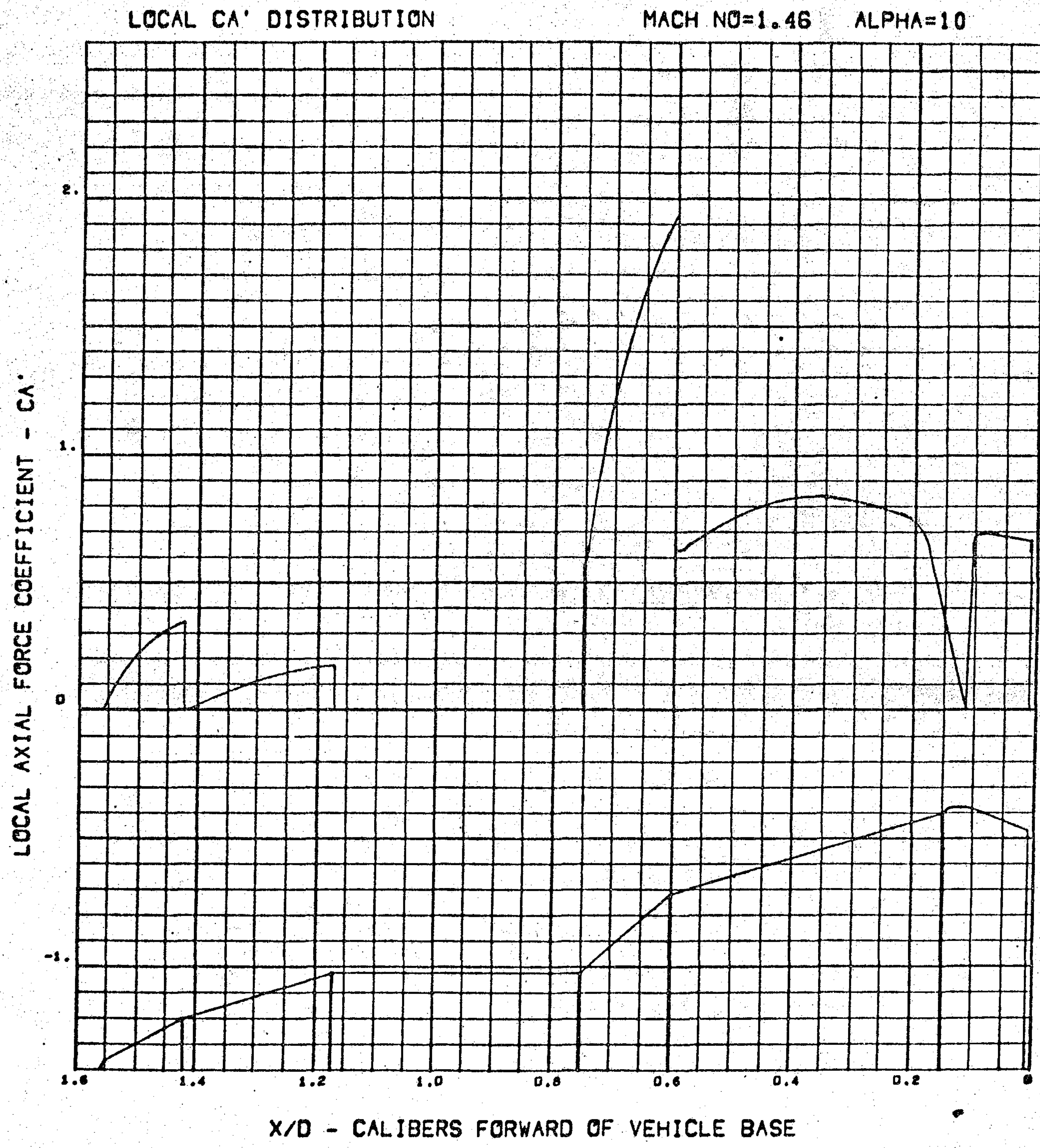
LOCAL CA' DISTRIBUTION
MACH NO=1.46 ALPHA=10
LOCAL AXIAL FORCE COEFFICIENT - CA'
2.
1.
0
-1.
1.6
1.4
1.2
1.0
0.8
0.6
0.4
0.2
0
X/D - CALIBERS FORWARD OF VEHICLE BASE

Figure F.1-24

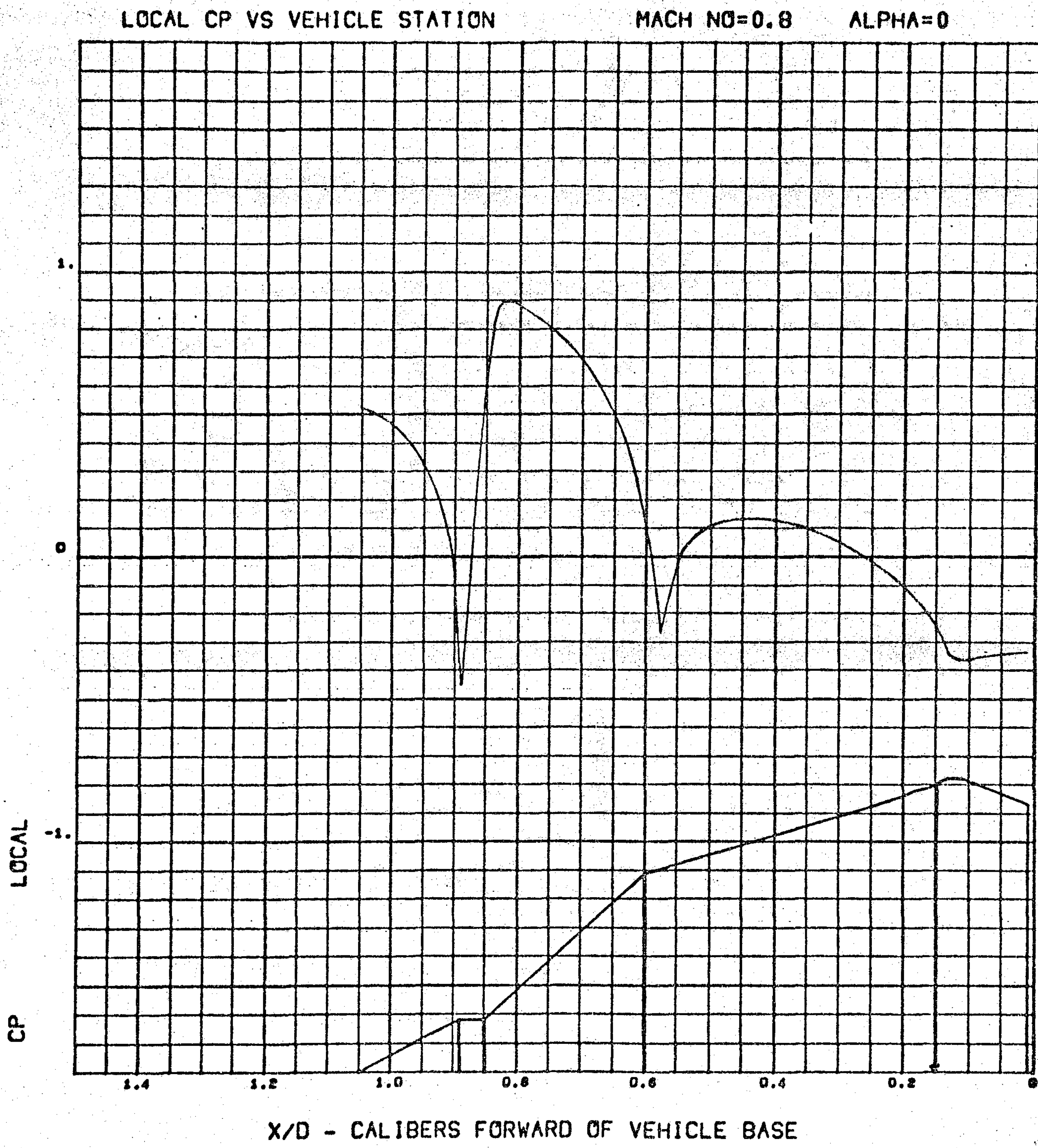
LOCAL CP VS VEHICLE STATION
MACH NO=0.8
ALPHA=0
1.
0
-1.
CP LOCAL
1.4
1.2
1.0
0.8
0.6
0.4
0.2
0
X/D - CALIBERS FORWARD OF VEHICLE BASE

Figure F.2-1

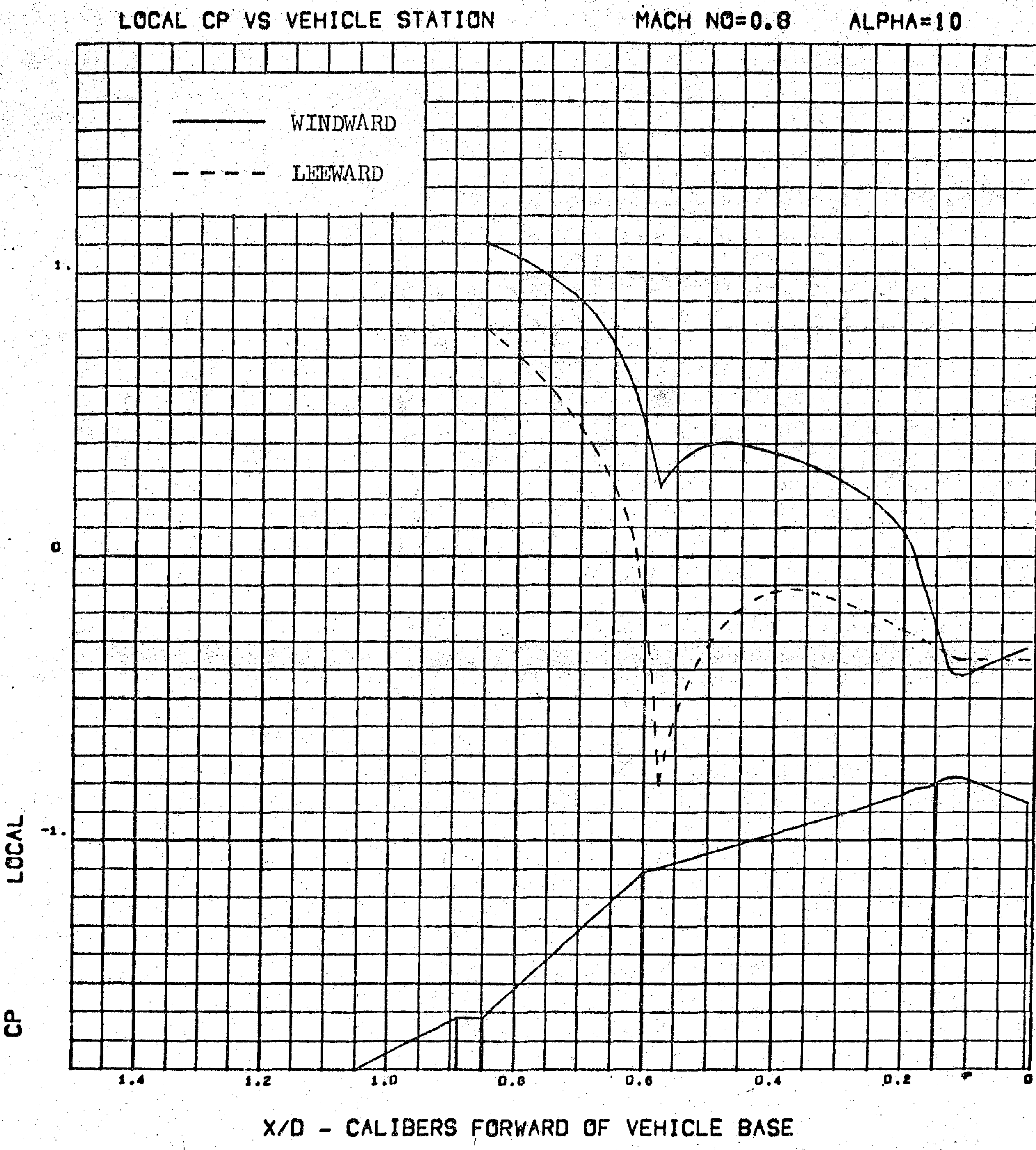

LOCAL CP VS VEHICLE STATION
MACH NO=0.8
ALPHA=10
WINDWARD
LEEWARD
1.
0
-1.
LOCAL
CP
1.4
1.2
1.0
0.8
0.6
0.4
0.2
0
X/D - CALIBERS FORWARD OF VEHICLE BASE

Figure F.2-2

B

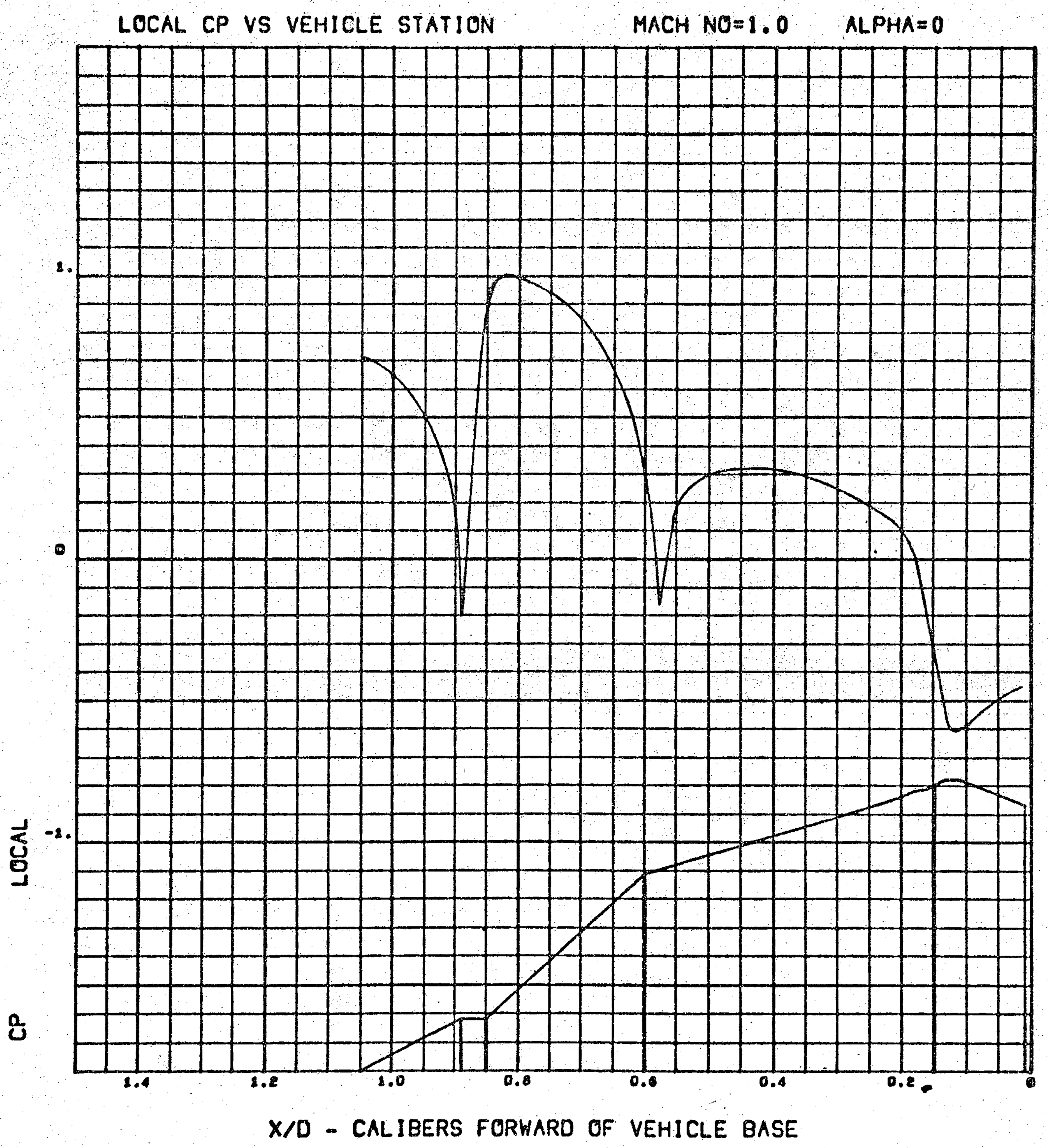

LOCAL CP VS VEHICLE STATION
MACH NO=1.0
ALPHA=0
1.
0
-1.
LOCAL
CP
1.4
1.2
1.0
0.8
0.6
0.4
0.2
0
X/D - CALIBERS FORWARD OF VEHICLE BASE

Figure F.2-3

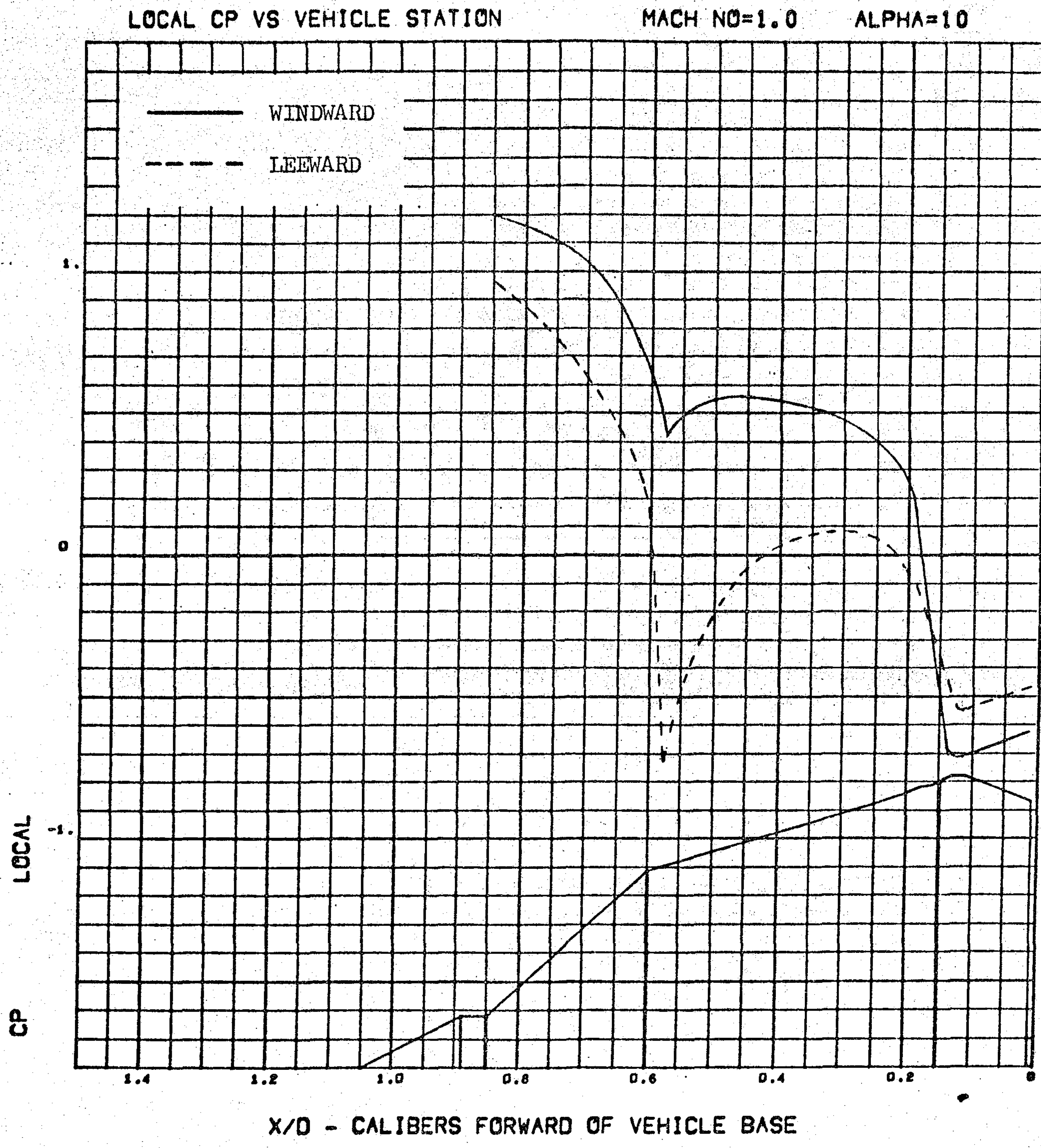
LOCAL CP VS VEHICLE STATION
MACH NO=1.0
ALPHA=10
WINDWARD
LEEWARD
1.
0
-1.
LOCAL
CP
1.4
1.2
1.0
0.8
0.6
0.4
0.2
0
X/D - CALIBERS FORWARD OF VEHICLE BASE

Figure F.2-4

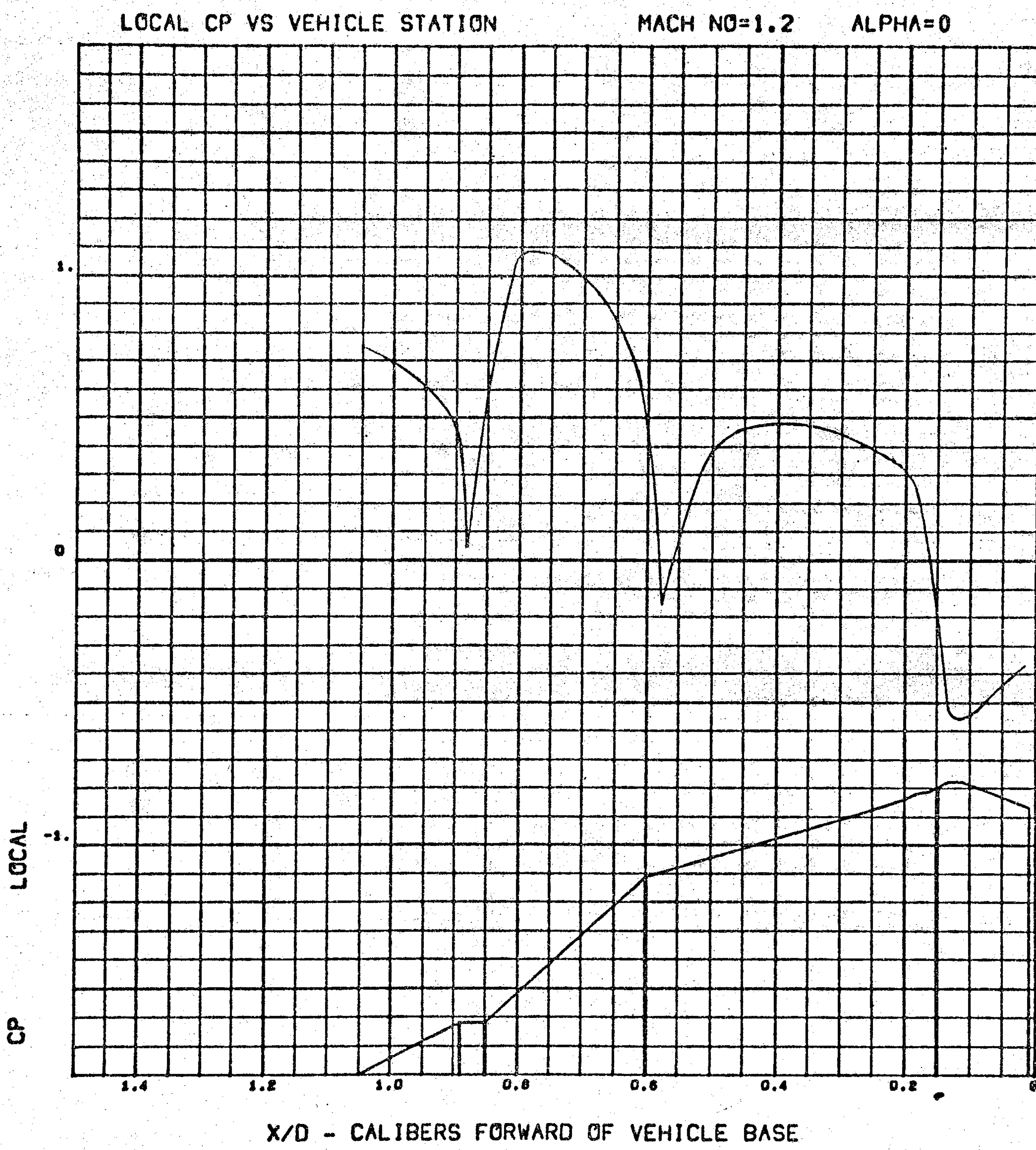
LOCAL CP VS VEHICLE STATION
MACH NO=1.2
ALPHA=0
1.
0
-1.
LOCAL
CP
1.4
1.2
1.0
0.8
0.6
0.4
0.2
0
X/D - CALIBERS FORWARD OF VEHICLE BASE

Figure F.2-5

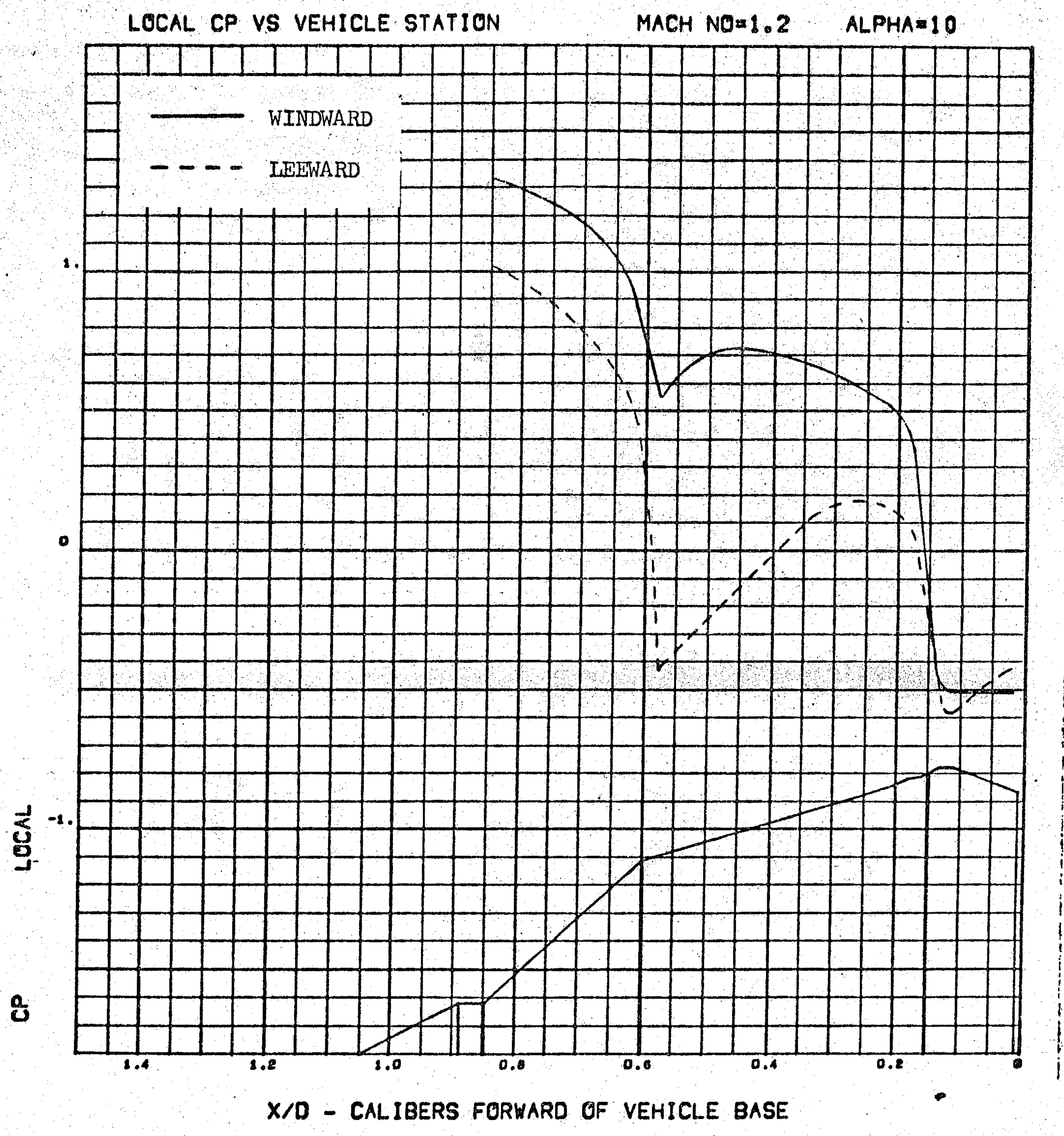
LOCAL CP VS VEHICLE STATION
MACH NO=1.2
ALPHA=10
WINDWARD
LEEWARD
1.
0
-1.
LOCAL
CP
1.4
1.2
1.0
0.8
0.6
0.4
0.2
0
X/D - CALIBERS FORWARD OF VEHICLE BASE

Figure F.2-6

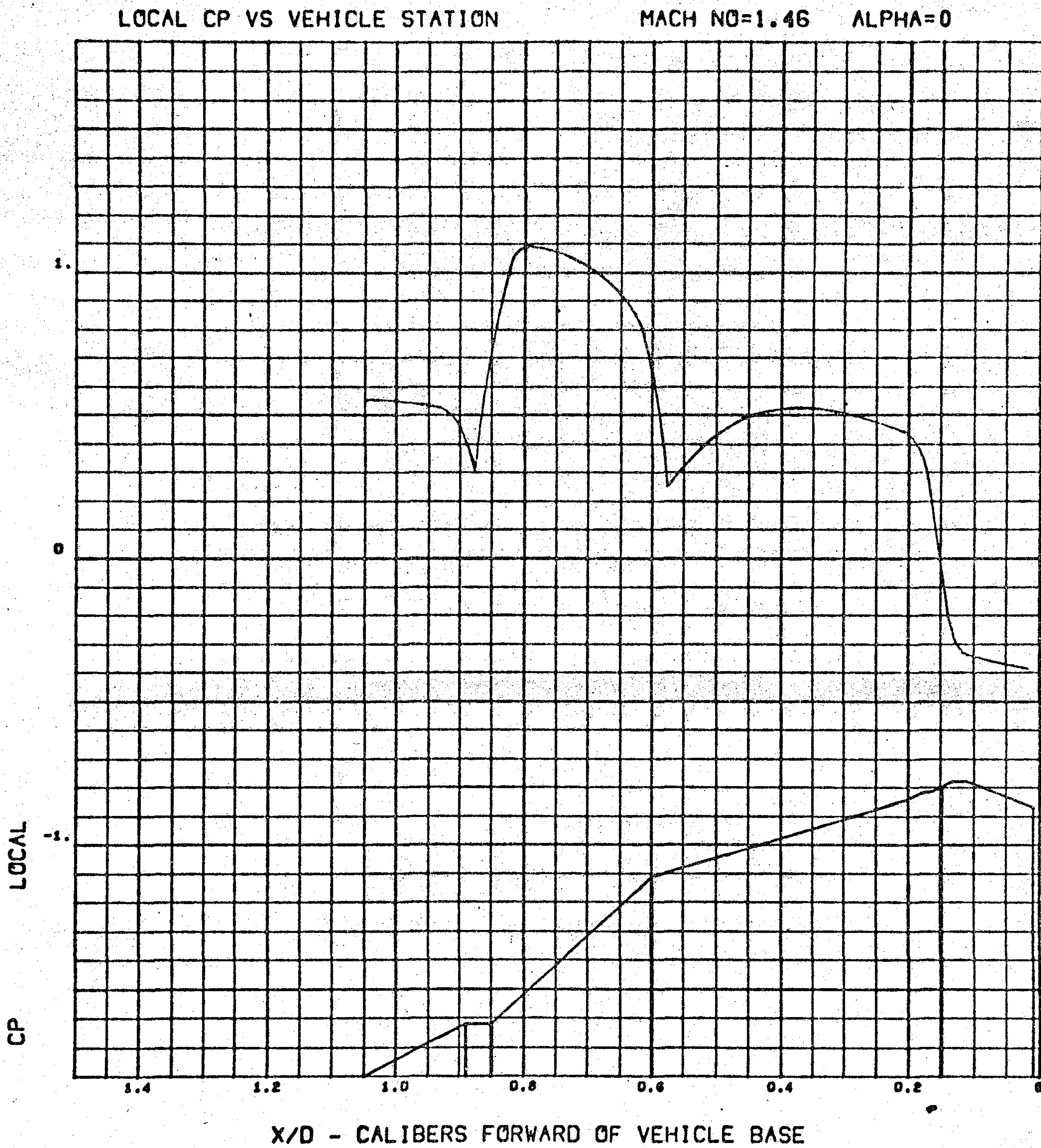

LOCAL CP VS VEHICLE STATION
MACH NO=1.46
ALPHA=0
1.
0
-1.
LOCAL
CP
1.4
1.2
1.0
0.8
0.6
0.4
0.2
0
X/D - CALIBERS FORWARD OF VEHICLE BASE

Figure F.2-7

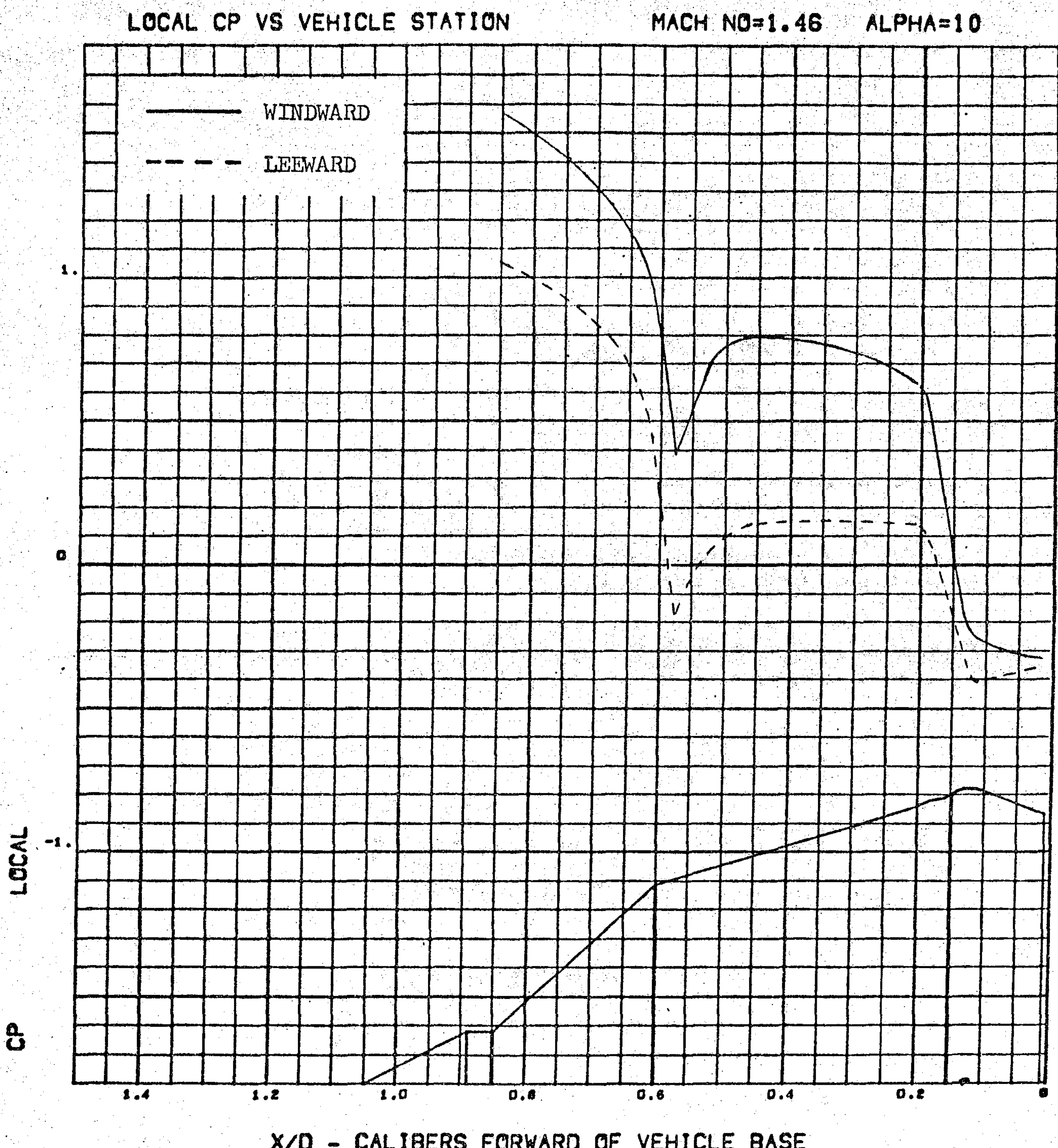

LOCAL CP VS VEHICLE STATION
MACH NO=1.46 ALPHA=10
WINDWARD
LEEWARD
1.
0
-1.
LOCAL CP
1.4
1.2
1.0
0.8
0.6
0.4
0.2
0
X/D - CALIBERS FORWARD OF VEHICLE BASE

Figure F.2-8

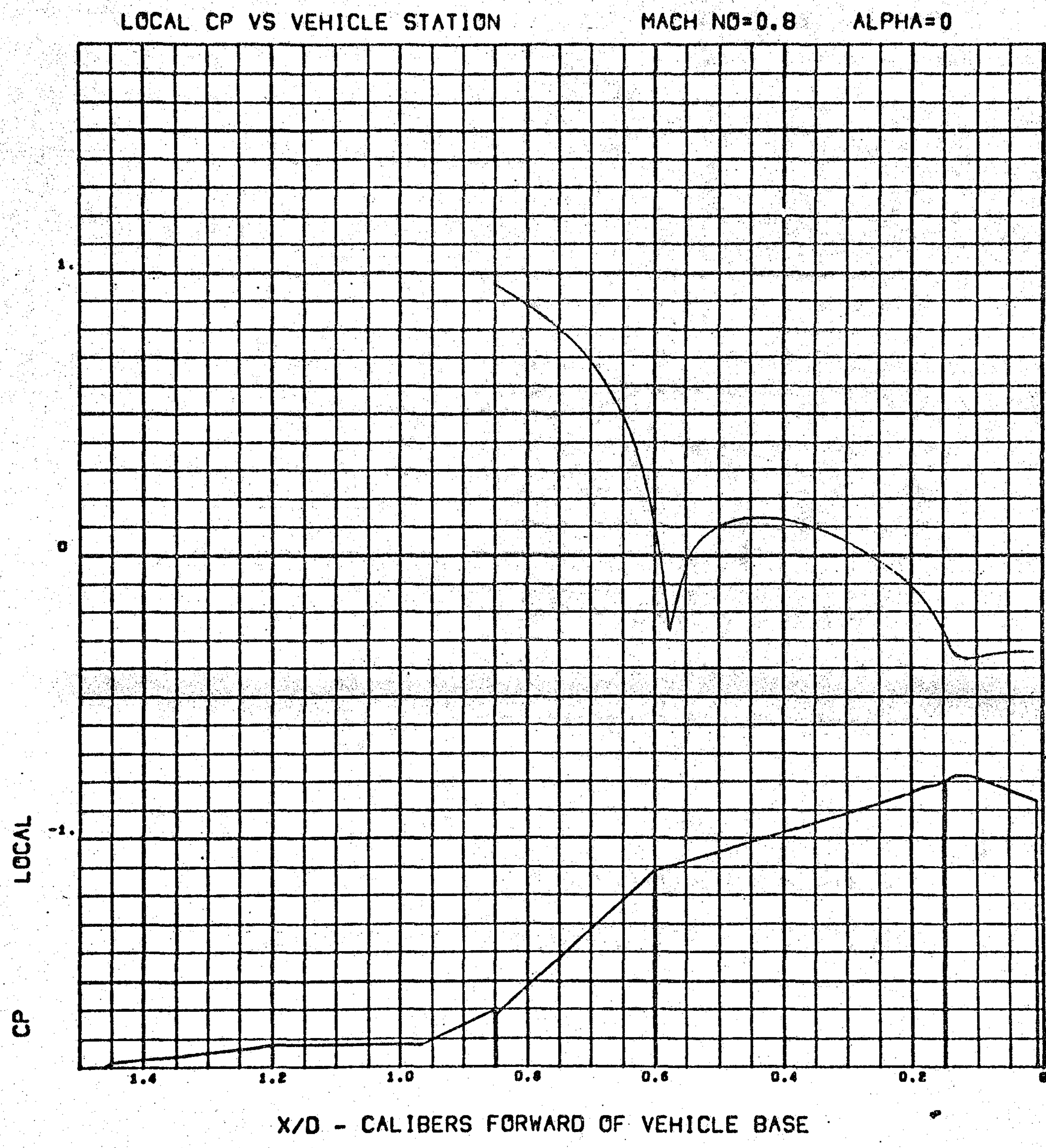
LOCAL CP VS VEHICLE STATION
MACH NO=0.8
ALPHA=0
1.
0
-1.
CP LOCAL
1.4
1.2
1.0
0.8
0.6
0.4
0.2
0
X/D - CALIBERS FORWARD OF VEHICLE BASE

Figure F.2-9

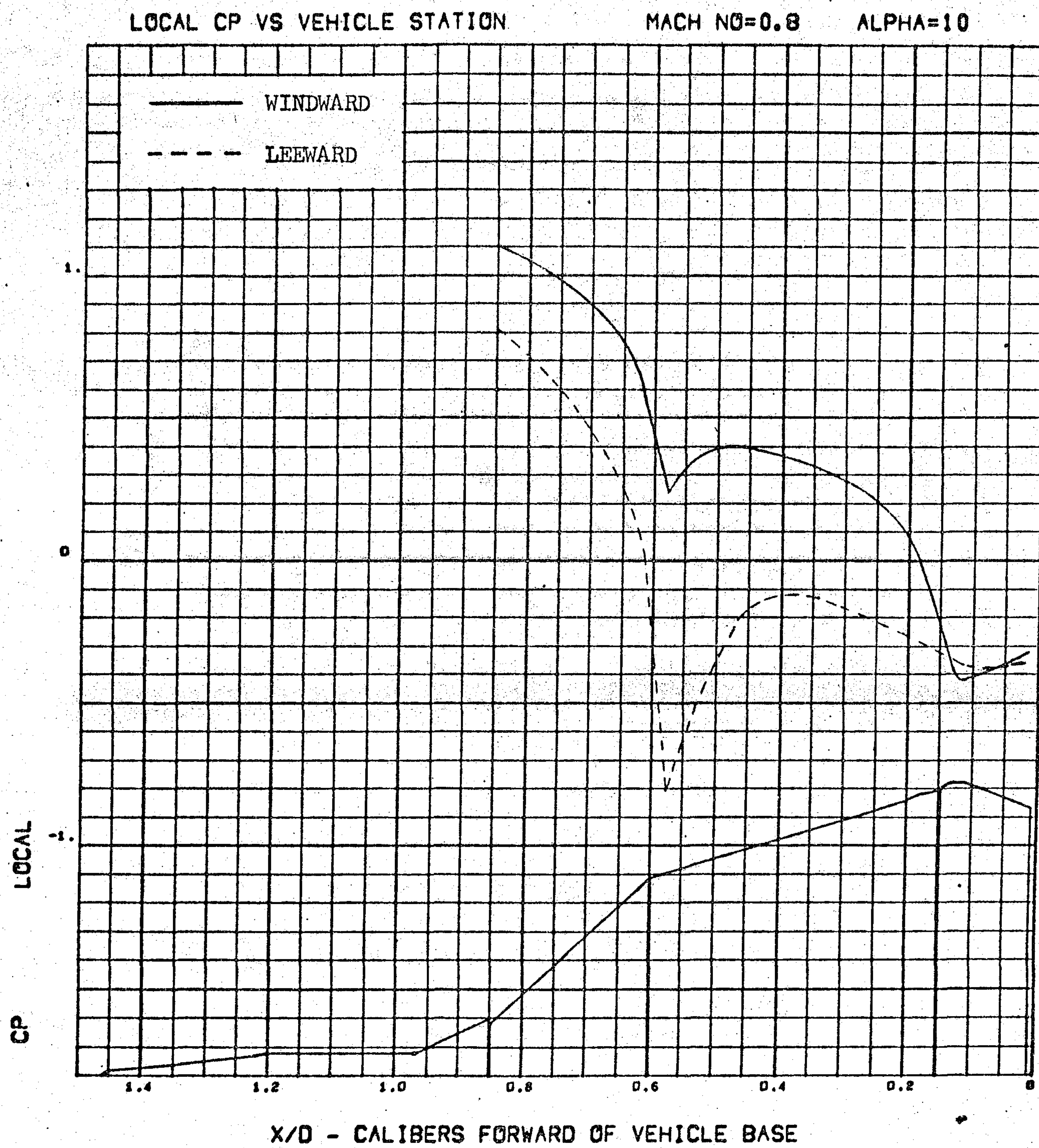

LOCAL CP VS VEHICLE STATION
MACH NO=0.8
ALPHA=10
WINDWARD
LEEWARD
1.
0
-1.
LOCAL
CP
1.4
1.2
1.0
0.8
0.6
0.4
0.2
0
X/D - CALIBERS FORWARD OF VEHICLE BASE

Figure F.2-10

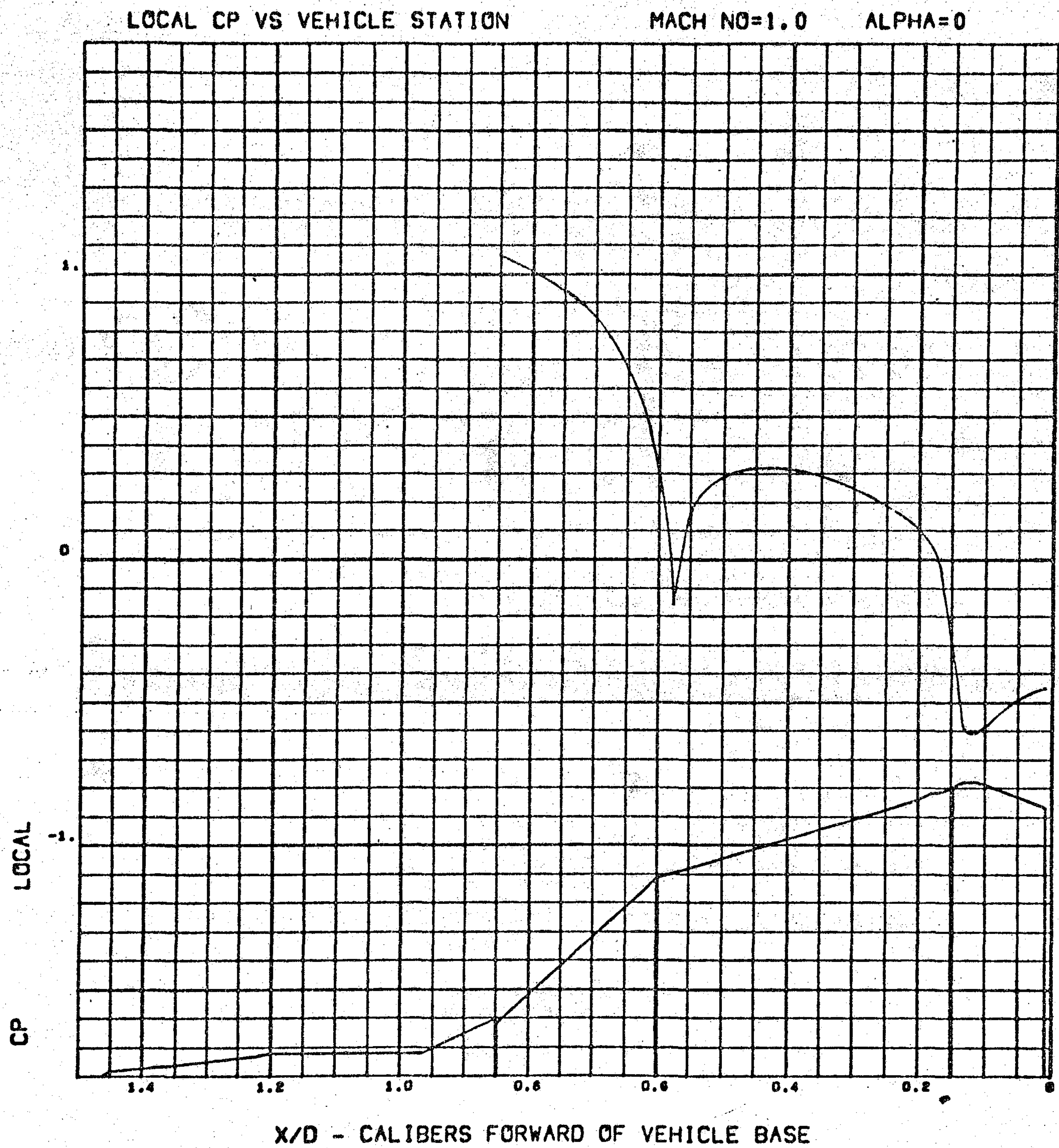

LOCAL CP VS VEHICLE STATION
MACH NO=1.0
ALPHA=0
1.
0
-1.
CP LOCAL
1.4
1.2
1.0
0.8
0.6
0.4
0.2
0
X/D - CALIBERS FORWARD OF VEHICLE BASE

Figure F.2-11

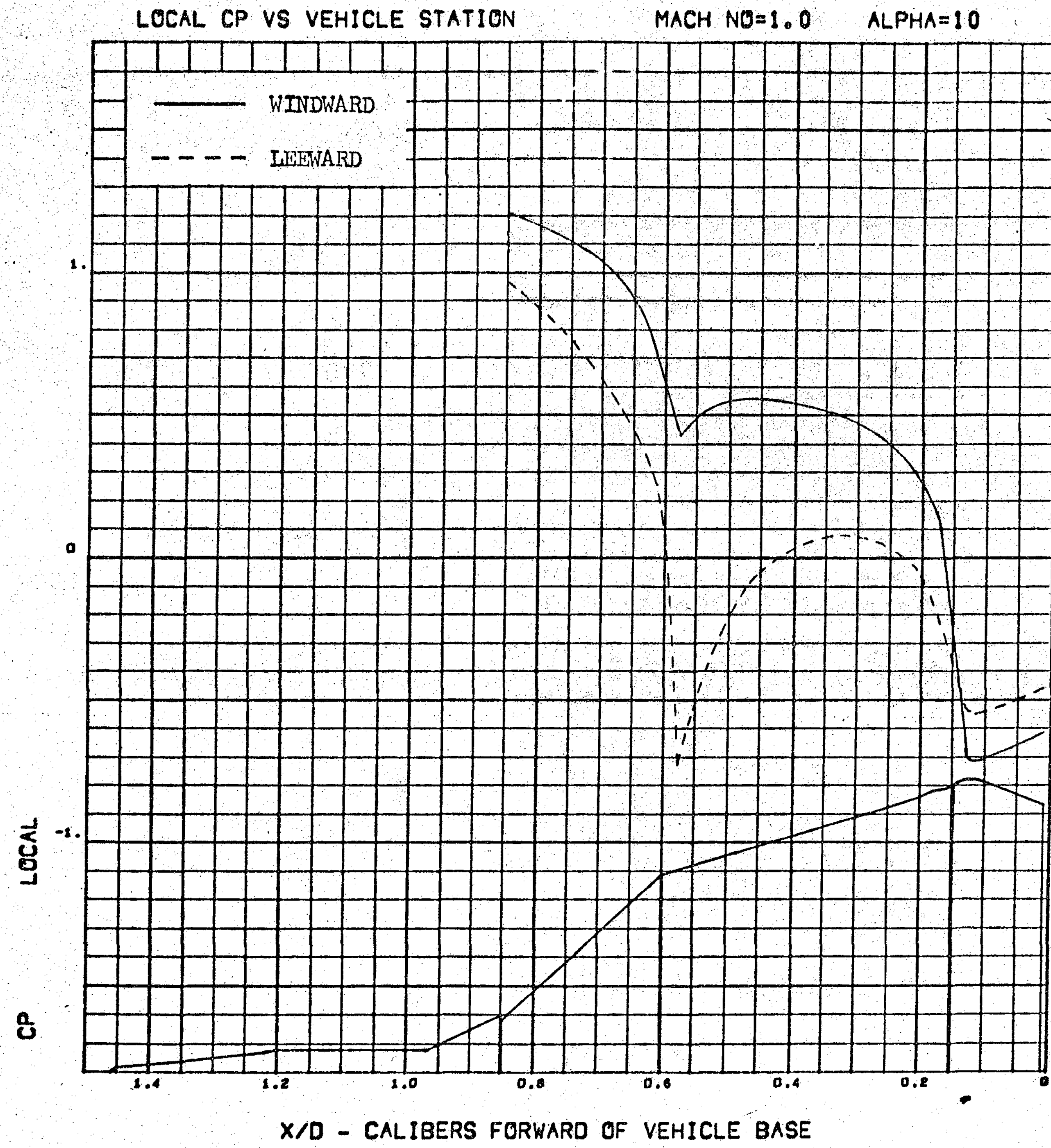

LOCAL CP VS VEHICLE STATION
MACH NO=1.0
ALPHA=10
WINDWARD
LEEWARD
1.
0
-1.
LOCAL CP
1.4
1.2
1.0
0.8
0.6
0.4
0.2
0
X/D - CALIBERS FORWARD OF VEHICLE BASE

Figure F.2-12

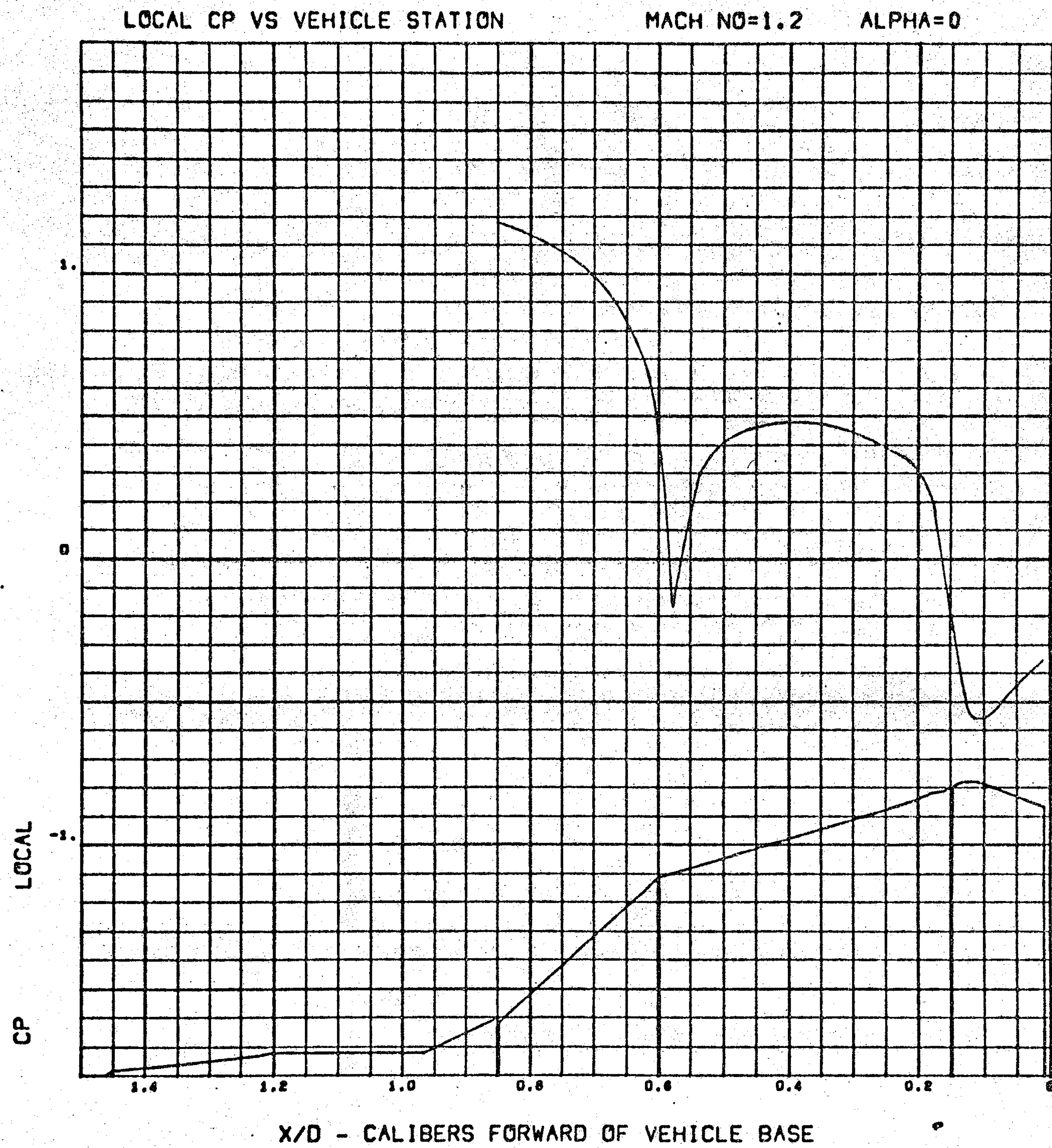
LOCAL CP VS VEHICLE STATION
MACH NO=1.2
ALPHA=0
1.
0
-1.
LOCAL
CP
1.4
1.2
1.0
0.8
0.6
0.4
0.2
0
X/D - CALIBERS FORWARD OF VEHICLE BASE

Figure F.2-13

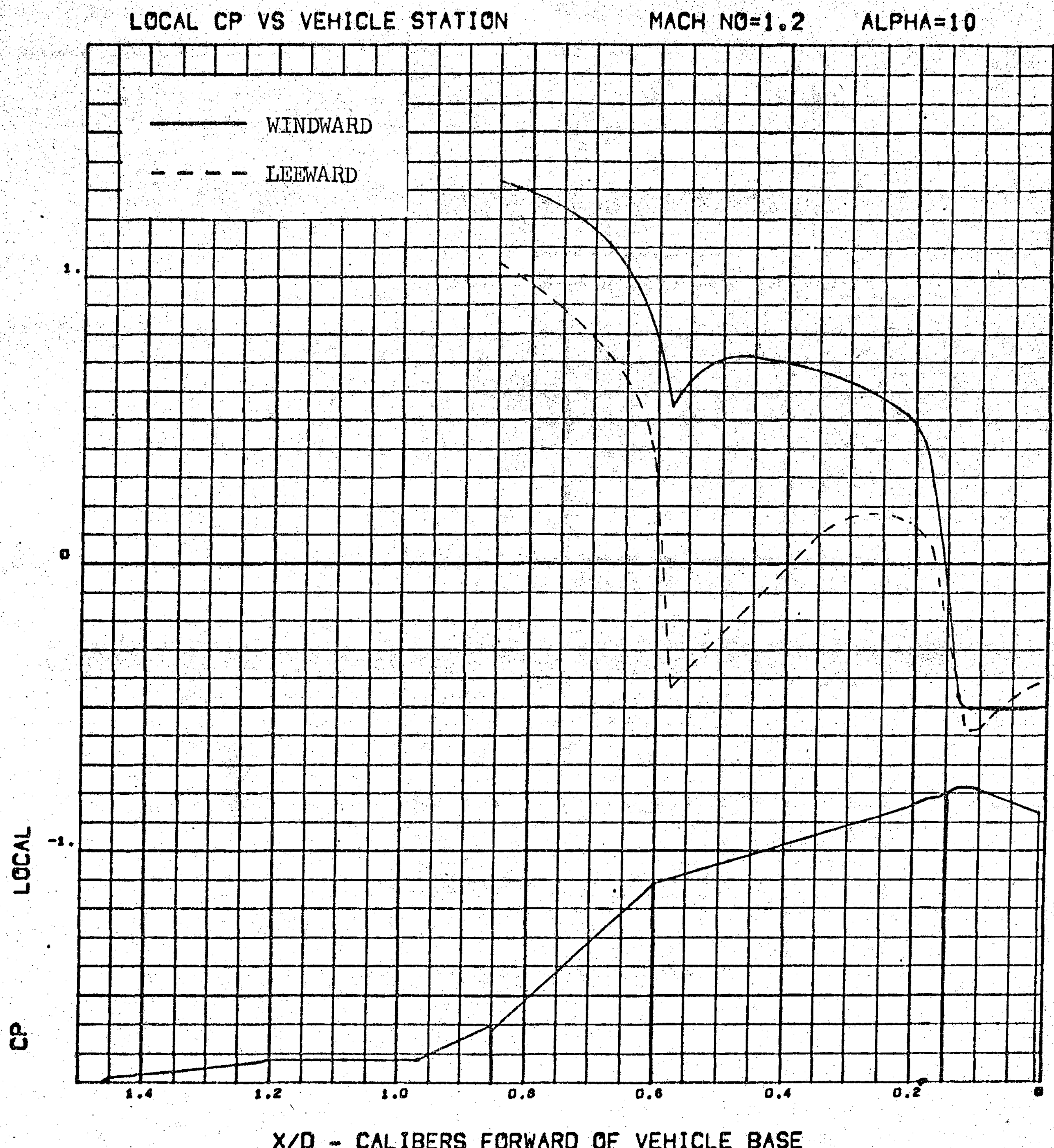

LOCAL CP VS VEHICLE STATION
MACH NO=1.2
ALPHA=10
WINDWARD
LEEWARD
1.
0
-1.
LOCAL
CP
1.4
1.2
1.0
0.8
0.6
0.4
0.2
0
X/D - CALIBERS FORWARD OF VEHICLE BASE

Figure F.2-14

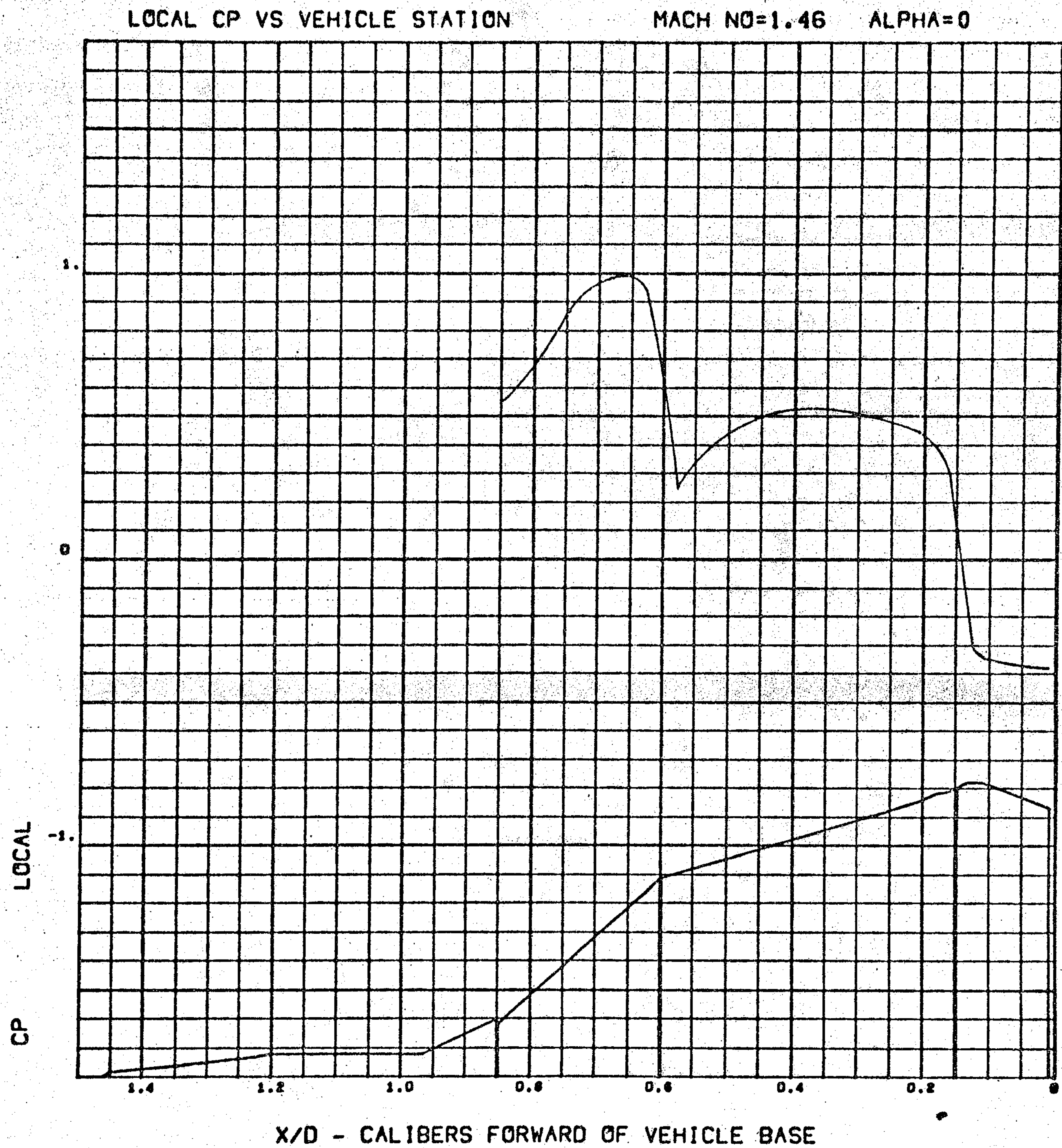
LOCAL CP VS VEHICLE STATION
MACH NO=1.46
ALPHA=0
1.
0
-1.
LOCAL
CP
1.4
1.2
1.0
0.8
0.6
0.4
0.2
0
X/D - CALIBERS FORWARD OF VEHICLE BASE

Figure F.2-15

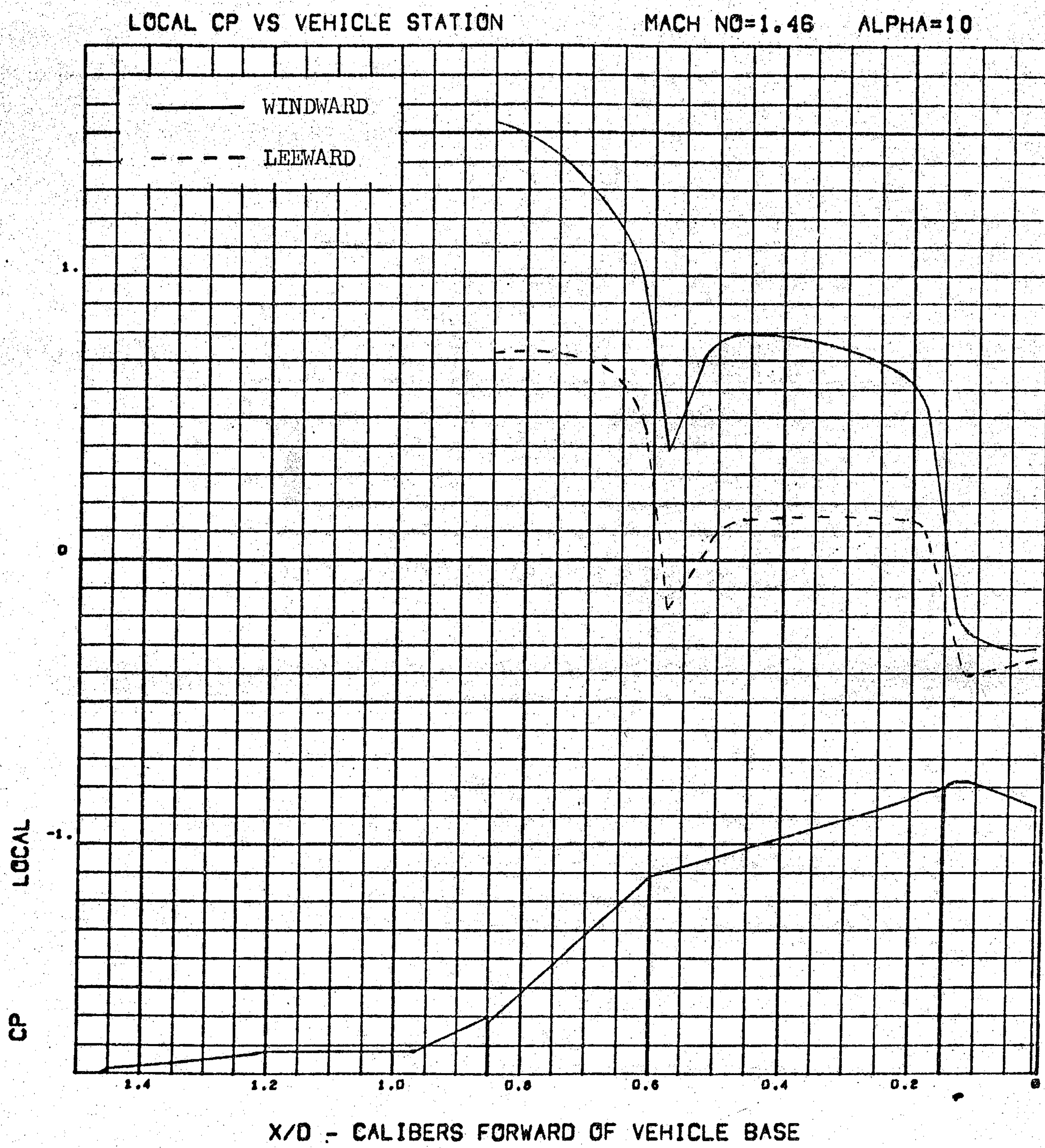
LOCAL CP VS VEHICLE STATION
MACH NO=1.46 ALPHA=10
WINDWARD
LEEWARD
1.
0
-1.
LOCAL CP
1.4
1.2
1.0
0.8
0.6
0.4
0.2
0
X/D - CALIBERS FORWARD OF VEHICLE BASE

Figure F.2-16

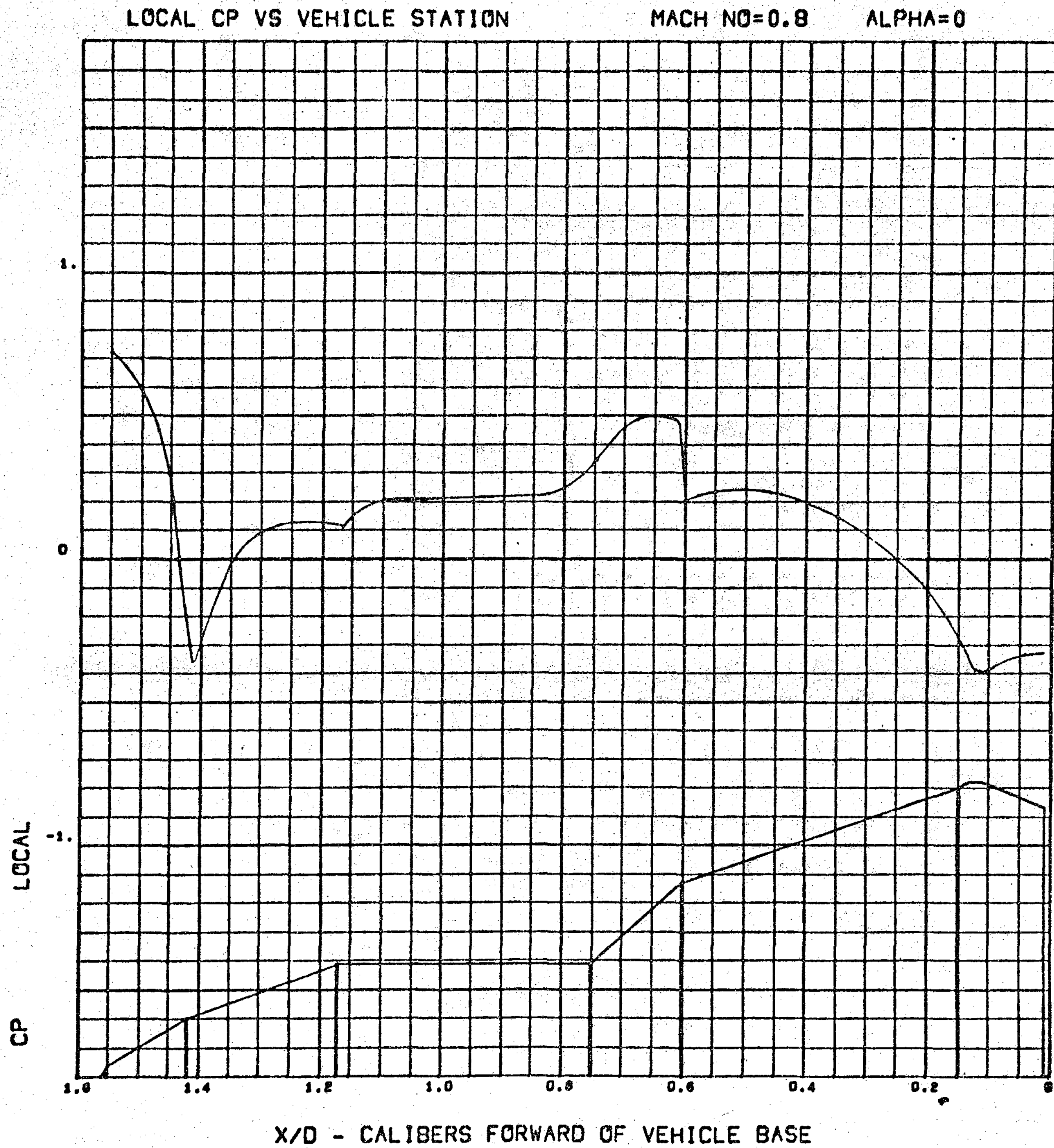
LOCAL CP VS VEHICLE STATION
MACH NO=0.8
ALPHA=0
1.
0
-1.
CP LOCAL
1.6
1.4
1.2
1.0
0.8
0.6
0.4
0.2
0
X/D - CALIBERS FORWARD OF VEHICLE BASE

Figure F.2-17

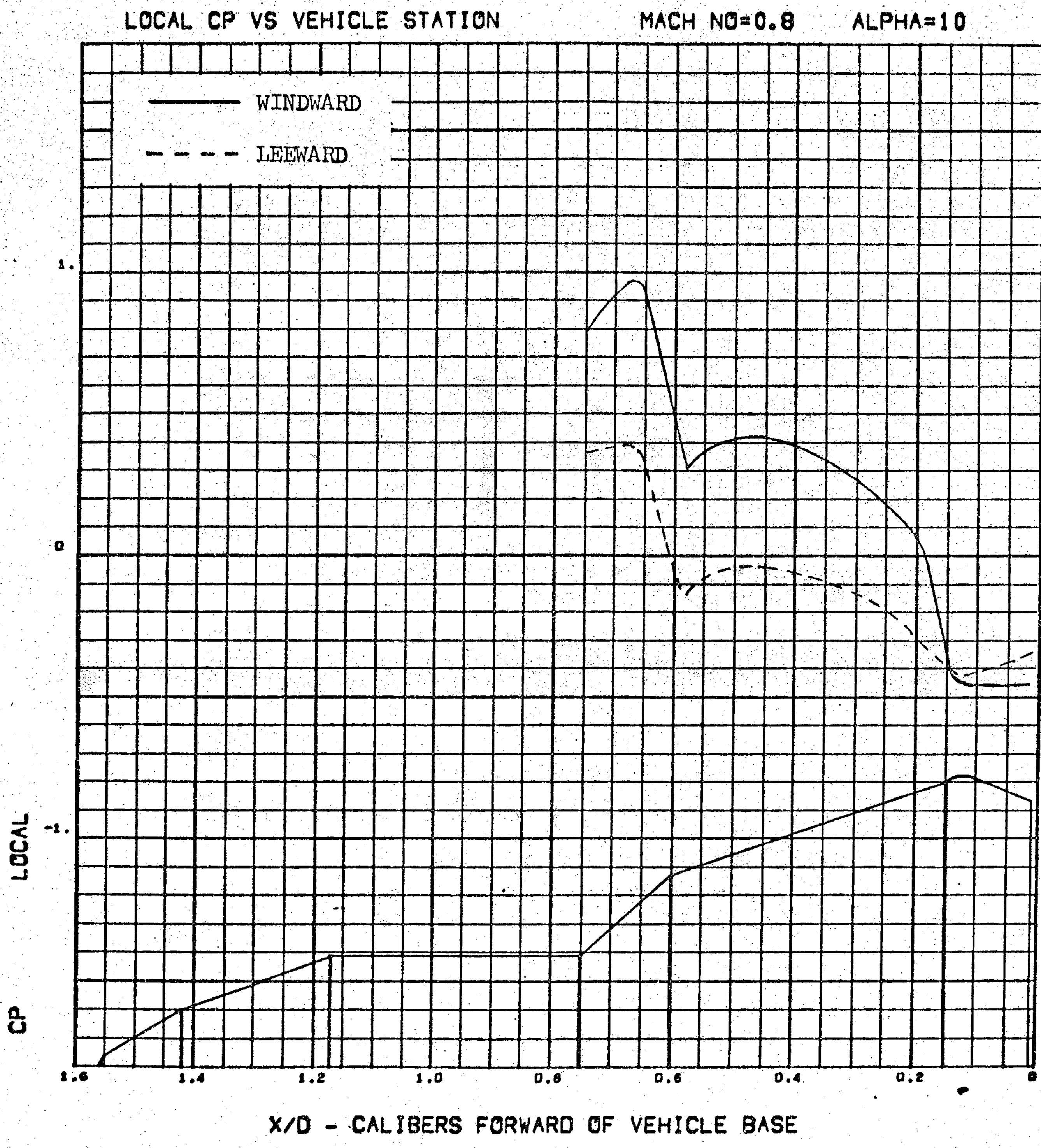

LOCAL CP VS VEHICLE STATION
MACH NO=0.8
ALPHA=10
WINDWARD
LEEWARD
1.
0
-1.
LOCAL
CP
1.6
1.4
1.2
1.0
0.8
0.6
0.4
0.2
0
X/D - CALIBERS FORWARD OF VEHICLE BASE

Figure F.2-18

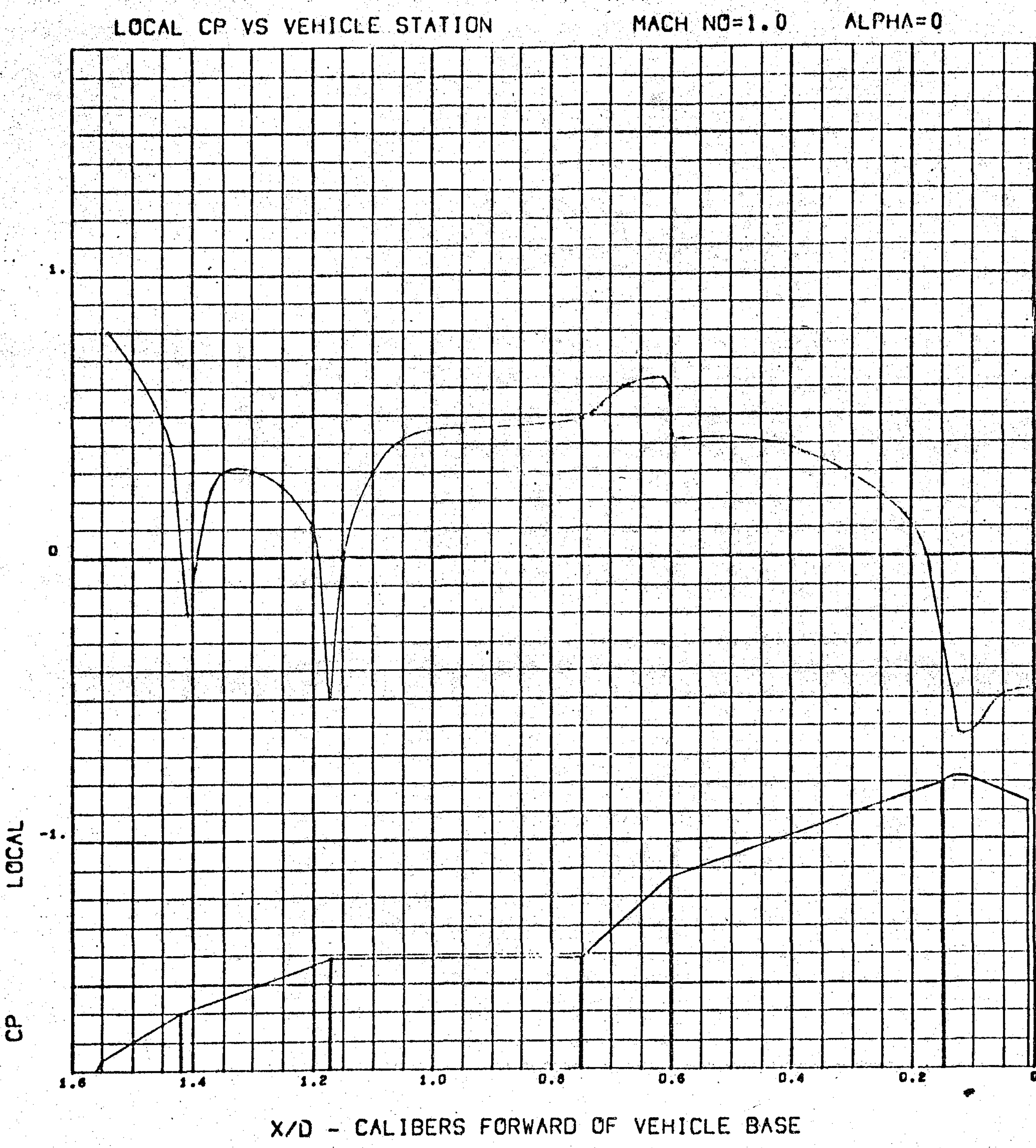

LOCAL CP VS VEHICLE STATION
MACH NO=1.0
ALPHA=0
1.
0
-1.
LOCAL CP
1.6
1.4
1.2
1.0
0.8
0.6
0.4
0.2
0
X/D - CALIBERS FORWARD OF VEHICLE BASE

Figure F.2-19

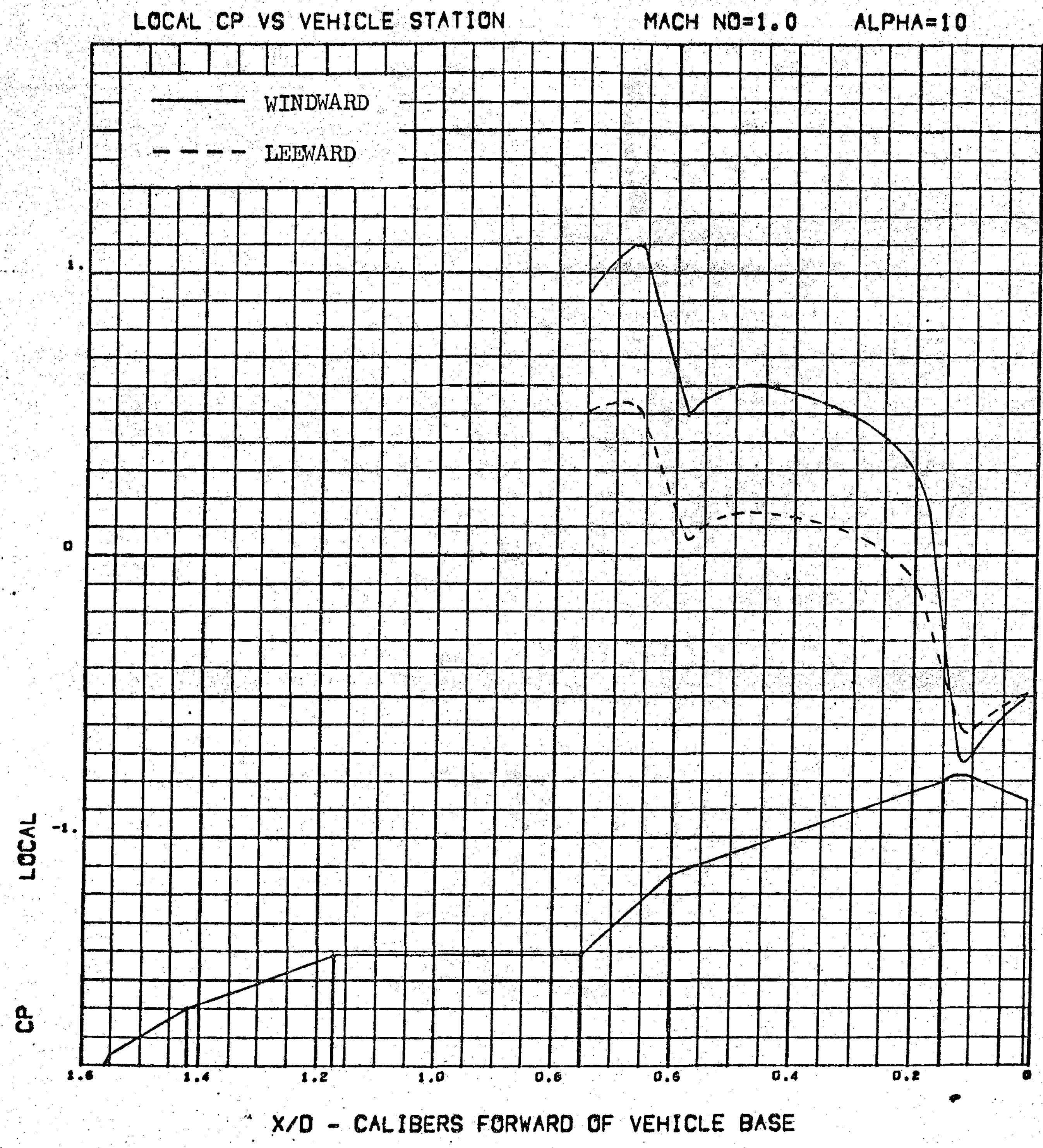

LOCAL CP VS VEHICLE STATION
MACH NO=1.0
ALPHA=10
WINDWARD
LEEWARD
1.
0
-1.
CP LOCAL
1.6
1.4
1.2
1.0
0.8
0.6
0.4
0.2
0
X/D - CALIBERS FORWARD OF VEHICLE BASE

Figure F.2-20

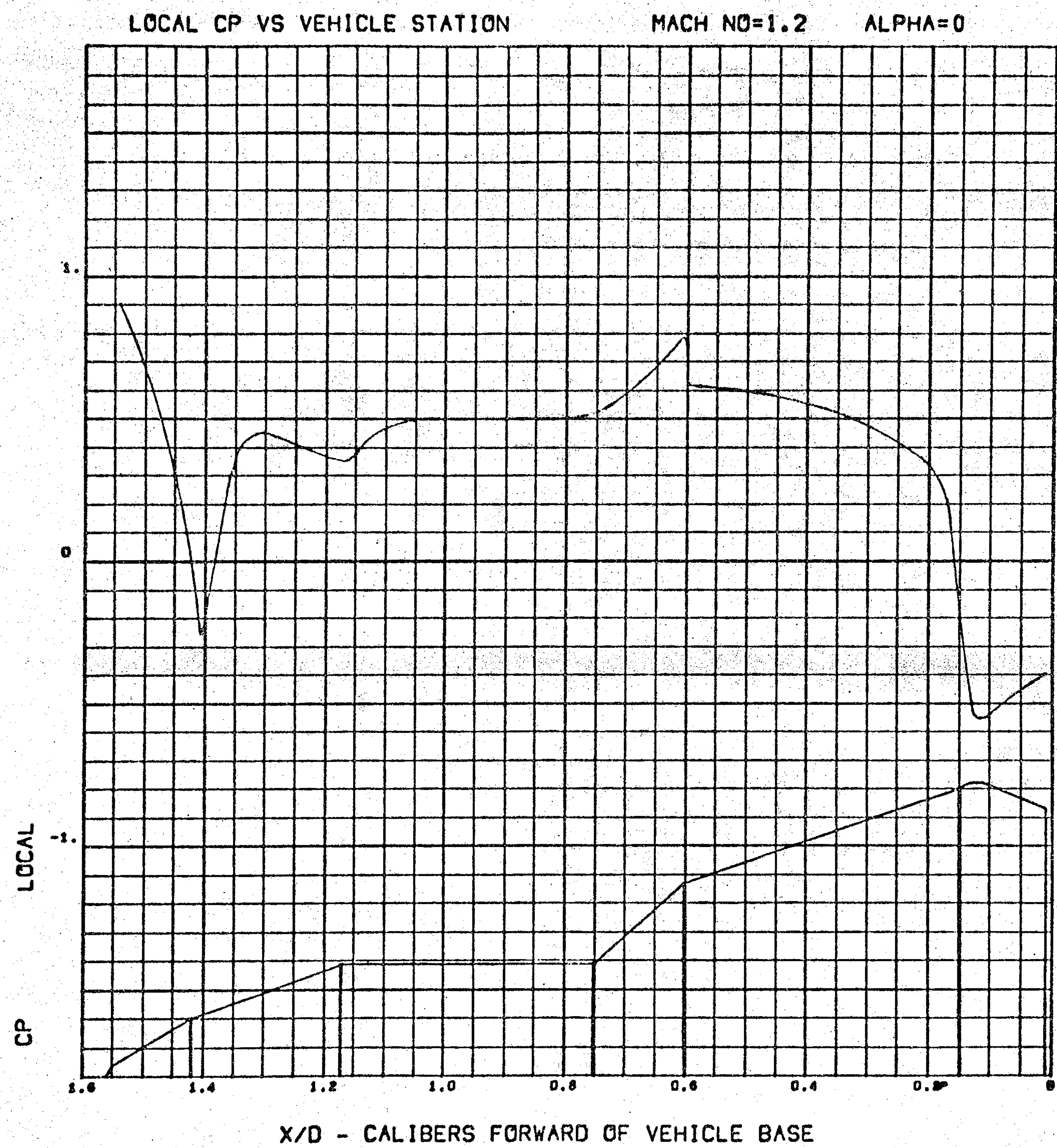

LOCAL CP VS VEHICLE STATION
MACH NO=1.2
ALPHA=0
1.
0
-1.
LOCAL CP
1.6
1.4
1.2
1.0
0.8
0.6
0.4
0.2
0
X/D - CALIBERS FORWARD OF VEHICLE BASE

Figure F.2-21

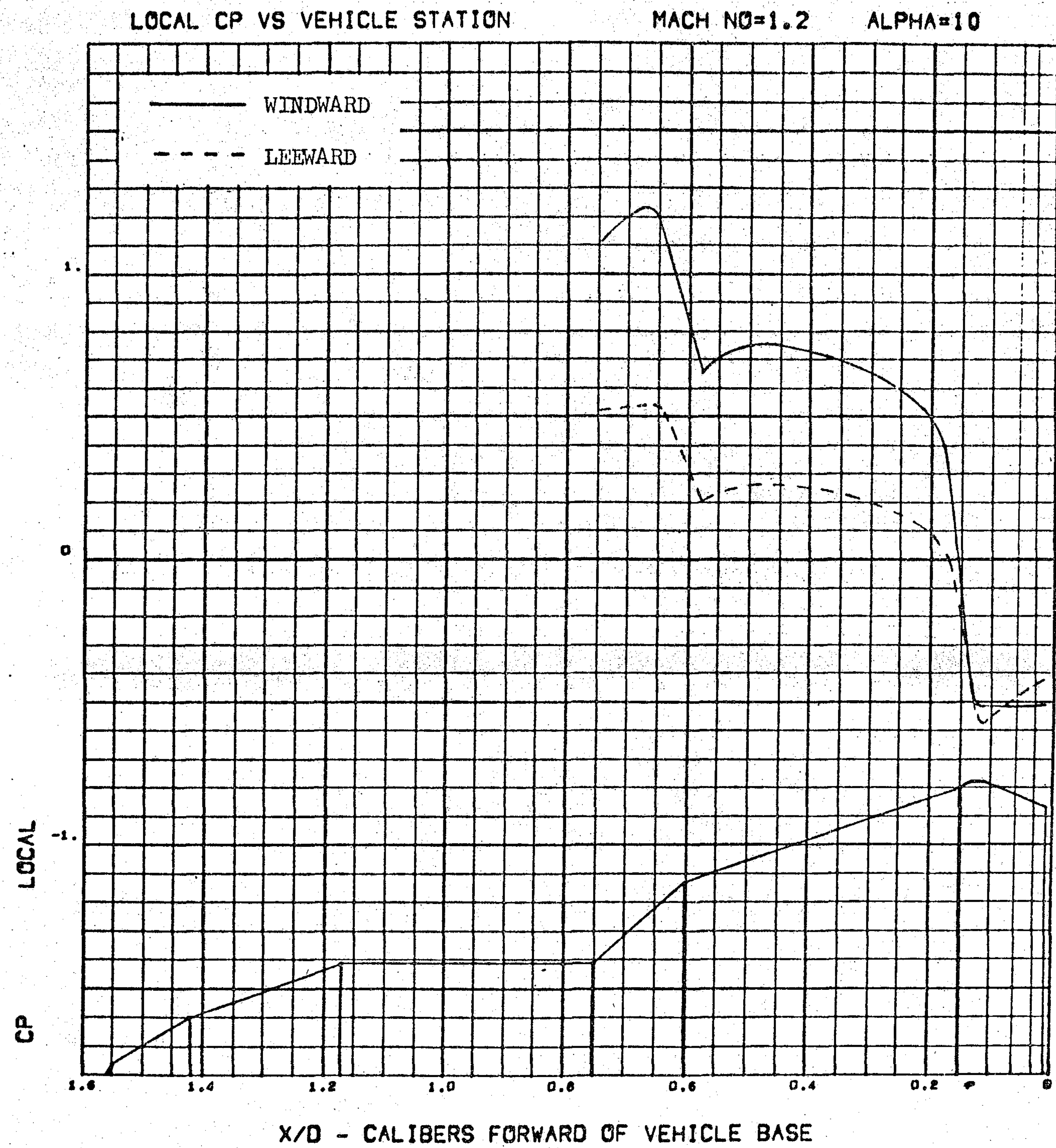
LOCAL CP VS VEHICLE STATION
MACH NO=1.2
ALPHA=10
WINDWARD
LEEWARD
1.
0
-1.
LOCAL CP
1.6
1.4
1.2
1.0
0.8
0.6
0.4
0.2
0
X/D - CALIBERS FORWARD OF VEHICLE BASE

Figure F.2-22

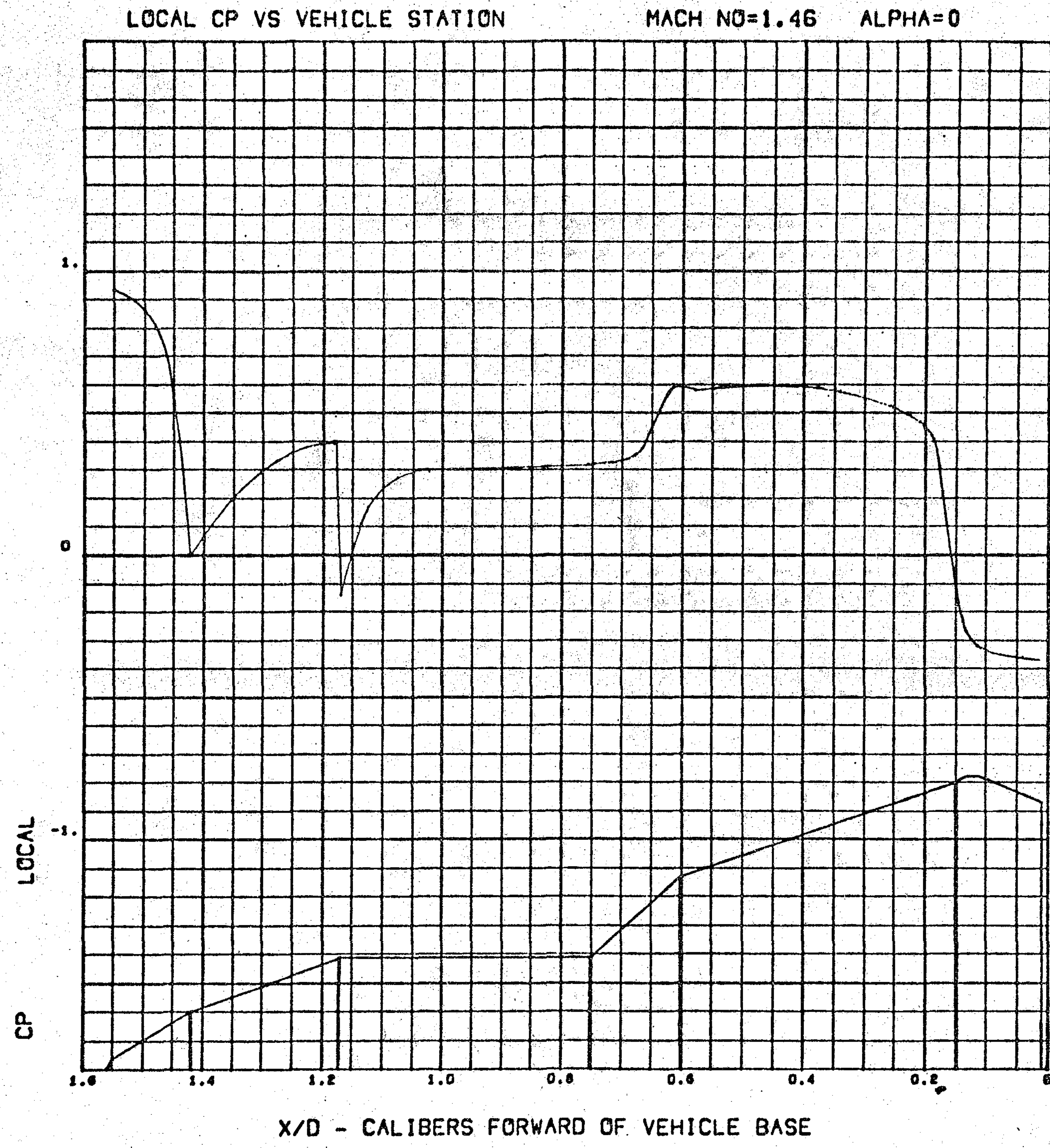
LOCAL CP VS VEHICLE STATION
MACH NO=1.46
ALPHA=0
1.
0
-1.
CP LOCAL
1.6
1.4
1.2
1.0
0.8
0.6
0.4
0.2
0
X/D - CALIBERS FORWARD OF VEHICLE BASE

Figure F.2-23

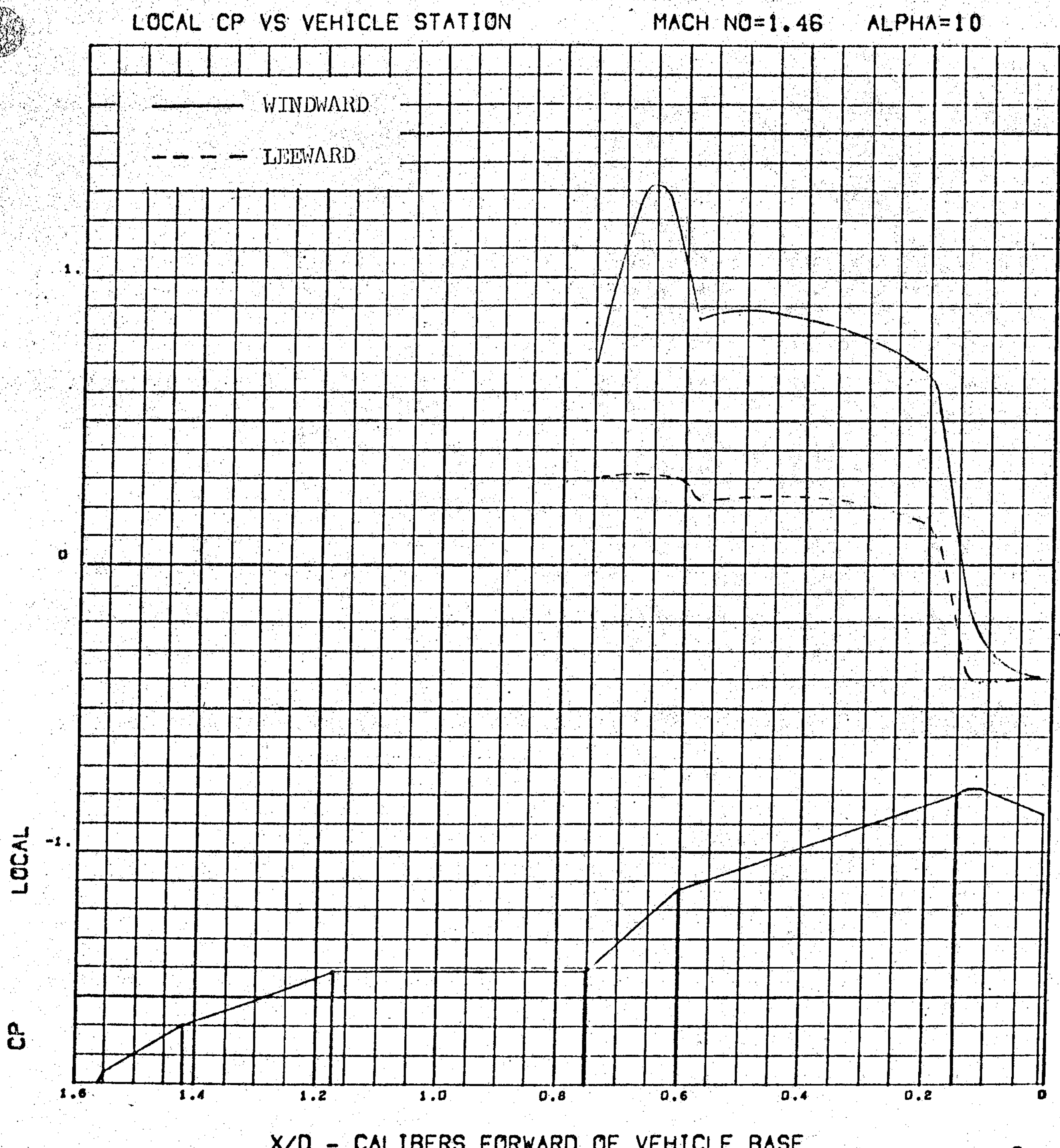
LOCAL CP VS VEHICLE STATION
MACH NO=1.46
ALPHA=10
WINDWARD
LEEWARD
1.
0
-1.
CP LOCAL
1.6
1.4
1.2
1.0
0.8
0.6
0.4
0.2
0
X/D - CALIBERS FORWARD OF VEHICLE BASE

Figure F.2-24

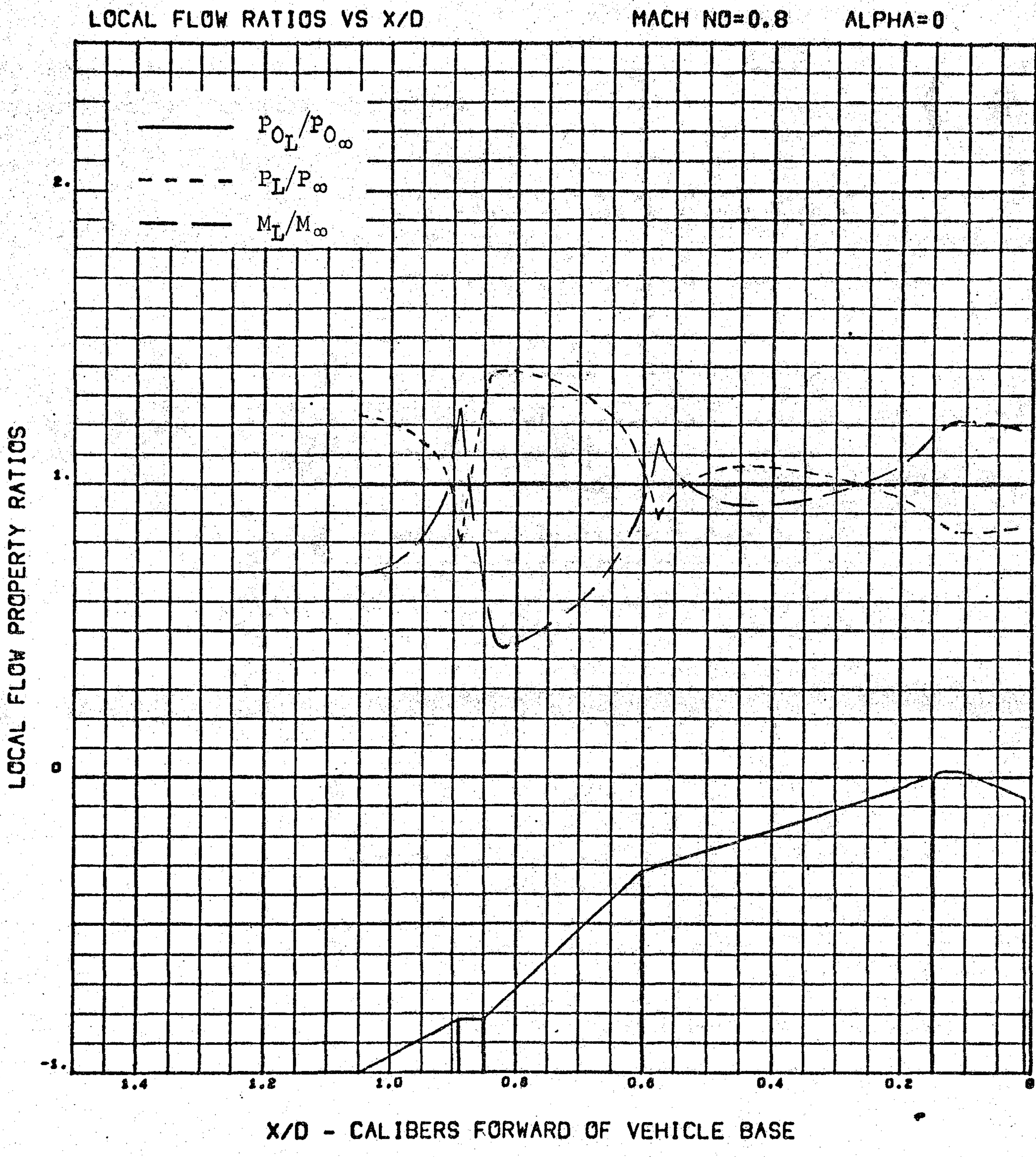

LOCAL FLOW RATIOS VS X/D
MACH NO=0.8
ALPHA=0
P_{O_L}/P_{O_∞}
P_L/P_∞
M_L/M_∞
LOCAL FLOW PROPERTY RATIOS
X/D - CALIBERS FORWARD OF VEHICLE BASE

Figure F.3-1

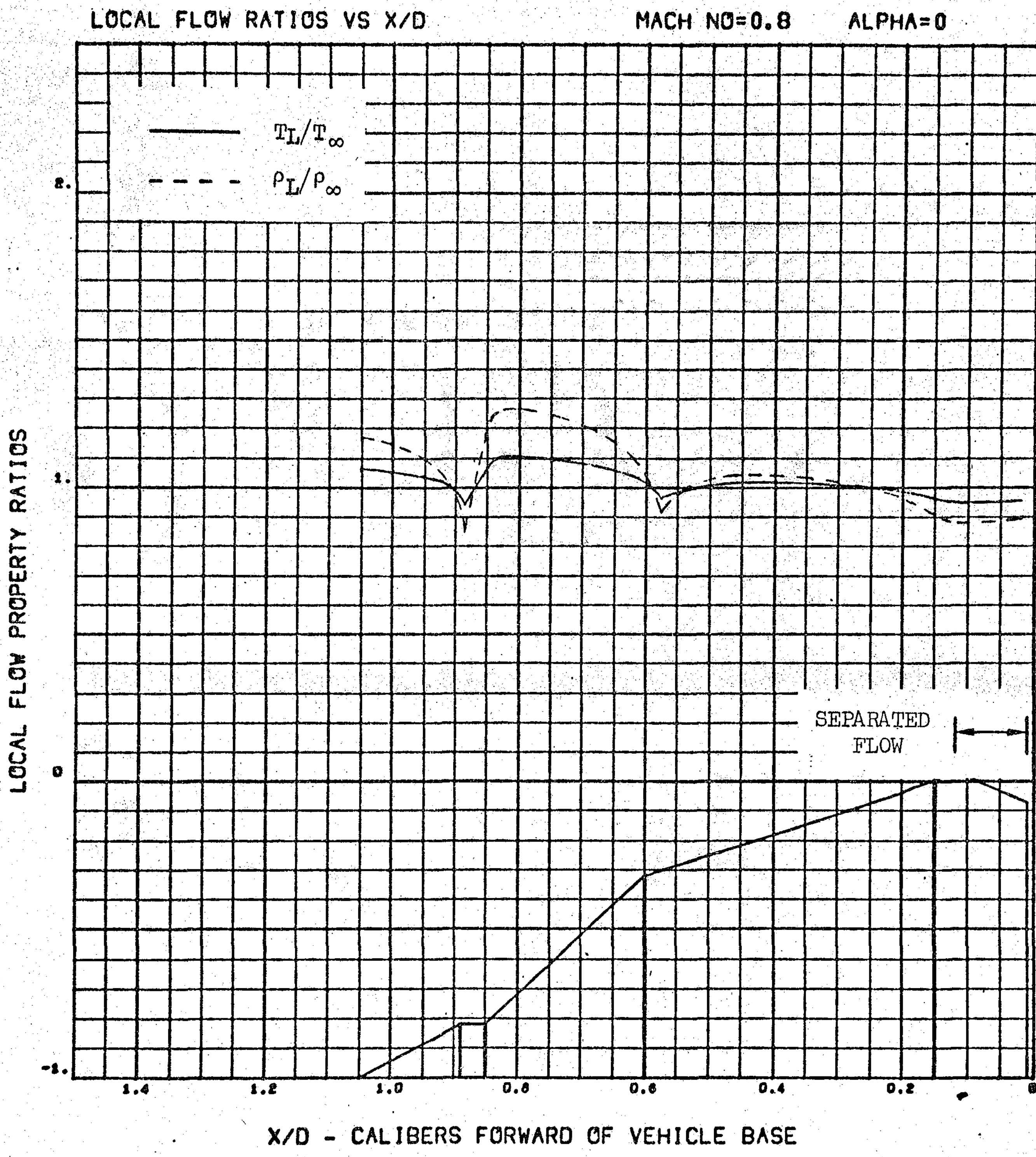
LOCAL FLOW RATIOS VS X/D
MACH NO=0.8
ALPHA=0
T_L/T_∞
ρ_L/ρ_∞
2.
1.
0
-1.
LOCAL FLOW PROPERTY RATIOS
SEPARATED FLOW
1.4
1.2
1.0
0.8
0.6
0.4
0.2
0
X/D - CALIBERS FORWARD OF VEHICLE BASE

Figure F.3-2

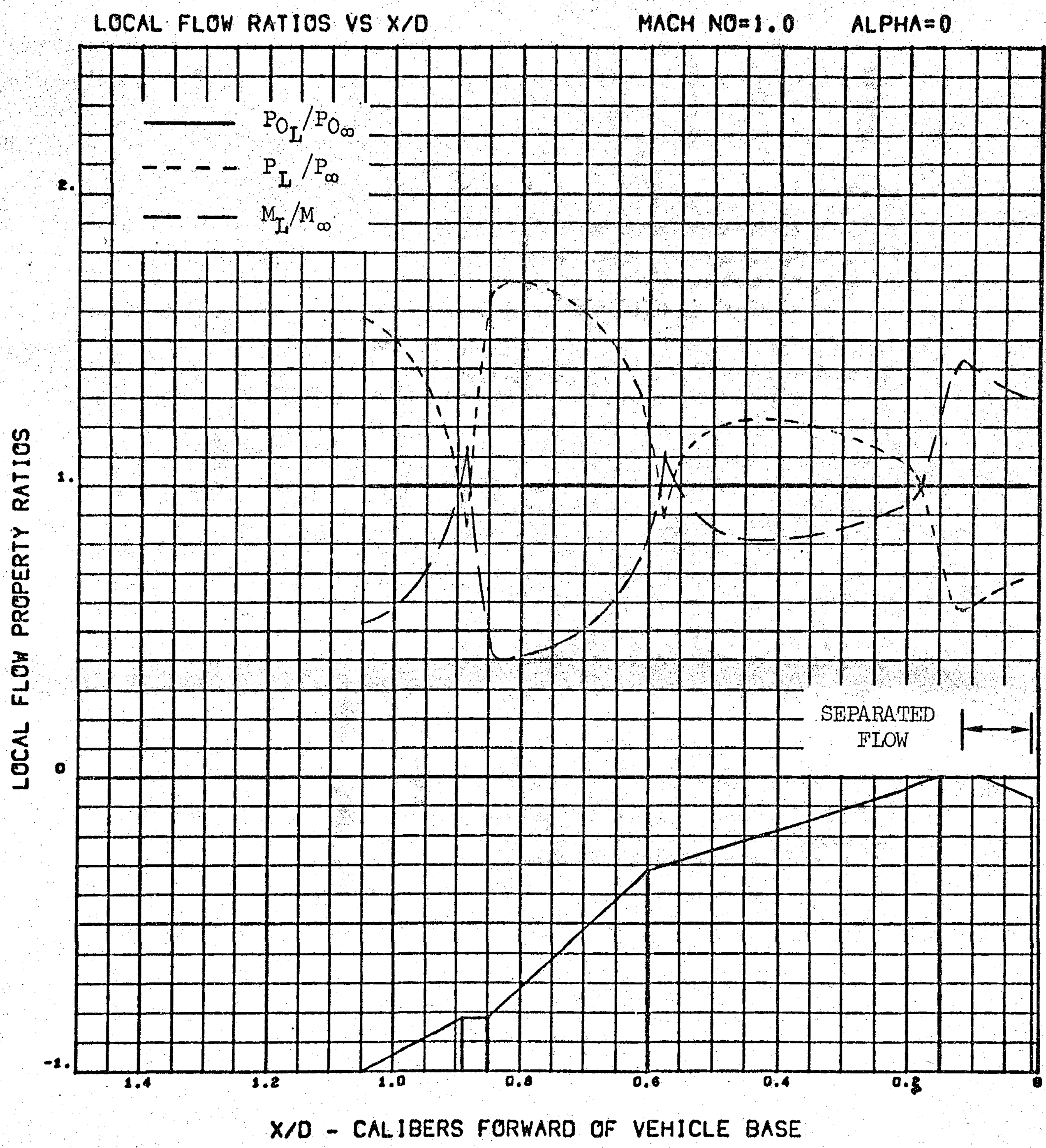
LOCAL FLOW RATIOS VS X/D
MACH NO=1.0
ALPHA=0
P_{O_L}/P_{O_∞}
P_L/P_∞
M_L/M_∞
SEPARATED FLOW
LOCAL FLOW PROPERTY RATIOS
2.
1.
0
-1.
1.4
1.2
1.0
0.8
0.6
0.4
0.2
0
X/D - CALIBERS FORWARD OF VEHICLE BASE

Figure F.3-3

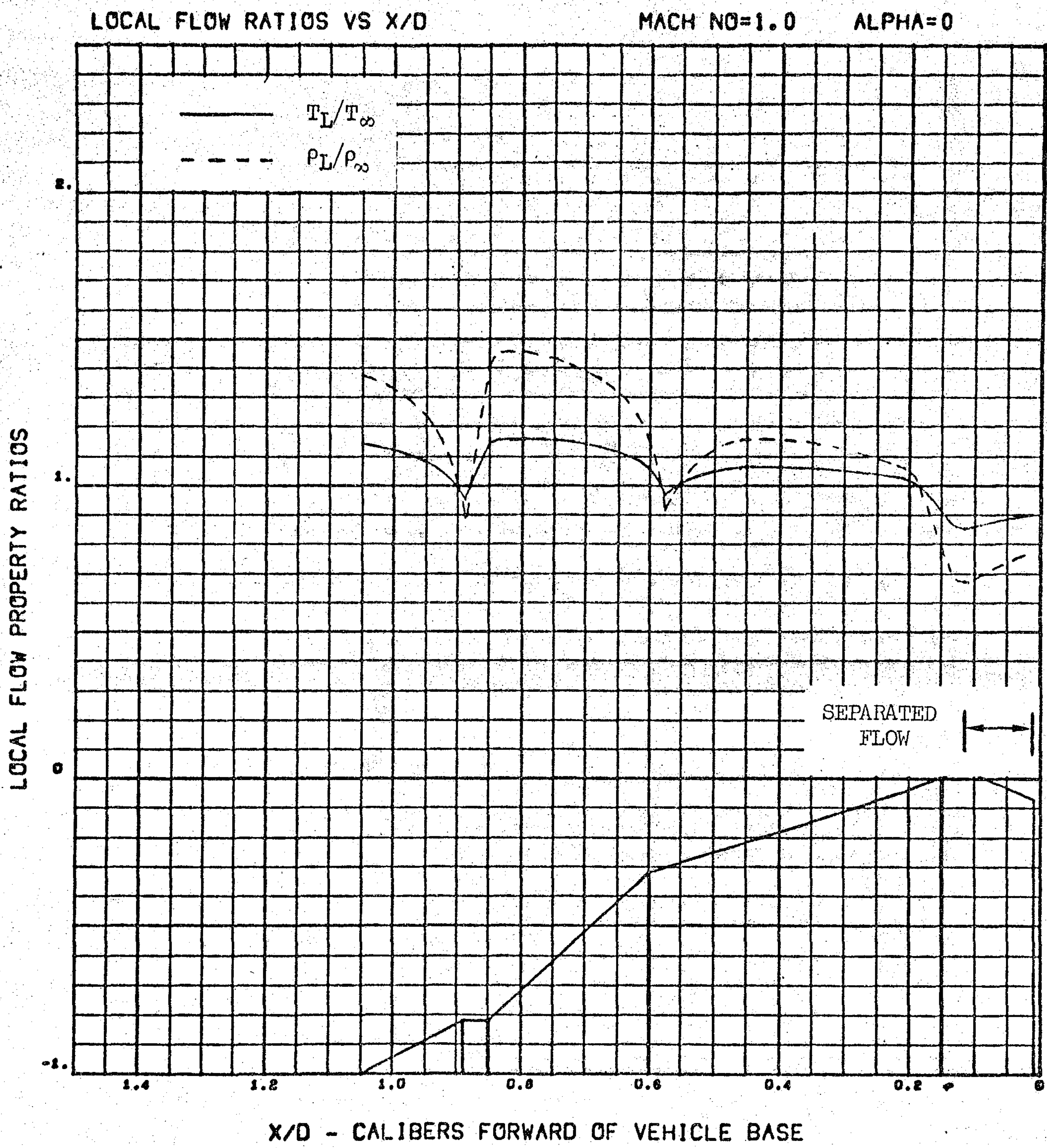
LOCAL FLOW RATIOS VS X/D
MACH NO=1.0
ALPHA=0
T_L/T_∞
ρ_L/ρ_∞
SEPARATED FLOW
LOCAL FLOW PROPERTY RATIOS
2.
1.
0
-1.
1.4
1.2
1.0
0.8
0.6
0.4
0.2
0
X/D - CALIBERS FORWARD OF VEHICLE BASE

Figure F.3-4

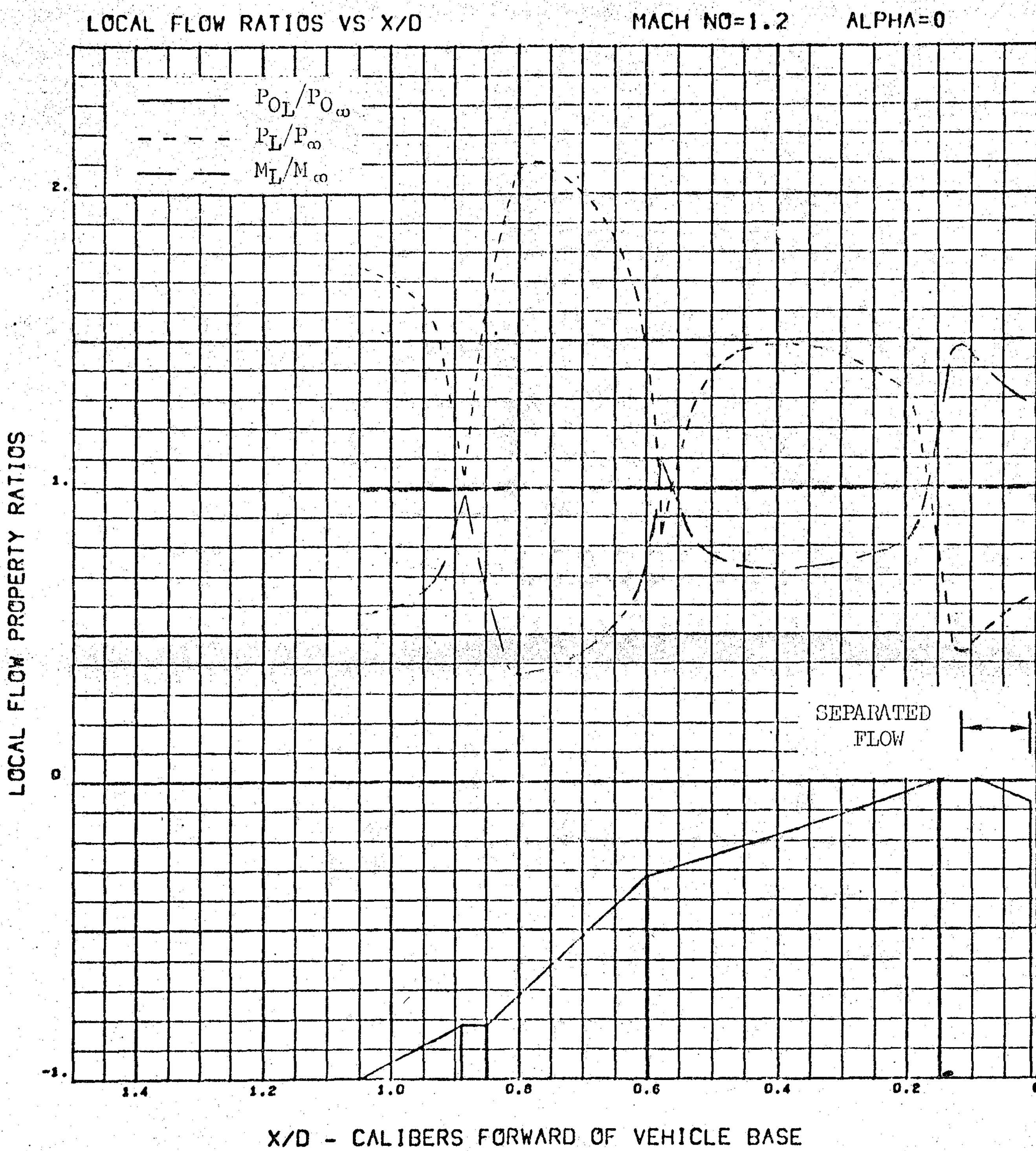
LOCAL FLOW RATIOS VS X/D
MACH NO=1.2
ALPHA=0
P_{O_L}/P_{O_∞}
P_L/P_∞
M_L/M_∞
SEPARATED FLOW
LOCAL FLOW PROPERTY RATIOS
2.
1.
0
-1.
1.4
1.2
1.0
0.8
0.6
0.4
0.2
0
X/D - CALIBERS FORWARD OF VEHICLE BASE

Figure F.3-5

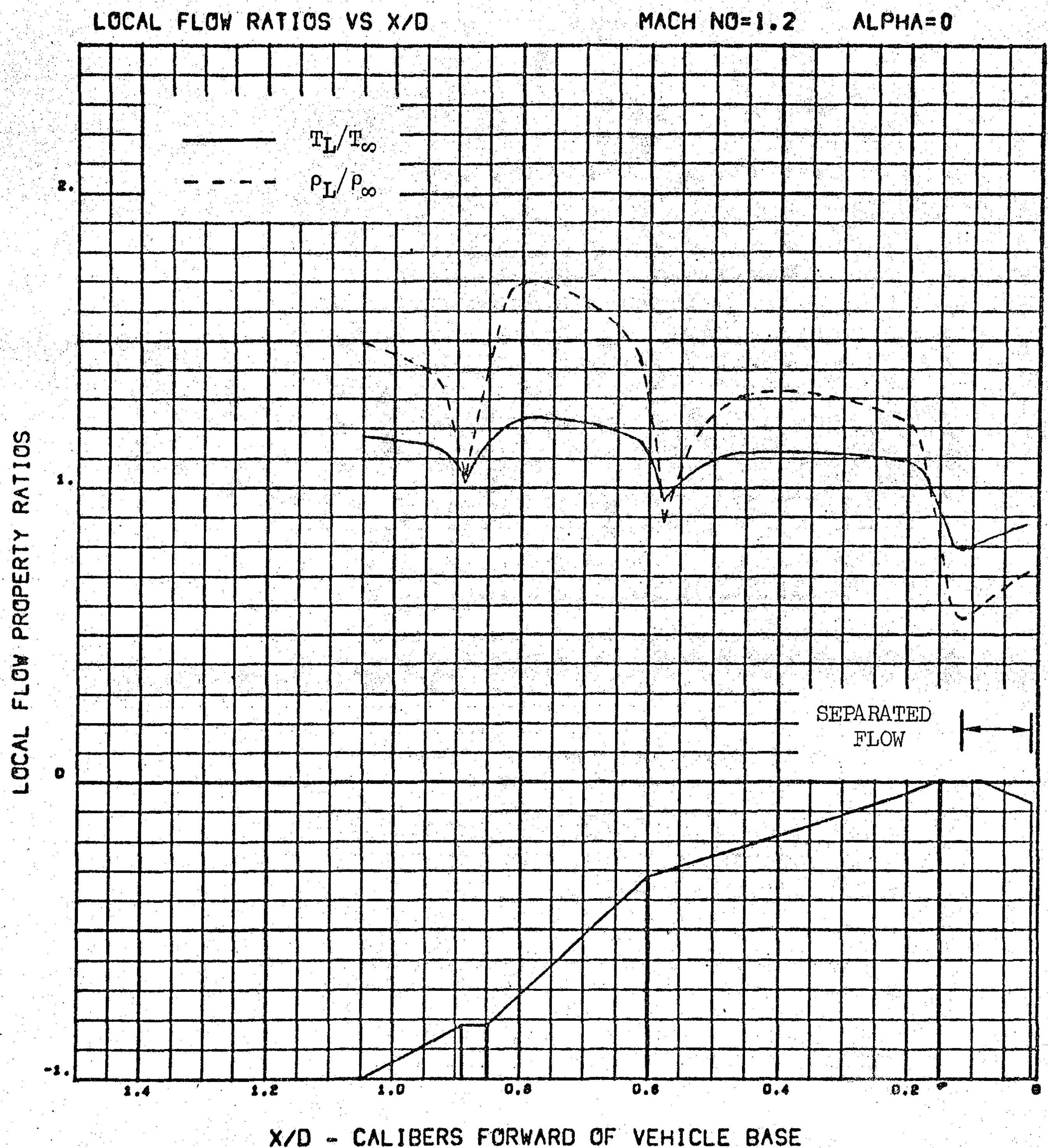
LOCAL FLOW RATIOS VS X/D
MACH NO=1.2
ALPHA=0
T_L/T_∞
ρ_L/ρ_∞
SEPARATED FLOW
LOCAL FLOW PROPERTY RATIOS
2.
1.
0
-1.
1.4
1.2
1.0
0.8
0.6
0.4
0.2
0
X/D - CALIBERS FORWARD OF VEHICLE BASE

Figure F.3-6

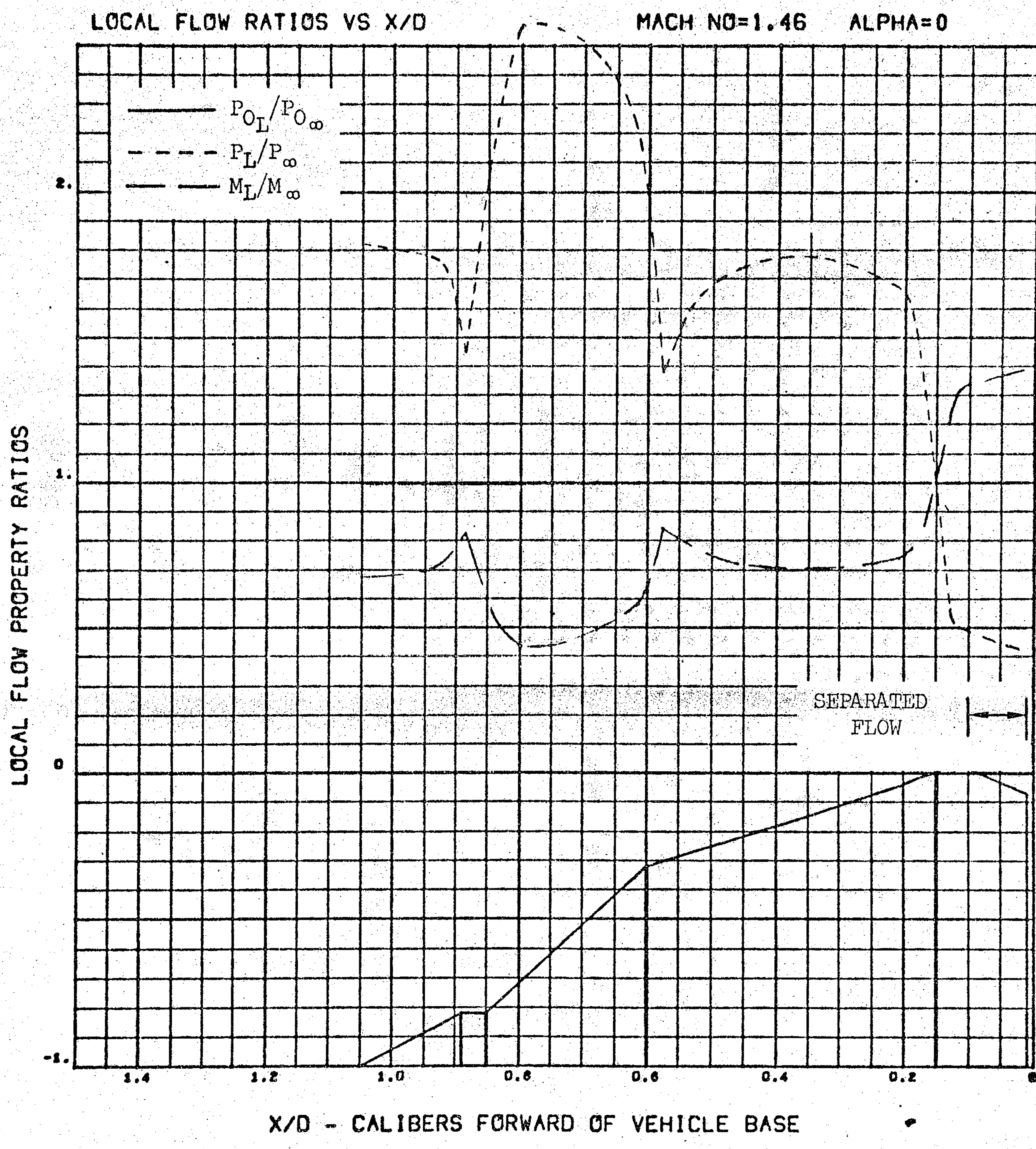

LOCAL FLOW RATIOS VS X/D
MACH NO=1.46 ALPHA=0
P_{O_L}/P_{O_∞}
P_L/P_∞
M_L/M_∞
SEPARATED FLOW
2.
1.
0
-1.
1.4
1.2
1.0
0.8
0.6
0.4
0.2
0
LOCAL FLOW PROPERTY RATIOS
X/D - CALIBERS FORWARD OF VEHICLE BASE

Figure F.3-7

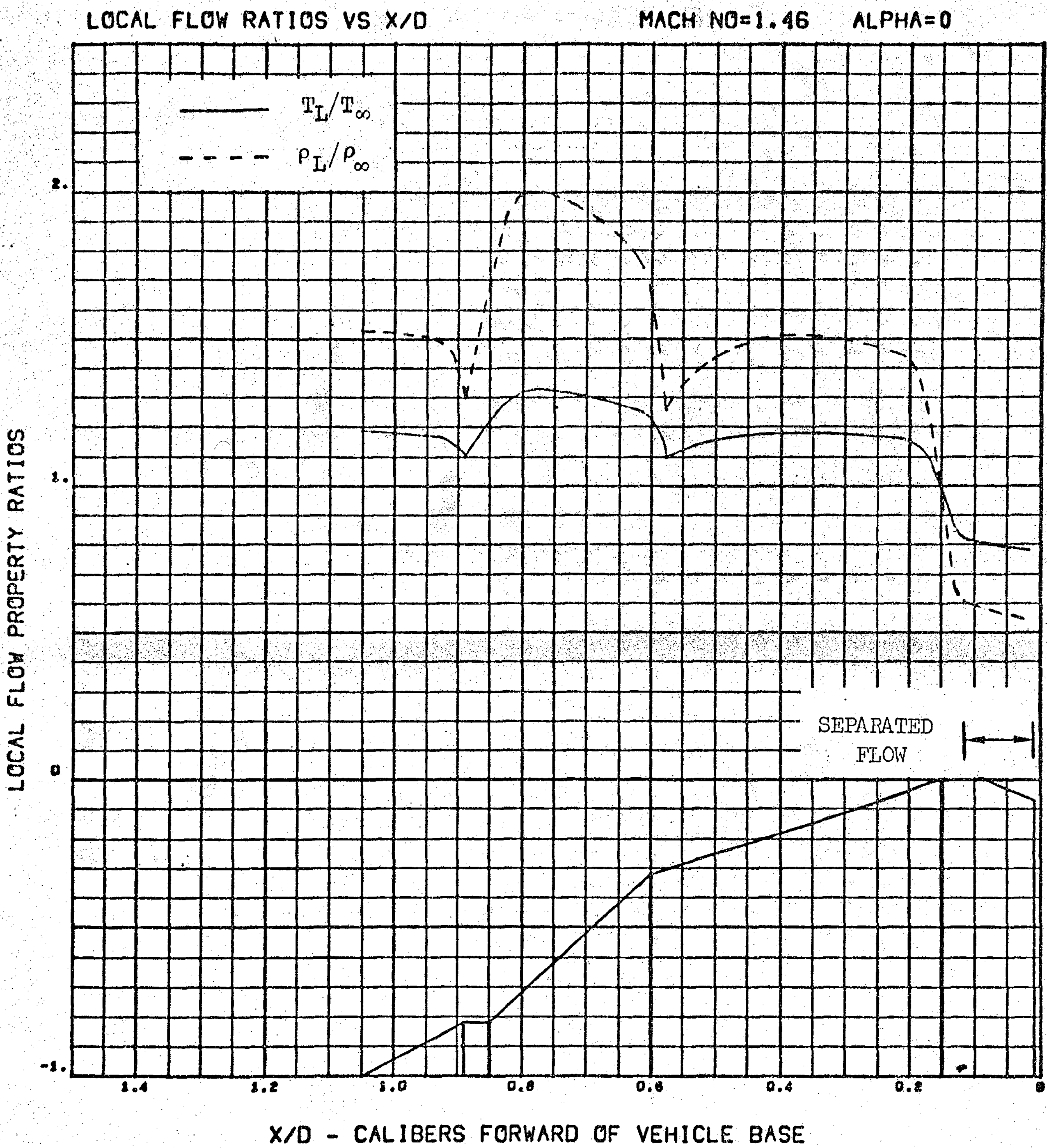
LOCAL FLOW RATIOS VS X/D
MACH NO=1.46 ALPHA=0
T_L/T_∞
ρ_L/ρ_∞
SEPARATED FLOW
LOCAL FLOW PROPERTY RATIOS
2.
1.
0
-1.
1.4
1.2
1.0
0.8
0.6
0.4
0.2
0
X/D - CALIBERS FORWARD OF VEHICLE BASE

Figure F.3-8

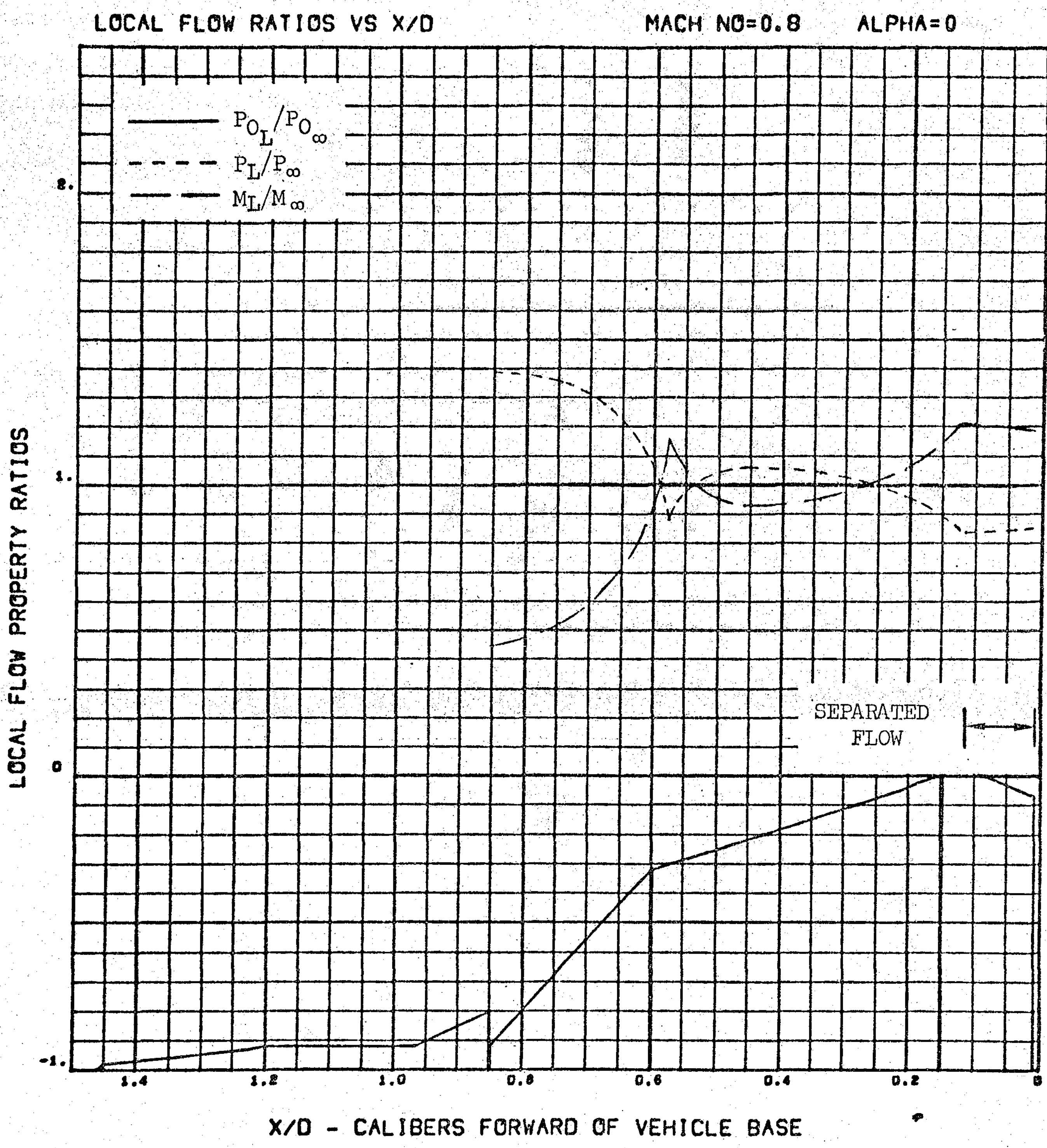

LOCAL FLOW RATIOS VS X/D
MACH NO=0.8
ALPHA=0
P_{O_L}/P_{O_∞}
P_L/P_∞
M_L/M_∞
2.
1.
0
-1.
LOCAL FLOW PROPERTY RATIOS
SEPARATED FLOW
1.4
1.2
1.0
0.8
0.6
0.4
0.2
0
X/D - CALIBERS FORWARD OF VEHICLE BASE

Figure F.3-9

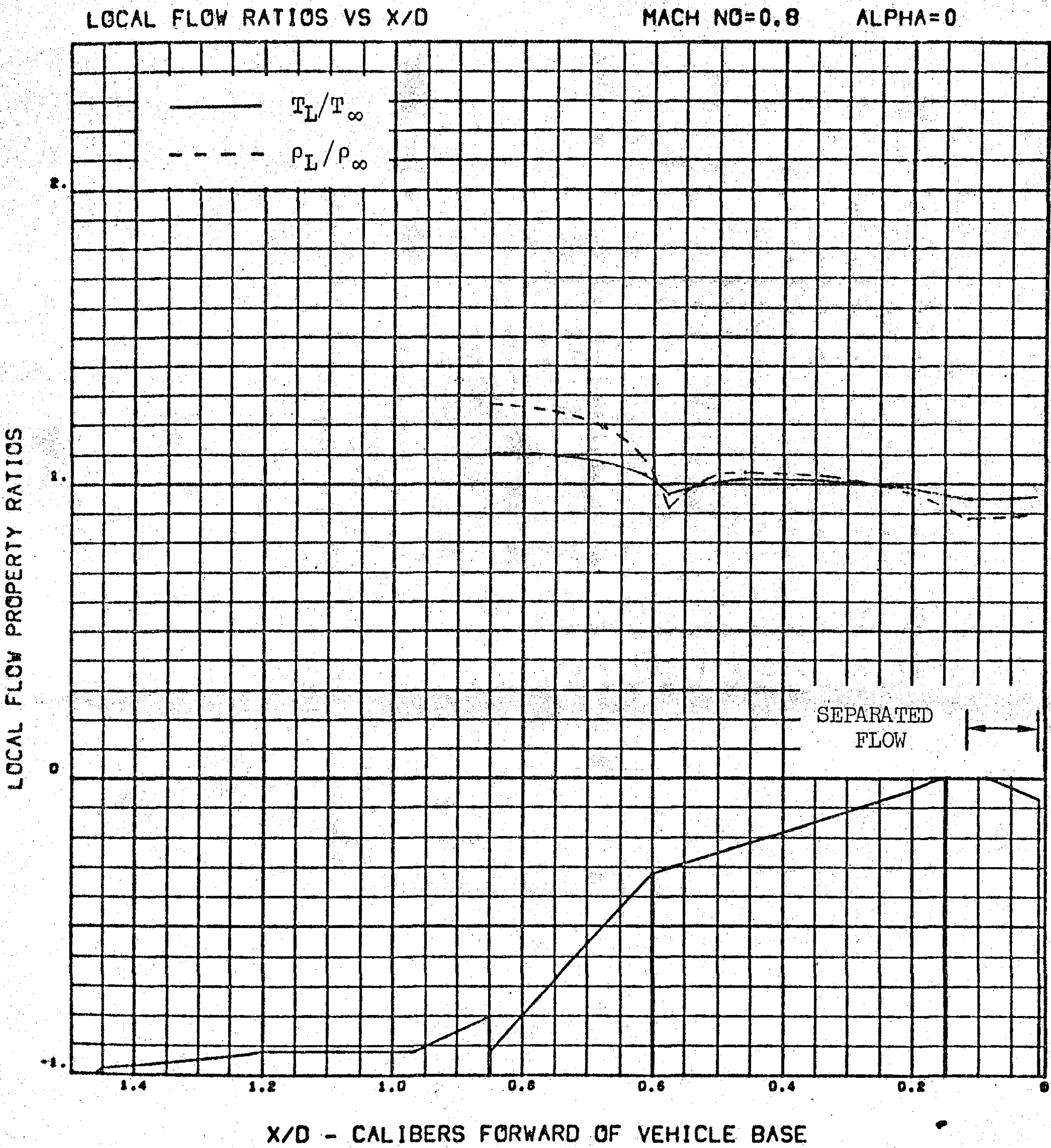
LOCAL FLOW RATIOS VS X/D
MACH NO=0.8
ALPHA=0
T_L/T_∞
ρ_L/ρ_∞
SEPARATED FLOW
LOCAL FLOW PROPERTY RATIOS
X/D - CALIBERS FORWARD OF VEHICLE BASE

Figure F.3-10

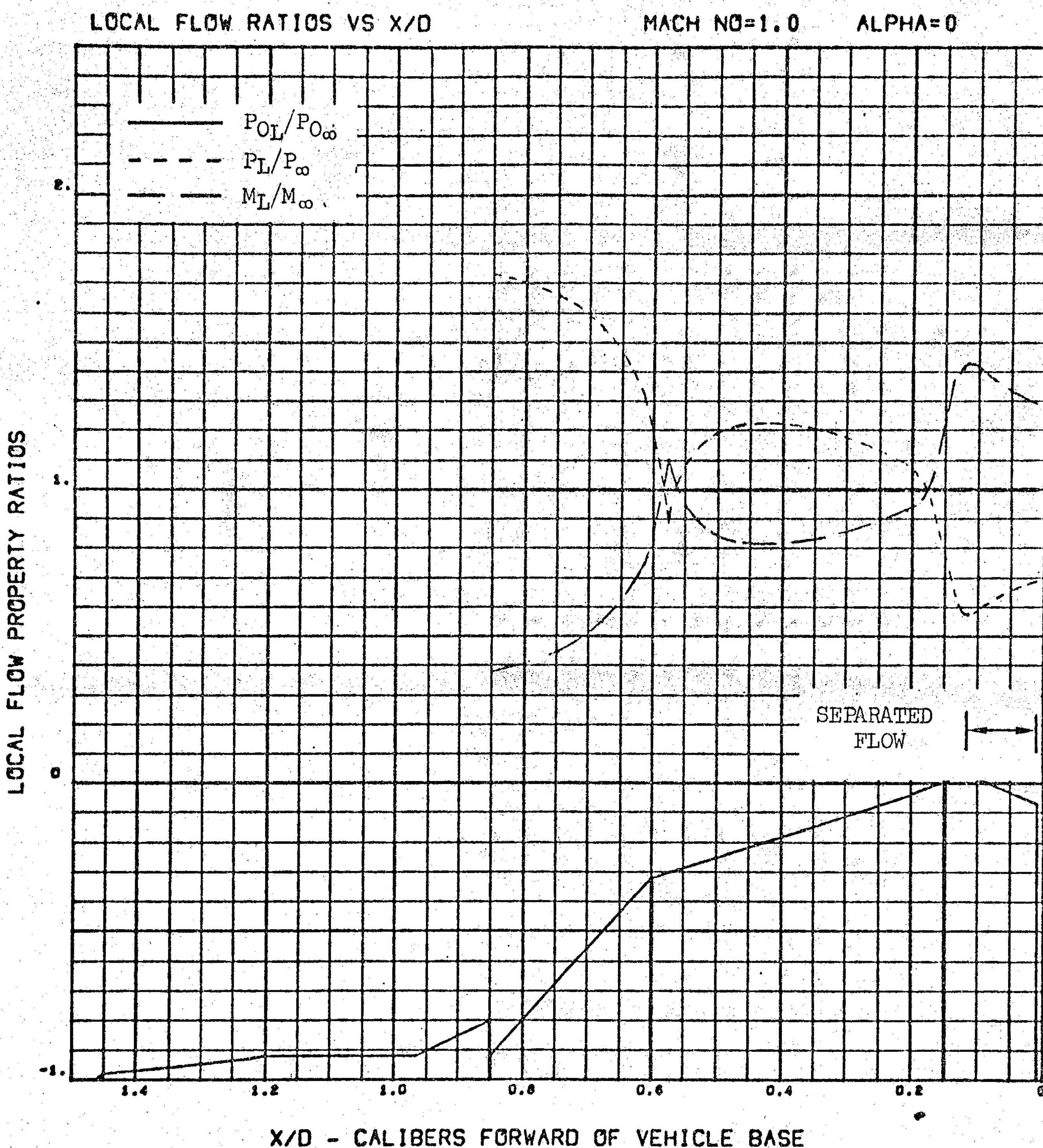
LOCAL FLOW RATIOS VS X/D
MACH NO=1.0
ALPHA=0
P_{O_L}/P_{O_∞}
P_L/P_∞
M_L/M_∞
SEPARATED FLOW
LOCAL FLOW PROPERTY RATIOS
2.
1.
0
-1.
1.4
1.2
1.0
0.8
0.6
0.4
0.2
0
X/D - CALIBERS FORWARD OF VEHICLE BASE

Figure F.3-11

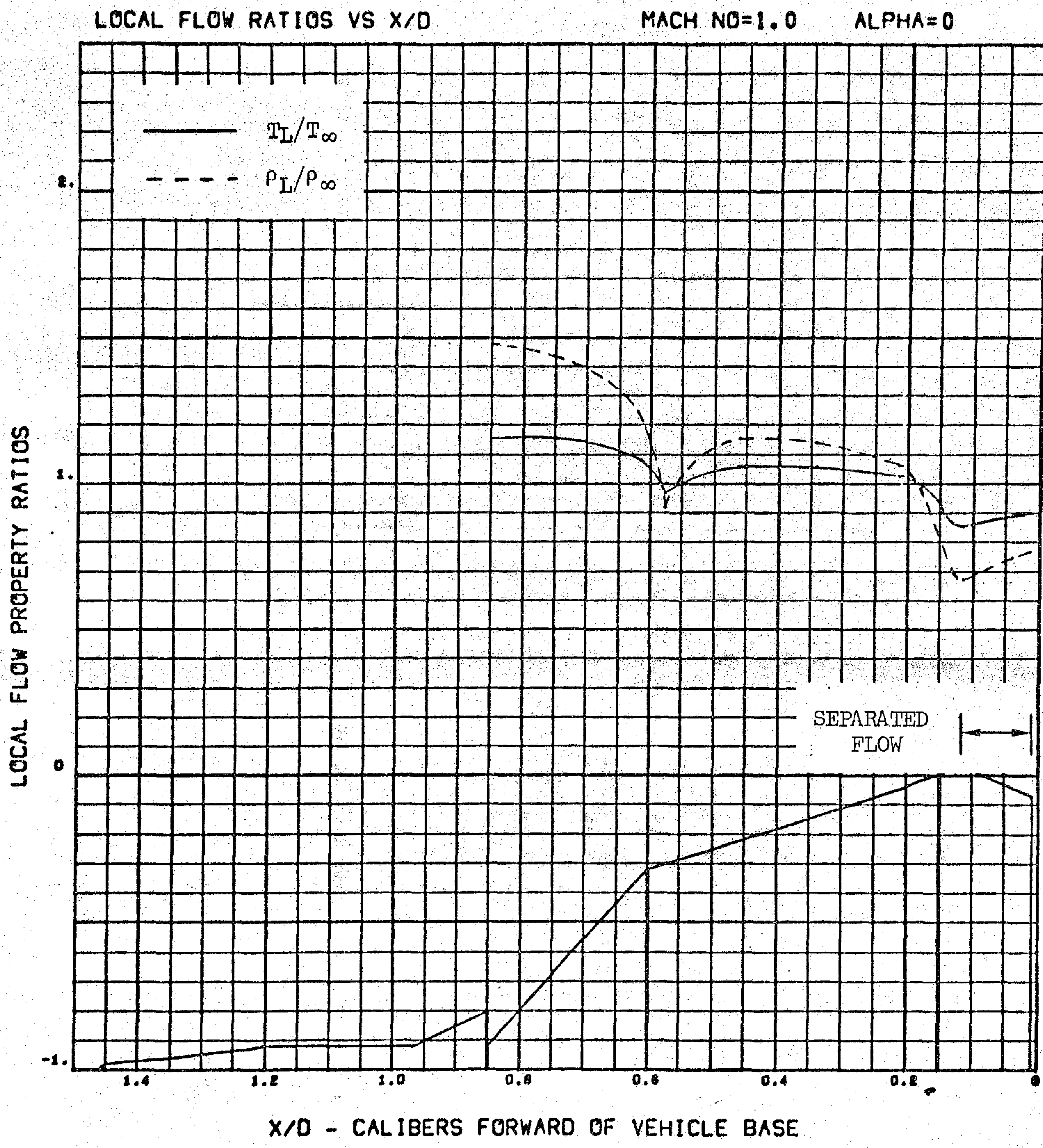

LOCAL FLOW RATIOS VS X/D
MACH NO=1.0
ALPHA=0
T_L/T_∞
ρ_L/ρ_∞
SEPARATED FLOW
LOCAL FLOW PROPERTY RATIOS
2.
1.
0
-1.
1.4
1.2
1.0
0.8
0.6
0.4
0.2
0
X/D - CALIBERS FORWARD OF VEHICLE BASE

Figure F.3-12

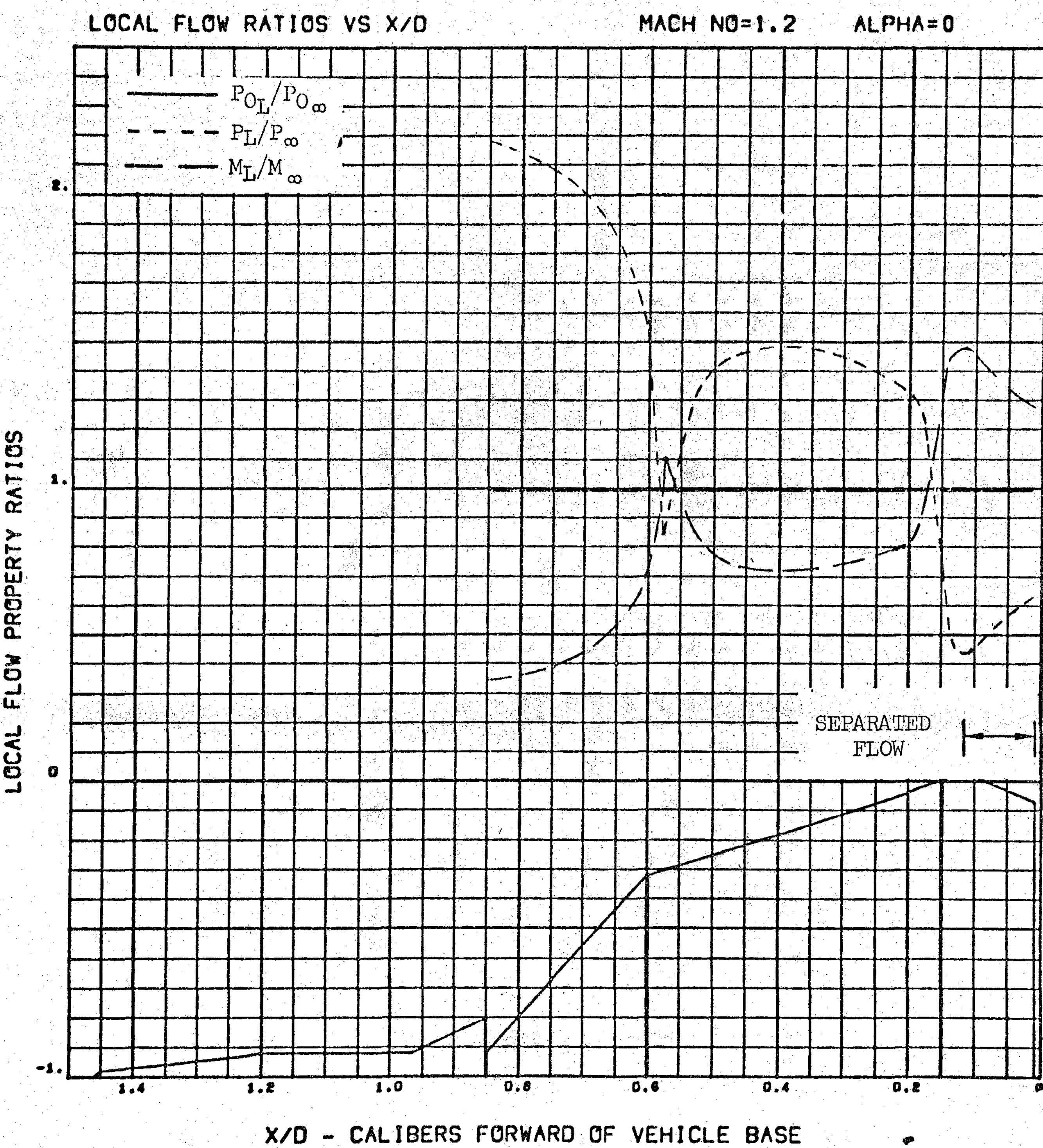

LOCAL FLOW RATIOS VS X/D
MACH NO=1.2
ALPHA=0
P_{O_L}/P_{O_∞}
P_L/P_∞
M_L/M_∞
SEPARATED FLOW
LOCAL FLOW PROPERTY RATIOS
2.
1.
0
-1.
1.4
1.2
1.0
0.8
0.6
0.4
0.2
0
X/D - CALIBERS FORWARD OF VEHICLE BASE

Figure F.3-13

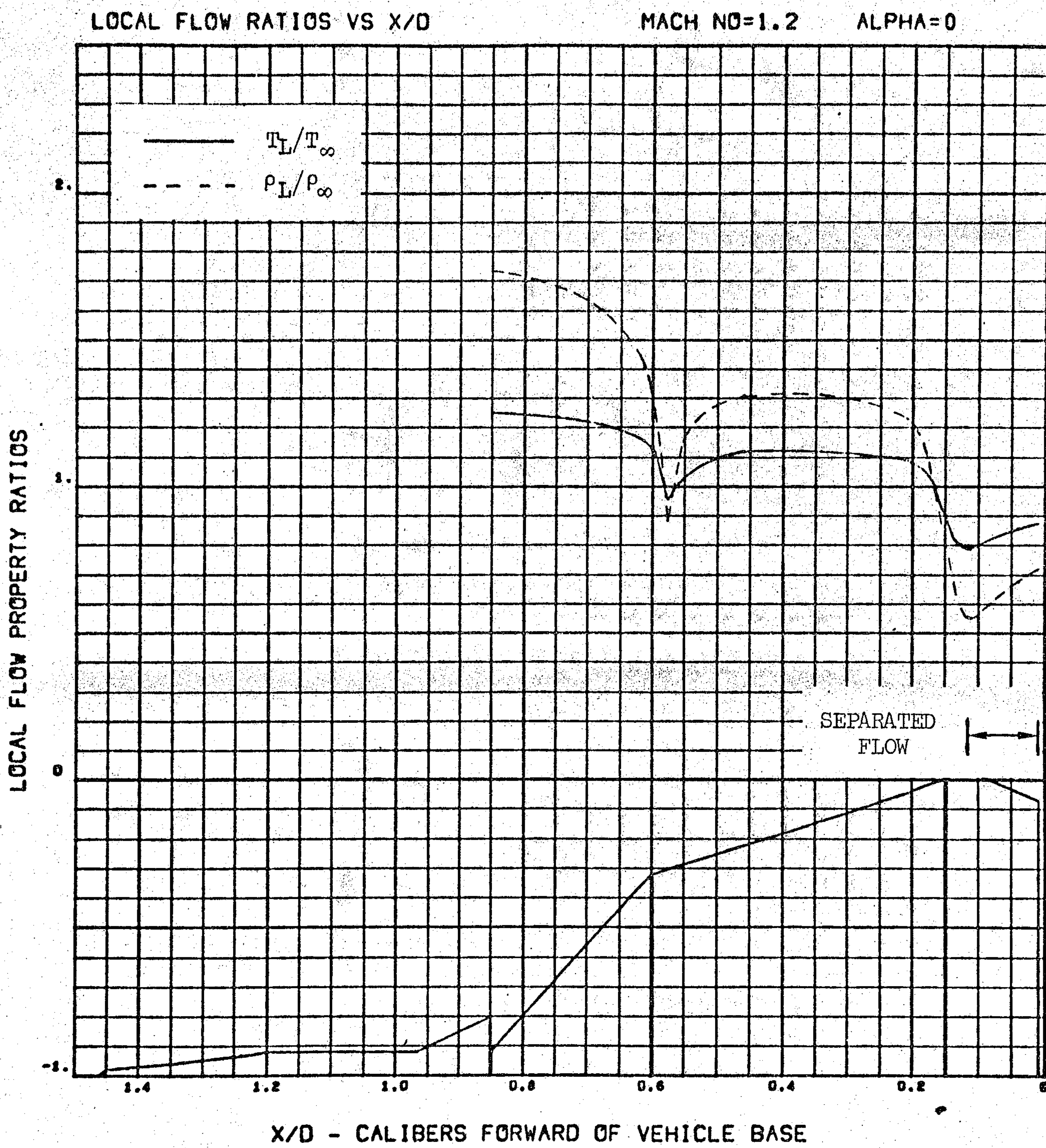
LOCAL FLOW RATIOS VS X/D
MACH NO=1.2
ALPHA=0
T_L/T_∞
ρ_L/ρ_∞
SEPARATED FLOW
LOCAL FLOW PROPERTY RATIOS
2.
1.
0
-1.
1.4
1.2
1.0
0.8
0.6
0.4
0.2
0
X/D - CALIBERS FORWARD OF VEHICLE BASE

Figure F.3-14

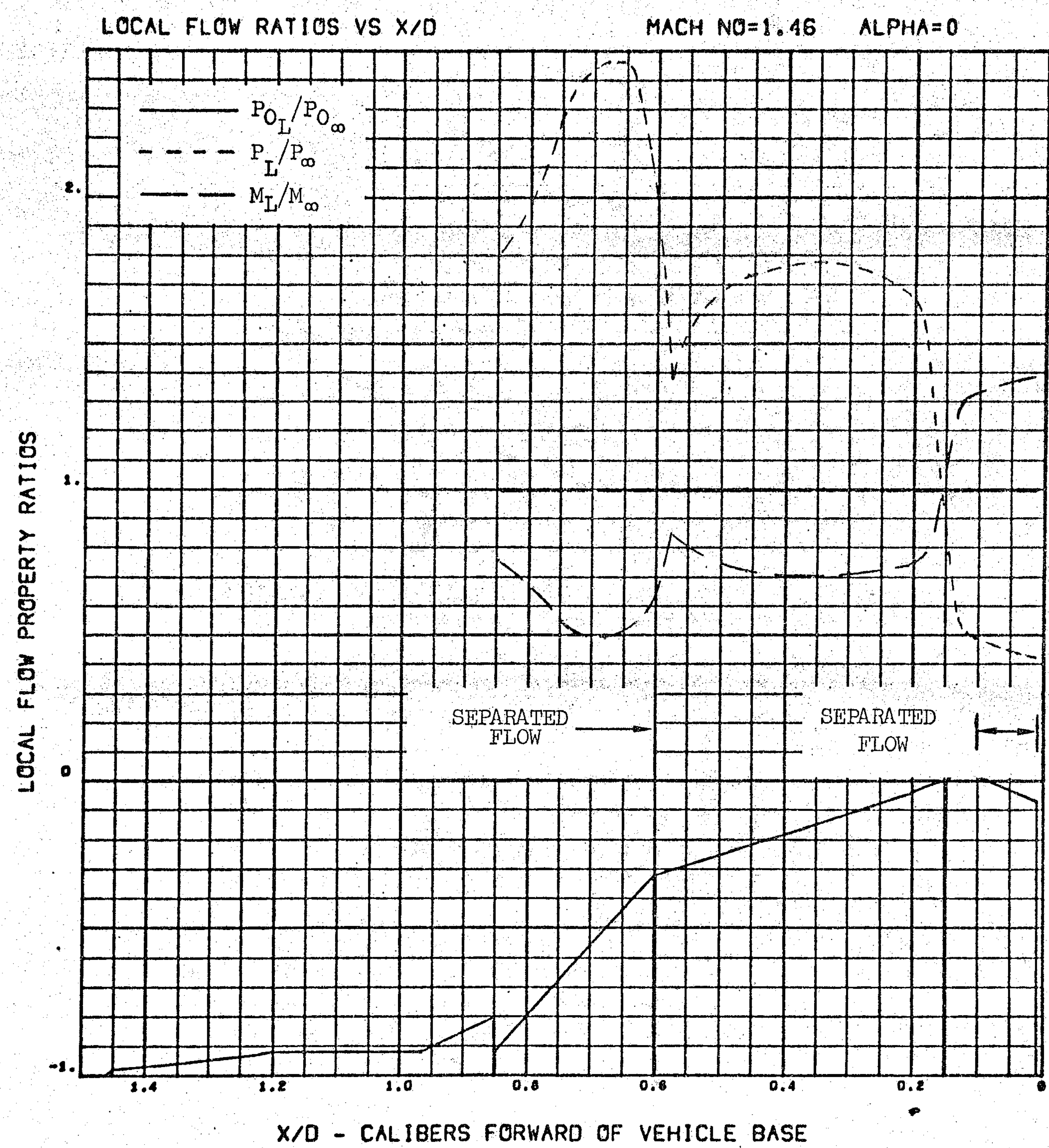

LOCAL FLOW RATIOS VS X/D
MACH NO=1.46 ALPHA=0
P_{O_L}/P_{O_∞}
P_L/P_∞
M_L/M_∞
2.
1.
0
-1.
LOCAL FLOW PROPERTY RATIOS
SEPARATED FLOW
SEPARATED FLOW
1.4
1.2
1.0
0.8
0.6
0.4
0.2
0
X/D - CALIBERS FORWARD OF VEHICLE BASE

Figure F.3-15

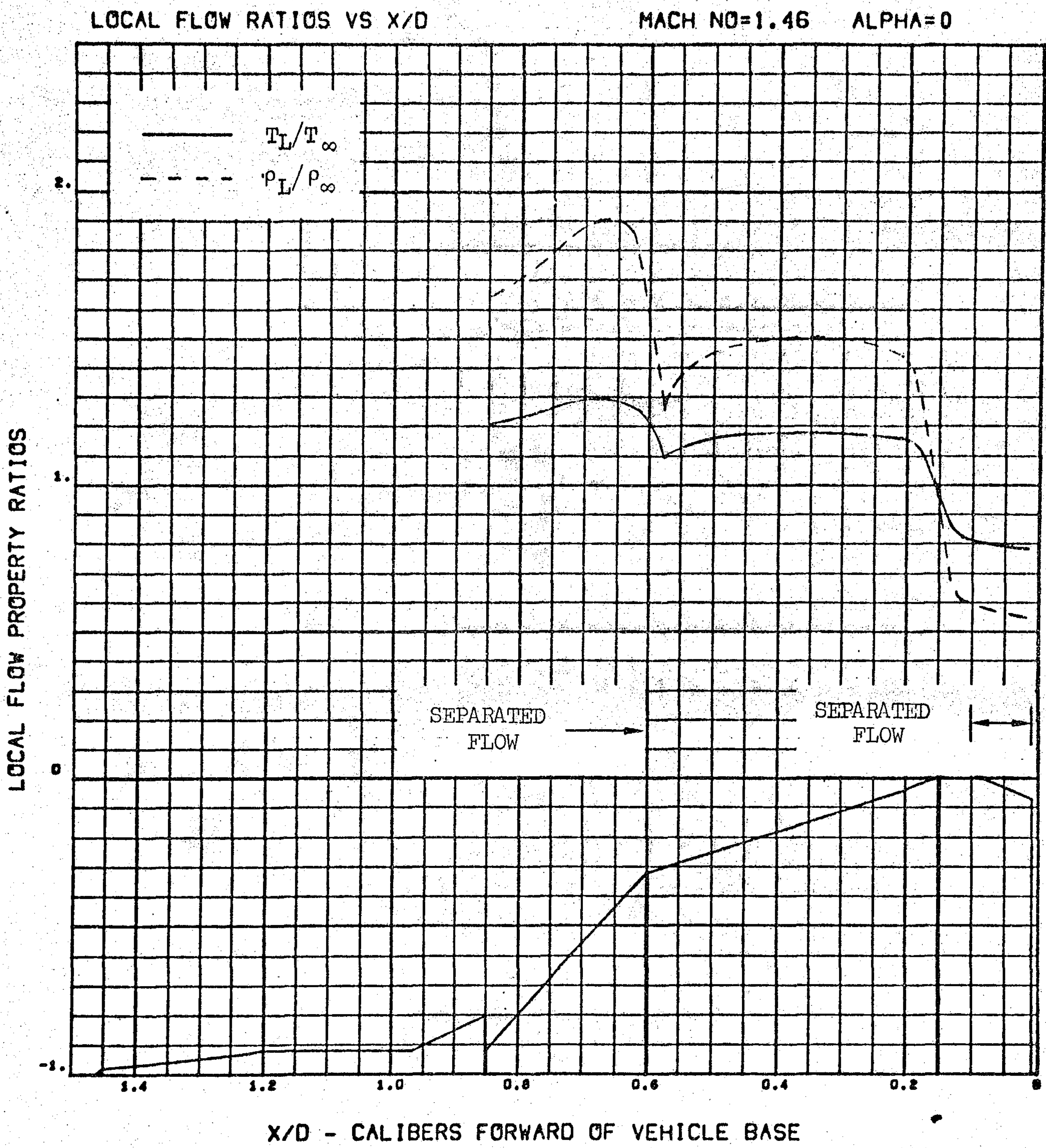
LOCAL FLOW RATIOS VS X/D
MACH NO=1.46 ALPHA=0
T_L/T_∞
ρ_L/ρ_∞
SEPARATED FLOW
SEPARATED FLOW
LOCAL FLOW PROPERTY RATIOS
2.
1.
0
-1.
1.4
1.2
1.0
0.8
0.6
0.4
0.2
0
X/D - CALIBERS FORWARD OF VEHICLE BASE

Figure F.3-16

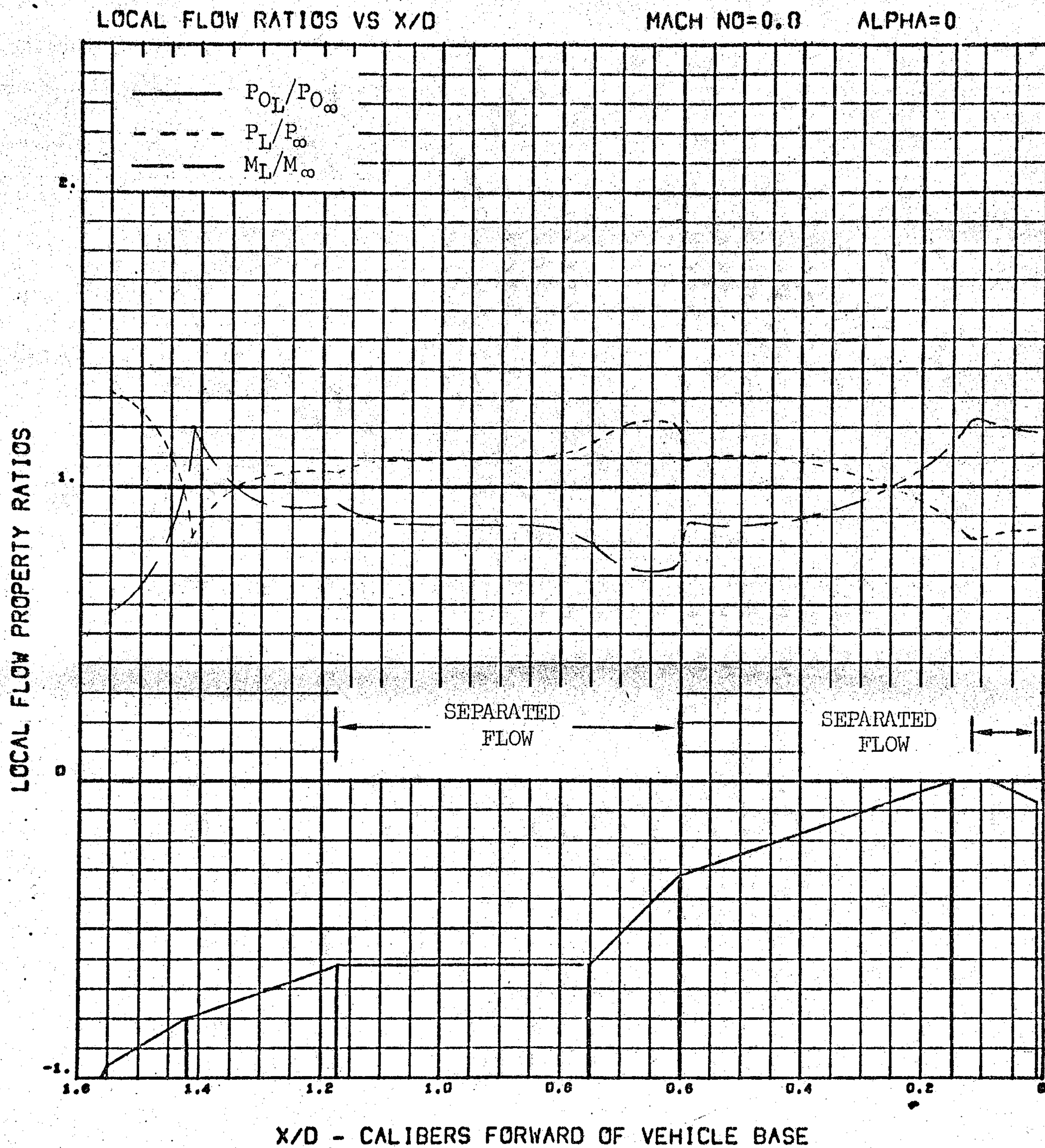
LOCAL FLOW RATIOS VS X/D
MACH NO=0.8
ALPHA=0
P_{O_L}/P_{O_∞}
P_L/P_∞
M_L/M_∞
SEPARATED FLOW
SEPARATED FLOW
LOCAL FLOW PROPERTY RATIOS
2.
1.
0
-1.
1.6
1.4
1.2
1.0
0.8
0.6
0.4
0.2
0
X/D - CALIBERS FORWARD OF VEHICLE BASE

Figure F.3-17

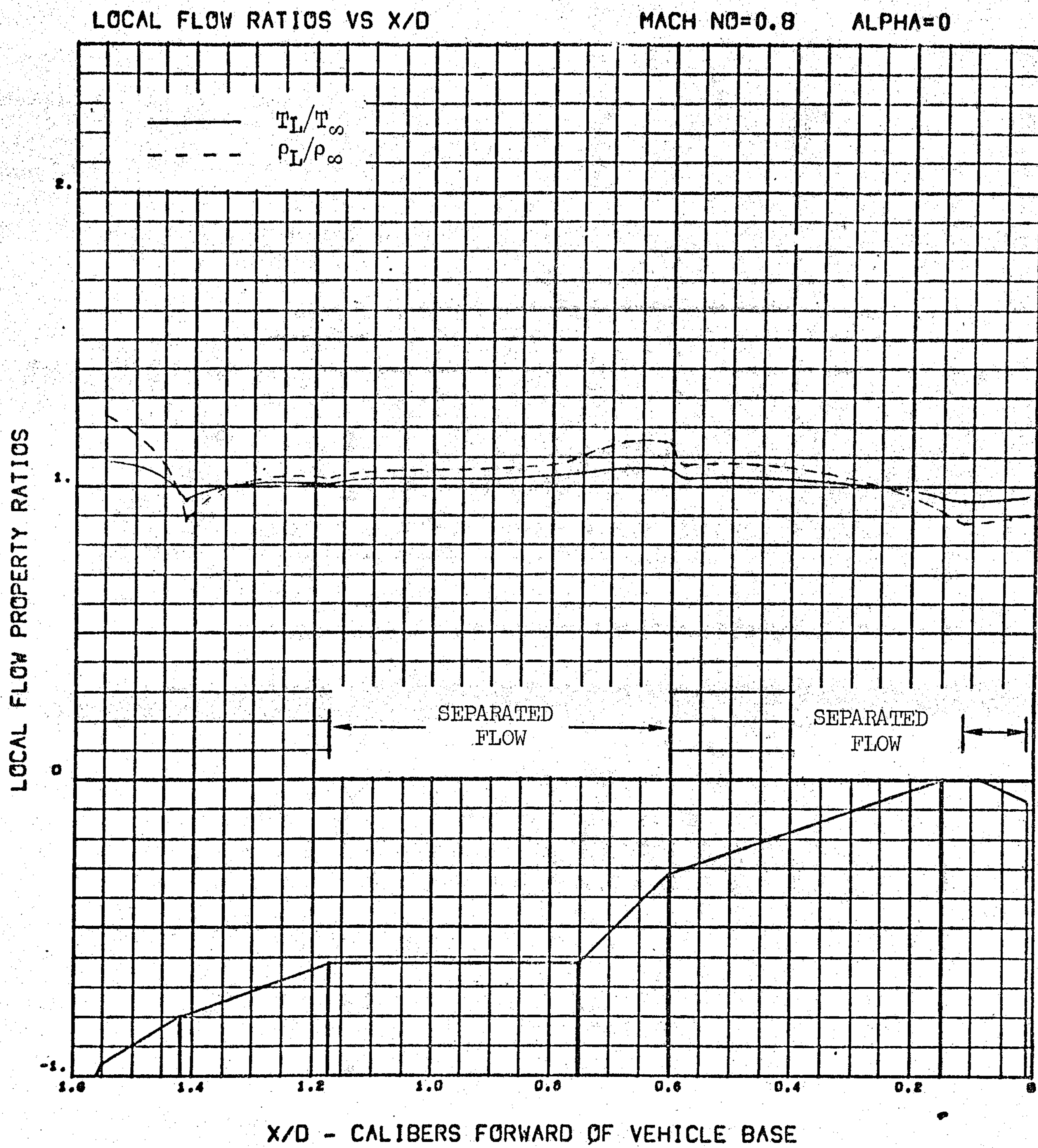

LOCAL FLOW RATIOS VS X/D
MACH NO=0.8
ALPHA=0
T_L/T_∞
ρ_L/ρ_∞
2.
1.
0
-1.
LOCAL FLOW PROPERTY RATIOS
SEPARATED FLOW
SEPARATED FLOW
1.6
1.4
1.2
1.0
0.8
0.6
0.4
0.2
0
X/D - CALIBERS FORWARD OF VEHICLE BASE

Figure F.3-18

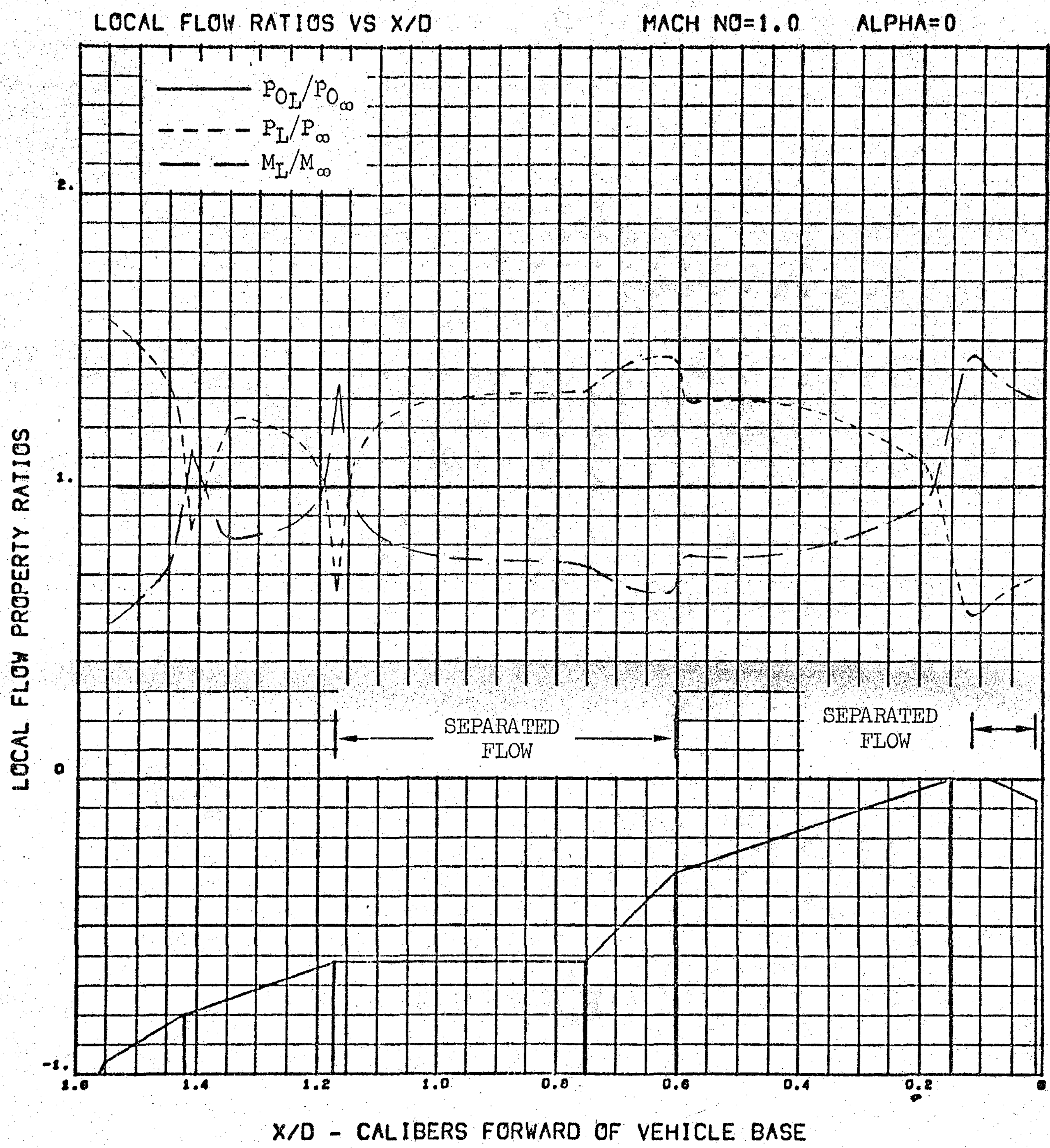

LOCAL FLOW RATIOS VS X/D
MACH NO=1.0
ALPHA=0
P_{O_L}/P_{O_∞}
P_L/P_∞
M_L/M_∞
LOCAL FLOW PROPERTY RATIOS
2.
1.
0
-1.
SEPARATED FLOW
SEPARATED FLOW
1.6
1.4
1.2
1.0
0.8
0.6
0.4
0.2
0
X/D - CALIBERS FORWARD OF VEHICLE BASE

Figure F.3-19

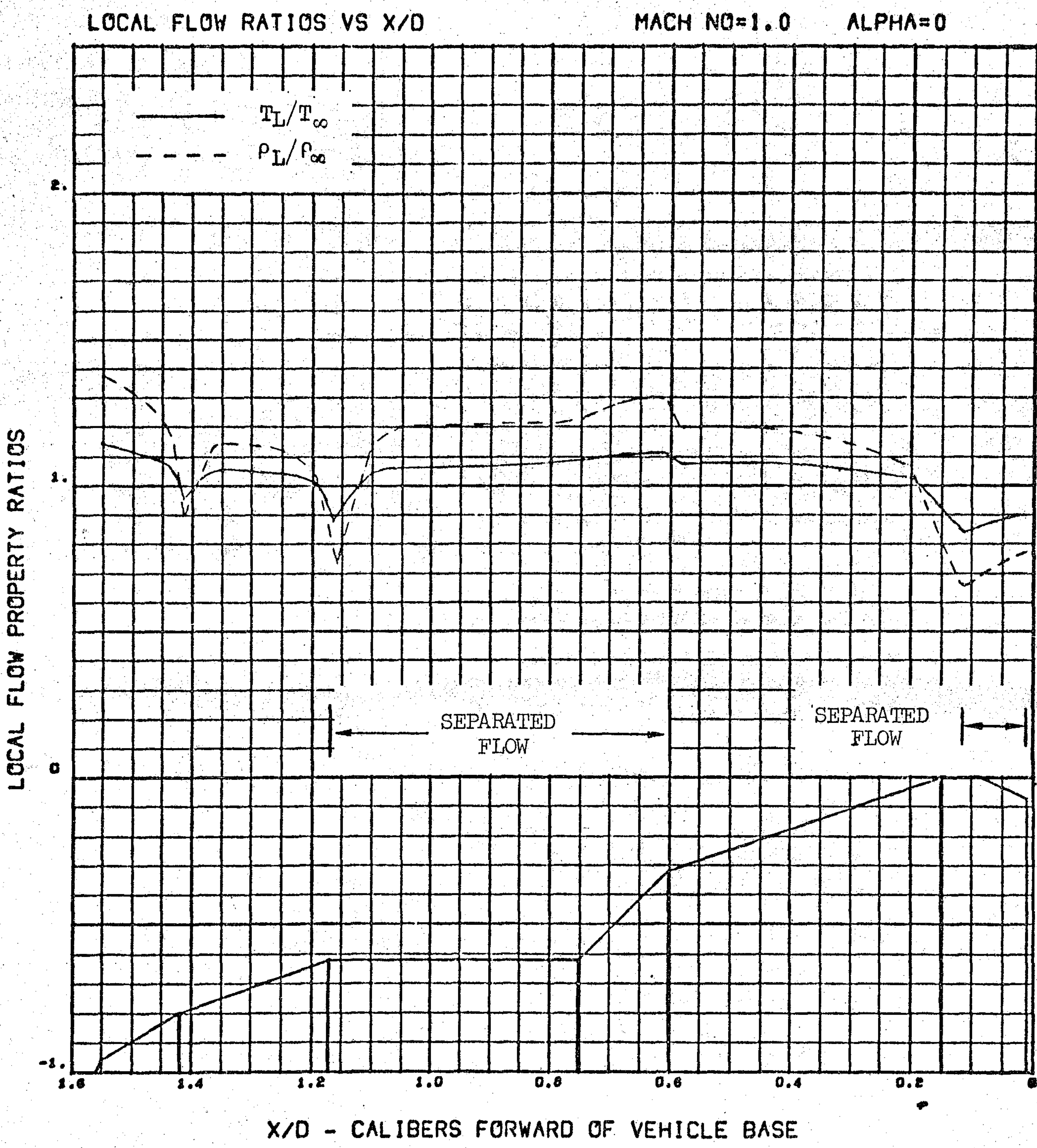

Figure F.3-20

E

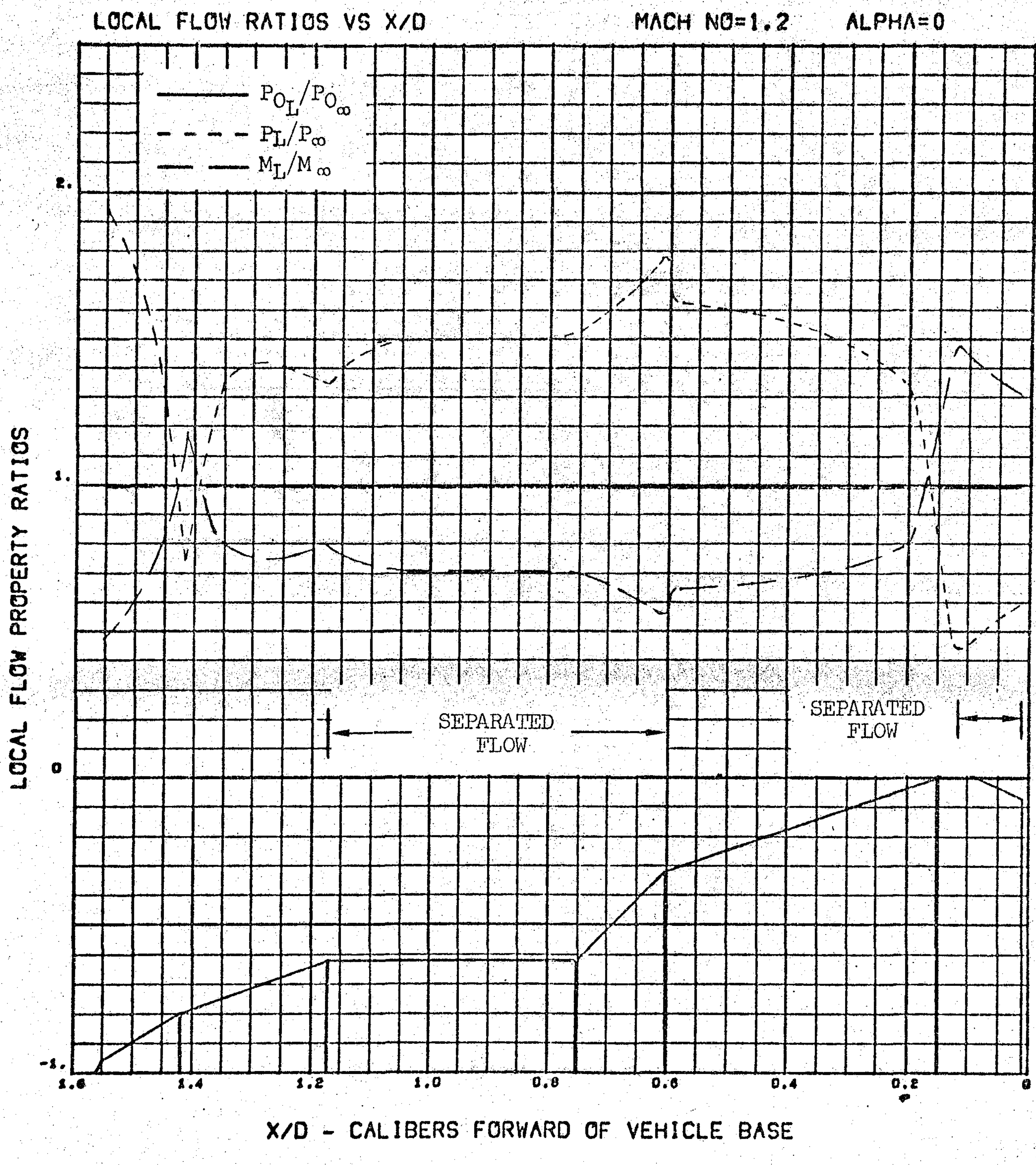

LOCAL FLOW RATIOS VS X/D
MACH NO=1.2 ALPHA=0
P_{O_L}/P_{O_∞}
P_L/P_∞
M_L/M_∞
SEPARATED FLOW
SEPARATED FLOW
LOCAL FLOW PROPERTY RATIOS
2.
1.
0
-1.
1.6
1.4
1.2
1.0
0.8
0.6
0.4
0.2
0
X/D - CALIBERS FORWARD OF VEHICLE BASE

Figure F.3-21

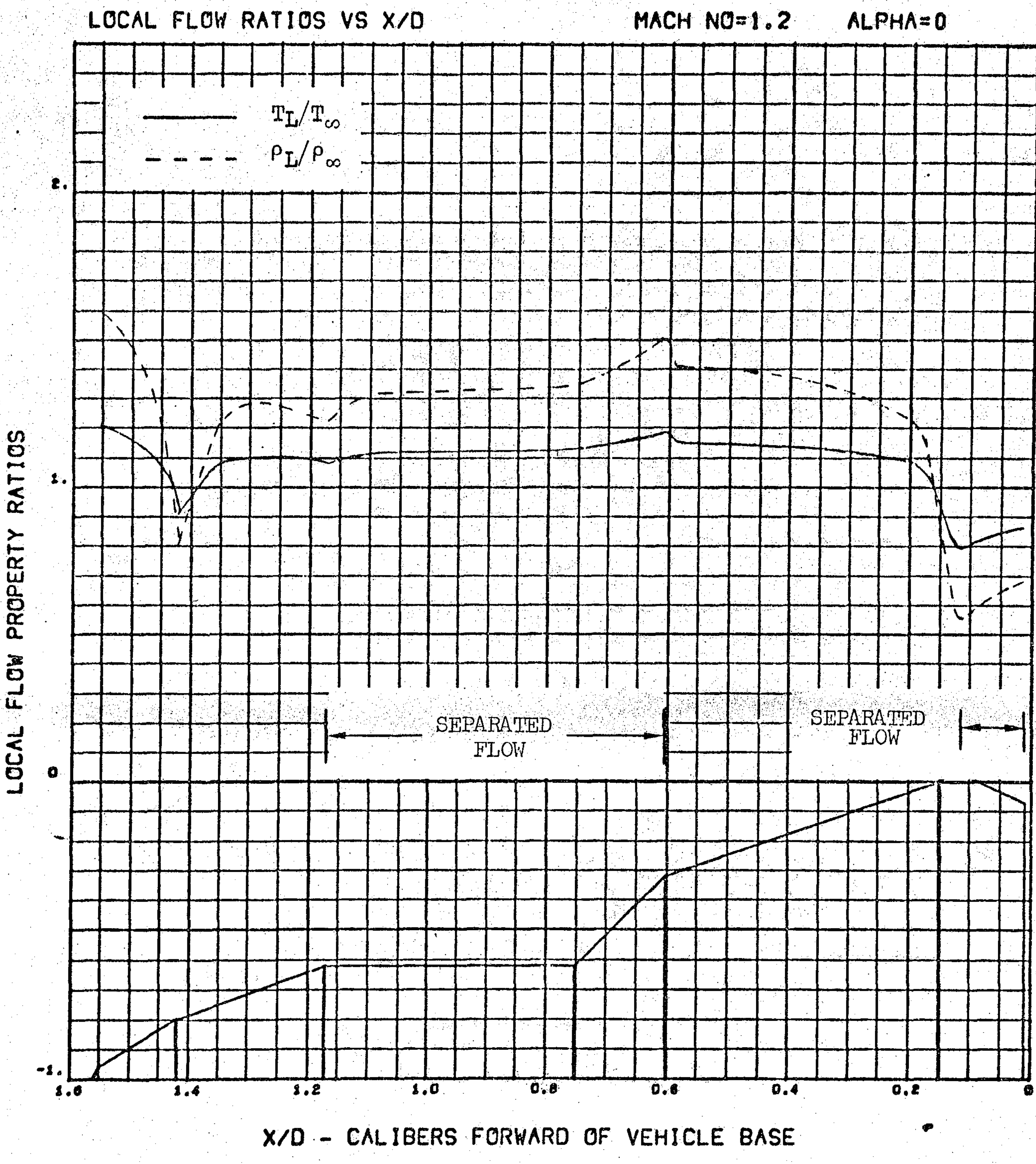
LOCAL FLOW RATIOS VS X/D
MACH NO=1.2
ALPHA=0
T_L/T_∞
ρ_L/ρ_∞
LOCAL FLOW PROPERTY RATIOS
2.
1.
0
-1.
SEPARATED FLOW
SEPARATED FLOW
1.6
1.4
1.2
1.0
0.8
0.6
0.4
0.2
0
X/D - CALIBERS FORWARD OF VEHICLE BASE

Figure F.3-22

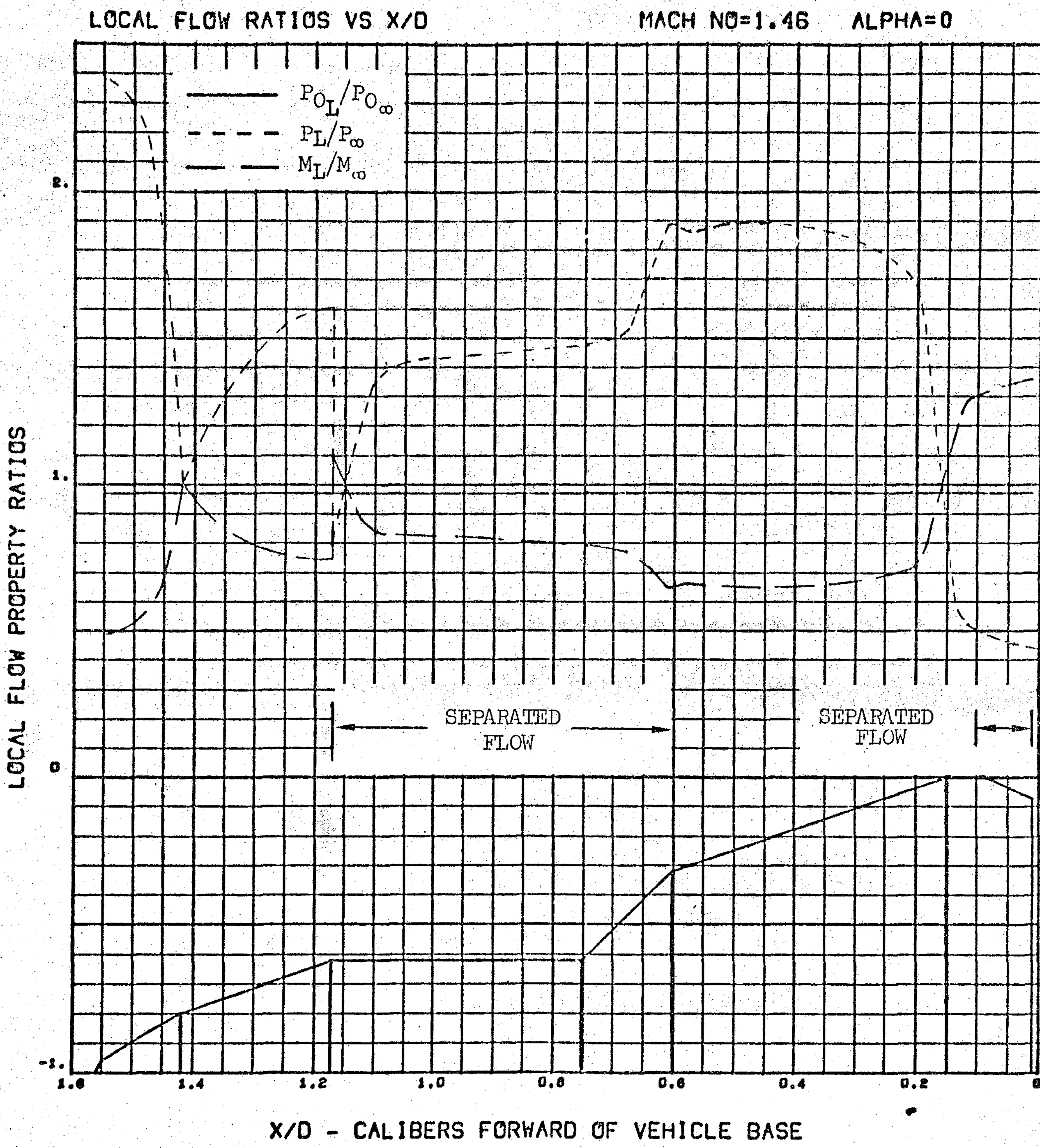
LOCAL FLOW RATIOS VS X/D
MACH NO=1.46 ALPHA=0
P_{O_L}/P_{O_∞}
P_L/P_∞
M_L/M_∞
LOCAL FLOW PROPERTY RATIOS
2.
1.
0
-1.
SEPARATED FLOW
SEPARATED FLOW
1.6
1.4
1.2
1.0
0.8
0.6
0.4
0.2
0
X/D - CALIBERS FORWARD OF VEHICLE BASE

Figure F.3-23

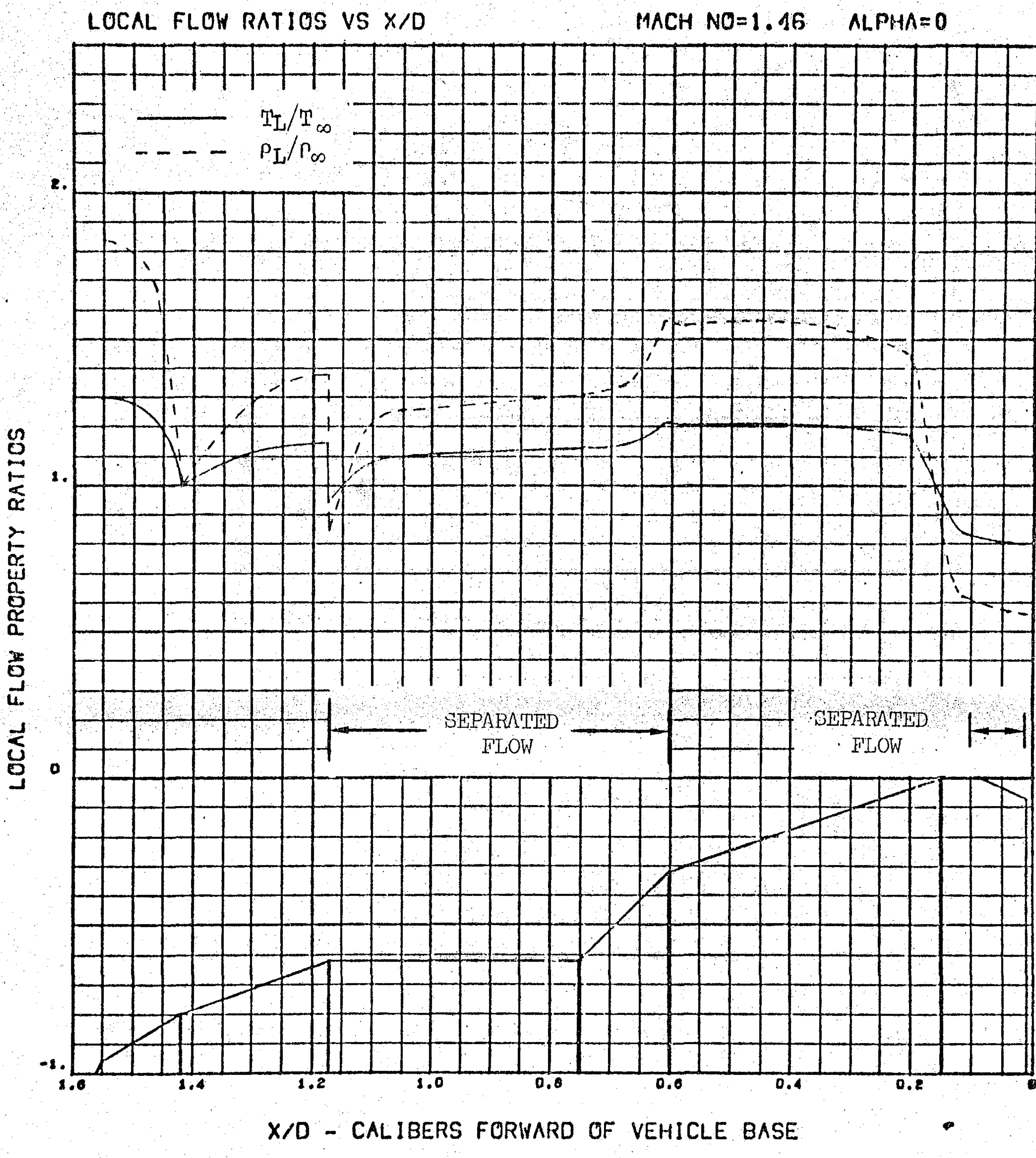

LOCAL FLOW RATIOS VS X/D
MACH NO=1.46 ALPHA=0
T_L/T_∞
ρ_L/ρ_∞
SEPARATED FLOW
SEPARATED FLOW
LOCAL FLOW PROPERTY RATIOS
2.
1.
0
-1.
1.6
1.4
1.2
1.0
0.8
0.6
0.4
0.2
0
X/D - CALIBERS FORWARD OF VEHICLE BASE

Figure F.3-24

APPENDIX G

FINAL WEIGHTS REPORT

Table G-1.

GROUP WEIGHT STATEMENT — PAGE 01 OF 05

CONFIGURATION: FINAL SERV-MURP/HYBRID — BY — DATE 6/25/71

01. WING GROUP				N/A
02. TAIL GROUP				N/A
03. BODY GROUP				207359
INTEGRAL TANKAGE			134800	
FUEL TANK		41454		
OXIDIZER TANK		57131		
BETWEEN TANKS (COMMON BKHD)		36215		
STRUCTURE FORWARD OF TANKS			2659	
STRUCTURE AFT OF TANKS			55883	
SIDEWALLS		12243		
RE-ENTRY BULKHEAD		13635		
THRUST STRUCTURE (MAIN ASCENT ENGINE)		14158		
THRUST STRUCTURE (LANDING ENGINE)		6702		
HOLDDOWN STRUCTURE		2974		
STRUCTURAL TIES, FASTENERS, ETC		6171		
SECONDARY STRUCTURE			14017	
MAIN ASCENT ENGINE DOORS		10005		
LANDING ENGINE INTAKE DOORS		1300		
LANDING ENGINE EXHAUST DOORS		1009		
LANDING GEAR DOORS		180		
INSTRUMENT ACCESS DOORS		220		
FAIRINGS		1303		
04. INDUCED ENVIRONMENTAL PROTECTION				24695
THERMAL PROTECTION			24695	

	UPPER CONE	LOWER CONE	BASE
SURFACE PROTECTION	(4631)	(6915)	(13149)
ABLATIVE			13149
RADIATIVE PANELS	-	-	-
INSULATION	4631	6915	

SOUND PROTECTION	-

Table G-1 (Continued)

GROUP WEIGHT STATEMENT

CONFIGURATION: FINAL SERV-MURP/HYBRID BY DATE 6/25/71

05.LANDING,DOCKING				10395
ALIGHTING GEAR			10395	
GEAR		9301		
DEPLOYMENT SYSTEM		909		
INSTALLATION		185		
HYDRAULIC FLUID		1260*		
* (NOT INCLUDED IN TOTAL-SEE CODES 23-26)				
DOCKING			-	
06.PROPULSION - MAIN ASCENT				134253
ENGINE AND ACCESSORIES			110804	
DOOR ACTUATION SYSTEM			6101	
PROPELLANT SYSTEM	FUEL (8935)	OXID (8413)	17348	
FILL AND DRAIN	2099	1658		
PRESSURIZATION	1026	2022		
VENT SYSTEM	354	484		
FEED SYSTEMS	5140	3843		
RECIRCULATION AND PURGE SYSTEMS	316	406		
07.PROPULSION - LANDING				58603
ENGINE AND ACCESSORIES			51991	
ENGINE		48845		
START SYSTEM		1760		
CONTROL SYSTEM		1386		
INSTALLATION,DUCTS,SHROUD			4122	
AIR DUCTS AND DEFLECTION VANES		2664		
EXHAUST DOOR ACTUATING MECHANISM		721		
INTAKE DOOR ACTUATING MECHANISM		737		
PROPELLANT SYSTEMS			702	
PRESSURIZATION AND VENT SYSTEM		74		
FEED AND TRANSFER LINES		503		
SUPPORTS/INSTALLATION		125		
TANKAGE-NONINTEGRAL			1788	

Table G-1. (Continued)

GROUP WEIGHT STATEMENT

CONFIGURATION: FINAL SERV-MURP/HYBRID BY DATE 6/25/71

08.PROPULSION - AUXILIARY			6071
THRUSTER INSTALLATION		1086	
PROPELLANT SYSTEMS		2284	
DISTRIBUTION SYSTEM	1190		
CONDITIONING SYSTEM	1094		
TANKAGE AND PRESSURIZATION		2701	
09.PRIME POWER			2140
FUEL CELLS AND PLUMBING		600	
TURBINE ALTERNATORS		800	
BATTERIES		340	
INSTALLATION		400	
10.ELECTRICAL			3164
DISTRIBUTORS		805	
VOLTAGE CONDITIONER/CONTROL ELECTRONICS		559	
CABLING AND INSTALLATION		1800	
11.HYDRAULIC EQUIPMENT			N/A
12.SURFACE CONTROLS			N/A

13.AVIONICS	UNITS	CABLING	COOLING	ANTENNAS	INSTALL.	
	(989)	(95)	(50)	(43)	(200)	1377
GUID./NAVIGATION	573	10	30	33	107	
FLIGHT CONTROL	40	-	-	-	10	
DATA MANAGEMENT	271	75	20	-	62	
COMMUNICATION	105	10	-	10	21	
INSTRUMENTATION	*	*	*	*	*	

* INSTRUMENTATION INCLUDED IN SYSTEMS WEIGHTS

Table G-1. (Continued)

GROUP WEIGHT STATEMENT PAGE 04 OF 05

CONFIGURATION: FINAL SERV-MURP/HYBRID BY DATE 6/25/71

14. ENVIRONMENTAL CONTROL				*
* (REQUIRED ENVIRONMENTAL CONTROL PROVISIONS INCLUDED WITH APPLICABLE SYSTEMS.)				
15. PERSONNEL PROVISIONS				N/A
16. RANGE SAFETY AND ABORT				0
17. BALLAST				0
18. GROWTH/UNCERTAINTY				44932
19. OPEN				
SUBTOTAL (DRY)				492989
20. PERSONNEL				N/A
21. PAYLOAD		ASCENT (88933)	DESCENT (46758)	88933
MURP SPACECRAFT		61651		
PERSONNEL MODULE			21758	
CARGO		27282	25000	
22. ORDNANCE				0
23. RESIDUAL AND UNUSEABLE FLUIDS	INERT (1260)	FUEL (4085)	OXID (20440)	25785
MAIN ASCENT PROPULSION SYSTEM		2114	16363	
MAIN TANK PRESSURANT		566	4077	
LANDING PROPULSION SYSTEM		300	-	
AUXILIARY PROPULSION SYSTEM		1105*		
HYDRAULIC FLUID (LANDING GEAR SYSTEM)	1260			
* (FOR LH2 TANK REPRESSURIZATION)				
SUBTOTAL (INERT WEIGHT)				607707

Table G-1. (Continued)

GROUP WEIGHT STATEMENT — PAGE 05 OF 05

CONFIGURATION: FINAL SERV-MURP/HYBRID BY DATE 6/25/71

25. RESERVE FLUIDS	FUEL	OXID	
	(17737)	(12750)	30487
MAIN ASCENT PROPULSION SYSTEM	2117	12700	
LANDING PROPULSION SYSTEM	15610		
AUXILIARY PROPULSION SYSTEM	0	0	
ELECTRICAL POWER SYSTEM	10	50	
26. INFLIGHT LOSSES	FUEL	OXID	
	(408)	(2450)	2858
MAIN ASCENT PROPULSION SYSTEM	308	1850	
LANDING PROPULSION SYSTEM	0	-	
AUXILIARY PROPULSION SYSTEM	0	0	
ELECTRICAL POWER SYSTEM	100	600	
27. PROPELLANT-ASCENT			5358429
MAINSTAGE UTILIZATION		5353076	
FUEL	764725		
OXIDIZER	4588351		
THRUST VECTOR CONTROL		5353	
FUEL	765		
OXIDIZER	4588		
28. PROPELLANT - LANDING			17235
29. PROPELLANT - AUXILIARY PROPULSION SYSTEM			32206
MANEUVER		27523	
ATTITUDE CONTROL		4683	
TOTAL (GROSS WEIGHT)			6048922

NOTE-DRY WEIGHT AND INERT MASSES OBTAINED FROM FINAL STAGE SIZING RUN. PAYLOAD AND PROPELLANT UTILIZATION WERE EXTRACTED FROM FINAL FLIGHT PERFORMANCE ANALYSIS.

Table G-2. Current Inventory of Fluids and Propellants (Lb)

CONFIGURATION	FINAL SERV-MURP HYBRID	BY		DATE: 6-25-71
SYSTEM	**EXPENDABLES (NOMINAL)**	**RESERVES**	**RESIDUALS**	**TOTAL**
PROPULSION - ASCENT	*(5,360,587)	(14,817)	(23,120)	(5,398,524)
OXIDIZER (LOX)	4,594,789	12,700	16,363	4,623,852
FUEL (LH)	765,798	2,117	2,114	770,029
PRESSURANT (GH_2, GOX)			4,643	4,643
PROPULSION - LANDING	(17,235)	(15,610)	(300)	(33,145)
FUEL (JP4)	17,235	15,610	300	33,145
PRESSURANT				
PROPULSION - AUXILIARY	(32,206)		(1,105)	(33,311)
OXIDIZER (LOX)	(27,605)	0	0	(27,605)
MANEUVER	23,591			23,591
ATTITUDE CONTROL	4,014			4,014
FUEL (LH)	(4,601)	0	1,105**	(4,601)
MANEUVER	3,932			3,932
ATTITUDE CONTROL	669			669
PRESSURANT				
MANEUVER				
ATTITUDE CONTROL				
ENVIRONMENTAL CONTROL				
(REQUIRED ENVIRONMENTAL				
CONTROL FLUID INCLUDED				
W/APPLICABLE SYSTEMS)				
PRIME POWER				
FUEL CELL REACTANTS	(700)	(60)		(760)
OXIDIZER (LOX)	600	50		650
FUEL (LH)	100	10		110
BATTERY ELECTROLITE				
HYDRAULIC SYSTEM - LANDING GEAR			(1,260)	(1,260)
HYDRAULIC FLUID			1,260	1,260
MISCELLANEOUS				

*INCLUDES MAINSTAGE, TVC AND THRUST DECAY PROPELLANTS

**LH_2 TANK REPRESSURIZATION

APPENDIX H

FINAL TRAJECTORIES

Table H-1.
SERV-MURP FINAL REFERENCE TRAJECTORY
50 X 100 NMI INJECTION ORBIT
28.5 DEGREE INCLINATION

PROJECT APOLLO STANDARD COORDINATE SYSTEM 1

FLIGHT TIME (SEC)	GEOCENTRIC RADIUS (FT)	INERTIAL VELOCITY (FT/S)	INERTIAL PATH ANGLE (DEG)	INERTIAL AZIMUTH (DEG)	GEOCENTRIC LATITUDE (DEG)	LONGITUDE (POS. EAST) (DEG)
.00	20909846.	1341.8	.00	90.00	28.36	-80.56
5.00	20909940.	1342.3	1.64	90.00	28.36	-80.56
10.00	20910234.	1344.0	3.41	89.99	28.36	-80.56
15.00	20910745.	1347.2	5.33	89.98	28.36	-80.56
20.00	20911492.	1352.4	7.40	89.98	28.36	-80.56
25.00	20912492.	1361.6	9.60	89.97	28.36	-80.56
30.00	20913767.	1377.2	11.89	89.97	28.36	-80.56
35.00	20915336.	1399.7	14.25	89.96	28.36	-80.56
40.00	20917219.	1429.3	16.64	89.95	28.36	-80.56
45.00	20919435.	1467.7	19.01	89.95	28.36	-80.56
50.00	20922005.	1516.7	21.28	89.94	28.36	-80.56
55.00	20924944.	1577.4	23.37	89.94	28.36	-80.56
60.00	20928265.	1650.3	25.22	89.94	28.36	-80.56
62.00	20929703.	1682.7	25.87	89.94	28.36	-80.55
64.00	20931202.	1716.7	26.45	89.94	28.36	-80.55
66.00	20932761.	1752.3	26.97	89.94	28.36	-80.55
68.00	20934380.	1789.2	27.42	89.94	28.36	-80.55
70.00	20936056.	1827.6	27.80	89.94	28.36	-80.55
72.00	20937787.	1866.4	28.09	89.95	28.36	-80.55
74.00	20939569.	1905.3	28.28	89.95	28.36	-80.55
76.00	20941396.	1944.1	28.38	89.95	28.36	-80.54
78.00	20943263.	1982.7	28.39	89.96	28.36	-80.54
80.00	20945166.	2022.4	28.35	89.96	28.36	-80.54
82.00	20947104.	2063.4	28.26	89.97	28.36	-80.54
84.00	20949074.	2106.3	28.14	89.97	28.36	-80.53
86.00	20951077.	2151.5	27.99	89.98	28.36	-80.53
88.00	20953112.	2198.9	27.80	89.99	28.36	-80.53
90.00	20955179.	2248.5	27.59	89.99	28.36	-80.52
92.00	20957277.	2300.7	27.35	90.00	28.36	-80.52
94.00	20959406.	2356.4	27.09	90.01	28.36	-80.51
96.00	20961571.	2417.9	26.85	90.02	28.36	-80.51
98.00	20963776.	2485.2	26.61	90.03	28.36	-80.50
100.00	20966025.	2558.3	26.37	90.03	28.36	-80.50
105.00	20971867.	2767.1	25.76	90.06	28.36	-80.48
110.00	20978060.	3010.3	25.07	90.08	28.36	-80.46

Table H-1. (Continued)
SERV-MURP FINAL REFERENCE TRAJECTORY
50 X 100 NMI INJECTION ORBIT
28.5 DEGREE INCLINATION

PROJECT APOLLO STANDARD COORDINATE SYSTEM 1

FLIGHT TIME (SEC)	GEOCENTRIC RADIUS (FT)	INERTIAL VELOCITY (FT/S)	INERTIAL PATH ANGLE (DEG)	INERTIAL AZIMUTH (DEG)	GEOCENTRIC LATITUDE (DEG)	LONGITUDE (POS. EAST) (DEG)
115.00	20984626.	3285.8	24.29	90.11	28.36	-80.44
120.00	20991571.	3590.3	23.41	90.15	28.36	-80.41
125.00	20998888.	3922.7	22.48	90.18	28.36	-80.38
130.00	21006560.	4281.4	21.50	90.22	28.36	-80.34
135.00	21014568.	4666.4	20.50	90.25	28.36	-80.30
140.00	21022891.	5076.9	19.50	90.30	28.36	-80.25
145.00	21031500.	5504.7	18.50	90.34	28.36	-80.19
150.00	21040339.	5936.0	17.52	90.39	28.36	-80.13
155.00	21049345.	6370.5	16.55	90.44	28.36	-80.06
160.00	21058461.	6807.9	15.60	90.49	28.36	-79.98
170.00	21076820.	7691.1	13.81	90.60	28.35	-79.80
180.00	21094960.	8584.6	11.90	90.80	28.35	-79.60
190.00	21112092.	9489.4	10.05	91.08	28.35	-79.37
200.00	21128059.	10403.6	8.50	91.35	28.34	-79.11
210.00	21142823.	11325.8	7.18	91.62	28.33	-78.82
220.00	21156358.	12254.7	6.05	91.89	28.32	-78.50
230.00	21168645.	13189.2	5.07	92.16	28.31	-78.15
240.00	21179681.	14128.7	4.23	92.45	28.30	-77.78
250.00	21189471.	15072.5	3.49	92.74	28.28	-77.37
260.00	21198036.	16020.0	2.85	93.03	28.26	-76.94
270.00	21205407.	16970.9	2.29	93.34	28.23	-76.47
280.00	21211628.	17924.6	1.81	93.66	28.20	-75.98
290.00	21216756.	18880.8	1.40	93.99	28.17	-75.46
300.00	21220861.	19839.2	1.05	94.33	28.13	-74.91
310.00	21224025.	20799.3	.75	94.68	28.09	-74.33
320.00	21226344.	21760.9	.51	95.04	28.04	-73.73
330.00	21227926.	22723.8	.32	95.41	27.99	-73.09
340.00	21228893.	23687.5	.17	95.80	27.93	-72.43
350.00	21229380.	24651.8	.07	96.19	27.86	-71.74
360.00	21229537.	25616.5	.01	96.60	27.78	-71.02
362.89	21229543.	25895.7	.00	96.72	27.76	-70.80

Table H-1. (Continued)

SERV-MURP FINAL REFERENCE TRAJECTORY
50 X 100 NMI INJECTION ORBIT
28.5 DEGREE INCLINATION

PROJECT APOLLO STANDARD COORDINATE SYSTEM 1

FLIGHT TIME (SEC)	ALTITUDE (FT)	VELOCITY (FT/S)	EARTH - FIXED PATH ANGLE (DEG)	AZIMUTH (DEG)	RANGE (NMI)	GEODETIC LATITUDE (DEG)
.00	0.	.0	.00	.00	.00	28.52
5.00	94.	38.3	89.83	337.86	.00	28.52
10.00	388.	80.0	89.79	321.58	.00	28.52
15.00	900.	125.3	89.75	310.77	.00	28.52
20.00	1646.	174.2	89.71	303.56	.00	28.52
25.00	2647.	227.0	89.77	45.57	.00	28.52
30.00	3921.	283.8	88.84	82.06	.00	28.52
35.00	5490.	344.9	87.59	86.25	.01	28.52
40.00	7373.	410.3	86.20	87.67	.03	28.52
45.00	9590.	480.3	84.59	88.41	.06	28.52
50.00	12160.	554.9	82.67	88.87	.10	28.52
55.00	15098.	634.5	80.45	89.18	.17	28.52
60.00	18420.	719.1	77.96	89.39	.28	28.52
62.00	19857.	753.9	76.89	89.46	.33	28.52
64.00	21356.	789.0	75.78	89.52	.39	28.52
66.00	22916.	824.2	74.63	89.58	.46	28.52
68.00	24534.	859.6	73.45	89.63	.54	28.52
70.00	26211.	895.1	72.23	89.67	.62	28.52
72.00	27942.	929.6	70.97	89.71	.71	28.52
74.00	29723.	962.6	69.68	89.75	.82	28.52
76.00	31550.	994.1	68.36	89.79	.93	28.52
78.00	33417.	1024.2	66.99	89.82	1.06	28.52
80.00	35320.	1054.7	65.59	89.85	1.20	28.52
82.00	37258.	1085.7	64.15	89.88	1.35	28.52
84.00	39228.	1118.1	62.68	89.91	1.51	28.52
86.00	41231.	1152.4	61.18	89.93	1.68	28.52
88.00	43266.	1188.5	59.65	89.96	1.87	28.52
90.00	45333.	1226.6	58.10	89.98	2.08	28.52
92.00	47431.	1267.0	56.53	90.00	2.30	28.52
94.00	49561.	1311.0	54.95	90.02	2.54	28.52
96.00	51725.	1360.9	53.36	90.05	2.80	28.52
98.00	53930.	1417.0	51.78	90.06	3.07	28.52
100.00	56179.	1479.1	50.21	90.08	3.37	28.52
105.00	62021.	1661.5	46.37	90.13	4.23	28.52
110.00	68214.	1879.6	42.73	90.17	5.26	28.52

Table H-1. (Continued)

SERV-MURP FINAL REFERENCE TRAJECTORY

50 X 100 NMI INJECTION ORBIT

28.5 DEGREE INCLINATION

PROJECT APOLLO STANDARD COORDINATE SYSTEM 1

FLIGHT TIME (SEC)	ALTITUDE (FT)	EARTH - FIXED VELOCITY (FT/S)	EARTH - FIXED PATH ANGLE (DEG)	EARTH - FIXED AZIMUTH (DEG)	EARTH - FIXED RANGE (NMI)	GEODETIC LATITUDE (DEG)
115.00	74781.	2131.6	39.34	90.21	6.50	28.52
120.00	81725.	2414.3	36.22	90.25	7.97	28.52
125.00	89042.	2726.6	33.37	90.29	9.70	28.52
130.00	96714.	3067.2	30.76	90.33	11.71	28.52
135.00	104722.	3435.9	28.40	90.37	14.03	28.52
140.00	113044.	3831.8	26.25	90.41	16.67	28.52
145.00	121653.	4246.6	24.29	90.46	19.66	28.52
150.00	130491.	4666.2	22.51	90.51	23.01	28.52
155.00	139497.	5090.3	20.88	90.56	26.71	28.52
160.00	148612.	5518.4	19.38	90.62	30.78	28.52
170.00	166969.	6385.8	16.70	90.73	40.03	28.52
180.00	185106.	7265.5	14.10	90.96	50.76	28.51
190.00	202234.	8159.0	11.71	91.26	63.02	28.51
200.00	218196.	9065.2	9.76	91.55	76.81	28.50
210.00	232952.	9981.5	8.15	91.84	92.13	28.50
220.00	246476.	10906.0	6.80	92.13	108.97	28.49
230.00	258751.	11837.3	5.65	92.41	127.35	28.47
240.00	269771.	12774.3	4.68	92.71	147.27	28.46
250.00	279543.	13716.3	3.84	93.01	168.73	28.44
260.00	288087.	14662.4	3.11	93.32	191.72	28.42
270.00	295432.	15612.3	2.49	93.63	216.26	28.39
280.00	301624.	16565.3	1.96	93.96	242.35	28.37
290.00	306718.	17521.0	1.51	94.30	269.98	28.33
300.00	310784.	18479.0	1.12	94.65	299.16	28.29
310.00	313904.	19439.0	.80	95.01	329.90	28.25
320.00	316173.	20400.5	.54	95.38	362.19	28.20
330.00	317700.	21363.4	.34	95.76	396.04	28.15
340.00	318604.	22327.2	.18	96.15	431.45	28.09
350.00	319023.	23291.7	.07	96.56	468.42	28.02
360.00	319103.	24256.5	.01	96.97	506.96	27.94
362.89	319085.	24535.7	.00	97.09	518.40	27.92

Table H-1. (Continued)
SERV-MURP FINAL REFERENCE TRAJECTORY
50 X 100 NMI INJECTION ORBIT
28.5 DEGREE INCLINATION

FLIGHT TIME (SEC)	THRUST (LB)	WEIGHT (LB)	LONGITUDINAL ACCELERATION (G'S)	INERTIAL ATTITUDE ANGLES PITCH (DEG)	YAW (DEG)	INCLINATION (DEG)
.00	7453152.	6075705.	1.2267	90.00	.00	28.36
5.00	7446326.	5968626.	1.2471	90.00	.00	28.36
10.00	7446265.	5861548.	1.2685	90.00	.00	28.36
15.00	7454580.	5754469.	1.2907	90.00	.00	28.36
20.00	7473279.	5647391.	1.3142	90.00	.00	28.36
25.00	7504556.	5540312.	1.3392	89.02	.00	28.36
30.00	7541866.	5433234.	1.3644	88.04	.00	28.36
35.00	7588189.	5326155.	1.3900	87.07	.00	28.36
40.00	7643647.	5219077.	1.4163	86.09	.00	28.36
45.00	7702629.	5111998.	1.4424	84.43	.00	28.36
50.00	7762570.	5004920.	1.4680	82.49	.00	28.36
55.00	7843860.	4897841.	1.4952	80.25	.00	28.36
60.00	7896483.	4790763.	1.5118	77.73	.00	28.36
62.00	7925293.	4747931.	1.5142	76.65	.00	28.36
64.00	7938154.	4705100.	1.5126	75.54	.00	28.36
66.00	7945901.	4662268.	1.5093	74.38	.00	28.36
68.00	7957442.	4619437.	1.5064	73.19	.00	28.36
70.00	7973028.	4576606.	1.4952	71.96	.00	28.36
72.00	7985490.	4533774.	1.4652	70.70	.00	28.36
74.00	8004384.	4490943.	1.4376	69.40	.00	28.36
76.00	8014626.	4448111.	1.4004	68.06	.00	28.36
78.00	8031568.	4405280.	1.3847	66.69	.00	28.36
80.00	8052721.	4362449.	1.3840	65.28	.00	28.36
82.00	8064963.	4319617.	1.3837	63.83	.00	28.36
84.00	8089169.	4276786.	1.4024	62.35	.00	28.36
86.00	8095353.	4233954.	1.4181	60.84	.00	28.36
88.00	8089880.	4191123.	1.4344	59.30	.00	28.36
90.00	8084321.	4148292.	1.4529	57.74	.00	28.36
92.00	8078678.	4105460.	1.4778	56.16	.00	28.36
94.00	8223165.	4062629.	1.5419	54.56	.00	28.36
96.00	8377743.	4019797.	1.6205	52.96	.00	28.36
98.00	8522754.	3976966.	1.6987	51.37	.00	28.36
100.00	8670678.	3934135.	1.7755	49.78	.00	28.36
105.00	9005232.	3827056.	1.9675	45.91	.00	28.36
110.00	9260175.	3719977.	2.1384	42.24	.00	28.36

Table H-1. (Continued)
SERV-MURP FINAL REFERENCE TRAJECTORY
50 X 100 NMI INJECTION ORBIT
28.5 DEGREE INCLINATION

FLIGHT TIME (SEC)	THRUST (LB)	WEIGHT (LB)	LONGITUDINAL ACCELERATION (G'S)	INERTIAL ATTITUDE ANGLES PITCH (DEG)	YAW (DEG)	INCLINATION (DEG)
115.00	9448708.	3612899.	2.2895	38.81	.00	28.36
120.00	9602472.	3505820.	2.4383	35.65	.00	28.36
125.00	9722106.	3398742.	2.5747	32.74	.00	28.36
130.00	9804476.	3291663.	2.7103	30.09	.00	28.36
135.00	9850582.	3184585.	2.8460	27.67	.00	28.36
140.00	9874302.	3077506.	2.9853	25.45	.00	28.36
145.00	9503376.	2972372.	3.0000	23.43	.00	28.36
150.00	9103685.	2871859.	3.0000	21.58	.00	28.36
155.00	8723928.	2775788.	3.0000	19.86	.00	28.36
160.00	8371912.	2683893.	3.0000	18.27	.00	28.36
170.00	7745578.	2511049.	3.0000	15.41	.00	28.36
180.00	7194799.	2350781.	3.0000	8.74	-1.36	28.36
190.00	6699829.	2201720.	3.0000	7.67	-1.43	28.37
200.00	6250474.	2062735.	3.0000	6.59	-1.51	28.37
210.00	5801830.	1933943.	3.0000	5.51	-1.58	28.38
220.00	5439309.	1813103.	3.0000	4.43	-1.66	28.38
230.00	5099185.	1699728.	3.0000	3.35	-1.73	28.39
240.00	4780106.	1593369.	3.0000	2.27	-1.81	28.40
250.00	4480795.	1493598.	3.0000	1.18	-1.88	28.40
260.00	4200053.	1400018.	3.0000	.09	-1.95	28.41
270.00	3936749.	1312250.	3.0000	-1.00	-2.03	28.42
280.00	3689819.	1229940.	3.0000	-2.09	-2.10	28.42
290.00	3458263.	1152754.	3.0000	-3.18	-2.17	28.43
300.00	3241137.	1080379.	3.0000	-4.28	-2.24	28.44
310.00	3037555.	1012518.	3.0000	-5.37	-2.31	28.45
320.00	2846634.	948878.	3.0000	-6.47	-2.38	28.46
330.00	2667525.	889175.	3.0000	-7.56	-2.45	28.47
340.00	2499514.	833171.	3.0000	-8.66	-2.52	28.48
350.00	2341934.	780645.	3.0000	-9.75	-2.58	28.49
360.00	2194156.	731385.	3.0000	-10.85	-2.65	28.50
362.89	2153147.	717716.	3.0000	-11.17	-2.67	28.50

Table H-1. (Continued)

SERV-MURP FINAL REFERENCE TRAJECTORY
50 X 100 NMI INJECTION ORBIT
28.5 DEGREE INCLINATION

FLIGHT TIME (SEC)	MACH NO.	DYNAMIC PRESSURE (LB/FT2)	NORMAL FORCE (LB)	AXIAL FORCE (LB)	ANGLE OF ATTACK (DEG)	AERO. HEATING INDICATOR (LB-FT/FT2)	AERO. LOAD INDICATOR (LB-DEG/FT2)
.00	.000	0.	.0	.0	.000	0.	0.
5.00	.034	2.	.0	2567.8	.047	51.	0.
10.00	.070	7.	.0	11140.7	.091	888.	1.
15.00	.110	18.	.0	27002.6	.132	4931.	2.
20.00	.154	33.	.0	51335.9	.170	17028.	6.
25.00	.201	55.	.0	85111.5	.722	45298.	40.
30.00	.253	83.	.0	128959.9	.700	101680.	58.
35.00	.309	117.	.0	184968.5	.401	202058.	47.
40.00	.369	156.	.0	251924.4	.032	366279.	5.
45.00	.435	200.	.0	328969.9	.002	618529.	0.
50.00	.507	246.	.0	415098.8	.002	986132.	1.
55.00	.585	293.	.0	520474.2	.004	1497362.	1.
60.00	.671	339.	.0	653732.9	.005	2180283.	2.
62.00	.708	356.	.0	735787.1	.006	2506625.	2.
64.00	.745	372.	.0	821328.8	.006	2864599.	2.
66.00	.783	386.	.0	909211.5	.007	3254338.	3.
68.00	.823	399.	.0	998607.5	.008	3675519.	3.
70.00	.863	410.	.0	1130242.3	.009	4127548.	4.
72.00	.904	418.	.0	1342649.2	.010	4608569.	4.
74.00	.944	422.	.0	1548394.5	.011	5114680.	5.
76.00	.984	423.	.0	1785346.9	.012	5641607.	5.
78.00	1.023	421.	.0	1931526.9	.013	6184254.	6.
80.00	1.063	417.	.0	2015097.2	.015	6739233.	6.
82.00	1.105	412.	.0	2087709.0	.016	7304876.	7.
84.00	1.148	406.	.0	2091544.4	.017	7879067.	7.
86.00	1.194	399.	.0	2091304.9	.019	8460935.	7.
88.00	1.241	391.	.0	2077962.7	.020	9049272.	8.
90.00	1.290	381.	.0	2057206.4	.022	9642551.	8.
92.00	1.341	371.	.0	2011595.6	.023	10239193.	9.
94.00	1.394	360.	.0	1959039.6	.025	10838059.	9.
96.00	1.451	349.	.0	1863674.4	.026	11440670.	9.
98.00	1.513	339.	.0	1767187.0	.027	12049311.	9.
100.00	1.579	329.	.0	1685679.5	.029	12665479.	9.
105.00	1.754	302.	.0	1475615.5	.032	14238532.	10.
110.00	1.961	279.	.0	1305344.1	.035	15871269.	10.

Table H-1. (Continued)
SERV-MURP FINAL REFERENCE TRAJECTORY
50 X 100 NMI INJECTION ORBIT
28.5 DEGREE INCLINATION

FLIGHT TIME (SEC)	MACH NO.	DYNAMIC PRESSURE (LB/FT2)	NORMAL FORCE (LB)	AXIAL FORCE (LB)	ANGLE OF ATTACK (DEG)	AERO. HEATING INDICATOR (LB-FT/FT2)	AERO. LOAD INDICATOR (LB-DEG/FT2)
115.00	2.199	255.	.0	1176840.2	.038	17573472.	10.
120.00	2.466	232.	.0	1054249.5	.041	19332477.	10.
125.00	2.763	207.	.0	971362.2	.045	21124604.	9.
130.00	3.077	182.	.0	882957.7	.048	22915316.	9.
135.00	3.407	156.	.0	787212.0	.051	24658592.	8.
140.00	3.752	132.	.0	686999.2	.054	26320446.	7.
145.00	4.102	110.	.0	586260.2	.058	27872817.	6.
150.00	4.445	90.	.0	488109.3	.061	29285600.	6.
155.00	4.786	73.	.0	396563.0	.065	30544306.	5.
160.00	5.131	59.	.0	320233.0	.069	31651083.	4.
170.00	5.917	39.	.0	212431.1	.078	33463408.	3.
180.00	6.889	26.	.0	142454.3	4.027	34892282.	105.
190.00	7.971	17.	.0	94670.0	2.540	35983501.	44.
200.00	9.141	11.	.0	62270.3	1.545	36778408.	18.
210.00	.000	0.	.0	.0	1.360	0.	0.
220.00	.000	0.	.0	.0	1.550	0.	0.
230.00	.000	0.	.0	.0	1.704	0.	0.
240.00	.000	0.	.0	.0	1.797	0.	0.
250.00	.000	0.	.0	.0	1.830	0.	0.
260.00	.000	0.	.0	.0	1.810	0.	0.
270.00	.000	0.	.0	.0	1.748	0.	0.
280.00	.000	0.	.0	.0	1.653	0.	0.
290.00	.000	0.	.0	.0	1.539	0.	0.
300.00	.000	0.	.0	.0	1.421	0.	0.
310.00	.000	0.	.0	.0	1.317	0.	0.
320.00	.000	0.	.0	.0	1.251	0.	0.
330.00	.000	0.	.0	.0	1.248	0.	0.
340.00	.000	0.	.0	.0	1.323	0.	0.
350.00	.000	0.	.0	.0	1.477	0.	0.
360.00	.000	0.	.0	.0	1.697	0.	0.
362.89	.000	0.	.0	.0	1.770	0.	0.

Table H-2.
SERV-MURP FINAL REFERENCE TRAJECTORY
50 X 110 NMI INJECTION ORBIT
55 DEGREE INCLINATION

PROJECT APOLLO STANDARD COORDINATE SYSTEM I

FLIGHT TIME (SEC)	GEOCENTRIC RADIUS (FT)	INERTIAL VELOCITY (FT/S)	INERTIAL PATH ANGLE (DEG)	INERTIAL AZIMUTH (DEG)	GEOCENTRIC LATITUDE (DEG)	LONGITUDE (POS. EAST) (DEG)
.00	20909846.	1341.8	.00	90.00	28.36	-80.56
5.00	20909943.	1342.3	1.67	90.00	28.36	-80.56
10.00	20910243.	1344.1	3.49	89.99	28.36	-80.56
15.00	20910766.	1347.5	5.45	89.98	28.36	-80.56
20.00	20911528.	1352.9	7.55	89.98	28.36	-80.56
25.00	20912550.	1361.7	9.79	89.91	28.36	-80.56
30.00	20913850.	1375.7	12.14	89.72	28.36	-80.56
35.00	20915449.	1395.2	14.58	89.40	28.36	-80.56
40.00	20917367.	1420.8	17.06	88.94	28.36	-80.56
45.00	20919624.	1453.7	19.56	88.31	28.36	-80.56
50.00	20922238.	1495.3	21.98	87.45	28.36	-80.56
55.00	20925225.	1546.4	24.28	86.33	28.36	-80.56
60.00	20928598.	1607.6	26.36	84.94	28.36	-80.56
62.00	20930056.	1634.6	27.10	84.32	28.37	-80.56
64.00	20931576.	1662.9	27.79	83.65	28.37	-80.56
66.00	20933156.	1692.5	28.40	82.96	28.37	-80.56
68.00	20934795.	1723.3	28.95	82.23	28.37	-80.56
70.00	20936492.	1755.0	29.43	81.47	28.37	-80.55
72.00	20938243.	1786.8	29.80	80.70	28.37	-80.55
74.00	20940042.	1818.5	30.07	79.91	28.37	-80.55
76.00	20941885.	1849.9	30.24	79.13	28.37	-80.55
78.00	20943766.	1881.5	30.32	78.33	28.38	-80.55
80.00	20945683.	1914.1	30.36	77.52	28.38	-80.55
82.00	20947634.	1948.0	30.33	76.70	28.38	-80.55
84.00	20949618.	1983.8	30.28	75.85	28.38	-80.54
86.00	20951635.	2021.6	30.19	74.98	28.38	-80.54
88.00	20953684.	2061.5	30.06	74.10	28.39	-80.54
90.00	20955765.	2103.6	29.89	73.20	28.39	-80.54
92.00	20957877.	2148.3	29.69	72.29	28.39	-80.53
94.00	20960022.	2197.1	29.49	71.36	28.40	-80.53
96.00	20962204.	2251.4	29.28	70.38	28.40	-80.53
98.00	20964428.	2311.5	29.08	69.38	28.40	-80.53
100.00	20966698.	2377.2	28.86	68.36	28.41	-80.52
105.00	20972602.	2567.3	28.27	65.76	28.42	-80.51
110.00	20978865.	2791.9	27.53	63.22	28.43	-80.50

Table H-2. (Continued)
SERV-MURP FINAL REFERENCE TRAJECTORY
50 X 110 NMI INJECTION ORBIT
55 DEGREE INCLINATION

PROJECT APOLLO STANDARD COORDINATE SYSTEM 1

FLIGHT TIME (SEC)	GEOCENTRIC RADIUS (FT)	INERTIAL VELOCITY (FT/S)	INERTIAL PATH ANGLE (DEG)	INERTIAL AZIMUTH (DEG)	GEOCENTRIC LATITUDE (DEG)	LONGITUDE (POS. EAST) (DEG)
115.00	20985511.	3049.4	26.65	60.81	28.45	-80.48
120.00	20992542.	3337.6	25.64	58.61	28.47	-80.47
125.00	20999950.	3655.2	24.55	56.63	28.49	-80.45
130.00	21007719.	4001.0	23.40	54.87	28.52	-80.42
135.00	21015829.	4374.9	22.23	53.32	28.55	-80.40
140.00	21024259.	4776.1	21.06	51.97	28.58	-80.36
145.00	21032975.	5191.1	19.91	50.80	28.62	-80.33
150.00	21041913.	5611.0	18.77	49.82	28.67	-80.29
155.00	21051012.	6035.4	17.67	48.99	28.72	-80.24
160.00	21060214.	6464.0	16.61	48.27	28.77	-80.19
170.00	21078723.	7332.1	14.60	47.12	28.89	-80.08
180.00	21096979.	8212.7	12.51	46.20	29.03	-79.96
190.00	21114174.	9106.4	10.50	45.46	29.19	-79.81
200.00	21130154.	10012.0	8.83	44.89	29.37	-79.64
210.00	21144886.	10927.3	7.41	44.44	29.57	-79.46
220.00	21158347.	11850.6	6.21	44.10	29.79	-79.25
230.00	21170528.	12780.6	5.18	43.83	30.03	-79.03
240.00	21181427.	13716.2	4.29	43.64	30.29	-78.79
250.00	21191058.	14656.7	3.52	43.49	30.57	-78.52
260.00	21199446.	15601.5	2.86	43.40	30.86	-78.24
270.00	21206629.	16549.9	2.28	43.35	31.18	-77.93
280.00	21212656.	17501.5	1.79	43.35	31.51	-77.60
290.00	21217591.	18455.9	1.37	43.37	31.87	-77.25
300.00	21221509.	19412.6	1.02	43.43	32.24	-76.88
310.00	21224498.	20371.3	.72	43.52	32.63	-76.48
320.00	21226660.	21331.6	.48	43.64	33.03	-76.06
330.00	21228111.	22293.3	.29	43.79	33.46	-75.62
340.00	21228976.	23256.0	.15	43.96	33.90	-75.15
350.00	21229399.	24219.4	.06	44.17	34.36	-74.65
360.00	21229532.	25183.4	.01	44.40	34.84	-74.13
367.56	21229543.	25912.1	.00	44.59	35.21	-73.71

Table H-2. (Continued)

SERV-MURP FINAL REFERENCE TRAJECTORY
50 X 110 NMI INJECTION ORBIT
55 DEGREE INCLINATION

PROJECT APOLLO STANDARD COORDINATE SYSTEM 1

FLIGHT TIME (SEC)	ALTITUDE (FT)	EARTH - FIXED VELOCITY (FT/S)	EARTH - FIXED PATH ANGLE (DEG)	EARTH - FIXED AZIMUTH (DEG)	RANGE (NMI)	GEODETIC LATITUDE (DEG)
.00	0.	.0	.00	.00	.00	28.52
5.00	97.	39.2	89.83	338.11	.00	28.52
10.00	398.	81.8	89.80	321.91	.00	28.52
15.00	920.	128.0	89.75	311.10	.00	28.52
20.00	1683.	177.8	89.71	303.86	.00	28.52
25.00	2704.	231.6	89.48	358.75	.00	28.52
30.00	4004.	289.5	88.57	23.50	.01	28.52
35.00	5604.	351.6	87.33	29.71	.01	28.52
40.00	7522.	418.0	85.94	32.22	.03	28.52
45.00	9779.	489.0	84.31	33.69	.06	28.52
50.00	12394.	564.7	82.37	34.68	.11	28.52
55.00	15382.	645.3	80.13	35.39	.19	28.52
60.00	18756.	730.7	77.61	35.90	.30	28.53
62.00	20215.	765.8	76.54	36.07	.35	28.53
64.00	21736.	801.0	75.42	36.22	.42	28.53
66.00	23317.	836.4	74.27	36.35	.49	28.53
68.00	24958.	871.9	73.09	36.47	.57	28.53
70.00	26656.	907.3	71.86	36.58	.65	28.53
72.00	28408.	941.3	70.61	36.68	.75	28.53
74.00	30208.	974.0	69.31	36.77	.86	28.53
76.00	32053.	1004.8	67.98	36.85	.98	28.53
78.00	33936.	1034.9	66.61	36.93	1.11	28.54
80.00	35855.	1065.5	65.21	37.00	1.25	28.54
82.00	37808.	1096.8	63.77	37.06	1.40	28.54
84.00	39794.	1129.8	62.29	37.13	1.57	28.54
86.00	41813.	1164.7	60.79	37.19	1.75	28.55
88.00	43865.	1201.5	59.26	37.25	1.94	28.55
90.00	45949.	1240.3	57.71	37.30	2.15	28.55
92.00	48064.	1281.6	56.14	37.36	2.38	28.55
94.00	50212.	1327.4	54.56	37.41	2.62	28.56
96.00	52397.	1379.3	52.98	37.46	2.88	28.56
98.00	54626.	1437.4	51.40	37.51	3.16	28.56
100.00	56900.	1501.6	49.84	37.56	3.47	28.57
105.00	62816.	1689.3	46.03	37.68	4.35	28.58
110.00	69093.	1912.6	42.44	37.78	5.40	28.59

Table H-2. (Continued)
SERV-MURP FINAL REFERENCE TRAJECTORY
50 X 110 NMI INJECTION ORBIT
55 DEGREE INCLINATION

PROJECT APOLLO STANDARD COORDINATE SYSTEM 1

FLIGHT TIME (SEC)	ALTITUDE (FT)	EARTH - FIXED VELOCITY (FT/S)	EARTH - FIXED PATH ANGLE (DEG)	EARTH - FIXED AZIMUTH (DEG)	RANGE (NMI)	GEODETIC LATITUDE (DEG)
115.00	75756.	2169.4	39.09	37.88	6.67	28.61
120.00	82807.	2457.2	36.00	37.96	8.17	28.63
125.00	90239.	2774.4	33.18	38.04	9.94	28.65
130.00	98035.	3120.0	30.61	38.11	11.99	28.68
135.00	106178.	3493.9	28.27	38.18	14.34	28.71
140.00	114644.	3895.1	26.15	38.24	17.03	28.75
145.00	123401.	4309.8	24.21	38.30	20.07	28.79
150.00	132385.	4729.3	22.45	38.36	23.47	28.83
155.00	141534.	5153.2	20.82	38.42	27.22	28.88
160.00	150792.	5581.1	19.33	38.48	31.34	28.93
170.00	169427.	6448.1	16.66	38.59	40.68	29.06
180.00	187829.	7327.3	14.05	38.67	51.52	29.20
190.00	205192.	8220.5	11.65	38.73	63.88	29.36
200.00	221360.	9126.5	9.69	38.82	77.76	29.54
210.00	236302.	10042.7	8.07	38.92	93.18	29.74
220.00	249996.	10967.0	6.71	39.03	110.13	29.96
230.00	262429.	11898.2	5.57	39.16	128.61	30.20
240.00	273604.	12835.0	4.59	39.31	148.62	30.46
250.00	283532.	13776.7	3.75	39.47	170.18	30.74
260.00	292239.	14722.5	3.03	39.64	193.27	31.03
270.00	299764.	15672.0	2.41	39.83	217.90	31.35
280.00	306156.	16624.5	1.89	40.04	244.08	31.68
290.00	311477.	17579.8	1.44	40.26	271.80	32.04
300.00	315805.	18537.3	1.06	40.49	301.08	32.41
310.00	319228.	19496.7	.75	40.74	331.90	32.80
320.00	321846.	20457.7	.50	41.01	364.28	33.21
330.00	323775.	21420.0	.30	41.29	398.22	33.64
340.00	325142.	22383.2	.16	41.60	433.71	34.08
350.00	326088.	23347.1	.06	41.92	470.76	34.54
360.00	326769.	24311.4	.01	42.26	509.38	35.02
367.56	327209.	25040.3	.00	42.53	539.60	35.39

Table H-2. (Continued)

SERV-MURP FINAL REFERENCE TRAJECTORY
50 X 110 NMI INJECTION ORBIT
55 DEGREE INCLINATION

FLIGHT TIME (SEC)	THRUST (LB)	WEIGHT (LB)	LONGITUDINAL ACCELERATION (G'S)	INERTIAL ATTITUDE ANGLES PITCH (DEG)	YAW (DEG)	INCLINATION (DEG)
.00	7453152.	6048922.	1.2321	90.00	.00	28.36
5.00	7446189.	5941843.	1.2527	90.00	.00	28.36
10.00	7446157.	5834765.	1.2742	90.00	.00	28.36
15.00	7454732.	5727686.	1.2966	90.00	.00	28.36
20.00	7474004.	5620608.	1.3202	90.00	.00	28.36
25.00	7505649.	5513529.	1.3453	89.02	.00	28.36
30.00	7543743.	5406451.	1.3705	88.04	.00	28.36
35.00	7590666.	5299372.	1.3962	87.07	.00	28.37
40.00	7647608.	5192294.	1.4226	86.09	.00	28.38
45.00	7705720.	5085215.	1.4485	84.35	.00	28.41
50.00	7767025.	4978137.	1.4740	82.39	.00	28.47
55.00	7848910.	4871058.	1.5011	80.14	.00	28.58
60.00	7900886.	4763980.	1.5150	77.61	.00	28.78
62.00	7926489.	4721148.	1.5164	76.53	.00	28.88
64.00	7937195.	4678317.	1.5139	75.41	.00	29.01
66.00	7943681.	4635485.	1.5101	74.25	.00	29.16
68.00	7960641.	4592654.	1.5082	73.06	.00	29.33
70.00	7973908.	4549823.	1.4870	71.83	.00	29.52
72.00	7988121.	4506991.	1.4573	70.57	.00	29.74
74.00	8006715.	4464160.	1.4276	69.27	.00	29.97
76.00	8016033.	4421328.	1.3895	67.93	.00	30.22
78.00	8036942.	4378497.	1.3857	66.55	.00	30.49
80.00	8054621.	4335666.	1.3839	65.14	.00	30.79
82.00	8071717.	4292834.	1.3912	63.69	.00	31.11
84.00	8096118.	4250003.	1.4104	62.21	.00	31.45
86.00	8093789.	4207171.	1.4251	60.69	.00	31.82
88.00	8088270.	4164340.	1.4425	59.16	.00	32.21
90.00	8082665.	4121509.	1.4626	57.60	.00	32.63
92.00	8083190.	4078677.	1.4909	56.02	.00	33.07
94.00	8278224.	4035846.	1.5709	54.43	.00	33.54
96.00	8421953.	3993014.	1.6493	52.84	.00	34.04
98.00	8568501.	3950183.	1.7273	51.26	.00	34.58
100.00	8718097.	3907352.	1.8057	49.69	.00	35.15
105.00	9037927.	3800273.	1.9955	45.85	.00	36.68
110.00	9296374.	3693194.	2.1699	42.23	.00	38.28

Table H-2. (Continued)

SERV-MURP FINAL REFERENCE TRAJECTORY
50 X 110 NMI INJECTION ORBIT
55 DEGREE INCLINATION

FLIGHT TIME (SEC)	THRUST (LB)	WEIGHT (LB)	LONGITUDINAL ACCELERATION (G'S)	INERTIAL ATTITUDE ANGLES PITCH (DEG)	YAW (DEG)	INCLINATION (DEG)
115.00	9472171.	3586116.	2.3183	38.84	.00	39.86
120.00	9620156.	3479037.	2.4678	35.72	.00	41.37
125.00	9740156.	3371959.	2.6054	32.86	.00	42.78
130.00	9817606.	3264880.	2.7429	30.24	.00	44.06
135.00	9854731.	3157802.	2.8786	27.85	.00	45.21
140.00	9815027.	3050792.	3.0000	25.67	.00	46.24
145.00	9400390.	2946781.	3.0000	23.68	.00	47.14
150.00	9005290.	2847405.	3.0000	21.84	.00	47.90
155.00	8630535.	2752424.	3.0000	20.15	.00	48.57
160.00	8284727.	2661549.	3.0000	18.57	.00	49.14
170.00	7669577.	2490457.	3.0000	15.72	.00	50.09
180.00	7126313.	2331739.	3.0000	8.95	.63	50.87
190.00	6637984.	2184075.	3.0000	7.95	.62	51.52
200.00	6194476.	2046344.	3.0000	6.94	.62	52.05
210.00	5755695.	1918565.	3.0000	5.93	.61	52.49
220.00	5396022.	1798674.	3.0000	4.92	.61	52.85
230.00	5058574.	1686191.	3.0000	3.90	.61	53.16
240.00	4742008.	1580669.	3.0000	2.89	.60	53.43
250.00	4445059.	1481686.	3.0000	1.87	.60	53.66
260.00	4166535.	1388845.	3.0000	.86	.59	53.86
270.00	3905313.	1301771.	3.0000	-.16	.58	54.03
280.00	3660338.	1220113.	3.0000	-1.18	.58	54.19
290.00	3430618.	1143539.	3.0000	-2.20	.57	54.32
300.00	3215215.	1071738.	3.0000	-3.22	.57	54.45
310.00	3013249.	1004416.	3.0000	-4.24	.56	54.55
320.00	2823833.	941278.	3.0000	-5.27	.55	54.65
330.00	2646134.	882045.	3.0000	-6.29	.55	54.74
340.00	2479449.	826483.	3.0000	-7.31	.54	54.82
350.00	2323115.	774372.	3.0000	-8.34	.53	54.89
360.00	2176508.	725503.	3.0000	-9.36	.52	54.96
367.56	2071799.	690600.	3.0000	-10.13	.52	55.00

Table H-2. (Continued)

SERV-MURP FINAL REFERENCE TRAJECTORY
50 X 110 NMI INJECTION ORBIT
55 DEGREE INCLINATION

FLIGHT TIME (SEC)	MACH NO.	DYNAMIC PRESSURE (LB/FT2)	NORMAL FORCE (LB)	AXIAL FORCE (LB)	ANGLE OF ATTACK (DEG)	AERO. HEATING INDICATOR (LB-FT/FT2)	AERO. LOAD INDICATOR (LB-DEG/FT2)
.00	.000	0.	.0	.0	.000	0.	0.
5.00	.034	2.	.0	2687.8	.047	54.	0.
10.00	.072	8.	.0	11644.5	.090	949.	1.
15.00	.113	18.	.0	28180.9	.130	5264.	2.
20.00	.157	35.	.0	53489.6	.167	18143.	6.
25.00	.206	57.	.0	88532.0	.668	48156.	38.
30.00	.258	86.	.0	134041.4	.656	107868.	56.
35.00	.315	121.	.0	191894.9	.395	213921.	48.
40.00	.377	161.	.0	260843.7	.244	387173.	39.
45.00	.443	206.	.0	339844.4	.247	652944.	51.
50.00	.516	253.	.0	429256.9	.265	1039086.	67.
55.00	.596	301.	.0	537066.6	.281	1574480.	85.
60.00	.683	347.	.0	683370.2	.296	2287266.	103.
62.00	.720	364.	.0	767384.9	.302	2626852.	110.
64.00	.758	379.	.0	854496.7	.307	2998595.	117.
66.00	.796	393.	.0	943644.5	.313	3402456.	123.
68.00	.836	405.	.0	1034135.2	.319	3837982.	129.
70.00	.877	415.	.0	1208136.4	.325	4304394.	135.
72.00	.917	422.	.0	1419938.4	.331	4798922.	139.
74.00	.958	425.	.0	1633502.5	.337	5317426.	143.
76.00	.997	425.	.0	1872432.8	.344	5855302.	146.
78.00	1.036	422.	.0	1969854.6	.352	6407523.	149.
80.00	1.077	418.	.0	2054504.6	.359	6971525.	150.
82.00	1.119	412.	.0	2099609.3	.366	7545535.	151.
84.00	1.163	406.	.0	2102094.7	.372	8127729.	151.
86.00	1.210	398.	.0	2098062.4	.377	8717284.	150.
88.00	1.258	389.	.0	2081258.5	.382	9312799.	149.
90.00	1.307	379.	.0	2054564.3	.385	9912685.	146.
92.00	1.358	368.	.0	2002124.7	.389	10515368.	143.
94.00	1.413	357.	.0	1938113.6	.390	11120246.	140.
96.00	1.472	347.	.0	1836208.9	.391	11729501.	136.
98.00	1.535	337.	.0	1745217.4	.389	12345178.	131.
100.00	1.602	327.	.0	1662559.5	.386	12968487.	126.
105.00	1.780	299.	.0	1454336.3	.375	14557494.	112.
110.00	1.992	276.	.0	1282690.0	.359	16207598.	99.

Table H-2. (Continued)
SERV-MURP FINAL REFERENCE TRAJECTORY
50 X 110 NMI INJECTION ORBIT
55 DEGREE INCLINATION

FLIGHT TIME (SEC)	MACH NO.	DYNAMIC PRESSURE (LB/FT2)	NORMAL FORCE (LB)	AXIAL FORCE (LB)	ANGLE OF ATTACK (DEG)	AERO. HEATING INDICATOR (LB-FT/FT2)	AERO. LOAD INDICATOR (LB-DEG/FT2)
115.00	2.235	252.	.0	1158355.9	.342	17924160.	86.
120.00	2.507	227.	.0	1034755.6	.324	19691656.	74.
125.00	2.808	203.	.0	954804.4	.307	21484403.	62.
130.00	3.124	176.	.0	862396.2	.291	23264788.	51.
135.00	3.457	151.	.0	764705.1	.275	24987142.	41.
140.00	3.804	127.	.0	662649.8	.260	26618806.	33.
145.00	4.151	105.	.0	560048.1	.247	28130511.	26.
150.00	4.492	85.	.0	463075.3	.236	29493894.	20.
155.00	4.832	69.	.0	373264.1	.225	30699478.	15.
160.00	5.178	55.	.0	300079.4	.216	31753010.	12.
170.00	5.989	36.	.0	198206.7	.200	33468265.	7.
180.00	6.977	24.	.0	131094.9	3.977	34805694.	96.
190.00	8.077	16.	.0	85759.1	2.357	35809318.	37.
200.00	9.263	10.	.0	55443.1	1.166	36526568.	12.
210.00	.000	0.	.0	.0	5.747	0.	0.
220.00	.000	0.	.0	.0	5.344	0.	0.
230.00	.000	0.	.0	.0	5.024	0.	0.
240.00	.000	0.	.0	.0	4.754	0.	0.
250.00	.000	0.	.0	.0	4.510	0.	0.
260.00	.000	0.	.0	.0	4.278	0.	0.
270.00	.000	0.	.0	.0	4.050	0.	0.
280.00	.000	0.	.0	.0	3.823	0.	0.
290.00	.000	0.	.0	.0	3.594	0.	0.
300.00	.000	0.	.0	.0	3.365	0.	0.
310.00	.000	0.	.0	.0	3.138	0.	0.
320.00	.000	0.	.0	.0	2.919	0.	0.
330.00	.000	0.	.0	.0	2.713	0.	0.
340.00	.000	0.	.0	.0	2.528	0.	0.
350.00	.000	0.	.0	.0	2.375	0.	0.
360.00	.000	0.	.0	.0	2.265	0.	0.
367.56	.000	0.	.0	.0	2.218	0.	0.

Table H-3.

SERV-MURP FINAL REFERENCE TRAJECTORY
50 X 100 NMI INJECTION ORBIT
104 DEGREE INCLINATION

PROJECT APOLLO STANDARD COORDINATE SYSTEM 1

FLIGHT TIME (SEC)	GEOCENTRIC RADIUS (FT)	INERTIAL VELOCITY (FT/S)	INERTIAL PATH ANGLE (DEG)	INERTIAL AZIMUTH (DEG)	GEOCENTRIC LATITUDE (DEG)	LONGITUDE (POS. EAST) (DEG)
.00	20909846.	1341.8	.00	90.00	28.36	-80.56
5.00	20909948.	1342.4	1.76	90.00	28.36	-80.56
10.00	20910263.	1344.3	3.66	89.99	28.36	-80.56
15.00	20910812.	1348.1	5.71	89.98	28.36	-80.56
20.00	20911611.	1354.0	7.91	89.98	28.36	-80.56
25.00	20912680.	1361.9	10.24	90.05	28.36	-80.56
30.00	20914038.	1371.8	12.73	90.27	28.36	-80.56
35.00	20915708.	1384.1	15.35	90.66	28.36	-80.56
40.00	20917707.	1399.3	18.08	91.22	28.36	-80.56
45.00	20920057.	1417.5	20.92	92.06	28.36	-80.56
50.00	20922774.	1438.7	23.83	93.25	28.36	-80.56
55.00	20925873.	1463.4	26.78	94.85	28.36	-80.56
60.00	20929368.	1491.4	29.68	96.95	28.36	-80.56
62.00	20930876.	1503.4	30.79	97.93	28.35	-80.56
64.00	20932445.	1515.7	31.86	99.01	28.35	-80.56
66.00	20934075.	1528.3	32.89	100.16	28.35	-80.56
68.00	20935764.	1541.1	33.86	101.41	28.35	-80.57
70.00	20937508.	1553.6	34.74	102.73	28.35	-80.57
72.00	20939303.	1565.5	35.52	104.12	28.35	-80.57
74.00	20941144.	1576.6	36.20	105.57	28.35	-80.57
76.00	20943025.	1587.0	36.77	107.08	28.34	-80.57
78.00	20944943.	1597.7	37.29	108.67	28.34	-80.57
80.00	20946896.	1608.9	37.75	110.36	28.34	-80.57
82.00	20948883.	1620.9	38.17	112.14	28.34	-80.57
84.00	20950902.	1634.3	38.55	114.04	28.33	-80.57
86.00	20952955.	1648.9	38.87	116.03	28.33	-80.57
88.00	20955041.	1665.1	39.14	118.13	28.33	-80.57
90.00	20957160.	1683.0	39.36	120.33	28.32	-80.58
92.00	20959311.	1703.6	39.52	122.63	28.32	-80.58
94.00	20961497.	1728.7	39.67	125.11	28.32	-80.58
96.00	20963726.	1758.6	39.79	127.73	28.31	-80.58
98.00	20966001.	1793.7	39.86	130.48	28.31	-80.58
100.00	20968326.	1834.3	39.87	133.33	28.30	-80.58
105.00	20974382.	1961.8	39.52	140.70	28.29	-80.59
110.00	20980817.	2127.0	38.58	147.95	28.27	-80.60

Table H-3. (Continued)
SERV-MURP FINAL REFERENCE TRAJECTORY
50 X 100 NMI INJECTION ORBIT
104 DEGREE INCLINATION

PROJECT APOLLO STANDARD COORDINATE SYSTEM 1

FLIGHT TIME (SEC)	GEOCENTRIC RADIUS (FT)	INERTIAL VELOCITY (FT/S)	INERTIAL PATH ANGLE (DEG)	INERTIAL AZIMUTH (DEG)	GEOCENTRIC LATITUDE (DEG)	LONGITUDE (POS. EAST) (DEG)
115.00	20987646.	2330.2	37.10	154.62	28.25	-80.60
120.00	20994871.	2571.3	35.25	160.50	28.22	-80.61
125.00	21002480.	2848.9	33.18	165.51	28.20	-80.62
130.00	21010456.	3162.1	31.04	169.73	28.16	-80.64
135.00	21018776.	3509.6	28.92	173.25	28.12	-80.65
140.00	21027417.	3886.6	26.88	176.16	28.08	-80.67
145.00	21036327.	4275.7	24.96	178.52	28.03	-80.69
150.00	21045436.	4673.9	23.15	180.44	27.97	-80.71
155.00	21054684.	5079.8	21.47	182.03	27.91	-80.73
160.00	21064010.	5492.6	19.90	183.37	27.84	-80.75
170.00	21082691.	6335.5	17.08	185.48	27.69	-80.81
180.00	21101017.	7195.0	14.34	187.13	27.52	-80.87
190.00	21118222.	8071.6	11.85	188.48	27.32	-80.94
200.00	21134161.	8964.8	9.82	189.54	27.09	-81.03
210.00	21148806.	9870.9	8.15	190.40	26.84	-81.12
220.00	21162139.	10787.2	6.75	191.10	26.57	-81.22
230.00	21174154.	11711.7	5.57	191.68	26.27	-81.33
240.00	21184855.	12643.0	4.56	192.17	25.95	-81.44
250.00	21194260.	13580.0	3.70	192.59	25.61	-81.57
260.00	21202399.	14521.9	2.97	192.94	25.24	-81.70
270.00	21209314.	15467.9	2.34	193.25	24.84	-81.85
280.00	21215060.	16417.5	1.81	193.51	24.42	-82.00
290.00	21219705.	17370.1	1.36	193.74	23.98	-82.16
300.00	21223329.	18325.2	.98	193.94	23.51	-82.33
310.00	21226027.	19282.6	.67	194.11	23.02	-82.50
320.00	21227903.	20241.8	.43	194.26	22.50	-82.68
330.00	21229079.	21202.5	.24	194.39	21.96	-82.88
340.00	21229686.	22164.3	.10	194.50	21.40	-83.07
350.00	21229871.	23127.0	.01	194.60	20.80	-83.28
360.00	21229791.	24090.3	-.04	194.69	20.19	-83.49
370.00	21229620.	25054.0	-.03	194.76	19.55	-83.72
378.73	21229542.	25895.7	-.00	194.82	18.97	-83.91

Table H-3. (Continued)

SERV-MURP FINAL REFERENCE TRAJECTORY
50 X 100 NMI INJECTION ORBIT
104 DEGREE INCLINATION

PROJECT APOLLO STANDARD COORDINATE SYSTEM 1

FLIGHT TIME (SEC)	ALTITUDE (FT)	* * * EARTH - FIXED VELOCITY (FT/S)	PATH ANGLE (DEG)	AZIMUTH (DEG) * * *	RANGE (NMI)	GEODETIC LATITUDE (DEG)
.00	0.	.0	.00	.00	.00	28.52
5.00	102.	41.2	89.83	338.66	.00	28.52
10.00	418.	85.9	89.80	322.67	.00	28.52
15.00	966.	134.2	89.76	311.84	.00	28.52
20.00	1765.	186.2	89.72	304.52	.00	28.52
25.00	2834.	242.2	89.51	237.91	.00	28.52
30.00	4193.	302.3	88.57	212.05	.00	28.52
35.00	5862.	366.7	87.32	205.96	.01	28.52
40.00	7861.	435.5	85.92	203.53	.03	28.52
45.00	10210.	508.8	84.20	202.05	.07	28.52
50.00	12926.	586.8	82.18	201.07	.12	28.52
55.00	16025.	669.8	79.86	200.39	.20	28.52
60.00	19517.	757.0	77.27	199.91	.32	28.52
62.00	21024.	792.5	76.17	199.75	.37	28.52
64.00	22592.	828.2	75.03	199.62	.44	28.51
66.00	24221.	863.9	73.85	199.49	.52	28.51
68.00	25908.	899.7	72.64	199.38	.60	28.51
70.00	27651.	934.2	71.39	199.28	.69	28.51
72.00	29445.	967.3	70.11	199.20	.80	28.51
74.00	31284.	998.8	68.79	199.12	.91	28.51
76.00	33163.	1028.9	67.43	199.05	1.03	28.51
78.00	35079.	1059.3	66.03	198.99	1.17	28.50
80.00	37029.	1090.4	64.60	198.93	1.32	28.50
82.00	39013.	1122.9	63.13	198.87	1.48	28.50
84.00	41030.	1157.4	61.63	198.81	1.65	28.50
86.00	43080.	1193.8	60.10	198.76	1.84	28.49
88.00	45163.	1232.1	58.55	198.71	2.04	28.49
90.00	47278.	1272.8	56.98	198.66	2.26	28.49
92.00	49424.	1317.0	55.40	198.62	2.50	28.48
94.00	51607.	1367.3	53.82	198.57	2.75	28.48
96.00	53831.	1423.9	52.23	198.53	3.03	28.47
98.00	56101.	1486.6	50.66	198.48	3.33	28.47
100.00	58421.	1555.5	49.10	198.44	3.65	28.46
105.00	64463.	1755.1	45.34	198.34	4.57	28.45
110.00	70879.	1990.3	41.79	198.26	5.68	28.43

Table H-3. (Continued)
SERV-MURP FINAL REFERENCE TRAJECTORY
50 X 100 NMI INJECTION ORBIT
104 DEGREE INCLINATION

PROJECT APOLLO STANDARD COORDINATE SYSTEM 1

FLIGHT TIME (SEC)	ALTITUDE (FT)	EARTH - FIXED VELOCITY (FT/S)	PATH ANGLE (DEG)	AZIMUTH (DEG)	RANGE (NMI)	GEODETIC LATITUDE (DEG)
115.00	77687.	2258.2	38.50	198.19	7.01	28.41
120.00	84886.	2557.4	35.47	198.12	8.59	28.39
125.00	92466.	2885.9	32.70	198.07	10.43	28.36
130.00	100406.	3243.2	30.18	198.03	12.57	28.32
135.00	108687.	3628.8	27.89	197.99	15.03	28.28
140.00	117283.	4038.3	25.80	197.96	17.83	28.24
145.00	126142.	4454.6	23.89	197.93	20.99	28.19
150.00	135194.	4875.6	22.14	197.91	24.50	28.13
155.00	144379.	5301.0	20.53	197.88	28.37	28.07
160.00	153637.	5730.4	19.04	197.87	32.61	28.00
170.00	172165.	6600.4	16.37	197.83	42.20	27.85
180.00	190313.	7482.9	13.78	197.87	53.29	27.67
190.00	207317.	8379.3	11.41	197.97	65.91	27.47
200.00	223032.	9288.1	9.48	198.04	80.07	27.25
210.00	237431.	10207.0	7.88	198.09	95.75	27.00
220.00	250496.	11133.8	6.54	198.13	112.97	26.72
230.00	262220.	12067.1	5.40	198.16	131.73	26.43
240.00	272610.	13006.0	4.43	198.18	152.03	26.10
250.00	281683.	13949.6	3.60	198.19	173.86	25.76
260.00	289469.	14897.2	2.89	198.20	197.24	25.39
270.00	296013.	15848.2	2.29	198.20	222.17	24.99
280.00	301369.	16802.3	1.77	198.19	248.64	24.57
290.00	305607.	17758.9	1.33	198.17	276.66	24.12
300.00	308807.	18717.7	.96	198.16	306.23	23.65
310.00	311066.	19678.4	.66	198.13	337.36	23.16
320.00	312489.	20640.6	.42	198.11	370.05	22.64
330.00	313198.	21604.0	.23	198.08	404.30	22.10
340.00	313327.	22568.5	.09	198.05	440.11	21.53
350.00	313024.	23533.6	.01	198.01	477.49	20.93
360.00	312447.	24499.1	-.04	197.98	516.43	20.31
370.00	311772.	25464.9	-.03	197.94	556.94	19.67
378.73	311250.	26308.3	-.00	197.91	593.59	19.08

Table H-3. (Continued)

SERV-MURP FINAL REFERENCE TRAJECTORY

50 X 100 NMI INJECTION ORBIT

104 DEGREE INCLINATION

FLIGHT TIME (SEC)	THRUST (LB)	WEIGHT (LB)	LONGITUDINAL ACCELERATION (G'S)	INERTIAL ATTITUDE ANGLES PITCH (DEG)	YAW (DEG)	INCLINATION (DEG)
.00	7453152.	5988787.	1.2445	90.00	.00	28.36
5.00	7445846.	5881708.	1.2654	90.00	.00	28.36
10.00	7445881.	5774630.	1.2872	90.00	.00	28.36
15.00	7455098.	5667551.	1.3099	90.00	.00	28.36
20.00	7475656.	5560473.	1.3339	90.00	.00	28.36
25.00	7508073.	5453394.	1.3591	89.01	.00	28.36
30.00	7547963.	5346316.	1.3845	88.03	.00	28.36
35.00	7596349.	5239237.	1.4102	87.04	.00	28.37
40.00	7656842.	5132159.	1.4371	86.06	.00	28.38
45.00	7712166.	5025080.	1.4621	84.12	.00	28.43
50.00	7777625.	4918002.	1.4875	82.09	.00	28.53
55.00	7850994.	4810923.	1.5123	79.78	.00	28.74
60.00	7909392.	4703845.	1.5214	77.19	.00	29.13
62.00	7925260.	4661013.	1.5199	76.09	.00	29.36
64.00	7933320.	4618182.	1.5162	74.95	.00	29.64
66.00	7945202.	4575350.	1.5128	73.78	.00	29.98
68.00	7962753.	4532519.	1.4991	72.56	.00	30.38
70.00	7975883.	4489688.	1.4680	71.32	.00	30.86
72.00	7994925.	4446856.	1.4393	70.03	.00	31.41
74.00	8007693.	4404025.	1.4007	68.71	.00	32.03
76.00	8025476.	4361193.	1.3874	67.35	.00	32.72
78.00	8048840.	4318362.	1.3869	65.95	.00	33.51
80.00	8062151.	4275531.	1.3882	64.52	.00	34.39
82.00	8086526.	4232699.	1.4072	63.05	.00	35.39
84.00	8095894.	4189868.	1.4239	61.55	.00	36.50
86.00	8090381.	4147036.	1.4407	60.02	.00	37.73
88.00	8084779.	4104205.	1.4596	58.47	.00	39.08
90.00	8079091.	4061374.	1.4857	56.90	.00	40.55
92.00	8210412.	4018542.	1.5478	55.32	.00	42.16
94.00	8369975.	3975711.	1.6307	53.73	.00	43.93
96.00	8516267.	3932879.	1.7103	52.14	.00	45.87
98.00	8665566.	3890048.	1.7890	50.57	.00	47.96
100.00	8818129.	3847217.	1.8706	49.01	.00	50.18
105.00	9105740.	3740138.	2.0549	45.23	.00	56.10
110.00	9354862.	3633059.	2.2280	41.67	.00	62.13

Table H-3. (Continued)
SERV-MURP FINAL REFERENCE TRAJECTORY
50 X 100 NMI INJECTION ORBIT
104 DEGREE INCLINATION

FLIGHT TIME (SEC)	THRUST (LB)	WEIGHT (LB)	LONGITUDINAL ACCELERATION (G'S)	INERTIAL ATTITUDE ANGLES PITCH (DEG)	YAW (DEG)	INCLINATION (DEG)
115.00	9518618.	3525981.	2.3778	38.36	.00	67.82
120.00	9654162.	3418902.	2.5241	35.31	.00	72.89
125.00	9762274.	3311824.	2.6636	32.52	.00	77.26
130.00	9838281.	3204745.	2.8068	29.97	.00	80.96
135.00	9861884.	3097667.	2.9440	27.63	.00	84.05
140.00	9612665.	2991505.	3.0000	25.51	.00	86.62
145.00	9202512.	2889738.	3.0000	23.55	.00	88.69
150.00	8814047.	2792527.	3.0000	21.75	.00	90.39
155.00	8449992.	2699619.	3.0000	20.08	.00	91.80
160.00	8114566.	2610680.	3.0000	18.53	.00	92.98
170.00	7517222.	2443029.	3.0000	15.71	.00	94.85
180.00	6987012.	2287427.	3.0000	9.38	-1.18	96.32
190.00	6509892.	2142616.	3.0000	8.48	-1.22	97.53
200.00	6076119.	2007511.	3.0000	7.59	-1.26	98.49
210.00	5646391.	1882130.	3.0000	6.69	-1.30	99.27
220.00	5293470.	1764490.	3.0000	5.80	-1.34	99.91
230.00	4962367.	1654122.	3.0000	4.90	-1.38	100.46
240.00	4651761.	1550587.	3.0000	4.01	-1.42	100.93
250.00	4360411.	1453470.	3.0000	3.11	-1.45	101.33
260.00	4087144.	1362381.	3.0000	2.21	-1.49	101.69
270.00	3830859.	1276953.	3.0000	1.31	-1.53	102.00
280.00	3590521.	1196840.	3.0000	.42	-1.57	102.28
290.00	3365152.	1121717.	3.0000	-.48	-1.61	102.53
300.00	3153833.	1051278.	3.0000	-1.39	-1.65	102.76
310.00	2955693.	985231.	3.0000	-2.29	-1.68	102.96
320.00	2769838.	923279.	3.0000	-3.19	-1.72	103.15
330.00	2595486.	865162.	3.0000	-4.09	-1.76	103.32
340.00	2431946.	810649.	3.0000	-5.00	-1.79	103.48
350.00	2278568.	759523.	3.0000	-5.90	-1.83	103.63
360.00	2134737.	711579.	3.0000	-6.81	-1.86	103.77
370.00	1999874.	666625.	3.0000	-7.71	-1.90	103.90
378.73	1888274.	629658.	3.0000	-8.51	-1.93	104.00

Table H-3. (Continued)

SERV-MURP FINAL REFERENCE TRAJECTORY
50 X 100 NMI INJECTION ORBIT
104 DEGREE INCLINATION

FLIGHT TIME (SEC)	MACH NO.	DYNAMIC PRESSURE (LB/FT2)	NORMAL FORCE (LB)	AXIAL FORCE (LB)	ANGLE OF ATTACK (DEG)	AERO. HEATING INDICATOR (LB-FT/FT2)	AERO. LOAD INDICATOR (LB-DEG/FT2)
.00	.000	0.	.0	.0	.000	0.	0.
5.00	.036	2.	.0	2971.4	.045	63.	0.
10.00	.076	8.	.0	12833.6	.086	1100.	1.
15.00	.118	20.	.0	30956.1	.125	6076.	3.
20.00	.165	38.	.0	58552.7	.161	20858.	6.
25.00	.215	62.	.0	96550.3	.521	55088.	32.
30.00	.270	93.	.0	145944.6	.518	122809.	48.
35.00	.329	130.	.0	208070.7	.309	242424.	40.
40.00	.393	173.	.0	281587.6	.353	436917.	61.
45.00	.462	220.	.0	365026.2	.296	733436.	65.
50.00	.537	269.	.0	462174.3	.320	1161247.	86.
55.00	.620	318.	.0	575488.6	.342	1750364.	109.
60.00	.710	363.	.0	752739.4	.363	2528315.	132.
62.00	.747	380.	.0	840923.9	.372	2896345.	141.
64.00	.786	394.	.0	931443.7	.381	3297347.	150.
66.00	.826	407.	.0	1023407.3	.389	3730947.	159.
68.00	.867	418.	.0	1168079.7	.398	4196467.	167.
70.00	.907	426.	.0	1385047.9	.408	4691760.	174.
72.00	.948	430.	.0	1594484.8	.418	5212660.	180.
74.00	.987	431.	.0	1838990.1	.429	5754630.	185.
76.00	1.026	429.	.0	1974921.7	.441	6312346.	189.
78.00	1.067	425.	.0	2059551.6	.452	6882501.	192.
80.00	1.109	420.	.0	2126801.8	.464	7463386.	195.
82.00	1.152	413.	.0	2130482.5	.474	8052937.	196.
84.00	1.198	406.	.0	2130133.7	.484	8650332.	196.
86.00	1.246	397.	.0	2115686.1	.493	9254351.	196.
88.00	1.295	387.	.0	2094283.2	.502	9863413.	194.
90.00	1.346	377.	.0	2045031.2	.509	10475865.	192.
92.00	1.400	365.	.0	1990668.8	.516	11090481.	188.
94.00	1.458	355.	.0	1886881.4	.520	11708666.	184.
96.00	1.520	344.	.0	1789977.2	.522	12332883.	180.
98.00	1.587	334.	.0	1706097.8	.522	12964615.	174.
100.00	1.657	323.	.0	1621652.8	.521	13604630.	168.
105.00	1.844	296.	.0	1420076.4	.513	15236279.	152.
110.00	2.067	272.	.0	1260443.6	.500	16934444.	136.

Table H-3. (Continued)

SERV-MURP FINAL REFERENCE TRAJECTORY
50 X 100 NMI INJECTION ORBIT
104 DEGREE INCLINATION

FLIGHT TIME (SEC)	MACH NO.	DYNAMIC PRESSURE (LB/FT2)	NORMAL FORCE (LB)	AXIAL FORCE (LB)	ANGLE OF ATTACK (DEG)	AERO. HEATING INDICATOR (LB-FT/FT2)	AERO. LOAD INDICATOR (LB-DEG/FT2)
115.00	2.319	248.	.0	1134580.8	.486	18697330.	120.
120.00	2.602	223.	.0	1024442.7	.472	20505206.	105.
125.00	2.913	197.	.0	940903.4	.459	22328940.	91.
130.00	3.236	170.	.0	843205.8	.447	24125324.	76.
135.00	3.577	145.	.0	742280.3	.436	25851435.	63.
140.00	3.928	121.	.0	638148.2	.426	27475819.	52.
145.00	4.272	99.	.0	533298.6	.420	28964853.	42.
150.00	4.612	80.	.0	436465.6	.415	30296124.	33.
155.00	4.953	65.	.0	351136.2	.413	31467122.	27.
160.00	5.304	52.	.0	282525.4	.412	32488089.	21.
170.00	6.149	35.	.0	188134.1	.412	34155008.	14.
180.00	7.155	23.	.0	124729.4	3.630	35453293.	83.
190.00	8.267	15.	.0	82043.6	1.983	36425759.	30.
200.00	9.459	10.	.0	53585.9	.817	37124750.	8.
210.00	.000	0.	.0	.0	8.079	0.	0.
220.00	.000	0.	.0	.0	7.452	0.	0.
230.00	.000	0.	.0	.0	6.985	0.	0.
240.00	.000	0.	.0	.0	6.620	0.	0.
250.00	.000	0.	.0	.0	6.321	0.	0.
260.00	.000	0.	.0	.0	6.062	0.	0.
270.00	.000	0.	.0	.0	5.825	0.	0.
280.00	.000	0.	.0	.0	5.601	0.	0.
290.00	.000	0.	.0	.0	5.381	0.	0.
300.00	.000	0.	.0	.0	5.163	0.	0.
310.00	.000	0.	.0	.0	4.944	0.	0.
320.00	.000	0.	.0	.0	4.724	0.	0.
330.00	.000	0.	.0	.0	4.503	0.	0.
340.00	.000	0.	.0	.0	4.283	0.	0.
350.00	.000	0.	.0	.0	4.066	0.	0.
360.00	.000	0.	.0	.0	3.854	0.	0.
370.00	.000	0.	.0	.0	3.650	0.	0.
378.73	.000	0.	.0	.0	3.484	0.	0.